UNCLASSIFIED

AD NUMBER

AD803008

NEW LIMITATION CHANGE

TO

Approved for public release, distribution unlimited

FROM

Distribution authorized to U.S. Gov't. agencies and their contractors; Administrative/Operational Use; May 1966. Other requests shall be referred to Commanding Officer, U.S. Army Research Office, Box CM, Duke Station, Durham, NC.

AUTHORITY

USARO ltr, 5 Jul 1967

THIS PAGE IS UNCLASSIFIED

ARO-D Report 66-2

803008

PROCEEDINGS OF THE ELEVENTH CONFERENCE ON THE DESIGN OF EXPERIMENTS IN ARMY RESEARCH DEVELOPMENT AND TESTING

Sponsored by
The Army Mathematics Steering Committee
on Behalf of
THE OFFICE OF THE CHIEF OF RESEARCH AND DEVELOPMENT

U. S Army Research Office - Durham
Report No. 66-2
May 1966

PROCEEDINGS OF THE ELEVENTH CONFERENCE ON THE DESIGN OF EXPERIMENTS IN ARMY RESEARCH, DEVELOPMENT AND TESTING

Sponsored by the Army Mathematics Steering Committee

Host

Headquarters, U. S. Army Munitions Command
Dover, New Jersey
20-22 October 1965

U. S. Army Research Office - Durham
Box CM, Duke Station
Durham, North Carolina

PAGES _____

ARE

MISSING

IN

ORIGINAL

DOCUMENT

FOREWORD

The Army Munitions Command headed by Major General F. A. Hanson hosted the Eleventh Conference on the Design of Experiments in Army Research, Development and Testing. This three-day meeting starting 20 October 1965 was conducted at Stevens Institute of Technology in Hoboken, New Jersey. Colonel Thomas W. McGrath, Deputy Commander at Headquarters Army Munitions Command, issued the following letter:

> "It is my privilege to welcome you to the Eleventh Conference on the Design of Experiments in Army Research, Development and Testing. We consider it a great honor to be selected to serve as host to this important meeting.
>
> We hope that each participant finds this conference both enjoyable and professionally rewarding."

The Army Mathematics Steering Committee, sponsors of this conference on behalf of the Office of Chief of Research and Development, would like to thank Colonel McGrath for his welcoming remarks. Members of this committee would also like to thank General Hanson for making available personnel under his command to help conduct this conference. In particular, many thanks are due to Mr. Henry DeCicco, who had the main responsibility as Chairman on Local Arrangements for coordinating the conference arrangements at the Command Headquarters.

The program of this meeting included 6 general, 11 technical, and 4 clinical sessions. The invited speakers in the general sessions featured the following addresses:

Confidence Limits for the Reliability of Complex Systems
Dr. Joan R. Rosenblatt, National Bureau of Standards

Non-Linear Models: Estimation and Design
Dr. J. Stuart Hunter, Princeton University

Selecting the Population with the Largest Parameter
Professor Robert E. Bechhofer, Cornell University

Selecting a Subset Containing the Population with the Largest Parameter
Professor Shanti S. Gupta, Purdue University

Target Coverage Problems
Professor William C. Guenther, University of Wyoming

Maximum Likelihood Estimates for the General Mixed Analysis of a Variance Model
Professor H. O. Hartley, Texas A&M University .

The conference was highlighted by the banquet held on Thursday evening, 21st of October, at Stevens Center with Mrs. Samuel Wilks as guest of honor. On this occasion Professor John W. Tukey of Princeton University was presented the first Wilks Memorial Medal Award.

This volume of the proceedings contains 26 of the papers which were presented at this meeting. The Army Mathematics Steering Committee has asked that these articles on modern principles on the design of experiments, as well as applications of these ideas, be made available in the form of this technical manual.

The Eleventh Conference was attended by more than 150 registrants and participants from over 57 different organizations. Speakers and panelists came from the National Bureau of Standards, Princeton University, Rocketdyne (A Division of North American Aviation, Inc.), National Institute of Mental Health, Virginia Polytechnic Institute, North Carolina State University at Raleigh, University of Oklahoma, George C. Marshall Space Flight Center (NASA), Cornell University, University of Georgia, University of Tennessee, Purdue University, Texas A&M University, University of Chicago, University of Wyoming, George Washington University, and thirteen Army facilities.

The chairman wishes to take this occasion to thank his Advisory Committee (Henry DeCicco, F. G. Dressel, Walter Foster, Fred Frishman, Bernard Greenberg, Boyd Harshbarger, William Kruskal, H. L. Lucas, Clifford Maloney, Henry Mann, and W. Y. Youden) for their assistance in formulating the program and their help in selecting the invited speakers. He is also grateful to the authors of contributed papers, chairmen, and panelists. Without their help this meeting could never have succeeded in its scientific purposes.

F. E. Grubbs
Conference Chairman

TABLE OF CONTENTS

	Page
Foreword	i
Table of Contents	iii
Program	vii
Confidence Limits for the Reliability of Complex Systems Joan R. Rosenblatt	*
Estimation and Design for Non-Linear Models J. Stuart Hunter	1
A Problem of Deterioration in Reliability Henry DeCicco	29
Game Theory Techniques for System Analysis and Design Jerome H. N. Selman	*
Systematic Methods for Analyzing $2^n 3^m$ Factorial Experiments Barry H. Margolin	31
Construction and Comparison of Non-Orthogonal Incomplete Factorial Designs S. R. Webb	61
Statistical Analysis of Automatically Recorded Physiograph Data John Atkinson	77
An Application of Experimental Design in Ergonomics: Heart Rate as a Function of Work Stress and Time Henry B. Tingey and William H. Kirby, Jr.	81
Strategy for the Optimal Use of Weapons by Area Coverage J. A. Nickel, J. D. Palmer and F. J. Kern	117
Variability of Lethal Area Bruce D. Barnett	155

*This paper was presented at the conference. It does not appear in these Proceedings.

Page

Decision Procedure for Minimizing Costs of Calabrating Liquid Rocket Engines
E. L. Bombara and S. H. Lishman 173

The Theoretical Strength of Titanium Calculated from the Cohesive Energy
Perry R. Smoot 203

Ten Snake Venoms: A Study of Their Effects on Physiological Parameters and Survival
J. A. Vick, H. F. Cichta, and J. H. Manthei 223

Piricularia Oryzae - Relationship Between Lesion Counts and Spore Counts
Thomas H. Barksdale, William D. Brener, Walter D. Foster, and Marian W. Jones 263

Extreme Vertices Design of Mixture Experiments
R. A. McLean, and V. L. Anderson 273

Design of a High-Voltage-Breakdown-In-Vacuum Experiment
M. M. Chrepta, J. Weinstein, G. W. Taylor and M. H. Zinn 285

Model Simulation of Bio-Cellular Systems
George I. Lavin . . . . . *

Some Inferential Statistics Which are Relatively Compatible with an Individual Organism Methodology
Samuel H. Revusky 299

Control of Data-Support Quality
Fred S. Hanson 313

Designs and Analyses for Inverse Response Problems in Sensitivity Testing
M. J. Alexander and D. Rothman 337

*This paper was presented at the conference. It does not appear in these Proceedings.

Page

Monte Carlo Investigation of the Probability Distributions of Dixon's Criteria for Testing Outlying Observations
Walter L. Mowchan 367

A Simplified Technique for Estimating Degrees of Freedom for a Two Population "T" Test when the Standard Deviations are Unknown and Not Necessarily Equal
E. Dutoit and R. Webster 415

Deleting Observations from a Least Squares Solution
Charles A. Hall 449

Precision and Bias Estimates for Data from Cinetheodolite and AN/FPS-16 Radar Trajectory Measuring Systems
Burton L. Williams and Oliver L. Kingsley 469

Thermal Cycles in Welding
Mark M. D'Andrea, Jr. 487

Statistical Analysis of Tensile-Strength Hardness Relationships in Thermomechanically Treated Steels
Albert A. Anctil 493

Comments on the Presentation by Albert A. Anctil
Joan R. Rosenblatt 509

Some Problems in Statistical Inference for Generalized Multinomial Populations
Bernard Harris 511

Statistics in the Calibration Laboratory
Joseph M. Cameron . . . . . *

Application of Numerical Techniques to Experimentally Model an Aerodynamic Function
Andrew H. Jenkins 519

Selecting the Population with the Largest Parameter
Robert E. Bechhofer . . . . . *

*This paper was presented at the conference. It does not appear in these Proceedings.

Page

Selecting a Subset Containing the Population with the Largest Parameter
Shanti S. Gupta . . . . . *

Presentation and Acceptance of the First Samuel S. Wilks Memorial Award
Frank E. Grubbs, John W. Tukey 569

Target Coverage Problems
William C. Guenther 573

Maximum Likelihood Estimates for Unbalanced Factorial Data
H. O. Hartley 597

List of Attendees 607

*This paper was presented at the conference. It does not appear in these Proceedings.

ELEVENTH CONFERENCE ON THE DESIGN OF EXPERIMENTS
IN ARMY RESEARCH, DEVELOPMENT AND TESTING

20-22 October 1965

Wednesday, 20 October

0900-1100 REGISTRATION - - Lobby of Stevens Center

0930-0945 CALLING OF CONFERENCE TO ORDER - - 4th Floor Seminar Room
Henry DeCicco, Chairman on Local Arrangements

0945-1200 GENERAL SESSION 1

Chairman: Dr. Walter D. Foster, U. S. Army Biological Laboratories, Fort Detrick, Frederick, Maryland

CONFIDENCE LIMITS FOR THE RELIABILITY OF COMPLEX SYSTEMS
Dr. Joan R. Rosenblatt, National Bureau of Standards

BREAK

NON-LINEAR MODELS: ESTIMATION AND DESIGN
Dr. J. Stuart Hunter, Princeton University

1200-1330 LUNCH

Technical Sessions I and II and Clinical Session A will start at 1330 and run to 1500. After the break Technical Sessions III and IV and Clinical Session B will convene at 1530 and run to 1700.

1330-1500 TECHNICAL SESSION I - - 4th Floor Seminar Room

Chairman: Joseph Mandelson, Directorate of Quality Assurance, U. S. Army Edgewood Arsenal, Edgewood, Maryland

A PROBLEM OF DETERIORATION IN RELIABILITY
Henry DeCicco, Quality Assurance Directorate, U. S. Army Munitions Command

TECHNICAL SESSION I (continued)

GAME THEORY TECHNIQUES FOR SYSTEM ANALYSIS AND DESIGN
Jerome H. N. Selman, Headquarters, U. S. Army Munitions Command, Dover, New Jersey

1330-1500 TECHNICAL SESSION II - - 3rd Floor Conference Room

Chairman: Badrig Kurkjian, Harry Diamond Laboratories, Washington, D. C.

SYSTEMATIC METHODS TO CALCULATE FACTOR EFFECTS AND FITTED VALUES FOR A 2^n3^m FACTORIAL EXPERIMENT
Barry H. Margolin, U. S. Army Electronics Command, Fort Monmouth, New Jersey

CONSTRUCTION AND COMPARISON OF NON-ORTHOGONAL INCOMPLETE FACTORIAL DESIGNS
S. R. Webb, Mathematics and Statistics Group, Rocketdyne, A Division of North American Aviation, Inc., Canoga Park, California. Rep. Aerospace Research Laboratories, Office of Aerospace Research, U. S. Air Force

1330-1500 CLINICAL SESSION A - - 4th Floor BCD Room

Chairman: David Jacobus, Walter Reed Army Institute of Research, Walter Reed Army Medical Center, Washington, D. C.

Panelists:

Dr. Walter D. Foster, Biometrics Division, U. S. Army, Biological Warfare Laboratories, Fort Detrick, Maryland

Dr. Samuel W. Greenhouse, National Institute of Mental Health, Bethesda, Maryland

Dr. Bernard Harris, Mathematics Research Center, U. S. Army, University of Wisconsin, Madison, Wisc.

Panelists (continued)

Professor Boyd Harshbarger, Virginia Polytechnic Institute, Blacksburg, Virginia

Professor H. L. Lucas, North Carolina State University at Raleigh, Raleigh, North Carolina

STATISTICAL ANALYSIS OF AUTOMATICALLY RECORDED PHYSIOGRAPH DATA
John Atkinson, Dir/Medical Research, CRDL, Edgewood Arsenal, Maryland

AN APPLICATION OF EXPERIMENTAL DESIGN IN ERGONOMICS: A CARDIOVASCULAR RESPONSE TO WORK STRESS
Henry B. Tingey and William H. Kirby, Jr., Terminal Ballistic Laboratory, Ballistic Research Laboratories, Aberdeen Proving Ground, Maryland

1500-1530 BREAK

1530-1700 TECHNICAL SESSION III - - 4th Floor Seminar Room

Chairman: O. P. Bruno, Surveillance Branch, Ballistic Research Laboratories, Aberdeen Proving Ground, Md.

STRATEGY FOR THE OPTIMAL USE OF WEAPONS BY AREA COVERAGE
J. A. Nickel, J. D. Palmer and F. J. Kern, Systems Research Center, University of Oklahoma, Norman, Okla. (Representing the U. S. Army Edgewood Arsenal)

VARIABILITY OF LETHAL AREA
Bruce D. Barnett, Data Processing Systems Office, Picatinny Arsenal, Dover, New Jersey

1530-1700 TECHNICAL SESSION IV - - 3rd Floor Conference Room

Chairman: Joseph Weinstein, Mathematics Division, U. S. Army Electronic R and D Laboratory, Fort Monmouth, New Jersey

TECHNICAL SESSION IV (continued)

DECISION PROCEDURE FOR MINIMIZING COSTS OF CALABRATING LIQUID ROCKET ENGINES
E. L. Bombara, National Aeronautics and Space Administration, George C. Marshall Space Flight Center, Huntsville, Alabama

CALCULATION OF THE THEORETICAL STRENGTH OF TITANIUM BY MEANS OF THE COHESIVE ENERGY
Perry R. Smoot, U. S. Army Materials Research Agency, Watertown, Massachusetts

1530-1700 CLINICAL SESSION B - - 4th Floor BCD Room

Chairman: Captain Douglas Tang, Walter Reed Army Institute of Research, Walter Reed Army Medical Center, Washington, D.C.

Panelists:

Professor Robert E. Bechhofer, Cornell University, Ithaca, New York

Professor A. C. Cohen, Jr., University of Georgia, Athens, Georgia

Professor Boyd Harshbarger, Virginia Polytechnic Institute, Blacksburg, Virginia

Professor H. L. Lucas, North Carolina State University at Raleigh, Raleigh, North Carolina

THE PATHOPHYSIOLOGY OF POISONOUS SNAKE VENOMS
J. A. Vick, H. P. Ciuchta, and J. H. Manthei, U. S. Army Chemical and Research Development Laboratories, Edgewood Arsenal, Maryland

CLINICAL SESSION B (continued)

RELATIONSHIP BETWEEN LESION COUNTS AND SPORE COUNTS
Thomas H. Barksdale, William D. Brener, Walter D. Foster, and Marian W. Jones, Biological Laboratories, Fort Detrick, Frederick, Maryland

Thursday, 21 October

Technical Sessions V, VI, and VII will run from 0830 to 1000. Following the break, Technical Sessions VIII and IX together with Clinical Session C will start at 1030 and end at 1200. After lunch Technical Session IX and X along with Clinical Sessions D will be held during the time interval 1330-1420. The Panel Discussion is scheduled to be conducted from 1500 to 1700. The banquet starts at 1830.

0830-1000 TECHNICAL SESSION V - - 4th Floor BCD Room

Chairman: Henry Ellner, Directorate for Quality Assurance, U. S. Army Edgewood Arsenal, Edgewood, Maryland

EXTREME VERTICES DESIGN OF MIXTURE EXPERIMENTS
R. A. McLean, Purdue University and the University of Tennessee, and V. L. Anderson, Purdue University. Representing Army Research Office-Durham

DESIGN OF A VACUUM-BREAKDOWN EXPERIMENT
M. M. Chrepta, J. Weinstein, G. W. Taylor, and M. H. Zinn, Electronic Components Laboratory, U. S. Army Electronics Command, Fort Monmouth, New Jersey

0830-1000 TECHNICAL SESSION VI - - 3rd Floor Seminar Room

Chairman: Albert Parks, Harry Diamond Laboratories, Washington, D. C.

MODEL SIMULATION OF BIO-CELLULAR SYSTEMS
George I. Lavin, Terminal Ballistic Laboratory, Ballistic Research Laboratories, Aberdeen Proving Ground, Md.

TECHNICAL SESSION VI (continued)

SOME INFERENTIAL STATISTICS WHICH ARE RELATIVELY COMPATIBLE WITH AN INDIVIDUAL ORGANISM METHODOLOGY
Samuel H. Revusky, U. S. Army Medical Research Laboratory, Fort Knox, Kentucky

0830-1000 TECHNICAL SESSION VII - - 4th Floor Seminar Room

Chairman: A. Bulfinch, Picatinny Arsenal, Dover, N. J.

CONTROL OF DATA-SUPPORT QUALITY
Fred S. Hanson, Plans and Operations Directorate, White Sands Missile Range, New Mexico

DESIGNS AND ANALYSES FOR THE INVERSE RESPONSE PROBLEM IN SENSITIVITY TESTING
M. J. Alexander, and D. Rothman, Mathematics and Statistics Group, Rocketdyne, A Division of North American Aviation, Inc., Canoga Park, California. Representing George C. Marshall Space Flight Center, NASA, Huntsville, Alabama

1000-1030 BREAK

1030-1200 TECHNICAL SESSION VIII - - 4th Floor BCD Room

Chairman: F. L. Carter, U. S. Army Biological Laboratories, Fort Detrick, Frederick, Maryland

MONTE CARLO INVESTIGATION OF THE PROBABILITY DISTRIBUTIONS OF DIXON'S CRITERIA FOR TESTING OUTLYING OBSERVATIONS
Walter L. Mowchan, Surveillance Branch, Ballistic Research Laboratories, Aberdeen Proving Ground, Maryland

TABLES AND CURVES FOR ESTIMATING DEGREES OF FREEDOM FOR A TWO POPULATION "T" TEST WHEN THE STANDARD DEVIATIONS ARE UNKNOWN AND UNEQUAL
E. Dutoit and R. Webster, Quality Assurance Directorate, Ammunition Reliability Division, Mathematics and Statistics Branch, Picatinny Arsenal, Dover, New Jersey

1030-1200 TECHNICAL SESSION IX - - 4th Floor Seminar Room

Chairman: Paul C. Cox, Reliability and Statistics Office, Army Missile Test and Evaluation Directorate, White Sands Missile Range, New Mexico

DELETING OBSERVATIONS FROM A LEAST SQUARES SOLUTION
Charles A. Hall, 2nd Lieutenant, Technical Services Division, White Sands Missile Range, New Mexico

PRECISION AND BIAS ESTIMATES FOR DATA FROM CINETHEODOLITE AND FPS-16 RADARS
Burton L. Williams, Range Instrumentation Systems Office, White Sands Missile Range, New Mexico

1030-1200 CLINICAL SESSION C - - 3rd Floor Seminar Room

Chairman: Dr. Fred Hanson, Plans and Operations Directorate, White Sands Missile Range, New Mexico

Panelists:

Professor H. O. Hartley, Texas A and M University, College Station, Texas

Professor J. Stuart Hunter, Princeton University, Princeton, New Jersey

Professor William Kruskal, University of Chicago, Chicago, Illinois

Dr. Henry B. Mann, Mathematics Research Center, U. S. Army, University of Wisconsin, Madison, Wisc.

Dr. Joan Rosenblatt, Statistical Engineering Laboratory, National Bureau of Standards, Washington, D. C.

THERMAL CYCLES IN WELDING
Mark M. D'Andrea, Jr., U. S. Army Materials Research Agency, Watertown, Massachusetts

CLINICAL SESSION C (continued)

STATISTICAL ANALYSIS OF TENSILE-STRENGTH HARDNESS RELATIONSHIPS IN THERMOMECHANICALLY TREATED STEELS
Albert A. Anctil, U. S. Army Materials Research Agency, Watertown, Massachusetts

1200-1330 LUNCH

1330-1420 TECHNICAL SESSION X - - 4th Floor Seminar Room

Chairman: Professor A. C. Cohen, Jr., The University of Georgia, Athens, Georgia

SOME PROBLEMS IN STATISTICAL INFERENCE FOR GENERALIZED MULTINOMIAL POPULATIONS
Bernard Harris, Mathematics Research Center, University of Wisconsin, Madison, Wisconsin

1330-1420 TECHNICAL SESSION XI - - 4th Floor BCD Room

Chairman: Professor W. Y. Youden, George Washington University, Washington, D. C.

STATISTICS IN THE CALIBRATION LABORATORY
Joseph M. Cameron, Statistical Laboratory (IBS), National Bureau of Standards, Washington, D. C.

1330-1420 CLINICAL SESSION D - - 3rd Floor Seminar Room

Chairman: Dr. Seigfried H. Lehnigk, Research and Development Directorate, U. S. Army Missile Command, Redstone Arsenal, Huntsville, Alabama

Panelists:

O. P. Bruno, Surveillance Branch, Ballistic Research Laboratories, Aberdeen Proving Ground, Maryland

Paul C. Cox, Army Missile Test and Evaluation Directorate, White Sands Missile Range, New Mexico

Panelists (continued)

Professor H. O. Hartley, Texas A and M University, College Station, Texas

Professor H. L. Lucas, North Carolina State University at Raleigh, Raleigh, North Carolina

Professor Henry B. Mann, Mathematics Research Center, U. S. Army, University of Wisconsin, Madison, Wisc.

APPLICATION OF NUMERICAL TECHNIQUES TO AN EXPERIMENTAL MODEL AND AERODYNAMIC FUNCTION
Andrew H. Jenkins, U. S. Army Missile Command

1420-1500 BREAK

1500-1700 GENERAL SESSION 2 - - 4th Floor Seminar Room

PANEL DISCUSSION ON SELECTING THE BEST TREATMENT
Chairman: Professor R. E. Bechhofer

Panelists and Titles of their addresses:

SELECTING THE POPULATION WITH THE LARGEST PARAMETER
Professor Robert E. Bechhofer, Cornell University

SELECTING A SUBSET CONTAINING THE POPULATION WITH THE LARGEST PARAMETER
Professor Shanti S. Gupta, Purdue University

1830 SOCIAL HOUR and BANQUET

THE SAMUEL S. WILKS AWARD

Presentation: Dr. Frank E. Grubbs, Ballistics Research Laboratories

Friday, 22 October

The Subcommittee on Probability and Statistics of the Army Mathematics Steering Committee will hold an open meeting from 0830 to 0915. All members attending the conference are invited to attend this meeting. General Session 4 will start at 0930 and run to 1200.

0830-0915 GENERAL SESSION 3 - - 4th Floor Seminar Room

OPEN MEETING OF THE SUBCOMMITTEE ON PROBABILITY AND STATISTICS
Chairman: Dr. Walter D. Foster, Biometric Division, U. S. Army Biological Warfare Laboratories, Fort Detrick, Frederick, Maryland

0915-0930 BREAK

0930-1200 GENERAL SESSION 4 - - 4th Floor Seminar Room

Chairman: Dr. Frank E. Grubbs, Chairman of the Conference, Ballistics Research Laboratories, Aberdeen Proving Ground, Maryland

TARGET COVERAGE PROBLEMS
Professor William C. Guenther, University of Wyoming, Laramie, Wyoming

MAXIMUM LIKELIHOOD ESTIMATES FOR THE GENERAL MIXED ANALYSIS OF A VARIANCE MODEL
Professor H. O. Hartley, Texas A and M University, College Station, Texas

ESTIMATION AND DESIGN FOR NON-LINEAR MODELS

J. S. Hunter
Princeton University

The object of this paper is to survey current work in estimation and design for non-linear models. The problems of estimation for linear models are first reviewed, taking recourse to geometric arguments, and the distinctions between linear and non-linear estimation problems described. Techniques for the estimation of parameters in non-linear models are then discussed: linearization of the model and the Gaussian Iterant, linearization of the sums of squares function, direct search, elimination of linear parameters, and linearization of the Normal equations. Borrowing heavily from the papers of G. E. P. Box and his co-workers, the problems of non-linear design are next discussed, both for the number of observations fixed, and for sequential non-linear designs. The emergence of intrinsic designs appropriate to individual non-linear models is noted.

Consider a response function expressed in terms of the general model

$$\eta = f(\xi_1, \xi_2, \ldots, \xi_k; \theta_1, \theta_2, \ldots, \theta_p) \tag{1}$$

where η is a response, the ξ_i, $i = 1, 2, \ldots, k$ are k variables or factors under the control of the experimenter and the θ_j, $j = 1, 2, \ldots, p$ are p parameters whose values are unknown.

Two classes of models will be discussed in this paper: linear and non-linear. Some examples of <u>linear</u> models are:

$$\eta = \theta_o + \sum_{j=1}^{p-1} \theta_j \xi_j \quad \text{or} \quad \eta = \theta_o + \sum_{j=1}^{p-1} \theta_j g_j(\xi).$$

where $g_j(\xi)$ are functions solely of the ξ_i as, for example, ξ_i^2 or $\xi_i \xi_j$. Examples of <u>non-linear</u> models are:

$$\eta = \theta_1(1-e^{\theta_2\xi_1}) \quad \text{or} \quad \eta = \theta_1 - \frac{\theta_2}{\theta_3-\xi_1} \quad \text{or} \quad \eta = \sum_{j=1}^{m} \theta_{1j} e^{-\theta_{2j}\xi_1}$$

the growth curve, the Clausius-Clapyion equation from thermodynamics, and the sum of exponential decay curves respectively. A clear distinction between linear and non-linear models will be made shortly.

Consider now $u = 1, 2, \ldots, n$ settings of the controlled variables and the corresponding responses $\eta_u = f(\xi_{1u}, \xi_{2u}, \ldots, \xi_{ku}; \theta_1, \theta_2, \ldots, \theta_p)$ or, in matrix notation

$$\eta_u = f(\underset{\sim}{\xi}_u, \underset{\sim}{\theta}) \tag{2}$$

where $\underset{\sim}{\xi}_u$ = (1 x k) row vector of the u^{th} setting of the controlled variables and $\underset{\sim}{\theta}$ = (p x 1) column vector of unknown parameters. The total array of settings of the controlled variables generates an n x k matrix $\underset{\sim}{\xi}$ consisting of the n row vectors $\underset{\sim}{\xi}_u$.

Of course, for a $\underset{\sim}{\xi}_u$ we will not observe the true response η_u but rather record an observation y_u where $y_u = \eta_u + \epsilon_u$, or,

$$\underset{\sim}{\chi} = \underset{\sim}{\eta} + \underset{\sim}{\epsilon} \tag{3}$$

where $\underset{\sim}{\chi}$ = n x 1 vector of observations

$\underset{\sim}{\eta}$ = n x 1 vector of responses

$\underset{\sim}{\epsilon}$ = n x 1 vector of disturbances.

In all that follows the individual disturbances ϵ_u are considered to be random events. Normally distributed with zero mean and homogeneous variance σ^2, that is, $E(\underset{\sim}{\epsilon}) = \underset{\sim}{0}$; $E(\underset{\sim}{\epsilon}\underset{\sim}{\epsilon}^T) = \underset{\sim}{I}_N \sigma^2$. Thus the joint probability density function for the observations y_u is:

$$p(\underset{\sim}{\chi}) = \left(\frac{1}{\sqrt{2n\sigma}}\right)^n e^{-\sum_{u=1}^{n}(y_u-\eta_u)^2/2\sigma^2} = \left(\frac{1}{\sqrt{2n\sigma}}\right)^n e^{-\frac{1}{2\sigma^2}(\underset{\sim}{\chi}-\underset{\sim}{\eta})^T(\underset{\sim}{\chi}-\underset{\sim}{\eta})}$$

Once the model $\eta_u = f(\underset{\sim}{\xi}_u, \underset{\sim}{\theta})$ is given we obtain:

$$(4) \qquad p(\underset{\sim}{y} \mid \underset{\sim}{\xi}, \underset{\sim}{\theta}, \sigma^2) = \left(\frac{1}{\sqrt{2n\sigma}}\right)^n e^{-\sum_{u=1}^{n} [y_u - f(\underset{\sim}{\xi}_u, \underset{\sim}{\theta})]^2/2\sigma^2}.$$

Since we will know $\underset{\sim}{y}$, $\underset{\sim}{\xi}$ and σ^2 the <u>likelihood function</u> for the parameters $\underset{\sim}{\theta}$ in the model are given by

$$(5) \qquad L(\underset{\sim}{\theta} \mid \underset{\sim}{y}, \underset{\sim}{\xi}, \sigma^2) = \left(\frac{1}{\sqrt{2n\sigma}}\right)^n e^{-\sum_{u=1}^{n} [y_u - f(\underset{\sim}{\xi}_u, \underset{\sim}{\theta})]^2/2\sigma^2}.$$

Our objective now is to find those values $\hat{\underset{\sim}{\theta}}$ of the parameters which maximize the likelihood function, or, equivalently, the logarithm of the likelihood function

$$(6) \qquad \ell = \ell n L = -\frac{n}{2} \ell n(2n\sigma^2) - \frac{1}{2\sigma^2} \sum_{u=1}^{n} [y_u - f(\underset{\sim}{\xi}_u, \underset{\sim}{\theta})]^2.$$

Thus, the maximum likelihood estimates $\hat{\theta}$ are obtained when the sum of squares function

$$(7) \qquad S(\theta) = \sum_u [y_u - f(\underset{\sim}{\xi}_u, \underset{\sim}{\theta})]^2$$

is minimized, e.g., when the least squares estimates $\hat{\underset{\sim}{\theta}}$ are obtained, thus

$$(8) \qquad S(\theta)_{min} = S(\hat{\theta}) = \sum_u [y_u - f(\underset{\sim}{\xi}_u, \hat{\underset{\sim}{\theta}})]^2 = \sum_u (y_u - \hat{y}_u)^2$$

where $\hat{y}_u = f(\underset{\sim}{\xi}_u, \hat{\underset{\sim}{\theta}})$ are the predicted values [1].

It will be helpful now to discuss least squares geometrically [2]. In this discussion, in order to "see" what is happening, we will restrict ourselves to problems in which the number of observations

$n = 3$ and the number of parameters $p = 2$. For $n > 3$ and $p > 2$, $(n \geq p)$, the reader is asked to use his imagination and remember that the rules of geometry employed will apply whatever the number of dimensions. Suppose an experimenter wishes to fit the linear model $y_u = \theta_o \xi_o + \theta_1 \xi_{1u} + \epsilon_u$ and that for each of three settings of ξ_o and ξ_1 he records a single observation y_u as given in Table I and displayed in Figure 1.

TABLE I

ξ_o	ξ_1	$\underset{\sim}{y}$	$\dot{\underset{\sim}{y}}$ for $\theta_o = 10, \theta_1 = 4$	$y - \dot{y}$
1	2	18.4	18.0	0.4
1	1	14.2	14.0	0.2
1	4	24.8	26.0	-1.2

The elements of the observation vector $\underset{\sim}{y}$ provide the coordinates of a point in the $n = 3$ dimensional "observation space" as illustrated in Figure 1a. The line segment joining this point to the origin is called the observation vector. Since there are $k = 2$ unknown parameters in the postulated model we can imagine a second coordinate system called the "parameter space" as illustrated in Figure 1b. Suppose now the experimenter chooses for his initial values of the parameters $\theta_o = 10$ and $\theta_1 = 4$, thus locating the point $\dot{\underset{\sim}{\theta}}$ in the parameter space. Associated with $\dot{\underset{\sim}{\theta}}$ will be the point $\dot{\underset{\sim}{y}}$ in the observation space determined by the prediction equation $\dot{y}_u = 10\xi_o + 4\xi_{1u}$ as illustrated in Figure 1c. (The coordinates for $\dot{\underset{\sim}{y}}$ are also given in Table I.) In fact, for every point $\underset{\sim}{\theta}$ in parameter space an associated point, $\underset{\sim}{y}$, can be located in the observation space. Remarkably, the surface generated by the predicted values $\dot{\underset{\sim}{y}}$ will be flat. In this simple example they form a $k = 2$ dimensional plane as illustrated in Figure 1c. The distance squared from the point $\underset{\sim}{y}$ to the point $\dot{\underset{\sim}{y}}$ is given by

$$S(\dot{\underset{\sim}{\theta}}) = \sum_u (y_u - \dot{y}_u)^2 = \sum_u [y_u - f(\underset{\sim}{\xi}_u, \dot{\underset{\sim}{\theta}})]^2 .$$

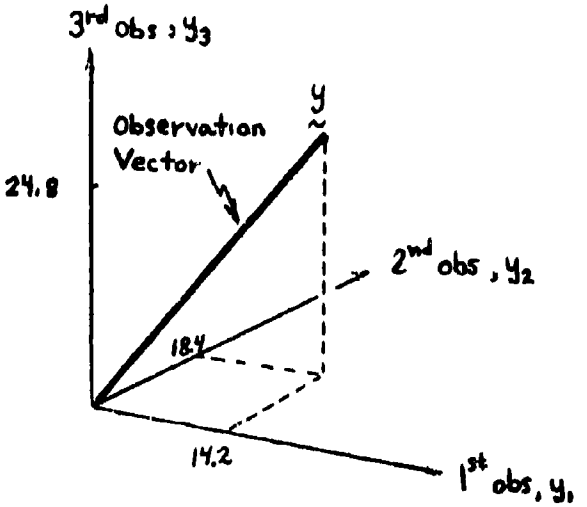

OBSERVATION SPACE

Figure 1a

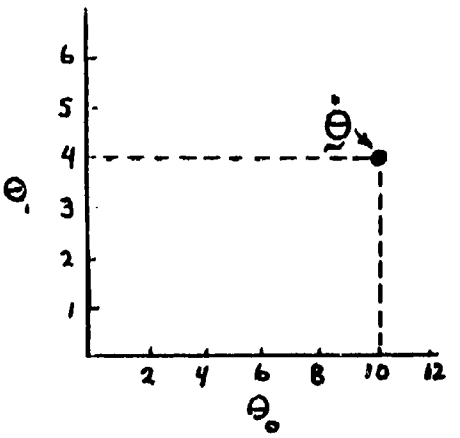

PARAMETER SPACE

Figure 1b

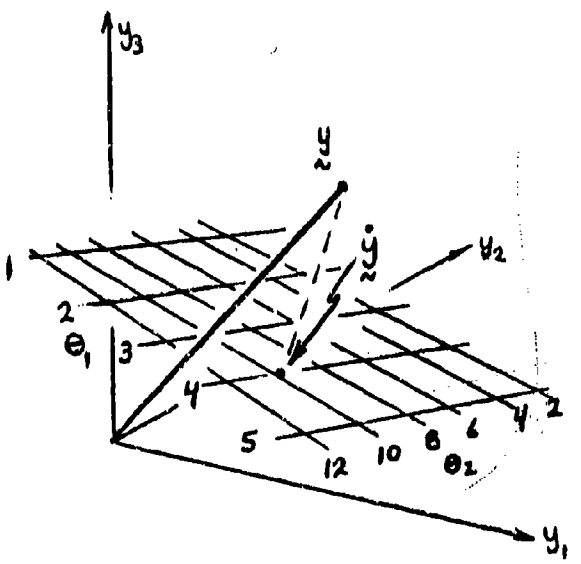

OBSERVATION SPACE

Figure 1c

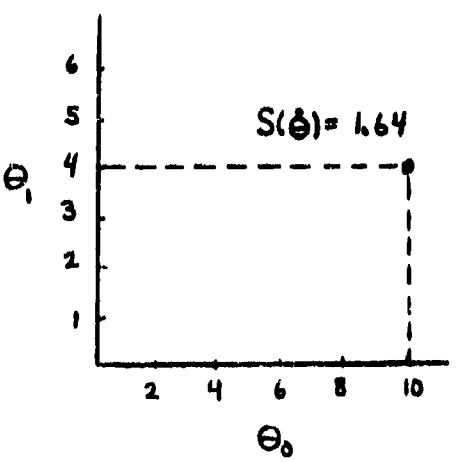

PARAMETER SPACE

Figure 1d

From Table I we see that $S(\dot{\theta}) = 1.64$. This sum of squares is recorded in Figure 1d at the point $\dot{\theta}$.

Our objective now is to locate the point $\hat{\underset{\sim}{y}}$ on the prediction surface closest to the observation point $\underset{\sim}{y}$, or equivalently, of finding the point $\hat{\underset{\sim}{\theta}}$ in the parameter space such that $S(\hat{\underset{\sim}{\theta}}) = \sum_u (y_u - \hat{y}_u)^2$ the length squares of the vector $(\underset{\sim}{y} - \hat{\underset{\sim}{y}})$, is smallest. (The symbol $\hat{\underset{\sim}{\theta}}$ indicates the least squares point and $\underset{\sim}{\theta}$ any other point in the parameter space. Similarly $\hat{y}$ and $\dot{y}$ are the associated points on the prediction sub-surface in the n-space of the observations.) Differentiating $S(\underset{\sim}{\theta})$ with respect to each the p parameters $\underset{\sim}{\theta}$ and setting these expressions equal to zero gives the p "normal" equations:

$$(9) \qquad \frac{\partial(S(\underset{\sim}{\theta}))}{\partial\theta_j} = 2 \sum_u [y_u - f(\underset{\sim}{\xi}_u, \underset{\sim}{\theta})] \left[\frac{\partial}{\partial\theta_j} f(\underset{\sim}{\xi}_u, \underset{\sim}{\theta})\right] = 0 \quad j=1,2,\ldots,p$$

or in matrix notation:

$$(10) \qquad \underset{\sim}{X}^T[y - \hat{y}] = 0$$

where $\underset{\sim}{X}$ = n x p matrix of derivatives whose elements are

$$\frac{\partial f(\underset{\sim}{\xi}_u, \theta)}{\partial\theta_j},$$

$\underset{\sim}{y}$ = n x 1 vector of observations,

$\hat{\underset{\sim}{y}}$ = n x 1 vector of predicted values.

The "normal" equations guarantee that the vector $\underset{\sim}{y} - \hat{\underset{\sim}{y}}$ will be perpendicular (normal) to the prediction surface and hence that the length squared of this vector $S(\hat{\theta})$ is a minimum. Now when the model $\eta_u = f(\underset{\sim}{\xi}_u, \underset{\sim}{\theta})$ is <u>linear</u>, the response vector $\underset{\sim}{\eta}$ may be written as $\underset{\sim}{\eta}_u = \underset{\sim}{\xi}_u \underset{\sim}{\theta}$. Further, Eq. (9) may now be written $S(\underset{\sim}{\theta}) = (\underset{\sim}{y} - \underset{\sim}{\xi}\underset{\sim}{\theta})^T(\underset{\sim}{y} - \underset{\sim}{\xi}\underset{\sim}{\theta})$. When we construct the normal equations, the elements of the <u>uth</u> row

of the matrix of derivatives $\underset{\sim}{X}$ are simply $-\frac{\partial f(\underset{\sim}{\xi}_u, \underset{\sim}{\theta})}{\partial \theta_j} = \underset{\sim}{\xi}_u$. The parameters $\underset{\sim}{\theta}$ disappear upon differentiation and we have simply that the matrix of derivatives $\underset{\sim}{X} = \underset{\sim}{\xi}$. Since $\hat{\underset{\sim}{\chi}} = \underset{\sim}{\xi}\,\hat{\underset{\sim}{\theta}}$ equation (10) becomes

$$\underset{\sim}{\xi}^T[\underset{\sim}{\chi} - \underset{\sim}{\xi}\hat{\underset{\sim}{\theta}}] = 0 \quad \text{or} \quad (\underset{\sim}{\xi}^T\underset{\sim}{\xi})\hat{\underset{\sim}{\theta}} = \underset{\sim}{\xi}^T\underset{\sim}{\chi} \,. \tag{11}$$

Solving for $\hat{\underset{\sim}{\theta}}$ gives

$$\hat{\underset{\sim}{\theta}} = (\underset{\sim}{\xi}^T\underset{\sim}{\xi})^{-1}\underset{\sim}{\xi}^T\underset{\sim}{\chi} \tag{12}$$

the familiar least squares solution for the coefficients in a linear model.

The analysis of variance table now becomes nothing more than the resolution of the observation vector $\underset{\sim}{\chi}$ into orthogonal components, the degrees of freedom column merely keeping track of the number of dimensions in which the corresponding vectors are free to move. Thus we have in general (n observations, p parameters):

(13) Analysis of Variance Table

	Sum of Square	Degrees of Freedom
Total Sum of Squares (Length Squared Observation Vector)	$\underset{\sim}{\chi}^T\underset{\sim}{\chi}$	n
Regression Sum of Squares (Length square, Vector of Predicted Values)	$\hat{\underset{\sim}{\chi}}^T\hat{\underset{\sim}{\chi}} = \hat{\underset{\sim}{\theta}}^T\underset{\sim}{\xi}^T\underset{\sim}{\xi}\hat{\underset{\sim}{\theta}}$	p
Residual Sum of Squares (Length Squared of Vector of Residuals)	$S(\hat{\underset{\sim}{\theta}}) = (\underset{\sim}{\chi}-\hat{\underset{\sim}{\chi}})^T(\underset{\sim}{\chi}-\hat{\underset{\sim}{\chi}})$	p=n-p

FIGURE 2

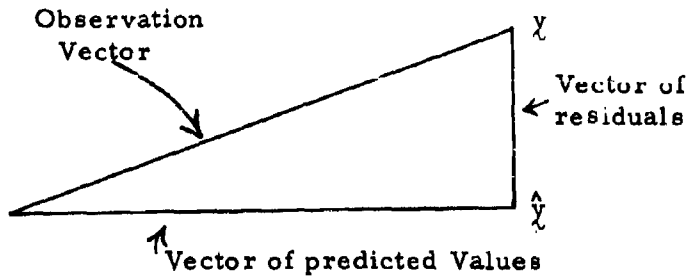

In our example we have (remembering that for this linear model $\underset{\sim}{X} = \underset{\sim}{\xi}$)

$$\underset{\sim}{\xi} = \underset{\sim}{X} = \begin{bmatrix} 1 & 2 \\ 1 & 1 \\ 1 & 4 \end{bmatrix} ; \quad \underset{\sim}{y} = \begin{bmatrix} 18.4 \\ 14.2 \\ 24.8 \end{bmatrix} \quad ; \quad (\underset{\sim}{X}^T\underset{\sim}{X}) = \underset{\sim}{X}^T\underset{\sim}{y} \; ; \; \begin{bmatrix} 3 & 7 \\ 7 & 21 \end{bmatrix} \begin{bmatrix} \hat{\theta}_o \\ \hat{\theta}_1 \end{bmatrix} = \begin{bmatrix} 57.4 \\ 150.2 \end{bmatrix}$$

$$\hat{\underset{\sim}{\theta}} = (\underset{\sim}{X}^T\underset{\sim}{X})^{-1}\underset{\sim}{X}^T\underset{\sim}{y} \; ; \; \begin{bmatrix} \hat{\theta}_o \\ \hat{\theta}_1 \end{bmatrix} = \frac{1}{14} \cdot \begin{bmatrix} 21 & -7 \\ -7 & 21 \end{bmatrix} \begin{bmatrix} 57.4 \\ 150.2 \end{bmatrix} = \begin{bmatrix} 11.0000 \\ 3.4857 \end{bmatrix}$$

$$\hat{\underset{\sim}{y}} = \underset{\sim}{\xi}\,\hat{\underset{\sim}{\theta}} = \begin{bmatrix} 1 & 2 \\ 1 & 1 \\ 1 & 4 \end{bmatrix} \begin{bmatrix} 11.0000 \\ 3.4857 \end{bmatrix} = \begin{bmatrix} 17.9714 \\ 14.4857 \\ 24.9428 \end{bmatrix} \; ; (\underset{\sim}{y} - \hat{\underset{\sim}{y}}) = \begin{bmatrix} 0.4286 \\ -0.2857 \\ -0.1428 \end{bmatrix}$$

Total SSq.	$\underset{\sim}{y}^T\underset{\sim}{y}$	= 1155.2400	3
Regression SSq.	$\hat{\underset{\sim}{y}}^T\hat{\underset{\sim}{y}}$	= 1154.9500	2
Residual SSq.	$(\underset{\sim}{y}-\hat{\underset{\sim}{y}})^T(\underset{\sim}{y}-\hat{\underset{\sim}{y}})$	= 0.2900	1

The residual sum of squares $S(\hat{\underset{\sim}{\theta}}) = 0.2900$ in the Analysis of Variance Table is obtained by subtraction. Using our vector of estimated residuals $\underset{\sim}{y}-\hat{\underset{\sim}{y}}$, $S(\hat{\underset{\sim}{\theta}}) = 0.2857$. The failure of these two values of $S(\hat{\underset{\sim}{\theta}})$ to agree exactly is due only to rounding errors.

Granting the model is correct, and that the observations $y_u = N(\eta_u, \sigma^2)$ then $S(\hat{\underset{\sim}{\theta}})/\nu = s^2$ estimates σ^2 with $\nu = (n-p)$ degrees of freedom. Further $E(\hat{\underset{\sim}{\theta}}) = \underset{\sim}{\theta}$; $V(\hat{\underset{\sim}{\theta}}) = (X^T X)^{-1}\sigma^2$ and in fact the $\hat{\theta}$ are distributed in a multivariate Normal: $N(\underset{\sim}{\theta}; [\underset{\sim}{X}^T\underset{\sim}{X}]^{-1}\sigma^2)$. Let $\dot{\underset{\sim}{\theta}}$ be specific values for the parameters postulated by the experimenter. To determine whether the least squares estimates $\hat{\underset{\sim}{\theta}}$ are reasonable in the light of this hypothesis we may now perform the $F_{p,\nu}$ test

$$(14) \qquad F_{p,\nu} = \frac{S(\dot{\underset{\sim}{\theta}})/p}{S(\hat{\underset{\sim}{\theta}})/\nu} = \frac{[(\dot{\underset{\sim}{\theta}}-\hat{\underset{\sim}{\theta}})^T \underset{\sim}{\xi}^T \underset{\sim}{\xi}(\dot{\underset{\sim}{\theta}}-\hat{\underset{\sim}{\theta}})]/p}{S(\hat{\underset{\sim}{\theta}})/\nu} .$$

If this observed value of $F_{p,\nu}$ is such that Prob $\{F_{p,\nu} \geq F_{p,\nu,\alpha}\} \leq \alpha$ we reject the hypothesis that the parameters could in fact equal $\dot{\underset{\sim}{\theta}}$. A geometric view of this testing procedure is given in Figure 3. Here we see the observation point $\underset{\sim}{y}$, the point on the solution locus $\hat{\underset{\sim}{y}}$ which is closest to $\underset{\sim}{y}$, and, finally, the point $\dot{\underset{\sim}{\eta}}$ determined from the model $\dot{\underset{\sim}{\eta}} = \underset{\sim}{\xi}\dot{\underset{\sim}{\theta}}$.

FIGURE 3

The resulution of the observation vector $\underset{\sim}{y}$ having its origin at the point $\dot{\underset{\sim}{\eta}} = \underset{\sim}{\xi}\dot{\underset{\sim}{\theta}}$

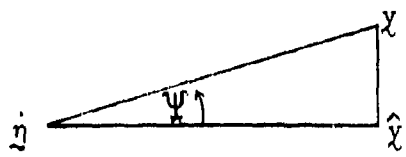

Accepting the hypothesis that $\underset{\sim}{\eta} = \underset{\sim}{\xi}\dot{\underset{\sim}{\theta}}$ is correct, then the vector $\underset{\sim}{\chi} - \dot{\underset{\sim}{\eta}}$ is due to random variability alone. The length squared of this vector $(\underset{\sim}{\chi} - \dot{\underset{\sim}{\eta}})^T(\underset{\sim}{\chi} - \dot{\underset{\sim}{\eta}})$ is then distributed as a χ^2 with n degrees of freedom. Since $\underset{\sim}{\chi} - \hat{\underset{\sim}{\chi}}$ is normal to the solution locus which contains $\dot{\underset{\sim}{\eta}} - \hat{\underset{\sim}{\chi}}$ we have, thanks to Pythagorous:

$$(\underset{\sim}{\chi} - \dot{\underset{\sim}{\eta}})^T(\underset{\sim}{\chi} - \dot{\underset{\sim}{\eta}}) = (\underset{\sim}{\chi} - \hat{\underset{\sim}{\chi}})^T(\underset{\sim}{\chi} - \hat{\underset{\sim}{\chi}}) + (\dot{\underset{\sim}{\eta}} - \hat{\underset{\sim}{\chi}})^T(\dot{\underset{\sim}{\eta}} - \hat{\underset{\sim}{\chi}})$$

or

$$S(\dot{\underset{\sim}{\theta}}) = S(\hat{\underset{\sim}{\theta}}) + (\dot{\underset{\sim}{\theta}} - \hat{\underset{\sim}{\theta}})^T \underset{\sim}{\xi}^T \underset{\sim}{\xi} (\dot{\underset{\sim}{\theta}} - \hat{\underset{\sim}{\theta}})$$

(15)

or

$$S(\dot{\underset{\sim}{\theta}}) = S(\hat{\underset{\sim}{\theta}}) + S(\dot{\underset{\sim}{\theta}} - \hat{\underset{\sim}{\theta}})$$

and since the errors are independent $S(\hat{\underset{\sim}{\theta}})$ is distributed as an χ^2 with $\nu = n-p$ degrees of freedom and $S(\dot{\underset{\sim}{\theta}} - \hat{\underset{\sim}{\theta}})$ distributed as χ^2 with p degrees of freedom. Thus the ratio given in Eq. (14) is distributed as $F_{p,n-p}$. We also observe that with the exception of the constant p and n-p that the F ratio is in fact equivalent to the $\cot^2 \psi$, where ψ is the angle between $\underset{\sim}{\chi} - \dot{\underset{\sim}{\eta}}$ and $\dot{\underset{\sim}{\eta}} - \hat{\underset{\sim}{\chi}}$. When the angle ψ is small (and hence $\dot{\underset{\sim}{\eta}}$ far from $\hat{\underset{\sim}{\chi}}$ or equivalently $\dot{\underset{\sim}{\theta}}$ far from $\hat{\underset{\sim}{\theta}}$), F will be large.

The boundary of the (1-α)% confidence region of $\underset{\sim}{\theta}$ is obtained by substituting in Eq. (14) the $F_{p,\nu,\alpha}$ critical value and solving the resulting expression for $\dot{\underset{\sim}{\theta}}$, thus

$$(\dot{\underset{\sim}{\theta}} - \hat{\underset{\sim}{\theta}})^T \underset{\sim}{\xi}^T \underset{\sim}{\xi} (\hat{\underset{\sim}{\theta}} - \dot{\underset{\sim}{\theta}}) = p \frac{S(\hat{\underset{\sim}{\theta}})}{\nu} F_{p,\nu,\alpha} \quad (16)$$

a quadratic form in the $\dot{\underset{\sim}{\theta}}$; (1), (3). An illustration of this boundary (for p=2) is displayed in Figure 4 by the dashed ellipse.

FIGURE 4

Sum of Squares Contours plotted in Parameter Space.

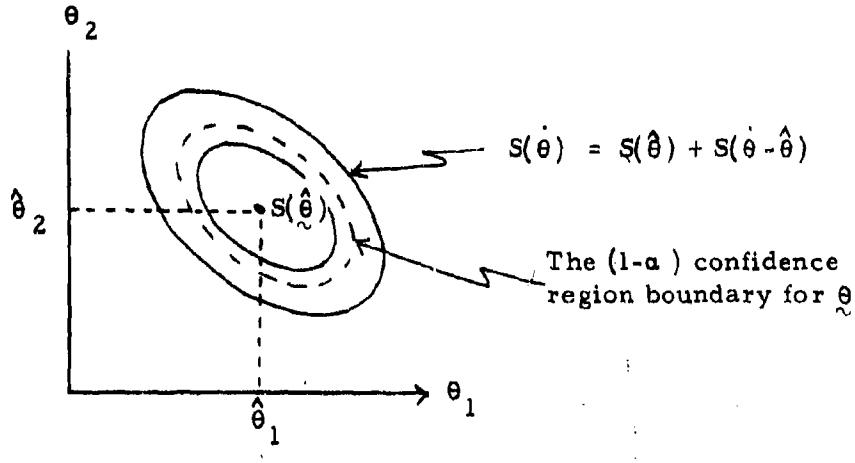

The length squared of the residual vector is $S(\hat{\theta})$. The length squared of the vector $\underset{\sim}{y}-\dot{\underset{\sim}{\eta}}$ is $S(\underset{\sim}{\theta}) = S(\hat{\underset{\sim}{\theta}}) + S(\underset{\sim}{\theta}-\hat{\underset{\sim}{\theta}})$. The ellipses shown in the figure are contour lines giving the sum of squares. The dashed contour line is the $S(\dot{\theta})$ that gives the critical value of $F_{p,\nu,\alpha}$. Thus, on the parameter space we can superimpose contour lines (surfaces for $k>2$) giving the sum of squares $S(\dot{\theta})$ for <u>any</u> choice of $\underset{\sim}{\theta}$.

<u>Fitting a Non-Linear Model</u>

We now consider the case where the model $\eta_u = f(\underset{\sim}{\xi}_u, \underset{\sim}{\theta})$ is <u>non</u>-linear. Suppose, for example, an experimenter wished to fit the model $\eta_u = \theta_1 e^{\theta_2 \xi_u}$ to the data given earlier for the linear model example. We can, as before, consider the $n=3$ observation space, the vector $\underset{\sim}{y}$, and a $p=2$ dimensional parameter space. Once again, for each point $\underset{\sim}{\theta}$ in the parameter space there will be an analogous point $\dot{\underset{\sim}{y}}$ in the observation space where $\dot{y}_u = \theta_1 e^{\theta_2 \xi_u}$. However, the locus of points

$\dot{\chi}$ produced for various values of the $\underset{\sim}{\theta}$ will now produce a curved prediction subspace as illustrated in Figure 5a. In the parameter space, the contours of the sums of squares $S(\theta)$ will produce elongated and

FIGURE 5

Geometric Interpretation of Non-Linear Least Squares

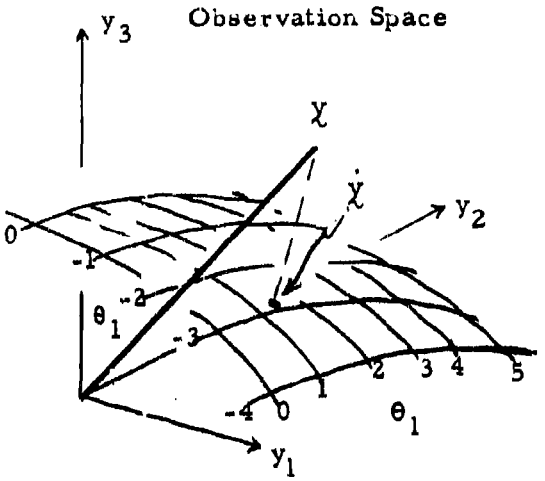

Figure 5a

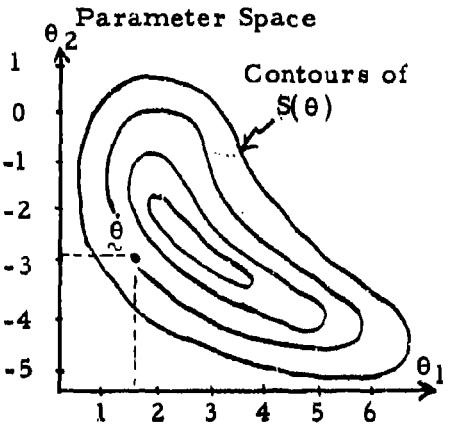

Figure 5b

twisted elliptical shapes as illustrated in Figure 5b. However, the maximum likelihood estimates of the parameters still require that we locate the point in the prediction subspace closest to χ, or equivalently, find the point $\hat{\theta}$ in the parameter space where $S(\theta)$ is smallest.

Thus, we form the normal equations $\underset{\sim}{X}^T[\chi - \hat{\chi}] = 0$ except that this time the derivative matrix $\underset{\sim}{X}$ consists of elements x_{uj}, $u=1,\ldots,n$; $j=1,\ldots,p$ containing the θ's. In general, we have

$$(17) \qquad \underset{\sim}{X} = \begin{bmatrix} x_{11} & x_{21} & \cdots & x_{k1} \\ x_{12} & x_{22} & & x_{k2} \\ \cdot & \cdot & & \cdot \\ \cdot & \cdot & & \cdot \\ \cdot & \cdot & & \cdot \\ x_{1n} & x_{2n} & & x_{kn} \end{bmatrix} \quad \text{where } x_{uj} = -\frac{\partial f(\underset{\sim}{\xi}_u, \underset{\sim}{\theta})}{\partial \theta_j}$$

or, for our example, since $\eta_u = \theta_1 e^{\theta_2 \xi_u}$ and $\underset{\sim}{\xi}^T = [2, 1, 4]$ we obtain

$$(18) \qquad \underset{\sim}{X} = \begin{bmatrix} e^{\theta_2 \xi_1} & \theta_1 \xi_1 e^{\theta_2 \xi_1} \\ e^{\theta_2 \xi_2} & \theta_1 \xi_2 e^{\theta_2 \xi_2} \\ e^{\theta_2 \xi_3} & \theta_1 \xi_3 e^{\theta_2 \xi_3} \end{bmatrix} = \begin{bmatrix} e^{2\theta_2} & 2\theta_1 e^{2\theta_2} \\ e^{\theta_2} & \theta_1 e^{\theta_2} \\ e^{4\theta_2} & 4\theta_1 e^{4\theta_2} \end{bmatrix}$$

To find those values $\hat{\theta}_1$ and $\hat{\theta}_2$ that will satisfy the conditions of the normal equation $\underset{\sim}{X}^T(\underset{\sim}{y}-\underset{\sim}{\hat{y}}) = 0$ is, usually, a very difficult task. We now discuss some of the various methods proposed for locating the point $\hat{\theta}$.

Linearize the Model:

Since the model is non-linear, we convert it to a linear model (approximately) by expanding the model in a 1st order Taylors series about some set of initial guessed values of the parameters $\underset{\sim}{\theta}^{(0)}$. Thus

$$(19) \qquad y_u = f(\xi_u, \theta^{(0)} + \sum_{j=1}^{p} (\theta_j - \theta_j^{(0)}) \left[\frac{\partial f(\underset{\sim}{\xi}_u, \underset{\sim}{\theta})}{\partial \theta_j}\right]_{\underset{\sim}{\theta}=\underset{\sim}{\theta}^\circ}$$

or

$$(20) \qquad y_u - y_u^{(0)} = \sum_{j=1}^{p} (\theta_j - \theta_j^{(0)}) \, x_{uj}$$

a set of n linear equations in the p unknowns $(\theta_j - \theta_j^{(0)})$ where $y_u^{(0)}$ is the predicted value of the response for the initial guessed values $\underset{\sim}{\theta}^{(0)}$, and x_{uj} are the derivatives evaluated at $\underset{\sim}{\theta}^{(0)}$. In matrix notation we have

$$(21) \qquad \underset{\sim}{\delta y} = \underset{\sim}{X}(\underset{\sim}{\delta \theta})$$

where $(\underset{\sim}{\delta y})$ = (n x 1) vector of deviations $(\underset{\sim}{y}-\underset{\sim}{y}^{\circ})$

$\underset{\sim}{X}$ = (n x p) matrix of derivatives x_{uj}

$(\underset{\sim}{\delta}\,\underset{\sim}{\theta})$ = (p x 1) matrix of corrections $(\theta_j-\theta_j^{(0)})$.

Since our model is now a linear one we can solve for $\underset{\sim}{\delta}\,\underset{\sim}{\theta}$ giving

$$\underset{\sim}{\delta}\,\hat{\underset{\sim}{\theta}} = (\underset{\sim}{X}^T\underset{\sim}{X})^{-1}\ \underset{\sim}{X}^T(\underset{\sim}{\delta y}) \quad .$$

Once we have the estimated corrections $(\hat{\underset{\sim}{\delta}}\underset{\sim}{\theta})$ we begin anew with new values of the parameters $\underset{\sim}{\theta}^{(1)} = \underset{\sim}{\theta}^{(0)} + \hat{\underset{\sim}{\delta}}\underset{\sim}{\theta}$ and continue the iteration until the estimated corrections $\hat{\underset{\sim}{\delta}}\underset{\sim}{\theta}$ are not different from zero. In actual practice the full correction $\hat{\underset{\sim}{\delta}}\underset{\sim}{\theta}$ is usually not employed but rather corrections proportional to $\hat{\underset{\sim}{\delta}}\underset{\sim}{\theta}$, that is $v\,\hat{\underset{\sim}{\delta}}\underset{\sim}{\theta}$ where $0 \leq v \leq 1$; (4), (5). This method of locating $\hat{\underset{\sim}{\theta}}$ is often called the Gauss-Newton or simply the Gaussian Iterant.

For example, suppose we are given the model $\eta_u = \theta_1 + e^{-\theta_2 \xi_u}$ and that we record three observations $y_u = \eta_u + \epsilon_u$ where the ϵ_u are Normal and independently distributed $N(0,\sigma^2)$. The vector $\underset{\sim}{\xi}$, giving the levels of the controlled variable, and the associated response vector $\underset{\sim}{y}$ are given in the following table. Let the initial estimates $\underset{\sim}{\theta}^{(0)}$ be $\theta_1^{(0)} = 10$ and $\theta_2^{(0)} = 1.1$. The vector of predicted values $\underset{\sim}{y}^{(0)}$ and deviations $\underset{\sim}{\delta y}$ are also given in the table.

TABLE 2

$\underset{\sim}{\xi}$	$\underset{\sim}{y}$	$y^{(0)}=10+e^{-1.1\xi}$	$\underset{\sim}{\delta y}=\underset{\sim}{y}-\underset{\sim}{y}^{(0)}$	
1.1	12	13.35	-1.35	$\underset{\sim}{y}^T\underset{\sim}{y} = \Sigma y^2 = 1561$
0.7	11	12.16	-1.16	$S(\underset{\sim}{\theta}^{\circ})=\Sigma(\delta y)^2=383.085$
1.7	36	16.49	19.51	

The derivatives of the model $\theta_1 + e^{-\theta_2 \xi_u}$ with respect to the parameters are:

$$\left.\frac{\partial f(\xi_u, \underset{\sim}{\theta})}{\partial \theta_1}\right|_{\underset{\sim}{\theta}^{(0)}} = x_{u1} = 1; \quad \left.\frac{\partial f(\xi_u, \underset{\sim}{\theta})}{\partial \theta_2}\right|_{\underset{\sim}{\theta}^{(0)}} = x_{u2} = -\xi_u e^{-\theta_1^{(0)} \xi_u}$$

giving for the matrix of derivatives:

$$\underset{\sim}{X} = \begin{bmatrix} 1 & 3.6889 \\ 1 & 1.5119 \\ 1 & 11.0301 \end{bmatrix}$$

Solving now for the corrections $\underset{\sim}{\hat{\delta\theta}} = (\underset{\sim}{X}^T \underset{\sim}{X})^{-1} \underset{\sim}{X}^T (\underset{\sim}{\delta y})$ gives

$$\underset{\sim}{\hat{\delta\theta}} = \begin{bmatrix} -7.0084 \\ 2.3427 \end{bmatrix}$$

and hence a new set of values for $\underset{\sim}{\theta}$, that is $\underset{\sim}{\theta}^{(1)} = \underset{\sim}{\theta}^{(0)} + (\underset{\sim}{\hat{\delta\theta}})$

$$\begin{bmatrix} \theta_1^{(1)} \\ \theta_2^{(1)} \end{bmatrix} = \begin{bmatrix} 10.1 \\ 1.1 \end{bmatrix} + \begin{bmatrix} -7.0084 \\ 2.3427 \end{bmatrix} = \begin{bmatrix} 2.9916 \\ 3.4427 \end{bmatrix}.$$

These values $\underset{\sim}{\theta}^{(1)}$ are now employed in another iteration, and the process is repeated until (hopefully) the estimated correction $\hat{\delta\theta}$ vanish. In this example the fifth, sixth and seventh iteration gave

$$\underset{\sim}{\theta}^{(5)} = \begin{bmatrix} 4.971 \\ 2.030 \end{bmatrix}; \quad \underset{\sim}{\theta}^{(6)} = \begin{bmatrix} 5.033 \\ 2.014 \end{bmatrix}; \quad \underset{\sim}{\theta}^{(7)} = \begin{bmatrix} 5.035 \\ 2.013 \end{bmatrix}$$

$$S(\underset{\sim}{\theta}^{(5)}) = 9.1117 \qquad S(\underset{\sim}{\theta}^{(6)}) = 8.4131 \qquad S(\underset{\sim}{\theta}^{(7)}) = 8.4128 .$$

The fitted model was taken to be

$$\hat{y} = 5.035 + e^{-2.013\xi} \quad .$$

These calculations are taken from introduction material appearing in a Master's Thesis by Norman Dahl, Princeton University, 1963[6].

Linearize the Sum of Squares Function

To locate the values of the θ's which reduces the sum of squares function $S(\theta)$ to a minimum, we may use standard response surface techniques (7), (8). Here the sum of squares function is approximated locally by a polynominal linear in the parameters. The response is the sum of squares $S(\theta)$ for each chosen set of the p parameters $\underset{\sim}{\theta}$, as illustrated for p = 2 parameters in Figure 6.

FIGURE 6

Locating $S(\hat{\underset{\sim}{\theta}})$ by Response Surface Methods

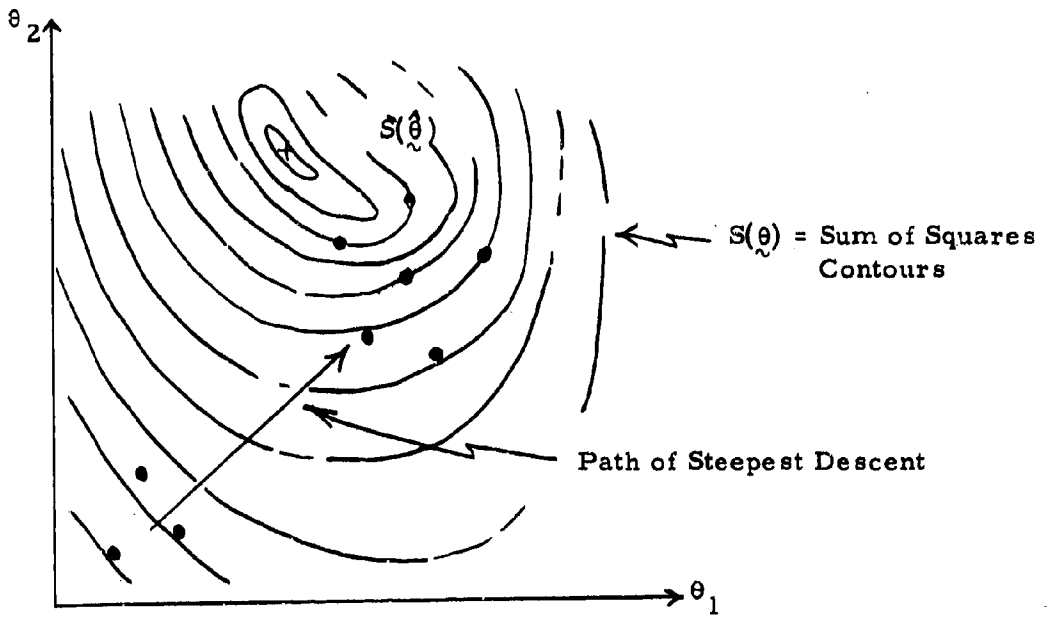

Suppose the experiment began with the guessed values of $\underset{\sim}{\theta}$ illustrated by the simplex design in the lower left hand portion of Figure 6. Upon computing $S(\underset{\sim}{\theta})$ at each of these settings the path of steepest descent can then be determined as indicated by the arrow in the figure. Trials along this path lead to the bottom of the trough. In practice, the size of the steps along the gradient can seriously effect the speed of convergence of the iteration, and several proposals have been made for adjusting the size of the steps to be taken [9], [10]. It is occasionally possible, as illustrated in Figure 6, to employ a second order design, and approximating polynomial in the $\underset{\sim}{\theta}$'s, and empirically determine the curved nature of the $S(\underset{\sim}{\theta})$ contours. This additional information is useful in determining the direction of the trough.

For the case where $p = 2$ or 3 it is often possible to determine $S(\underset{\sim}{\theta})$ everywhere on a grid of values of θ, thus permitting the contours of $S(\underset{\sim}{\theta})$ to be sketched in by hand. The position of $S(\hat{\underset{\sim}{\theta}})$ can then be determined directly. This brute force method is admissible only for p small, and where computation is both very fast and economical.

Direct Search

Direct Search [1] is a method for determining $S(\theta)$ which does not employ any one strategy unless there is a demonstrable reason for doing so. One direct search routine, called 'pattern search' has proved useful. Initially a 'good' point $\underset{\sim}{\theta}$ is chosen in the parameter space and $S(\underset{\sim}{\theta})$ computed. Then the p individual values of $\underset{\sim}{\theta}$ are changed a 'basic' step in a one at a time fashion and $S(\underset{\sim}{\theta})$ evaluated each time. This information is used to design a pattern indicative of the likely direction for successful moves. A pattern move is now made. If successful, (that is, $S(\underset{\sim}{\theta})$ is reduced) each of the p values of $\underset{\sim}{\theta}$ at the new base point are changed a basic step to see if the pattern may be improved. All steps indicative of an improvement are now added to all the previous steps to form a new pattern and the pattern move employed anew. The originators of the method (R. Hooke and T. A. Jeeves) note that once a pattern becomes established it will often grow until the pattern moves are as much as 100 times as large as the basic steps. When a pattern move fails to reduce $S(\underset{\sim}{\theta})$ the authors propose starting a completely new pattern off the current best point.

Elimination of Linear Parameters

Often a model $\eta = f(\underset{\sim}{\xi}, \underset{\sim}{\theta})$ contains parameters that may be defined as "linear", that is, upon differentiating the function $f(\underset{\sim}{\xi}, \underset{\sim}{\theta})$ with respect

to a "linear" parameter, all the parameters disappear in the derivative. For example, consider the model

$$\eta = \theta_1 + e^{\theta_2 \xi}$$

and its associated sum of squares function

$$S(\theta) = \sum_u (y_u - \theta_1 - e^{\theta_2 \xi_u})^2 \quad . \tag{22}$$

The derivative matrix $\underset{\sim}{X}$ consists of the elements $x_{u1} = \frac{\partial S(\underset{\sim}{\theta})}{\partial \theta_1}$ and $x_{u2} = \frac{\partial S(\underset{\sim}{\theta})}{\partial \theta_2}$. Clearly the elements x_{u1} contain neither parameter and hence θ_1 is said to enter the model "linearly". The normal equations associated with this model are

$$\begin{aligned} \eta \theta_1 + \sum_u e^{\theta_2 \xi_u} &= \sum_u y_u \\ \sum \xi_u \theta_1 e^{\theta_2 \xi_u} + \sum \xi_u e^{2\theta_2 \xi_u} &= \sum_u \xi_u y_u e^{\theta_2 \xi_u} \end{aligned} \quad . \tag{23}$$

The first of these equations may be solved for θ_1 to give

$$\theta_1 = \bar{y} - \frac{1}{n} \sum_u e^{\theta_2 \xi_u} \quad . \tag{24}$$

This expression for θ_1 may be used in several ways. For example, we can substitute for θ_1 in the second normal equation in Eq. (23) and then solve for θ_2 by trial and error. Or, since we now have an expression in θ_2 only, we might attempt to linearize this normal equation using a Taylor Series about some guessed value θ_2 and determine, in a fashion analogous to the Gaussian Iterant, corrections on the guessed values. Upon substituting θ_1 in $S(\theta)$ we obtain

$$(25) \qquad S(\theta) = \sum_u [y_u - \bar{y} - (e^{\theta_2 \xi_u} - \frac{1}{n} \sum e^{\theta_2 \xi_u})]^2 .$$

It is now easy to calculate $S(\theta)$ for various values of θ_2 and to determine the minimum $S(\theta)$ as illustrated in Figure 7.

FIGURE 7

The Non-Linear Parameter

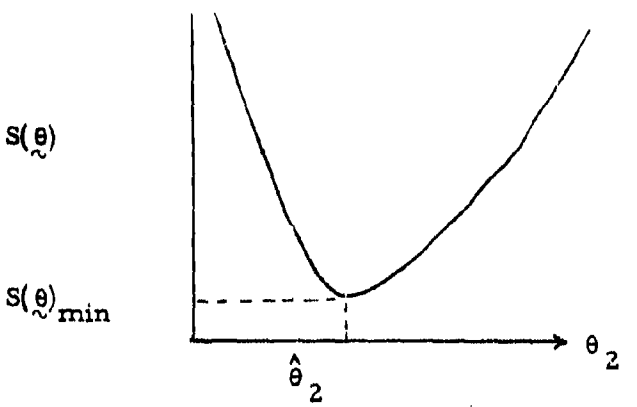

Once $\hat{\theta}_2$, the estimate of θ_2 giving the minimum $S(\theta)$ is obtained, $\hat{\theta}_1$ can be determined using equation (22). In general, it is always possible to solve for all the linear parameters in terms of the non-linear parameters and thus reduce the search for the minimum of $S(\underset{\sim}{\theta})$ to one involving only the non-linear parameters (12).

Confidence Regions for $\underset{\sim}{\theta}$

The confidence region for $\underset{\sim}{\theta}$ can be determined (13) as in the case of linear models, by first determining that value of the $S(\underset{\sim}{\theta})$ which would just produce a critical value of $F_{p,\nu,\alpha}$. The problem then becomes one of locating the contour for this critical value of $S(\theta)$. This can be accomplished if $S(\theta)$ has been determined over a reasonably fine lattice of points throughout the parameter space. However,

as mentioned earlier, the evaluation of $S(\theta)$ over a large lattice can be quite expensive in computation time.

An approximate confidence region can be constructed by first converting the non-linear model into an approximate linear model about the least squares estimate $\hat{\underset{\sim}{\theta}}$. The variances and covariance of the estimated parameters is then given, approximately, by $(\underset{\sim}{X}^T\underset{\sim}{X})^{-1}\sigma^2$ where the derivative matrix is evaluated at the point $\hat{\underset{\sim}{\theta}}$. The approximate confidence region for the $\underset{\sim}{\theta}$ is then given by the quadratic form

$$(\dot{\theta}-\hat{\theta})^T X^T X(\dot{\theta}-\hat{\theta})^T = p\,\frac{S(\hat{\theta})}{\nu}\,F_{p,\nu,\alpha}. \tag{26}$$

Design for Non-Linear Models

The problems of estimating the parameters $\underset{\sim}{\theta}$ in a non-linear model $y_u = f(\underset{\sim}{\xi}_u, \underset{\sim}{\theta}) + \epsilon$ have been briefly reviewed. We turn now to the problem of choosing the settings of the variables $\underset{\sim}{\xi}$ so that our estimates of the $\underset{\sim}{\theta}$ are, in some sense, best. One criterion for a good design is to choose the levels of the $\underset{\sim}{\xi}$, that is, construct the design matrix, so that $(\underset{\sim}{X}^T\underset{\sim}{X})^{-1}$ is as small as possible. This directs us then to choose $\underset{\sim}{\xi}$ so that the determinant $|\underset{\sim}{X}^T\underset{\sim}{X}|$ is as large as possible. G. E. P. Box and H. L. Lucas [14] employed this criteria for the construction of a non-linear design in an early paper by considering the special case where $n = p$, the number of runs equals the number of parameters. For this special case $|\underset{\sim}{X}^T\underset{\sim}{X}| = |\underset{\sim}{X}|^2$. Thus the problem becomes one of determining the levels of $\underset{\sim}{\xi}$ so as to maximize the determinante $|X|$.

For example, suppose the model is $\eta = \theta_1 e^{\theta_2 \xi}$. Then the determinant of the matrix of derivatives $\underset{\sim}{X}$ becomes

$$|\underset{\sim}{X}| = \begin{vmatrix} e^{\theta_2 \xi_1} & \theta_1 \xi_{11} e^{\theta_2 \xi_1} \\ e^{\theta_2 \xi_2} & \theta_1 \xi_{12} e^{\theta_2 \xi_2} \end{vmatrix} = [\xi_2 - \xi_1]\theta_1 e^{\theta_2(\xi_1+\xi_2)} \tag{26}$$

where ξ_1 and ξ_2 are the two settings of ξ to be determined. Clearly, initial guesses of the parameters θ_1^* and θ_2^* are necessary before these levels of ξ can be determined. Let $\xi_{min} < \xi < \xi_{max}$ be the admissible range of ξ. Then if the model represents an exponential decay (θ_2 is negative) we find that $|\underset{\sim}{X}|$ is maximized when $\xi_1 = \xi_{(min)}$ and $\xi_2 = \xi_{(min)} + 1/\theta_2^*$. Thus if η_1 is the response at $\xi_{(min)}$, the initial response, the experimenter is instructed to take the next observation when $\eta = e^{-1} = 36.8\%$ of η. If the model represents exponential growth (θ_2 is positive), then $|X|$ is maximized by setting $\xi_2 = \xi_{max}$ and $\xi_1 = \xi_{max} - 1/\theta_2^*$. Thus we should take our first observation when $\eta = e^{-1} = 36.8\%$ of the response at ξ_{max}. Box and Lucas discuss design problems associated with other simple non-linear models. In another paper [15], Box and W. G. Hunter discuss the general problem of experimental design for non-linear models with the two objectives of i) establishing the form of the model and the ii) estimating the parameters in the model most precisely.

Of course, for $n = p$ the values ξ_1 and ξ_2 that maximize $|X|$ could have been determined by trial and error using a fast computer once θ_1^* and θ_2^* were given by choosing a lattice of values ξ_1 and ξ_2 and determining the contours of $|X|$ as illustrated in Figure 8.

FIGURE 8

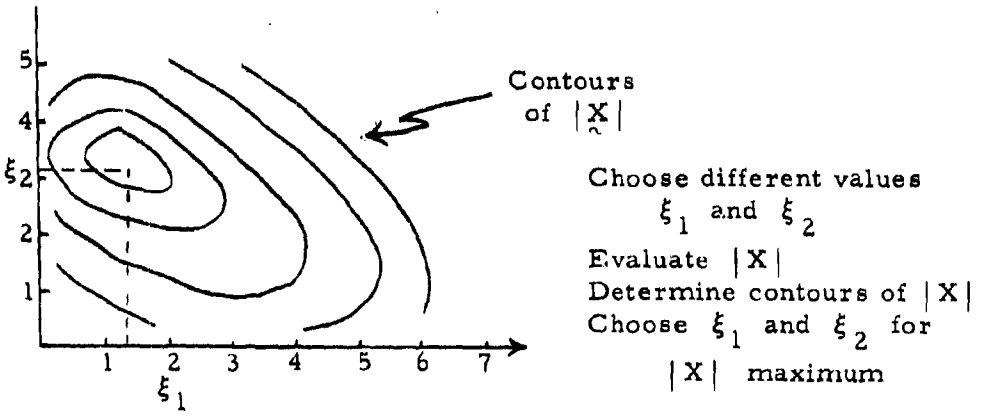

This brute force method can easily be extended to more settings of ξ. In fact, those doing such computations will find that the levels of ξ will usually merely replicate themselves for $n > 2$. Further, models with p parameters will produce designs with $n = p$ points. In all of this, the initial guessed values $\underset{\sim}{\theta}^{*}$ must be available.

In a second report [16] Box and W. G. Hunter discuss the problem of sequential non-linear designs. Here we begin with n observations $\underset{\sim}{y}$, the results of a model $\underset{\sim}{y} = f(\underset{\sim}{\xi}_u, \underset{\sim}{\theta}) + \underset{\sim}{\epsilon}$ and the n x k design matrix $\underset{\sim}{\xi}$. By the methods of non-linear estimation we can then determine the least squares estimate $\hat{\theta}$ of the p parameters. Knowing $\hat{\theta}$ we may compute the n predicted values $\hat{y}_u = f(\underset{\sim}{\xi}_u, \hat{\theta})$ and finally the n x 1 vector of residuals $\underset{\sim}{R} = \underset{\sim}{y} - \hat{\underset{\sim}{y}}$. We may also compute the n x p elements of the derivative matrix $\underset{\sim}{X}_n$ evaluated for $\underset{\sim}{\theta} = \hat{\underset{\sim}{\theta}}$. Let $\underset{\sim}{C}_n = |\underset{\sim}{X}_n^T \underset{\sim}{X}_n|$ be the determinant of the p x p matrix $\underset{\sim}{X}_n^T \underset{\sim}{X}_n$. We now require $\underset{\sim}{\xi}_{n+1}$, the settings of the k controlled variables for experiment n+1. As earlier, subject to the experimental constraints on the variables $\underset{\sim}{\xi}$, we wish to maximize the determinant

$$C_{n+1} = |\underset{\sim}{X}_{n+1}^T \underset{\sim}{X}_{n+1}| \quad . \tag{27}$$

Now $C_{n+1} = C_n + \underset{\sim}{x}_{n+1} \underset{\sim}{x}_{n+1}^T$ where $\underset{\sim}{x}_{n+1}$ is the (1xp) row vector

$$\underset{\sim}{x}_{n+1} = [x_{n+1,1}, x_{n+1,2}, \cdots, x_{n+1,p}]$$

and where the $j^{\underline{th}}$ element $x_{n+1,j}$ is the derivative of the function $f(\xi, \underset{\sim}{\theta})$ with respect to θ_j evaluated at $\hat{\theta}$, that is $x_{n+1,j} = \left.\frac{\partial f(\underset{\sim}{\xi}_{n+1}, \underset{\sim}{\theta})}{\partial \theta_j}\right|_{\hat{\underset{\sim}{\theta}}}$.

To determine the settings $\underset{\sim}{\xi}_{n+1}$ to maximize C_{n+1} we now choose a lattice of points in the space of the k controlled variables $\underset{\sim}{\xi}$, and by determining C_{n+1} at each of these lattice points, locate that setting which minimizes C_{n+1}. Since we already know C_n this calculation is not quite as onerous as might at first seem.

The following example is from the Box and W. G. Hunter report. The non-linear model under study is

$$\eta = \frac{\theta_1 \theta_3 \xi_1}{1+\theta_1 \xi_1 + \theta_2 \xi_2} \quad . \tag{28}$$

The two controlled variables, ξ_1 and ξ_2, are constrained to lie in the interval 0 to 3. An initial experimental design, consisting of a 2^2 factorial, was first employed to obtain data to help estimate the three parameters. The design levels and response were:

(29)

ξ_1	ξ_2	χ
1	1	0.126
2	1	0.219
1	2	0.076
2	2	0.126

To begin the non-linear estimation computation the initial guessed values of the parameters were $\theta_1^{(0)} = 2.9$; $\theta_2^{(0)} = 12.2$ and $\theta_3^{(0)} = 0.69$. The least square estimates $\hat{\underset{\sim}{\theta}}^{(1)}$ were $\hat{\theta}_1 = 10.39$; $\hat{\theta}_2 = 48.83$ and $\hat{\theta}_3 = 0.74$. These estimates of the parameters were then used to compute the elements in the derivative matrix $\underset{\sim}{X}_n$.

To determine the location of the fifth experiment the determinant C_{n+1} was estimated for a grid of values of ξ_1 and ξ_2.

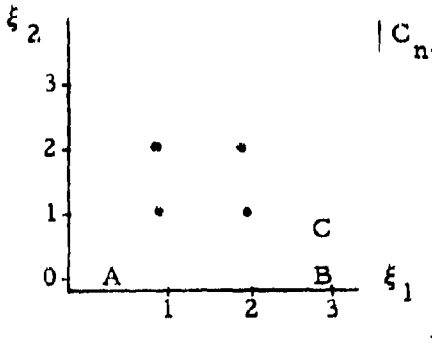

$$|C_{n+1}| = \begin{vmatrix} C_{11}+x_{15}^2 & C_{12}+x_{15}x_{25} & C_{13}+x_{15}x_{35} \\ & C_{22}+x_{25}^2 & C_{23}+x_{25}x_{35} \\ \text{Symmetric} & & C_{33}+x_{35}^2 \end{vmatrix}$$

FIGURE 9

The maximum of C_5 occurs at $\xi_{51} = 0.1$ and $\xi_{52} = 0.0$. The next experiment gave $y_5 = 0.186$ and the new estimates (using the $\hat{\underset{\sim}{\theta}}^{(1)}$ as the initial guessed values in the iteration) were $\hat{\theta}_1 = 3.11$; $\hat{\theta}_2 = 15.19$ and $\hat{\theta}_3 = 0.79$. We now begin anew. C_6 was maximum at $\xi_{61} = 3.0$ and $\xi_{62} = 0$. The new observation was $y_6 = 0.606$ and the newest estimates $\hat{\theta}_1 = 3.96$; $\hat{\theta}_2 = 15.32$ and $\hat{\theta}_3 = 0.66$. Box and Hunter proceeded until n = 13. Of very considerable interest is the fact that the nine experiments following the initial 2^2, grouped themselves into three regions in the space of ξ_1 and ξ_2. These regions: A, B, and C are noted in Figure 9. These three regions roughly define the "intrinsic" design configuration for the model and proposed experimental region.

The criteria, maximize $|\underset{\sim}{X}^T\underset{\sim}{X}|$ is certainly not the only one an experimenter might propose. For example, an experimenter might wish to minimize the trace of $|\underset{\sim}{X}^T\underset{\sim}{X}|^{-1}$, or propose values for various elements in the $\underset{\sim}{X}^T\underset{\sim}{X}$ matrix. The problem now would be one of choosing the settings of the $\underset{\sim}{\xi}_u$, for n fixed, to satisfy these constraints, that is, given $\underset{\sim}{X}^T\underset{\sim}{X}$ can we determine $\underset{\sim}{\xi}$? Box and W. G. Hunter solve this important problem for the special case of p = k+1 in their report.

Although the way forward to the construction of non-linear designs has been indicated by the work of G.E.P. Box and W.G. Hunter, the applications of these methods is only begun. It is evident that designs will have to be constructed for each model and experimenter, since initial guessed values of the non-linear parameters are required. The question of how sensitive a derived design is to fluctuations in the initial guesses is largely unanswered, and many more questions could be posed. One thing is certain the arts of experimental design continue to grow rapidly.

BIBLIOGRAPHY

[1] Box, G.E.P., "Fitting Empirical Data", Annals N.Y. Acad. of Science 80, pp. 792-816 (1960).

[2] Bartlett, M. S., "The Vector Representation of a Sample", Proc. Cambridge Philos. Soc. 30 pp. 327-40 (1934).

[3] Scheffé, H., The Analysis of Variance, John Wiley & Sons, Inc. (1959).

[4] Hartley, H.O., "The Modified Gauss-Newton Method for the Fitting of Non Linear Regression Functions by Least Squares", Technometrics 3, No. 2 p. 269-280 (1961).

[5] Box, G.E.P., "Use of Statistical Methods in the Elucidation of Basic Mechanisms", Bull., Inst. Internat'l Statistics, 36, pp. 215 (1957).

[6] Dahl, N.E., "Some Iterative Methods for Non Linear Estimation", Masters Theis, Department of Chemical Engineering, Princeton University (1963).

[7] Box, G.E.P., "The Exploration and Exploitation of Response Surfaces: Some General Considerations and Examples", Biometrics, 10, p. 16-60 (1954).

[8] Box, G.E.P., and Coutie, H.A., "Application of Digital Computers in the Exploration of Functional Relationships", Proc. I.E.E. 103 B Suppl. 1, pp. 100-17 (1956).

[9] Levenberg, K., "A Method for the Solution of Certain Non Linear Problems in Least Squares", Quart. Applied Mathematics 2, pp 164-8, (1944).

[10] Marquardt, D.W., "An Algorithm for Least Squares Estimation of Nonlinear Parameters", Jour. Industrial & Applied Mathematics, 11, No. 2, pp. 431-41 (1963).

[11] Hooke R. and Jeeves, T.A., "Direct Search Solution of Numerical and Statistical Problems", JACM 8 pp 212-29 (1961).

[12] Williams, E.J., Regression Analysis, John Wiley, N. Y. (1959).

[13] Beale, E.M.L., "Confidence Regions in Non Linear Estimation", J. R. Stat. Soc. B, 22, pp. 41-76 (1960).

[14] Box, G.E.P. and Lucas, H.L., "Design of Experiments in Non-Linear Situations", Biometrika, 46, pp. 77-90 (1959)

[15] Box, G.E.P. and Hunter, W.G., "The Experimental Study of Physical Mechanisms", Technometrics 7, pp 23-42 (1965).

[16] Box, G.E.P., and Hunter, W.G., "Sequential Design of Experiments in Non Linear Situations", Tech. Report 21, Department of Statistics, University of Wisconsin (1963).

A PROBLEM OF DETERIORATION IN RELIABILITY

Henry DeCicco
Quality Assurance Directorate
U. S. Army Munitions Command
Dover, New Jersey

ABSTRACT. A technique is discussed for framing a reliability model in terms of variables data rather than attribute data. A particular model is developed in terms of a Gamma process; it is believed that the model may prove applicable to items undergoing long term storage, especially where continuous observations are not feasible. Estimates of the parameters of the model, along with a discussion of procedures for control and verfication are included.

NOTE: For a fuller discussion of the contents of this paper, please refer to the following article:

"Estimation, Control and Verfication Procedures for a Reliability Model Based on Variable Data", by S. Ehrenfeld and H. DeCicco, Management Science, Vol. 10, No. 2, January 1964.

SYSTEMATIC METHODS FOR ANALYZING 2^n3^m FACTORIAL EXPERIMENTS*

Barry H. Margolin
Harvard University and U. S. Army Electronics Command

ABSTRACT. Two systematic procedures to facilitate the analysis of a complete 2^n3^m factorial experiment are presented. The methods are applicable when all the quantitative three-level factors are equally spaced and when the contrasts involving qualitative three-level factors appear as if the three-level factors were in fact quantitative and equally spaced. Algorithm I systematizes the calculation of the factor effects for the 2^n3^m series of designs. Algorithm II yields the set of fitted values, and hence the residuals, based on those factor effects which have been judged to be non-negligible. The two algorithms have additional and possibly more important uses in studying fractionated 2^n3^m factorial experiments. Algorithm I can be used to facilitate the writing down of the cross-product matrix for a desired set of factor effects for a specified set of treatment combinations. For the special case of the standard fractionated 2^{n-p} series of designs the two algorithms can be used to find the set of defining contrasts corresponding to a given set of treatment combinations or to find the set of treatment combinations corresponding to a given set of defining contrasts.

1. INTRODUCTION. In his oft-quoted bulletin in 1937 on the design and analysis of factorial experiments Yates [7] presented two systematic tabular algorithms for the 2^n series of factorial designs, i.e., designs for studying n two-level factors. The algorithms presented were for the calculation of the factor effects and the calculation of the fitted (predicted) values based on those factor effects judged to be non-negligible. Davies [4] extended the first procedure for calculating factor effects to the 3^m series of designs, i.e., designs for studying m three-level factors. These methods have enabled the factorial experimenter who lacks a high speed computer to save a considerable amount of time and effort in his data analysis. Even where a computer has been available, it has usually proven beneficial to program the algorithms as opposed to the standard method of analysis. This paper presents two procedures for calculating

*This work was begun while the author was a summer employee of the United States Army Electronics Command, Fort Monmouth, during the period 6/65 - 9/65.

factor effects and fitted values for the 2^n3^m series of complete factorial designs. In addition, the algorithms have further applications to the study of fractionated 2^n3^m factorial designs and specifically to the 2^{n-p} series of designs.

2. THE MODEL. Throughout this paper we will be dealing with a factorial experiment in which n factors are studied at two levels each and m factors are studied at three levels each. Unless it is stated to the contrary the experiments will be complete factorials. In addition, the effects attributable to a three-level factor and its interactions will be broken into the usual single degree of freedom components, namely, a linear component, a quadratic component, and interactions involving these components. This breakdown of an effect into its single degree of freedom components is discussed elsewhere by Davies [4].

Let us adopt the following notation: Designate the n two-level factors by letters A, B, ..., and the m three-level factors by letters R, S, ... The main effects of the two-level factors will be indicated by the same capital letters used to indicate the factors. Thus, for example, A will indicate either factor A or the main effect of factor A. It will always be clear from the context of the discussion which interpretation is desired. The two main effect components of a three-level factor will be indicated by the capital letter indicating the factor plus a subscript L or Q, depending upon whether we wish to denote the linear or quadratic component, e.g., R_L will denote the linear effect of factor R. A single degree of freedom component of a multi-factor interaction effect will be designated by a "word" consisting of the capital letters with subscripts where necessary, corresponding to the factors interacting. Thus, ABR_LS_Q will denote the single degree of freedom effect corresponding to the interaction

(A) X (B) X (linear R) X (quadratic S).

Finally, μ will designate the grand mean, i.e., the average of the expected values of all treatment combinations in the full factorial.

In the model, the expected value of the response to the (i)th treatment combination, say $E(y_i)$, $i = 1, 2, \ldots, 2^n3^m$, is expressible as a linear combination of all the main and multi-factor interaction effects

plus the grand mean. To illustrate the model for the $2^2 3^1$ design, let A, B and R be the two two-level factors and the three-level factor respectively. Then we assume:

$$E(y_i) = \mu X_{\mu i} + (A)X_{Ai} + (B)X_{Bi} + (R_L)X_{R_L i} + (R_Q)X_{R_Q i} + (AB)X_{ABi}$$

$$+ (AR_L)X_{AR_L i} + (AR_Q)X_{AR_Q i} + (BR_L)X_{BR_L i} + (BR_Q)X_{BR_Q i}$$

$$+ (ABR_L)X_{ABR_L i} + (ABR_Q)X_{ABR_Q i} \quad , \quad i = 1, 2, \ldots, 12 \ .$$

We also assume that the variance of each observation y_i is constant, say σ^2, and that the observations are independent.

The values of the coefficients $X_{\mu i}, X_{Ai}, \ldots, X_{ABR_Q i}$, $i = 1, 2, \ldots, 12$, are determined by the settings of the factors A, B and R for the (i)th treatment combination as follows:

1) $X_{\mu i} = 1$, $i = 1, \ldots, 12$.

2) If factor A is at its low level, $X_{Ai} = -1$; otherwise, $X_{Ai} = 1$.

3) If factor B is at its low level, $X_{Bi} = -1$; otherwise, $X_{Bi} = 1$.

4) If factor R is at its low level, $X_{R_L i} = -1$ and $X_{R_Q i} = 1$.

5) If factor R is at its intermediate level, $X_{R_L i} = 0$ and $X_{R_Q i} = -2$.

6) If factor R is at its high level, $X_{R_L i} = 1$ and $X_{R_Q i} = 1$.

7) The coefficient corresponding to any interaction will have a value equal to the product of the coefficients of those factor effect components which are interacting, e.g., $X_{ABR_Q i} = X_{Ai} X_{Bi} X_{R_Q i}$.

If we let $\underset{\sim}{E(Y)} = (E(y_i), \ldots, E(y_{12}))$, $\underset{\sim}{\beta} = (\mu, A, B, \ldots, ABR_Q)$, (i.e., $\underset{\sim}{\beta}$ is the vector of effects) and

$$\underset{\sim}{X} = \begin{pmatrix} X_{\mu 1} & X_{A1} & \cdots & X_{ABR_Q 1} \\ \cdot & \cdot & & \cdot \\ \cdot & \cdot & & \cdot \\ \cdot & \cdot & & \cdot \\ X_{\mu 12} & X_{A12} & \cdots & X_{ABR_Q 12} \end{pmatrix},$$

then the model can be reformulated as: $\underset{\sim}{E(Y)} = \underset{\sim}{\beta X'}$, with independent observations of common variance.

Algorithm I, presented in the next section, enables the calculation of $\underset{\sim}{\hat{\beta}}$, the estimate of $\underset{\sim}{\beta}$, in just one tabular operation.

3. CALCULATION OF THE FACTOR EFFECTS. We revert to the general case of a $2^n 3^m$ design. For the levels of the factors, we need the following notation: Let 0 and 1 designate the low level and high level respectively for each two-level factor. Let 0,1 and 2 designate the low, intermediate and high levels respectively for each three-level factor.

Now every treatment combination can be identified with an (n+m)-place integer, possibly beginning with zero. The integral value corresponding to a treatment combination will have a 0 or 1 in the first place, depending upon the level of the A factor; it will have a 0 or 1 in the second place, depending upon the level of the B factor, and so on for the first n places corresponding to the n two-level factors. The (n+1)st place will contain a 0,1, or 2, depending upon the level of the R factor, and so on for the m places corresponding to the m three-level factors.

We now define a column of treatment combinations to be in standard order if the corresponding column of (n+m)-place "integers" is in ascending order of magnitude. The systematic method for the calculation of the factor effects is a direct combination of the methods known

for the 2^n and 3^m series [7,4]. Write down in a column the treatment combinations in standard order. In the adjacent column enter the observed responses. Consider this column of observed responses, usually called column zero, and each of the succeeding m-1 columns as consecutive sets of three values. Then:

(i) For each set, form the sum of the three numbers $(y_1 + y_2 + y_3)$ and enter these values in order in the next column (column I).

(ii) Form the difference: the third element minus the first element $(y_3 - y_1)$ for every set, and enter these values in order in column I under the sums just calculated.

(iii) Form the sum of the first and third values minus twice the second value in every set $(y_1 - 2y_2 + y_3)$ and enter these numbers in order in column I, which is now completed.

(iv) Repeat the above three-step operation m-1 times, so that it has been performed m times in all.

Now consider this last column arrived at after (iv) and the following n-1 columns as consecutive sets of two elements.

(v) For each set form the sum of the two values $(x_1 + x_2)$ and enter these values in order in the next column.

(vi) Then form the difference: the second number minus the first $(x_2 - x_1)$ for each set, and enter these values in order under the sums just calculated in (v).

(vii) Repeat this two-step operation n-1 times, so that it has been performed n times in all.

The final column now contains the contrast sums (not effects) for the factor effects in standard order. Standard order of the factor effects for a $2^2 3^2$, for example, is: total, S_L, S_Q, R_L, $R_L S_L$, $R_L S_Q$, R_Q, $R_Q S_L$, $R_Q S_Q$, B, BS_L, $\cdots$, $BR_Q S_Q$, A, AS_L, $\cdots$, $ABR_Q S_Q$ [4].

To calculate the factor effects (not the standardized factor effects) one must divide each contrast sum by its appropriate divisor. This divisor is given by

$$\text{Divisor} = 2^{n+i}\,3^{m-p}$$

where i = number of three-level factors in the effect, e.g., for ABR_LS_Q, i = 2; and where p = number of linear terms of three level factors in the effect, e.g., for ABR_LS_Q, p = 1.

To calculate the sum of squares for any effect, square the corresponding contrast sum and divide by the above divisor, or square the effect and multiply by the above divisor.

By way of clarification of the above exposition consider the following tabular analysis of a contrived $2^2\,3^1$:

Example I

A	B	R	Response	I	II	III	Divisor	Effect	Effect Name	Sum of Squares
0	0	0	28	99	234	360	12	30	Mean	10,800
0	0	1	27	135	126	64	8	8	R_L	512
0	0	2	44	21	52	120	24	5	R_Q	600
0	1	0	36	105	12	120	12	10	B	1,200
0	1	1	27	16	72	56	8	7	BR_L	392
0	1	2	72	36	48	72	24	3	BR_Q	216
1	0	0	14	-12	36	-108	12	-9	A	972
1	0	1	5	24	84	-40	8	-5	AR_L	200
1	0	2	2	18	20	-24	24	-1	AR_Q	24
1	1	0	30	54	36	48	12	4	AB	192
1	1	1	21	6	36	16	8	2	ABR_L	32
1	1	2	54	42	36	0	24	0	ABR_Q	0
								Total sum of squares =		15,140

Two final comments on this algorithm are in order:

(i) To calculate standardized effects (constant variance), to be used, for example, in half-normal plotting [3], one must divide the elements of the column of contrast sums by the square root of the appropriate divisor presented previously.

(ii) If m = 0, this procedure reduces to the Yates method for the 2^n series; if n = 0, this procedure reduces to the Davies technique for the 3^m series [7,4].

4. CALCULATION OF THE FITTED VALUES. We observed previously that the result of the first algorithm is a column of factor effects in standard order. One can then judge these effects as to their significance, either by a half-normal plot employing the standardized effects, or by the usual analysis of variance using the calculated sums of squares. One need next calculate the fitted values and the set of residuals (the observed response minus the fitted value). This enables one to check in detail the fit of the equation based on the significant effects to the observed data. For this purpose we propose the following tabular algorithm:

(i) Write down the column of effects (contrast sums divided by appropriate divisor) in standard order, replacing those judged to be negligible by a zero.

(ii) As in the first algorithm, regard the numbers in this column and the succeeding m-1 columns as consecutive sets of three values. For each set, form the sum of the first and third elements minus the second element $(y_1-y_2+y_3)$ and enter these values in order in the next column.

(iii) Next, form the difference: the first element minus twice the third element in each set $(y_1 - 2y_3)$, and enter these numbers in order under the values calculated in the previous step.

(iv) Form the sum of the elements in each set $(y_1+y_2+y_3)$ and enter these values in order in the remaining spaces in the next column.

(v) Repeat this three-step operation m-1 times, so that it has been performed m times in all.

(vi) Invert this last column.

(vii) Consider this new column and the succeeding n-1 columns as consecutive sets of two numbers. For each set, form the sum of the two values $(x_1 + x_2)$ and enter these values in order in the next column.

(viii) Form the difference: the second number minus the first number in each set $(x_2 - x_1)$, and enter these values in order under the sums calculated in (vii).

(ix) Repeat this two-step operation n-1 times, so that it has been performed n times in all.

(x) Invert this last column.

The resulting column contains the fitted values in standard order.

If our procedure is valid, applying it to the calculated effects of the earlier example should yield the initial observations or responses in their standard ordering. This is presented below:

Example 2

Effect		I	I inverted	II	III	III inverted = Fitted Value
Mean	30	27	6	-9	54	28
R_L	8	6	-15	63	21	27
R_Q	5	-5	20	-3	30	44
B	10	2	43	24	2	36
BR_L	7	20	4	-3	5	27
BR_Q	3	4	-7	33	14	72
A	-9	-7	4	-21	72	14
AR_L	-5	4	20	23	27	5
AR_Q	-1	43	2	-11	36	2
AB	4	20	-5	16	44	30
ABR_L	2	-15	6	-7	27	21
ABR_Q	0	6	27	21	28	54

Thus, the original set of responses is recovered, and it is in standard order. Hence, algorithms I and II operate in an inverse manner.

Observe that for the 2^n series, i.e., $m = 0$, this procedure reduces to the method presented by Yates [7] for calculating fitted values. One first inverts a column of factor effects in standard order, where zeros have replaced the negligible effects. Then one performs the calculations required in algorith I for the 2^n series. Finally, another column inversion is required. The end result is a column of fitted values based on the significant effects and it appears in standard order.

Algorithms I and II have been presented without proof, but their validity can be verified by a rather untidy argument using matrix theory, or by an inductive argument. While the proofs have been omitted, one should observe that the relationship between algorithms I and II is much more direct than it appears. Consider steps (i) - (iii) in algorithm I; they can be summarized in matrix notation as:

$$(y_1, y_2, y_3) \cdot \begin{pmatrix} 1 & -1 & 1 \\ 1 & 0 & -2 \\ 1 & 1 & 1 \end{pmatrix} .$$

Next, steps (ii)-(iv) in algorithm II can be summarized as:

$$(y_1, y_2, y_3) \cdot \begin{pmatrix} 1 & 1 & 1 \\ -1 & 0 & 1 \\ 1 & -2 & 1 \end{pmatrix} .$$

Observe then that the second 3X3 matrix is merely the transpose of the first 3X3 matrix. In a similar fashion, steps (v) and (vi) in algorithm I can be summarized as:

$$(x_1, x_2) \cdot \begin{pmatrix} 1 & -1 \\ 1 & 1 \end{pmatrix} .$$

Also, steps (vi) - (viii) and (x) in algorithm II can be summarized as:

$$(x_1, x_2) \cdot \begin{pmatrix} 0 & 1 \\ 1 & 0 \end{pmatrix} \cdot \begin{pmatrix} 1 & -1 \\ 1 & 1 \end{pmatrix} \cdot \begin{pmatrix} 0 & 1 \\ 1 & 0 \end{pmatrix} .$$

The product of the three 2X2 matrices directly above is: $\begin{pmatrix} 1 & 1 \\ -1 & 1 \end{pmatrix}$.

This is the transpose of the first 2X2 matrix above. This matrix relationship is not accidental; it generalizes as follows: Let $\underset{\sim}{M}$ denote the matrix of coefficients which operates on the right of the $1X2^n3^m$ data matrix in a complete factorial and produces the matrix of contrast sums. Then $\underset{\sim}{M}'$ operating on the right of the $1X2^n3^m$ matrix of the grand mean and the set of effects (not standardized), where zeros have replaced the negligible effects, produces the matrix of fitted values.

5. FRACTIONATED 2^n3^m FACTORIAL EXPERIMENTS. Fractionating the 2^n3^m series of factorial designs has not proven to be an easy proposition. Webb [8] has presented a fairly thorough review of the work that has been done in this area; however, there appears to be room for further exploration and study. No attempt will be made in this paper to produce new fractions of the 2^n3^m series. We present, rather, a procedure based on algorithm I for writing down the cross-produce or normal matrix for any desired set of factor effect estimates broken into the usual single degree of freedom components, given a specified fractional set of treatment combinations. The method presented is far superior to the tedious sums of squares and cross-products calculation usually used to determine the elements of the cross-product matrix each time an altered set of factor effects is to be considered. This will speed the evaluation of new designs by criteria to be discussed later, and will facilitate the calculation of the desired estimates and evaluation of the proposed model.

We retain the model presented for the full factorial; however, in a fractionated experiment we are restricted to obtaining estimates of only a subset of the set of all single degree of freedom effects possible in the full factorial. Note that in a full factorial one may be interested also in only a subset of the set of effects possible, but that is by choice.

Those effects which are of no interest or cannot be estimated are then suppressed by assuming them to be zero in the model. In addition, in a fractionated experiment we no longer have $2^n 3^m$ treatment combinations to run, but a smaller number, say N. Hence, if we are interested in the subset of effects, both main and interaction, designated by $(\mu, \alpha, \beta, \ldots, \omega)$, the model is

$$E(y_i) = \mu X_{\mu i} + \alpha X_{\alpha i} + \beta X_{\beta i} + \ldots + \omega X_{\omega i}, \quad i = 1, \ldots, N,$$

where μ is the grand mean, and the observations are independent with variance σ^2. The coefficients $X_{\mu i}, X_{\alpha i}, \ldots, X_{\omega i}$ are determined as before by the settings of the factors for the (i)th treatment combination.

DEFINITION. $X_\alpha = (X_{\alpha 1}, \ldots, X_{\alpha N})$ will be called the <u>indicator variable</u> corresponding to the effect α.

DEFINITION. Two indicator variables X_α and X_β will be said to be <u>orthogonal</u> for the fractional factorial if

$$\sum_{i=1}^{N} X_{\alpha i} X_{\beta i} = 0 ;$$

otherwise, they will be said to be <u>entangled</u>. (We have purposefully avoided using the ambiguous term "confounding".) As a consequence of our particular model, X_α and X_β are orthogonal if and only if

$$\sum_{i=1}^{N} X_{\alpha\beta i} = 0 , \quad \text{since} \quad \sum_{i=1}^{N} X_{\alpha\beta i} = \sum_{i=1}^{N} X_{\alpha i} X_{\beta i} .$$

To be able to handle the case where both α and β have factor components in common, e.g., $\alpha = AR_L S_L$ and $\beta = ABR_L S_Q$, we need to extend the notation of an indicator variable to allow subscripts containing such meaningless symbols as R_L^2, $S_L S_Q$, and A^2. This will be purely for convenience so that, for example, we can write

$$X_{AR_LS_L} X_{ABR_LS_Q} = X_{A^2BR_L^2S_LS_Q} .$$

DEFINITION. Effects α and β will be said to be entangled for the fractional factorial if their corresponding indicator variables are entangled.

Note that aliasing of effects α and β is the special case of entangling where either $X_\alpha = X_\beta$ or $X_\alpha = -X_\beta$.

DEFINITION. If $\sum_{i=1}^{N} X_{\alpha i} \neq 0$, then X_α will be said to be an entangling contrast for the design.

It is clear that if X_α is an entangling contrast, then X_α is entangled with X_μ , and hence, α is entangled with the grand mean μ . It should also be clear that defining contrasts, as defined for the fractionated 2^{n-p} series of designs in [2] , are merely special cases of entangling contrasts where either $X_{\alpha i} = 1$ for $i = 1, \ldots, N$, or $X_{\alpha i} = -1$ for $i = 1, \ldots, N$, and hence

$$\sum_{i=1}^{2^{n-p}} X_{\alpha i} = \pm 2^{n-p} .$$

6. CORRELATION AND ORTHOGONALITY. The normal or cross-product matrix for a fractional factorial, necessary for least squares estimation, requires simply the sums of squares and cross-products of the indicator variables corresponding to the desired subset of effect estimates. The normal matrix is singular if and only if the set of indicator variables involved is linearly dependent. In this case we say that the set of effects is non-estimable. The only way to circumvent this problem and achieve unique estimates is to suppress a sufficient number of effects to destroy all linear dependencies.

Let us assume that the normal matrix is non-singular. Then one is interested in the inverse of the normal matrix for purposes of estimation

and determining the correlation between estimates. The inverse of the normal matrix is in fact the covariance matrix between effect estimates. It is well known (see [4], for example) that if the set of indicator variables is completely orthogonal, i.e., any two indicator variables corresponding to different effects are orthogonal, then the normal matrix and the covariance matrix are both diagonal. Hence, the correlation between any two estimates of factor effects is zero. It is less well known and deserves repeating that orthogonality of a pair of indicator variables is neither necessary nor sufficient for the corresponding pair of estimates to have zero correlation. The following two small examples will illustrate this:

I.

Design				Indicator Variables			
Run	A	B	C	X_μ	X_A	X_B	X_C
1	0	0	0	1	-1	-1	-1
2	0	1	0	1	-1	1	-1
3	1	0	0	1	1	-1	-1
4	1	1	1	1	1	1	1

The normal matrix is:

$$\begin{pmatrix} 4 & 0 & 0 & -2 \\ 0 & 4 & 0 & 2 \\ 0 & 0 & 4 & 2 \\ -2 & 2 & 2 & 4 \end{pmatrix}$$

and its inverse, the covariance matrix is:

$$\begin{pmatrix} \frac{1}{2} & -\frac{1}{4} & -\frac{1}{4} & \frac{1}{2} \\ -\frac{1}{4} & \frac{1}{2} & \frac{1}{4} & -\frac{1}{2} \\ -\frac{1}{4} & \frac{1}{4} & \frac{1}{2} & -\frac{1}{2} \\ \frac{1}{2} & -\frac{1}{2} & -\frac{1}{2} & 1 \end{pmatrix} .$$

Thus, even though $\sum_{i=1}^{4} X_{Ai}X_{Bi} = 0$, $\text{cov}(\hat{A}, \hat{B}) = \frac{1}{4}\sigma^2$, where $\hat{A}$ and $\hat{B}$ denote the estimated effects.

II.

Design				Indicator Variables			
Run	R	S	A	X_μ	X_{R_L}	X_{S_L}	X_A
1	1	0	0	1	0	-1	-1
2	0	1	0	1	-1	0	-1
3	1	1	1	1	0	0	1
4	2	2	1	1	1	1	1

The normal and covariance matrices are respectively:

$$\begin{pmatrix} 4 & 0 & 0 & 0 \\ 0 & 2 & 1 & 2 \\ 0 & 1 & 2 & 2 \\ 0 & 2 & 2 & 4 \end{pmatrix} \qquad \begin{pmatrix} \frac{1}{4} & 0 & 0 & 0 \\ 0 & 1 & 0 & -\frac{1}{2} \\ 0 & 0 & 1 & -\frac{1}{2} \\ 0 & -\frac{1}{2} & -\frac{1}{2} & 3/4 \end{pmatrix} .$$

Thus, $\mathrm{cov}(\hat{R}_L, \hat{S}_L) = 0$, but $\sum_{i=1}^{4} X_{R_L i} X_{S_L i} = 1$. Both these small designs were intended solely for illustrative purposes, but either might conceivably arise at an early stage of some experiment in which the factors are introduced sequentially and the results become available sequentially.

7. USES OF THE ENTANGLING CONTRASTS. One needs to be able to calculate the normal matrix for a design for any conceivable set of desired estimates for both estimation and evaluation of the design. It is with respect to this task that the entangling contrasts prove useful. Consider the set of entangling contrasts corresponding to the set of all possible effects for the fractional factorial under consideration. Then this set contains succinctly the information needed to write down the normal matrix corresponding to any desired set of effect estimates. For example, suppose that α, β and γ are three of the single degree of freedom effects we are interested in for a particular fractionated $2^n 3^m$ experiment. Suppose further that the only entangling contrast for the experiment, regardless of the set of desired effects, is $X_{\alpha\beta\gamma}$. Thus,

$$\sum_{i=1}^{N} X_{\alpha\beta\gamma i} = c \neq 0, \quad \text{whence,} \quad \sum_{i=1}^{N} X_{\alpha i} X_{\beta\gamma i} = c.$$

Since we are interested in α, β and γ, it then follows that X_α is entangled with $X_{\beta\gamma}$, and that the cross-product of X_α and $X_{\beta\gamma}$ is equal to c. We will denote the cross-product of X_α and $X_{\beta\gamma}$ by $(X_\alpha, X_{\beta\gamma})$. Hence, $(X_\alpha, X_{\beta\gamma}) = c$. Similarly, $(X_\beta, X_{\alpha\gamma}) = (X_\gamma, X_{\alpha\beta}) = (X_\mu, X_{\alpha\beta\gamma}) = c$. We shall call c the value of the entangling contrast.

Finally, we know that since $X_{\alpha\beta\gamma}$ is the only entangling contrast, no other non-zero cross-products are possible. Hence, we can write down the complete normal matrix for any desired set of effects just from the knowledge of the entire set of entangling contrasts. It turns out that we don't even need the entire set of entangling contrasts. This reduction can be accomplished by use of the following easily verified identities:

i) $X_{A^2_a} = X_a$, where A is a two-level factor;

ii) $X_{R^2_{L_a}} = (2/3)X_a + (1/3)X_{R_{Q^a}}$, where R is a three-level factor;

iii) $X_{R^2_{Q_a}} = 2X_a - X_{R_{Q^a}}$, where R is a three-level factor; and

iv) $X_{R_L R_{Q^a}} = X_{R_{L^a}}$, where R is a three-level factor.

Hence, we need not calculate directly any entangling contrast which has squared components or both the linear and quadratic components of the same factor as part of its subscript. The remaining subset of entangling contrasts will be called the generating set of entangling contrasts. Thus, once we have determined our desired effects, we can process to write down the corresponding normal matrix from the generating set of entangling contrast.

There is a second related use of the set of entangling contrasts for any desired set of effects. Frequently the normal matrix can be rearranged so that there are square submatrices (proper) of non-zero elements down the main diagonal and zeros elsewhere. Webb [8] has termed such designs clumpwise-orthogonal designs. Such a rearrangement, if possible, makes it easier to evaluate the determinant of the entire normal matrix as the product of the determinants of the submatrices. Thus, if the normal matrix is singular, one can localize the linear dependencies by determining which submatrices are singular. The inversion of the normal matrix is also facilitated, for one need only invert each of the smaller submatrices. Finally, the rearrangement allows us to state immediately that if X_α and X_β are indicator variables whose sums of squares are found in different submatrices, then cov $(\hat{\alpha}, \hat{\beta}) = 0$ [4].

The breakdown of the normal matrix is accomplished as follows: Define $\sim$ to be a relation between indicator variables X_α and X_β such that $X_\alpha \sim X_\beta$ if and only if X_α is entangled with X_β, or if there is a finite chain of indicator variables in the desired model, say $X_{A_1}, \ldots, X_{A_n}$, such that X_α is entangled with X_{A_1}, X_{A_i} is entangled with $X_{A_{i+1}}$, $i = 1, \ldots, n-1$, and X_{A_n} is entangled with X_β.

It should be clear that this relation is an equivalence relation for the desired set of indicator variables corresponding to the desired set of effect estimates. Hence, it determines equivalence classes or disjoint subsets of the set of desired indicator variables. The corresponding rearrangement of the normal matrix by equivalence classes will accomplish the desired clumpwise-orthogonalization of the normal matrix. In practice this is an easy operation to perform.

8. DETERMINING THE GENERATING SET OF ENTANGLING CONTRASTS. We intend to make use of algorithm I for calculating the generating set of entangling contrasts. For any effect α, algorithm I forms the contrast sum

$$\sum_{i=1}^{2^{n_3 m}} y_i X_{\alpha i} \quad ,$$

Where y_i is the response entry in the (i)th position in column zero. The contrast sum appears in the final column in the position designated for α in the standard ordering of all possible effects in the full factorial. Let us consider what would happen if, instead of using $(y_1, \ldots, y_{2^{n_3 m}})'$ as column zero, we choose to have $(z_1, \ldots, z_{2^{n_3 m}})'$ as column zero, where

$z_i = 1$ if the (i)th treatment combination in the standard order was run as part of the fractional factorial, $i = 1, \ldots, 2^{n_3 m}$,

$= 0$ otherwise.

Then one would find $\sum_{i=1}^{2^{n_3 m}} z_i X_{\alpha i}$ appearing in the position for α in the final column. However,

$$\sum_{i=1}^{2^{n_3 m}} z_i X_{\alpha i} = \sum_{j \in S} X_{\alpha j} \quad ,$$

where S is the set of those treatment combinations forming the given fractional factorial. Thus, $\sum_{j \in S} X_{\alpha j}$ is simply the calculation we need to determine whether or not X is an entangling contrast for the fractional factorial. Thus, algorithm I can be employed to find the generating set of entangling contrasts in any fraction of a 2^n3^m design, since one sweep of algorithm I performs the calculation of $\sum_{j \in S} X_{\alpha j}$ for all possible effects α which are meaningful. Practically speaking, if the number 2^n3^m is relatively small, say 81 or less, this procedure works well, and the bookkeeping does not become unreasonable even when calculating by hand.

To summarize then the procedure in this case, one writes down all the treatment combinations in the full factorial in standard order. One places a one in the response column next to each treatment combination which was run in the fractional factorial and a zero in each of the remaining positions in column zero. One then proceeds with algorithm I as if this dummy response column were a true response column for a full 2^n3^m factorial. As in a full 2^n3^m factorial, one identifies the final column with a column of effects in standard order. Now, however, the interpretation of the final column will differ from that of a column of calculated contrasts. If there is a non-zero element in the final column next to any effect, then the corresponding indicator variable is an entangling contrast in the generating set with the value of the non-zero element. For example, consider the following fraction of a $2^2 3^2$ consisting of 12 runs:

Run number / Factor	1	2	3	4	5	6	7	8	9	10	11	12
A	0	0	0	0	0	0	1	1	1	1	1	1
B	0	0	0	1	1	1	0	0	0	1	1	1
R	0	1	2	0	1	2	0	1	2	0	1	2
S	0	1	2	1	2	0	1	2	1	2	0	1

Here A and B designate as usual the two-level factors and R and S designate the three-level factors.

This fraction was formed by setting $A + B + R \equiv S \pmod 3$.

Then the procedure to find the generating set of entangling contrasts is demonstrated below:

A	B	R	S	0	I	II	III	IV	Contrast name
0	0	0	0	1	1	3	6	12	Total
0	0	0	1	0	1	3	6	0	S_L
0	0	0	2	0	1	3	0	0	S_Q
0	0	1	0	0	1	3	0	0	R_L
0	0	1	1	1	1	0	0	-1	$R_L S_L$
0	0	1	2	0	1	0	0	3	$R_L S_Q$
0	0	2	0	0	1	0	0	0	R_Q
0	0	2	1	0	1	0	0	-3	$R_Q S_L$
0	0	2	2	1	1	0	1	-3	$R_Q S_Q$
0	1	0	0	0	1	0	-2	0	B
0	1	0	1	1	1	0	3	0	BS_L
0	1	0	2	0	1	0	0	0	BS_Q
0	1	1	0	0	-1	0	0	0	BR_L
0	1	1	1	0	0	0	0	-3	$BR_L S_L$
0	1	1	2	1	1	0	-3	-3	$BR_L S_Q$
0	1	2	0	1	0	0	0	0	BR_Q
0	1	2	1	0	1	2	3	3	$BR_Q S_L$
0	1	2	2	0	-1	-1	-6	-9	$BR_Q S_Q$
1	0	0	0	0	0	-1	0	0	A
1	0	0	1	1	1	-1	0	0	AS_L
1	0	0	2	0	-1	0	0	0	AS_Q
1	0	1	0	0	1	3	0	0	AR_L
1	0	1	1	0	-1	3	0	-3	$AR_L S_L$
1	0	1	2	1	0	-3	0	-3	$AR_L S_Q$
1	0	2	0	1	1	0	0	0	AR_Q
1	0	2	1	0	-2	0	0	3	$AR_Q S_L$
1	0	2	2	0	1	0	-3	-9	$AR_Q S_Q$
1	1	0	0	0	-2	0	0	0	AB
1	1	0	1	0	1	0	3	0	ABS_L
1	1	0	2	1	1	-3	-6	0	ABS_Q
1	1	1	0	1	-2	-3	0	0	ABR_L
1	1	1	1	0	1	3	0	3	$ABR_L S_L$
1	1	1	2	0	1	6	-3	-9	$ABR_L S_Q$
1	1	2	0	0	1	-3	6	0	ABR_Q
1	1	2	1	1	1	-3	-9	9	$ABR_Q S_L$
1	1	2	2	0	-2	-3	0	9	$ABR_Q S_Q$

Hence, the generating set of entangling contrasts is as follows:

$R_L S_L = -1$, $R_L S_Q = 3$, $R_Q S_L = -3$, $R_Q S_Q = -3$, $BR_L S_L = -3$,

$BR_L S_Q = -3$, $BR_Q S_L = 3$, $BR_Q S_Q = -9$, $AR_L S_L = -3$, $AR_L S_Q = -3$,

$AR_Q S_L = 3$, $AR_Q S_Q = -9$, $ABR_L S_L = 3$, $ABR_L S_Q = -9$,

$ABR_Q S_L = 9$, $ABR_Q S_Q = 9$.

Thus, we find that there are even two letter entangling contrasts, such as $R_L S_L$, in this design. One could now proceed to write down the normal matrix for any desired set of effect estimates based on these twelve runs.

If $2^n 3^m$ is a relatively large number so as to make the foregoing procedure unwieldy, a variation of the above may be more suitable, provided one can identify a set of "live" factors in the fractional factorial, i.e., factors which, when the remaining factors are suppressed in the design, form a full factorial. Thus, in the fractional $2^2 3^2$ in twelve runs presented above, factors A, B and R may be considered "live". The run numbers are already in standard order for the full factorial on A, B and R as they are presented. Consider then that we are dealing with a full $2^2 3^1$ design. Now, instead of a column of ones and zeros, enter in column zero next to each treatment combination the $X_{S_L i}$ corresponding to the run. Proceed with algorithm I for this dummy response column for a $2^2 3^1$ design. Then identify the last column with the effects in the $2^2 3^1$ on A, B and R. Note that we are actually calculating

$$\sum_{i=1}^{12} X_{S_L i} X_{ai} = X_{S_L a}$$

for all effects a involving A, B and R as components. Then non-zero elements in the last column of the algorithm will indicate which generating entangling contrasts in this design involve S_L as a component of

the subscript. Similarly, by taking as the zero column $(X_{S_Q 1}, \ldots, X_{S_Q 12})'$, one can find those entangling contrasts in the generating set which involve S_Q as a component of the subscript. Clearly, every entangling contrast will involve either S_L or S_Q or both as a component of the subscript, since A, B and R form a "live" full factorial and hence, no entangling contrast can exist solely involving A, B and R. We have then found the entire generating set of entangling contrasts in this plan by two applications of algorithm I, each individually smaller in size than the application of algorithm I presented earlier. The above variation is demonstrated below:

"Live" Factors			Suppressed Factors	S_L	I	II	III	Contrasts involving A, B and R
A	B	R	S					
0	0	0	0	-1	0	0	0	Total
0	0	1	1	0	0	0	-1	R_L
0	0	2	2	1	0	1	-3	R_Q
0	1	0	1	0	0	-2	0	B
0	1	1	2	1	2	-3	-3	BR_L
0	1	2	0	-1	-1	0	3	BR_Q
1	0	0	1	0	-1	0	0	A
1	0	1	2	1	-1	0	-3	AR_L
1	0	2	0	-1	0	-3	3	AR_Q
1	1	0	2	1	-3	0	0	AB
1	1	1	0	-1	-3	-3	3	ABR_L
1	1	2	1	0	3	6	9	ABR_Q

Thus, we find the subset of the generating set of entangling contrasts involving S_L to be:

$R_L S_L = -1$, $R_Q S_L = -3$, $BR_L S_L = -3$, $BR_Q S_L = 3$, $AR_L S_L = -3$, $AR_Q S_L = 3$, $ABR_L S_L = 3$, $ABR_Q S_L = 9$. This checks with our previous calculation of the generating set of entangling contrasts. A similar computation for S_Q would complete the generating set of entangling contrasts for this design.

9. YATES' 3^{3-1} DESIGNS. One specific investigation of the entangling of single degree of freedom effects in a fractional $2^n 3^m$ deserves mention. In [7] , Yates presented twelve distinct 3^{3-1} designs, illustrated below with R, S and T representing the three factors and W, X, Y and Z being Yates' own notation:

		W_1	W_2	W_3	X_1	X_2	X_3	Y_1	Y_2	Y_3	Z_1	Z_2	Z_3
R	S	T	T	T	T	T	T	T	T	T	T	T	T
0	0	0	2	1	0	1	2	0	2	1	0	1	2
0	1	1	0	2	2	0	1	1	0	2	2	0	1
0	2	2	1	0	1	2	0	2	1	0	1	2	0
1	0	2	1	0	1	2	0	1	0	2	2	0	1
1	1	0	2	1	0	1	2	2	1	0	1	2	0
1	2	1	0	2	2	0	1	0	2	1	0	1	2
2	0	1	0	2	2	0	1	2	1	0	1	2	0
2	1	2	1	0	1	2	0	0	2	1	0	1	2
2	2	0	2	1	0	1	2	1	0	2	2	0	1

The following generating sets of entangling contrasts have been found for the twelve different 3^{3-1} designs:

W_1 : $R_L S_L T_L = -3$, $R_L S_Q T_L = -3$, $R_Q S_L T_L = 3$, $R_Q S_Q T_L = -9$,

$R_L S_L T_Q = 3$, $R_L S_Q T_Q = -9$, $R_Q S_L T_Q = 9$, $R_Q S_Q T_Q = 9$.

W_2: $R_L S_L T_L = 3$, $R_L S_Q T_L = -3$, $R_Q S_L T_L = 3$, $R_Q S_Q T_L = 9$,
$R_L S_L T_Q = 3$, $R_L S_Q T_Q = 9$, $R_Q S_L T_Q = -9$, $R_Q S_Q T_Q = 9$.

W_3: $R_L S_Q T_L = 6$, $R_Q S_L T_L = -6$, $R_L S_L T_Q = -6$, $R_Q S_Q T_Q = -18$.

X_1: $R_L S_L T_L = -3$, $R_L S_Q T_L = 3$, $R_Q S_L T_L = -3$, $R_Q S_Q T_L = -9$,
$R_L S_L T_Q = 3$, $R_L S_Q T_Q = 9$, $R_Q S_L T_Q = -9$, $R_Q S_Q T_Q = 9$.

X_2: $R_L S_Q T_L = -6$, $R_Q S_L T_L = 6$, $R_L S_L T_Q = -6$, $R_Q S_Q T_Q = -18$.

X_3: $R_L S_L T_L = 3$, $R_L S_Q T_L = 3$, $R_Q S_L T_L = -3$, $R_Q S_Q T_L = 9$,
$R_L S_L T_Q = 3$, $R_L S_Q T_Q = -9$, $R_Q S_L T_Q = 9$, $R_Q S_Q T_Q = 9$.

Y_1: $R_L S_L T_L = -3$, $R_L S_Q T_L = 3$, $R_Q S_L T_L = 3$, $R_Q S_Q T_L = 9$,
$R_L S_L T_Q = -3$, $R_L S_Q T_Q = -9$, $R_Q S_L T_Q = -9$, $R_Q S_Q T_Q = 9$.

Y_2: $R_L S_Q T_L = -6$, $R_Q S_L T_L = -6$, $R_L S_L T_Q = 6$, $R_Q S_Q T_Q = -18$.

Y_3: $R_L S_L T_L = 3$, $R_L S_Q T_L = 3$, $R_Q S_L T_L = 3$, $R_Q S_Q T_L = -9$,
$R_L S_L T_Q = -3$, $R_L S_Q T_Q = 9$, $R_Q S_L T_Q = 9$, $R_Q S_Q T_Q = 9$.

Z_1: $R_L S_Q T_L = 6$, $R_Q S_L T_L = 6$, $R_L S_L T_Q = 6$, $R_Q S_Q T_Q = -18$.

Z_2: $R_L S_L T_L = -3$, $R_L S_Q T_L = -3$, $R_Q S_L T_L = -3$, $R_Q S_Q T_L = 9$,
$R_L S_L T_Q = -3$, $R_L S_Q T_Q = 9$, $R_Q S_L T_Q = 9$, $R_Q S_Q T_Q = 9$.

Z_3: $R_L S_L T_L = 3$, $R_L S_Q T_L = -3$, $R_Q S_L T_L = -3$, $R_Q S_Q T_L = -9$,
$R_L S_L T_Q = -3$, $R_L S_Q T_Q = -9$, $R_Q S_L T_Q = -9$, $R_Q S_Q T_Q = 9$.

The main thing to observe is that there are four designs which have only four entangling contrasts in the generating set and that there are eight designs containing eight entangling contrasts in the generating set. Thus, the twelve designs are by no means equal in their degrees or patterns of entanglement for the particular model we are assuming. Note, however, all entangling contrasts involve three-letter words.

For example, suppose we are interested in estimating R_L, R_Q, S_L, S_Q, T_L, T_Q, R_LS_L and R_LT_L, and hypothesize that $\mu = 0$. Suppose further that we have some prior estimate of σ^2 and that we are interested in considering designs W_1, W_2 and W_3 as possible experimental designs. Then the normal matrices for W_1, W_2 and W_3 are respectively:

$$\begin{pmatrix} 6 & 0 & 0 & 0 & 0 & 0 & 0 & 0 \\ 0 & 18 & 0 & 0 & 0 & 0 & 0 & 0 \\ 0 & 0 & 6 & 0 & 0 & 0 & 0 & -3 \\ 0 & 0 & 0 & 18 & 0 & 0 & 0 & -3 \\ 0 & 0 & 0 & 0 & 6 & 0 & -3 & 0 \\ 0 & 0 & 0 & 0 & 0 & 18 & 3 & 0 \\ 0 & 0 & 0 & 0 & -3 & 3 & 4 & 1 \\ 0 & 0 & -3 & -3 & 0 & 0 & 1 & 4 \end{pmatrix}, \quad \begin{pmatrix} 6 & 0 & 0 & 0 & 0 & 0 & 0 & 0 \\ 0 & 18 & 0 & 0 & 0 & 0 & 0 & 0 \\ 0 & 0 & 6 & 0 & 0 & 0 & 0 & 3 \\ 0 & 0 & 0 & 18 & 0 & 0 & 0 & -3 \\ 0 & 0 & 0 & 0 & 6 & 0 & 3 & 0 \\ 0 & 0 & 0 & 0 & 0 & 18 & 3 & 0 \\ 0 & 0 & 0 & 0 & 3 & 3 & 4 & 1 \\ 0 & 0 & 3 & -3 & 0 & 0 & 1 & 4 \end{pmatrix}$$

and

$$\begin{pmatrix} 6 & 0 & 0 & 0 & 0 & 0 & 0 & 0 \\ 0 & 18 & 0 & 0 & 0 & 0 & 0 & 0 \\ 0 & 0 & 6 & 0 & 0 & 0 & 0 & 0 \\ 0 & 0 & 0 & 18 & 0 & 0 & 0 & 6 \\ 0 & 0 & 0 & 0 & 6 & 0 & 0 & 0 \\ 0 & 0 & 0 & 0 & 0 & 18 & -6 & 0 \\ 0 & 0 & 0 & 0 & 0 & -6 & 4 & -2 \\ 0 & 0 & 0 & 6 & 0 & 0 & -2 & 4 \end{pmatrix},$$

where the ordering of the cross-product terms corresponds to the order of the listing of the desired effects above. Two examples of the calculations required for the normal matrix are:

$$\text{i)}\ (R_L S_L\ ,\ R_L S_L) = X_{R_L^2 S_L^2} = (2/3)X_{S_L^2} + (1/3)X_{R_Q S_L^2}$$

$$= (4/9)X_{\mu} + (2/9)X_{R_Q} + (2/9)X_{S_Q} + (1/9)X_{R_Q S_Q}\ ,$$

$$\text{ii)}\ (R_L S_L\ ,\ R_L T_L) = X_{R_L^2 S_L T_L} = (2/3)X_{S_L T_L} + (1/3)X_{R_Q S_L T_L}\ .$$

Hence, for all three designs we find, since $X_{\mu} = 9$, that

$$(R_L S_L,\ R_L S_L) = (4/9) \cdot 9 + 0 + 0 + 0 = 4\ .$$

Moreover, for W_1 and W_2,

$$(R_L S_L\ ,\ R_L T_L) = 0 + (1/3) \cdot 3 = 1\ ,$$

whereas for W_3

$$(R_L S_L\ ,\ R_L T_L) = 0 + (1/3) \cdot (-6) = -2\ .$$

A criterion for differentiating among a group of designs utilizing a given number of treatment combinations, none of which is completely orthogonal with respect to a desired set of effect estimates has been discussed by Webb [8]. He proposes that the design which has the smallest determinant of the covariance matrix might be optimal. This is equivalent to choosing the design which maximizes the determinant of

the normal matrix, and minimizes the volume of the confidence ellipsoid on the parameters estimated [6].

The values of the determinants of the normal matrix for W_1, W_2 and W_3 are $3^{10}2^6$, $3^{10}2^6$ and 0. By methods discussed earlier, one can easily localize the linear dependency in design W_3 to the subset $(X_{S_Q}, X_{R_LT_L}, X_{R_LS_L}, X_{T_Q})$. In fact it is easily verified that for W_3,

$$X_{S_Q} = 3X_{R_LT_L} + 3X_{R_LS_L} + X_{T_Q} .$$

We might define a measure of the relative efficiency in general of a design D_1 to a design D_2 with respect to a particular desired set of effect to be

$$\frac{\det(\text{normal matrix for } D_1)}{\det(\text{normal matrix for } D_2)} \times 100\% .$$

In our consideration of W_1, W_2 and W_3 for the particular desired set of effects, we would eliminate W_3 because of the linear dependency. Then, the efficiency of W_1 relative to W_2 is 100%, so that they are equally desirable according to our criterion.

10. DETERMINING DEFINING CONTRASTS IN A 2^{n-p} DESIGN.

The 2^{n-p} series of fractionated equal frequency designs (as opposed, for example, to designs of proportional frequency presented by Addelman [1]) deserves special consideration. In this case, as we have already pointed out, the concept of an entangling contrast reduces to that of a defining contrast. Thus, the procedure presented for finding the set of entangling contrasts will yield the set of defining contrasts in a standard 2^{n-p} design. Gorman [5] observed this fact previously and independently of this work. Solely for purposes of illustration, we consider the following 2^{3-2} design:

Factor:	A	B	C
Run 1	0	0	1
Run 2	1	1	0

The procedure presented then is:

A	B	C	0	I	II	III	Defining contrast
0	0	0	0	1	1	2	Total
0	0	1	1	0	1	0	C
0	1	0	0	0	1	0	B
0	1	1	0	1	-1	-2	BC
1	0	0	0	1	-1	0	A
1	0	1	0	0	1	-2	AC
1	1	0	1	0	-1	2	AB
1	1	1	0	-1	-1	0	ABC

Thus, the set of defining contrasts is:

$$I = -BC = -AC = AB \ ,$$

where the sign of the defining contrast is also determined by the last column of the algorithm.

11. DETERMINING THE SET OF TREATMENT COMBINATIONS IN A 2^{n-p} DESIGN. Frequently one knows the set of defining contrasts for a chosen 2^{n-p} factorial design and desires to know which treatment combinations form the desired fractional factorial. Begin with the column of effects for a full 2^n design, where the dummy effect column contains a plus or minus one next to those desired defining contrasts and zeros elsewhere. The sign of each one is determined by the sign of the corresponding defining contrast. The result of an application of algorithm II is usually a set of fitted values for the complete 2^n design; for our

purpose, the non-zero "fitted values" correspond to runs contained in the desired 2^{n-p} design. This procedure is illustrated below:

Suppose I = -BC = -AC = AB; then ,

Defining contrast	0	0 inverted	I	II	III	III inverted	Treatment A	B	C
Total	1	0	1	0	0	0	0	0	0
C	0	1	-1	0	4	4	0	0	1
B	0	-1	-1	2	0	0	0	1	0
BC	-1	0	1	2	0	0	0	1	1
A	0	-1	1	-2	0	0	1	0	0
AC	-1	0	1	2	0	0	1	0	1
AB	1	0	1	0	4	4	1	1	0
ABC	0	1	1	0	0	0	1	1	1

We thus find that the runs for this particular fraction are:

	A	B	C
Run 1	0	0	1
Run 2	1	1	0

as we knew to be the case.

This procedure can be justified by remembering that algorithms I and II perform inverse operations. Hence, the validity of the above procedure follows from the validity of the procedure presented in section 10.

12. ACKNOWLEDGEMENTS. I am deeply indebted to C. Daniel for his suggestions and encouragement to write this paper. I also wish to thank J. Weinstein for the fruitful discussions we had while I was at Ft. Monmouth, and to express my gratitude to Professor W. G. Cochran for his thorough reading of the final draft of this paper.

REFERENCES

1. Addelman, S., "Orthogonal Main-Effect Plans for Asymmetrical Factorial Experiments". Technometrics, 4(1962), 21-46.

2. Cochran, W. G., and Cox, G., Experimental Designs. Second Edition. New York: Wiley, 1957.

3. Daniel, C., "Use of Half-Normal Plots in Interpreting Factorial Two-Level Experiments". Technometrics, 1(1959), 311-341.

4. Davies, O. L., Editor, Design and Analysis of Industrial Experiments. Second Edition. London, England: Oliver and Boyd, 1958.

5. Gorman, J. W., communicated via C. Daniel.

6. Mood, A. M., "On Hotelling's Weighing Problem". Annals Math. Stat., 17(1946), 432-446.

7. Yates, F., The Design and Analysis of Factorial Experiments. Harpenden, England: Imperial Bureau of Soil Science, 1937.

8. Webb, S., "Design, Testing and Estimation in Complex Experimentation: Part I. Expansible and Contractible Factorial Designs and the Application of Linear Programming to Combinatorial Problems". Aerospace Research Labs. Techn. Doc. 65-116 (1965).

CONSTRUCTION AND COMPARISON OF NON-ORTHOGONAL INCOMPLETE FACTORIAL DESIGNS*

Steve Webb
Rocketdyne, A Division of North American Aviation, Inc.

ABSTRACT. Experience in industrial consulting indicates that the requirements of a real test plan often differ from the textbook examples in the number of levels of the factors, the interactions which can be ignored, and the number of runs in the experiment.. The statistical consultant must either convince the experimenter to compromise his original goals, or develop an ad hoc design based on existing designs and the former's intuition.

This paper is concerned with methods for constructing such designs and criteria for comparing alternatives. Various construction techniques are illustrated by examples. Two criteria are developed, and a convenient computer routine for evaluating them is described. Examples of designs are given which were constructed for actual experimental situations.

INTRODUCTION AND SUMMARY. Very often in industrial research an experimental program must be planned for which existing fractional factorial designs are inadequate. The most common reasons for this inadequancy are

1) the available designs contain too many runs,

2) the factors to be evaluated in the experiment do not all appear at the same numbers of levels, and

3) the particular set of interactions which cannot be ignored in the analysis of the experimental results does not appear in any of the published designs.

In such cases the consulting statistician may have a tendency to try and alter the thinking of the experimenter so that one of the standard published designs can be used. This is, of course, undesirable from

*Research sponsored by the Aerospace Research Laboratories, Office of Aerospace Research United States Air Force, under Contract AF33 (615)-2818, monitored by Dr. H. Leon Harter.

the experimenter's point of view and increases the probability that the design will not be carried out as originally planned. As an alternative, the statistician is faced with the problem of developing an ad hoc test plan which satisfies the actual objectives and constraints of the real situation. Using his intuition supplemented by a meager amount of theory he must come up with a design with satisfactory statistical properties.

CRITERIA FOR COMPARING DESIGNS. The response from an experiment will be denoted by the N-component vector Y, and its expected value by $EY = X\beta$, where β is a p-component vector of parameters. Generally speaking, a good design will have low parameter-estimate variances, which are proportional to the diagonal elements of $(X'X)^{-1}$. For a given experimental situation, that is, specification of the number of factors, numbers of levels for each factor, and the interactions to be estimated, a particular finite set of designs is available. In case one of these designs leads to the minimization of the variance of each estimate, then there is no selection problem. This does not often happen, however, except for fractional factorials with all factors at two levels.

In rare cases the relative importance of the parameters to be estimated may be known quantitatively well enough in advance so that a realistic criterion can be established based on the variances. This would usually take the form of a weighted average of the variances. Most often, however, the relative importance of estimating the parameters with low variances will depend on their as yet unknown values.

A criterion for selecting the design often proposed is the generalized variance, defined as the determinant of $(X'X)^{-1}$. A confidence set for the parameters is the set for which $(\beta-\hat{\beta})'(X'X)(\beta-\hat{\beta}) \leq K$. The volumn of this ellipsiod is

$$V = \frac{2\pi^{\frac{1}{2}p} K^{\frac{1}{2}p}}{p\Gamma(\frac{1}{2}p)\sqrt{\det(X'X)}} ,$$

which is seen to be related to the design only through the determinant of the cross-product matrix. It is convenient to consider the determinant in the form of an index, called the estimation index, defined by

$$I_E = \det(X'X)/(N^p \Pi_{i=1}^p w_i) \quad .$$

The weights w_i are defined as follows. Let Z be the coefficient matrix associated with the full factorial; that is, if Y^* were a vector of response for a full factorial then $EY^* = Z\theta$. (The standard parameterization is such that $Z'Z$ is a diagonal matrix.) Let d_i represent the i-th diagonal entry of $Z'Z$ and let M represent the total number of runs in the full factorial. Then $w_i = d_i/M$.

Often the purpose of an experiment is to obtain overall information about the response. In these cases the appropriate criterion is based on the average variance of a fitted response, where the average is taken over all M points of the full factorial. The average variance is proportional to $\Sigma w_i V_i$, where the V_i are the diagonal elements of $(X'X)^{-1}$. A convenient representation is through the "fitting index"

$$I_F = p/(N\Sigma_{i=1}^p w_i V_i) \quad .$$

More generally, an index could be based on the integrated variance of a fitted response. Such an index would in general involve off-diagonal elements of $(X'X)^{-1}$, and would be difficult to define in a way which is general enough for both quantitative and qualitative factors. Experience has showed I_F to be a very useful index.

Consider the class of models which is "complete" in the sense that if any interactions between a pair of factors appear in the model, then all interactions between them appear. It has been proved [1] that for models which are complete in this sense, the maximum value of both I_E and I_F is unity. In [2] it is shown that the maximum is achieved if certain combinations of levels appear with equal frequency. An equivalent criterion is that the cross-product matrix X'X is proportional to the cross-product matrix Z'Z for the full factorial. All

regular fractional factorials have this property. If interaction parameters do not appear in complete sets, either or both indices may be greater than unity.

Thus far nothing has been said about the parameterization used to describe the response, that is, how β is defined in terms of the expected responses at the various treatment combinations, or equivalently, how the elements of the X matrix are defined. Since the parameterization is to a large extent arbitrary, a particularly appealing property of the two indices is that they are invariant under nonsingular reparameterizations. That is, suppose $EY = X\beta = XA\alpha$, and similarly $EY^* = Z\beta = XA\alpha$, where A is nonsingular. It can be demonstrated that I_F and I_E are identical whether calculated under the parameterization β or α. Thus, the parameterization is immaterial as far as these criteria are concerned.

Without the use of electronic computers, the computation of the indices would be extremely tedious. A computer code has been written for routine and convenient comparison of alternative incomplete factorial designs. A detailed description of this code and its use is available [3]. Any number of designs may be evaluated simultaneously by reading in to the computer the treatment combinations in each. The evaluation will be made for up to five models (specification of interaction terms to be included in the model). A number of options is available to the user, including changing the parameterization used for two-, three-, or four-level factors, or changing the weights used in computing the indices. A Fortran listing is included in reference [3].

METHODS OF CONSTRUCTION.

1. Exhaustive Enumeration. For a few simple experimental situations it is feasible to enumerate all possible designs. The optimum design can then easily be chosen. As an example, consider as an experimental situation a 2^3 in 5 runs with no interactions. There are exactly eleven nonsingular designs, which together with their properties are given in Table I. Clearly, the best designs are the eighth and ninth, for which each variance is minimized.

2. One Parameter at a Time. It is always possible to construct a saturated design (although they are very inefficient) by allocating one run to the estimation of each parameter. For example, a $3^2 \times 2^2$ with

EXHAUSTIVE ENUMERATION OF 2 CUBED IN 5 RUNS

PARAMETER	1ST DESIGN	2ND DESIGN	3RD DESIGN	4TH DESIGN	5TH DESIGN	6TH DESIGN
MEAN	0.875000	0.500000	0.875000	0.375000	0.500000	0.375000
A1	0.375000	0.375000	0.500000	0.875000	0.875000	0.500000
B1	0.375000	0.500000	0.500000	0.375000	0.500000	0.500000
C1	0.375000	0.375000	0.375000	0.375000	0.375000	0.375000
ESTIMATION INDEX	0.204800	0.204800	0.204800	0.204800	0.204800	0.204800
FITTING INDEX	0.400000	0.457143	0.355556	0.400000	0.355556	0.457143
N	5	5	5	5	5	5
DESIGNS	1) 0 0 0 2) 0 0 0 3) 0 0 1 4) 0 1 0 5) 1 0 0	1) 0 0 0 2) 0 0 0 3) 0 0 1 4) 0 1 1 5) 1 0 0	1) 0 0 0 2) 0 0 1 3) 0 0 1 4) 0 1 0 5) 1 0 0	1) 0 0 0 2) 0 0 0 3) 0 0 1 4) 0 1 0 5) 1 1 1	1) 0 0 0 2) 0 0 0 3) 0 0 1 4) 0 1 1 5) 1 1 0	1) 0 0 0 2) 0 0 1 3) 0 0 1 4) 0 1 0 5) 1 1 0

TABLE I

TABLE I (Continued)

EXHAUSTIVE ENUMERATION OF 2 CUBED IN 5 RUNS

PARAMETER	1ST DESIGN	2ND DESIGN	3RD DESIGN	4TH DESIGN	5TH DESIGN
MEAN	0.437500	0.218750	0.218750	0.250000	0.375000
A1	0.437500	0.218750	0.218750	0.250000	0.500000
B1	0.250000	0.218750	0.218750	0.437500	0.500000
C1	0.250000	0.218750	0.218750	0.437500	0.875000
ESTIMATION INDEX	0.409600	0.819200	0.819200	0.409600	0.204800
FITTING INDEX	0.581818	0.914286	0.914286	0.581818	0.355556
N	5	5	5	5	5
DESIGNS	1) 0 0 0 2) 0 0 1 3) 0 1 0 4) 0 1 1 5) 1 0 0	1) 0 0 0 2) 0 0 0 3) 0 1 1 4) 1 0 1 5) 1 1 0	1) 0 0 0 2) 0 0 1 3) 0 1 0 4) 1 0 0 5) 1 1 1	1) 0 0 0 2) 0 0 1 3) 0 1 0 4) 1 0 1 5) 1 1 0	1) 0 0 1 2) 0 0 1 3) 0 1 0 4) 1 0 0 5) 1 1 0

the linear-by-linear interaction between the two three-level factors is as follows

0 0 0 0	mean
1 0 0 0	effect of first factor
2 0 0 0	
0 1 0 0	effects of second factor
0 2 0 0	
2 2 0 0	interaction
0 0 1 0	effect of third factor
0 0 0 1	effect of fourth factor ,

where we have indicated the parameter estimated from each run. The fitting and estimation indices are .24 and .025, respectively.

3. Correspondence. The theory for mixed factorial designs is less well developed than that for designs in which all factors appear at the same number of levels. A useful technique is to construct a design with all factors at the same number of levels, then replace some of the factors with ones of real interest using a fixed correspondence between sets of levels. The best-known examples of this technique are the proportional-frequency designs of Addelman [4]. To demonstrate this approach consider a Latin Square of side 3.

0	0	0	0
0	1	1	1
0	2	2	2
1	0	1	2
1	1	2	0
1	2	0	1
2	0	2	1
2	1	0	2
2	2	1	0 .

The last two factors may be replaced by two-level factors by using the correspondence

$$0 \rightarrow 0$$
$$1 \rightarrow 1$$
$$2 \leftarrow 1 \quad ,$$

which results in the design

$$\begin{array}{cccc} 0 & 0 & 0 & 0 \\ 0 & 1 & 1 & 1 \\ 0 & 2 & 1 & 1 \\ 1 & 0 & 1 & 1 \\ 1 & 1 & 1 & 0 \\ 1 & 2 & 0 & 1 \\ 2 & 0 & 1 & 1 \\ 2 & 1 & 0 & 1 \\ 2 & 2 & 1 & 0 \end{array} \quad .$$

This design is quite efficient, having a fitting index of .93 and an estimation index of .79. A number of different types of correspondences is given by Addelman in [4].

4. Permutation-Invariant Designs. The salient property of permutation-invariant designs, defined in [5], is that estimates involving factors which appear at the same number of levels have the same variance properties. More formally, the cross-product matrix $X'X$ remains unaltered if factors appearing at the same number of levels are permuted. An example of a $3^2 \times 2^3$ main effect design, for which $I_F = .80$ and $I_E = .47$, is:

$$\begin{array}{ccccc} 0 & 0 & 1 & 0 & 0 \\ 0 & 1 & 0 & 0 & 1 \\ 0 & 2 & 0 & 1 & 0 \\ 1 & 0 & 0 & 0 & 0 \\ 1 & 1 & 1 & 1 & 1 \\ 1 & 2 & 1 & 1 & 1 \\ 2 & 0 & 0 & 1 & 1 \\ 2 & 1 & 1 & 1 & 0 \\ 2 & 2 & 1 & 0 & 1 \end{array} \quad .$$

Using a standard parameterization, the X and $X'X$ matrices for this design are:

$$X = \begin{bmatrix} 1 & -1 & -1 & 1 & 1 & 1 & -1 & -1 \\ 1 & -1 & 0 & 1 & -2 & -1 & -1 & 1 \\ 1 & -1 & 1 & 1 & 1 & -1 & 1 & -1 \\ 1 & 0 & -1 & -2 & 1 & -1 & -1 & -1 \\ 1 & 0 & 0 & -2 & -2 & 1 & 1 & 1 \\ 1 & 0 & 1 & -2 & 1 & 1 & 1 & 1 \\ 1 & 1 & -1 & 1 & 1 & -1 & 1 & 1 \\ 1 & 1 & 0 & 1 & -2 & 1 & 1 & -1 \\ 1 & 1 & 1 & 1 & 1 & 1 & -1 & 1 \end{bmatrix}, \quad (X'X) = \begin{bmatrix} 9 & 0 & 0 & 0 & 0 & 1 & 1 & 1 \\ 0 & 6 & 0 & 0 & 0 & 2 & 2 & 2 \\ 0 & 0 & 6 & 0 & 0 & 2 & 2 & 2 \\ 0 & 0 & 0 & 18 & 0 & -2 & -2 & -2 \\ 0 & 0 & 0 & 0 & 18 & -2 & -2 & -2 \\ 1 & 2 & 2 & -2 & -2 & 9 & 1 & 1 \\ 1 & 2 & 2 & -2 & -2 & 1 & 9 & 1 \\ 1 & 2 & 2 & -2 & -2 & 1 & 1 & 9 \end{bmatrix}.$$

Permutation of factors appearing at the same numbers of levels has the effect of permuting rows and columns of the submatrices in the partitioned cross-product matrix. Since the submatrices are invariant, the design is permutation-invariant.

This principle has been used* to construct a series of as yet unpublished saturated second-order designs for three-level factors. For five factors the design contains the treatment combination 0 0 0 0 0, the five treatment combinations which are permutations of 1 1 1 1 0, the five permutations of 2 2 2 2 0, and the ten permutations of 2 2 0 0 0. For this design the fitting index is .66 and the estimation index is 2.35. Relative to the full factorial but adjusting for the difference in the number of runs, the efficiency of the estimate off the mean is 82%, of the linear main effects is 114%, of the quadratic main effects if 25%, and of the linear by linear interactions is 171%. The reason that the linear effects and interactions are so efficient is that the points of the design tend to be concentrated around the outside of the hypercube.

5. Balancing Levels. A very useful technique for constructing designs is to start with an ordinary factorial structure for the first group of factors, and then insert the remaing factors in such a way that pairs of levels appear together with nearly equal frequencies. For example, the following two designs are obtained by adding another two-level factor to a basic 2x3 full factorial:

*This work was carried out by R. L. Rechtschaffner of Rocketdyne's Statistical Test Design Unit.

Design 1	Design 2
0 0 0	0 0 0
0 1 1	0 1 1
1 0 1	1 0 1
1 1 0	1 1 1
2 0 0	2 0 1
2 1 1	2 1 0

There variance properties are given in Table II.

EXAMPLES. Three ad hoc designs which have been used successfully at Rocketdyne will be mentioned briefly. The first involved determination of char formation rate in ablative heat-shield material under simulated reentry conditions. The testing was done in a small stationary hydrogen-oxygen rocket engine. The experimental variables were rocket engine combustion chamber pressure, propellant mixture ratio, and the angle of the sample in the rocket exhaust. The experimental design chosen was one of the optimum 2^3 designs in 5 runs discussed earlier.

Run Number	Target Chamber Pressure (Psia)	Target Mixture Ratio	Inclination Angle (degrees)
1	170	4	0
2	250	4	$12\frac{1}{2}$
3	170	16	$12\frac{1}{2}$
4	250	16	0
5	250	16	$12\frac{1}{2}$

Another such design was used on a Signal Corps battery program. The experimental work involved screening 4 cathode materials, 3 solvents, and 4 salts. The design was constructed by balancing the levels of the second four-level factor within the framework of the 12-run 3 x 4 factorial.

3x2x2 'BALANCED' DESIGNS

PARAMETER	1ST DESIGN	2ND DESIGN
MEAN	0.166667	0.194444
A1	0.250000	0.250000
A2	0.083333	0.111111
B1	0.187500	0.166667
C1	0.187500	0.250000
ESTIMATION INDEX	0.888889	0.666667
FITTING INDEX	0.952381	0.833333
N	6	6

TABLE II

Run Number	Cathode	Solvent	Salt
1	0	0	0
2	0	1	1
3	0	2	3
4	1	0	1
5	1	1	0
6	1	2	2
7	2	0	2
8	2	1	3
9	2	2	1
10	3	0	3
11	3	1	2
12	3	2	0

Although there was no justification for assuming interactions did not exist, they could reasonably be expected to be less important than main effects. It was intended that this experiment be used to eliminate from contention some of the candidate materials with just a few tests, so that later tests could concentrate on the better ones. The actual decision made from these tests was that none of the four cathode materials was satisfactory, and later testing should be directed at finding additional materials. If all interactions had been considered, 48 tests, using these four unsatisfactory materials, would be required.

The balancing technique was used effectively to construct a $3^4 \times 2^3$ design in 27 runs for a program concerned with the valuation of fiber-reinforced plastic laminates. The variables are as follows:

Variable	Code	Levels
Bonding Pressure	A	3
Bonding Temperature	B	3
Resin Concentration	C	3
Post-Cure Temperature	D	3
Bonding Time	E	2
Post-Cure Time	F	2
Fiber Quality	G	2

DESIGN NUMBER 1	DESIGN NUMBER 2	DESIGN NUMBER 3	DESIGN NUMBER 4	DESIGN NUMBER 5
1) 0 0 0 0 0 0 0 0	1) 0 0 0 0 0 0 0	1) 0 0 0 0 0 0 0	1) 0 0 0 0 0 0 0	1) 0 0 0 0 0 0 0
2) 0 0 1 2 1 1 1	2) 0 0 1 2 0 0 1	2) 0 0 1 2 1 0 0	2) 0 0 1 2 1 0 0	2) 0 0 1 1 1 1 1
3) 0 0 2 1 0 0 0	3) 0 0 2 1 1 1 0	3) 0 0 2 1 0 1 0	3) 0 0 2 1 0 1 0	3) 0 0 2 2 1 0 0
4) 0 1 0 2 1 0 1	4) 0 1 0 2 1 1 1	4) 0 1 0 2 1 0 0	4) 0 1 0 2 1 0 0	4) 0 1 0 2 1 0 1
5) 0 1 1 1 0 0 1	5) 0 1 1 1 0 0 1	5) 0 1 1 1 1 1 0	5) 0 1 1 1 1 1 0	5) 0 1 1 0 0 0 1
6) 0 1 2 0 1 0 1	6) 0 1 2 0 1 1 1	6) 0 1 2 0 1 1 1	6) 0 1 2 0 1 1 1	6) 0 1 2 1 1 1 0
7) 0 2 0 1 1 1 0	7) 0 2 0 1 0 0 0	7) 0 2 0 1 0 1 0	7) 0 2 0 1 0 1 0	7) 0 2 0 1 1 1 1
8) 0 2 1 0 1 1 1	8) 0 2 1 0 1 0 1	8) 0 2 1 0 1 1 1	8) 0 2 1 0 1 1 1	8) 0 2 1 2 0 1 1
9) 0 2 2 2 0 1 0	9) 0 2 2 2 0 1 0	9) 0 2 2 2 0 0 1	9) 0 2 2 2 0 0 1	9) 0 2 2 0 0 1 0
10) 1 0 0 2 0 0 1	10) 1 0 0 2 1 0 1	10) 1 0 0 2 1 0 0	10) 1 0 0 2 1 0 0	10) 1 0 0 2 1 1 1
11) 1 0 1 1 0 0 1	11) 1 0 1 1 0 1 1	11) 1 0 1 1 1 1 0	11) 1 0 1 1 1 1 0	11) 1 0 1 0 0 1 1
12) 1 0 2 0 1 0 1	12) 1 0 2 0 0 1 1	12) 1 0 2 0 1 1 1	12) 1 0 2 0 1 1 1	12) 1 0 2 1 0 1 0
13) 1 1 0 1 0 1 1	13) 1 1 0 1 0 0 1	13) 1 1 0 1 1 1 0	13) 1 1 0 1 1 1 0	13) 1 1 0 1 0 0 0
14) 1 1 1 0 1 1 0	14) 1 1 1 0 1 1 0	14) 1 1 1 0 0 0 0	14) 1 1 1 0 0 0 0	14) 1 1 1 2 1 1 1
15) 1 1 2 2 0 1 0	15) 1 1 2 2 1 0 0	15) 1 1 2 2 1 0 1	15) 1 1 2 2 1 0 1	15) 1 1 2 0 1 0 0
16) 1 2 0 0 0 1 1	16) 1 2 0 0 1 0 1	16) 1 2 0 0 1 1 1	16) 1 2 0 0 1 1 1	16) 1 2 0 0 1 0 1
17) 1 2 1 2 1 0 0	17) 1 2 1 2 0 1 0	17) 1 2 1 2 1 0 1	17) 1 2 1 2 1 0 1	17) 1 2 1 1 0 0 1
18) 1 2 2 1 0 0 0	18) 1 2 2 1 0 1 1	18) 1 2 2 1 0 1 1	18) 1 2 2 1 0 1 1	18) 1 2 2 2 1 1 0
19) 2 0 0 1 1 1 0	19) 2 0 0 1 1 1 0	19) 2 0 0 1 0 1 0	19) 2 0 0 1 0 1 0	19) 2 0 0 1 1 0 1
20) 2 0 1 0 1 1 1	20) 2 0 1 0 0 1 1	20) 2 0 1 0 1 1 1	20) 2 0 1 0 1 1 1	20) 2 0 1 2 0 0 1
21) 2 0 2 2 0 1 0	21) 2 0 2 2 1 1 0	21) 2 0 2 2 0 0 1	21) 2 0 2 2 0 0 1	21) 2 0 2 0 1 1 0
22) 2 1 0 0 0 1 1	22) 2 1 0 0 1 1 1	22) 2 1 0 0 1 1 1	22) 2 1 0 0 1 1 1	22) 2 1 0 0 1 1 1
23) 2 1 1 2 1 0 0	23) 2 1 1 2 1 0 0	23) 2 1 1 2 1 0 1	23) 2 1 1 2 1 0 1	23) 2 1 1 1 0 1 1
24) 2 1 2 1 0 1 1	24) 2 1 2 1 1 0 0	24) 2 1 2 1 0 1 1	24) 2 1 2 1 0 1 1	24) 2 1 2 2 0 1 0
25) 2 2 0 2 1 1 0	25) 2 2 0 2 0 1 0	25) 2 2 0 2 0 0 1	25) 2 2 0 2 0 0 1	25) 2 2 0 2 0 0 0
26) 2 2 1 1 1 0 0	26) 2 2 1 1 0 0 0	26) 2 2 1 1 0 1 1	26) 2 2 1 1 0 1 1	26) 2 2 1 0 1 1 1
27) 2 2 2 0 1 0 1	27) 2 2 2 0 1 0 1	27) 2 2 2 0 0 0 0	27) 2 2 2 0 0 0 0	27) 2 2 2 1 1 0 0

3X3X3X3X2X2X2 IN 27 RUNS.

PARAMETER	1ST DESIGN	2ND DESIGN	3RD DESIGN	4TH DESIGN	5TH DESIGN
MEAN	0.040023	0.038683	**********	**********	0.039227
A1	0.065645	0.066797	0.101365	0.101365	0.060946
A2	0.023191	0.021691	0.045917	0.045917	0.024405
B1	0.068331	0.144732	0.101365	0.101365	0.057834
B2	0.021630	0.033605	0.043643	0.043643	0.019690
C1	0.101666	0.071088	0.101365	0.101365	0.196730
C2	0.030675	0.026362	0.045917	0.045917	0.100966
D1	0.068076	0.136054	**********	**********	0.060441
D2	0.021945	0.034868	**********	**********	0.018519
E1	0.065291	0.067670	0.535088	0.535088	0.081871
F1	0.077900	0.094148	**********	**********	0.046593
G1	0.052820	0.071160	0.367325	0.367325	0.293654
A1B1	0.147604	0.095345	0.186404	0.186404	0.177751
A1C1	0.095526	0.146515	0.175439	0.175439	0.115574
B1C1	0.102529	0.089120	0.186404	0.186404	0.093785
B1E1	0.090778	0.287987	0.078947	0.078947	0.080452
D1F1	0.139308	0.166098	**********	**********	0.094064
ESTIMATOR INDEX	0.070734	0.022297	0.000000	0.000000	0.036923
FITTING INDEX	0.669524	0.510378	0.000000	0.000000	0.480730
N	27	27	27	27	27

It was established that the linear interactions AB, AC, BC, BE, and DF are expected to be important. Since the factor D does not interact with the other three three-level factors, the starting point was a 1/3 replicate of a 3^4 using as defining contrast $I = A^2 B^2 C^2 D$. For the 2^3 part of the design three replications of the 2^3 plus three additional points were used. The 2^3 part was associated with the 3^4 part a number of ways, and the best design selected. The third and fourth designs were singular. The first, and best, design in presently being implemented.

REFERENCES

[1] Webb, S. R. (1964). Otimality properties of orthogonal designs. Presented at the annual meeting of the American Statistical Association, Chicago. (Appendix C of ARL 65-116, Part I.)

[2] Webb, S. R. (1964). Orthogonal incomplete factorial designs and their construction using linear programming. Research Report RR 64-20, Rocketdyne, Canoga Park. (Appendix A of ARL 65-116, Part I.)

[3] Webb, S. R. and Galley, S. W. (1965). A computer routine for evaluating incomplete factorial designs. Technical Documentary Report ARL 65-116, Part IV, Aerospace Research Laboratories, Wright-Patterson Air Force Base.

[4] Addelman, S. (1962). Orthogonal main-effect plans for asymmetrical factorial experiments. Technometrics 4, 21-46.

[5] Webb, S. R. (1964). Characterization of non-orthogonal incomplete factorial designs. Research Report RR 64-18, Rocketdyne, Canoga Park. (Appendix B of ARL 65-116, Part I.)

STATISTICAL ANALYSIS OF AUTOMATICALLY RECORDED PHYSIOGRAPH DATA

J. C. Atkinson
Directorate of Medical Research, CRDL,
Edgewood Arsenal, Maryland

The Directorate of Medical Research, CRDL, Edgewood Arsenal, Maryland has the mission of investigating the physiological effects of certain chemical substances on both human and animal subjects. One of the machines used to measure these effects is a physiograph. This machine which is commonly used in hospitals measures temperature, pulse, breathing rate and both systolic and diastolic blood pressure.

The common hospital versions displays the information only, however, in our scientific work a permanent recording was desired so an analog to digital converter and a punch paper tape output was installed on a unit by the manufacturer, Air Shields of Hatboro, Pennsylvania. Originally a flexowriter was used for the output device; later, a Frieden SP-2 tape punch was substituted to reduce noise.

This machine can be used on both human and animal subjects. It was first used by our Clinical Division with humans. It was shut down for some months when difficulties were encountered with the sensors picking up the signal from the subject. Later with better sensors it was put to use again this time with dogs. The speed of recording can be adjusted. So far we have run at a rate where a complete set of 5 measurements are recorded every 5 seconds. Lower rates are possible and in many cases desirable particularly where changes occur only gradually.

When the paper tape is received by the computer section what is seen is a series of 4 digit numbers followed by a stop code where every 5th number is of the same kind. The numbers are first checked by the computer for magnitude. For human's temperature is assumed to be at least 90, pulse 50, breathing 5, systolic blood pressure 50, and diastolic 20. If all readings are at least as large as those above, the readings are reduced by the above for internal computations. Otherwise, an error stop occurs. It is felt that if the physiograph ever gets out of sequence the above checks would bring it to a rapid halt since, for instance, reading breathing rate for blood pressure would bring an error halt.

After reading a predetermined number of enteries, or from a signal on the input tape, computations are begun. The mean, 95% confidence limits, standard error and coefficient of variations are computed for each of the 5 types of measurements together with all ten 2 factor correlation coefficients.

It is hoped that the mean values and their standard errors will indicate longer term effects of the chemical. For instance, significant changes might be shown to occur from 1 to 4 hours after administration, and apparent recovery thereafter. The correlations are hoped to show up more subtle changes. For instance a negative correlation between pulse and blood pressure is considered abnormal.

Unfortunately the change from a flexowriter to an SP-2 punch output took longer than anticipated and to date we have only data from early human runs with inaccurate sensors but no drug runs. It is hoped that dog drug runs will start this month. An output from a test run is shown as Figure 1 to illustrate format.

FIGURE 1

0987*	768*	129*	1010*	610*
986*	743*	141*	1010*	610*
986*	755*	140*	1016*	610*
986*	738*	150*	1016*	615*
986*	739*	165*	1017*	619*
985*	749*	150*	1011*	610*
982*	760*	160*	1009*	610*
983*	770*	149*	1010*	610*
982*	770*	161*	1010*	611*
983*	770*	170*	1008*	610*

F*

	MEAN	95% CONFIDENCE LIMITS		STANDARD ERROR	COEFF OF VARIATION
TEMPERATURE	98.46000	98.32547	98.59453	.06038	.00613
PULSE	75.62000	74.68645	76.55354	.41900	.05540
BREATHING	15.15000	14.25679	16.04321	.40090	.26462
SYSTOLIC	101.17000	100.93699	101.40301	.10458	.01033
DIASTOLIC	61.15000	60.93478	61.36523	.09660	.01579

CORRELATION COEFFICIENT

	PULSE	BREATHING	SYSTOLIC	DIASTOLIC
TEMPERATURE	-.58672	-.64727	.57735	.31997
PULSE		.05096	-.69729	-.63695
BREATHING			-.08100	.35415
SYSTOLIC				.74324

AN APPLICATION OF EXPERIMENTAL DESIGN IN ERGONOMICS: HEART RATE AS A FUNCTION OF WORK STRESS AND TIME

H. B. Tingey* and W. H. Kirby, Jr.
Ballistic Research Laboratories
Aberdeen Proving Ground, Maryland

ABSTRACT: This presentation concerns the establishment of a relationship between heart rate and imposed physical workloads for a given time period for a small group of young males. A hypothesis was developed, experiments designed, data collected under controlled conditions, and the results analyzed using classical statistical methods. The results demonstrate that the underlying functional relationship alters as the stimulus changes. In this case the alterations may be defined over five segments of time.

1. INTRODUCTION. Studies of changes in the human circulation have been made from many points of view. Physiologists and others have long been interested in the effects of physical work on the circulatory system. Many of these studies have used heart rate behavior as an indication of the circulatory system's capacity to respond to physical workloads. Heavy, medium and light workloads have been considered under various environmental conditions of temperature and humidity.

However, to the best of our knowledge, there has been no attempt to study these clinical and physical relationships using more classical statistical procedures in association with pre-experimental hypothesis formulation. The usual approach is to collect large amounts of data, tabulate it and/or plot it on a graph. Then generalized clinical interpretations are made. Occasionally, a statistician is asked to assist in doing something with the data following its collection.

This study was done as an exploratory exercise not only to investigate the possibility of an underlying relationship between heart rate and physical load, but as a means of bringing the engineer, physician, and statistician together on a problem of common interest. We wanted to consider each other's viewpoints in reference to a physical-medical problem. There are also a common interest to employ more scientific method in this area of research.

*Now Assistant Professor of Statistics and Computer Science, University of Delaware, Newark, Delaware.

We all knew that heart rate would increase with physical exertion and decrease following the cessation of it. However, we were interested in knowing the more precise nature of the rise and fall for different degrees of work intensity. As simplifications we decided to hold the work period and environment constant. The physical workloads were chosen in this first study for convenience and measurability.

Our longer range objectives include the development of predictive functions relating more generalized stress situation on the human system using this type of approach. Additional cardiovascular system phenomena which are also of potential interest to other researchers, clinicians, and those concerned with the effects of various forms of stress are being considered. Such phenomena may include, among others, coagulation factors, measure of hypoxia, and biochemical constituents.

2. METHODS.

2.1 Scope and Procedure.

The purpose of this experiment was to assess the reaction of the human heart rate to work stimulation. The conduct of the experiment took the following line.

A method of work was selected which may be described as a form of weight lifting. Preliminary trials were made to determine a set of weights, number of repetitions and frequency which could be accomplished by the five involved subjects. It was decided that available bar-bell weights, namely 21.6 lbs., 26.6 lbs., and 31.6 lbs. would be used. Each bar-bell was to be raised from the chest position to maximum vertical height and lowered with minimum restraint to the starting position. This cycle was repeated 30 times at a timed (metronome) rate of two seconds resulting in approximately one minute of intensive physical activity. The subjects themselves were a non-random sample of available personnel.

A brief physical description of the five subjects who were healthy males is as follows:

No.	Age	Weight	Height
1.	35	175	5'-9"
2.	30	230	6'-4"
3.	44	180	5'-9"
4.	24	135	5'-7"
5.	25	155	5'-9"

The experiment was conducted over three successive days for three successive weeks. Each repetition of the experiment started on Sunday and terminated on Tuesday of the week. On each day the experiment was started at the same time of day and the subjects performed in the same sequence. On the first day the 21.6-lb. weight was used with the 26.6-lb. and 31.6-lb. weights used on the second and third days, respectively. The room was air conditioned and temperature and humidity were essentially constant throughout the investigation.

Five minutes prior to the initiation of the weight-lifting exercise each subject was seated in a chair adjacent to the apparatus. Small patch electrodes had already been positioned on each side of the bare chest at the mid-clavicular line just above the lower costal border for the continuous recording of the electrocardiogram. The recording was accomplished using a telemetering apparatus and commenced immediately after the subject was seated. This first phase which began at -300 seconds terminated at -60 seconds.

The subject then arose, stepped onto the force platform, moved into a predetermined standing position with the forearms against the chest, elbows acutely flexed, and hands positioned to receive the bar-bell from others. At approximately -5 seconds he was handed the bar-bell and at zero seconds he began the exercise, ending with the termination of the 30th. cycle at +60 seconds. Others relieved him of the bar-bell immediately following the cessation of exercise. The subject then stepped down from the platform and sat in a chair resting for the remaining 540 seconds. Then he was removed from the experiment and the continuous monitoring of the electrocardiogram ceased.

This sequence of events led to five time zones to consider for curve fitting, namely, (1) a rest phase with essentially constant heart rate (time: -300 sec. to -60 sec.); (2) a preparation phase with linear increase

in heart rate (time: -60 sec. to -40 sec.); (3) a short recovery phase with linear decrease in heart rate (time: -35 sec. to -5 sec.);* (4) the measured work phase with linear increase (time: actually 0 sec. to 60 sec. but heart rate changes occurred between -5 sec. to 55 sec. - the latter is used); and (5) the recovery phase with exponential decrease (time: 55 sec. to 600 sec.). As mentioned, heart rate was recorded continuously (via telemetered ECGs) and the distance of each lift recorded photographically. Apparatus and measurement equipment are discussed in Section 2.5.

2.2 Hypothesis.

The general hypothesis initially considered expressed heart rate to be some function of workload and time. Symbolically, it was stated, H.R. = f(L,T). One could make the expression more explicit by adding a constant of proportionality and giving both L (measured load) and T (measured time) exponentials. Because of the sequence of events which took place, the initial hypothesis was modified to consider the five time periods during which the individuals were measured. This led us to the following:

H_o: (a) The regression relationship between a workload and heart rate is given over each of the five segments as a function of time.

(1) $H.R. = k$ $\quad k > 0, -300 < t < -120,$

(2) $H.R. = k_1 + \beta t$ $\quad k_1, \beta > 0, -60 < t < -40,$

(3) $H.R. = k_2 + \beta_1 t$ $\quad k_2 > 0, \beta_1 < 0, -35 < t < -5,$

(4) $H.R. = k_3 + \beta_2 t$ $\quad k_3 > 0, \beta_2 > 0, 0 < t < 55,$

(5) $H.R. = k_4 t^{\alpha} e^{-\beta_3 t}$ $\quad k_4 > 0, \alpha > 0, \beta_3 > 0, 60 < t < 600.$

Note: The actual relationship might be specified by a single relationship but more careful planning in the light of this this experiment is required. One might state the overall relationship as:

*One might be led to considering this interval as two segments whereas our original hypothesis was that over a short interval our heart rate decrease could be considered linear.

$$H.R. = Kt^{\alpha} e^{-\beta t^2}$$

(b) The regression relationship between a time and heart rate is given as a function of load:

$$H.R. = \alpha(t) + \beta(t)L \quad .$$

Initially the data are subjected to the analysis of variance for a three-way layout and appropriate tests for the significance of main effects (and the particular intervals over which they are significant) and to detect possible interactions which may be present. The hypothesis tests have followed the standard F-test procedure and are indicated in the ANOVA (Analysis of Variance) Table III.

2.3 Design.

The basic design employed for each replicate of the experiment is a two-way layout using time and theoretical load as controlled variables with heart rate as the response variable. The general formulas are given in Table 1.

TABLE I

General Formulas for Two-Way Layout

Source	SS	df	E(ms)
Time	$SS_t = JK\sum_i (y_{i..} - y_{...})^2$	I-1	$\sigma^2 + JK\sigma_t^2$
Load	$SS = IK\sum_j (y_{i..} - y_{...})^2$	J-1	$\sigma^2 + IK\sigma_\ell^2$
Time X Load	$SS_{t\ell} = K\sum_i \sum_j (y_{ij..} - y_{i..} - y_{j..} \cdot y_{...})^2$	(I-1)(J-1)	$\sigma^2 + K\sigma_{t\ell}^2$
Error	$SS_e = \sum_i \sum_j \sum_k (y_{ijk} - y_{ij.})^2$	IJ(K-1)	σ^2
Total	$SS_T = \sum_i \sum_j \sum_k (y_{ijk} - y_{...})^2$	IJK-1	

It is, perhaps more desirable to analyze the data over the three trials of the experiment by introducing another main effect for repetitions of the experiment. Hence the analysis of variance takes on the pattern of a three-way layout with several (say n) observations per cell. The general formulas for this situation are presented in Table II.

The data from the experiment are used according to the formulas in Table II to calculate the results given in Table III. The error sum of squares should indicate the approximate value of the residual error after fitting the regression lines proposed in the original hypothesis. One may, as a matter of interest, test the significance of the mean squares for main effects and interactions. This would then lead the investigator to an analysis to determine the regression which might exist over each of the five intervals.

Additionally, results from the mean squares fitting for the fixed time-load variable and the fixed load-time variable are presented in Tables IV and V.

2.4 Instrumentation and Equipment.

The weights used in this equipment were obtained from a commercially available bar-bell (dumb bell) set, the components of which were weighed to the nearest tenth of a pound. The components were assembled in three combinations to give the test weights of 21.6, 26.6, and 31.6 pounds.

The experiment was conducted on the surface of a force-platform of special design capable of making accurate measurements of forces in the three orthogonal axes and of moments about these three axes. While the platform impulses were measured, discussion concerning them are beyond the scope of this presentation.

Heart rates were obtained from a TELEMEDICS Radio-Electrocardiograph known commercially as the RKG 100 System which is composed of a receiver Model MCM and transmitter Model 100 A. The associated electrodes, as mentioned previously, were positioned in order to minimize muscular noise and prevent premature loosening of them. Very sharp QRS complexes were obtained. The e.c.g. profiles were recorded simultaneously with impulses from the platform on both a Sanborn 8-channel Paper Recording System, Model 858-5460 and a Sanborn-Ampex Magnetic Data Recording System, Model 2007.

TABLE II

General Formulas for Three-Way Layout

Source	SS	df	E(ms)
Time	$SS_t = JKN\Sigma_i(y_{i...} - y_{....})^2$	I-1	$\sigma^2 + JKN\sigma^2_t$
Load	$SS_\ell = IKN\Sigma_j(y_{j...} - y_{....})^2$	J-1	$\sigma^2 + JKN\sigma^2_\ell$
Repetitions	$SS_r = IJN\Sigma_k(y_{..k.} - y_{....})^2$	k-1	$\sigma^2 + IJN\sigma^2_r$
Time X Load	$SS_{t\ell} = KN\Sigma_i\Sigma_j(y_{ij..} - y_{j...} - y_{....})^2$	(I-1)(J-1)	$\sigma^2 + KN\sigma^2_{tx\ell}$
Load X Reps	$SS_{\ell xr} = IN\Sigma_j\Sigma_k(y_{.jk.} - y_{j...} - y_{..k.} - y_{....})^2$	(J-1)(K-1)	$\sigma^2 + IN\sigma^2_{\ell xr}$
Time X Reps	$SS_{txr} = JN\Sigma_i\Sigma_k(y_{i.k.} - y_{i...} - y_{..k.} - y_{....})^2$	(I-1)(K-1)	$\sigma^2 + IN\sigma^2_{txr}$
Time X Load X Reps	$SS_{tx\ell xr} = N\Sigma_i\Sigma_j\Sigma_k(y_{ijk.} - y_{ij..} - y_{i.k.} - y_{.jk.} + y_{i...} + y_{.j..} + y_{..k.} - y_{....})^2$	(I-1)(J-1)(K-1)	$\sigma^2 + N\sigma^2_{tx\ell xr}$
Error	$SS_e = \Sigma_i\Sigma_j\Sigma_k\Sigma_n(y_{ijkn} - y_{ijk.})^2$	IJK(N-1)	σ^2
Total	$\Sigma_i\Sigma_j\Sigma_k\Sigma_n(y_{ijkn} - y_{....})^2$		

The metronome was a battery-powered electromechanical oscillator with amplifier and speaker calibrated to give the desired frequency (one pulse per second).

16mm motion pictures were taken of each subject during each exercise. The camera was located in order to record the appropriate movements of each subject in association with fiducial markers.

3. RESULTS.

3.1 Results and Interpretations.

The computations noted in Tables I and II were carried out and are shown in Table III.

It was found that there were significant differences in the response due to different loads. This was, of course, a gratifying result inasmuch as the increment between levels of load was rather small. The resulting F-ratio is more than adequate for the stated significance level. This effect can be appreciated graphically by referring to Figure 1.

The next control variable, time, is again highly significant as was to be expected. The significance here, as well as the previous effect, i.e. load, may well stimulate the analyst to consider the functional fit to the data proposed in the original hypothesis.

A difficulty encountered from the analytical point of view occurs when one observes that both the Repetitions by Load interaction and Load by Time interaction are both significant. Considering the former, Repetitions by Load, the explanation here must come more from clinical considerations than from statistical interpretations alone. While the entire experiment was considered to be one that could be repeated, one can note that the subjects under consideration, although healthy, were not in top physical condition. As the experimental series progressed, an improvement (or degradation) in the physical condition probably occurred. Techniques also improved during the conduct of the experiment. In addition, there were one or two minor changes in apparatus which might account for this effect. Additionally, the subjects were not isolated from normal daily routine before and during the experiment. Perhaps the effect of psychological factors operating through the autonomic nervious system may be more important than can be identified at this time.

TABLE III

Analysis of Variance

Source	DF	SS	MS	F-Ratio	Significance
Replications	2	2026.58	1013.29	8.64	None
Load	2	7504.00	3752.00	31.99	*
Time	43	317105.39	7374.54	62.87	**
RxL	4	5462.93	1365.73	11.67	*
RxT	86	4874.66	56.68	0.483	None
LxT	86	15868.31	184.52	1.573	88
RxLxT	172	9693.96	56.36	0.480	None
Error	1584	185808.71	117.30		
Total	1979	548344.54			

* Significant at 5% Level.

**Significant at 1% Level.

HEART RATE CHANGE BEFORE, DURING, AND AFTER PRESCRIBED WEIGHT-LIFTING EXERCISE USING THE FOLLOWING WEIGHTS

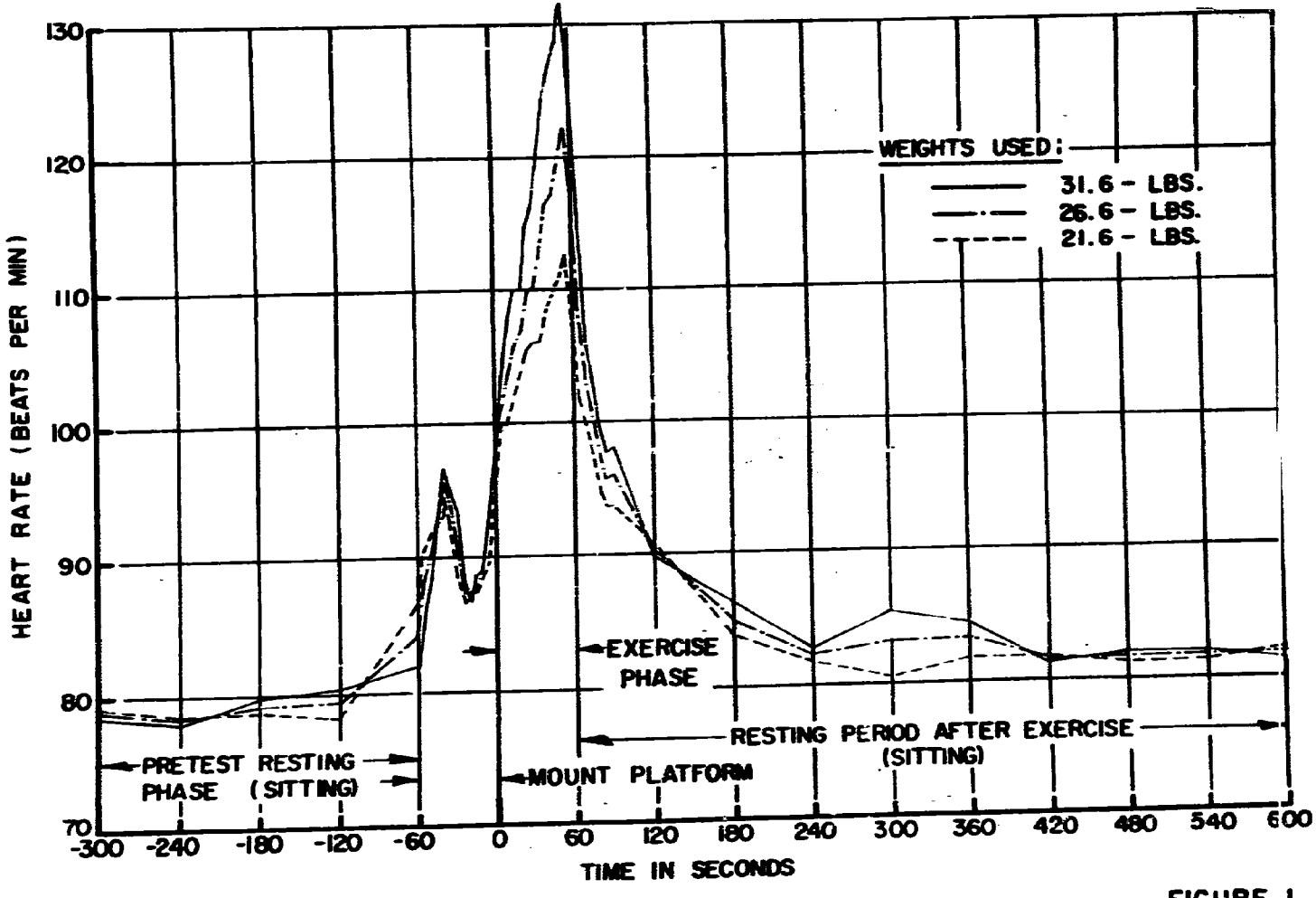

FIGURE 1

The Load by Time interaction probably receives its largest contribution from the differences in heart rate accelerations and peak values which occur over the working phase. In comparison with the close similarity of the curves of the other time segments of the experimental cycle, this interaction could perhaps be avoided in subsequent experimentation by considering measurements only over the working phase. However, this approach cannot be taken until reasonable baselines are established for pre- and post-work periods.

In view of the purpose of the experiment and the original hypothesis presented, an attempt is made to perform the regression analysis set forth under the null hypothesis. Table IV indicates the linear regression functions in reference to time. One may observe that the residual error after fitting closely resembles, on the average, the error mean square from the analysis of variance. Table V indicates the regression functions in reference to load. In like manner, the residual error after fitting resembles the error mean square from the analysis of variance.

Tests of significance have not been performed on the individual constants listed in Tables IV and V in that the appearance of interaction effects does not allow the combining of all the data or the three replicates as was done for these calculations. We have not formulated the precise nature of the multiple test procedure implied here. The basic intent again was to develop an idea of the form to assist in future designs.

4. DISCUSSION.

4.1 Subtle Observations.

a. Heart rate prior to leaving the sitting rest position.

It is interesting to observe (Figure 1) the resting heart rate patterns. Fluctuations for a given subject on a given experimental run were essentially similar for the different loads and repetitions. Thus there was an identifiable pattern for each of the participating subjects. One would judge that some of the fluctuation in general might be lessened if subjects were isolated and testing singly in an environment in which external stimuli were essentially nil. Statistically, of course, we have treated the values in this phase as constants.

TABLE IV

Table of Linear Regression Functions:
Heart Rate vs. Time

Time (Seconds)	$\hat{\alpha}$	$\hat{\beta}$	ERMS	$\hat{\sigma}_{\alpha}$	$\hat{\sigma}_{\alpha}$
-300.	79.244444	- .05333333	7.0593	1.6639	.25777
-240.	78.655555	- .06000000	6.3054	1.4862	.23024
-180.	78.777777	.13333335	5.6110	1.3225	.20488
-120.	78.222222	.28000001	7.0641	1.6650	.25795
- 60.	86.499999	- .41999997	9.7390	2.2955	.35562
- 55.	90.899999	- .55333331	13.227	3.1178	.48300
- 50.	91.977777	- .35999996	11.914	2.8081	.43503
- 45.	92.655555	.00666670	12.102	2.8524	.44190
- 40.	94.411110	.23333336	13.937	3.2849	.50890
- 35.	92.622222	.26666670	12.917	3.0446	.47166
- 30.	88.433333	.52666668	13.759	3.2431	.50242
- 25.	86.388888	.15333334	11.775	2.7755	.42997
- 20.	87.199999	- .07999997	11.938	2.8139	.43592
- 15.	87.333333	.10666670	10.728	2.5286	.39172
- 10.	88.755555	.02666669	9.5600	2.2533	.34908
- 5.	89.677777	.40666669	8.5388	2.0126	.31179
0.	95.911110	.12000002	7.8273	1.8449	.28581
5.	99.966666	.32666671	8.1022	1.9097	.29585
10.	99.899999	.72666669	8.7247	2.0564	.31858
15.	101.44444	.86666670	9.4751	2.2333	.34598
20.	103.70000	.60666668	9.6506	2.2747	.35239
25.	105.47778	.91333333	11.449	2.6985	.41805
30.	106.04444	1.0133333	11.570	2.7271	.42248
35.	106.05555	1.4733333	11.876	2.7993	.43366
40.	108.48889	1.5866667	12.465	2.9380	.45515
45.	109.68889	1.5600000	13.738	3.2382	.50166
50.	110.62222	1.8000000	12.613	2.9729	.46056
55.	112.45555	1.9266667	13.713	3.2321	.50072
60.	107.64444	2.0133334	13.540	3.1914	.49441
65.	101.70000	1.3133334	10.333	2.4355	.37731
70.	99.799999	.66666669	10.289	2.4251	.37569
75.	97.411110	.55333335	8.1311	1.9165	.29691
80.	94.766666	.47333335	8.8753	2.0919	.32408
85.	93.644444	.42666669	8.9016	2.0981	.32504
90.	93.766666	.43333337	9.8854	2.3300	.36096
120.	90.755555	- .10666665	8.9511	2.1098	.32685
180.	83.622222	.25333335	8.1302	1.9163	.29687
240.	81.633333	.11333336	8.2653	1.9482	.30181
300.	80.422222	.49333335	8.5371	2.0122	.31173
360.	81.888888	.25333336	8.5314	2.0109	.31152
420.	81.866666	- .05333333	6.9260	1.6325	.25290
480.	81.011110	.07333336	5.7840	1.3633	.21120
540.	81.033333	.07333334	6.5464	1.5430	.23904
600.	82.266666	- .10666665	5.9303	1.3978	.21655

TABLE V

Table of Regression Functions
Heart Rate vs. Load

Time Segment	21.6 lbs.	25.6 lbs.	31.6 lbs.
I	79.7	79.7	79.7
II	82.6 + .55Δt*	82.6 + .55Δt*	82.6 + .55Δt*
IIIa	92.5 - .61Δt*	92.5 - .61Δt*	98.5 - .61Δt*
IIIb	83.6 + .15Δt*	83.6 + .15Δt*	83.6 + .15Δt*
IV	96.2 + .32t**	96.7 + .43t**	99.2 + .62t**
V	$e^{4.68}{}_t{}^{.0011}{}_e{}^{-.087t}$**	$e^{4.74}{}_t{}^{.0014}{}_e{}^{-.1t}$**	$e^{4.82}{}_t{}^{.0019}{}_e{}^{.13t}$**

* Start Δt at zero at the beginning of the respective segments and increase by 5 for each interval.

** Start t at zero at the beginning of the respective segments and increase by 1 for each 5 seconds.

b. Heart rate during immediate pre-work phase.

After the subjects left their resting chairs, they took several paces and took a single step up to the work platform and assumed a predetermined work position. The subject then remained in this position to await the signal to receive the bar-bell and commence the excercise. It was this phase that caused us some unexpected concern from an analytical point of view in that we lost control of the individual in transferring him from the resting phase to the working phase. More careful planning should avoid this problem in the future. The same kinds of variations mentioned in (a) above likewise were found in this phase. These were also treated in linear fashion.

c. Heart rate during work.

While it was expected that the heart rate would rise rapidly with the sudden onset and continuation of intensive physical exercise, a more precise statement on how it would rise was desired. This, hopefully, would give some insight in reference to the possibility of an underlying functional relationship between workload and heart rate response. The data points for each of the three loads for the five subjects are shown graphically in Figures 2, 3, and 4. These data were fitted with linear regression lines as shown also on the graphs. It is interesting to look now at the individual pattern for this phase of the experiment. Figures 5, 6, and 7 show their characteristics. To us these were very interesting observations for they provided additional insight on the manner that individuals respond to a physical stress in a physiological way using a set of quantitative measures as opposed to the more common but less rigorous clinical impressions. However, we are mindful of the exploratory nature of this project as well as its being a small non-random sample.

d. Heart rate during recovery.

It is very interesting that heart rate falls so rapidly following the cessation of physical work. This well known exponential fall, the greater part of which takes place within approximately the first 10 to 15 seconds, was demonstrated in association with the raw data points for the various loads shown in Figures 8, 9, and 10. According to the results in this study heart rate began to fall several seconds prior to

HEART RATE CHANGE DURING 60-SECONDS OF PRESCRIBED WORK

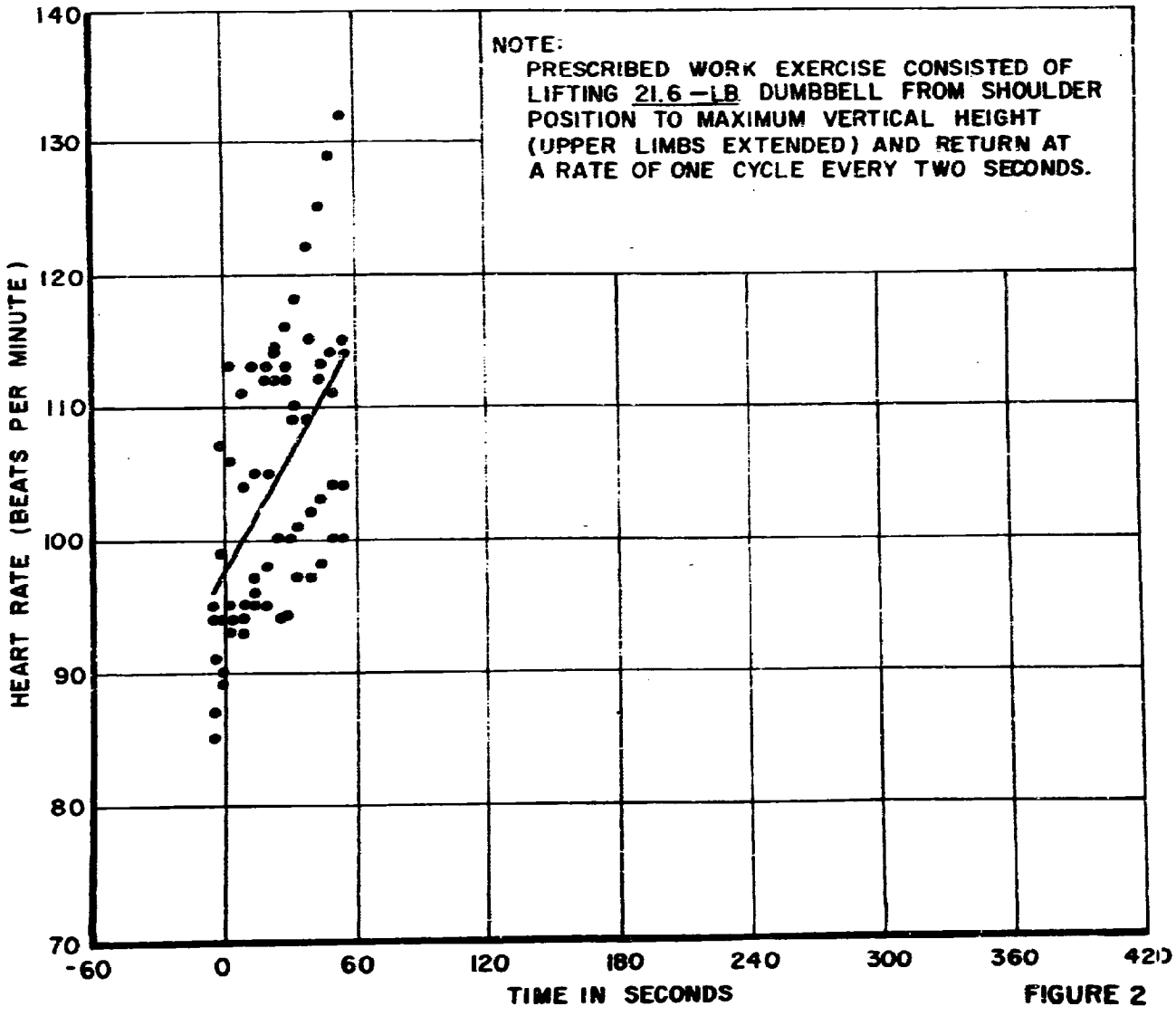

FIGURE 2

PRECEDING
PAGE BLANK

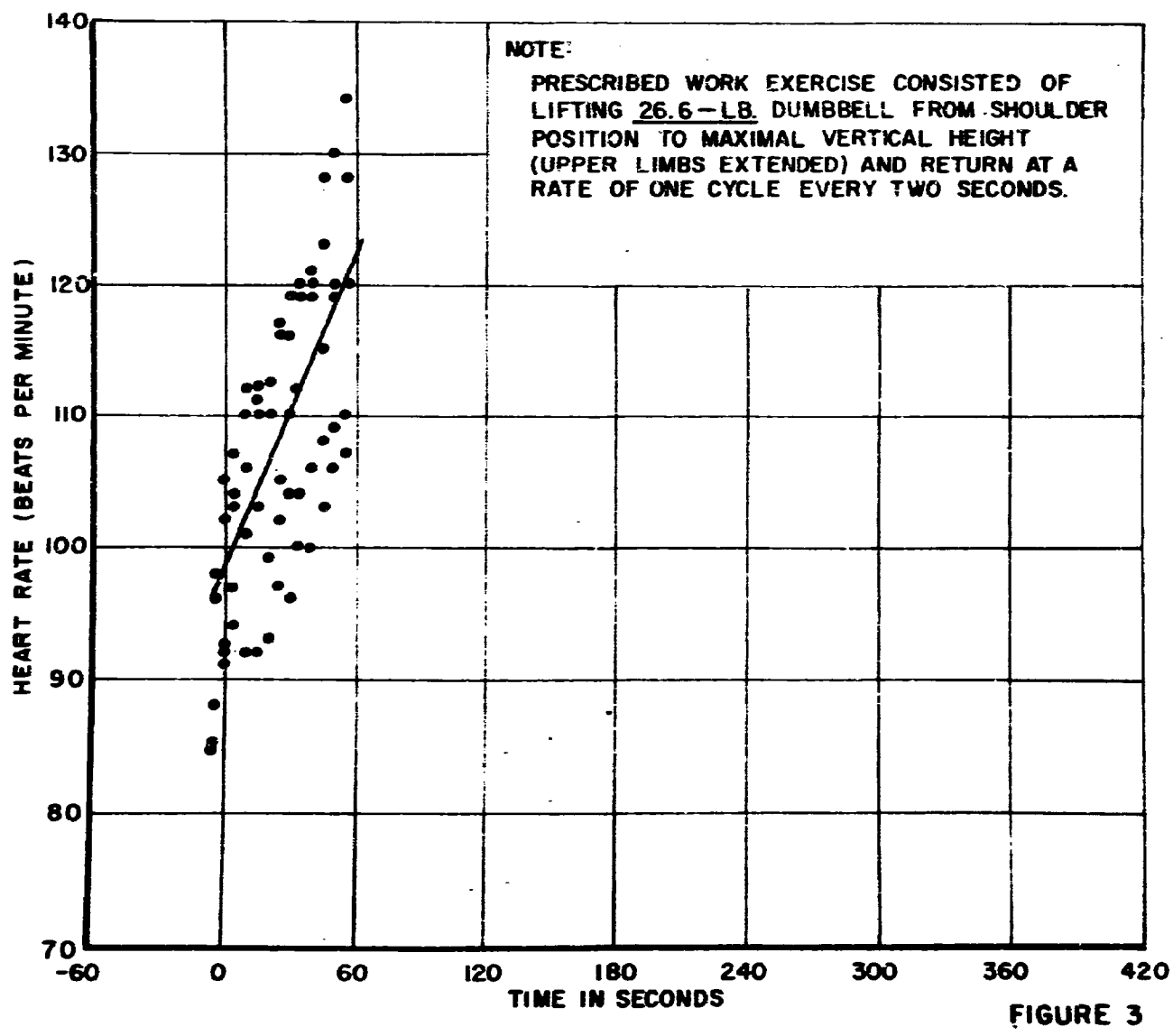
HEART RATE CHANGE DURING 60-SECONDS OF PRESCRIBED WORK
NOTE:
PRESCRIBED WORK EXERCISE CONSISTED OF LIFTING 26.6—LB. DUMBBELL FROM SHOULDER POSITION TO MAXIMAL VERTICAL HEIGHT (UPPER LIMBS EXTENDED) AND RETURN AT A RATE OF ONE CYCLE EVERY TWO SECONDS.
HEART RATE (BEATS PER MINUTE)
140
130
120
110
100
90
80
70
-60
0
60
120
180
240
300
360
420
TIME IN SECONDS

FIGURE 3

PRECEDING
PAGE BLANK

HEART RATE CHANGE DURING 60-SECONDS OF PRESCRIBED WORK

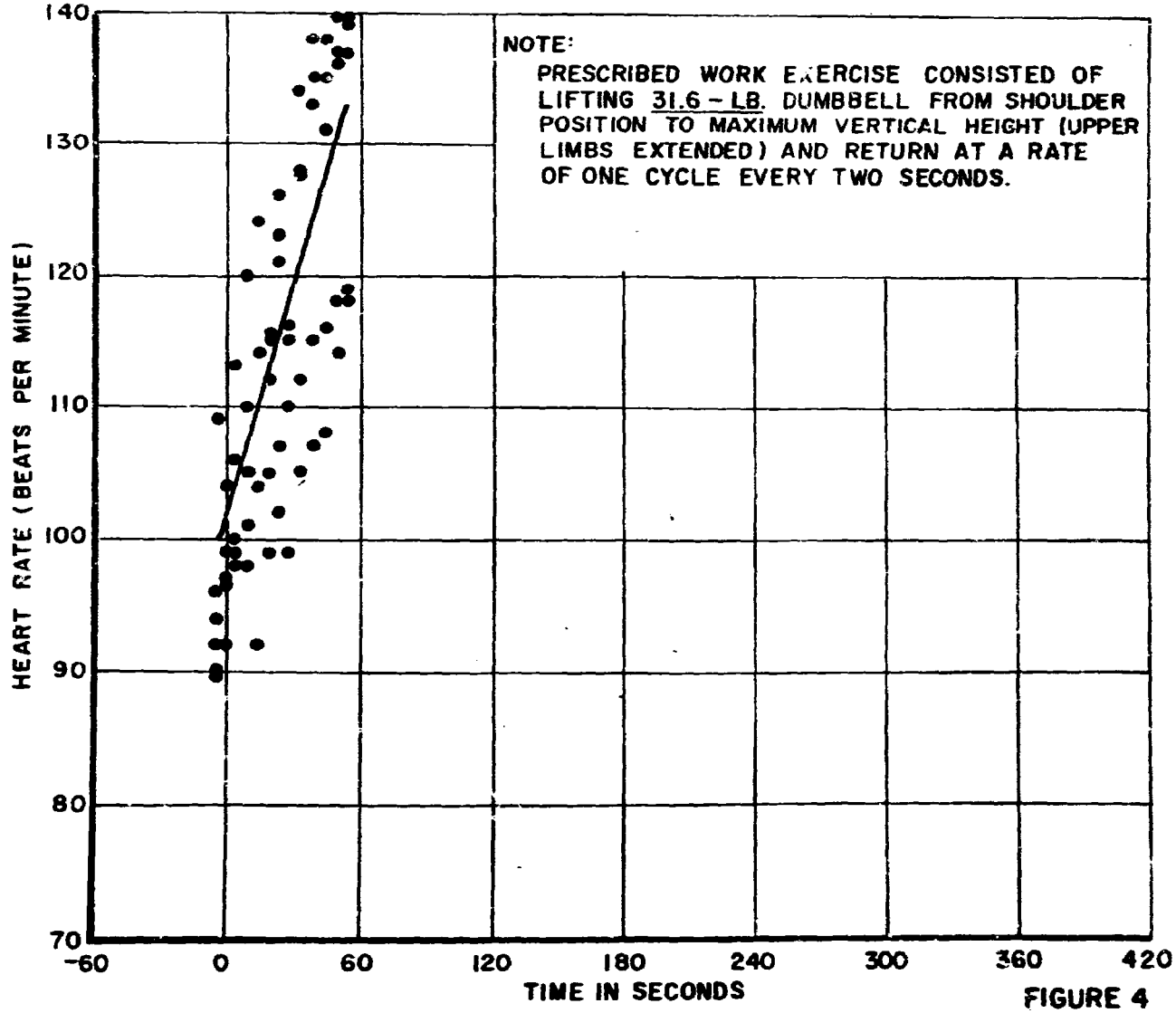

FIGURE 4

BLANK

HEART RATE CHANGE OF INDIVIDUAL SUBJECTS DURING 60-SECOND WORK PERIOD USING 21.6 LB DUMBBELL (AVERAGE OF 3 TRIALS)

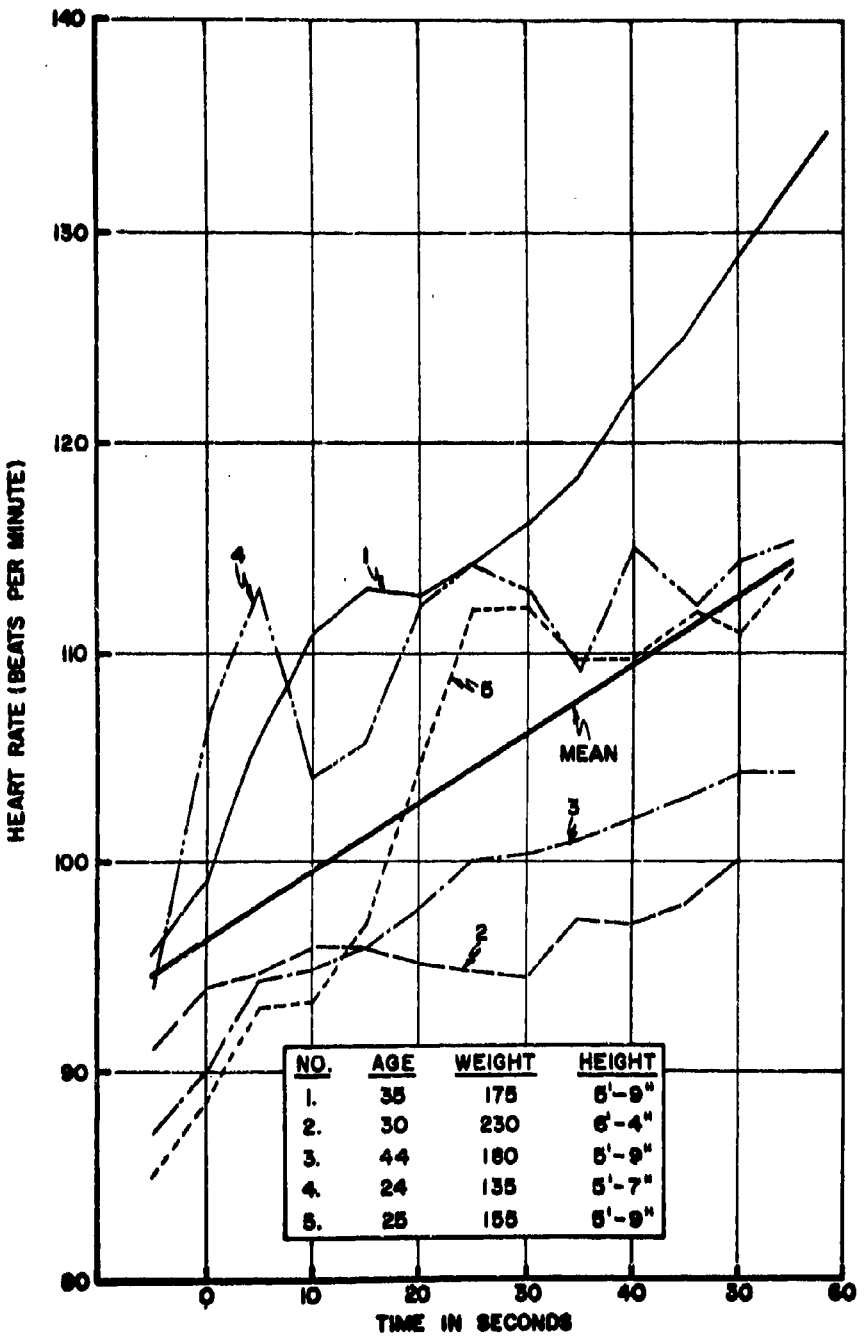

FIGURE 8

PRECEDING
PAGE BLANK

HEART RATE CHANGE OF INDIVIDUAL SUBJECTS
DURING 60-SECOND WORK PERIOD USING 26.6 LB
DUMBBELL (AVERAGE OF 3 TRIALS)

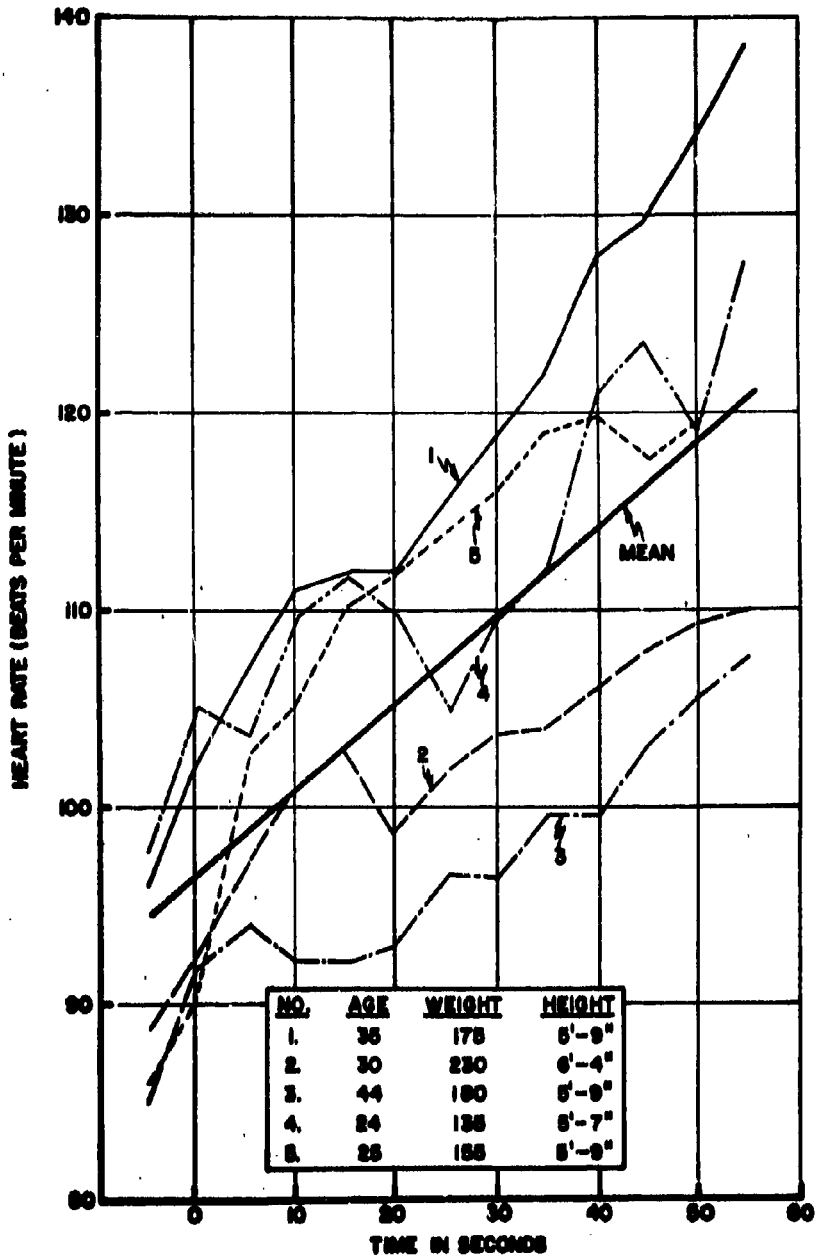

FIGURE 6

PRECEDI
PAGE . BLA

HEART RATE CHANGE OF INDIVIDUAL SUBJECTS DURING 60-SECOND WORK PERIOD USING 31.6 LB DUMBBELL (AVERAGE OF 3 TRIALS)

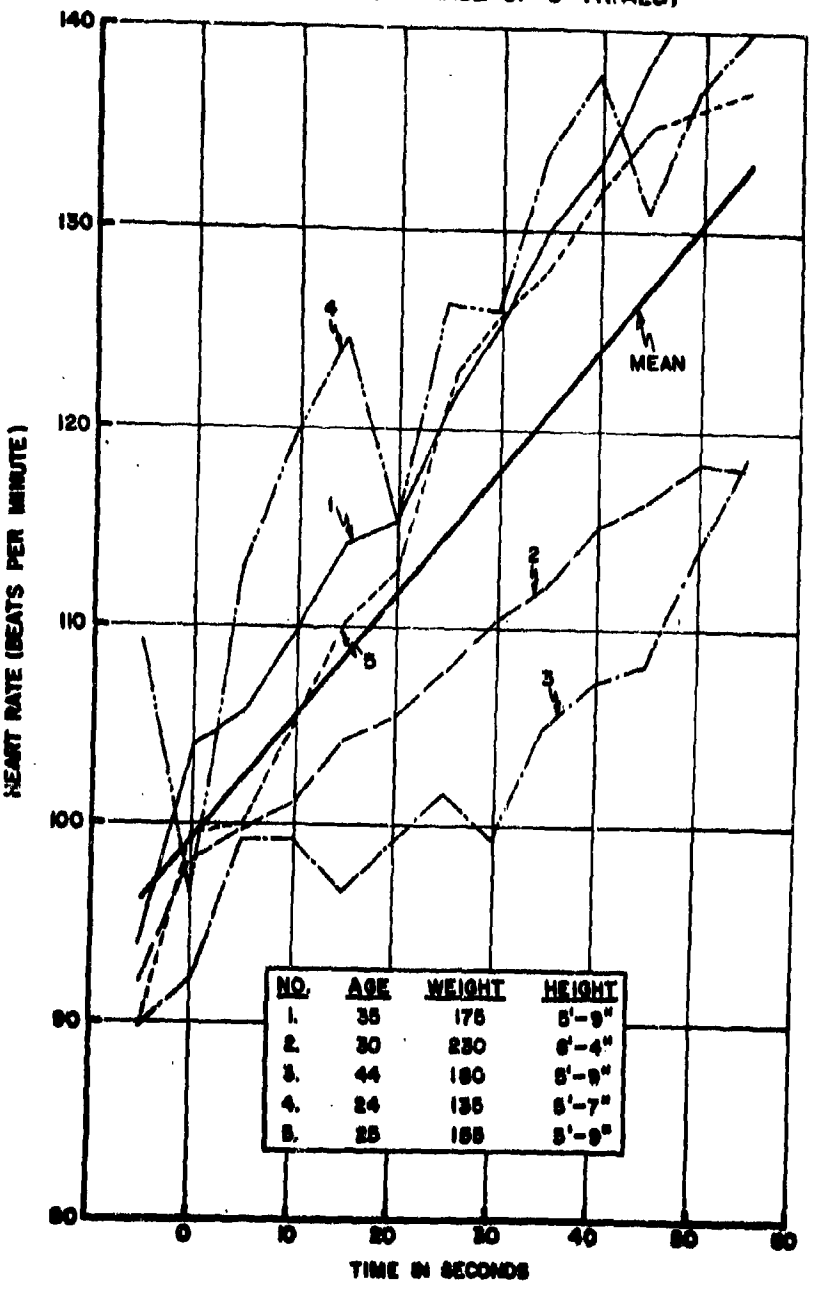

FIGURE 7

the cessation of the work. Our explanation for this is that it may in part be anticipation by the individual toward the end of the work cycle and, in part, due to the method of discretizing the data. Since the participants in this investigation were considered to be clinically healthy males in a somewhat restricted age range, no inferences are made regarding variations in the return of individual heart rates to the normal or resting baselines. The fitted exponential regression curves shown in the figures mentioned above are treated statistically. Variations are attributed to circulatory system characteristics and their nervous system interactions. Presumably external stimuli which may influence heart rates in the resting and the final stages of recovery would be less significant during intensive physiological stress derived from physical work.

e. Heart rate over the experimental cycle.

A summary or heart rate profile over all phases of the experimental cycle averaged for each load is recalled as shown in Figure 1. It is interesting to observe the slopes of the surves showing heart rate increase in that they are clearly different even for the small increments of work intensity. The same may be said in reference to the peak values.

4.2 Direction of Subsequent Investigation.

In brief the following are being considered for subsequent investigations:

a. Longer work periods in order to understand more about heart rate behavior at maximum range under prolonged work stress.

b. The utilization of an open system in order to accomplish a. above. Weight lifting, unlike bicycling or tasks utilizing more of the muscles tends to generate exhaustion prior to the onset of peak heart rate.

c. Certain biochemical parameters associated with circulatory system response to work stress may be useful particularly as it may, in turn, be related to such medical conditions as shock. Here then we become concerned with multivariate models and analysis.

d. Planning of experiments for additional insight on roles of other physical and psychological factors.

e. An ultimate objective is to relate "stress" to cardiovascular system changes associated with early signs of cardiovascular deterioration and a particular condition known as hemorrhagic shock.

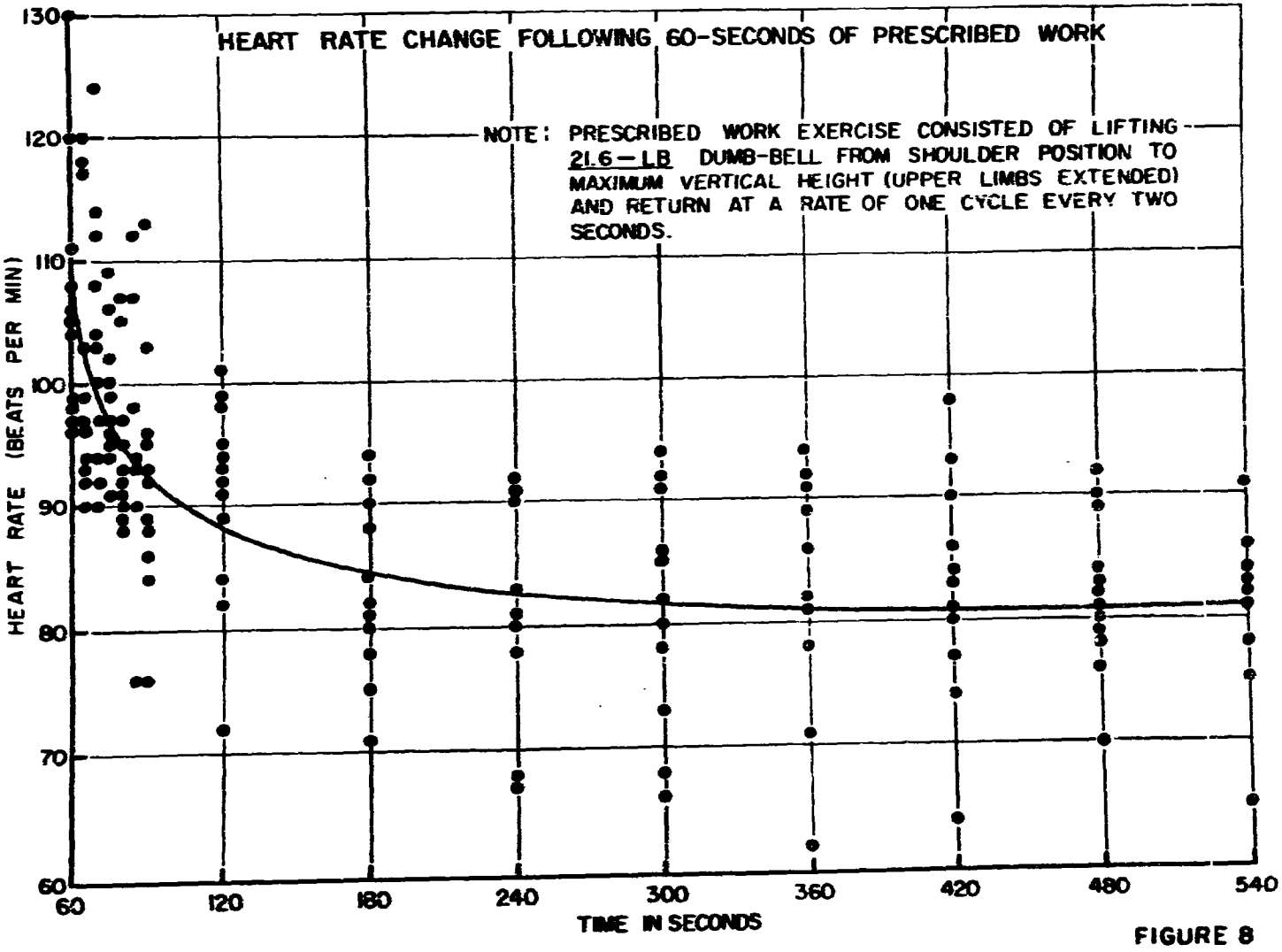
HEART RATE CHANGE FOLLOWING 60-SECONDS OF PRESCRIBED WORK
NOTE: PRESCRIBED WORK EXERCISE CONSISTED OF LIFTING 21.6 – LB DUMB-BELL FROM SHOULDER POSITION TO MAXIMUM VERTICAL HEIGHT (UPPER LIMBS EXTENDED) AND RETURN AT A RATE OF ONE CYCLE EVERY TWO SECONDS.
HEART RATE (BEATS PER MIN)
130
120
110
100
90
80
70
60
60
120
180
240
300
360
420
480
540
TIME IN SECONDS

FIGURE 8

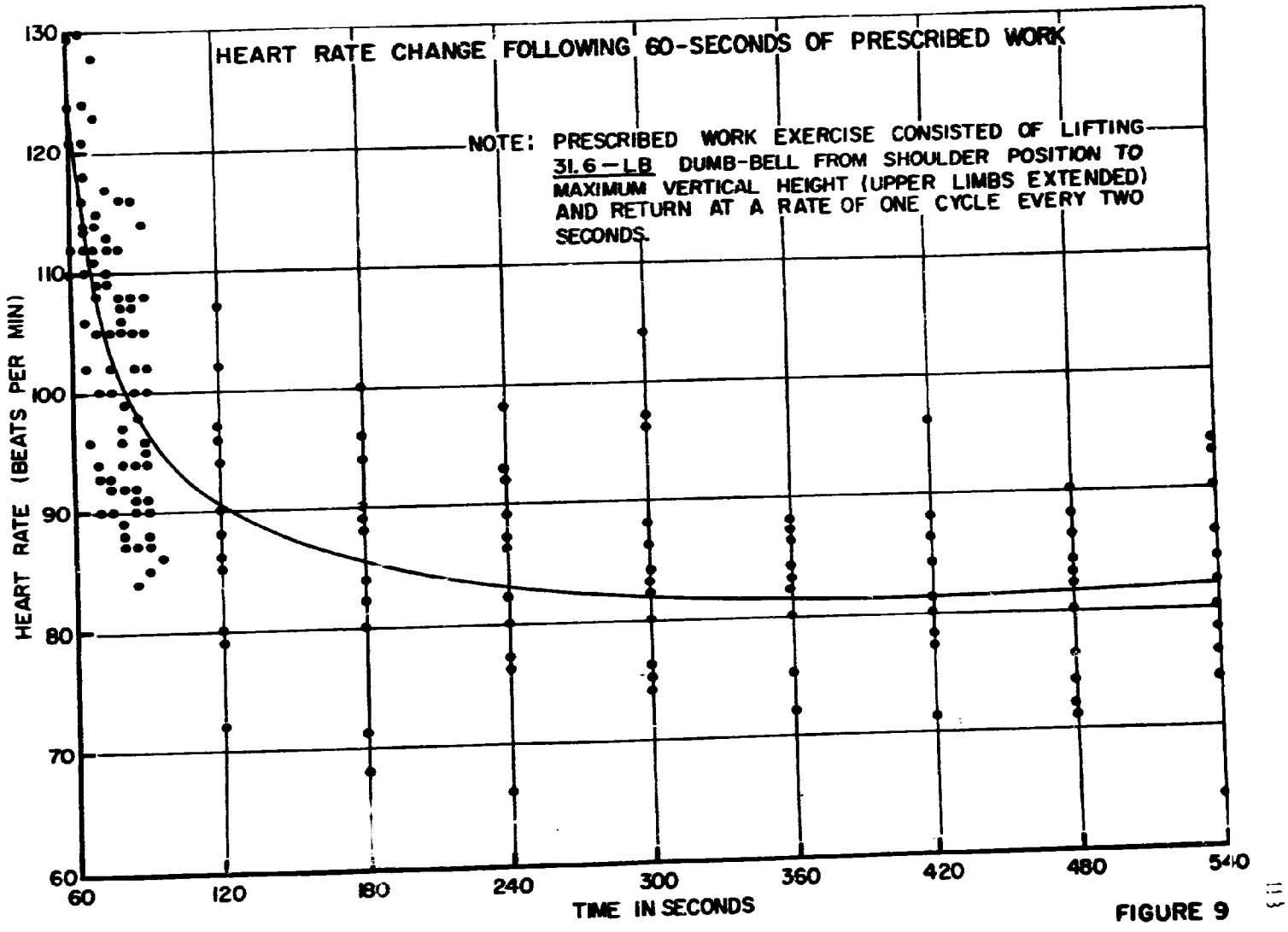
HEART RATE CHANGE FOLLOWING 60-SECONDS OF PRESCRIBED WORK
NOTE: PRESCRIBED WORK EXERCISE CONSISTED OF LIFTING 31.6 – LB DUMB-BELL FROM SHOULDER POSITION TO MAXIMUM VERTICAL HEIGHT (UPPER LIMBS EXTENDED) AND RETURN AT A RATE OF ONE CYCLE EVERY TWO SECONDS.
HEART RATE (BEATS PER MIN)
130
120
110
100
90
80
70
60
60
120
180
240
300
360
420
480
540
TIME IN SECONDS

FIGURE 9

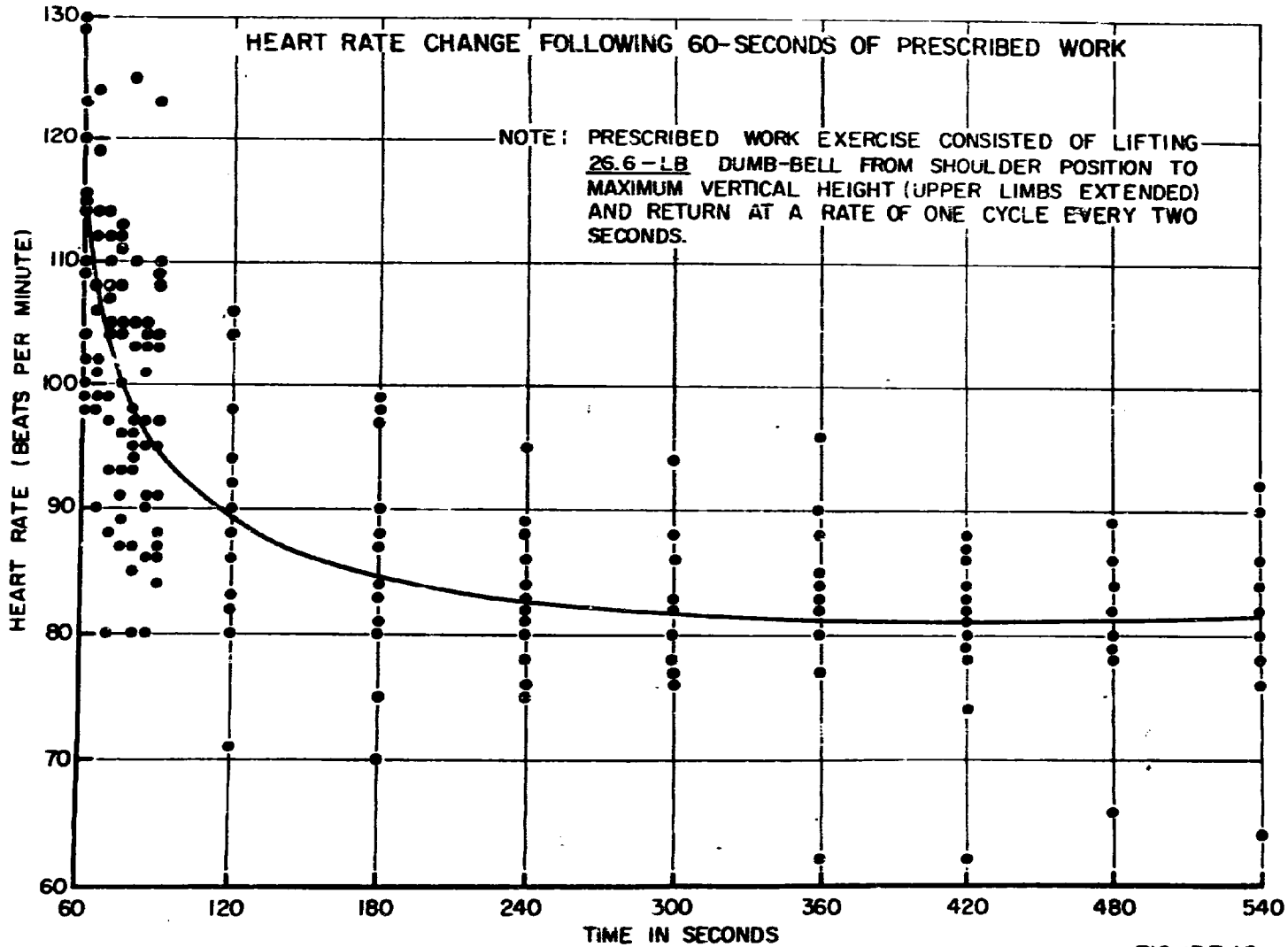
HEART RATE CHANGE FOLLOWING 60-SECONDS OF PRESCRIBED WORK
NOTE: PRESCRIBED WORK EXERCISE CONSISTED OF LIFTING 26.6-LB DUMB-BELL FROM SHOULDER POSITION TO MAXIMUM VERTICAL HEIGHT (UPPER LIMBS EXTENDED) AND RETURN AT A RATE OF ONE CYCLE EVERY TWO SECONDS.
HEART RATE (BEATS PER MINUTE)
130
120
110
100
90
80
70
60
60
120
180
240
300
360
420
480
540
TIME IN SECONDS

FIGURE 10

STRATEGY FOR THE OPTIMAL USE OF WEAPONS BY AREA COVERAGE*

J. A. Nickel, J. D. Palmer, and F. J. Kern
University of Oklahoma, Norman, Oklahoma
(Representing the U. S. Army Edgewood Arsenal)

ABSTRACT. The development of non-nuclear ground-based weapons systems in a historical perspective is briefly reviewed. The implications of this development to target acquisition and logistics in terms of efficiency of coverage are included.

By defining a new concept termed Efficiency of Target Destruction as the ratio of expected area destruction of a target complex to the maximum theoretical area destruction possible, the authors have demonstrated that a delivery of a number of small effects patterns can be most efficient. Through use of the SADI Mark IV, Statistical Additive Density Integrator, it was found that the delivery error (standard deviation of delivery) must be in the neighborhood of 50% of the target radius for maximum efficiency. It was further found that the efficiency is not appreciably reduced if the actual aim point is within 30% of the target's radius of the center.

These results clearly indicate that for certain classes of targets a decided advantage is attained in terms of efficiency of the weapons system, reduction of target locator accuracy requirements, and a lessening of the impact of logistics support.

INTRODUCTION. In the generations of ground based weapons systems since World War II, three readily identifiable stages have existed in the development of non-nuclear weapons. In the first instance, the attempt was to develop a warhead with the greatest possible damage or effects pattern which required larger and larger lethal radii for each particular system. During this initial phase, it was tacitly assumed that if one could develop a larger effects pattern, this was most easily delivered on target. A major effort during this period was toward warhead design and development, with little effort toward determining the accuracy requirements. It was further assumed that once the warhead was available, delivery on target would be readily achieved.

*This acticle appeared earlier as a University of Oklahoma Research Institute Technical Report: Contract DA 18-035-AMC-116(A); Internal Memorandum 1454-1-2, July 1965.

The second phase initiates with the realization that the warhead could not be delivered on target with a high degree of reliability, that is with a high assurance level. This led into the second phase which was the development of more accurate locators and target acquisition devices for sophisticated target acquisition--techniques such as infrared, radar, radiometers, acoustics, etc. In this phase the dependence of any system on the inherent ability of a locator to not only locate the target, but also locate itself relative to the weapon was realized. This presented the third problem with even more difficulties for designers and tacticians. The situation now becomes that of large lethal area weapons with a relatively low accuracy yielding the resultant of the net amount of lethal pattern placed on a target being less than that which could be achieved should a highly accurate method of firing be developed. With the realization that these two viewpoints were mutally opposing, atte pts have been made to develop closely coordinated systems involving locators and weapons. Considerable research has been performed in an attempt to formulate a methodology which would serve to alleviate this inherent difficulty.

In establishing minimum criteria for target location and firing patterns, the objectives have been aimed at generating more accurate locating systems and larger effects patterns. Target requirements have become more and more stringent. More potent effects patterns (non-nuclear) have been developed with the rather obvious end result of requiring greater locator accuracy to achieve a maximum effective firepower per unit. Most recent studies have been directed to ascertaining error sources and attempting to provide a maximum assurance level of target coverage for a given system. This has usually resulted in going to larger and larger total effects patterns as a consequence of the inability to supply more accurate target location methods. Tests to determine the maximum allowable error for multiple effects patterns have resulted in a promulgation of this same trend. Hence, a higher required assurance value of target destruction has resulted in specifications for more accuracy in location.

The problems which accrue from this trend are many. They include the requirement for more accuracy and mobility in target location systems, logistic difficulties associated with increased firing rates, loss of target during "zero-in" fire due to target mobility, and high initial and maintenance costs associated with larger more complex weapons systems. The results have been the generation of requirements for more accurate radars,

infrared devices, and optical detectors with accompanying data processing equipment, weapons selectors as well as more accurate delivery systems.

A re-examination of simulation data originally run to determine minimum accuracy requirements to yield maximim area coverage has resulted in a number of factors which point toward an entirely different assessment of applicable criteria contradicting previous concepts. In attempting to determine the "efficiency" of various weapons systems against standard target sizes, it was found that maximum efficiency seemed to occur when use was made of smaller values of R_D/R_T (lethal patterns) and that a deliberate error of up to 15% R_T had only a minor effect on area coverage at the maximum efficiency levels and further that a sacrifice in assurance level could be made and yet have a better system than is presently available against certain classes of targets under the previous optimization requirements.

Through the use of the OURI-SADI Mark IV, a systematic study of effects patterns and their effectiveness on area targets has been under investigation. An analysis of the data has brought forward several observations. Foremost among the observations is that the effectiveness in use of munitions can be increased by reducing the size of the effects pattern of a given round and distributing a number of these with a delivery error that is bounded away from zero, i.e., not perfectly accurate, as well as having an upper bound on the weapons errors.

For flame technology, this is particularly important since by not attempting to cover the entire target with fuel, the insulation effect of unburned fuels is minimized. The desirability of small portable flame devices increases since on the criteria enumerated they are tactically sound. Furthermore, multiple bursts with each component yielding a small effects pattern, requires less delivery accuracy than a single larger burst having the same potential of destruction.

The SADI Mark IV, Statistical Additive Density Integrator, as developed by the personnel of the Systems Research Center, University of Oklahoma Research Institute, permits the evaluation of lethality to a target by simulation techniques. Through such studies, several factors influencing the effectiveness of multiple firings on a target have come to light. Area coverage affected by flame devices is particularly well-modeled by this simulation technique.

At this juncture of study, the basic configuration has been the random placement of six circular "cookie-cutter" effects regions. Each component, with total destruction or lethality throughout the circle, is distributed about a point on a circular target. Circular effects regions have been employed since in a first approximation, this is approximately the shape experienced under actual firings. Circular targets have been used since maximum efficiency could be designed into the SADI Mark IV with this coniiguration. It is known, however, that a topological equivalence exists between this configuration and any other for which the boundaries of the target and lethality region are simple closed curves. It should be further observed that the numerical discrepancy between using circular patterns and rectangular patterns is negligible. (Ewing, George. Predicting the Effects of Multiple Firing on an Area Target and Related Questions. OCDD, USA AMS, Ft. Sill, 1955). Implicit in the foregoing equivalence are questions of approximated symmetry and other regulatory conditions which will not be considered.

APPROXIMATING CONVOLUTION OF THE MOMENT GENERATING INTEGRAL. In trying to estimate a suitable approximation to the probability density function f(x) of a population from which samples are drawn, the following scheme approximating the density function from the empirical moments is proposed.

It is known in statistical theory, that if the Moment Generating Function, M(x), is known for a sampling distribution, then the moments of that distribution are readily obtained from the derivatives.

For simplicity it is assumed that the probability density f(x) at a continuous variable has a convergent McLaurin expansion on the unit interval (0, 1) and is zero elsewhere, i.e.,

$$f(x) = \sum_{k=0}^{\infty} b_k x^k \qquad 0 \leq x \leq 1$$

$$= 0 \qquad \text{elsewhere.}$$

This assumption permits the Moment Generating Function M(x) to be expressed as an integral over the unit interval, i.e.,

$$M(x) = \int_{-\infty}^{+\infty} e^{xt} \cdot f(t)dt = \int_{0}^{1} e^{xt} f(t)dt \quad .$$

This function can furthermore be expressed as a power series

$$M(x) = 1 + \sum_{k=1}^{\infty} \frac{x^k \nu_k}{k!}$$

where ν_k is the k^{th} moment about the origin.

A second possible interpretation is available by considering M(x) as an Integral Transform instead of an expected value. As an Integral Transform, the following needed properties can be established.

(1) $M(ax + by) = aM(x) + bM(y)$

(2) $M\left[f'(x)\right] + xM\left[f(x)\right] = e^x f(1) - f(0)$

(3) $M(0) = 0$

(4) $M(1) = \sum_{k=0}^{\infty} \frac{x^k}{(k+1)!}$

(5) $M(x) = \sum_{k=0}^{\infty} \left[\frac{1}{(k+1)!} - \frac{1}{(k+2)!}\right] \cdot x^k$

(6) $M(x^2) = \sum_{k=0}^{\infty} \left[\frac{1}{(k+1)!} - \frac{2}{(k+2)!} + \frac{2}{(k+3)!}\right] x^k$

and in general

(7) $M(x^n) = \frac{1}{x} \sum_{k=0}^{\infty} \frac{x^k}{k!} - \frac{n}{x} M\left[x^{n-1}\right]$.

Using the assumed power series expansion for the probability density $f(x)$

$$M\left[f(x)\right] = M\left[\sum_{k=0}^{\infty} b_k x^k\right]$$

$$= \sum_{k=0}^{\infty} b_k \, M\left[x^k\right] \quad .$$

When the transforms of x^k are substituted into this last expression a second power series expansion is obtained for the Moment Generating Function, this time in terms of the McLaurin coefficients of $f(x)$. Two power series converging to the same function necessarily have identical coefficients. From this, it follows that

$$\nu_{k-1} = \sum_{j=1}^{\infty} \frac{b_{j-1}}{k + j - 1} \qquad k = 1, 2, \ldots$$

where $\nu_o = 1$. These constitute an infinite system of equations in the variables b_{j-1}, $j = 1, 2, \ldots$

Letting B denote the column matrix of the McLaurin coefficients b_{i-1}, N the column matrix of the moments ν_{i-1} calculated from the sample, and A the Hilbert matrix

$$A = \left(\frac{1}{i + j - 1}\right) \quad .$$

The foregoing system of equations can be written

$$AB = N \quad .$$

The matrix A is singular and has no inverse. However, if the system is truncated so as to utilize only a specific number (n) of moments, the resulting $(n + 1)$ by $(n + 1)$ square matrix A_n does have an inverse A_n^{-1}.

The approximating polynomial coefficients can then readily be obtained as

$$B = A_n^{-1} N \ .$$

It should be observed that the matrix A_n, and hence, its inverse is independent of the sampling distribution, hence, one A_n^{-1} can be used for all samples at that degree of approximation.

From a casual observation of the data it is apparent that the density function is not uniform, normal, or even symmetrical. It follows that any admissible polynomial approximation should be by a polynomial of degree greater than two. To allow for the possibility of symmetry it is reasonable to consider an approximating polynomial of degree four (4). If a least squares analysis were to be employed in determining the coefficients for such a polynomial, it would be necessary to use eight (8) moments of the relative areas. Since the basis for accepting the polynomial of degree four as a good approximation to the density function is not established, an abbreviated procedure over a least squares evaluation is desired.

A polynomial approximation to the probability density function was developed through the use of an approximating convolution of the Moment Generating Integral. If the approximating density function is given by

$$f(x) = b_o + b_1 x + b_2 x^2 + b_3 x^3 + b_4 x^4 \ ,$$

where x is the relative area reduced to the unit interval. The above approximating convolution gives the following formulas for the coefficients.

$$b_o = 25 - 300\nu_1 + 1050\nu_2 - 1400\nu_3 + 630\nu_4$$

$$b_1 = -300 + 4800\nu_1 - 18900\nu_2 + 26880\nu_3 - 12600\nu_4$$

$$b_2 = 1050 - 18900\nu_1 + 79380\nu_2 - 117600\nu_3 + 56700\nu_4$$

$$b_3 = -1400 + 26880\nu_1 - 117600\nu_2 + 179200\nu_3 - 88200\nu_4$$

$$b_4 = 630 - 12600\nu_1 + 56700\nu_2 - 88200\nu_3 + 44100\nu_4$$

where ν_1, ν_2, ν_3, and ν_4 are the moments of the relative areas of coverage about the origin reduced (or scaled) so that the maximum relative area is one (1). This calculation only requires the use of four moments of the distribution to give an approximating polynomial. The only segment of the ensuing polynomial used is that part lying above the axis and corresponding to the range of values of the original sampling distribution.

For the purposes of the original problem, the cumulative probability distribution is needed. This is readily approximated by the polynomial

$$P = b_o x + (1/2)b_1 x^2 + (1/3)b_2 x^3 + (1/4)b_3 x^4 + (1/5)b_4 x^5,$$

obtained from integrating the approximating density polynomial. This again is used only over the domain corresponding to the observed area input obtained from the simulator. As a statistical control, a kolmogorov-Smirnov Test was applied to the empirical distribution and the calculated approximating cumulative probability polynomial.

SYSTEMATICALLY INTRODUCED BIAS. It has long been recognized that a knowledge of the exact position of a target relative to the weapon is generally not initially known. This raises the question of bias effects in the assumed target location relative to the actual target center. A study has been initiated to investigate the systematic introduction of bias in the location of ground zero. The actual procedure used is probably best described through the use of the flow chart of Figure 1.

Initially, in the study of bias effects, the parameters considered have been $\sigma = 0.5$ and $r = 0.2\sqrt{5}$. For this particular case, it became apparent in preliminary investigations that a bias less than or equal to 0.3 of the target radius produced minor decrease in the expected area coverage. The fall off to a first approximation is parabolic and the area coverage can be approximated by multiplying the expected area coverage of a symmetrical distribution by the factor.

$$1 - \sqrt{0.925X} \qquad 0 \leq X \leq 0.4 \quad .$$

In this factor, the bias X is the ratio of the distance between the target center and aim point, and the target radius. For $X = 0.3$, the fall off

FIGURE 1

Bias Effect Analysis on a Sampling Distribution of a Composite of N Effects Patterns

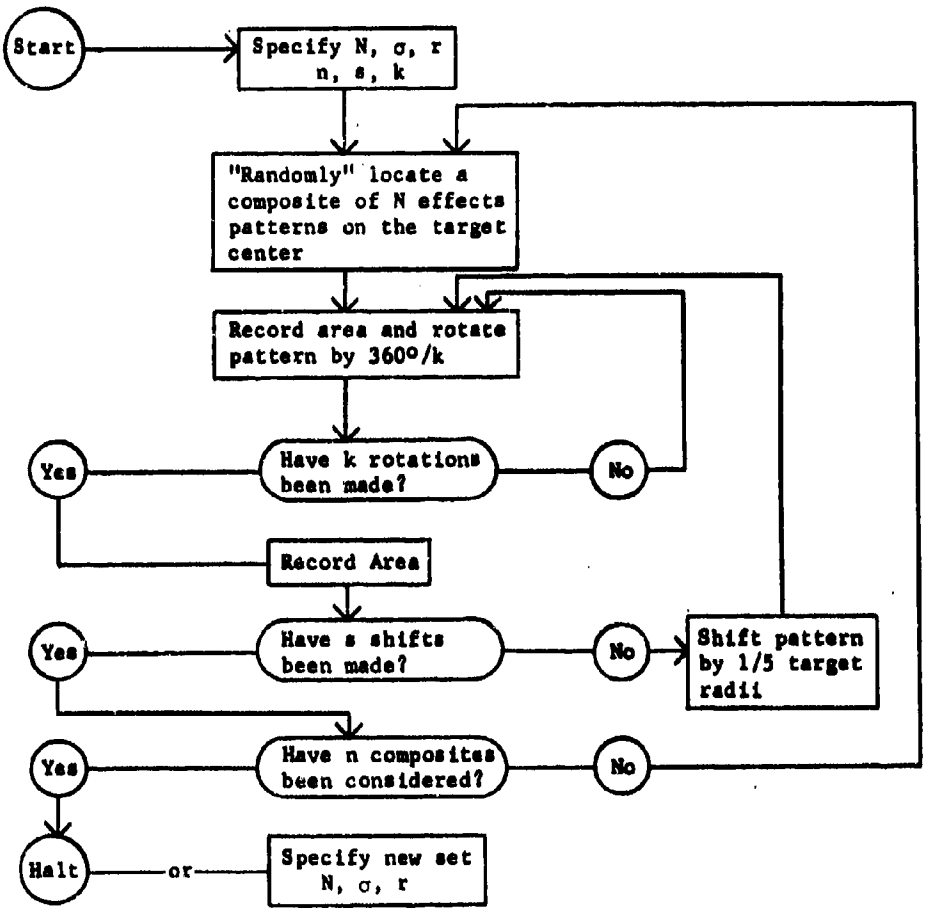

Dictionary of Symbols

N = number of effects patterns (component) in composite

σ = standard deviation of delivery

r = relative radius of effects pattern (component)

n = total number of composite patterns to be considered

s = total number of shifts to be considered (bias effects in terms of 1/5 target radii)

k = total number of rays to be considered

FIGURE 8

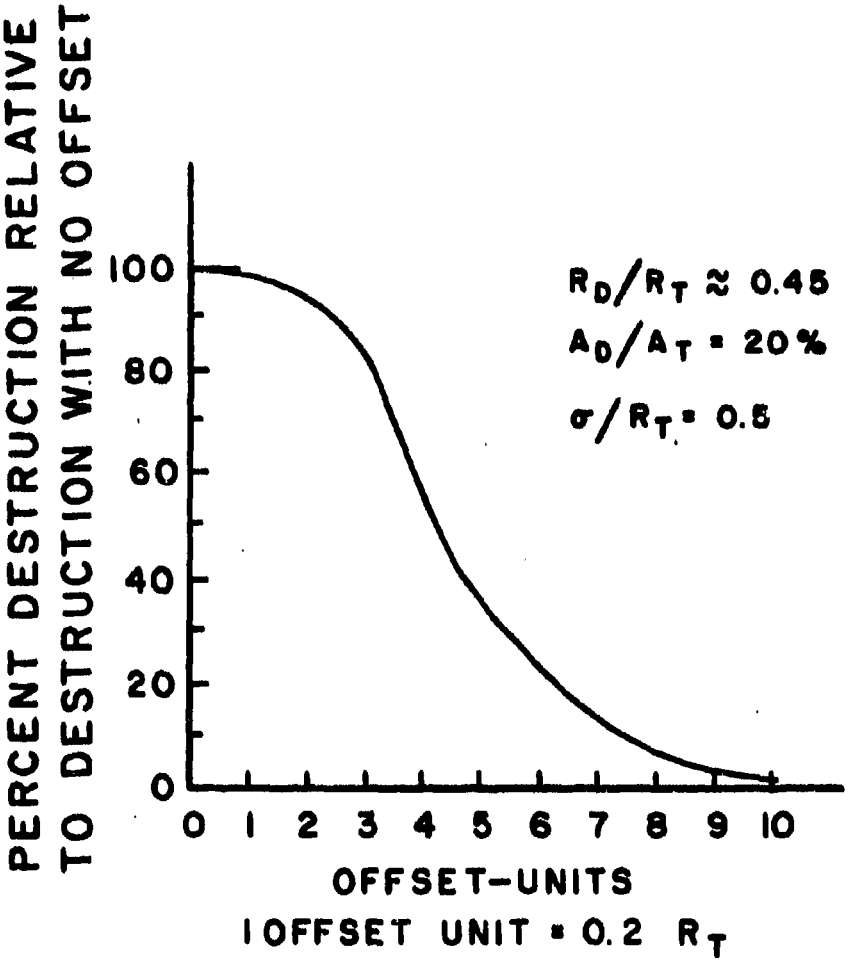

DECREMENT IN DESTRUCTION AS A FUNCTION OF OFFSET

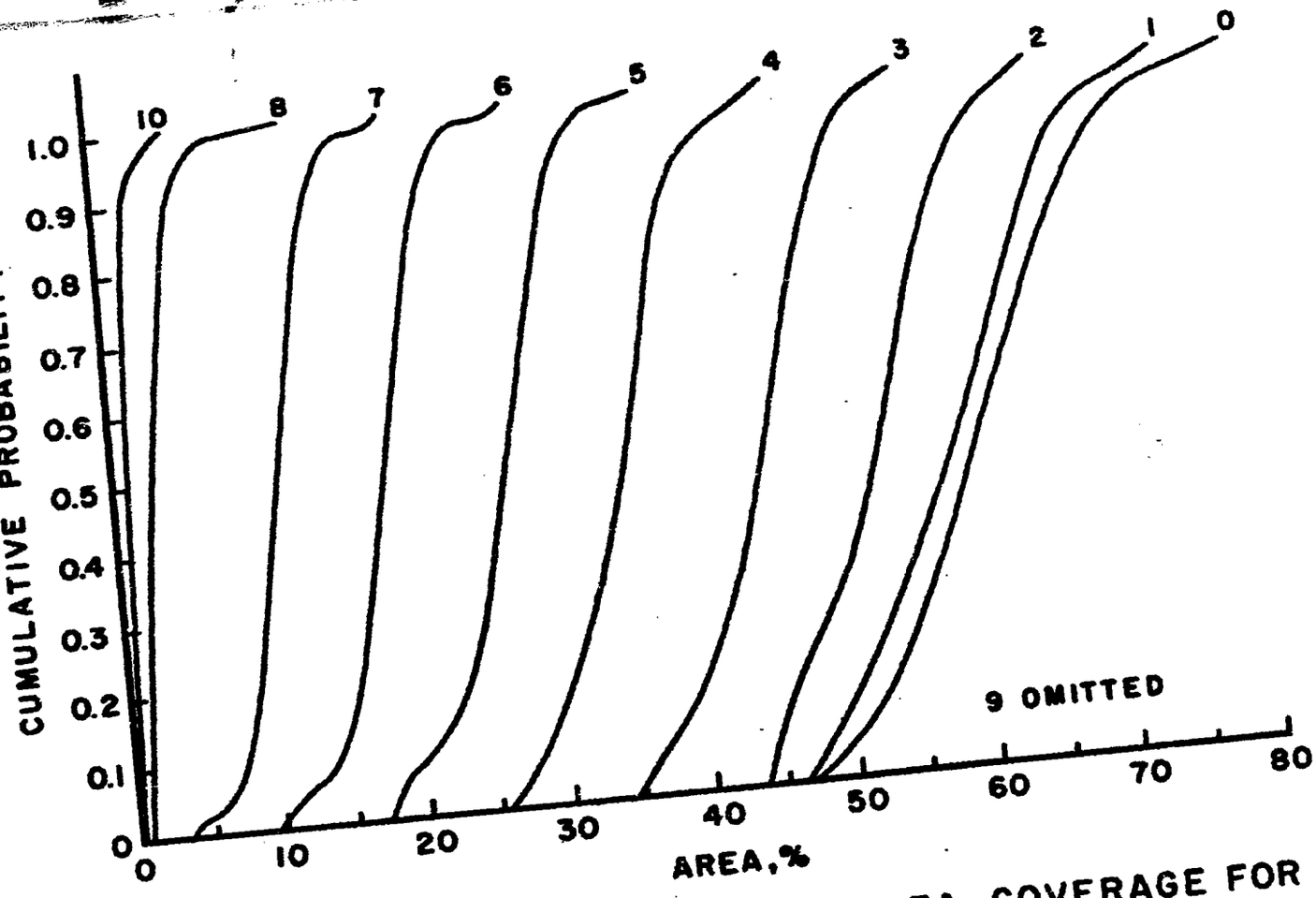

CUMULATIVE PROBABILITY OF AREA COVERAGE FOR SYSTEMATIC DISPLACEMENT OF TARGET AIM POINT

FIGURE 9

FIGURE 10

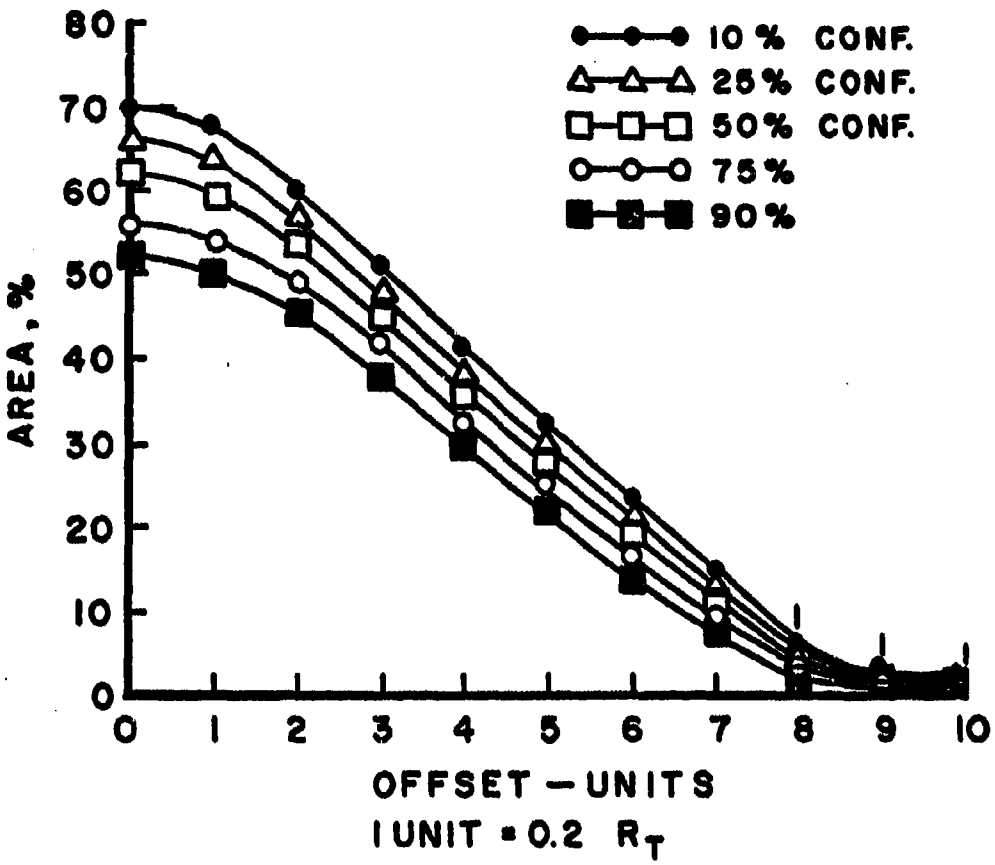

AREA COVERAGE AS A FUNCTION OF DISPLACEMENT OF TARGET AIM POINT

is approximately 15%, and hence for smaller bias, the correction is quite insignificant. It must be again pointed out that the foregoing correction is based upon the observations of one pair of parameters. A larger set of parameters must be considered before general conclusions can be drawn with a high degree of certainty.

One conclusion inferred from the foregoing observation is that for multiple firings on an area target, the accompanying target acquisition problem is not of major significance, since minor inaccuracies in the target location will not significantly affect the expected amount of destruction when all rounds are aimed at what is considered to be the target center.

SYMMETRICAL PROBLEM. The first study to be considered consisted of six rounds being aimed at the center of a circular target and distributed with a circular normal probability distribution about the aim point. Standard deviations equal to one-half and three-fourths of the target radius were used with a larger variety of effects circles. (Nickel, J. A., Palmer, J. D., Battlefield Simulation for First Round Accuracy Requirements of Simultaneous Multiple Firings. Proceedings of Winter Convention on Military Electronics, IRE, 1963; Nickel, J. A., Palmer, J. D., Gajjar, J. T., Kern, F. J., and Williams, D. R. Battlefield Simulation for First Round Accuracy Requirements of Simultaneous Multiple Firings. Data Supplement No. 1. DA 34-031-AIV-679, 1107-5-6, January 8, 1963.)

In all cases considered, it was observed that the smaller standard deviation consistently yielded a greater statistical area coverage. In other words, for a given size of the component effects circle, the standard deviation of one-half the target radius gave a greater area coverage than did the larger standard deviation of three-fourths the target radius. A local minimum area coverage is to be had with a standard deviation of zero, in which case all effects components would lie on top of each other, giving a total effective area equivalent to that produced by a single component.

Consider the statistical area coverage as a function of the standard deviation of delivery, σ, as well as the radius of the effects circle component, r. Notationally, this will be written as $A(\sigma, r)$. From the remarks of the preceding paragraph one observes that

$$A(0, r) < A(0.5, r) \qquad r < 1$$

$$A(0.75, r) < A(0.5, r) \quad .$$

Since σ can be varied continuously, it is reasonable to surmise that the area function also varies continuously. One now concludes from the mean value theorem of differential calculus that the area function achieves an expected maximum value for some σ in the neighborhood of $\sigma = 0.5$ for each value of r. The associated values are yet to be approximated by simulation studies. A fundamental conclusion to be drawn from these observations is that for a given size of effects components, there is a critical value for the standard deviation of delivery which will yield a maximum area coverage at a given statistical level, when the aim point is the target center. Figure 2 illustrates this fact by exhibiting a random delivery pattern, delivered with standard deviation of (a) $\sigma = 0.5$ and (b) $\sigma = 1.0$. In Figure (2a) there is considerable overlapping of lethality components. In Figure (2b) two of the lethality components are so far removed from the target center that no damage to the target is experienced by them and are not recorded in the figure.

A second observation based upon this modeling is that for a given number of effects components, the total effects or area coverage as measured on the simulator, increases with an increase in r, the radius of the component circles. However, an increase in r is accompanied with an increase in the areas shared by two or more components. This effect is illustrated in Figures 3a and 3b. These figures are composites showing the effect of distributing six rounds (lethal components) about the center of the target with $\sigma = 0.5$. The shaded set of circles correspond to an $r = 0.25$ whereas the larger boundary about these shaded circles correspond to $r = 0.5$.

From a tactical point of view, a weapon is most effective if it deploys to a given target only the minimum quantity of casualty producing material. Using this as a basis, it is proposed that an index of efficiency E, can be determined by

$$E = \frac{\text{Expected Target Area Coverage}}{\text{Theoretical Area Coverage}} \quad .$$

Figure 2a

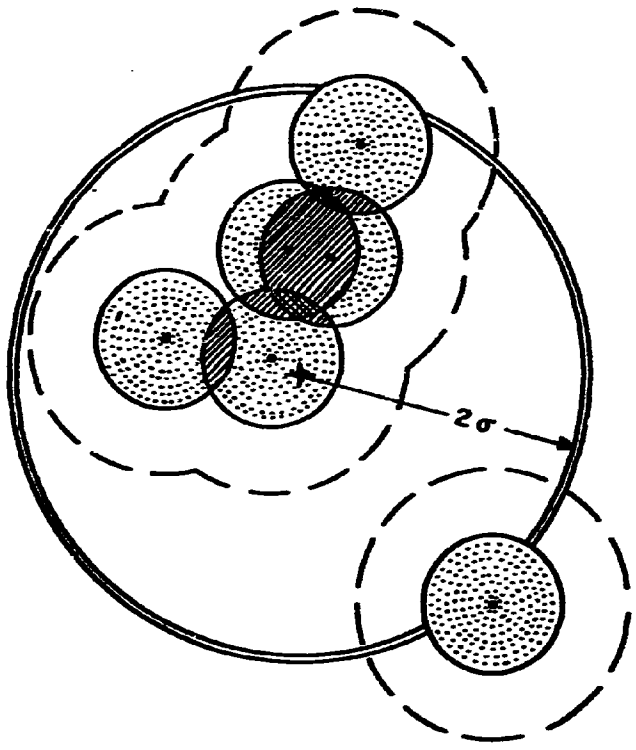

$\sigma/R_T = 0.5$

Figure 2b

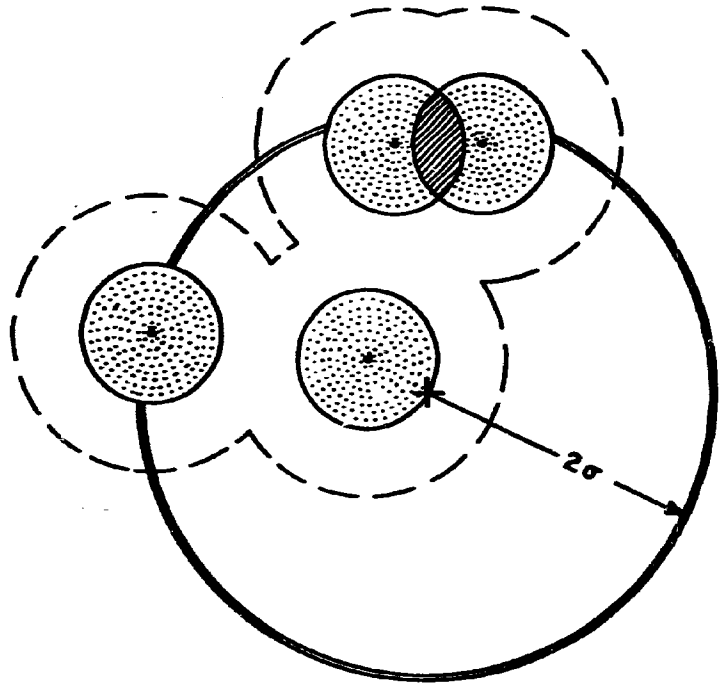

$\sigma/R_T = 1.0$

Two Random Distribution Patterns for a Six Round Salvo
($R_D/R_T = 0.25$ and $\sigma/R_T = 0.5$ and 1.0)

Figure 3a

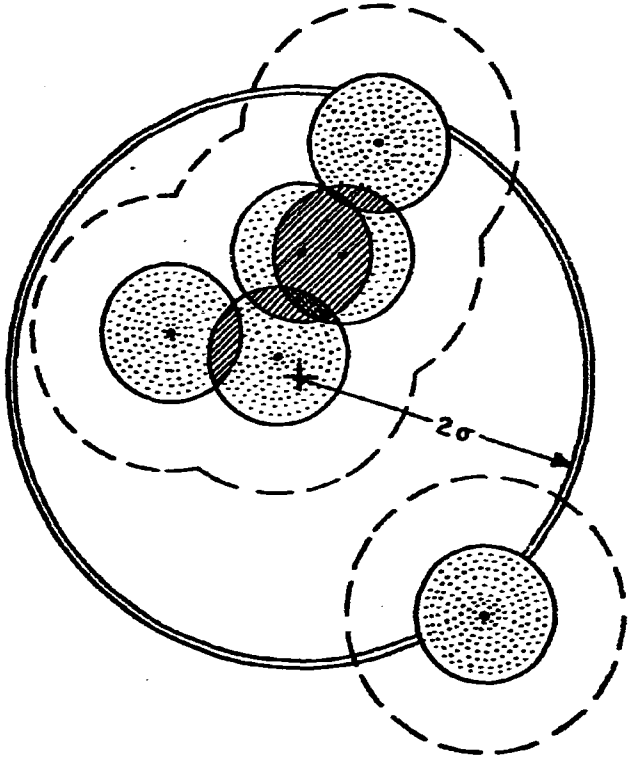

Figure 3b

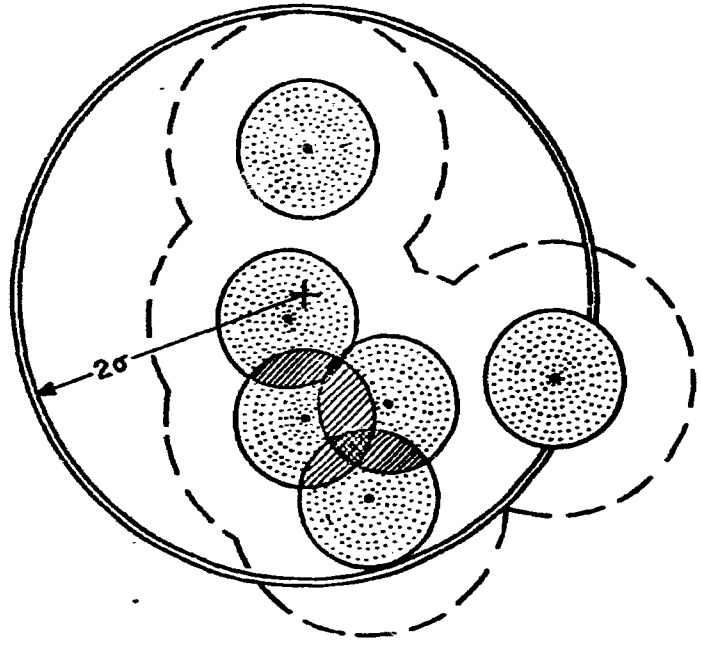

Two Random Distribution Patterns for a Six Round Salvo (σ/R_T = 0.5 and R_D/R_T = 0.25 and 0.50)

Figure 3a

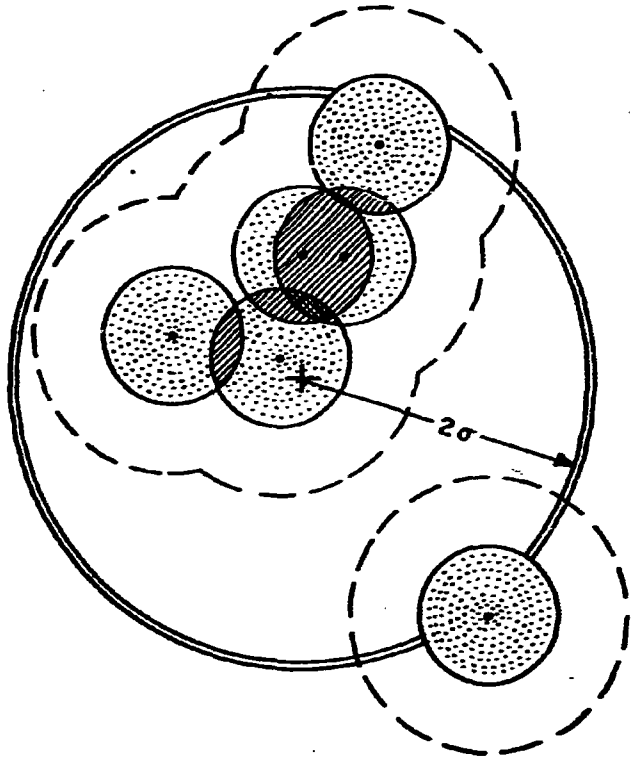

Figure 3b

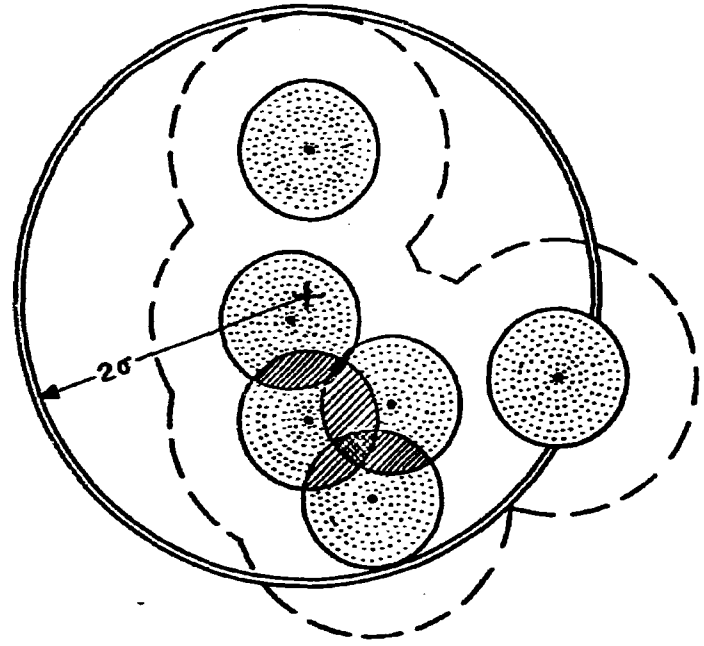

Two Random Distribution Patterns for a Six Round Salvo (σ/R_T = 0.5 and R_D/R_T = 0.25 and 0.50)

The Theoretical Area Coverage in the formula is defined as the total area that could be covered by the casualty producing material if it were distributed uniformly. This value, the Theoretical Area Coverage, may exceed the total area of the target. If A_L is the effects area produced by one component, then NA_L is the Theoretical Area Coverage, N being the number of effects areas used.

Defining efficiency as above, it is readily observable its efficiency decreases with an increase in the size of the effects components for a given number of components. The dependence on the standard deviation of the distribution again enters in with an apparent maximum again somewhere near $\sigma = 0.5$. This criteria of efficiency no longer demands extreme accuracy. The classical phrase "don't shoot until you see the whites of their eyes," is in general not applicable, excepting certain limited tactical situations.

At all levels of significance and for all σ, the efficiency curves appear to approach each other asymptotically for large component radii, r. Further, it should be observed that the limit value for the efficiency index on increasing r is 0. Figures 4 and 5 indicate the efficiencies for $\sigma = 0.5$ and $\sigma = 0.75$ respectively. From these curves, the following qualitative information is evident. First, the efficiency increases with a decrease in the level of assurance demanded. For small r and large σ there seems to be an achievable maximum of efficiency obtainable. This may, however, be an apparent condition peculiar to the particular sample set used. Further investigation is needed on this point. A flow chart describing the proposed investigation on the SADI Mark IV is found in Figure 6.

A conjecture resulting from these observations is that the efficiency can be increased by reducing the size of the effects circles to a critical size dependent upon the target size and the standard deviation of delivery σ. This implies an entirely new concept for matched weapons systems.

LOGISTICAL IMPLICATIONS. For tactical neutralization of destruction of area targets, a number of tentative conclusions can be formulated in light of the foregoing observations. If it is desirable to strike the target without forewarning, several features need to be considered. A single round could be used, but in such situations the effects of bias and delivery errors play a major role (Nickel, J. A.,

FIGURE 4

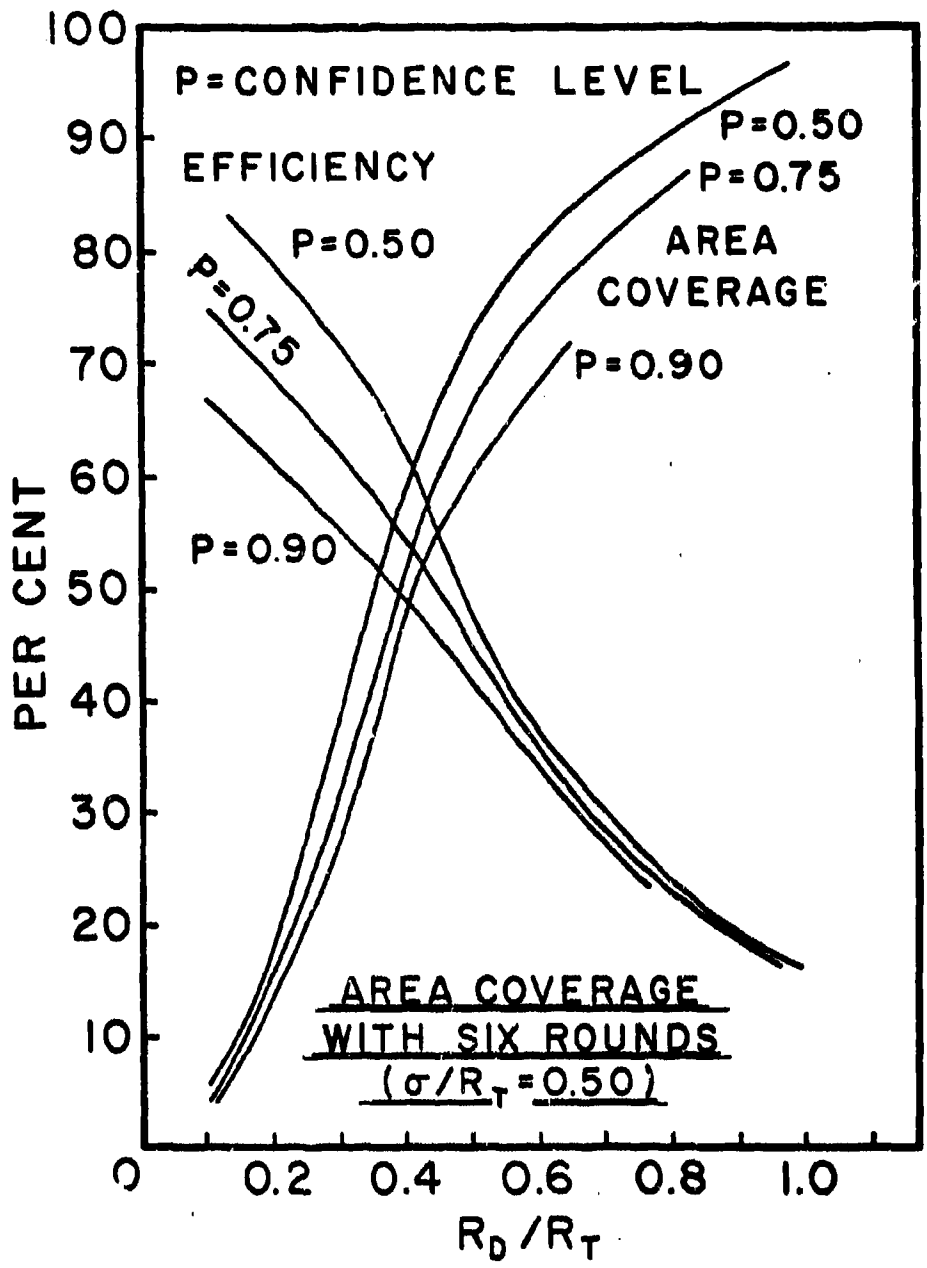

Area Coverage and Efficiency with Six Round Salvo ($\sigma/R_T = 0.50$)

FIGURE 5

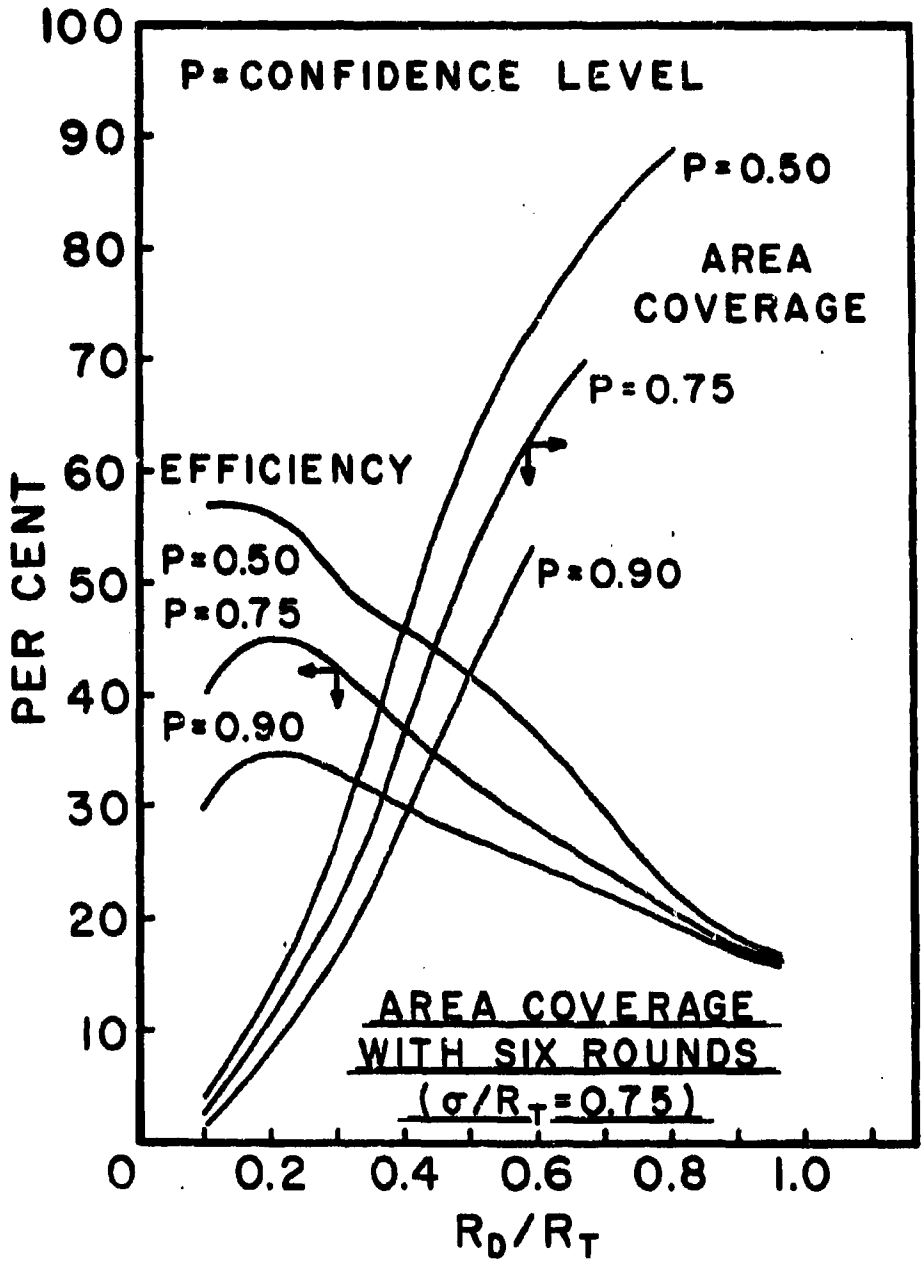

Area Coverage and Efficiency with Six Round Salvo ($\sigma/R_T = 0.75$)

FIGURE 6

Flow Chart for Sampling the Optimum Number of Rounds

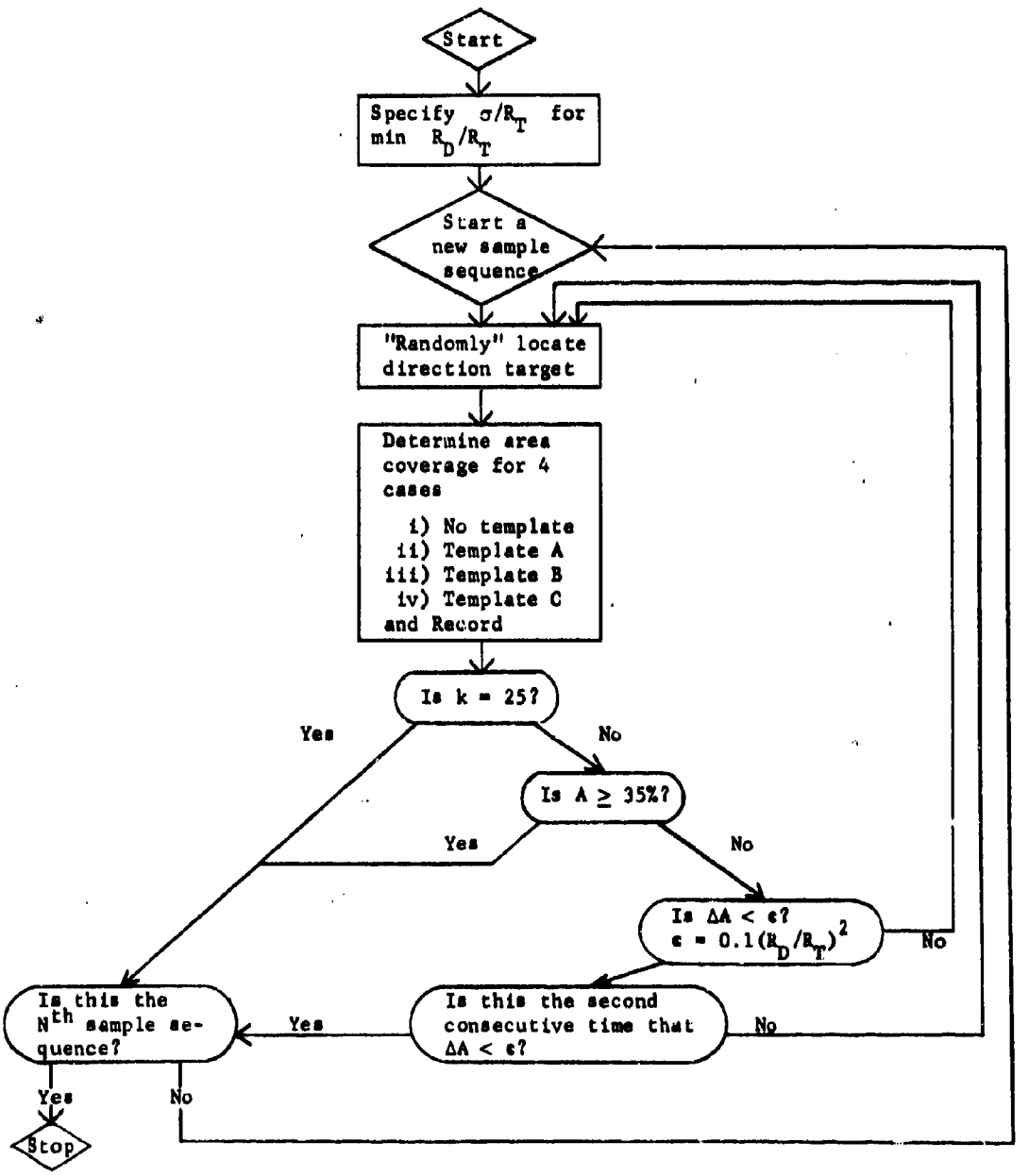

Palmer, J. D. Nomograph for the Determination of the Common Area of Intersection of Two Distributed Circles, DA 34-031-AIV-679, 1107-5-9, March, 1964.) in the relative effectiveness of that round, that is, target location problems are of paramount importance.

As an alternate approach, multiple rounds, each with a smaller effect pattern can be employed. In such a deployment of munitions, the effects of bias (if not too great) are minimized. Furthermore, the efficiency of effective area coverage can be increased for a suitable matching of effects radius and standard deviation of delivery to the target radius.

An immediate implication is that an effective weapons system to be employed against area targets for which protective procedures can be affected, such as mobile targets, personnel, etc., are those which can deliver a number of rounds, each with a small effects radius. The effectiveness of the system is optimized and does not require excessive accuracy. Such weapons presumably would include small caliber cannons, rocket launchers, and mortars, with a variety of warheads from HE to flame and other incendiary devices. Stated another way, minor inaccuracies in the location of a target under the fire of a volley will not significantly affect the expected amount of destruction.

Unloading a volley on a target before protective measures can be undertaken, may be tactically more efficient than attempting to zero in on a target by successive firings and corrections. Not only does the zeroing give forewarning, but increased accuracy in the knowledge of target location is not found. As an illustration consider the problem of using two rounds to bracket the target and the third for effect. First, in order to assure equivalent ballistic trajectories, missiles of the same size and mass must be used, and hence two rounds are wasted. To further assess the consequences of bracket firing, suppose the first round is fired short (deliberately), by an amount S. Due to errors inherent to the system, the round lands at P_2 instead of P_1. For symmetrical bracketing, Figure 7, the second round is aimed at P_3, a point symmetrically located with respect to the target point T. If P_1 had coordinates (0, -s), then P_2 has coordinates (-x, -y-s) where x and y are distributed by the appropriate error ellipse of the weapon. The intended coordinates of P_3 are (x, y + s), but in actuality the aim

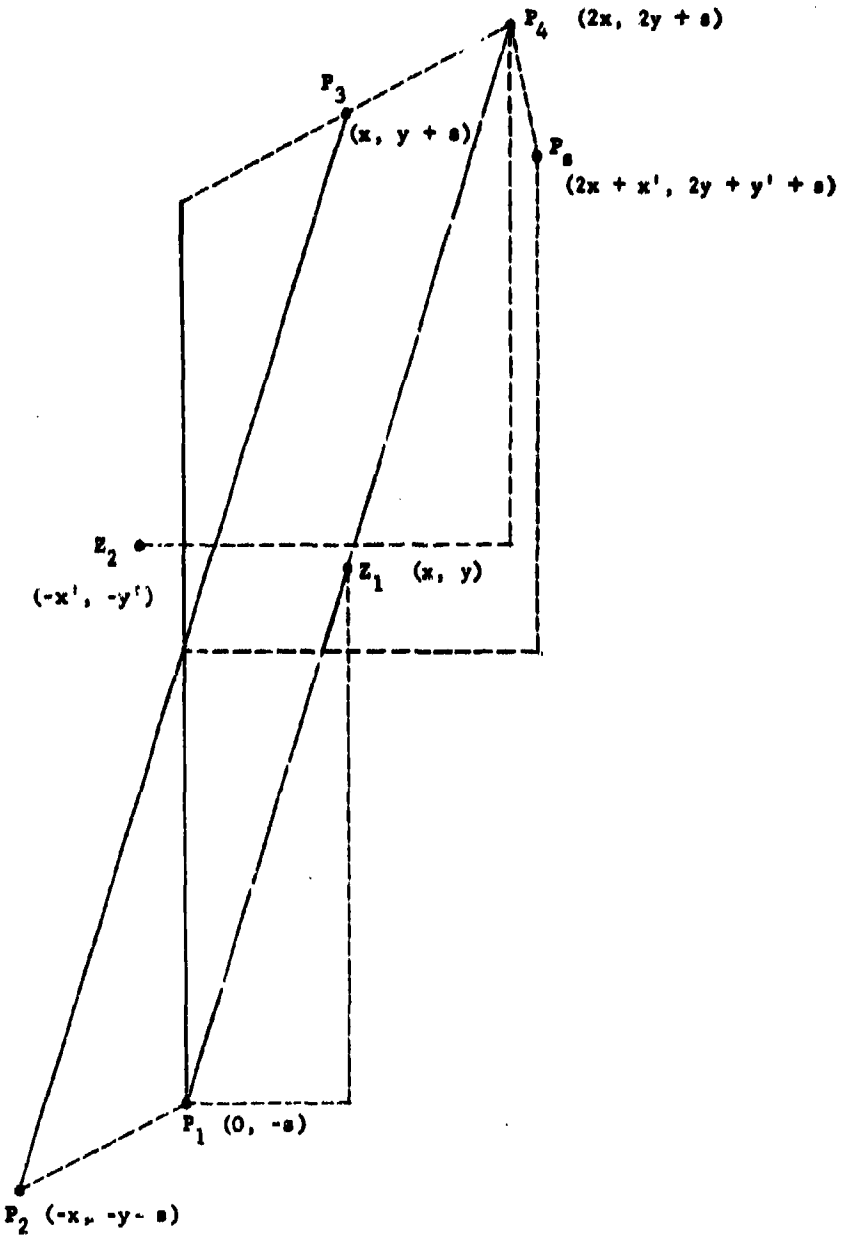

FIGURE 7

point is at P_4 with coordinates (2x, 2y + s). The second round actually aimed at P_4 lands at a point P_5 with coordinates (2x + x', 2y + y' + s) when x' and y' are again distributed according to the error ellipse of the weapon. From the coordinates of P_2 and P_5, the observed burst points, corrections are calculated for determining the target location T. The correction is applied either to the coordinate P_2 or P_5 where in actuality it should have been and actually is applied to the unknown coordinates of point P_1 and P_4. If the correction is applied to P_2, the aim point, Z_1, has coordinates (x, y), whereas if the correction is applied to P_5, the aim point, Z_1, has coordinates (x', y'). This is interpreted to being equivalent that the weapon can now "know" the location of the target to within the probability distribution of the weapon under bracket fire techniques, and hence in firing for effect, the location of the third round be distributed about the target with a probability distribution with twice the variance of the weapon.

It should be observed that successive rounds fired at the target without further correction will be distributed about an aim point offset from the target in some direction. This offset is an example of the unknown bias in the delivery of munitions. This further emphasizes the desirability of multiple small round firings in order to take advantage of insensitivity to bias in delivery effectiveness.

Manpower requirements and other aspects of logistical support, point to other desirable features of such systems. The importance of such consideration has been noted many times and has been particularly well-stated by Marshak and Mickey (Rand Corporation) when commenting on the optimal choice for weapons when they said,

> "We want to choose a weapon system that, subject to a given cost constraint, will maximize the mathematical expectation of a military utility (probability of victory)."

The foregoing model is based on the correlation of probability of victory to the target area coverage. Some further comments on the nature of cost constraints have been briefly considered by Nickel and Palmer

(Methodology Utilized in the Determination of Weapons System Accuracy Requirements, Proceedings of the Winter Convention on Military Electronics, IEEE, 1964.).

APPENDIX A

Data for studying the bias effects (lack of knowledge concerning target center) on a sampling distribution of a composit of N-effects patterns have been taken on the SADI Mark IV. A flow chart exhibiting the basic data taking procedure is presented in Figure 1. The data have been subsequently reduced to cumulative probability curves by means of the movement generator technique discussed in this paper. All parameters are normalized with respect to the radius of the target.

A preliminary analysis using six rounds distributed with a normalized standard deviation of 0.5, and a destructive component radius of 0.45 is shown in Figure 8. This curve exhibits the relative change in the average area of destruction for each displacement from the center and for which it was observed that small displacements had little effect on the area coverage.

In order to get a more detailed view of the results, another set of patterns was investigated. During this investigation the distribution error was specified in terms of circular probable error (CPE = 1.177σ), but the same circles of destruction ($R_D/R_T \cong 0.45$) were employed as in the preliminary investigation. Figure 9 exhibits the family of cumulative probability curves as functions of area coverage resulting from the set of more than 50 patterns. Each curve in the family specifies the displacement of intended aim point in terms of 0.2 of the target radius, i.e., each curve represents a shift of aim point by 20% of the target radius from the target center.

In considering these several curves, their similarity and ordering is as would be expected. It must be pointed out, however, that for displacements less than 30% of the target radius, the fall off in area coverage is small. To further clarify this point, Figure 10 illustrates the area coverage as a function of the aim point displacement for confidence levels of 10, 25, 50, 75, and 90%.

APPENDIX B

Data for determining the optimum number of rounds to be deployed against a target was obtained on the SADI Mark IV according to the scheme exhibited in the flow chart Figure 6. At the time of writing this report all of the desired data had not been generated and the analysis is not complete. Several sizes of destructive or lethal components and dispersion errors are under investigation with the hope of determining optimum parameters.

THE VARIABILITY OF LETHAL AREA

Bruce Barnett
Data Processing Systems Office,
Picatinny Arsenal, Dover, New Jersey

The purpose of this paper is to describe a statistical model that estimates the variability of lethal area when fragment mass and initial fragment velocity are allowed to randomly vary between specified limits. Prior to this development, the general lethal area equation will be derived to illustrate the nature of the equations involved and to show the assumptions made in its derivation.

The lethal area concept is usually applied to anti-personnel munitions that are of a fragmenting nature such as bombs, mines, grenades and shells. The lethal area is a number that yields a measure of effectiveness of the particular munition under investigation - the larger the lethal area the more effective the weapon. The usual mathematical definition is the following: "The lethal area of a weapon is that number which when multiplied by a constant density of targets will yield the expected number of incapacitations". Figure 1 illustrates a typical situation.

Shown here is a shell bursting over some area A containing N targets, uniformly distributed. Let h be the height of the shell at detonation, ω its angle of fall, and θ_1, θ_2 the zone angles within which fragments are ejected. These fragments are to incapacitate as many targets as possible. Let the position of each target temporarily be known, the coordinates of the ith target being (X_i, Y_i). The density of targets ρ_T is the ratio N/A. The lethal area, (A_L), can be written as

$$A_L = \frac{A}{N} E[N_c] \tag{1}$$

so that multiplying A_L by ρ_T yields $E[N_c]$ according to the definition. Here

N_c = random variable = the number of casualties

and $E[N_c]$ is the expected value of N_c.

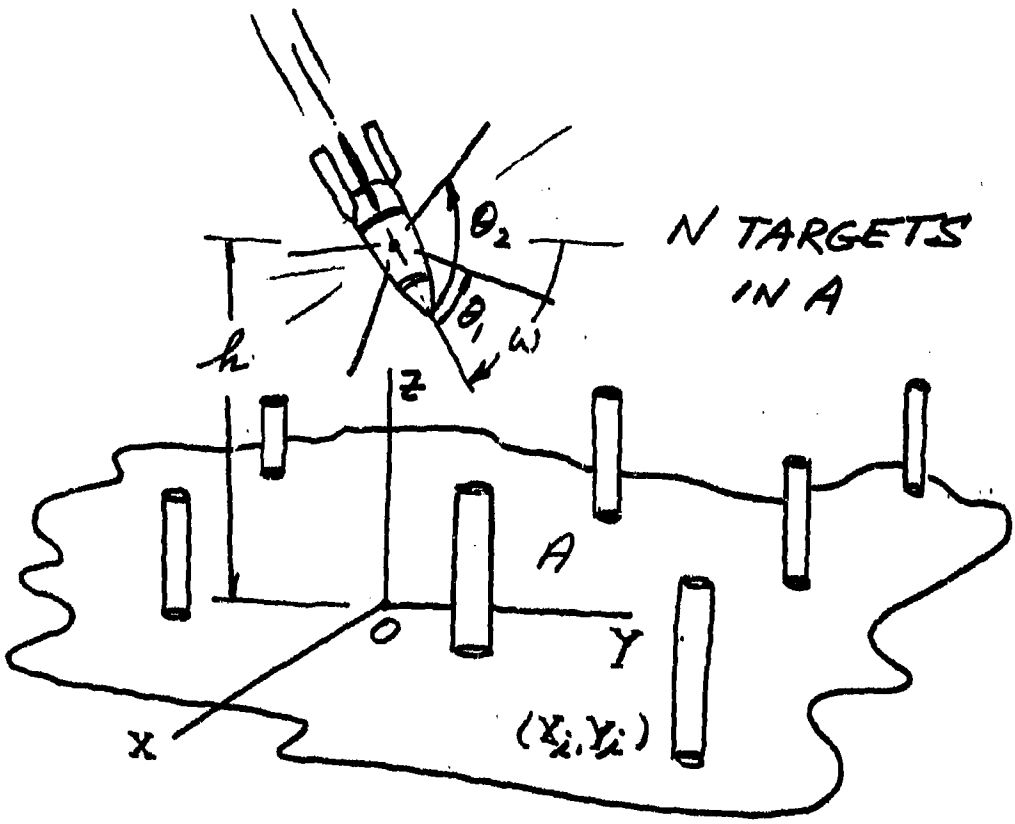

FIGURE 1

The lethal area equation is not useable, however, in the general form of equation (1). To refine this equation let

Y_i = random variable = 1 if the ith target is incapacitated

= 0 otherwise .

The number of casualties can, therefore, be expressed as

$$N_c = \sum_{i=1}^{N} Y_i \quad . \tag{2}$$

Defining P_{K_i} as the probability that $Y_i = 1$, it follows that

$$A_L = \frac{A}{N} \sum_{i=1}^{N} E[Y_i] = \frac{A}{N} \sum_{i=1}^{N} P_{K_i} \quad . \tag{3}$$

Refining the lethal area equation further let

N_i = random variable = number of fragments striking the ith target

P_{HK_i} = random variable = probability that any one fragment striking the ith target incapacitates that target

$X_j^{(i)}$ = random variable = 1 if the jth fragment to strike the ith target is the first fragment to incapacitate that target = 0 otherwise.

Expressing Y_i in terms of the $X_j^{(i)}$'s, yields

$$Y_i = \sum_{j=1}^{N_i} X_j^{(i)} \quad . \tag{4}$$

Applying equation (5),

$$E[Y_i] = E[E[Y_i \mid P_{HK_i}, N_i]] \tag{5}$$

it follows that

$$E[Y_i] = E[E[\sum_{j=1}^{N_i} X_j^{(i)} \mid P_{HK_i}, N_i]]$$

$$= E[\sum_{j=1}^{N_i} \cdot \text{Prob}\left\{ X_j^{(i)} = 1 \right\} \mid P_{HK_i}, N_i]$$

$$= E[\sum_{j=1}^{N_i} (1-P_{HK_i})^{j-1} P_{HK_i}] \quad . \tag{6}$$

Summing the geometrical series in the latter equation produces

$$E[Y_i] = E[1 - (1-P_{HK_i})^{N_i}] \quad . \tag{7}$$

Using the Poisson distribution as an approximation to the binomial, equation (7) becomes

$$E[Y_i] \doteq E[1-e^{-N_i P_{HK_i}}] \quad . \tag{8}$$

This equation is further approximated as follows

$$E[Y_i] \doteq 1 - e^{-E[N_i]\ E[P_{HK_i}]} \quad . \tag{9}$$

This is equivalent to expanding $1-e^{-x}$ about the point $E[X]$, $X = N_i P_{HK_i}$ and using the first term.

Letting

(10) $$N_i = \rho_i \cdot A_{P_i}$$

where

ρ_i = random variable = density of fragments at the ith target

A_{P_i} = random variable = presented area of the ith target

then

(11) $$E[N_i] = E[\rho_i] \; E \; [A_{P_i}]$$

so that finally

(12) $$A_L = \frac{A}{N} \sum_{i=1}^{N} E\,[Y_i] = \frac{A}{N} \sum_{i=1}^{N} 1 - e^{-E[\rho_i]E[A_{P_i}]\,E[P_{HK_i}]}$$

This equation can be used when the targets are at predetermined positions and should yield a good estimate of the lethal area. This is so, because the known target locations enable reasonable estimates for $E[\rho_i]$, $E[A_{P_i}]$, and $E[P_{HK_i}]$ to be assigned. Data for P_{HK_i}, the probability that a random fragment striking the ith target incapacitates that target, can be obtained experimentally depending in part on the mass and striking velocity of the fragment.

In a tactical situation, however, the target coordinates are rarely known and it is desirable to obtain an analogous lethal area equation to handle this typical case. To accomplish this, let

$E[Y_i] = P_{K_i}$ where now P_{K_i} is a function of (X_i, Y_i), X_i, Y_i being random variables defining the coordinates of the ith target.

In this case

$$E[Y_i] = E[E[P_{K_i} \mid X_i, Y_i]]$$

$$(12) \qquad = E[P_K(X_i, Y_i)]$$

$$= \iint_A P_K(X_i, Y_i)\, f(X_i, Y_i)\, dX_i dY_i \quad .$$

Since a uniform density of targets is assumed

$$(13) \qquad f(X_i, Y_i) = \frac{1}{A}$$

so that

$$(14) \qquad E[Y_i] = \frac{1}{A} \iint_A P_K(X_i, Y_i)\, dX_i dY_i \quad .$$

Substituting this equation in the lethal area equation produces

$$(15) \qquad A_L = \frac{A}{N} \left(\sum_{i=1}^{N} E[Y_i] \right) = \frac{A}{N} \cdot \frac{1}{A} \sum_{i=1}^{N} \iint_A P_K dX_i dY_i .$$

Each of these N integrals are identical, so that

$$(16) \qquad A_L = \frac{A}{N} \cdot \frac{1}{A}\, N \iint_A P_K dX dY = \iint_A P_K dX dY \quad .$$

This is the usual lethal area equation. It can be evaluated by judiciously selecting various points in the groundplane, evaluating P_K at these points and numerically obtaining the value of the integral.

This equation, however, does not allow for any of the parameters to be randomized; that is, it cannot be used directly to ascertain the variability of lethal area. Before describing the statistical model, it is worth-while to state several reasons for analyzing the variability of lethal area. Some are:

1. A quantitative measure of the variability of lethal area due to specific parameters is provided. A possible application of this is for establishing tolerances. For example, there are controlled and un-controlled variables associated with a shell. Fragment breakup and explosive weight being somewhat controlled, burst height (for an air burst) and angle of fall being uncontrolled. Tendencies exist to maintain tight tolerances on variables that can be controlled even at more expense. In lieu of the variability induced by parameters that cannot be controlled, these possibly tight tolerances may possibly be relaxed without significantly affecting the overall effectiveness. Conversely, variability can point out those parameters that need be better controlled to assure more uniform effectiveness.

2. Variability affects the design of optimum rounds. Briefly, rounds should not be designed to produce high effectiveness under ideal burst conditions, but decrease sharply in effectiveness when variations from these ideal conditions are present.

3. Variability analysis permits probabilistic bounds to be placed on the number of casualties. For example, it may be advantageous in some situations to have a minimum assurance level for incapacitating at least P% of the targets.

To study the variability of lethal area in the most general case would first necessitate establishing the independent random variables and those quantities in the lethal area equation that depend on them. For example, one may write

$$(17)\quad A_L = \int\int_A \left(1-e^{-\rho(m(\theta, V_o), h, \theta_1, \theta_2, \omega)}\, A_p(h) P_{HK}(m, V_o, \theta, a)\right) dA .$$

Here, it is assumed that the density ρ of fragments depends on the mass breakup, which in turn depends on the intial fragment velocity V_o, and the angle measured off the nose of the shell. The burst height,

spray angles and angle of fall also affect the density of fragments at a selected target. Similarly, for A_p and P_{HK}. As a first analysis, however, several simplifying assumptions will be made. Some of the assumptions are somewhat unrealistic; for example, the drag coefficient α is assumed independent of the fragment mass. It is for this reason that the results from this analysis should not be strictly interpreted. However, what may be of importance is to see how well the statistical model estimates the variability, for then in the favorable case, the possibility exists of generalizing the model to include more realism.

The assumptions used in this analysis are listed below.

1. Only the fragment mass m and initial fragment velocity V_o will be considered as random variables. This means that the burst height, angle of fall, weight of fragmenting material, etc., are precisely known in advance.

2. A 90° fall angle is assumed.

3. The fragments are all of the same mass and initial velocity, although the particular m and V_o are random variables.

4. m, V_o are independent random variables, both uniformly distributed. α, the drag coefficient is independent of both m and V_o.

5. Inverse square law for density is assumed.

6. A_p, the presented area of a target is a known function of h and R (R is the ground range to the target under consideration).

7. P_{HK} is specified by an exact formula given as a function of m and V, the striking velocity.

8. The maximum effective range of a fragment depends on m and $E[V_o]$.

As a result of these assumptions, one may write

$$A_L = 2\pi \int_0^{R_{max}} \left(1 - e^{-\rho(m)\cdot E[A_p]\cdot P_{HK}(m,V)}\right) R\,dR \quad . \tag{18}$$

This is the lethal area equation written in polarcoordinates, making use of the fact that $\omega = 90^{o}$ yields radial symmetry. The density ρ is

$$\rho = \frac{\omega}{2\pi m r^{2}[\cos\theta_{1} - \cos\theta_{2}]} \tag{19}$$

where r is the range from the burst point to the target under consideration and ω = weight of fragmenting material. The relation

$$N_{f} = \frac{\omega}{m} \tag{20}$$

N_{f} being the number of fragments, was used in obtaining equation (19).

$A_{p} = f_{1}(h, R)$ a known quantity

$P_{HK} = f_{2}(m, V)$; $V = V_{o}e^{-aRm^{-1/3}}$

A typical plot of P_{HK} is shown in Figure 2.

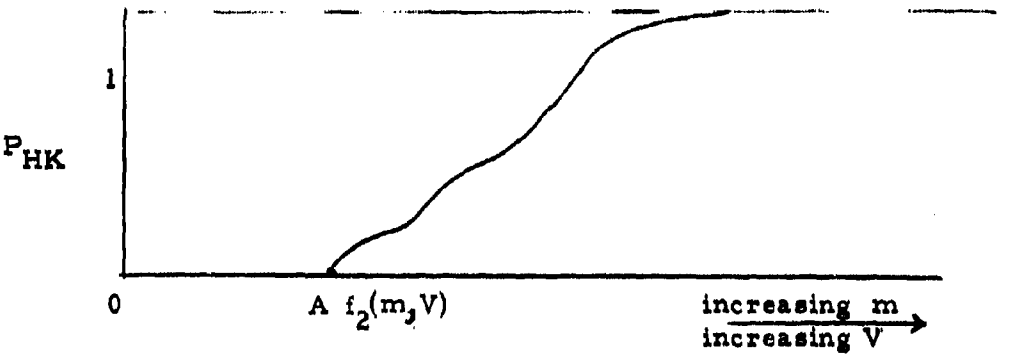

FIGURE 2

Note that a certain cut-off point A exists such that for $f_2(m,V) \leq A$, $P_{HK} \equiv 0$. P_{HK} is non-differentiable at this point A.

To obtain the variability of lethal area, it is first convenient to reduce the integral form of the lethal area equation to one that is purely algebraic. This is accomplished by selecting a numerical scheme to evaluate the integral. In this case the Trapezoidal rule was used. Thus

$$A_L = 2\pi \Delta R \sum_{i=1}^{M} R_i P_{K_i} \quad . \tag{21}$$

Here it is assumed that $R_o = 0$ and m is so large that

$$P_{K_M} = P_K(R_M) = 0 \quad . \tag{22}$$

Clearly

$$E[A_L] = 2\pi \Delta R \sum_{i=1}^{M} R_i \, E[P_{K_i}] \tag{23}$$

and

$$V[A_L] = 4\pi^2 (\Delta R)^2 \; V[\sum_{i=1}^{M} R_i \, P_{K_i}] \quad . \tag{24}$$

The latter equation can be put in the more convenient form by employing equation (25).

$$V\left[\sum_{i=1}^{M} R_i P_{K_i}\right] \equiv E\left[\sum_{i=1}^{M} R_i P_{K_i} - E\left[\sum_{i=1}^{M} R_i P_{K_i}\right]\right]^2$$

(25)

$$= \sum_{i=1}^{M} R_i^2 V[P_{K_i}] + 2 \sum_{i<j} R_i R_j \left(E[P_{K_i} \cdot P_{K_j}] - E[P_{K_i}] \cdot E[P_{K_j}]\right) .$$

Since $V[P_{K_i}] = E\left[\left[P_{K_i} - E[P_{K_i}]\right]^2\right.$

equations (23) and (24) require only that expressions of the form

$$E[P_{K_i}] \ , \ E[P_{K_i}^2] \ , \text{ and } E[P_{K_i} \cdot P_{K_j}] \quad \text{to}$$

be evaluated to ascertain the end result. This is described next.

Following Reference 1 a logical method of proceeding would be to expand P_{K_i} in a Taylor series in the independent random variables m and V_o.

Thus

$$P_K = P_K + P_{Km}(m-\overline{m}) + \rho_{KV_o}(V_o-\overline{V}_o)$$

$$+ \frac{1}{2!}\left(P_{Kmm}(m-\overline{m})^2 + 2\,P_{KmV_o}(m-\overline{m})(V_o-\overline{V}_o)\right.$$

(27)

$$\left. + P_{KV_oV_o}(V_o-\overline{V}_o)^2\right) .$$

In the right members of (27) P_K, $P_{Km} \equiv \partial P_K/\partial m$, ..., are each understood evaluated at the point $(\overline{m}, \overline{V}_o)$.

Here the subscript i has been omitted. Unfortunately a deficiency in the above expansion exists in that P_K may take on negative values and thus becomes meaningless. This is illustrated in Figure 3.

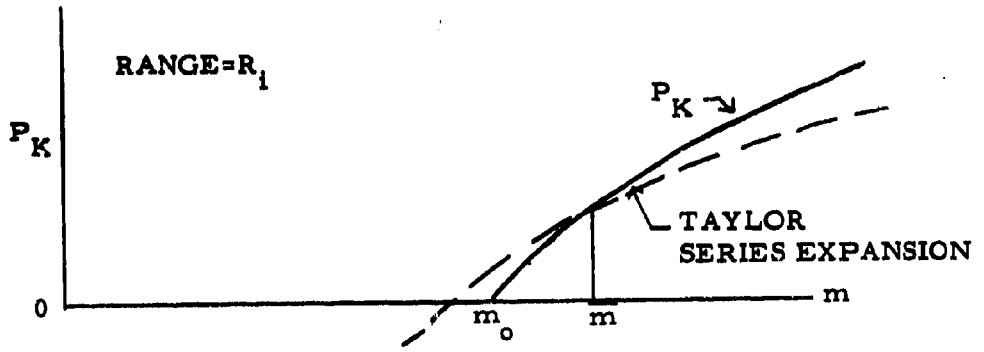

FIGURE 3

In addition a second deficiency results when using this expansion in that for any given initial velocity V_o there is a corresponding mass ($=m_o$) where P_K is non-differentiable. This arises from the point of non-differentiability in the P_{HK} equation which is subsequently carried through to the P_K equation. (By assumption (8) $E[V_o]$ will be used instead of the random variable V_o to determine m_o).

Both difficulties are overcome, however, if one forms two separate expansions for P_K, namely;

for $m \geq m_o$

$$(28) \qquad P_K = \sum_{n=o}^{2} \frac{1}{n!} \left((m-\overline{m}^*) \frac{\partial}{\partial m} + (V_o - \overline{V}_o) \frac{\partial}{\partial V_o} \right)^n P_K$$

for $m < m_o$

$$P_K \equiv 0$$

where for algebraic simplicity $\overline{m}^*$ is chosen by

$$\overline{m}^* = E\,[m \mid m \geq m_o(R)\,] \tag{29}$$

so that

$$E\,[m-\overline{m}^* \mid m \geq m_o(R)\,] = 0$$

since

$$E[Y] = E[Y \mid X < X_o\,] \cdot \text{Prob}\,\{X < X_o\} + E\,[Y \mid X \geq X_o] \cdot \text{Prob}\,\{X \geq X_o\}\,. \tag{30}$$

One may write for P_K

$$E[P_K] = (P_K + \tfrac{1}{2}\,P_{Kmm}\,E\,[m-\overline{m}^*]^2 + \tfrac{1}{2}\,P_{KV_oV_o}\,E\,[V_o-\overline{V}_o]^2 \mid m \geq m_o) \cdot \text{Prob}\,\{m \geq m_o\}. \tag{31}$$

Similarly

$$V[P_K] = E[\,[\,P_K - E[\,P_K]\,]^2 \mid m \geq m_o]\ \text{Prob}\,\{m \geq m_o\} \tag{32}$$

each term of which is easily evaluated.

The covariance terms are handled by expanding $P_{K_i}\ P_{K_j}$ about a selected point and formally taking the expected value of the product. For example

$$P_{K_i} P_{K_j} = (P_{K_i}[P_{K_j} + P_{K_j m}(m-\overline{m^*}) + \ldots]$$

$$+ P_{K_i m}(m-\overline{m^*})[P_{K_j} + P_{K_j m}(m-\overline{m^*}) + \ldots]$$

$$+ \ldots) \cdot \text{Prob} \left\{ m \geq m_o(R_j) \right\}$$

so that

$$E[P_{K_i} P_{K_j}] = P_{K_i} P_{K_j} + \ldots + P_{K_i m} P_{K_j m} E[m-\overline{m^*}]^2$$

$$+ \ldots) \cdot \text{Prob} \left\{ m \geq m_o \right\} .$$

For the uniform distribution

$$f(X) = \frac{1}{b-a}$$

it is easily verified that

$$E[X-\overline{X}] = 0$$

$$E[X-\overline{X}]^2 = \frac{(b-a)^2}{12}$$

$$E[X-\overline{X}]^3 = 0$$

$$E[X-\overline{X}]^4 = \frac{(b-a)^4}{80} .$$

Equations (23) and (24) are thus completely determined.

These equations were used to obtain numerical estimates for the variability of lethal area. These results were compared with a Monte

Carlo evaluation whereby m and V_o were sampled from their respective distributions. The results of the comparison are shown in Table 1.

TABLE 1

	$E[A_L]$	$\sigma[A_L]$
STATISTICAL MODEL	4519	178.9
MONTE CARLO MODEL	4516	179.8

% Difference in $E[A_L]$ = .06%

% Difference in $\sigma[A_L]$ = .50%

In ascertaining these results the following variances were assigned; $V[m]$ = .75 and $V[V_o]$ = 75, also 200 simulations were used in the Monte Carlo evaluation.

The next Table shows a comparison of $E[P_K]$ and $V[P_K]$ at selected ranges.

TABLE II

	$E[P_K]$		$V[P_K] \times 10^3$	
RANGE	M.C.*	S.M.	M.C.*	S. M.
10	.9366	.9370	.1572	.1658
20	.5482	.5491	.5372	.6667
30	.2967	.2974	.2839	.2958
40	.1736	.1740	.1068	.1112
50	.1103	.1105	.0429	.0447
100	.0222	.0222	.0011	.0012
200	.0028	.0028	0	0
270	.0008	.0008	0	0
300	.0004	.0004	.00001	.00001
370	0	0	0	0

*Based on a sample size of 100

A review of these results indicate that the statistical model does provide a good approximation to the variability of lethal area - a method which may possibly be generalized to include more realism in the model.

It is of interest to note that the covariance terms contributed as high as 87% of the total variance of lethal area. The final table also included for interest, shows the effect of step size used in the numerical integration scheme on the results.

TABLE III

	R = 5	R = 10	R = 20
$E[A_L]$	4554.	4519.	4304.
$\sigma[A_L]$	179.4	178.9	185.5

In summary, therefore, it is not the numerical results of this paper that should be emphasized, but rather the possible application of a straight-forward technique to a complex problem involving the variability of lethal area.

REFERENCE

1. Picatinny Arsenal Technical Report 2508, "Variability of Lethal Area", by Sylvain Ehrenfeld, February 1959.

DECISION PROCEDURE FOR MINIMIZING COSTS OF CALIBRATING LIQUID ROCKET ENGINES

Sidney H. Lishman and E. L. Bombara
Engine Program Office, Marshall Space Flight Center

SUMMARY: Prior to acceptance of a liquid rocket engine for use in Saturn vehicles, the average thrust of two consecutive tests without an intervening calibration must satisfy specification requirements. The contractor may recalibrate after the first and subsequent tests if he so chooses, based upon decision limits, until the above requirement is met.

This paper provides a method for calculating decision limits such that the total number of tests required for acceptance is minimized. The model for calculating the decision limit takes into account operational reliability and life of the engine, ratio of cost of testing to cost of an engine, and correlation between tests as a function of engine-to-engine and run-to-run variance components.

INTRODUCTION. One of the requirements for NASA acceptance of a Saturn vehicle engine is that the thrust averaged from two successive tests without an intervening calbration fall within specification limits. In the past, most engines were accepted from the contractor after three tests, but when the specification was recently tightened it was estimated that more than 50% of all engines would have to be tested at least four times prior to acceptance. Their increase in number of tests per engine represented an appreciable increase in costs.

This paper presents the results of a study made to determine what could be done to reduce acceptance testing costs when the specification limits are held constant.

DISCUSSION. Engine testing is conducted in accordance with the following ground rules until the engine meets acceptance requiremtns or until it is scrapped:

1. If thrust in a test following a calibration is outside certain decision limits, the engine is successively recalibrated and tested until thrust falls inside the decision limits.

2. If thrust in a test following a calibration is inside the decision limits, no changes are made to the engine and another test is conducted in an attempt to satisfy acceptance requirements.

3. If the average thrust from two consecutive tests without intervening calibration falls outside of specification limits, the engine is recalibrated, and the test cycle is repeated.

It should be pointed out that the value in using a procedure such as described below is greatest when specification limits are tight. If specification limits are very wide, there is not much point in using decision limits at all, because the need for recalibration becomes remote.

ILLUSTRATIONS. For the purpose of applications herein, the following assumptions were made:

1. The engine is always calibrated after the first test (due to high variability of thrust prior to the first calibration).

2. There is no bias introduced in calibrating the engine.

3. After the initial calibration, ability to recalibrate does not improve between tests.

4. Cost of calibration is negligible compared to cost of a test.

5. The engine is scrapped after N tests that do not satisfy the criterion for acceptance described above.

6. The engine-to-engine and run-to-run variance components, σ^2_{EE} and σ^2_{RR}, respectively, are known; the mean thrust is also known.

7. σ^2_{RR} is the same for all engines.

8. Engine-to-engine and run-to-run deviates are normally and independently distributed.

The models described below can easily be altered to change assumptions 1 through 5.

Two models are considered herein:

1. Assume the engine is scrapped after nine unsuccessful tests, and operational reliability = 1.0. Operational reliability is defined as one minus the probability of any failure (hardware, facility, human error) that causes a single additional test and calibration. Assume that the cost of scrapping an engine is equal to the cost of 40 tests.

2. Assume the engine is scrapped after 5 unsuccessful tests and operational reliability $\leq$ 1.0.

Common to all models generated under the above assumptions, we define the following probabilities (figure 1):

Let P(i) be the probability of thrust exceeding the decision limits in the i^{th} test.

Let $P(\bar{i})$ be the conditional probability that the mean thrust, $(X_i+X_{i+1})/2$, of the i^{th} and $(i+1)^{th}$ tests exceeds the specification limits.

It is assumed that P(i) is the same for all i, and that $P(\bar{i})$ is the same for all i. Assuming normality, P(i) and $P(\bar{i})$ may be calculated from the bivariate normal density as illustrated in figure 1.

P(i) and $P(\bar{i})$ may be obtained from equations (1), (2), (3) below by using any table of the bivariate normal distribution, such as reference (1). It is convenient to express the correlation coefficient as a function of the run-to-run and engine-to-engine variance components, because of the advantage gained by utilizing all pertinent data. From the appendix, the standard deviation of X_i is:

(1) $$\sigma_{X_i} = \sqrt{\sigma_{RR}^2 + \sigma_{EE}^2} \quad .$$

The correlation coefficient between X_i and $(X_i+X_{i+1})/2$ is:

Figure 1

BIVARIATE NORMAL PROBABILITIES

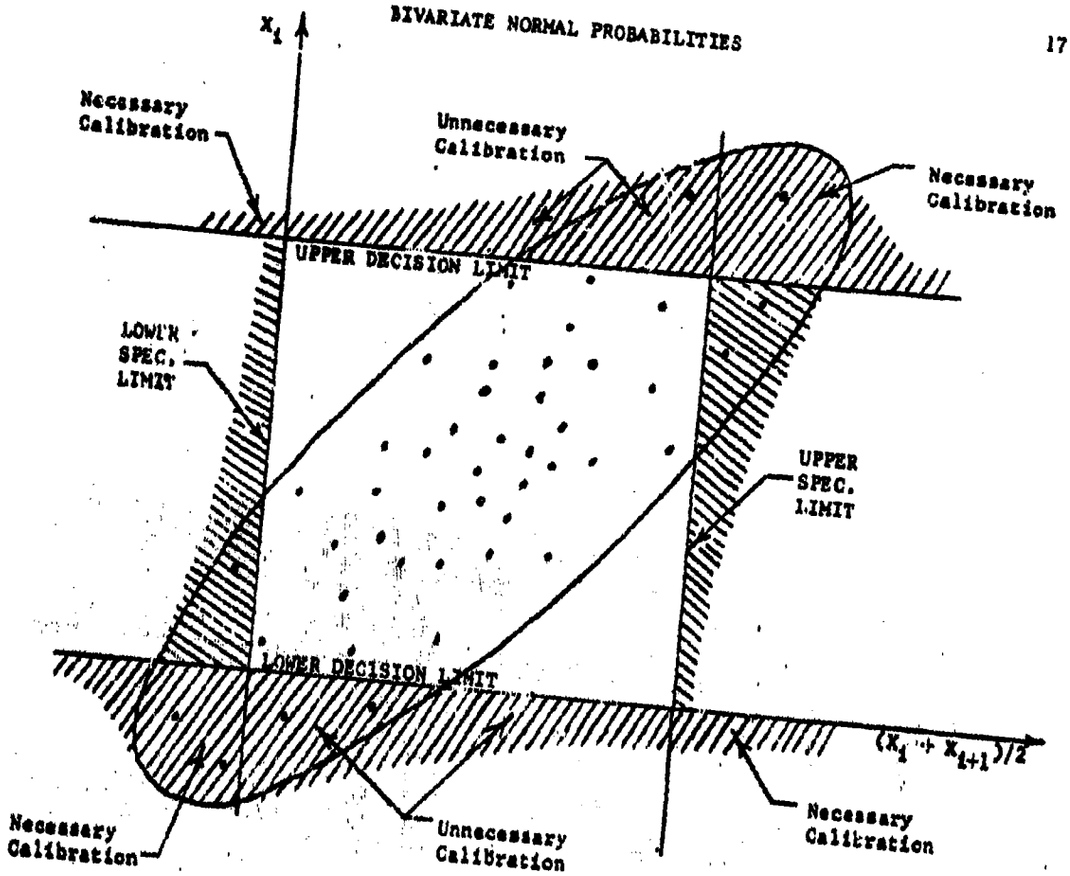

$P(1)$ =

$P(\bar{1})$ =

(2) $$\rho_{X_i \,,\, (X_i+X_{i+1})/2} = \sqrt{1 - \frac{\sigma_{RR}^2}{2\,\sigma_{X_i}^2}} \quad .$$

The standard deviation of $(X_i+X_{i+1})/2$ is:

(3) $$\sigma_{(X_i+X_{i+1})/2} = \sigma_{X_i}\, \rho_{X_i \,,\, (X_i+X_{i+1})/2} \quad .$$

MODEL 1; Reliability = 1.0; engine is scrapped after 9 unsuccessful tests.

Let the notation "2 $\overline{3}$" describe the event that thrust of the second test was within decision limits and that the average thrust of the second and third test was within specification limits. Let the notation "2_c 3 $\overline{4}_c$ 5 $\overline{6}$" describe the following event:

- Calibration after second test (thrust outside of decision limits).
- No calibration after third test (thrust within decision limits).
- Calibration after fourth test (mean thrust of third and fourth test outside of specification limits).
- Thrust in fifth test within decision limits.
- Average thrust of fifth and sixth tests within specification limits.

Using this notation and the notation of figure 1, probabilities for the various events are as follows:

TABLE I

EVENTS	PROBABILITY
$2\ \bar{3}$	$1-P(1)-P(\bar{1})$
$2_c\ 3\ \bar{4}$	$[1-P(1)-P(\bar{1})]\,P(1)$
$2\ \bar{3}_c\ 4\ \bar{5}$	$[1-P(1)-P(\bar{1})]\,P(\bar{1})\,[1-P(1)]$
$2_c\ 3_c\ 4\ \bar{5}$	$[1-P(1)-P(\bar{1})]\,[P(1)]^2$
$2\ \bar{3}_c\ 4_c\ 5\ \bar{6}$	$[1-P(1)-P(\bar{1})]\ P(1)\ P(\bar{1})\ [1-P(1)]$
$2_c\ 3\ \bar{4}_c\ 5\ \bar{6}$	$[1-P(1)-P(\bar{1})]\ P(1)\ P(\bar{1})\ [1-P(1)]$
$2_c\ 3_c\ 4_c\ 5\ \bar{6}$	$[1-P(1)-P(\bar{1})]\,[P(1)]^3$
$2\ \bar{3}_c\ 4\ \bar{5}_c\ 6\ \bar{7}$	$[1-P(1)-P(\bar{1})]\,[P(\bar{1})]^2\,[1-P(1)]^2$
$2\ \bar{3}_c\ 4_c\ 5_c\ 6\ \bar{7}$	$[1-P(1)-P(\bar{1})]\,[P(1)]^2\ P(\bar{1})[1-P(1)]$
$2_c\ 3\ \bar{4}_c\ 5_c\ 6\ \bar{7}$	$[1-P(1)-P(\bar{1})]\,[P(1)]^2\ P(\bar{1})[1-P(1)]$
$2_c\ 3_c\ 4\ \bar{5}_c\ 6\ \bar{7}$	$[1-P(1)-P(\bar{1})]\,[P(1)]^2\ P(\bar{1})[1-P(1)]$
$2_c\ 3_c\ 4_c\ 5_c\ 6\ \bar{7}$	$[1-P(1)-P(\bar{1})]\,[P(1)]^4$
$2\ \bar{3}_c\ 4\ \bar{5}_c\ 6_c\ 7\ \bar{8}$	$[1-P(1)-P(\bar{1})]\ P(1)\ [P(\bar{1})]^2[1-P(1)]^2$
$2\ \bar{3}_c\ 4_c\ 5\ \bar{6}_c\ 7\ \bar{8}$	$[1-P(1)-P(\bar{1})]\ P(1)\ [P(\bar{1})]^2[1-P(1)]^2$
$2\ \bar{3}_c\ 4_c\ 5_c\ 6_c\ 7\ \bar{8}$	$[1-P(1)-P(\bar{1})]\,[P(1)]^3\ P(\bar{1})\ [1-P(1)]$
$2_c\ 3\ \bar{4}_c\ 5\ \bar{6}_c\ 7\ \bar{8}$	$[1-P(1)-P(\bar{1})]\ P(1)\cdot\ [P(\bar{1})]^2\ [1-P(1)]^2$
$2_c\ 3\ \bar{4}_c\ 5_c\ 6_c\ 7\ \bar{8}$	$[1-P(1)-P(\bar{1})]\,[P(1)]^3\ P(\bar{1})\ [1-P(1)]$
$2_c\ 3_c\ 4\ \bar{5}_c\ 6_c\ 7\ \bar{8}$	$[1-P(1)-P(\bar{1})]\,[P(1)]^3\ P(\bar{1})\ [1-P(1)]$
$2_c\ 3_c\ 4_c\ 5\ \bar{6}_c\ 7\ \bar{8}$	$[1-P(1)-P(\bar{1})]\,[P(1)]^3\ P(\bar{1})\ [1-P(1)]$
$2_c\ 3_c\ 4_c\ 5_c\ 6_c\ 7\ \bar{8}$	$[1-P(1)-P(\bar{1})]\,[P(1)]^5$

TABLE I (Cont'd)

EVENTS	PROBABILITY
$2\ \bar{3}_c\ 4\ \bar{5}_c\ 6\ \bar{7}_c\ 8\ \bar{9}$	$[1 - P(_1) - P(\bar{1})]\ [P(\bar{1})]^3\ [1 - P(_1)]^3$
$2\ \bar{3}_c\ 4\ \bar{5}_c\ 6_c\ 7_c\ 8\ \bar{9}$	$[1 - P(_1) - P(\bar{1})]\ [P(_1)]^2\ [P(\bar{1})]^2\ [1 - P(_1)]^2$
$2\ \bar{3}_c\ 4_c\ 5\ \bar{6}_c\ 7_c\ 8\ \bar{9}$	$[1 - P(_1) - P(\bar{1})]\ [P(_1)]^2\ [P(\bar{1})]^2\ [1 - P(_1)]^2$
$2\ \bar{3}_c\ 4_c\ 5_c\ 6\ \bar{7}_c\ 8\ \bar{9}$	$[1 - P(_1) - P(\bar{1})]\ [P(_1)]^2\ [P(\bar{1})]^2\ [1 - P(_1)]^2$
$2\ \bar{3}_c\ 4_c\ 5_c\ 6_c\ 7_c\ 8\ \bar{9}$	$[1 - P(_1) - P(\bar{1})]\ [P(_1)]^4\ P(\bar{1})\ [1 - P(_1)]$
$2_c\ 3\ \bar{4}_c\ 5\ \bar{6}_c\ 7_c\ 8\ \bar{9}$	$[1 - P(_1) - P(\bar{1})]\ [P(_1)]^2\ [P(\bar{1})]^2\ [1 - P(_1)]^2$
$2_c\ 3\ \bar{4}_c\ 5_c\ 6\ \bar{7}_c\ 8\ \bar{9}$	$[1 - P(_1) - P(\bar{1})]\ [P(_1)]^2\ [P(\bar{1})]^2\ [1 - P(_1)]^2$
$2_c\ 3\ \bar{4}_c\ 5_c\ 6_c\ 7_c\ 8\ \bar{9}$	$[1 - P(_1) - P(\bar{1})]\ [P(_1)]^4\ P(\bar{1})\ [1 - P(_1)]$
$2_c\ 3_c\ 4\ \bar{5}_c\ 6\ \bar{7}_c\ 8\ \bar{9}$	$[1 - P(_1) - P(\bar{1})]\ [P(_1)]^2\ [P(\bar{1})]^2\ [1 - P(_1)]^2$
$2_c\ 3_c\ 4\ \bar{5}_c\ 6_c\ 7_c\ 8\ \bar{9}$	$[1 - P(_1) - P(\bar{1})]\ [P(_1)]^4\ P(\bar{1})\ [1 - P(_1)]$
$2_c\ 3_c\ 4_c\ 5\ \bar{6}_c\ 7_c\ 8\ \bar{9}$	$[1 - P(_1) - P(\bar{1})]\ [P(_1)]^4\ P(\bar{1})\ [1 - P(_1)]$
$2_c\ 3_c\ 4_c\ 5_c\ 6\ \bar{7}_c\ 8\ \bar{9}$	$[1 - P(_1) - P(\bar{1})]\ [P(_1)]^4\ P(\bar{1})\ [1 - P(_1)]$
$2_c\ 3_c\ 4_c\ 5_c\ 6_c\ 7_c\ 8\ \bar{9}$	$[1 - P(_1) - P(\bar{1})]\ [P(_1)]^6$

Assume that the cost of one engine is equivalent to the cost of $M = 40$ tests. Let P_j be the sum of probabilities in table 1 associated with those events requiring j tests. Then the expected number of tests per accepted engine is:

$$E(N) = \frac{\sum_{j=3}^{N} jP_j + M\left(1 - \sum_{j=3}^{N} P_j\right)}{\sum_{j=3}^{N} P_j} \qquad (4)$$

The quantity in parenthesis is the probability that more than 9 tests are required; i.e., the probability of scrapping the engine. Holding the specification limit constant, the decision limit (figure 1) is varied until $E(N)$ is minimized.

In illustration, this model was used to support contract negotiations in an engine program where reliability of the engine is very high. Practice is to scrap the engine after 9 unsuccessful tests. Data showed that the square root of the within-engine, or run-to-run variance component of thrust was 600 lbs., and the square root of the engine-to-engine variance component was between 1200 and 1500 lbs. Both extremes were analyzed, as follows:

Case 1: $\sigma_{EE} = 1200$ lbs. $\sigma_{RR} = 600$ lbs.

From equation (1), $\sigma_{X_i} = \sqrt{(600)^2 + (1200)^2} = 1340$ lbs.

From equation (2) $\rho_{X_i,\,(X_i + X_{i+1})/2} = \sqrt{1 - \frac{1}{2}\left(\frac{600}{1340}\right)^2} = .95$

From equation (3) $\sigma_{(X_i + X_{i+1})/2} = .95(1340) = 1270$ lbs.

Suppose the specification limits for thrust are nominal $\pm$ 2000 lbs. Then the number of standard deviations between nominal and the specification limit (two-sided) is $2000/1270 = 1.57$. By trial and error, equation (4) is minimized when the decision limits are nominal $\pm$ 1.7(1340) = nominal $\pm$ 2200 lbs, when $E(N) = [3.178 + 40(.0020)]/.998 = 3.26$ tests per accepted engine.

Case 2: σ_{EE} = 1500 lbs. σ_{RR} = 600 lbs.

From equation (1), $\sigma_{X_i} = \sqrt{(600)^2 + (1500)^2} = 1620$ lbs.

From equation (2), $\rho_{X_i,\,(X_i + X_{i+1})/2} = \sqrt{1 - \frac{1}{2}\left(\frac{600}{1620}\right)^2} = .965$

From equation (3), $\sigma_{(X_i + X_{i+1})/2} = .965(1620) = 1560$ lbs.

The number of standard deviations between nominal and the specification limit (two-sided) is 2000/1560 = 1.28. By trial and error, equation (4) is minimized when the decision limits are nominal $\pm$ 1.5(1620) = nominal $\pm$ 2430 lbs, when E(N) = [3.286 + 40(.0122)] /.988 = 3.8 tests per accepted engine. (Note that changing the ratio of σ_{RR}/σ_{X_i} from 600/1340 in case 1 to 600/1620 in case 2 changes the correlation coefficient by only .015, and merely changes the optimum decision limits from 1.7 to 1.5 standard deviations. E(N) changes significantly, from 3.3 to 3.8 tests per accepted engine.)

Other information of interest corresponding to decision limits is the following:

A. Prob. of acceptance after N tests = $\sum_{j=3}^{N} P_j$

B. Prob. of scrapping engine after N tests = $1 - \sum_{j=3}^{N} P_j$

C. Percent engines requiring calibration after second test = P(i) Of these, the four "corners" of the bivariate distribution are necessary (see figure 1).

Prior to this analysis, the contractor had been using arbitrary decision limits of nominal $\pm$ (2000-2 σ_{RR}). Advantages gained by minimizing expected number of tests are also obtained from A, B, and C above, as follows:

COMPARISON OF DECISION LIMITS

ASSUMING THAT AFTER 9 UNSUCCESSFUL TESTS THE ENGINE IS SCRAPPED

σ_{EE} = 1200 lbs. σ_{RR} = 600 lbs.

(Spec. = Nominal $\pm$ 1.6 Sigma)

(Assume 1 Engine = 40 Tests)	Decision Limit = nominal $\pm$ 0.6 σ_{Xi}		Optimum Dec. Limit = nominal $\pm$ 1.7σ_{Xi}
· Prob. of Acceptance after 3 Tests	.45		.87
· % Engines requiring calibration after 2nd test	55% (of these, 20% are necessary)		10% (of these, 77% are necessary)
· Average number of tests required for acceptance	4.11(due to recalibration) 0.61(due to scrapped engine) 4.72 (Total) Δ = 1.5 tests/engine		3.18 0.08 3.26
· Expected Number of Scrapped Engines Per 100 Tested	1.5		0.2
· % Engines Accepted after N Tests	45.1	N = 3	86.7
	69.9	N = 4	95.5
	83.5	N = 5	99.0
	90.0	N = 6	99.6
	95.0	N = 7	99.76
	97.3	N = 8	99.79
	98.5	N = 9	99.80

COMPARISON OF DECISION LIMITS
ASSUMING THAT AFTER 9 UNSUCCESSFUL TESTS
THE ENGINE IS SCRAPPED

σ_{EE} = 1500 lbs. σ_{RR} = 600 lbs.

(Spec. = Nominal $\pm$ 1.3 Sigma)

(Assume 1 Engine = 40 Tests)	Decision Limit = nominal $\pm$ 0.5 σ_{X_i}		Optimum Dec. Limit = nominal $\pm$ 1.5 σ_{X_i}
Prob. of Acceptance after 3 Tests.	.38		.78
%Engines Requiring Calibration After 2nd Test	62% (of these, 31% are necessary)		16% (of these, 84% are necessary)
Average Number of Tests Required for Acceptance	4.4 (due to recalibration) 1.4 (due to scrapped engine) 5.8 (Total) Δ = 2.0 Tests/Engine		3.3 0.5 3.8
Expected Number of Scrapped Engines per 100 Tested	3.5		1.2
% Engines Accepted after N Tests	38.0	N = 3	78.0
	61.9	N = 4	90.6
	76.4	N = 5	96.5
	85.4	N = 6	98.0
	91.0	N = 7	98.5
	94.4	N = 8	98.7
	96.5	N = 9	98.8

MODEL 2: Reliability ≤ 1.0; Engine is scrapped after 5 unsuccessful tests. Assume that the engine is scrapped when the contractor fails to meet requirements for acceptance after 5 successive tests with calibration. Let $1-R_1$ be the probability of failure in the first test, where "failure" is any event that causes a single additional test as in table 2, and similarly for $1-R_2$ in the seond test, etc. A curve of reliability vs. number of tests may be obtained from past experience, as in figure 2.

Figure 2

OPERATIONAL RELIABILITY VS. NUMBER OF TESTS

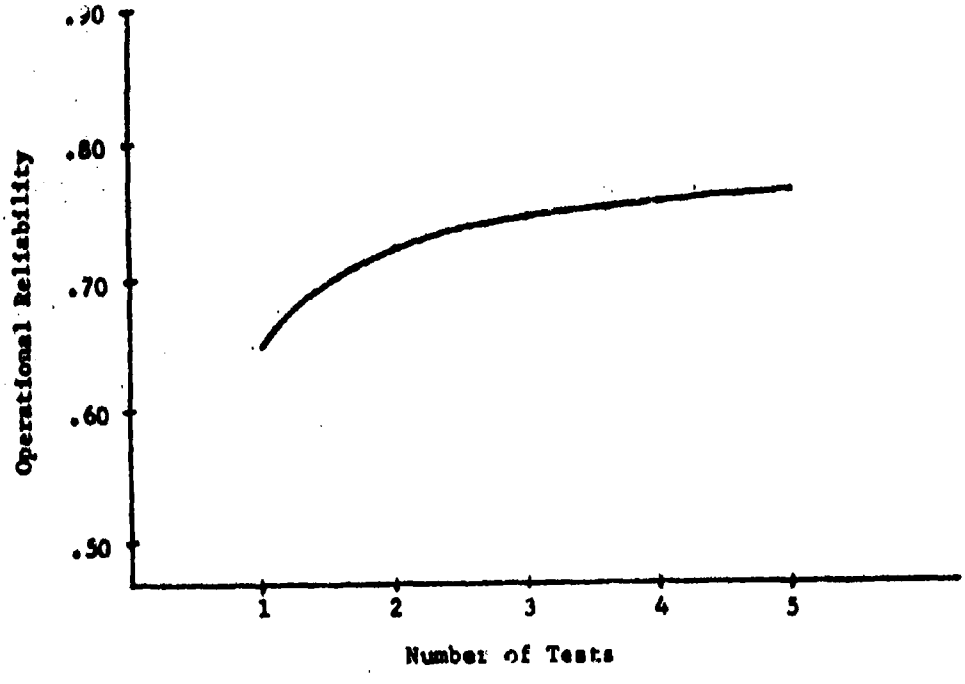

Let the notation "$1_c\ 2_{F2}\ 3_c\ 4\ \overline{5}$ describe the following event:

Calibration after first test.
Failure during second test.
Calibration after third test.
Thrust in fourth test within decision limits.
Average thrust of fourth and fifth tests within specification limits.

As before, the engine is always calibrated after the first test, unless failure occurs. Using the notation P(i) and $P(\overline{i})$ as in model 1, probabilities for the various events are as follows:

TABLE 2

EVENT	PROBABILITY
$1_c\ 2\ \overline{3}$	$R_1 R_2 R_3 [1 - P(i) - P(\overline{i})]$
$1_c\ 2_c\ 3\ \overline{4}$	$R_1 R_2 R_3 R_4 P(i) [1 - P(i) - P(\overline{i})]$
$1_{F1} 2_c\ 3\ \overline{4}$	$(1 - R_1) R_2 R_3 R_4 [1 - P(i) - P(\overline{i})]$
$1_c\ 2_{F2} 3\ \overline{4}$	$(1 - R_2) R_1 R_3 R_4 [1 - P(i) - P(\overline{i})]$
$1_c\ 2_c\ 3_c\ 4\ \overline{5}$	$R_1 R_2 R_3 R_4 R_5 [P(i)]^2 [1 - P(i) - P(\overline{i})]$
$1_c\ 2\ \overline{3}_c\ 4\ \overline{5}$	$R_1 R_2 R_3 R_4 R_5 [1-P(i)] [P(\overline{i})] [1 - P(i)-P(\overline{i})]$
$1_{F1} 2_{F2} 3_c\ 4\ \overline{5}$	$(1 - R_1) (1 - R_2) R_3 R_4 R_5 [1 - P(i) - P(\overline{i})]$
$1_{F1} 2_c\ 3_{F3} 4\ \overline{5}$	$(1 - R_1) (1 - R_3) R_2 R_4 R_5 [1 - P(i) - P(\overline{i})]$
$1_c\ 2_{F2} 3_{F3} 4\ \overline{5}$	$(1 - R_2)(1 - R_3) R_1 R_4 R_5 [1 - P(i) - P(\overline{i})]$
$1_{F1} 2_c\ 3_c\ 4\ \overline{5}$	$(1 - R_1) R_2 R_3 R_4 R_5 [P(i)]^2 [1 - P(i) - P(\overline{i})]$
$1_c\ 2_{F2}\ 3_c\ 4\ \overline{5}$	$(1 - R_2) R_1 R_3 R_4 R_5 P(i) [1 - P(i) - P(\overline{i})]$
$1_c\ 2_c\ 3_{F3} 4\ \overline{5}$	$(1 - R_3) R_1 R_2 R_4 R_5 P(i) [1 - P(i) - P(\overline{i})]$

Assuming that the cost of one engine is equivalent to the cost of M tests, and letting P_j be the sum of probabilities in table 2 associated with j tests, the expected number of tests per accepted engine is given by equation (4).

Case 1: Reliability < 1.0

In illustration suppose σ_{EE} = 1200 lbs., σ_{RR} = 600 lbs., specification limits are nominal ± 2000 lbs., and the cost of one engine is equivalent to the cost of 40 tests. Then as in model 1, case 1, we have:

$$\sigma_{X_i} = 1340 \text{ lbs.}$$

$$\rho_{X_i,\,(X_i + X_{i+1})/2} = .95$$

$$\sigma_{(X_i+X_{i+1})/2} = 1270 \text{ lbs.} \quad .$$

Number of standard deviations between nominal and specification limit = 1.57.

Calculate P_j from table 2 for j = 3, 4, 5, utilizing operational reliability values of figure 2. By trial and error, equation (4) is minimized when the decision limits are nominal ± 1.8 standard deviations, and E(N) = 24.6 tests per accepted engine.

Case 2: Reliability = 1.0 (Same correlation coefficient and standard deviations as in case 1)

It is of interest to observe the partial effect of reliability on the optimum decision limits and expected number of tests, E(N). Let R_1 through R_5 be 1.0. Then utilizing table 2, (or table 1 for j = 3, 4, 5) calculate P_j. The standard deviations of X_i and $(X_i+X_{i+1})/2$ and correlation coefficient are the same as in case 1. Equation (4) is minimized when the decision limits are nominal ± 1.5 standard deviations and E(N) = 3.6 tests per accepted engine. In comparing these values to those in case 1, note that the optimum decision limits become tighter, and the

number of tests per accepted engine decreases as reliability increases.

By comparison of results in Model 1, case 1 to those of Model 2, case 2, a measure of the effect of scrapping the engine after 9 versus 5 tests is obtained. The optimum decision limits are nominal $\pm$ 1.7 standard deviations in the former, and E(N) = 3.3 tests per accepted engine; in the latter, the optimum decision limits are nominal $\pm$ 1.5 standard deviations, and E(N) = 3.6 tests.

APPLICATIONS: The minimum expected number of tests per accepted engine, E(N), provides a convenient yardstick for trade-off studies. For example, one might want to determine whether or not the cost of overhauling test facilities in order to improve operational reliability by, say, 5%, is worthwhile. Or, one might want to determine whether the cost of reducing engine-to-engine variability by improving calibration techniques or equipment is offset by the reduced number of tests required for acceptance, etc.

REFERENCES

(1) Tables of the Bivariate Normal Distribution Function and Related Functions, National Bureau of Standards, U. S. Department of Commerce.

(2) Tables of Normal Probability Functions, National Bureau of Standards, U. S. Department of Commerce.

APPENDIX

$$\rho_{X_i,\ \frac{X_i + X_{i+1}}{2}} = \frac{\operatorname{cov}\left(\bar{x}_i, \frac{X_i + X_{i+1}}{2}\right)}{\sigma_{X_i},\ \sigma_{\frac{X_i + X_{i+1}}{2}}}$$

Substituting from equations (7) and (8), this is

$$(5) \qquad = \frac{\sigma_{X_i}^2 + \rho_{X_i,\ X_{i+1}}\ \sigma_{X_i}\ \sigma_{X_{i+1}}}{\sigma_{X_i}\ \sqrt{\sigma_{X_i}^2 + \sigma_{X_{i+1}}^2 + 2\rho_{X_i,\ X_{i+1}}\ \sigma_{X_i}\ \sigma_{X_{i+1}}}}$$

Substituting from equation (9),

$$= \frac{\sigma_{X_i}^2 + \frac{1}{2}\left(\sigma_{X_i}^2 + \sigma_{X_{i+1}}^2 - 2\sigma_{RR}^2\right)}{\sigma_{X_i}\ \sqrt{2\sigma_{X_i}^2 + 2\sigma_{X_{i+1}}^2 - 2\sigma_{RR}^2}}$$

$$(6) \qquad = \frac{3\sigma_{X_i}^2 + \sigma_{X_{i+1}}^2 - 2\sigma_{RR}^2}{\sigma_{X_i}\ \sqrt{8\left(\sigma_{X_i}^2 + \sigma_{X_{i+1}}^2 - \sigma_{RR}^2\right)}}$$

assuming $\sigma_i = \sigma_{i+1}$,

$$\rho_{X_i,\ \frac{X_i + X_{i+1}}{2}} = \frac{2\sigma_{X_i}^2 - \sigma_{RR}^2}{\sigma_{X_i}\sqrt{2(2\sigma_{X_i}^2 - \sigma_{RR}^2)}}$$

$$= \sqrt{1 - \frac{\sigma_{RR}^2}{2\sigma_{X_i}^2}} \tag{6A}$$

or, letting $\sigma_{X_i} = \sigma_{X_{i+1}}$ in equation (5), this result may be expressed as:

$$\rho_{X_i,\ \frac{X_i + X_{i+1}}{2}} = \frac{1}{\sqrt{2}}\sqrt{1 + \rho_{X_i,\ X_{i+1}}} \tag{6B}$$

Let σ_{EE}^2 be the engine-to-engine variance component. Using the relation $\sigma_{X_i} = \sqrt{\sigma_{EE}^2 + \sigma_{RR}^2}$ together with equations (6A) and (8B), the volume in the corners of figure 1 are computed from a bivariate normal distribution table. Using this result plus a univariate normal table, P(i) and $P(\bar{i})$ as defined pgs. 175 and 177 are calculated.

$$\operatorname{cov}\left(X_i,\ \frac{X_i + X_{i+1}}{2}\right)$$

$$= E\left[X_i\left(\frac{X_i + X_{i+1}}{2}\right)\right] - E(X_i)\,E\left(\frac{X_i + X_{i+1}}{2}\right)$$

$$= \frac{1}{2} \left\{ E(X_i^2) + E(X_i X_{i+1}) - \left[E(X_i)\right]^2 - E(X_i)\, E(X_{i+1}) \right\}$$

$$= \frac{1}{2} \left[\sigma_{X_i}^2 + \operatorname{cov}(X_i, X_{i+1}) \right]$$

(7) $$= \frac{1}{2} \left[\sigma_{X_i}^2 + \rho_{X_i, X_{i+1}}\, \sigma_{X_i}\, \sigma_{X_{i+1}} \right] .$$

If $\sigma_{X_i} = \sigma_{X_{i+1}}$, this becomes

(7A) $$\operatorname{cov}\left(X_i, \frac{X_i + X_{i+1}}{2}\right) = \frac{\sigma_{X_i}^2}{2} \left[1 + \rho_{X_i, X_{i+1}}\right]$$

---

(8) $$\sigma_{\frac{X_i + X_{i+1}}{2}} = \frac{1}{2} \sqrt{\sigma_{X_i}^2 + \sigma_{X_{i+1}}^2 + 2\rho_{X_i, X_{i+1}}\, \sigma_{X_i} \sigma_{X_{i+1}}} .$$

If $\sigma_{X_i} = \sigma_{X_{i+1}}$,

(8A) $$\sigma_{\frac{X_i + X_{i+1}}{2}} = \frac{\sigma_{X_i}}{\sqrt{2}} \sqrt{1 + \rho_{X_i, X_{i+1}}} .$$

From (6B), this becomes

(8B) $$\sigma_{\frac{X_i + X_{i+1}}{2}} = \sigma_{X_i} \rho_{X_i, \frac{X_i + X_{i+i}}{2}}$$

from equation (9A), (8A) becomes

(8C) $$\sigma_{\frac{X_i + X_{i+1}}{2}} = \sqrt{\sigma^2 - \sigma^2_{\frac{RR}{2}}}$$

Sum of squares run-to-run is

$$SS_{RR} = \frac{1}{2} \sum_{a=1}^{N} (X_{i_a} - X_{i+1_a})^2$$

$$= \frac{1}{2} \sum_{a=1}^{N} [(X_{i_a} - \mu_i) - (X_{i+1_a} - \mu_{i+1}) + (\mu_i - \mu_{i+1})]^2.$$

Assuming $\mu_i = \mu_{i+1}$, and since $MS_{SS} = \frac{SS_{RR}}{N}$,

$$MS_{RR} = \frac{1}{2} \left[\frac{\Sigma (X_i - \mu_i)^2}{N} + \frac{\Sigma (X_{i+1} - \mu_{i+1})^2}{N} - \frac{2 \Sigma (X_L - \mu_i)(X_{i+1} - \mu_{i+1})}{N} \right].$$

Taking expectations, the run-to-run variance component is:

$$\sigma^2_{RR} = \frac{1}{2} [\sigma^2_{X_i} + \sigma^2_{X_{i+1}} - 2 \operatorname{cov}(X_i, X_{i+1})]$$

$$= \frac{1}{2} [\sigma^2_{X_i} + \sigma^2_{X_{i+1}} - 2 \rho_{X_i, X_{i+1}} \sigma_{X_i} \sigma_{X_{i+1}}]$$

and

$$\rho_{X_i,\, X_{i+1}} = \frac{\sigma_{X_i}^2 + \sigma_{X_{i+1}}^2 - 2\sigma_{RR}^2}{2\,\sigma_{X_i}\,\sigma_{X_{i+1}}}. \tag{9}$$

If $\sigma_{X_i} = \sigma_{X_{i+1}}$

$$\rho_{X_i,\, X_{i+1}} = 1 - \frac{\sigma_{RR}^2}{\sigma_{X_i}^2}. \tag{9A}$$

LIMITS AND RELATIONSHIPS:

$$\rho_{X_i,\, X_{i+1}} = 2\rho^2_{X_i,\, \frac{X_i + X_{i+1}}{2}} - 1 = 1 - \frac{\sigma_{RR}^2}{\sigma_{X_i}^2}.$$

When $\sigma_{EE} = 0$, $\rho_{X_i,\, X_{i+1}} = 0$; when $\sigma_{RR} = 0$, $\rho = 1.0$.

$\rho_{X_i,\, \frac{X_i + X_{i+1}}{2}}$	$\rho_{X_i,\, X_{i+1}}$	$\frac{\sigma_{RR}^2}{\sigma_{X_i}^2}$	$\frac{\sigma_{RR}}{\sigma_{X_i}}$
1.00	1.00	0	0
.99	.96	.04	.20
.98	.92	.08	.28
.97	.88	.12	.35
.96	.84	.16	.40
.95	.80	.20	.45
.90	.62	.38	.62
.85	.44	.56	.75
.80	.28	.72	.85
.75	.12	.88	.94
$1/\sqrt{2} = .707$	0	1.00	1.00

FIGURE 3

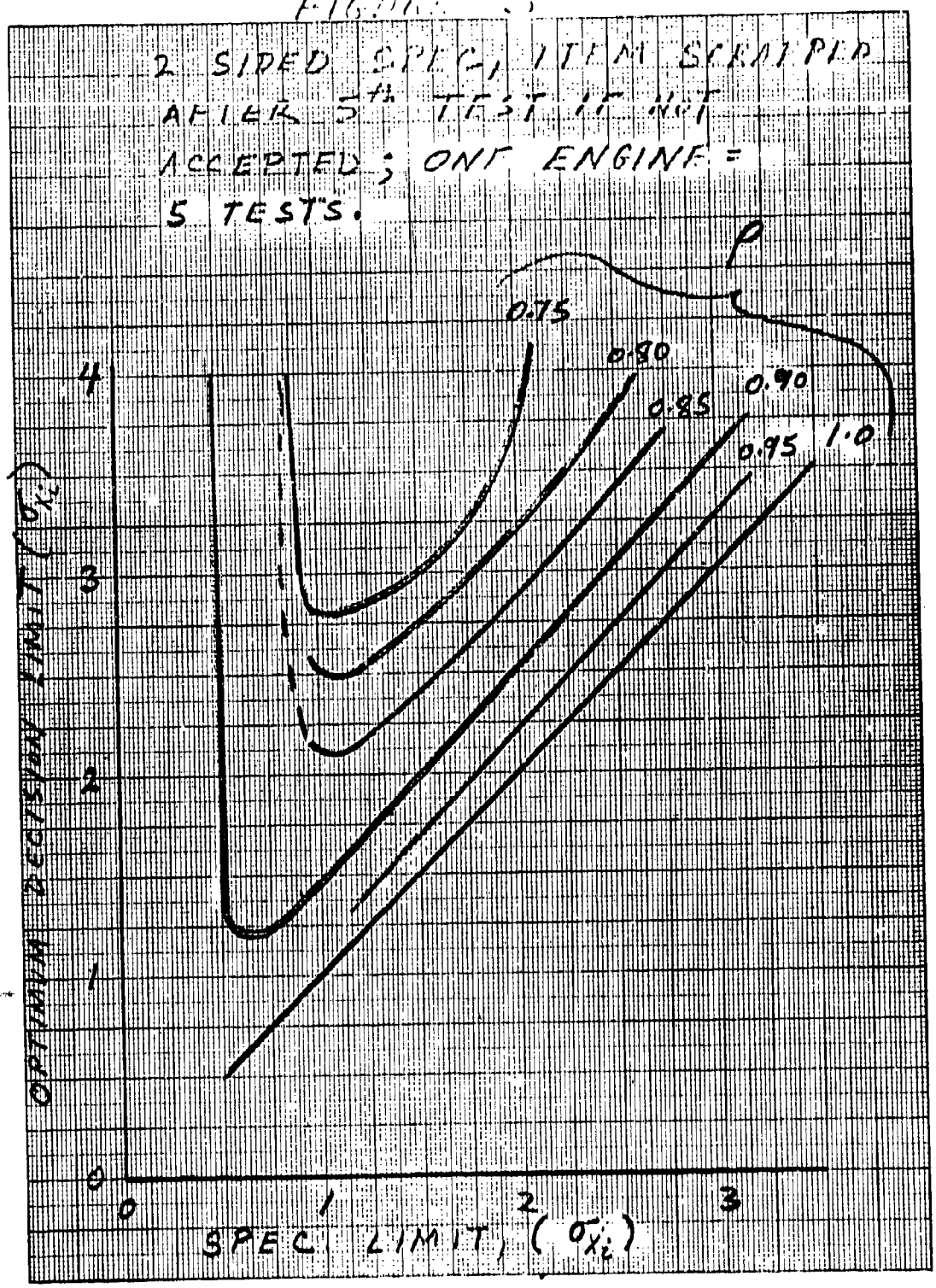
2 SIDED SPEC LIMIT SKIP LOT AFTER 5 TEST IF NOT ACCEPTED; ONE ENGINE = 5 TESTS.
P
0.75
0.80
0.85
0.90
0.95
1.0
4
3
2
1
0
0
1
2
3
OPTIMUM REJECTABLE LIMIT, ($\bar{x}_L$)
SPEC LIMIT, ($\bar{x}_L$)

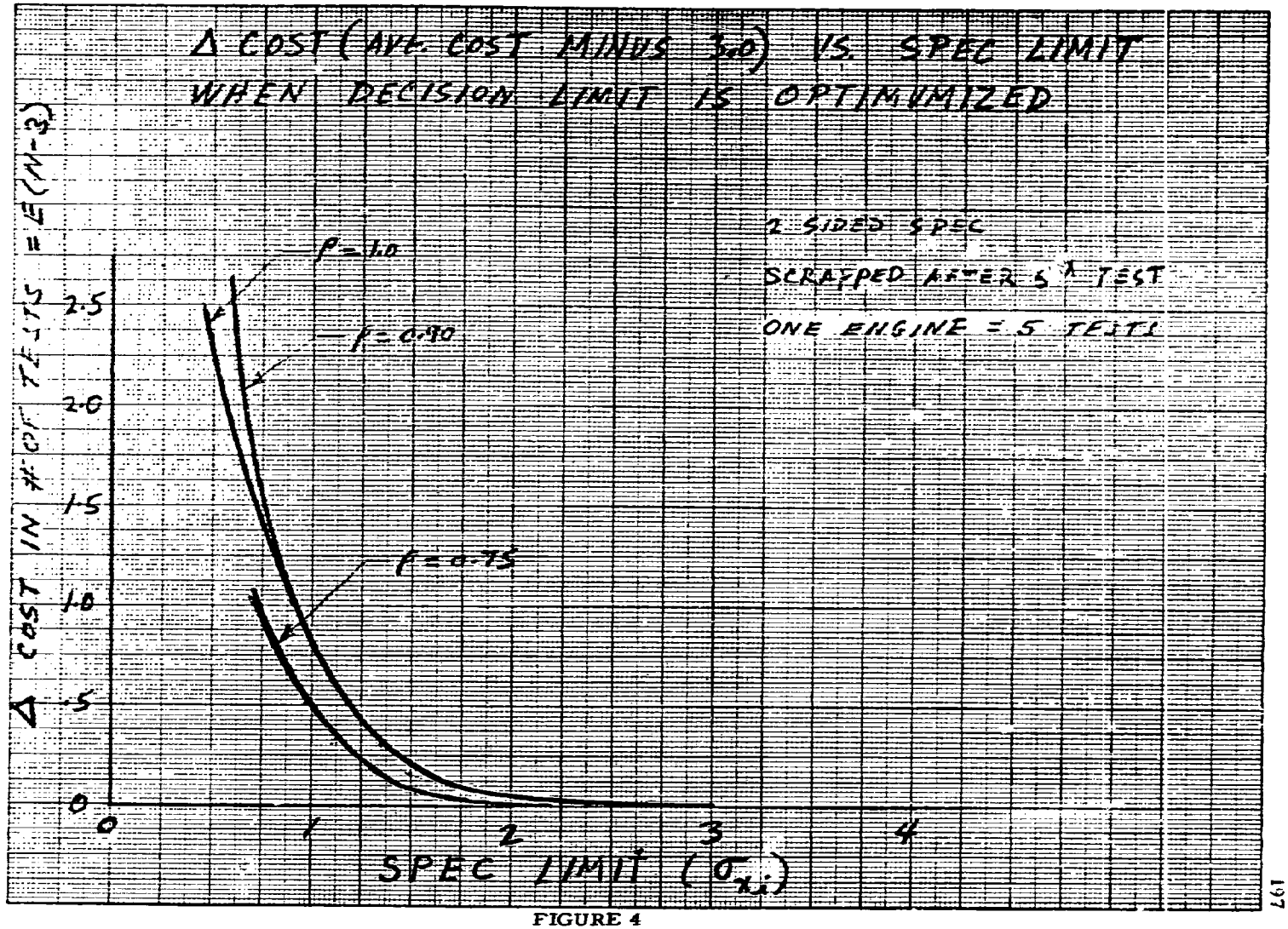
Δ COST (AVG. COST MINUS 3.0) VS. SPEC LIMIT
WHEN DECISION LIMIT IS OPTIMUMIZED
2 SIDED SPEC
SCRAPPED AFTER 5 TEST
ONE ENGINE = 5 TESTS
ρ = 1.0
ρ = 0.90
ρ = 0.75
Δ COST IN # OF TESTS = E(N-3)
0
.5
1.0
1.5
2.0
2.5
0
1
2
3
4
SPEC LIMIT (σx,y)

FIGURE 4

FIGURE 5

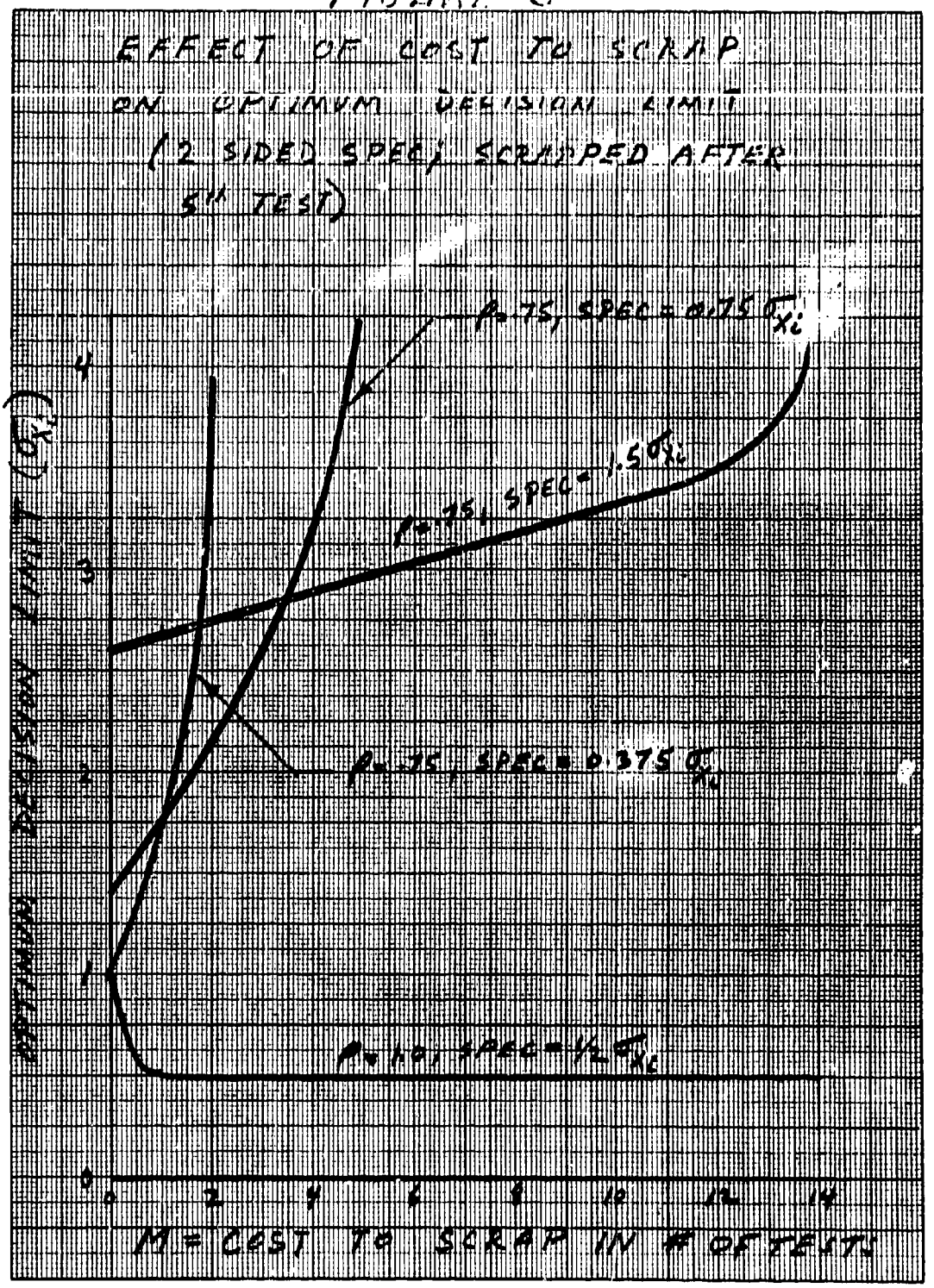
EFFECT OF COST TO SCRAP
ON OPTIMUM DECISION LIMIT
(2 SIDED SPEC, SCRAPED AFTER
5th TEST)
$\rho = .75$, SPEC = $0.75\,\sigma_{x_i}$
$\rho = .75$, SPEC = $1.50\,\sigma_{x_i}$
$\rho = .75$, SPEC = $0.375\,\sigma_{x_i}$
$\rho = 1.0$, SPEC = $\frac{1}{2}\,\sigma_{x_i}$
$\frac{\text{OPTIMUM DECISION LIMIT}}{\sigma_{x_i}}$
0
2
4
6
8
10
12
14
M = COST TO SCRAP IN # OF TESTS

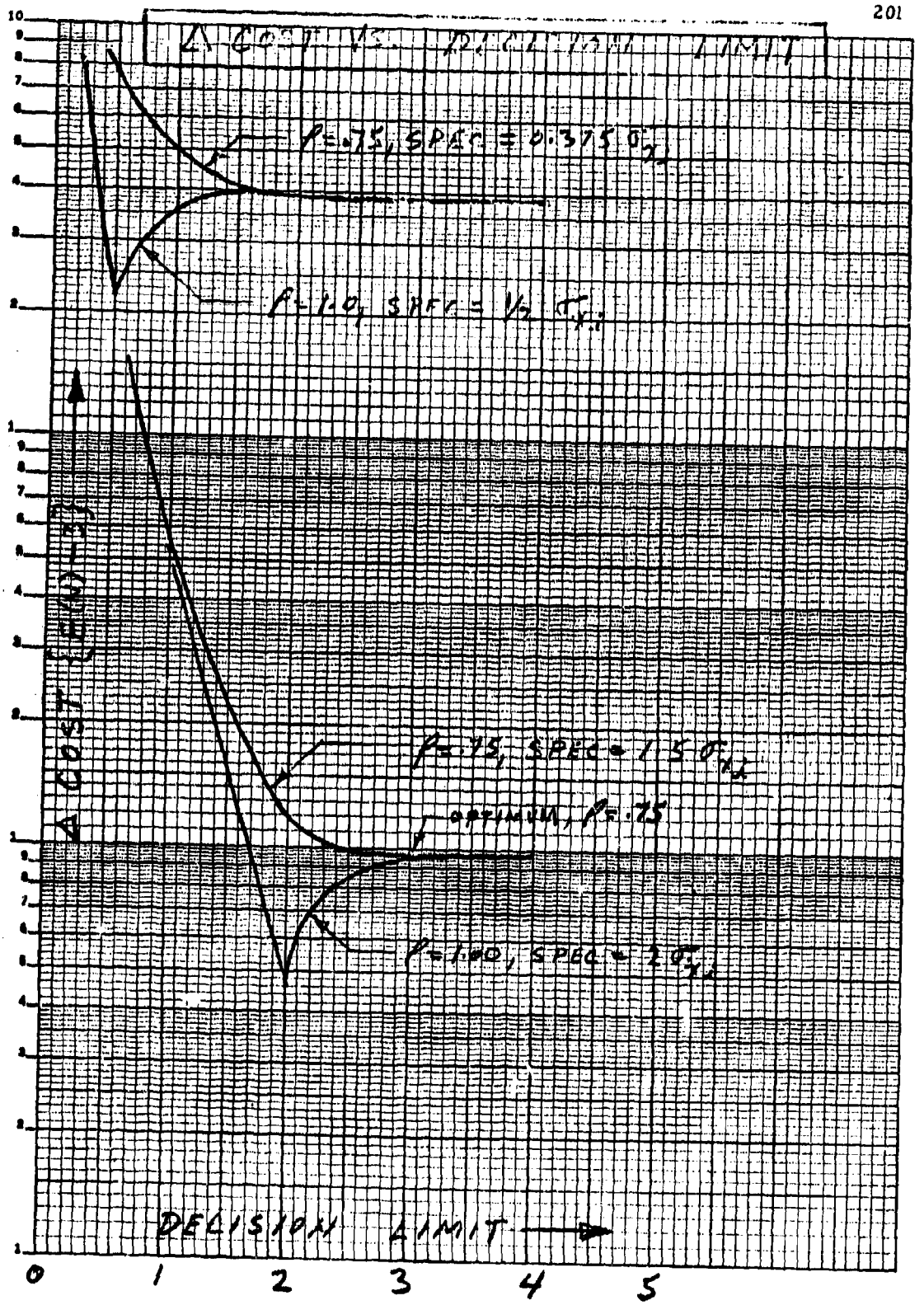
ρ=.75, SPEC = 0.375 σ_y
ρ=1.0, SPEC = ½ σ_y
ρ=.75, SPEC = 1.5 σ_y
OPTIMUM, ρ=.75
ρ=1.00, SPEC = 2 σ_y
DECISION LIMIT
0
1
2
3
4
5

THE THEORETICAL STRENGTH OF TITANIUM CALCULATED FROM THE COHESIVE ENERGY

Perry R. Smoot
Research Physical Metallurgist
U. S. Army Materials Research Agency
Watertown, Massachusetts

ABSTRACT. The derivation of the equation for theoretical strength $\sigma_{max} = \sqrt{\frac{4E\gamma}{r_e}}$ was reviewed, and certain assumptions made were considered questionable. Therefore, the accuracy of the equation was considered questionable, and a new method for calculating the theoretical strength of crystals was derived, utilizing the Morse potential equation and the cohesive energy. The theoretical strength of titanium calculated by this method was 3.28×10^6 psi.

I. INTRODUCTION. The U. S. Army Materials Research Agency is engaged in the development of strong, lightweight titanium alloys for use in Army weapons. In the course of this investigation, a question arose concerning the maximum strength theoretically obtainable, and how it might be obtained. It has been proposed for some time that the theoretical strength of metals is considerably higher than that normally observed. Polanyi[1] presented a method of calculating theoretical strength, in which the bonding force between atoms, as a function of internuclear separation, was taken to be approximately as shown in Figure 1. As a brittle crack progressed through the crystal in the manner shown in Figure 2, the interatomic bonds were extended and broken, and the work done against each bond was equal to the area under the curve from r_e to r_s in Figure 1. As the brittle crack progressed, new surfaces were created having a surface energy of 2S, and this energy was assumed equal to the work done against the interatomic bonds. On this basis, an algebraic solution for σ_{max}, the maximum theoretical stress at fracture was obtained, as follows:

$$\sigma_{max} = \sqrt{\frac{4E\gamma}{r_e}}$$

where E = the elastic modulus
S = the surface energy
r_e = the equilibrium atomic spacing .

The value of σ_{max} was ordinarily expected to be of the order of $\frac{E}{10}$, which was about 1 to 10 x 10^6 psi for most common metals[2]. Indeed, very high strength values of this order of magnitude have been obtained in metallic and ceramic whiskers.

In the deviation of this expression, the following energy balance is assumed:

Energy to fracture bonds = surface energy of new surface created by fracture .

No theoretical basis for this assumption is apparent, since the mechanism by which surface energy arises, and its relationship, if any, to the energy required to fracture the interatomic bonds is not known. Consequently, this expression for the theoretical strength is considered to be of questionable accuracy.

Another questionable aspect in the derivation of this method is the assumption that the interatomic force vs. displacement curve (Figure 1) is sinusoidal. In addition, there is a practical difficulty in calculating theoretical strengths by this method, since surface energy values for solids are not available for most elements (including titanium).

Because of these questions as to the correctness of this method, and because of the lack of surface energy data, it was desired to discover another method for calculating theoretical strength in which more confidence could be felt, perhaps by some means involving computation of the actual forces between atoms.

II. CALCULATIONS. As a result of an inquiry, Dr. R. J. Weiss[3] suggested a method for calculating the theoretical strength of metals by means of the Morse potential equation[4]:

$$V = D\left[e^{-2a(r-r_e)} - 2e^{-a(r-r_e)}\right]$$

where V(Ev) = potential energy

$D(\frac{Ev}{atom})$ = cohesive energy (the heat of vaporization, ΔH_V) per atom

$a(\frac{1}{\mathring{A}})$ = a constant

$r(\mathring{A})$ = the internuclear separation

$r_e(\mathring{A})$ = the equilibrium separation .

This equation related the bonding energy of two hydrogen atoms to the internuclear separation, as shown in Figure 3.

The energy values given by this function agreed well with:

a. experimental values of bonding energy vs separation for the H_2^+ molucule (except under compression; see Table I)[5],

b. theoretical values of bonding energy calculated in a few cases by quantum mechanics,[6]

c. experimental values for compressibility for sixteen metals (see Figure 4)[7].

It was therefore considered reasonable to assume that this relationship applied between the atoms in a crystal, with a modification consisting of multiplying the cohesive energy by a factor to take into account the division of the cohesive energy between nearest neighbors in a crystal. Differentiation of this equation yielded an expression for interatomic force, and it was suggested that this be used to calculate the maximum force between atoms and the theoretical strength of metals. The accuracy of the calculations was expected to be within a factor of two at worst, and probably much better.

As mentioned above, it was necessary to multiply the cohesive energy by a factor to take into account its division between N nearest neighbors. The energy contributed by each atom to each interatomic bond was $\frac{1}{N}D$. Since this contribution was made by one atom at each end of each bond, the total energy of one bond was $\frac{2}{N}D$. Therefore, the cohesive energy, D, was multiplied by $\frac{2}{N}$ when the Morse potential equation was applied to a crystal.

The theoretical strength of a titanium crystal was calculated by means of the method suggested above by Dr. Weiss. The Morse potential equation for a crystal was differentiated as follows:

$$V(Ev) = \frac{2}{N}D\left[e^{-2a(r-r_e)} - 2e^{-a(r-r_e)}\right] \quad \text{(Morse potential equation for a crystal)}$$

$$V = \frac{2}{N}D\left[e^{-2ar + 2ar_e} - 2e^{-ar + ar_e}\right] \tag{1}$$

$$V = \frac{2}{N}De^{-2ar}e^{2ar_e} - \frac{4}{N}De^{-ar}e^{ar_e}.$$

This equation was similar to:

$$y = k\,e^{bx}, \quad \text{where k and b are constants.}$$

Since $\frac{dy}{dx} = b\,k\,e^{bx}$, then

$$\frac{dV}{dr} = F\left(\text{interatomic force, } \frac{Ev}{\overset{\circ}{A}}\right) = -2ae^{2ar_e}\frac{2}{N}De^{-2ar} + 2ae^{ar_e}\frac{2}{N}De^{-ar} \tag{2}$$

$$F = \frac{4}{N}Da\cdot\left[-e^{2a(r_e-r)} + e^{a(r_e-r)}\right]$$

and

$$\frac{d^2V}{dr^2} = \frac{dF}{dr} = K\left(\text{interatomic spring constant, } \frac{Ev/\overset{\circ}{A}}{\overset{\circ}{A}}\right) =$$

$$4a^2e^{2ar_e}\frac{2}{N}De^{-2ar} - 2a^2e^{ar_e}\frac{2}{N}De^{-ar} \tag{3}$$

$$K = \frac{4}{N}Da^2\left[2e^{2a(r_e-r)} - e^{a(r_e-r)}\right].$$

It should be noted that when $r = r_e$,

$$K = \frac{4}{N} D a^2$$

and when K = 0

(4) $$4a^2 e^{2ar_e} \frac{2}{N} De^{-2ar} = 2a^2 e^{ar_e} \frac{2}{N} De^{-ar}$$

$$2e^{ar_e} e^{-ar} = 1$$

$$\frac{1}{e^{ar}} = \frac{1}{2e^{ar_e}}$$

$$e^{ar} = 2e^{ar_e}$$

$$ar \ln e = \ln 2 + ar_e \ln e$$

$$ar = \frac{\ln 2}{\ln e} + ar_e$$

and

(5) $$r = r_e + \frac{\ln 2}{a \ln e} = r_e + \frac{.693}{a} .$$

In order to utilize these equations to calculate the theoretical strength of a crystal, it was necessary to obtain numerical values for a, D, and r_e. Values for D and r_e were found in the literature as follows:

$$D = 4.74 \frac{Ev^8}{atom}$$

$$r_e = 2.95 \text{ A}^{o9} .$$

The value "a" was determined from the elastic modulus of the crystal. The structure of titanium is hexagonal close packed, and was considered to be an assembly of unit tensile cells, as shown in Figure 5. As a hypothetical stress was applied to the crystal in the [100] direction, an elastic strain occurred, as shown in Figure 6, so that bonds between atoms in the plane of atom A such as bond AS were extended, but bonds such as AT and AJ were not. Also, the bonds between atoms in the plane of atom A and the atoms above and below this plane were not extended. For example, bonds AG, AV and AO (Figure 7) were not extended. Trigonometric calculation demonstrated that this was possible without physical interference between atoms. As a result, the spring constant of the unit tensile cell was equal to the spring constant, K, of the single interatomic bond, AS. A numerical value for K was determined from Young's modulus, E, as follows:

$$E = 17.85 \times 10^{6} \text{ psi} = 7.67 \times 10^{-1} \frac{\text{Ev/Å}}{\text{Å}^2}$$

$$7.67 \times 10^{-1} \times \frac{6.24}{2.95} = 16.22 \times 10^{-1} \frac{\text{Ev/Å}}{\text{Å}} = K$$

where 6.24 = transverse area of unit tensile cell, Å^2

2.95 = length of unit tensile cell, Å .

From equation (4), above

$$K = \frac{4}{N} Da^2 = 16.22 \times 10^{-1}$$

and

$$a = 1.014 \frac{1}{\text{Å}} .$$

Having numerical values for all the constants required, the Morse potential energy and interatomic force were calculated as a function of internuclear displacement, r, and the results are shown in Figure 8. It will be noted that as a stress was applied and the interatomic bond

extended, the maximum force was reached at the internuclear separation for which $\frac{dF}{dr} = 0$. The internuclear separation at this point was calculated from the equation:

$$r - r_e + \frac{.693}{a} \quad \text{(equation 5, above)} \quad .$$

This separation was 3.63 Å, and the corresponding force was 0.402 $\frac{Ev}{Å}$ (0.645×10^{-4} dynes).

This data was then used to calculate the theoretical strength of a titanium crystal. A tensile force was considered to be applied in the [001] direction in the crystal, an equal part of which was transferred to each atom in the (001) plane (see Figure 9). These tensile forces on each atom are represented by the vectors AB and AF. The tensile vector AB is the resultant of the vectors AC, AD, and AE. These vectors arise from the extension of the interatomic bonds AC, AD and AE. As the applied tensile force increased, the bonds extended until they reached the fracture extension; and the force in each bond increased to equal the fracture force mentioned above. As the applied tensile increased still further, the bonds exceeded the fracture separation and the force in each one decreased in accordance with Figure 8. Thereafter, the sum of the bond forces was less than the applied force, so that the applied force was able to fracture the crystal on the (001) plane.

The theoretical maximum strength was attained immediately prior to fracture. The stress on the crystal at this time was determined by calculating the magnitude of the vector AB and dividing it by the area per atom in the (001) plane. The value so calculated was 3.28×10^6 psi. It should be noted that, in this theory of fracture, it was assumed that no slip occurred and no brittle crack propagated through the crystal at a stress lower than the theoretical maximum.

A calculation of the theoretical strength of a monatomic titanium filament was made by means of equations 1 and 2, letting N = 2, and the theoretical maximum strength of a monatomic filament was found to be 8,200,000 (8.2×10^6) psi, which was considerably higher than for the crystal. This increased strength was due to greater cohesive energy

per bond, since there were fewer nearest neighbors. The strength of a monatomic sheet would be above that of the crystal and below that of a filament, due to the same effect.

Using this method, the theoretical cleavage strength of iron in the [100] direction was calculated to be 12.7×10^6 psi. It is interesting to compare this value with the observed yield strength of iron whiskers in the [100] direction, which is $.664 \times 10^6$ psi[10]. The strength of the whiskers is considerably higher than normally observed in iron and iron-base alloys, showing that the material is capable of much higher strength than it normally exhibits. On the other hand, the whisker yield strength is considerably less than the calculated cleavage strength, due to the onset of plastic flow. If plastic flow could be prevented by some means, it is possible that the high cleavage strength predicted by the calculations could be attained.

III. DISCUSSION. The theoretical strength calculated for titanium, 3.28×10^6 psi, is much larger than the normally observed strength of about 200,000 psi. Greater confidence is felt in this method of calculating theoretical strength than in the method of Polanyi, because of the questionable aspects of the Polanyi deriviation mentioned in the Introduction.

High theoretical strengths may be obtainable in real materials if the necessary conditions can be maintained, namely, that no slip occur and no brittle crack propagate at a stress below the theoretical maximum strength. The method of obtaining these conditions is problematical, and several possible methods may be suggested. One method might be to grow whiskers of such perfection that no slip would occur and no brittle crack would propagate until a stress level approaching the theoretical were reached. Another method might be to simply produce very fine filaments (not necessarily whiskers) by some method, such as drawing from the melt. Slip in these filaments might be inhibited by alloying elements and brittle crack formation supressed by the small size. (There is some evidence that in filaments, the tendency for brittle cracks to nucleate and propagate is suppressed by decreasing the diameter.) Slip might also be inhibited by suitable control of crystal orientation, the production of very fine grain sizes, or by amorphous (vitreous) structures. The high strengths calculated for monatomic filaments and sheets may be approached if these or similar structures can be produced. There is some hope that these high strength levels may be attained in metals such as titanium, since strength levels of 3×10^6 psi have already been achieved with graphite whiskers[11].

IV. RECOMMENDATIONS FOR FURTHER WORK. Since this area of study offers considerable promise for the development of ultra-high strength materials, it is suggested that further work be undertaken to further develop the theory of the strength of solids, verify it experimentally, and find methods of applying it to the production of engineering materials having these high strengths. From a survey of the literature, it appears that further developments are necessary in the methods of quantum mechanics so that more accurate calculations of the energy vs. internuclear separation may be made. Experiments are required to verify the results obtained and to provide data for engineering application.

The materials offering the best combination of properties should be identified, and developmental programs initiated to establish methods of providing high strength engineering materials at acceptable cost and in the quantities required.

ACKNOWLEDGEMENT. The author is indebted to Dr. R. J. Weiss of the U. S. Army Materials Research Agency for providing the theoretical physical basis and guidance on which these calculations were based.

TABLE I

Bonding Energy and Interatomic Spacing for H_2^+

(Energy Unit: Rydbergs)

r	V Exact	V Calculated*
0.2	7.1426	0.9654
0.4	2.3984	0.5821
0.6	0.9903	0.3093
0.8	0.3910	0.1184
1.0	0.0964	-0.0122
1.2	-0.0579	-0.0989
1.4	-0.1399	-0.1536
1.6	-0.1819	-0.1854
1.8	-0.2005	-0.2010
2.0	-0.2053	-0.2053
2.2	-0.2017	-0.2020
2.4	-0.1931	-0.1937
2.6	-0.1817	-0.1824
2.8	-0.1687	-0.1693
3.0	-0.1551	-0.1556
3.2	-0.1415	-0.1417
3.4	-0.1282	-0.1282
3.6	-0.1154	-0.1153
3.8	-0.1034	-0.1033
4.0	-0.0922	-0.0922
5.0	-0.0489	-0.0502
6.0	-0.0240	-0.0264
7.0	-0.1002	-0.0134
8.0	-0.0051	-0.0070
9.0	-0.0024	-0.0036

*Calculated by means of the Morse potential equation.

Credit: From Quantum Theory of Molecules and Solids, by J. C. Slater, Copyright © 1963 by the McGraw Hill Book Co., Inc. Used by permission of McGraw Hill Book Co.

REFERENCES

1. Polanyi, M., Z. Phys. 7, 323, (1921)

2. J. W. Spretnak, A Summary of the Theory of Fracture in Metals, D.M.I.C. Report No. 157, 1961.

3. Dr. R. J. Weiss, private communication, U. S. Army Materials Research Agency.

4. Dr. R. J. Weiss, Solid State Physics for Metallurgists, Page 67, Permagon Press, Oxford, 1963.

5. Slater, J. C., Quantum Theory of Molecules & Solids, 1, Page 18.

6. Slater, J. C., Introduction to Chemical Physics, page 133.

7. Girifalco, L. A., Application of Morse Potential Function to Cubic Metals, Technical Report R-5, NASA, 1959, page 6.

8. Ref. 5, page 55.

9. Metals Handbook, 8th Edition, 1, American Society for Metals, 1961.

10. Doremus, R. H., Growth and Perfection of Crystals, pages 163 and 173. John Wiley and Sons, Inc.

11. Ibid, page 197.

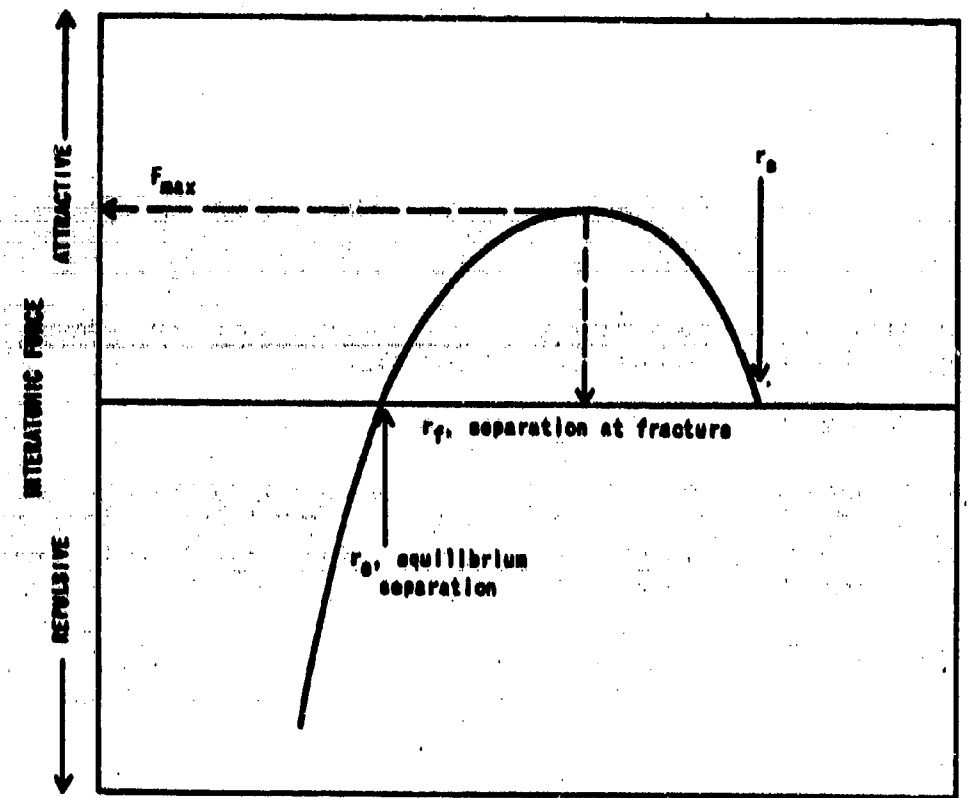

Figure 1. INTERATOMIC FORCE VERSUS INTERNUCLEAR SEPARATION
The curve was assumed to be sinusoidal between r_0 and r_s.
U. S. ARMY MATERIALS RESEARCH AGENCY

19-066-1915/AMC-64

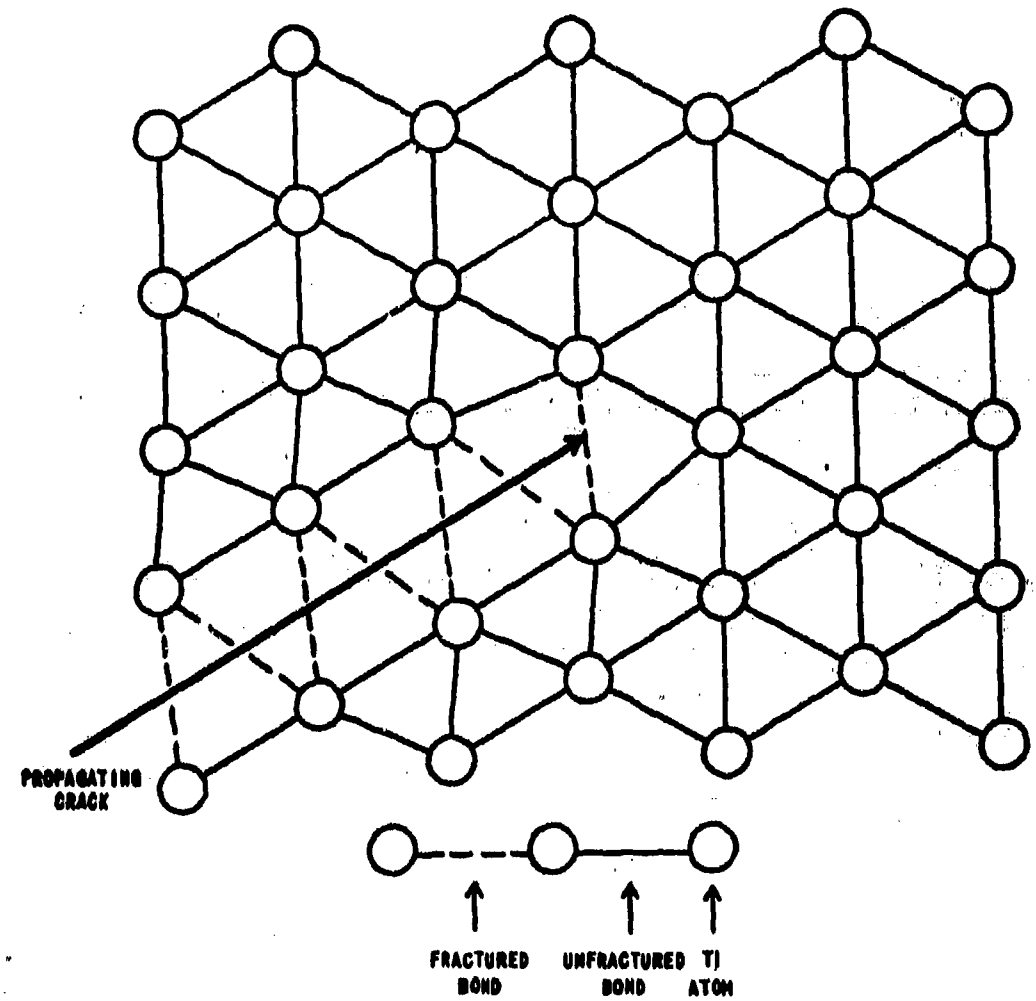

Figure 2. BRITTLE FRACTURE OF TITANIUM CRYSTAL
U. S. ARMY MATERIALS RESEARCH AGENCY

19-066-1913/AMC-64

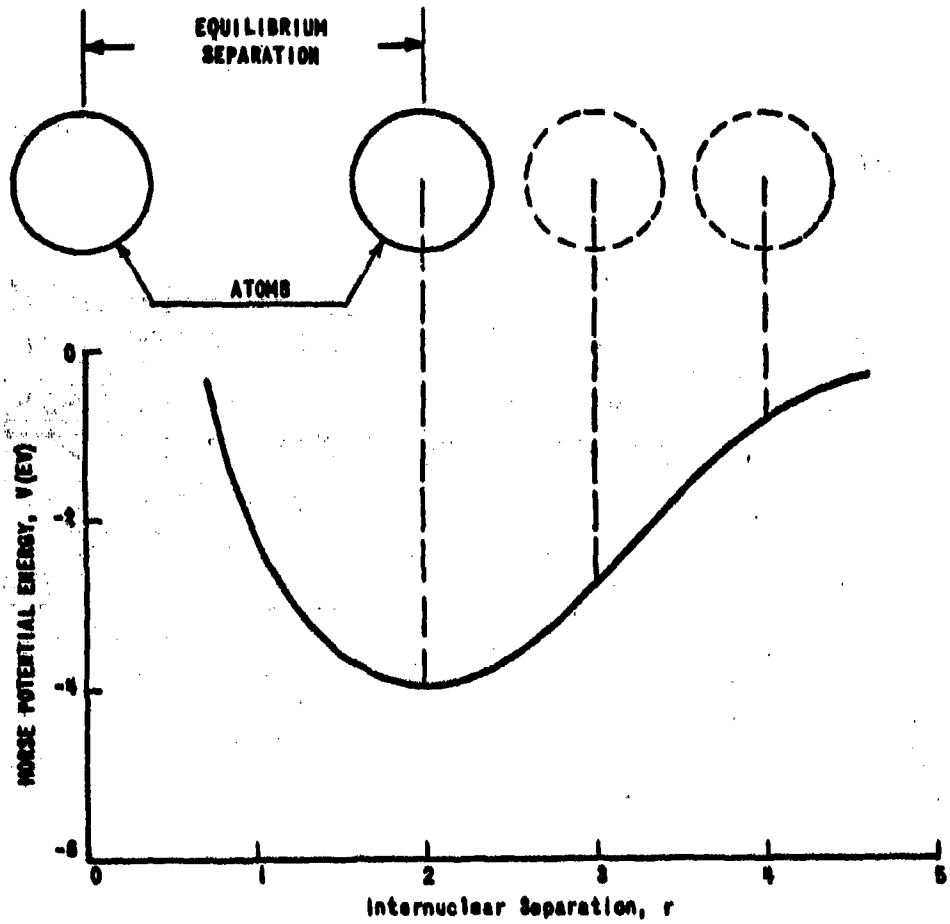

Figure 8. MORSE POTENTIAL ENERGY VERSUS INTERNUCLEAR SEPARATION (SCHEMATIC)

U. S. ARMY MATERIALS RESEARCH AGENCY

19-066-1916/AMC-64

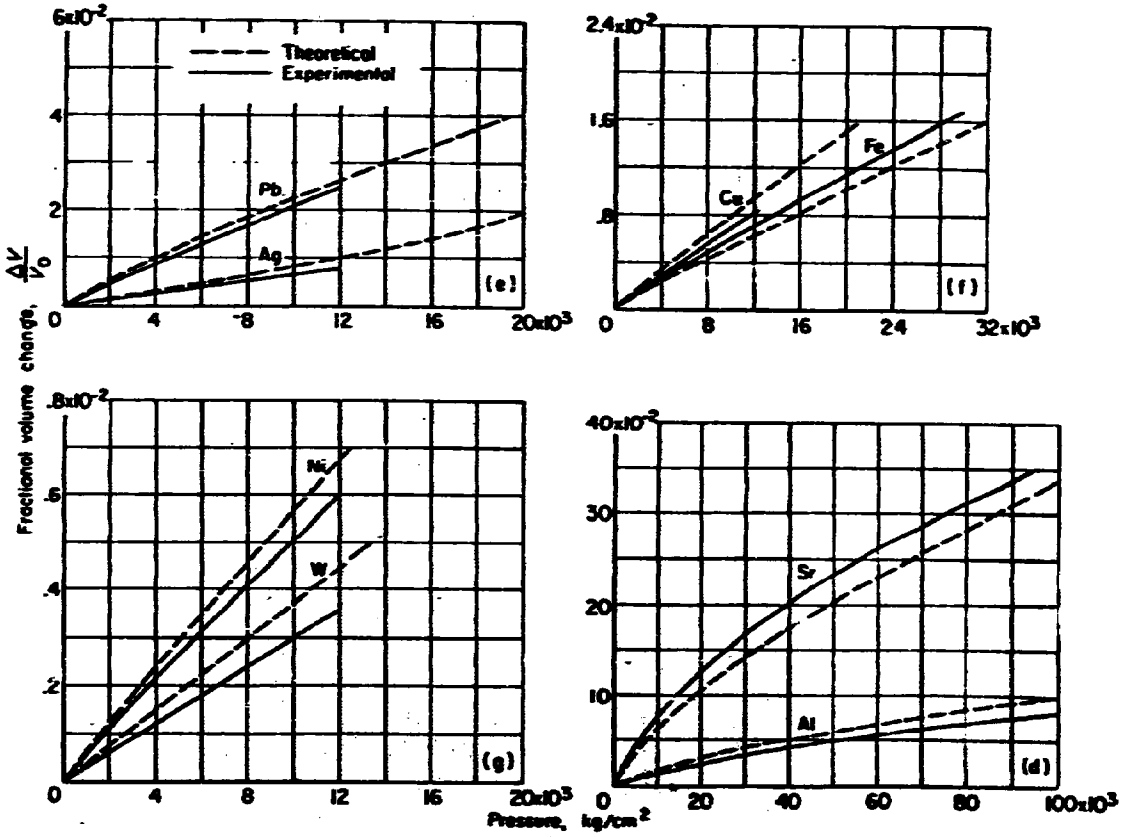

Figure 4. THEORETICAL AND EXPERIMENTAL COMPRESSIBILITY

19-066-590/MC-65

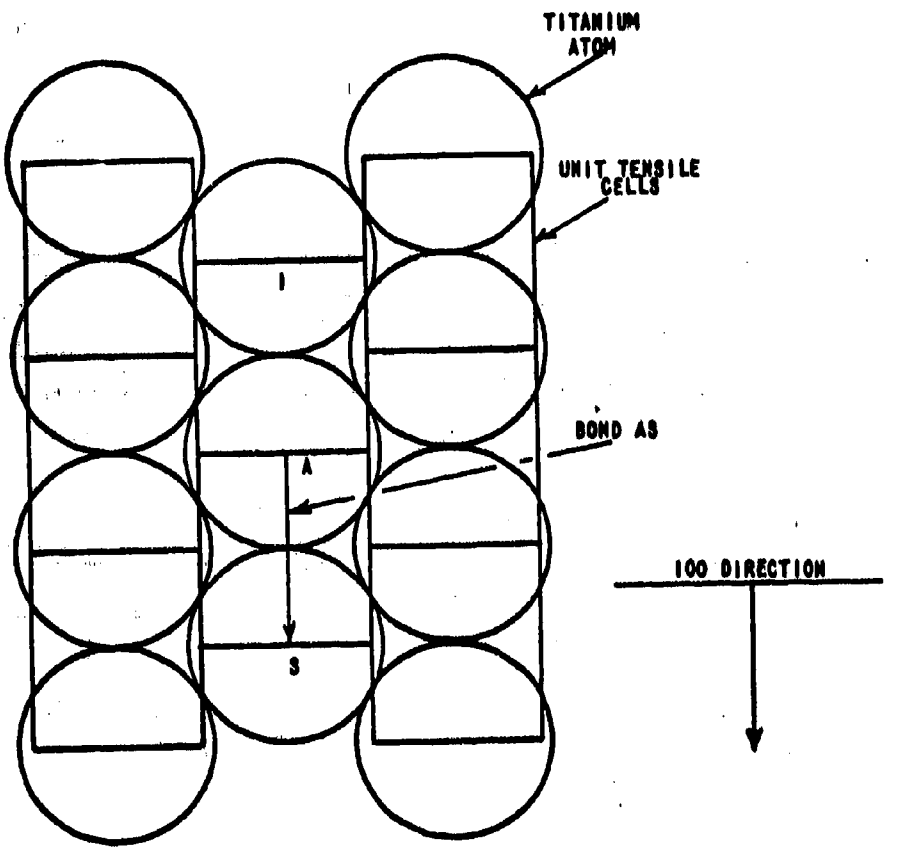

Figure 5. CRYSTAL STRUCTURE OF TITANIUM HEXAGONAL CLOSE PACKED

U. S. ARMY MATERIALS RESEARCH AGENCY

19-066-1917/AMC-64

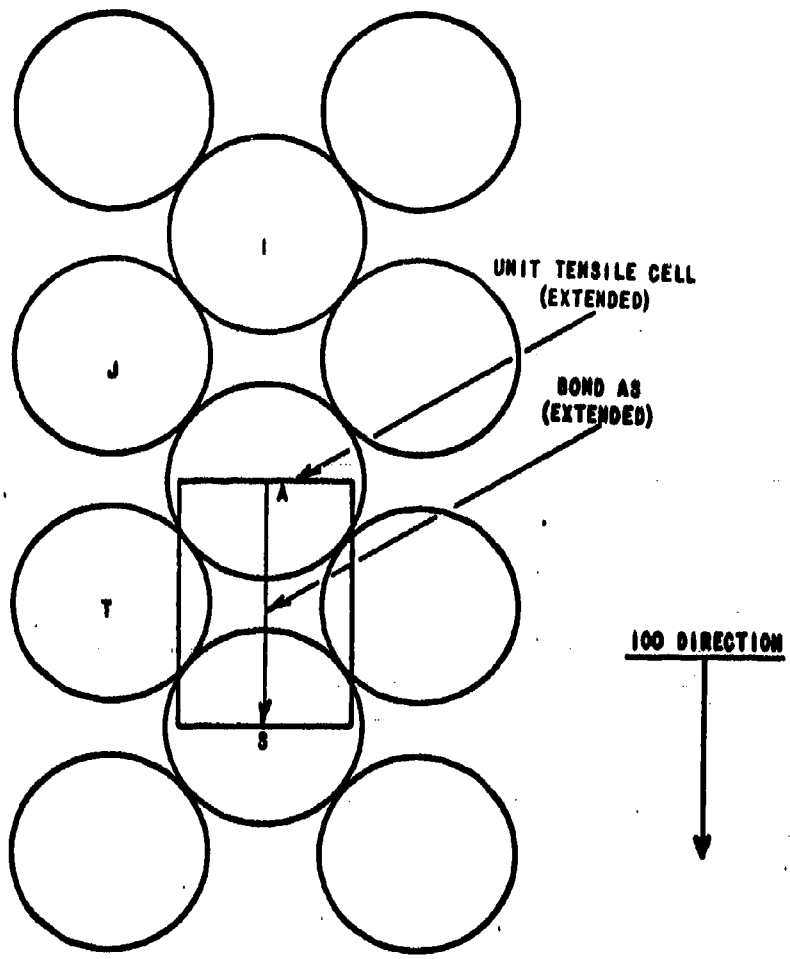

Figure 6. TITANIUM CRYSTAL,
ELASTICALLY STRAINED

U. S. ARMY MATERIALS RESEARCH AGENCY

19-066-1914/AMC-64

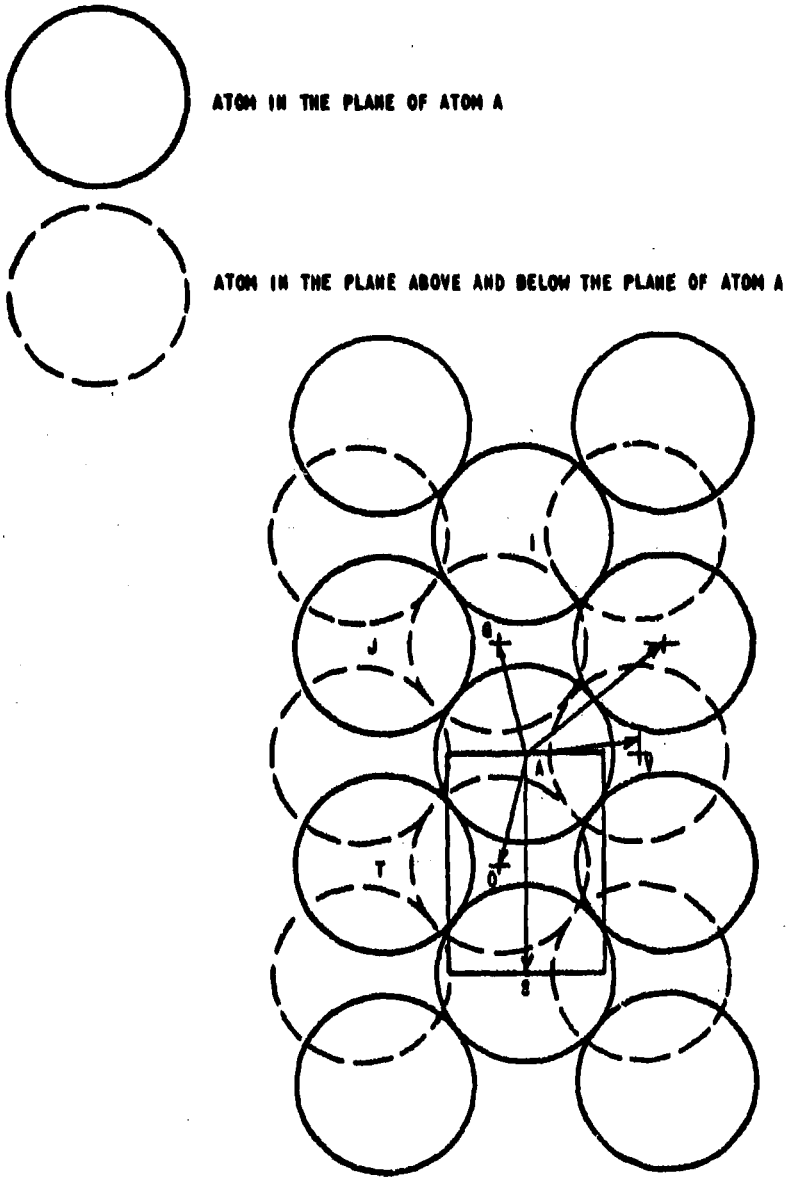

Figure 7. TITANIUM CRYSTAL, ELASTICALLY STRAINED

19-066-1918/AMC-64

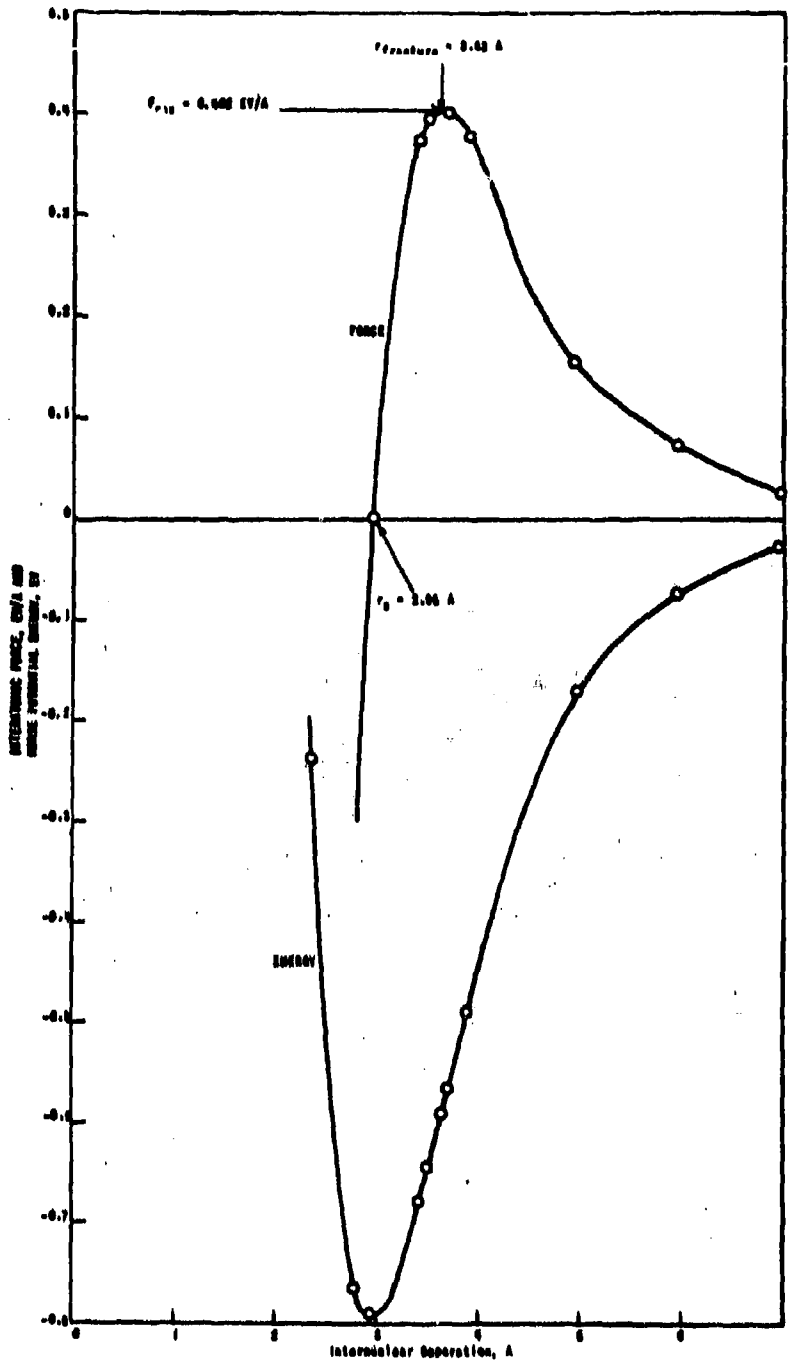

Figure 8. MORSE POTENTIAL ENERGY AND INTERATOMIC FORCE VERSUS INTERNUCLEAR SEPARATION

U. S. ARMY MATERIALS RESEARCH AGENCY

10-066-1383/AMC-65

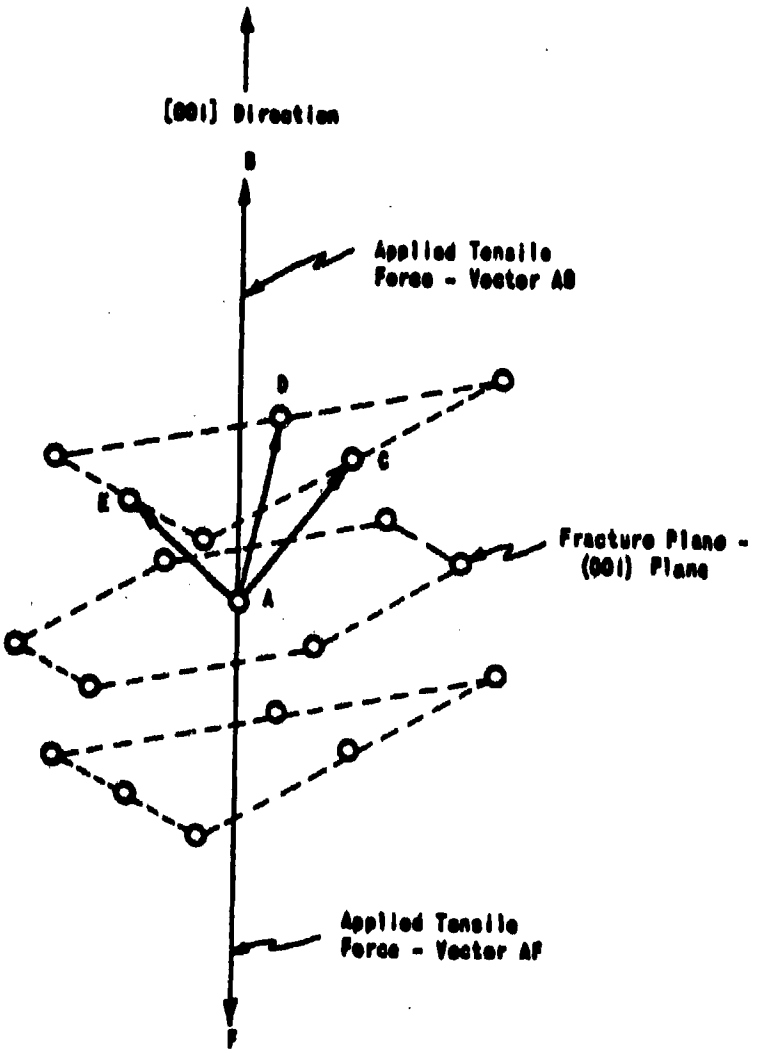

Figure 8. PORTION OF TITANIUM CRYSTAL (ORTHOGRAPHIC)
U. S. ARMY MATERIALS RESEARCH AGENCY

19-066-1340/AMC-65

TEN SNAKE VENOMS: A STUDY OF THEIR EFFECTS ON PHYSIOLOGICAL PARAMETERS AND SURVIVAL

James A. Vick, Henry P. Ciuchta, and James H. Manthei
Neurology Branch, Experimental Medicine Department
Medical Research Laboratory, U.S. Army Chemical and Research Labs,
Edgewood Arsenal, Maryland

The poisonous snakes and the venoms they produce have both fascinated and confounded the scientific world for a number of centuries. In the past inaccurate and incomplete descriptions of the physiologic changes observed following envenomation have aided the advance of folklore concerning the venomous snake. Even now there are numerous conflicting reports concerning the mechanism by which these venoms produce their lethality. It is no small wonder, therefore, that because of these reports many misgivings and misconceptions concerning the snake and its lethal and/or incapacitating capabilities have arisen.

With this background in mind a study was designed to determine the exact sequence of physiologic changes which follow the injection of a lethal dose of snake venom. Precise data concerning the minimum lethal dose for each of ten venoms was also determined, as well as a comparison of relative potencies in the mouse and dog.

MATERIALS AND METHODS. The snake venoms used in these experiments were obtained commercially from the Miami Serpentarium, Miami, Florida and from the Medical Research Laboratory at Ft. Knox, Kentucky. Each venom, which was collected by inducing the snake to strike a rubber covered jar, was mucous free and devoid of cellular debris. Bacteria were removed by high-speed centrifugation and the supernatant liquid was lyophilized. Ten venoms, representing three families of snakes, were studied. These were as follows:

Family - Crotalidae

1. Crotalus Adamanteus . . . . . Eastern Diamondback Rattlesnake
2. Agkistrodon Piscivorus . . . . . Cottonmouth Moccasin
3. Crotalus Atrox . . . . . Western Diamondback Rattlesnake
4. Agkistrodon Contortix Contortix . . . . . Southern Copperhead

5. Agkistrodon Contortix Mokeson . . . . . Northern Copperhead

Family - Elapidae

1. Bungarus Caeruleus . . . . . Indian Krait
2. Naja Naja . . . . . Indian Cobra
3. Micrurus Fulvius . . . . . Coral Snake

Family - Viperidae

1. Vipera Russelli . . . . . Russell's Viper
2. Bitis Arietans . . . . . Puff Adder

Initial toxicity of the ten venoms was determined using a total of 1864 mice. Just prior to administration, the lyophilized venom was dissolved in normal saline (1.0 mg/ml) for intravenous injection into the dorsal tail vein of the mouse. Table 1 shows the number of mice used to establish the LD_{99} and time to death for each venom.

Eighty adult mongrel dogs, anesthetized with 30 mg/kg pentobarbital sodium, were employed in the second phase of this study. Arterial blood pressure was monitored using a polyethylene catheter inserted into the femoral artery and connected to a statham pressure transducer and an E and M physiograph recorder. Portal venous pressure was recorded via a catheter inserted into the splenic vein and advanced into the portal circulation. Respiratory rate, electrocardiogram (EKG), and heart rate were continuously monitored using a pair of needle-tip electrodes placed in either side of the chest wall, and connected to the E and M physiograph through appropriate preamplifiers.

Cortical electrical activity (EEG) was monitored using four unipolar silver electrodes placed directly on the dura of each hemisphere of the brain and connected to hi-gain preamplifiers. Two of the electrodes were placed in the frontal area and two in the occipital region of the brain. Continuous recordings of EEG were made on a Model 5 grass polygraph.

The LD_{99}, as well as the approximate time to death, was determined for each venom. All data were statistically evaluated using standardized procedures (1).

Evisceration was performed in 20 dogs to determine if the initial fall in blood pressure observed following venom administration was due to the pooling of blood in the hepato-splanchnic bed. The surgical evisceration procedure was carried out as follows: the celiac, superior and inferior mesenteric arteries were ligated, and the stomach, spleen and intestines were removed after ligation of the esophagus and sigmoid colon. The portal vein was also ligated and sectioned. Blood flow to the adrenal glands and kidneys was carefully preserved and not impaired by the procedure.

Vagotomy was performed through an incision made at the level of the larynx. Both vagi were cut following a careful dissection from the tissues surrounding the carotid artery. A recovery period of 60 minutes was allowed before venom was administered.

RESULTS. The intravenous mouse LD_{99} with 95 per cent confidence limits for each of the ten venoms is shown in Table 1 [Figures and tables have been placed at the end of this article.] Comparative potencies for each venom are also graphically displayed in Figure 1. It is to be noted that the most lethal venom (Indian Krait) is approximately one hundred times more potent than the venoms of either the Northern or Southern Copperhead. Also shown in Table 1 is the average time to death for each venom. There appears to be no clear relationship between potency and survival in that the most potent venom (Krait) has the longest survival time.

The I. V. LD_{99} of each venom in the dog is shown in Table 2. Average time to death is also indicated for the ten venoms. Comparative potencies for all venoms are presented in Figure 2. In general, this data indicates that, on a mg/kg basis, the lethal dose of each venom in the dog is significantly less than the corresponding lethal dose of venom in the mouse ($p < .05$). This is not entirely true, however, because the lethal doses of Russell's Viper and Coral snake venoms are nearly identical in both the dog and mouse ($p > .05$). Relative potencies of the venoms are

quite similar in that the venom which is the most potent in the dog is also the one that is most potent in the mouse. Likewise, the venom which is the least potent in the dog is also the one that is the least potent in the mouse.

The specific effects of lethal injections of each venom on EEG, EKG, heart rate, respiration and blood pressure in the dog are shown in Figures 3-12:

Figure 3. Following a lethal injection of Eastern Diamondback rattlesnake venom, there occurred a precipitous fall in arterial blood pressure and a marked narrowing of the pulse pressure. This was followed at from 8 to 10 minutes by partial recovery of blood pressure to near normal levels and an increase in pulse pressure. Finally, just prior to death arterial pressure once again decreased sharply, terminating with cardiac arrest.

Respiration appeared unaffected during the first 2-5 minutes post injection at which time an abrupt cessation in ventilation occurred. Changes in EKG observed after the injection of the venom were consistant with progressive cardiac anoxia. Fast tracing during the post injection period showed depression of the ST segment, inversion of the spike segment, and finally, overwhelming cardiac hypoxia.

This venom produced marked bradycardia immediately post injection becoming progressively severe until just prior to death. At this time an anoxic tachycardia was observed leading to ventricular fibrillation.

Within 3-5 minutes after injection a complete loss of all cortical electrical activity occurred. This change was irreversible and appeared to occur prior to depression of respiratory movements.

Evisceration, for the most part, prevented the sharp fall in arterial blood pressure and the decrease in heart rate observed in the intact dog. Instead, a very moderate decrease in blood pressure occurred with an associated increase in heart rate.

Bilateral vagotomy did not prevent the drop in blood pressure but did allow for an increase in heart rate following a lethal injection of Eastern Diamondback rattlesnake venom.

Figure 4. The venom of the Cottonmouth moccasin also produced a precipitous fall in arterial blood pressure, however, an increase in pulse pressure rather than a decrease was noted. This was followed by partial recovery at from 3-5 minutes and a subsequent decline in both arterial and pulse pressures. Just prior to death a second marked increase in both arterial pressure and pulse pressure occurred. This appeared to be due to depressed respiratory movements and generalized cardiovascular hypoxia. Respiration was temporarily interrupted after injection of venom. This was followed by partial recovery and a subsequent decrease in both rate and volume over the following 10-20 minutes, leading to complete apnea. No significant changes in EKG were noted until severe respiratory embarrassment became apparent at which time changes consistent with generalized myocardial hypoxia appeared. Likewise, heart rate was only slightly affected by this venom until time of apnea when terminal tachycardia was noted. This was followed by cardiac arrest.

No significant changes in cortical electrical activity were noted immediately following the injection of venom. Only after prolonged hypotension were alterations in EEG noted. At time of apnea complete electrical silence was observed.

Evisceration did not prevent the precipitous decrease in blood pressure or the bradycardia produced by this venom. In contrast, vagotomy allowed for an increase in heart rate as the blood pressure fell following the injection of the venom.

Figure 5. The venom of the Western Diamondback rattlesnake produced a less dramatic fall in arterial blood pressure. Pulse pressure increased initially and returned to normal as blood pressure recovered. No anoxic rise in blood pressure was observed at any time prior to death. Rather, a slow progressive decline in both arterial and pulse pressures occurred during the 10-15 minutes preceeding cardiac arrest. Respiration was not significantly affected by the venom during the first 10 minutes post injection, however, an abrupt decrease in both respiratory rate and volume was noted, at approximately 15-20 minutes which quickly lead to complete cessation of respiration.

With this venom the EKG was relatively normal until the time at which both apnea and severe hypotension became prominent. When this occurred changes consistent with cardiac hypoxia were noted. The only

alteration in heart rate noted following injection of venom was a terminal bradycardia which occurred at time of cardiovascular collapse.

A decrease in cortical electrical activity was observed following Western Diamondback rattlesnake venom and occurred prior to any significant alterations in normal physiologic function. This change in cortical activity progressed to complete electrical silence just prior to death.

Evisceration partially prevented the decrease in arterial blood pressure observed with this venom and allowed for an increase in heart rate.

Vagotomy also eliminated the post venom bradycardia but did not prevent the sharp fall in blood pressure.

Figure 6. A lethal injection of Northern Copperhead venom produced an unusually sharp fall in arterial blood pressure and a remarkable increase in pulse pressure. Arterial pressure remained at a very low level (30-40 mm Hg) until respiratory arrest occurred at which time an anoxic-induced hypertension and subsequent cardiovascular failure occurred. This entire sequence of events required a total of from 8-12 minutes. Complete respiratory arrest occurred approximately 2-1/2 minutes after the injection of the venom. Changes in EKG and heart rate were observed only after prolonged apnea. This also is true for the change in cortical electrical activity. Loss of EEG appeared due primarily to prolonged cerebral hypoxia. Average time to death with this venom was approximately 2 hours.

Evisceration did not significantly alter the changes in heart rate and blood pressure observed in the intact dog.

Vagotomy did allow, however, for an increase in heart rate as arterial pressure fell following injection of venom.

Figure 7. Southern Copperhead snake venom produced changes in the dog similar to those observed with the venom of the Northern Copperhead. A precipitous fall in arterial blood pressure occurred with an associated increase in pulse pressure. At 5-10 minutes post injection pulse pressure narrowed as arterial pressure increased slightly. No significant changes in respiration, EKG, heart rate or EEG were noted during the initial post injection period. Progressive respiratory

depression was noted at from 30-60 minutes, terminating in apnea and a subsequent cardiovascular collapse. With this venom a slow progressive decline in cortical electrical activity was observed which occurred prior to any significant change in respiration. Time to death was approximately 1 - 1-1/2 hours.

The effect of evisceration and vagotomy was identical to that observed with Northern Copperhead.

Figure 8. The venom of the Indian Krait produced a gradual decrease in arterial blood pressure with little or no change in pulse pressure. Arterial pressure returned to normal at from 5-15 minutes and remained stable until the final anoxic rise and abrupt decline at death. Respiration remained affected by the venom until approximately 20-30 minutes post injection at which time a decrease in amplitude but not rate of respiration was observed. No significant change in heart rate or EKG were observed at any time prior to cessation of respiration. Cortical electrical activity also remained essentially normal following Indian Krait venom, decreasing abruptly only after prolonged apnea and following the onset of cardiovascular difficulties. Average time to death for this group was 2 hours.

Evisceration partially prevented the sharp fall in arterial pressure but did not affect the profound bradycardia observed in the intact dog.

Following vagotomy no significant decrease in arterial blood pressure was noted. The bradycardia previously noted in the intact and eviscerated animals was eliminated by vagotomy, being replaced by an actual increase in heart rate.

Figure 9. A lethal injection of Indian Cobra venom produced an immediate fall in arterial blood pressure and a narrowing of the pulse pressure. This was followed by a progressive increase in both arterial and pulse pressure to near normal levels reaching maximum recovery at from 20-25 minutes. With the onset of respiratory paralysis a sharp rise in both pressures was noted which terminated in cardiovascular collapse and death. The effect of cobra venom on the respiratory mechanism of the dog has previously been described in great detail. This study confirmed previous results in that there was a slow progressive decrease in respiratory rate and volume with complete arrest at

approximately 20-30 minutes post injection. Heart rate and EKG were not markedly affected by the venom until respiratory arrest at which time terminal anoxic changes were observed. A remarkable change in cortical electrical activity was noted following administration of the cobra venom. Within 30-60 seconds there was a complete and irreversible loss of all cortical electrical activity resulting in an isoelectric EEG tracing.

The initial fall in arterial pressure and decrease in heart rate was completely prevented by surgical evisceration. Instead, a marked increase in heart rate followed the administration of the venom and occurred as blood pressure fell slowly over the entire observation period of 1 to 2 hours.

Vagotomy had no significant effect upon the changes in heart rate and blood pressure previously noted in the intact dog.

Figure 10. The venom of the Coral snake produced an initial rise in arterial blood pressure. This was followed in 30 to 60 seconds by a sharp fall in arterial pressure and a decrease in pulse pressure. Both pressures then gradually increased reaching normal or near normal levels in 15-30 minutes post injection. At time of severe respiratory embarrassment arterial pressure fell off abruptly. The hypoxic rise in systemic pressure previously noted with other venoms at time of apnea was not seen. Immediately after venom administration a temporary period of apnea was also observed which lasted from 3 to 5 minutes. Breathing gradually returned to normal and remained such until time of respiratory failure. Heart rate decreased abruptly during the time of initial hypotension. Heart rate returned to normal in approximately 10 minutes and remained stable until terminal bradycardia was observed. EKG was not affected by the venom until time of respiratory arrest. A gradual decrease in cortical electrical activity was noted at from 3 to 5 minutes post injection. This change was reversible and EEG returned to normal or near normal 15 minutes post injection. A second loss of cortical activity was noted at the terminal stage at a time when severe respiratory difficulties were apparent. Average time to death with coral snake venom was 2.5 hours.

With this venom an increase in heart rate and a decrease in arterial blood pressure were noted in both the eviscerated and the vagotomized animals.

Figure 11. A lethal injection of Russell's Viper venom produced an immediate and irreversible decline in arterial blood pressure. Pulse pressure decreased as arterial pressure fell and remained narrow until death. No terminal signs of hypoxia were exhibited with this venom. Respiration was not affected during the initial post injection period. However, at approximately ten minutes there was an abrupt cessation of respiratory movements. Heart rate decreased as arterial blood pressure fell, showing some increase in rate just prior to death. Following respiratory arrest, however, profound bradycardia was noted.

Progressive hypoxic changes in EKG were noted after administration of the venom. At time of death electrical disassociation leading to cardiac arrest was seen. No alteration in electrical cortical activity was noted immediately post injection. Following the prolonged hypotension a gradual decrease in activity was observed. At no time prior to death, however, was a completely isoelectric tracing (EEG quiescence) recorded such as was observed with certain other venoms. Evisceration prevented the initial hypotension and bradycardia produced by Russell's Viper venom. A rather slow progressive decline in arterial blood pressure occurred over a 15-30 minute period of time. Death followed respiratory paralysis. Vagotomy did not prevent the sharp fall in arterial blood pressure previously noted in the intact animal, however, bradycardia was prevented and a significant increase in heart rate occurred.

Figure 12. The venom of the Puff Adder produced a somewhat transient fall in arterial blood pressure. Following the brief fall both blood pressure and heart rate decreased progressively over the 15-30 minutes preceeding death. An abrupt cessation of breathing was also noted with this venom. Sporadic irregular movements were observed at approximately 15 minutes post injection. This was followed by complete cessation of respiratory movements. Profound bradycardia and EKG changes were noted shortly after envenomation progressing rapidly to cardiac arrest. Cortical electrical activity decreased sharply at approximately 3 to 5 minutes, remaining "quite" until death. Evisceration did not prevent the initial fall in arterial blood pressure but did eliminate the sharp decrease in heart rate produced by the venom of the Puff Adder. Eviscerated animals went on to expire, however, in much the same manner as the intact envonomated dogs. Vagotomy eliminated the bradycardia, allowing for an increase in heart rate but did not prevent the initial fall in blood pressure.

DISCUSSION. The results of this study indicated that the toxicity of snake venom is not a species specific phenomenon. Even though the lethal dose of venom for the mouse is in many instances 5 to 10 times greater than that for the dog, relative potencies are remarkably similar. That is: venoms which appear most toxic in the mouse are likewise most potent in the dog -- the reverse of this is also true. As the potency of the venom decreases, however, the difference between the lethal dose, on a mg/kg basis, for the mouse and dog increases. This is most probably due to differences in the rate of the metabolism for each species which may be obscured in the extremely potent venoms. Our data would tend to substantiate this in that the mouse and dog LD_{99}'s are quite alike for two of the more potent venoms, I. E. Russell's Viper and Coral snake.

The injection of a lethal dose of snake venom produced a precipitous fall in arterial blood pressure and a marked decrease in heart rate. This is not unlike those changes observed following administration of certain other toxins where hypotension, bradycardia and decreased venous return have been observed and are attributed to the hepato-splanchnic pooling of blood (2, 3, 4). In this study surgical removal of the viscera prior to envenomation was seen to prevent the initial fall in blood pressure and apparent pooling of blood in dogs administered either cobra or Russell's Viper venoms. These data support the concept that these venoms produce a marked pooling of blood in the hepato-splanchnic bed of the dog. Evisceration, however, did not prevent death of the animals. With Rattlesnake and Krait venoms evisceration modified but did not prevent the initial fall in arterial blood pressure. This is most probably due to pooling of blood in the pulmonary tissues as well as in the hepato-splanchnic bed (5, 6). Pulmonary vascular pooling per se is also thought to occur with the venoms of the puff adder, coral snake, copperhead and cottonmouth moccasin. In these cases evisceration did not in any way modify the initial drop in blood pressure previously observed in the intact dog. Studies are currently underway in these laboratories to more closely examine this phenomenon.

A cholinergic-like response has been described following the injection of gram negative endotoxin in which a decrease in heart rate was noted and appeared to be due to an increase in parasympathetic tone (7). Lethal doses of venom also produced bradycardia in conjunction with the early fall in blood pressure. Bilateral vagotomy prior to administration of venom not only eliminated the slowing of the heart but actually allowed

for a significant increase in rate. Vagotomy in deference to evisceration did not, however, prevent the initial fall in blood pressure nor did it in any way alter the ultimate lethal effects of envenomation. The only exception in this study of venoms was found with that of the Indian Krait, which, if administered following vagotomy, did not result in either a decrease in heart rate or blood pressure. All animals treated in this manner did eventually expire, however.

The effect of certain venoms on cortical electrical activity has previously been described (8,9). This study confirmed the earlier reports in that a marked change in EEG was observed following the intravenous administration of crude cobra venom. This observation has been extended to include the venoms of the Eastern and Western Diamondback Rattlesnakes and the Puff Adder. No significant changes in EEG appeared to occur with the remaining venoms. The mechanism by which the venoms produced a quieting of cortical activity is as yet obscure.

The most nebulous aspect of this study was the apparent mode of death by which the venoms produced their lethal effects. For the most part the primary mechanism of death appeared to be of a respiratory nature. It is important to note, however, that the respiratory failure observed with certain venoms followed a prolonged period of hypotension. The apparent cause of respiratory failure may not in fact be due to the direct action of venom on the respiratory system but to a medullary hypoxia. None the less it has been proposed by some that cobra venom produces respiratory paralysis by interference with nerve impulse transmission at the myoneural junction of the diaphragm (10, 11). Others postulate that this phenomenon may be the result of increased nerve membrane permeability (12). Although other venoms may act in much the same manner as cobra venom preliminary observations would indicate that central respiratory involvement is indeed a possibility. Halmagyi et al have shown that rattlesnake venom decreases sensitivity of medullary respiratory neurons rather than affect either the peripheral nerve or neuromuscular apparatus (13). These possibilities have not yet been explored.

SUMMARY. Lethal doses of venom representing three families of poisonous snakes (Crotalidae, Elapidae and Viperidae) were administered intravenously to mice and dogs. The approximate lethal dose of ten venoms was established, as well as a characterization of the patho-

physiological events preceeding death in the anesthetized dog. Results indicate:

1. On a mg/kg basis the lethal dose of each venom for the dog is significantly less than that for the mouse.

2. The venom which is most potent in the dog is also the one that is most potent in the mouse. Likewise, the venom which is the least potent in the dog is also the one that is least potent in the mouse.

3. All venoms produced a precipitous fall in arterial blood pressure immediately post injection which appeared to be due to pooling of blood in the viscera and/or the pulmonary vasculature.

4. A significant decrease in heart rate occurred simultaneously with the drop in arterial blood pressure and can be completely eliminated by prior vagotomy.

5. The venoms of the Indian Cobra, Rattlesnake and the Puff Adder all produced a marked decrease in cortical activity immediately following injection.

6. The apparent mode of death with these venoms appeared to be respiratory in nature although the role of prolonged cardiovascular hypotension has not yet been fully evaluated.

REFERENCES

1. Snedecor, G. W.: Statistical Methods, Iowa State College Press, Ames, Iowa, 1946.

2. Vick, J. A.: Etiology of Early Endotoxin-Induced Bradycardia and Hypotension. Military Medicine, 129: 659, 1964.

3. Lillehei, R. C. and L. D. MacLean: The Intestinal Factor in Irreversible Endotoxin Shock. Ann. Surg., 148: 513, 1958.

4. Gilbert, R. P.: Mechanism of the Hemodynamic Effects of Endotoxin. Physiol. Rev., 40: 245, 1960.

5. Vick, J. A., R. J. Blanchard and J. F. Perry, Jr.: Effects of Epsilon Amino Caproic Acid on Pulmonary Vascular Changes Produced by Snake Venom. Proc. Soc. Exper. Biol. Med., 113: 841, 1963.

6. Feldberg, W. and C. H. Kellaway: Circulatory Effects of the Venom of the Indian Cobra. Ast. J. Exp. Biol. Med. Sci., 15: 81, 1937.

7. Trank, J. W. and M. B. Visscher: Carotid Sinus Baroreceptor Modifications Associated with Endotoxin Shock. Amer. J. Physiol., 202: 971, 1962.

8. Vick, J. A., H. P. Ciuchta and E. H. Polley: Effect of Snake Venom and Endotoxin on Cortical Electrical Activity. Nature, 203: 1387, 1964.

9. Bicher, H. I., C. Klibansky, J. Shiloah, S. Gitter and A. de Vriies: Isolation of Three Different Neurotoxins from Indian Cobra Venom and the Relation of their Action to Phospholipase A. Biochem. Pharma., 14: 1779, 1965.

10. Vick, J. A., H. P. Ciuchta and E. H. Polley: The Effect of Cobra Venom on the Respiratory Mechanism of the Dog. Arch. Inter. Pharmacol. et de Therapie, 153: 424, 1965.

11. Meldrum, B. S.: Depolarization of Skeletal Muscle by a Toxin From Cobra Venom. J. Physiol., 168: 49, 1963 (London).

12. Narahashi, T. and J. M. Tobias: Properties of Axon Membranes as Affected by Cobra Venom, Digitonin and Proteases. Amer. J. Physiol., 207: 1441, 1964.

13. Halmagyi, D. F. J., B. Starzecki and G. J. Horner: Mechanism and Pharmacology of Shock Due to Rattlesnake Venom in Sheep. J. Applied Physiol., 20: 709, 1965.

TABLE I

SNAKE VENOM*	NO. OF MICE USED	LD_{99} (mg/kg) (WITH 95 PER CENT CONFIDENCE LIMITS)	AVG. TIME TO DEATH
Russell's Viper	175	0.13(0.085-0.19)	3 min. (0.6-11.4)
Indian Krait	232	0.24(0.45-1.32)	498 " (202-1232)
Coral	220	0.62(0.52-0.73)	556 " (445-695)
Puff Adder	260	0.99(0.90-1.10)	271 " (181-407)
Indian Cobra	138	1.16(0.29-4.69)	117 " (49-277)
Eastern Diamondback Rattlesnake	162	2.49(2.13-2.92)	154 " (65-366)
Cottonmouth Moccasin	174	5.26(3.47-7.99)	98 " (42-228)
Western Diamondback Rattlesnake	185	5.56(2.05-15.10)	117 " (46-300)
Northern Copperhead	154	7.19(5.99-8.63)	129 " (50-337)
Southern Copperhead	164	9.52(7.72-11.75)	144 " (63-327)

* Listing of Snake Venoms Arranged According to Order of Decreasing Toxicity

TABLE II

NAME OF VENOM*	NO. OF DOGS	LO_{99} (mg/kg)	AVG. TIME TO DEATH	BLOOD PRESSURE			HEART RATE		
				Int	Evis	Vagot	Int	Evis	Vagot
Russell's Viper	14	0.10	720 min.	Dec	-	Dec	Dec	Inc	Inc
Indian Krait	20	0.12	120 - 180 min.	Dec	Sl Dec	-	Dec	Dec	Inc
Indian Cobra	44	0.15	60-120 "	Dec	-	Dec	Dec	Inc	-
Puff Adder	16	0.50	480 "	Dec	Dec	Dec	Dec	Sl Inc	Inc
Coral Snake	14	0.50	30-60 "	Dec	Dec	Dec	Dec	Inc	Inc
Eastern Diamondback Rattlesnake	14	0.50	27 "	Dec	Sl Dec	Dec	Dec	Inc	Inc
Western Diamondback Rattlesnake	25	0.50	15 "	Dec	Sl Dec	Dec	Sl Dec	Inc	Inc
Cottonmouth Moccasin	16	0.75	180 - 300 min.	Dec	Dec	Dec	Sl Dec	Dec	Inc
Northern Copperhead	10	0.75	120 "	Dec	Dec	Dec	Sl Dec	Dec	Inc
Southern Copperhead	24	0.75	60 "	Dec	Dec	Dec	Sl Dec	Dec	Inc

Int-intact normal dog; Evis-eviscerated; Vagot-vagotomized.

* Listing of Snake Venoms Arranged According to Order of Decreasing Toxicity.

MOUSE
LD99 WITH 95% CONFIDENCE LIMITS
mg/kg
NAME OF SNAKE VENOM

FIGURE 1

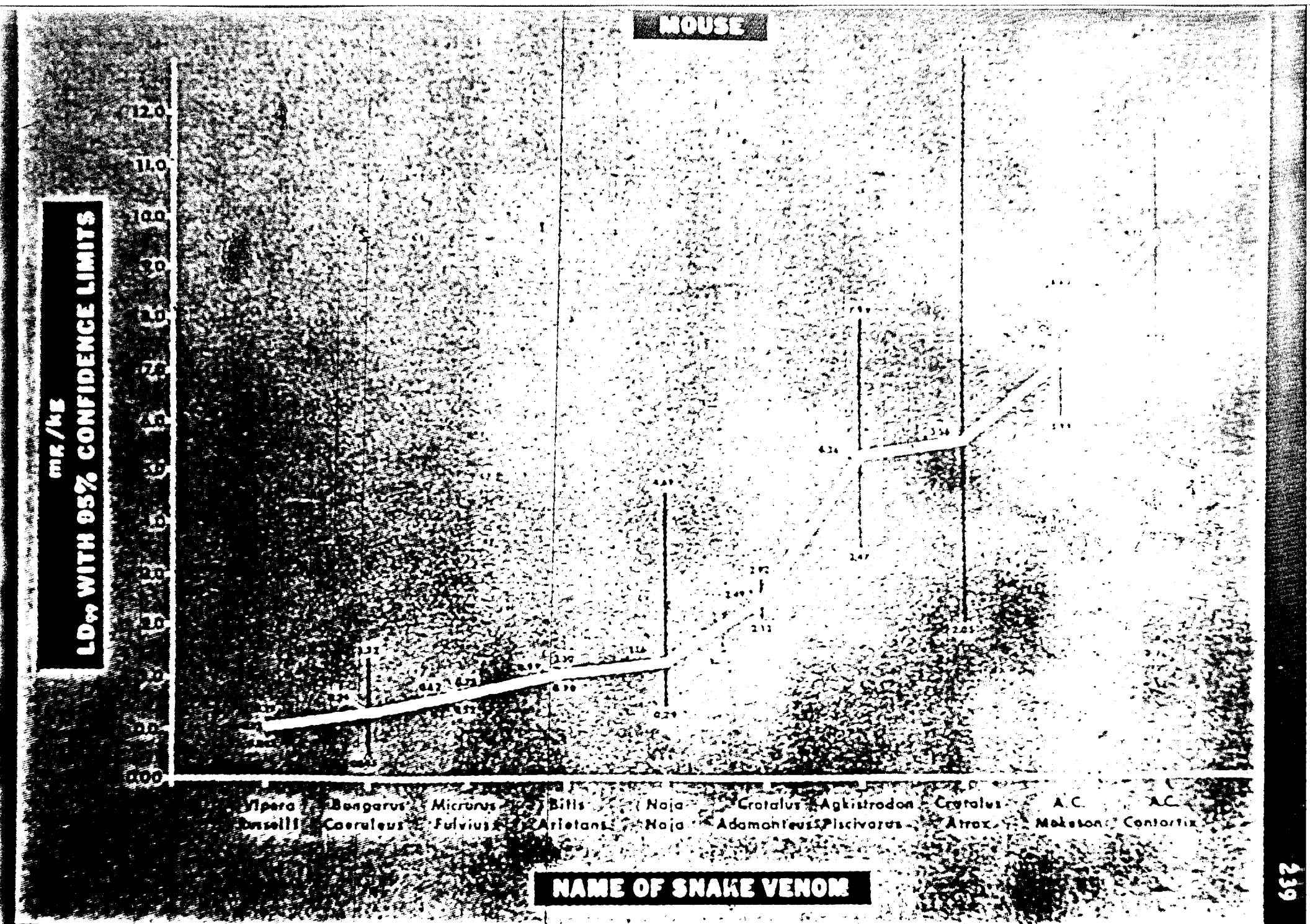
MOUSE
mg/kg
LD50 WITH 95% CONFIDENCE LIMITS
12.0
11.0
Vipera russelli
Bungarus coeruleus
Micrurus fulvius
Bitis arietans
Naja naja
Crotalus adamanteus
Agkistrodon piscivorus
Crotalus atrox
A.C. Moleson
A.C. Contortix
NAME OF SNAKE VENOM

FIGURE 1

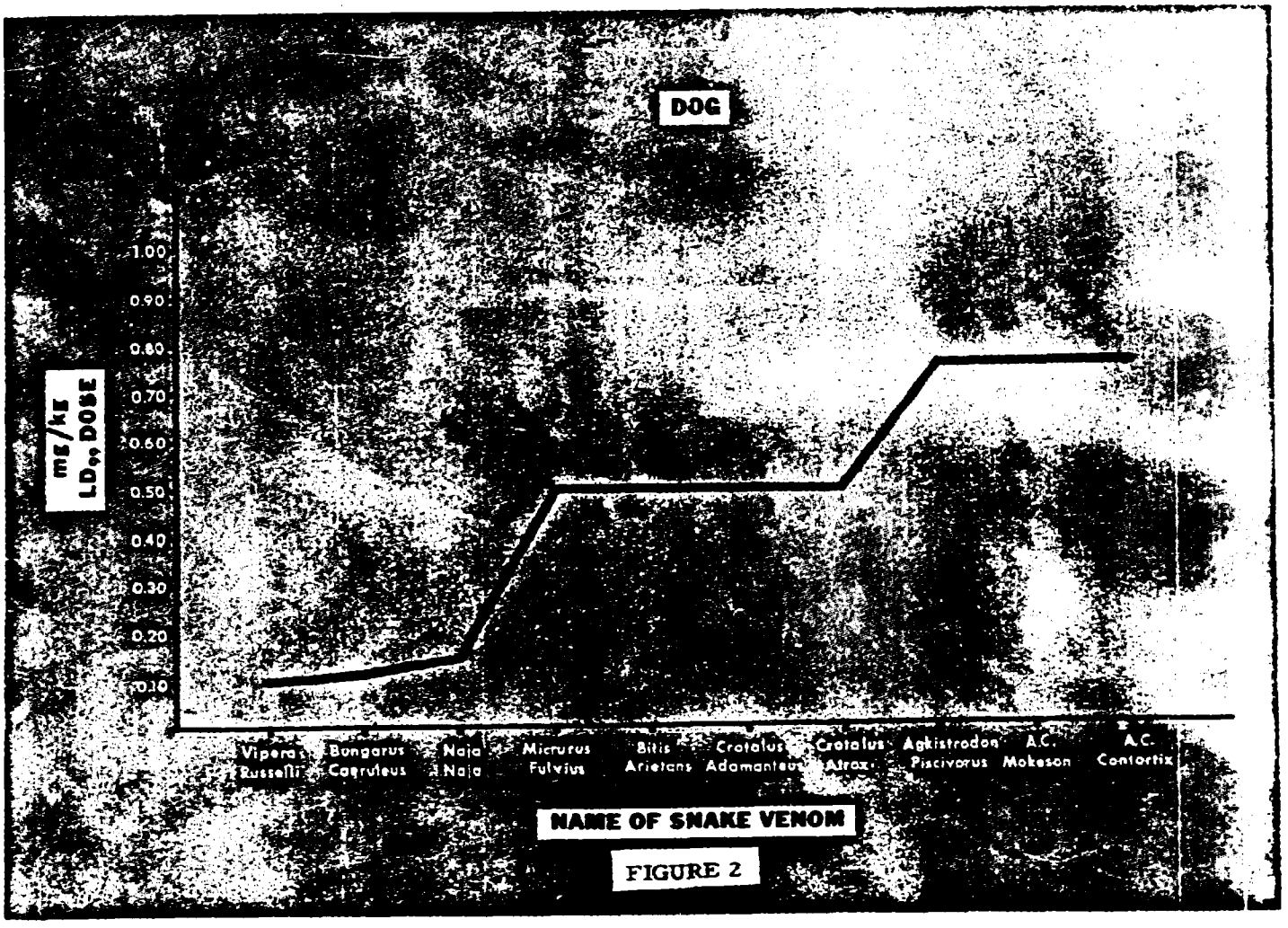
DOG
mg/kg
LD50 DOSE
1.00
0.90
0.80
0.70
0.60
0.50
0.40
0.30
0.20
0.10
Vipera Russelli
Bungarus Caeruleus
Naja Naja
Micrurus Fulvius
Bitis Arietans
Crotalus Adamanteus
Crotalus Atrox
Agkistrodon Piscivorus
A.C. Mokeson
A.C. Contortix
NAME OF SNAKE VENOM

FIGURE 2

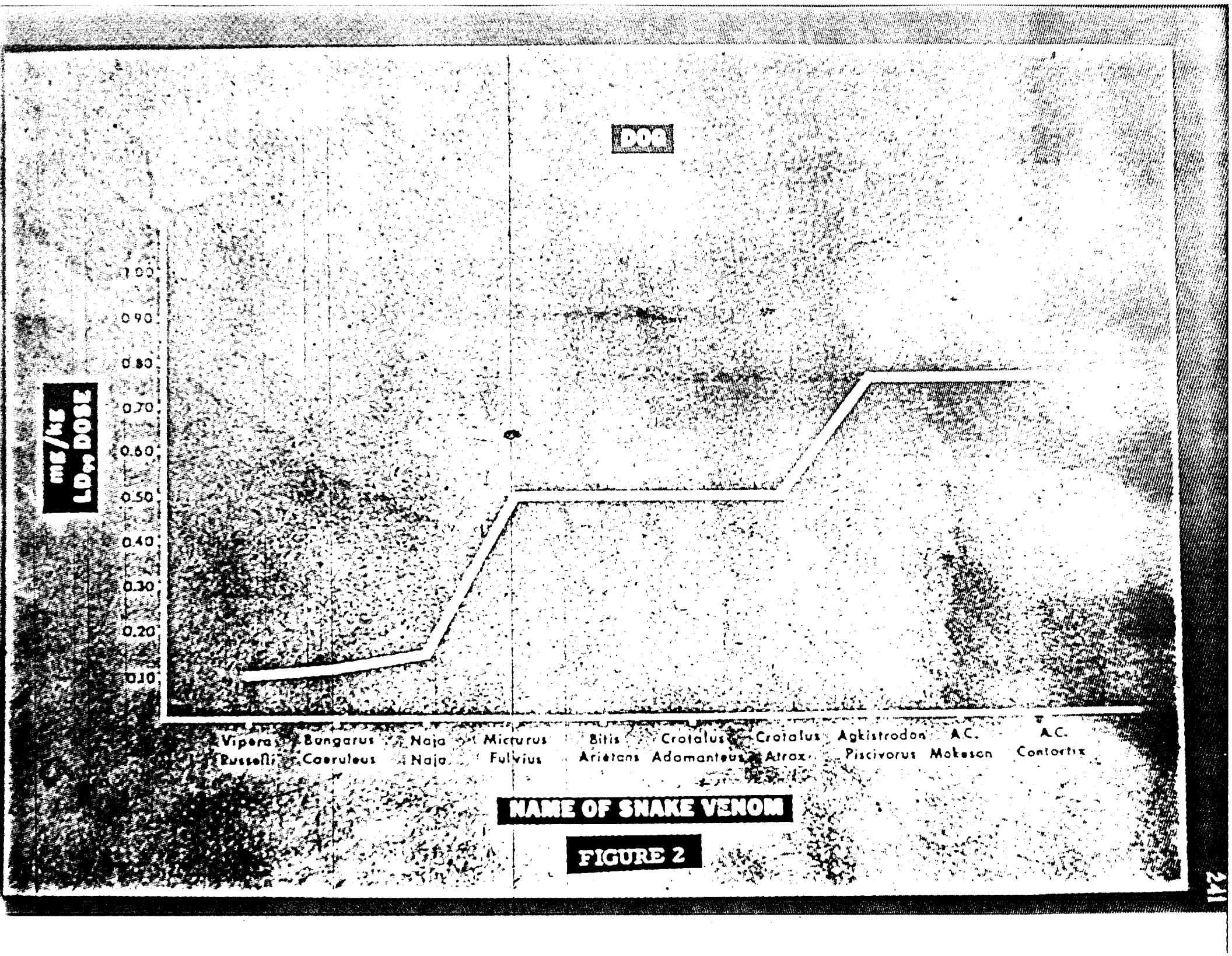
DOG
mg/kg LD50 DOSE
1.00
0.90
0.80
0.70
0.60
0.50
0.40
0.30
0.20
0.10
Vipera Russelli
Bungarus Caeruleus
Naja Naja
Micrurus Fulvius
Bitis Arietans
Crotalus Adamanteus
Crotalus Atrox
Agkistrodon Piscivorus
A.C. Mokeson
A.C. Contortix
NAME OF SNAKE VENOM

FIGURE 2

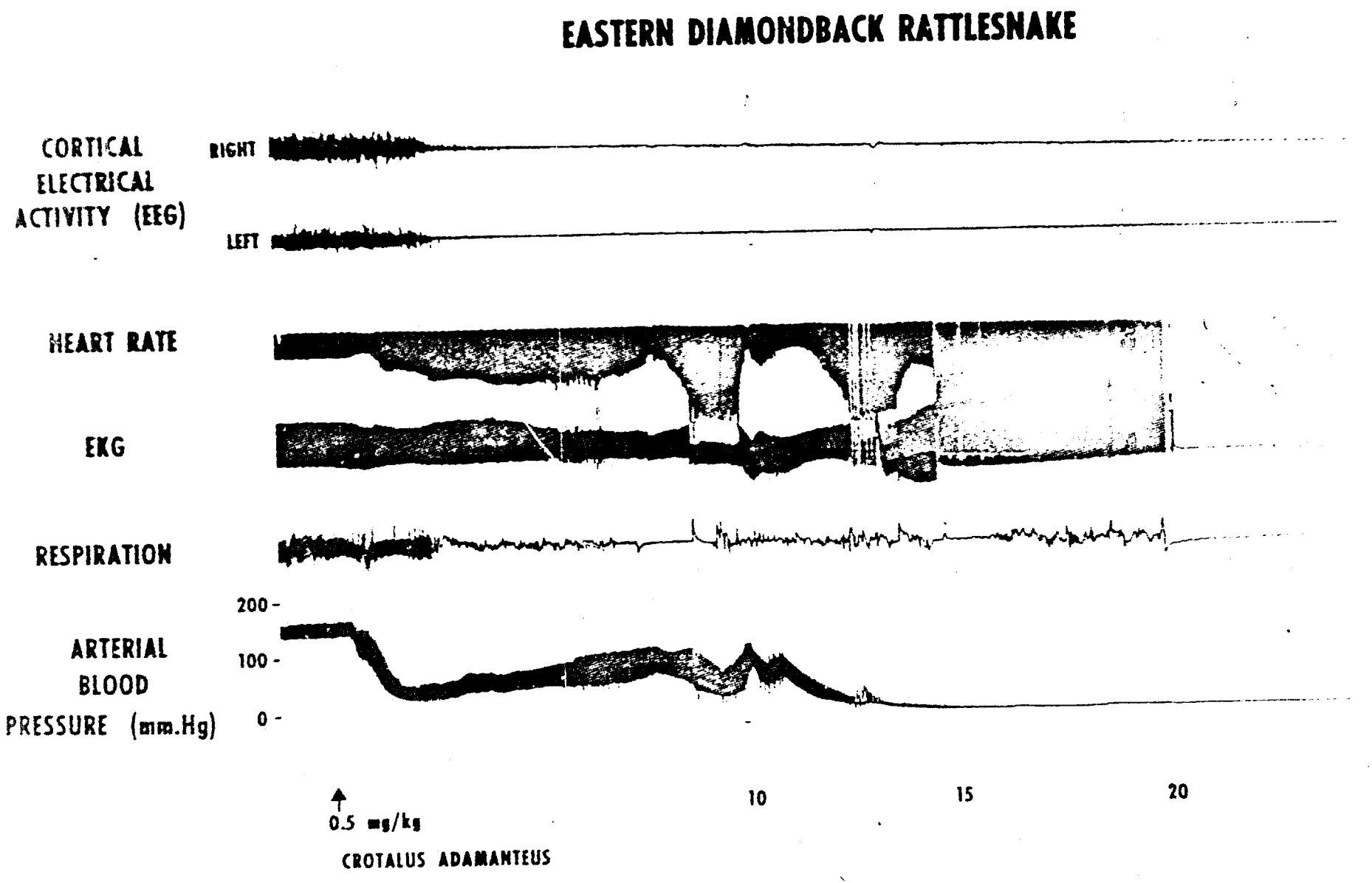
EASTERN DIAMONDBACK RATTLESNAKE
CORTICAL ELECTRICAL ACTIVITY (EEG)
RIGHT
LEFT
HEART RATE
EKG
RESPIRATION
ARTERIAL BLOOD PRESSURE (mm.Hg)
200
100
0
10
15
20
0.5 mg/kg
CROTALUS ADAMANTEUS
TIME POST INJECTION (Minutes)

FIGURE 3

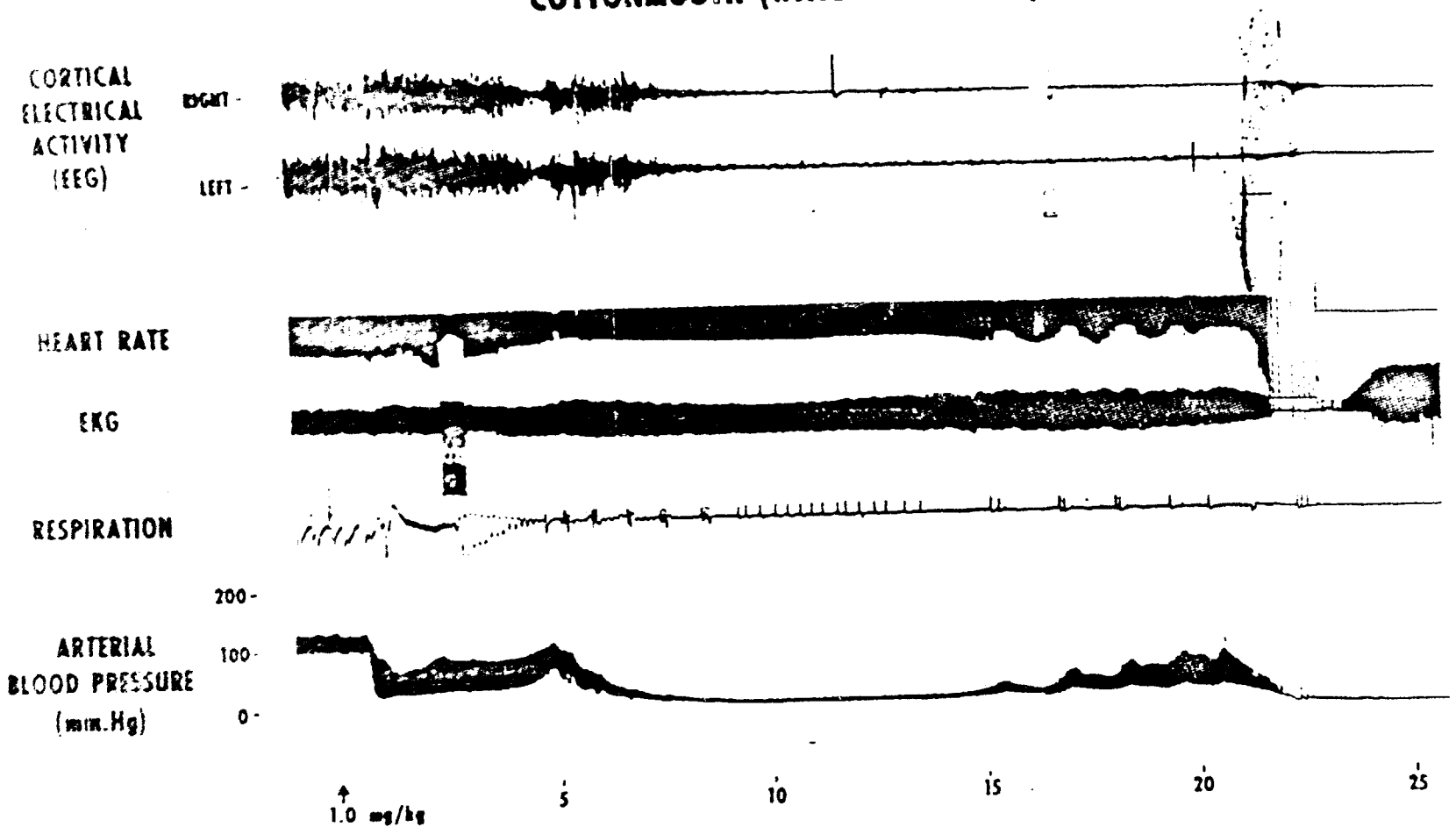
COTTONMOUTH (WATER MOCCASIN)
CORTICAL ELECTRICAL ACTIVITY (EEG)
RIGHT
LEFT
HEART RATE
EKG
RESPIRATION
200
100
0
ARTERIAL BLOOD PRESSURE (mm.Hg)
1.0 mg/kg
5
10
15
20
25
AGKISTRODON PISCIVORUS
TIME POST INJECTION (Minutes)

FIGURE 4

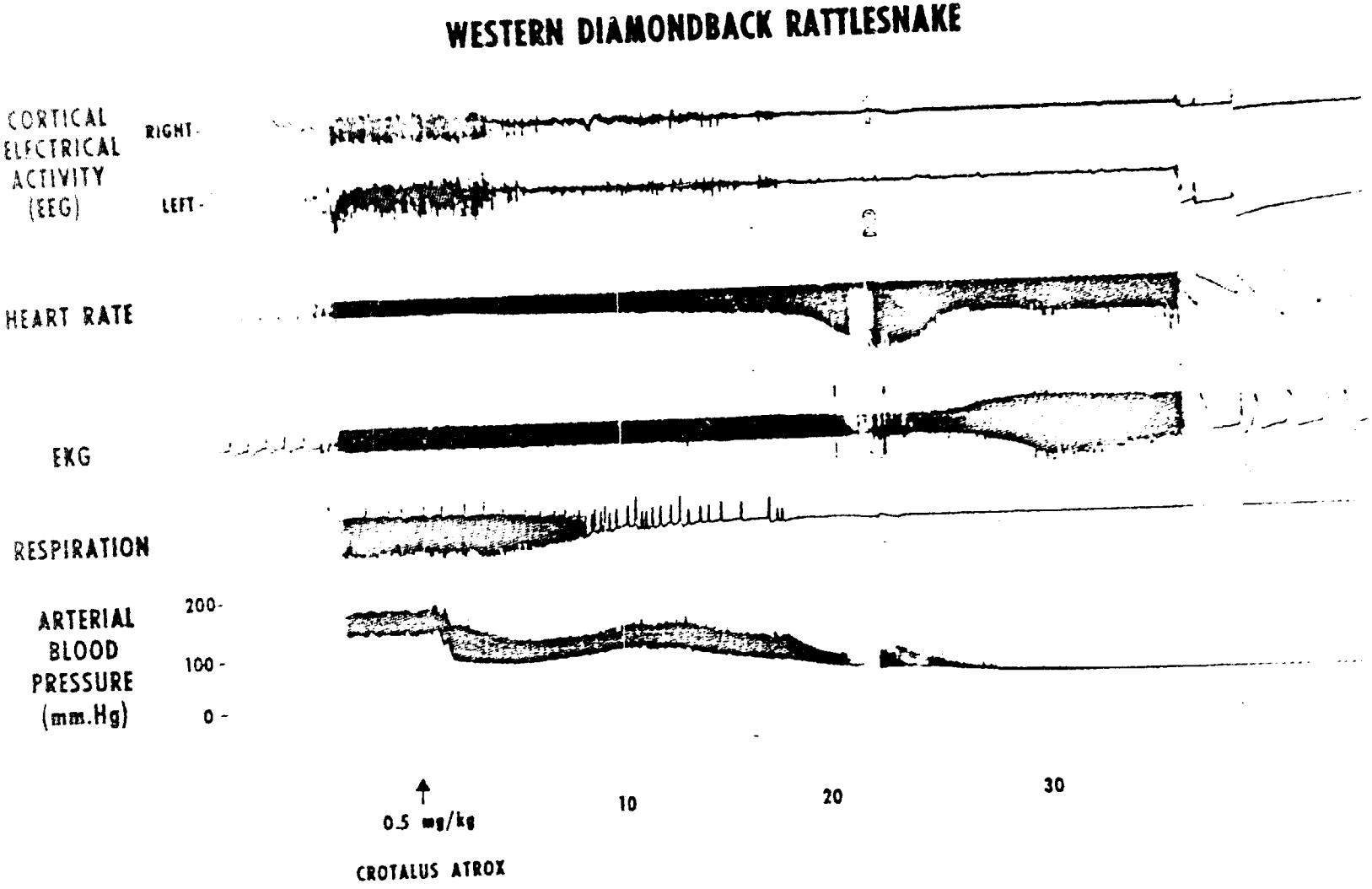
WESTERN DIAMONDBACK RATTLESNAKE
CORTICAL ELECTRICAL ACTIVITY (EEG)
RIGHT
LEFT
HEART RATE
EKG
RESPIRATION
ARTERIAL BLOOD PRESSURE (mm.Hg)
200
100
0
0.5 mg/kg
CROTALUS ATROX
10
20
30
TIME POST INJECTION (Minutes)

FIGURE 5

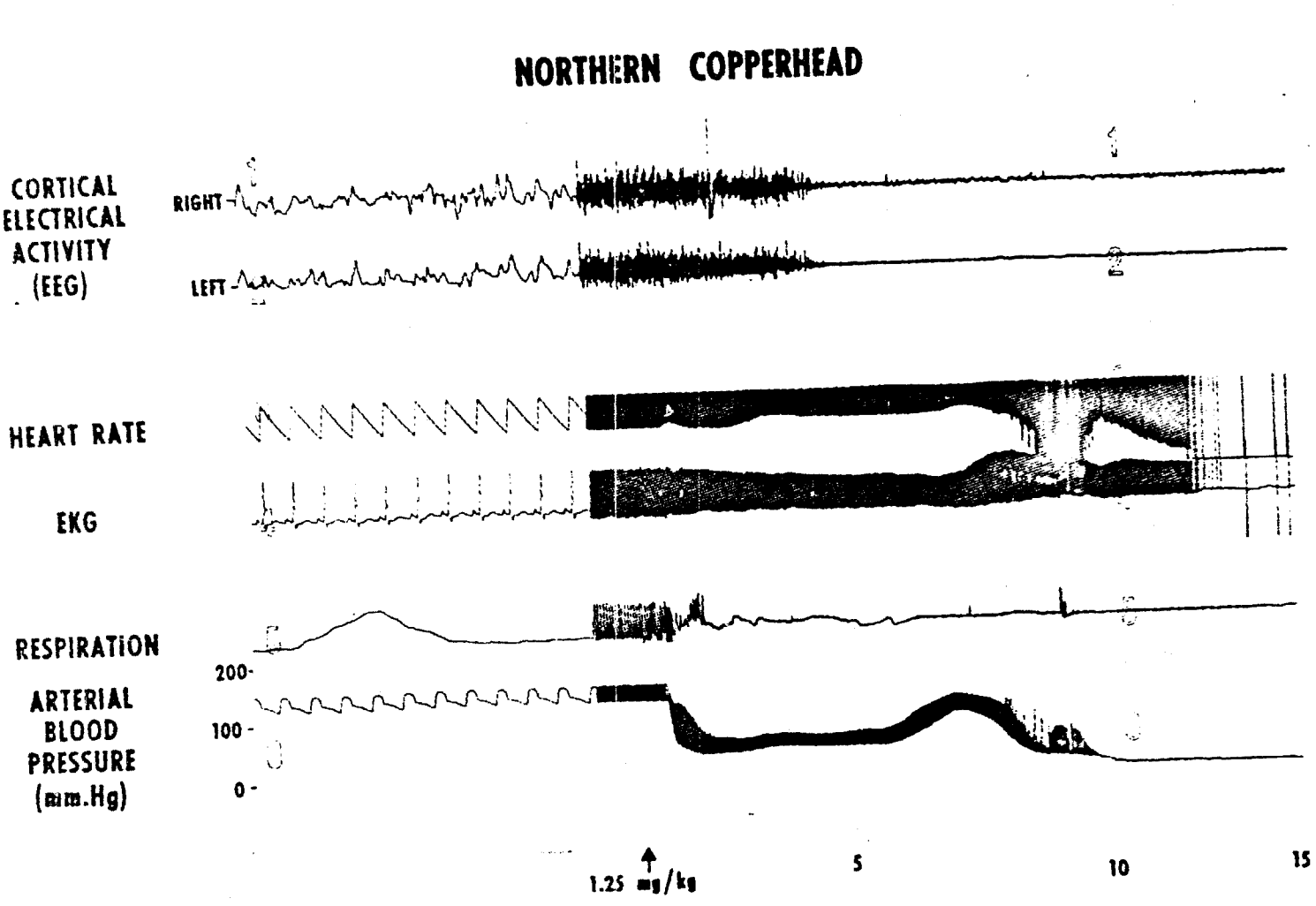
NORTHERN COPPERHEAD
CORTICAL ELECTRICAL ACTIVITY (EEG)
RIGHT
LEFT
HEART RATE
EKG
RESPIRATION
ARTERIAL BLOOD PRESSURE (mm.Hg)
200
100
0
1.25 mg/kg
5
10
15
AGKISTRODON CONTORTIX MOKESON
TIME POST INJECTION (Minutes)

FIGURE 6

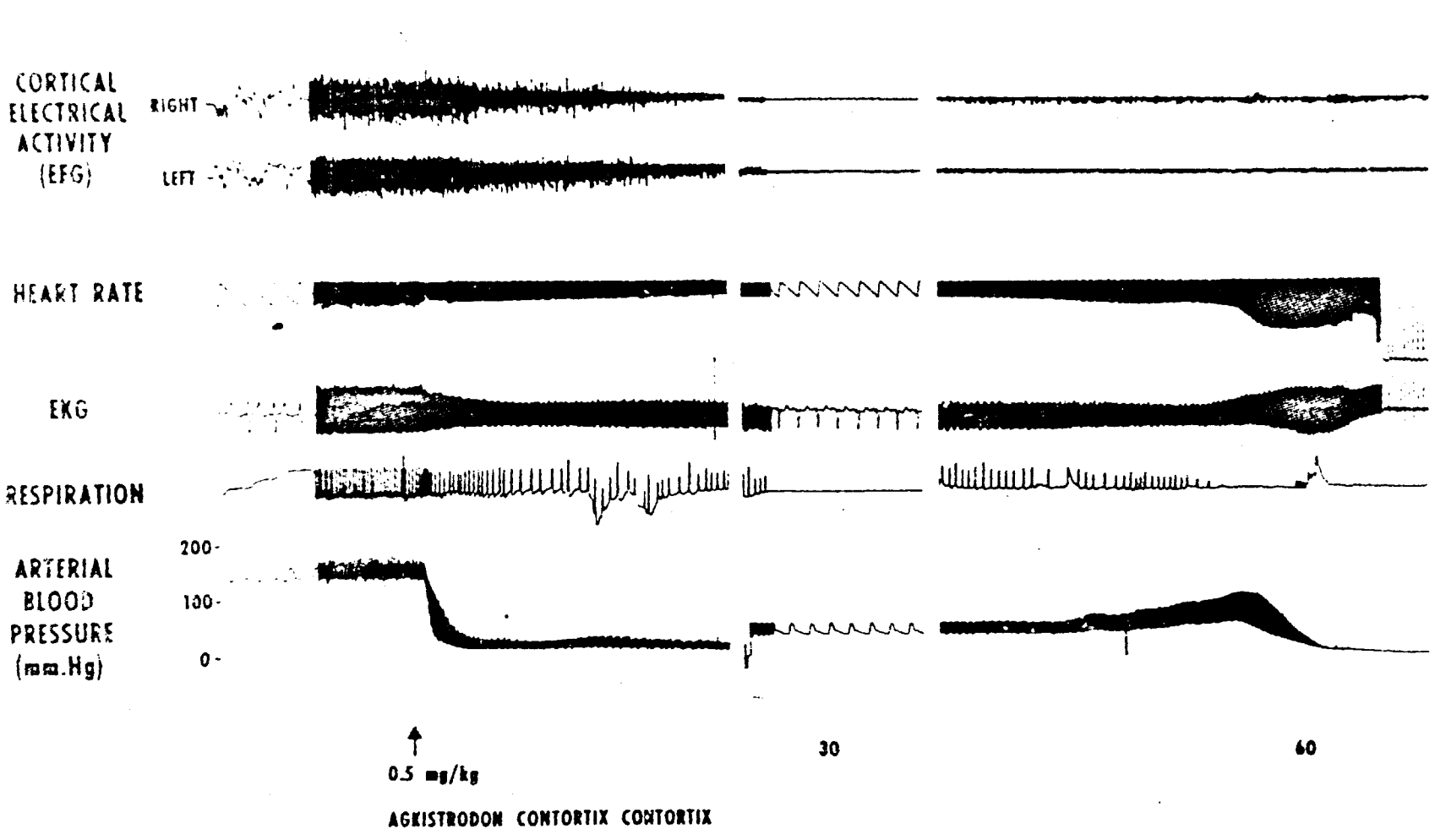
SOUTHERN COPPERHEAD
CORTICAL ELECTRICAL ACTIVITY (EEG)
RIGHT
LEFT
HEART RATE
EKG
RESPIRATION
ARTERIAL BLOOD PRESSURE (mm.Hg)
200
100
0
0.5 mg/kg
30
60
AGKISTRODON CONTORTIX CONTORTIX
TIME POST INJECTION (Minutes

FIGURE 7

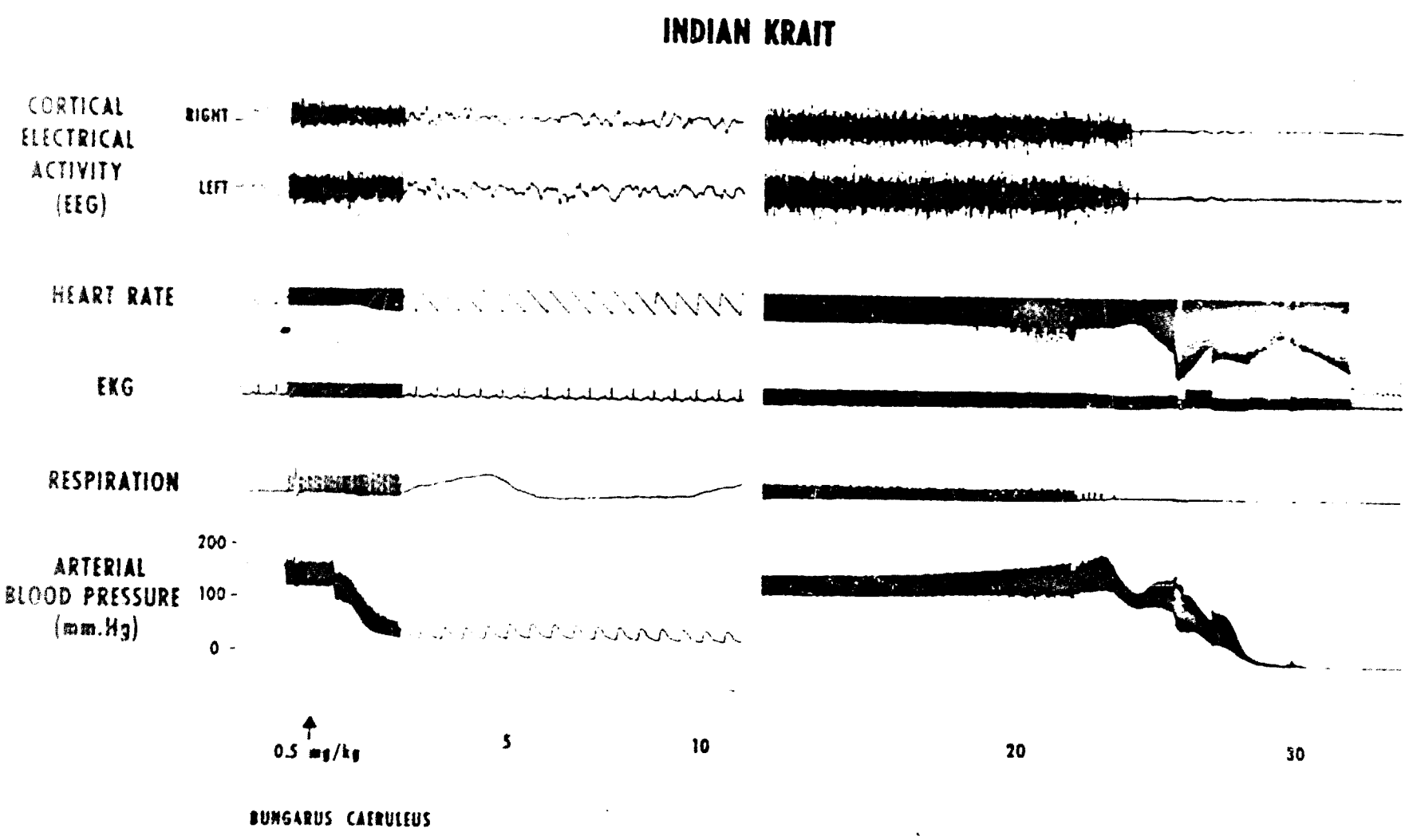
INDIAN KRAIT
CORTICAL ELECTRICAL ACTIVITY (EEG)
RIGHT
LEFT
HEART RATE
EKG
RESPIRATION
ARTERIAL BLOOD PRESSURE (mm.Hg)
200
100
0
0.5 mg/kg
5
10
20
30
BUNGARUS CAERULEUS
TIME POST INJECTION (Minutes)

FIGURE 8

INDIAN COBRA

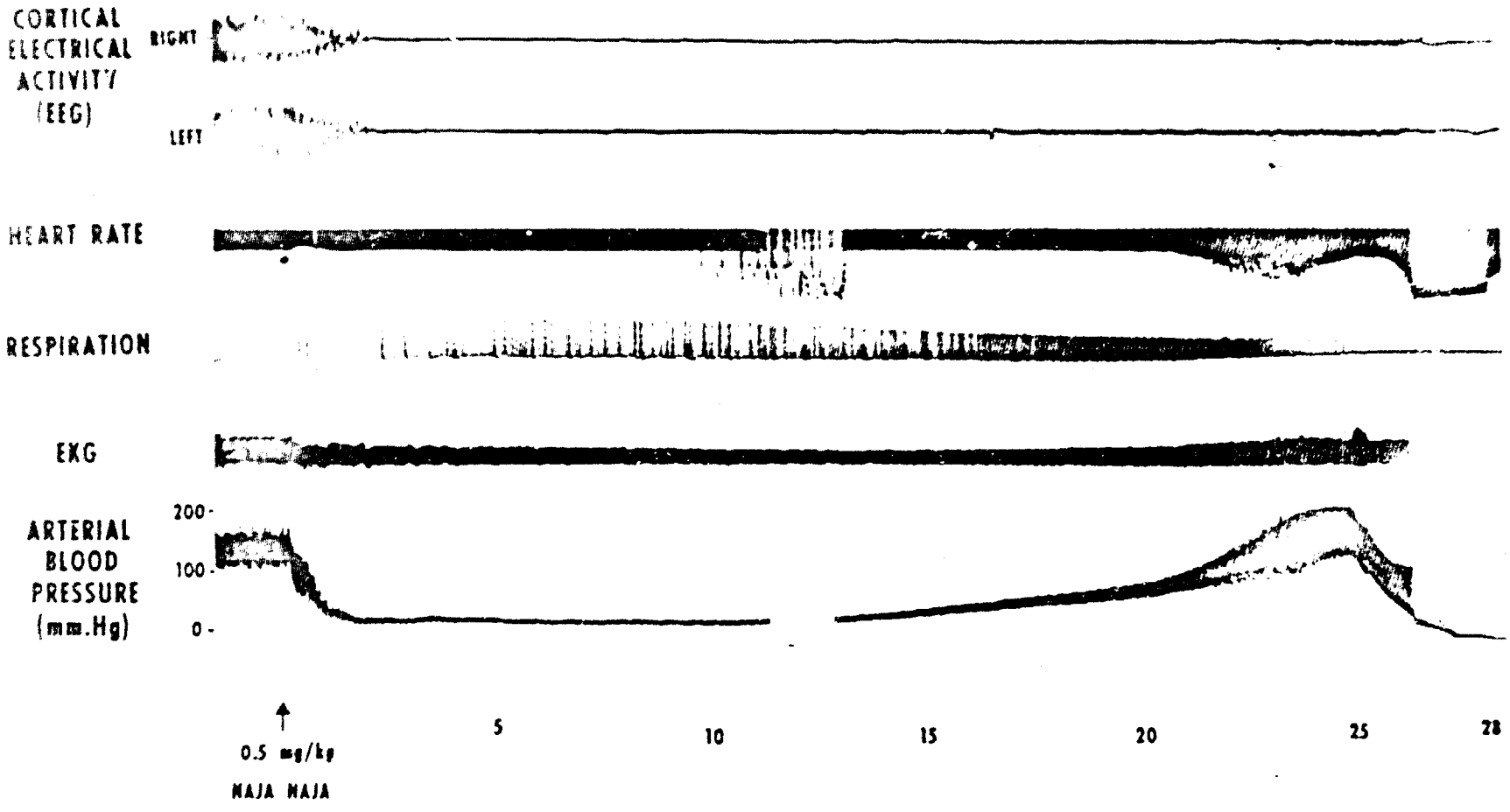

TIME POST INJECTION (Minutes)

FIGURE 9

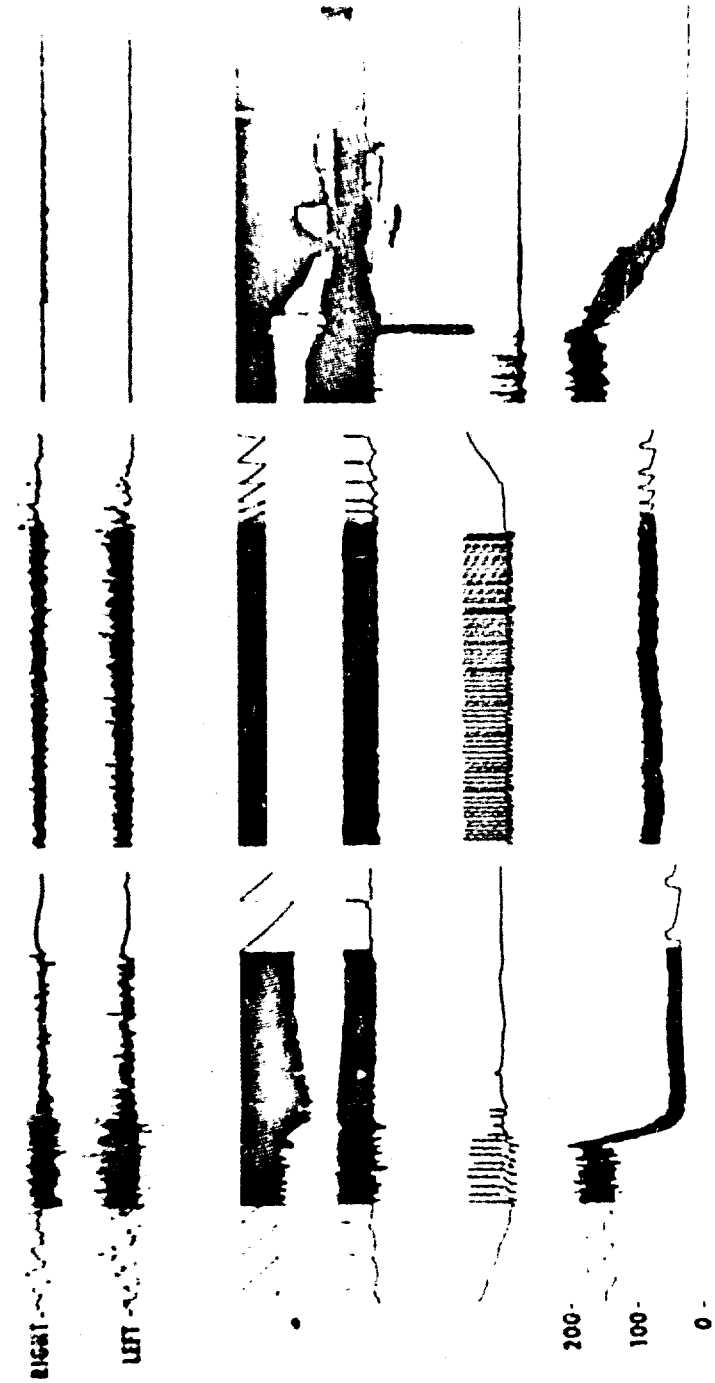
CORAL SNAKE
CORTICAL ELECTRICAL ACTIVITY (EEG)
RIGHT
LEFT
HEART RATE
EKG
RESPIRATION
ARTERIAL BLOOD PRESSURE (mm.Hg)
200
100
0
0.5 mg/kg
MICRURUS FULVIUS
15
30
TIME POST INJECTION (Minutes)

FIGURE 10

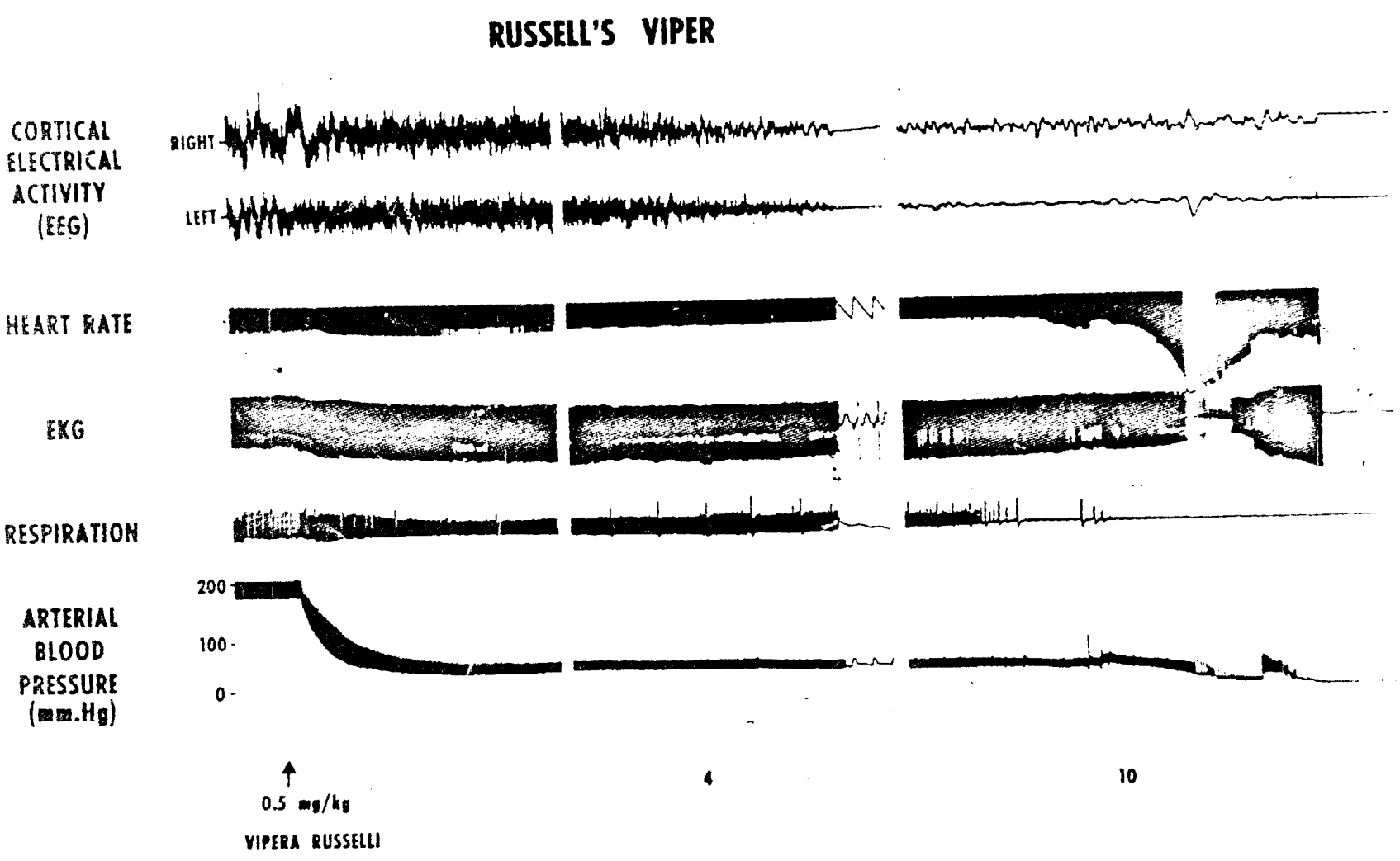
RUSSELL'S VIPER
CORTICAL ELECTRICAL ACTIVITY (EEG)
RIGHT
LEFT
HEART RATE
EKG
RESPIRATION
ARTERIAL BLOOD PRESSURE (mm.Hg)
200
100
0
4
10
0.5 mg/kg
VIPERA RUSSELLI
TIME POST INJECTION (Minutes)

FIGURE 11

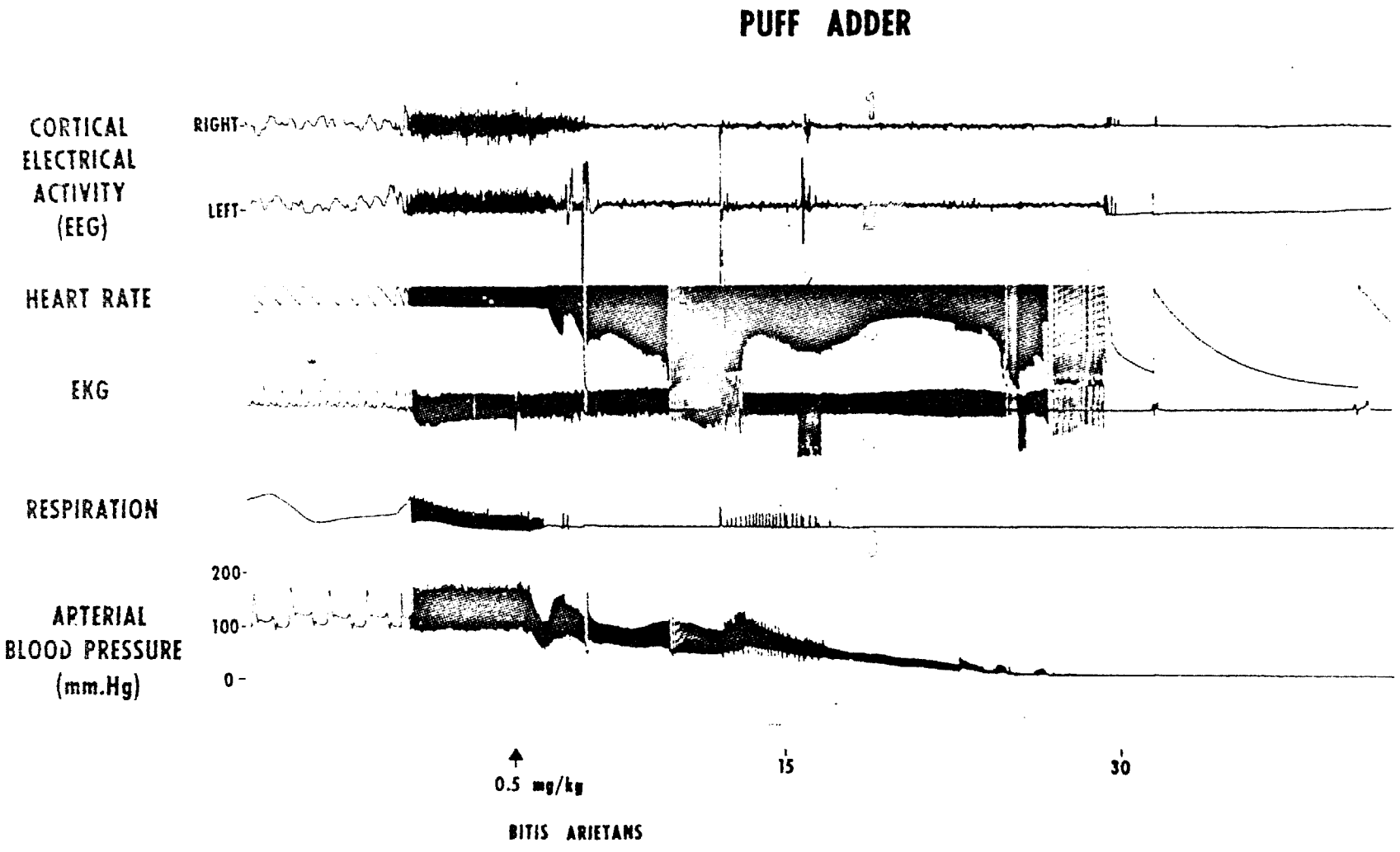
PUFF ADDER
CORTICAL ELECTRICAL ACTIVITY (EEG)
RIGHT
LEFT
HEART RATE
EKG
RESPIRATION
ARTERIAL BLOOD PRESSURE (mm.Hg)
200
100
0
0.5 mg/kg
15
30
BITIS ARIETANS
TIME POST INJECTION (Minutes)

FIGURE 12

PIRICULARIA ORYZAE - RELATIONSHIP BETWEEN LESION COUNTS AND SPORE COUNTS

Thomas H. Barksdale, William D. Brener,
Walter D. Foster, and Marian W. Jones
U. S. Army Biological Laboratories
Fort Detrick, Frederick, Maryland

INTRODUCTION: On theoretical grounds, one spore of Piricularia oryzae can cause one lesion on a rice leaf under suitable environmental conditions. In nature, however, when a plant population (that has leaves oriented in all possible planes) is exposed to a population of spores the ratio of spores to lesions is necessarily much greater than 1:1. This is true for a variety of reasons, e.g., (a) not all spores are viable, (b) not all spores land on leaves because most fall on soil or are carried away from fields by air currents, and (c) not all leaves are equally susceptible. It was desired to simulate natural conditions and to find the relationship between spore and plant populations in terms of a sample of a spore cloud and lesion counts, respectively. Of particular interest was an estimate of the range of spore counts below which lesions are not likely to form, and above which lesions will usually appear.

MATERIALS AND METHODS: Weighed amounts of a dry spore preparation (1) of Piricularia oryzae, Race 1, were discharged with a CO_2 pistol into a small closed chamber (30 x 18 inches x 26 inches high) placed flush against an ordinary chemical fume hood with a floor surface 35 inches across and 28 inches deep (Figure 1.).

After one minute was allowed for the cloud to equalize, the front and rear sides of the chamber were quickly removed, and the cloud was drawn through the hood. Pots of one-month-old Gulfrose rice plants were arranged in the hood to the front-left, front-right, rear-left, and rear-right of hood center where a rotobar spore sampler was located at plant height. Spores collected on the rotobar were counted after each run.

Four runs (designated A1, A2, B1, and B2) per day were made on each of five successive days. The following amounts of inoculum were used for runs designated "A": 2, 4, 8, 16, and 32 mg; for runs "B": 1, 5, 10, 25, and 50 mg were used. Following inoculations on a given day, plants were placed in dew chambers at 72 to 75°F for 16 hours,

after which they were placed on a greenhouse bench. Eight days later, data for each pot were taken in terms of (a) number of lesions, and (b) number of leaves.

ANALYSIS: Variables for analysis were "lesions per leaf" and "number of spores on rotobar". We had hoped to find transformations of spore counts and/or lesion counts that would linearize the relationship between the two variates, X-intercepts of tolerance limits for the regression line providing the desired range of spore counts, as shown in Figure 2.

Some of the mathematical models investigated are shown as follows:

Number	Equation
1	$\text{Log}\,[\text{Log}(\text{Lesions} + a_1) + a_2] = \alpha + \beta\,(\text{Log Spores})$
2	$\text{Log}\,[\text{Log}(\text{Lesions} + a_1) + a_2] = \alpha + \beta\,(\text{Spores})$
3	$\text{Log}\,[\text{Log}(\text{Lesions} - \text{Background} + a_1) + a_2] = \alpha + \beta\,(\text{Log Spores})$
4	$\text{Log}\,(\text{Lesions} - \text{Background} + a) = \alpha + \beta\,(\text{Spores})$
5	$(\text{Lesions})^{1/2} = \alpha + \beta\,(\text{Spores})$.

Preliminary tests based on a more limited range of spore counts indicated that Equation 1, which is a special case of the Weibull function, linearized the data for each individual test; however, parameters varied among tests. At that time the variation was attributed to non-standard experimental variables. For the tests discussed in this paper, particular emphasis was placed on standardization of experimental variables such as method of firing the CO_2 pistol, time elapsed between steps in the procedure, and plant age. Also, an extended range of spore counts was used. Equation 1 did not linearize the data obtained from these tests.

Equation 2 differs from Equation 1 in that original spore counts were not transformed. This equation resulted in linearity, but variation in the transformation of lesions increased with number of spores on rotobar, and a positive Y-intercept was obtained. When this equation was fitted to the data, approximately 52% of the variation in "lesions per leaf" was explained.

The positive Y-intercept of Equation 2 indicates that some lesions would have been formed in the absence of spores. This is not possible. The data could have resulted from use of previously infected plants, or if the chamber and/or hood were contaminated from previous runs. It was assumed that some background was present, and the average number of lesions obtained with very low spore counts was used as an estimate of this background, shown in Equation 3. A linear relationship in this transformation did not exist.

A plot of the data transformed as in Equation 4 gave results similar to those obtained with Equation 2; i.e., the function appeared to be linear, but with unequal variances in the transformation of lesions, and it appeared that a positive Y-intercept would still exist. Results from Equations 2 and 4 did, however, seem to imply that spores should remain untransformed.

Equation 5 gave the desired properties of linearity and homogeneity of variances. When this equation was fitted to the data, results shown in Figure 3 were obtained. This equation explained about 65% of the variation in "lesions per leaf". A positive Y-intercept is again evident. Untransformed data, together with the fitted equation and 80% tolerance limits for individual values are shown in Figure 4.

DISCUSSIONS AND PROBLEMS: Our problem is, of course, that we did not obtain the expected positive X-intercept from which tolerance limits for individual values would have given an estimate of the range of number of spores below which lesions would not form and above which lesions would usually appear.

Some deficiencies of the experimental design have occurred to us.

First, we should have included runs in which no spores were released as a check on methods and a measure of any background that may have been present.

Second, consideration should have been given to the ratio of leaf area (this involves orientation of the leaves among other factors) to volume of air sampled by the rotobar. An attempt should have been made to equalize the probability of obtaining one spore on the rotobar and the probability of one spore landing on any one leaf in the hood.

Detection of small numbers of spores presents a technical problem. Since our interest is in a range of counts that is probably low, perhaps it might be more accurate to estimate lesion counts expected from low spore counts by extrapolation of a function derived from a range of higher counts, in which we have more confidence.

We have been measuring number of spores collected at plant height. Perhaps this is not the measurement we need. Fallout would not be included in this measurement. Perhaps an additional measurement of spores collected from the floor of the hood should be made. We may need a measurement of the cloud before it reaches the plants, in which case should we go to a wind tunnel?

Suggestions for the design and analysis of an experiment to find the relationship between spore counts and lesion counts, particularly the range of spore counts below which lesions will not be likely to form and above which lesions will usually appear, will be appreciated.

REFERENCES

1. Andersen, A. L., B. W. Henry, and E. C. Tullis, 1947. Factors affecting infectivity, spread, and persistence of Piricularia oryzae Cav. Phytopathology 37: 94-110.

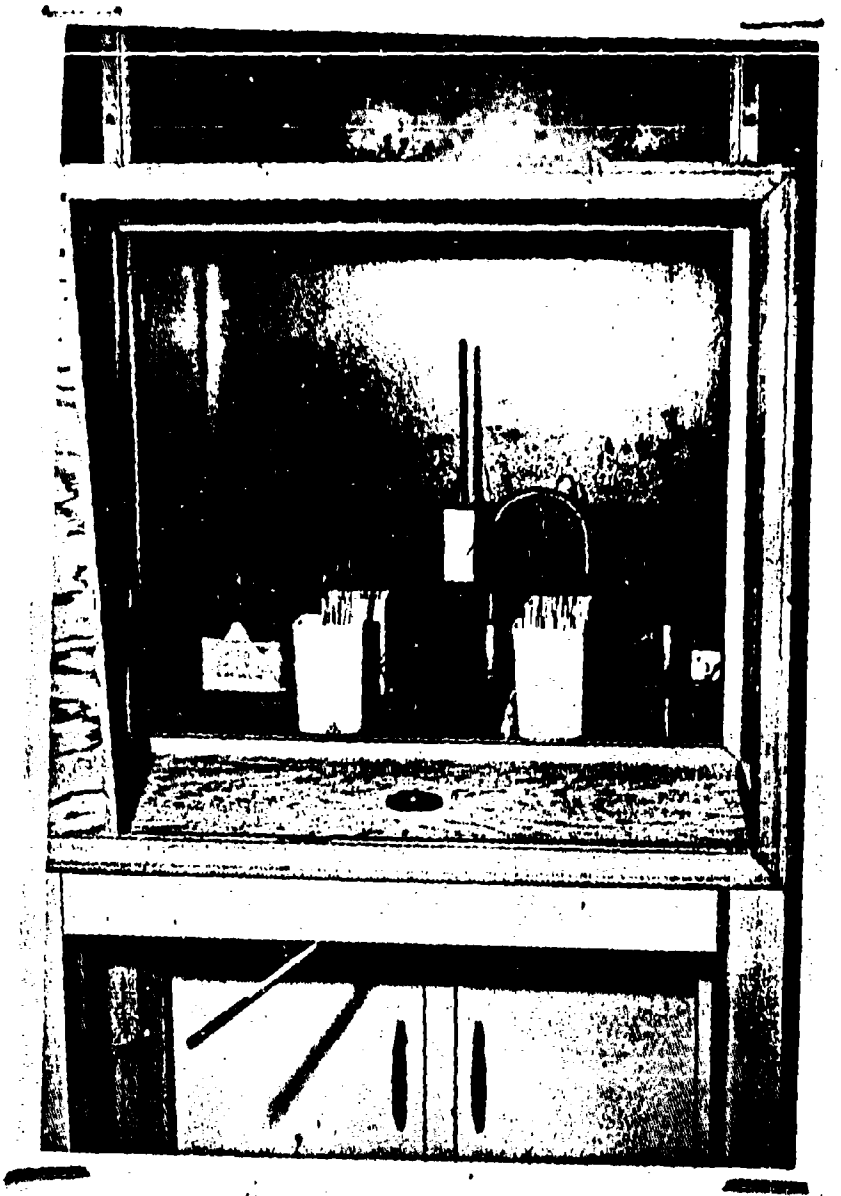

Figure 1: Inoculation Equipment

Showing location of plants and rotocar spore sampler in the fume hood, and the cloud chamber with removable sides in front of the hood.

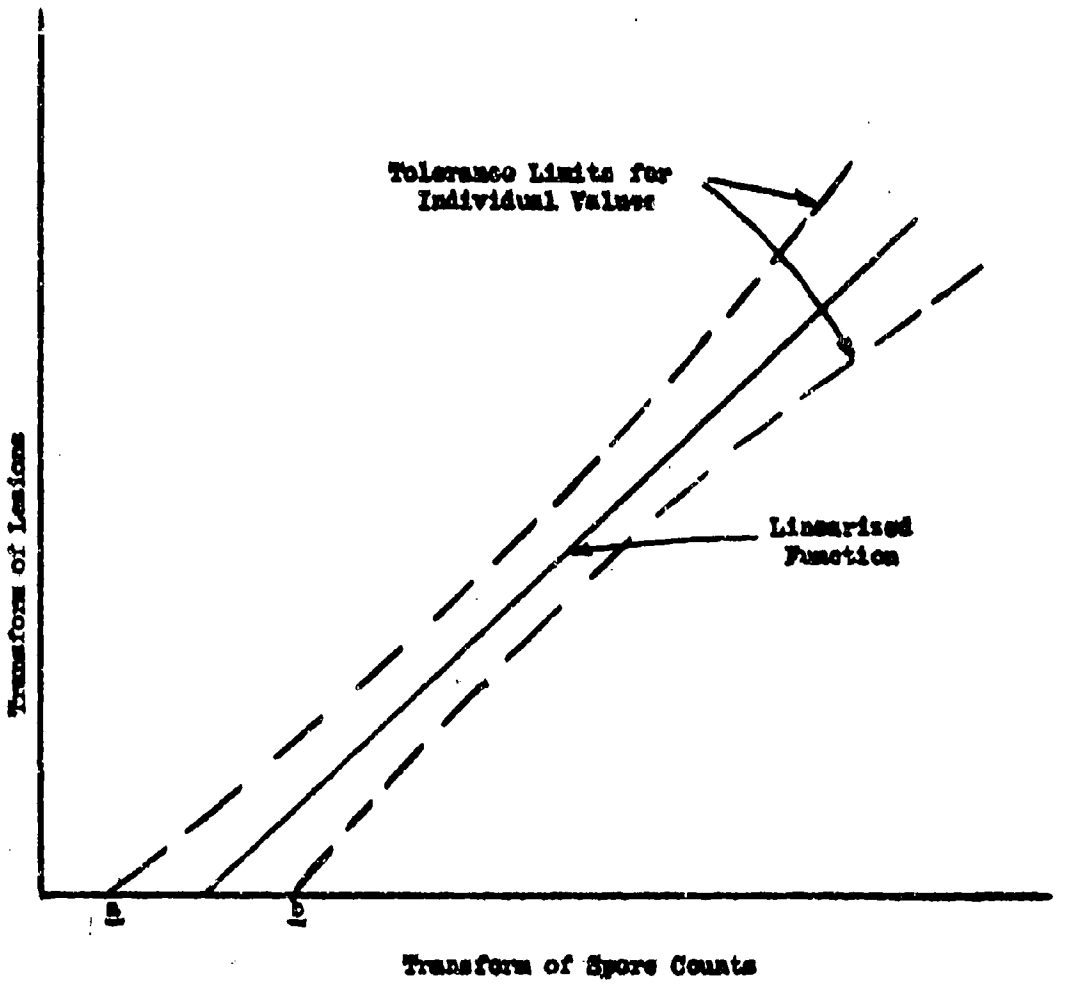

Point a is the desired value on the spore axis below which lesions will not be likely to form and point b is the value above which lesions will usually appear.

Figure 2

Figure 3

$(\text{Lesions/leaf})^{1/2}$ As a Function of Number of Spores on Rotobar

$(\text{Lesions/leaf})^{1/2} = 0.1671 + 0.002565\ (\text{Spores on Rotobar})$

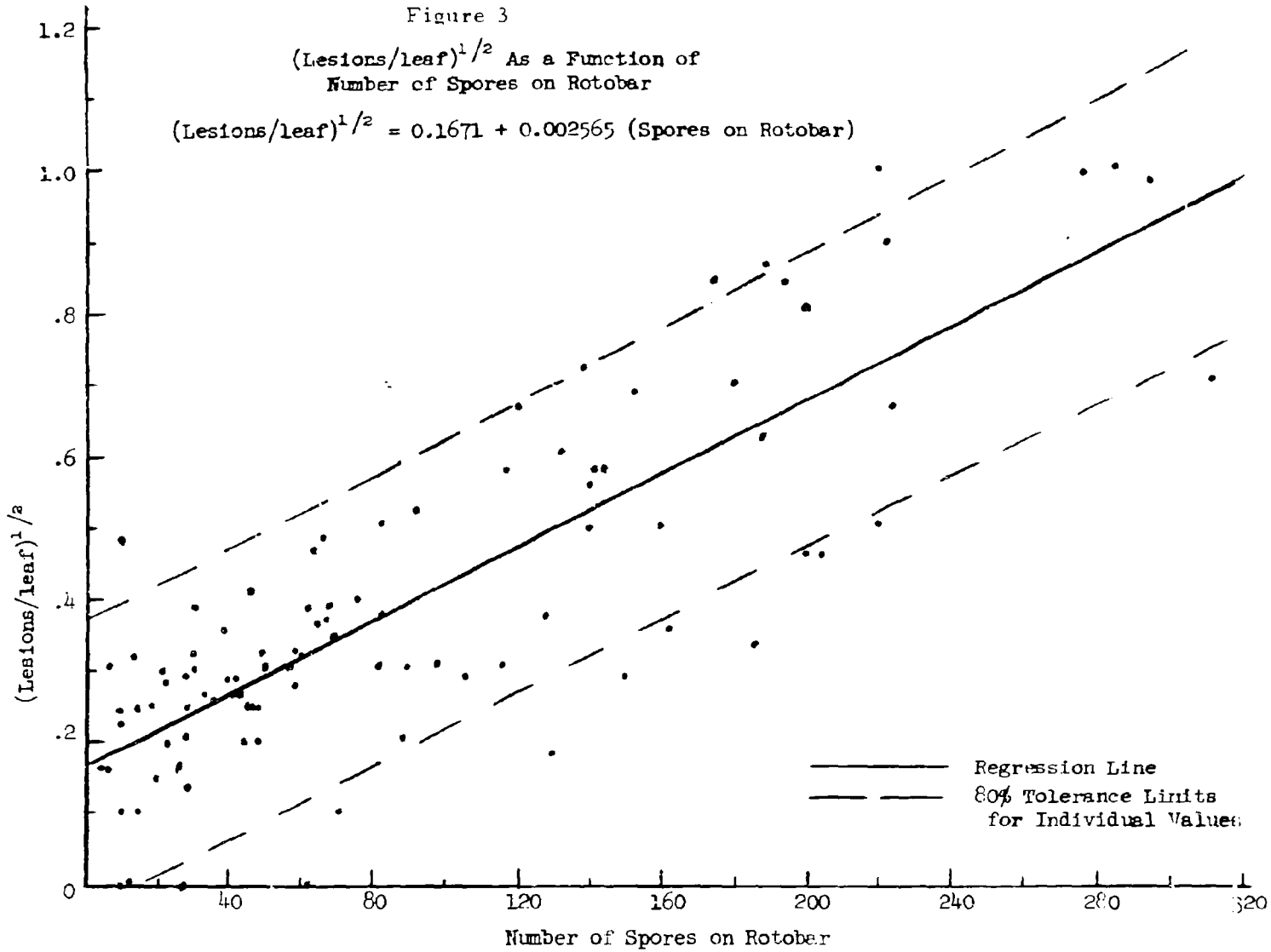

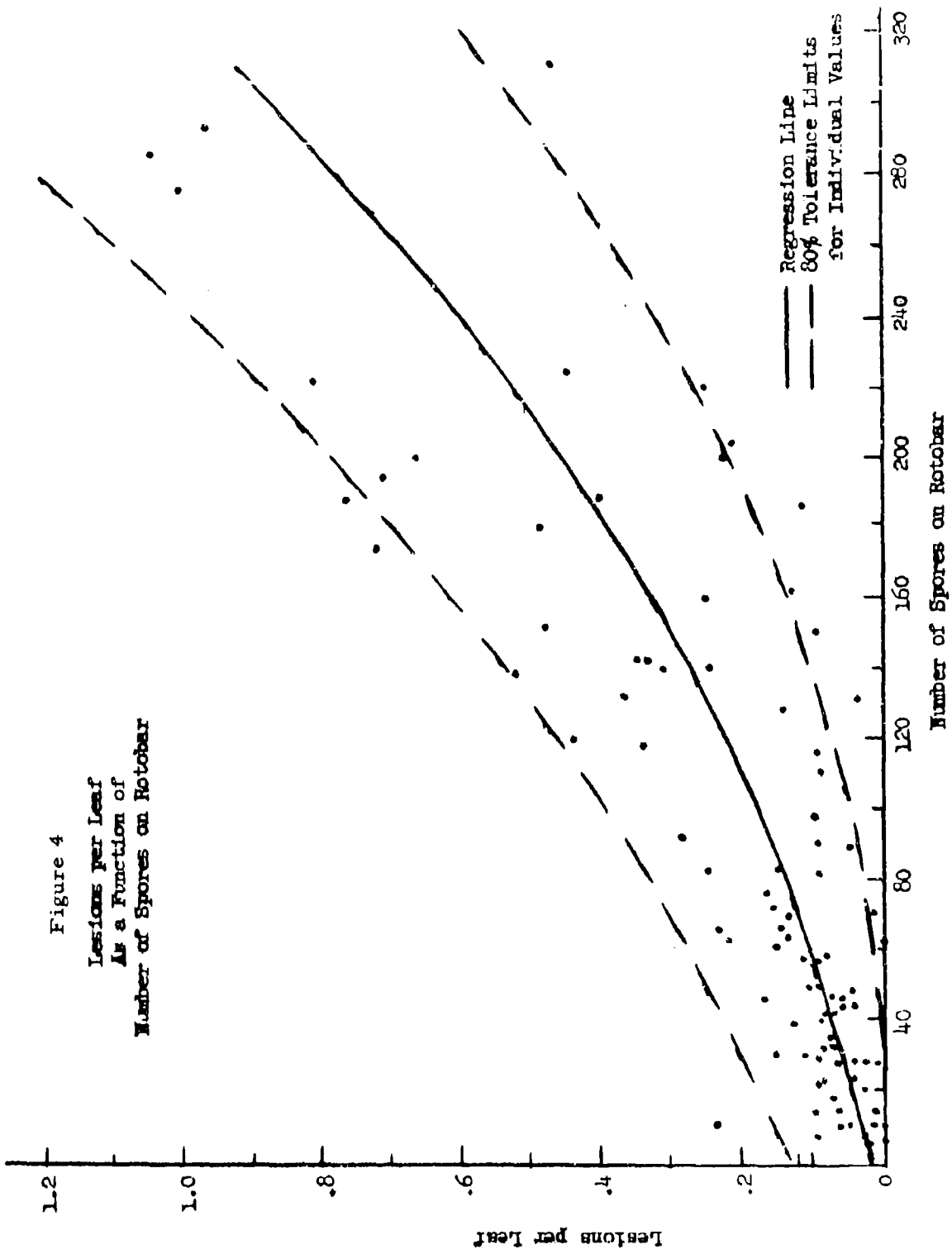

Figure 4
Lesions per Leaf
As a Function of
Number of Spores on Rotobar

EXTREME VERTICES DESIGN OF MIXTURE EXPERIMENTS*

R. A. McLean, University of Tennessee
and
V. L. Anderson, Purdue University

ABSTRACT. The extreme vertices design is developed as a procedure for conducting experiments with mixtures when several factors have constraints placed on them. The constraints so imposed reduce the size of the factor space which would result had the factor levels been restricted to only 0 to 100 per cent. The selection of the vertices and the various centroids of the resulting hyper-polyhedron as the design is a method of determining a unique set of treatment combinations. This selection is motivated by the desire to explore the extremes as well as the center of the factor space.

A non-linear programming procedure is used in determining the optimum treatment combination.

INTRODUCTION. In experiments dealing with mixtures one studies the response surface of a given dependent variable, y, (e.g., amount of illumination, in candles, for a given size flare) as a function of q factors ($q \geq 3$). The q factors (components) are all represented by a proportion, x_i, of the total mixture. Thus

$$\{1\} \qquad \sum_{i=1}^{q} x_i = 1 \qquad \text{and} \qquad 0 \leq a_i \leq x_i \leq b_i \leq 1$$

where $i = 1, \ldots, q$, and the a_i and b_i are constraints on the x_i imposed by the experimenter or by the physical situation involved.

Scheffé [6] introduced the topic of mixture experiments for the case $a_i = 0$ and $b_i = 1$ for $i = 1, \ldots, q$. He defined the $\{q, m\}$ simplex lattice design as a design which uniformly covers the factor space with each factor having $m+1$ equally spaced values from 0 to 1 such that $\sum_{i=1}^{q} x_i = 1$. A complete $\{3, 2\}$ lattice would consist of

*This paper has been submitted to Technometrics for publication.

ob rations taken at the following points (1,0,0), (0,1,0), (0,0,1), (0.5,0.5,0), (0.5,0,0.5), and (0,0.5,0.5) which are seen to lie on the plane $x_1 + x_2 + x_3 = 1$ in the first octant (Mason and Hazard [3]). This lattice is pictured in Figure 1 and redrawn in Figure 2 as a two-dimensional simplex. Since the example which is presented later contains four factors, a $\{4,3\}$ lattice is presented in Figure 3 as a three-dimensional simplex

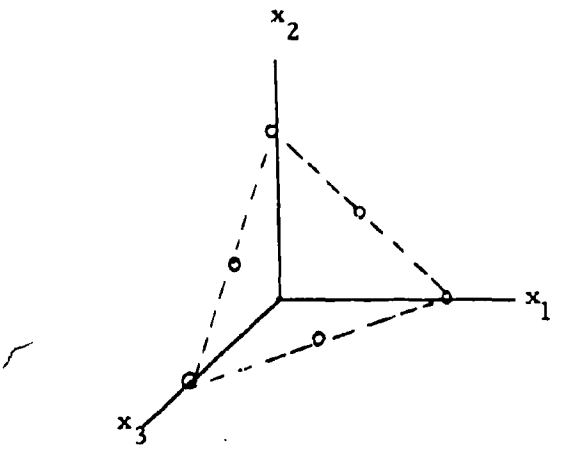

Figure 1 - $\{x_1+x_2+x_3 = 1\}$ plane

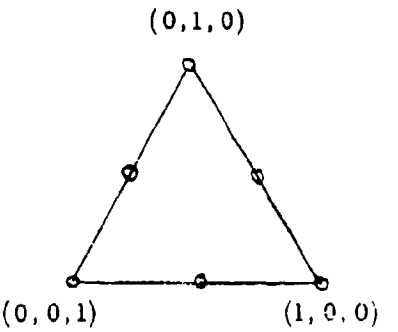

Figure 2 - $\{3,2\}$ lattice

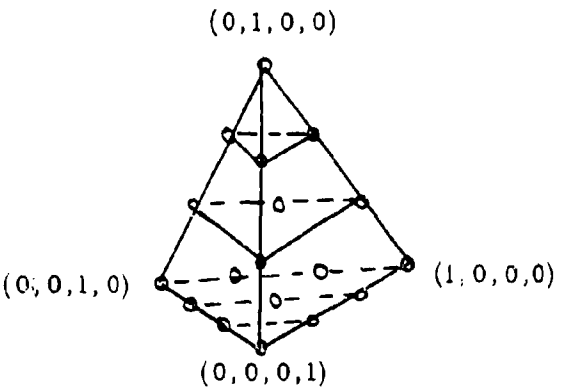

Figure 3 - $\{4,3\}$ lattice

(tetrahedron). In general the q dimensional factor space will reduce to a (q-1) dimensional polyhedron.

Scheffé discusses the use of a polynomial of degree n in estimating the response function defined on any $\{q, n\}$ lattice design. A simple procedure is derived for estimating the regression coefficients for these polynomials in the case of $\{q, 2\}$ and $\{q, 3\}$ lattice designs. This method was extended by Gorman and Hinman [2] to the case of a $\{q, 4\}$ lattice design and the corresponding quartic polynomials. Both of these papers give detailed information on testing the fit of the polynomial to the response surface and for determining the variance of a predicted response.

Scheffé briefly discusses the problem where one factor has an upper bound less than one, thus the restriction $x_i \leq b_i < 1$ for some i. The notion of a "pseudocomponent" (coding of the original variables) is introduced which permits the establishment of a regression equation in terms of the coded variables. It is pointed out that this procedure can be extended to more than one factor. It is also noted that the design of the experiment for this method has a shortcoming of not completely covering the factor space of interest.

It is the purpose of this paper to introduce a design which will allow each factor to be constrained as described in $\{1\}$ and cover the extremes of the factor space. It is assumed throughout that the degenerate situation of

$$\sum_{i=1}^{q} a_i \geq 1 \quad \text{or} \quad \sum_{i=1}^{q} b_i \leq 1$$

does not occur. In the case of either equality only one treatment combination would be feasible, i.e., either $(a_1, \ldots, a_q)$ or $(b_1, \ldots, b_q)$, respectively. In the case where $a_i = b_i$ for the ith factor, the dimensionality of the factor space is reduced by one and the remaining components must sum to $(1-a_i)$ which indicates that the design problem is essentially the same. Hence we also assume that $a_i \neq b_i$ for any $i = 1, \ldots, q$.

EXTREME VERTICES DESIGN. The constraints placed on the individual factors describe an irregular hyper-polyhedron (q-1 dimensions). The vertices and centroids of this figure describe a unique set of points (the design of the experiment) which may be used to estimate the response surface. Throughout the paper it will be assumed that there is a sufficient number and adequate placement of points in the design to permit estimation of all parameters in the polynomial that is used to approximate the response surface. In the case of the quadratic model

$$y = \sum_{i=1}^{q} \beta_i x_i + \sum_{1 \le i < j \le q} \beta_{ij} x_i x_j \qquad (2)$$

which is used exclusively in this paper, a minimum of $\frac{1}{2}q(q+1)$ points are required. Additional points would, of course, be necessary if an estimate of error is needed or if the lack of fit is to be tested. In case additional points are desired in any given design they may be obtained, for example, by using mid points of the edges of the hyper-polyherdon or repeating some of the existing points. A more elaborate description of the various polynomials that may be used can be found in the Gorman and Hinman paper.

Once the constraints for each factor are given all the points of the basic design are uniquely determined. The vertices of the design must fall on the boundary formed by upper or lower constraints of (q-1) factors. Hence, the vertices of the design may be found by using the two following rules:

(1) Write down all possible two level treatment combinations using the a_i and b_i levels for all but one factor which is left blank, e.g. $(a_1, b_2, a_3, —, a_5, b_6)$ for a six factor experiment. This procedure generates $q \cdot 2^{q-1}$ possible treatment combinations with one factor's level blank in each.

(2) Go through all $q \cdot 2^{q-1}$ possible treatment combinations and fill in those blanks that are admissible, i.e., that level (necessarily falling within the constraints of the

missing factor) which will make the total of the levels for that treatment combination add to one. Each of the admissible treatment combinations is a vertex; however, some vertices may appear more than once.

The hyper-polyhedron so constructed contains a variety of centroids. There is one located in each bounding 2-dimensional face, 3-dimensional face, . . . , r-dimensional face ($r \leq q - 2$), and the centroid of the hyper-polyhedron. The latter point being the treatment combination obtained by averaging all the factor levels of the existing vertices. The centroids of the 2-dimensional faces by isolating all sets of vertices for which each of (q-3) factor levels remains constant within a given set and by averaging the factor levels for each of the three remaining factors. All remaining centroids are found in a similar fashion using all vertices which have (q-r-1) factor levels constant within a set for an r-dimensional face where $3 \leq r \leq q - 2$. It should be noted that under the assumptions given above the dimensionality of the hyper-polyhedron formed by the extreme vertices will always be q-1.

EXAMPLE. In manufacturing one particular type of flare the chemical constituents are magnesium (x_1), sodium nitrate (x_2), strontium nitrate (x_3), and binder (x_4). Engineering experience has indicated that the following constraints on a proportion by weight basis should be utilized:

$$.40 \leq x_1 \leq .60,$$
$$.10 \leq x_2 \leq .50,$$
$$.10 \leq x_3 \leq .50,$$
$$\text{and } .03 \leq x_4 \leq .08 .$$

The problem is to find the treatment combination (x_1, x_2, x_3, x_4) which gives maximum illumination as measured in candles.

The vertices of the polyhedron consisting of all the admissible points of the factor space are found by applying rules (1) and (2) above.

The listing appears as

Treatment Combination	x_1	x_2	x_3	x_4	Treatment Combination	x_1	x_2	x_3	x_4
	.40	.10	.10	___	(1)	.40	.10	.47	.03
	.40	.10	.50	___	(2)	.40	.10	.42	.08
	.40	.50	.10	___		.40	.50	___	.03
	.40	.50	.50	___		.40	.50	___	.08
	.60	.10	.10	___	(3)	.60	.10	.27	.03
	.60	.10	.50	___	(4)	.60	.10	.22	.08
	.60	.50	.10	___		.60	.50	___	.03
	.60	.50	.50	___		.60	.50	___	.08
(5)	.40	.47	.10	.03		___	.10	.10	.03
(6)	.40	.42	.10	.08		___	.10	.10	.08
	.40	___	.50	.03		___	.10	.50	.03
	.40	___	.50	.08		___	.10	.50	.08
(7)	.60	.27	.10	.03		___	.50	.10	.03
(8)	.60	.22	.10	.08		___	.50	.10	.08
	.60	___	.50	.03		___	.50	.50	.03
	.60	___	.50	.08		___	.50	.50	.08

thus indicating eight admissible vertices and six faces. These eight treatment combinations are shown in Figure 4.

In order to complete the design, one must determine the six centroids for each face and the centroid for the polyhedron. To do this we list the treatment combinations that make up the six faces with the resulting centroids as follows:

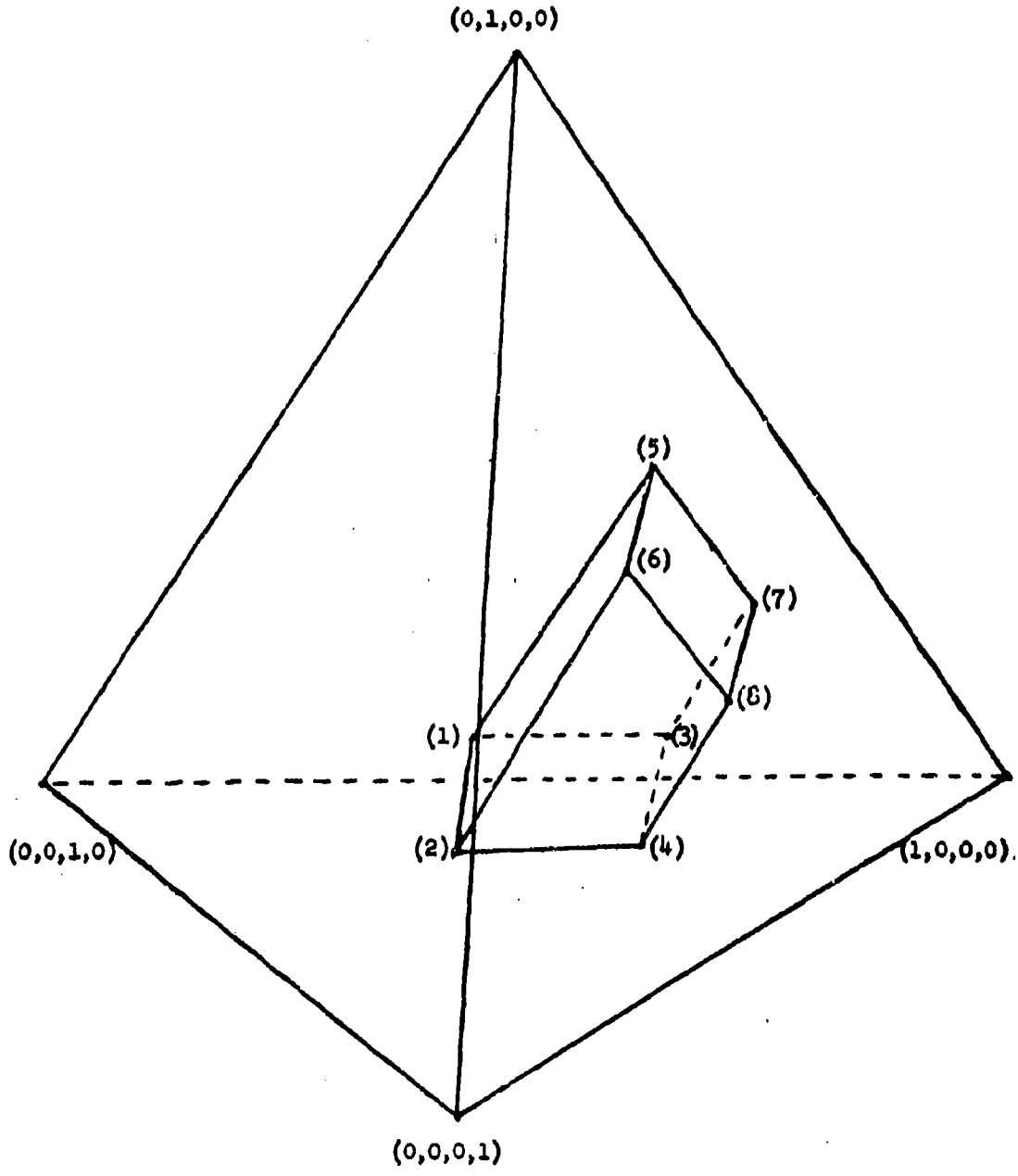

Figure 4 - Extreme vertices for flare experiment

Treatment Combination	Centroid	Treatment Combination which form the face
(9)	(.50, .1000, .3450, .055)	(1), (2), (3), (4)
(10)	(.50, .3450, .1000, .055)	(5), (6), (7), (8)
(11)	(.40, .2725, .2725, .055)	(1), (2), (5), (6)
(12)	(.60, .1725, .1725, .055)	(3), (4), (7), (8)
(13)	(.50, .2350, .2350, .030)	(1), (3), (5), (7)
(14)	(.50, .2100, .2100, .080)	(2), (4), (6), (8)

and the final centroid of the polyhedron, of course, comes from the average of all eight treatment combinations and is

(15) (.50, .2225, .2225, .055).

Fifteen flares assembled at each of the above treatment combinations produced, respectively, the following amounts of illumination (measured in 1000 candles):

(1)	75	(6)	230	(11)	190
(2)	180	(7)	220	(12)	310
(3)	195	(8)	350	(13)	260
(4)	300	(9)	220	(14)	410
(5)	145	(10)	260	(15)	425

Standard least squares techniques were used on the above data to obtain the complete quadratic model (equation (2) above)

$$y = -1,558x_1 - 2,351x_2 - 2,426x_3 + 14,372x_4 + 8,300x_1x_2 + 8,076x_1x_3 -$$

$$6,625x_1x_4 + 3,213x_2x_3 - 16,998x_2x_4 - 17,127x_3x_4 .$$

The squared multiple correlation coefficient (R^2) for this model is .9833, with only five degrees of freedom for residual. If only x_1, x_2, x_3, x_1x_2, x_1x_3, x_1x_4, x_2x_3 were used, the R^2 would be .9829, with eight degrees of freedom. Since all four variables still appeared in the latter model, the authors decided to retain the full model. The reader should recognize that, as in any model development problem, one must have stopping rules for evolving models from data. The purpose of this example, however, is merely to demonstrate the use of the regression model to determine the optimum treatment combination not to elaborate on model development, per se.

In an attempt to determine the optimum treatment combination, Lagrange multipliers were utilized to determine the maximum of the above equation subject to the constraint

$$\sum_{i=1}^{4} x_i = 1.$$

The resulting equations to be solved are

$$\begin{aligned}
8,300x_2 + 8,076x_3 - 6,625x_4 + \lambda &= 1,558 \\
8,300x_1 + 3,213x_3 - 16,998x_4 + \lambda &= 2,351 \\
8,076x_1 + 3,213x_2 - 17,127x_4 + \lambda &= 2,426 \\
-6,625x_1 - 16,998x_2 - 17,127x_3 + \lambda &= -14,372 \\
x_1 + x_2 + x_3 + x_4 &= 1
\end{aligned}$$

where λ is the unknown Lagrange factor. The solution to these equations indicates the optimum treatment combination is

$$(.5020, .2786, .2203, -.0009)$$

which is obviously incorrect since all factor levels must be positive. It should be noted that the above approach would only be valid if the resulting factor levels (for the maximum y) fell within their respective constraints.

In order to consider all the necessary constraints, a more appropriate tool was utilized in estimating the optimum treatment combination. A non-linear programming routine (SHARE program No. 1399 Gradient Projection (G P 90) by Ruth P. Merrill, Shell Development Co., Emeryville, California) was used to yield the treatment combination

$$(.5233, \quad .2299, \quad .1668, \quad .0800)$$

which is the desired solution to the problem. The predicted value of y for this optimum point is 397.48. It should be noted that this procedure only guarantees an optimum in the case where the response surface is a concave function.

It is quite feasible that one would like to further verify the initial estimate of the optimum condition. This could be done by applying anotherextreme vertices design to a localized region containing this initial point.

An additional comment on this experiment is that the fifteenth observation seems to be too large for the equation used. Further experimentation is necessary to investigate this feature thoroughly. It is hoped that this peculiarity does not detract from the purpose of the paper, namely to show a unique design of experiment for mixture problems.

FEATURES OF THE DESIGN. The extreme vertices design for mixture problems is uniquely determined once the investigator decides on the constraints for the chosen factors to be used in the experiment. In addition, the design allows investigation of the extreme points of the factor space as well as internal points in a manner similar to that used quite successfully in evolutionary operations. As pointed out in the example above, this design can be used sequentially to locate the optimum treatment combination.

As with all factorial type experiments the number of treatment combinations increases quite rapidly as the number of factors increases. As a guide to the number of treatment combinations which one might expect, Table I displays the minimum number of vertices and number of centroids in the 2-dimensional faces, 3-dimensional faces, etc., for use in designs containing up to 8 factors. Formulae for determining

these figures as well as conservative upper bounds on the number of treatment combinations are given in a paper by Saaty [5]. Additional readings on the geometry of this type of configuration is given in references [1] and [4]. It is seen in Table 1 that the number of the various dimensional faces rapidly increases as the number of necessary treatment combinations. One way of reducing the number of observations would be to delete certain centroids, say, those belonging to the even dimensional faces.

Table 1

Minimum design structure compared to number of parameters for a quadratic model

		Face dimension							
q	Vertices	2	3	4	5	6	7	Minimum design size	Number of Parameters
3	3	1						4*	6
4	4	4	1					9*	10
5	5	10	5	1				21	15
6	6	20	15	6	1			48	21
7	7	35	35	21	7	1		106	28
8	8	56	70	56	28	8	1	227	36

*Extreme vertices design would have to be augmented with additional points if these cases occur.

Another method for reducing the size of the design would be to compute a normalized distance between points of the design and randomly omit points that are less than a certain minimum distance from other design points. The minimum distance and the method of normalization, which would be required if certain components are much more sensitive than others, would have to be chosen by the experimenter. One possible means of normalization would be to define the distance between two points $(x_{i1},\ldots,x_{iq})$ and $(x_{j1},\ldots,x_{jq})$ as

$$d_{ij} = \left(\sum_{r=1}^{q} \left(\frac{x_{ir} - x_{jr}}{b_r - a_r} \right)^2 \right)^{\frac{1}{2}} .$$

This method of normalization would assume that the sensitivity for each factor is inversely proportional to the length of its constraint interval.

In light of the above discussion it is easily seen that a computer program for determining the various extreme vertices, centroids, and normalized distances between points would be highly desirable when q gets greater than 4 or 5. At the moment, no such program exists; however, writing such a program should not be too difficult.

ACKNOWLEDGEMENTS. The authors wish to thank Mr. Jerry L. Kemp of the R and D Department at the U. S. Naval Ammunitions Depot, Crane, Indiana, for providing the example on flares, and Mrs. Shirley Wolfe and Mrs. Louise Lui for handling the computations of the example.

REFERENCES

[1] Gass, Saul I., 1958, "Linear Programming: Methods and Applications", McGraw-Hill Book Co., Inc., New York.

[2] Gorman, J.W. and J.E. Hinman, 1962, "Simplex Lattice Designs for Multicomponent Systems", Technometrics, Vol. 4, p. 463-487.

[3] Mason, T.E. and C.T. Hazard, 1947, "Brief Analytic Geometry", second edition, Ginn and Company, Boston.

[4] Murdock, D.C., 1957, "Linear Algebra for Undergraduates", John Wiley & Sons, New York.

[5] Saaty, T.L., 1955, "The Number of Vertices of a Polyhedron", American Mathematical Monthly Vol. 62, p. 326-331.

[6] Scheffé, H., 1958, "Experiments with Mixtures", Journal of Royal Statistical Society, Series B, Vol. 20, p. 344-360

[7] Scheffé, H., 1963, "The Simplex Centroid Design for Experiments with Mixture", Journal of Royal Statistical Society, Series B, Vol. 25, p. 235-263.

THE DESIGN OF A HIGH-VOLTAGE-BREAKDOWN-IN-VACUUM EXPERIMENT*

M. M. Chrepta, J. Weinstein, G. W. Taylor, and M. H. Zinn
Electronic Components Laboratory
U. S. Army Electronics Command, Fort Monmouth, New Jersey

INTRODUCTION. Present-day requirements for extremely high-power radar and communication systems, high-energy particle accelerators, and ion-propulsion systems demand reliable operation of components at voltages up to a million volts. The demand is greatest in components such as vacuum tubes, vacuum capacitors, and ion-propulsion systems where high voltage must be insulated by vacuum in small spaces. Therefore, a reliable relation between the hold-off voltage and the factor or factors that affect an electrical breakdown in vacuum is needed for the design of these components.

The mechanism of voltage breakdown in a vacuum medium has been the object of wide investigation for many years. In spite of the voluminous literature on the subject, there are insufficient data available to permit a straight-forward approach to the design of high-voltage sections of high-power electron tubes or other types of devices. In a study of the available literature, one finds a wide divergence in both the data and the theories that have been generated from the data. Fig. 1 shows the spread of the scattered data:

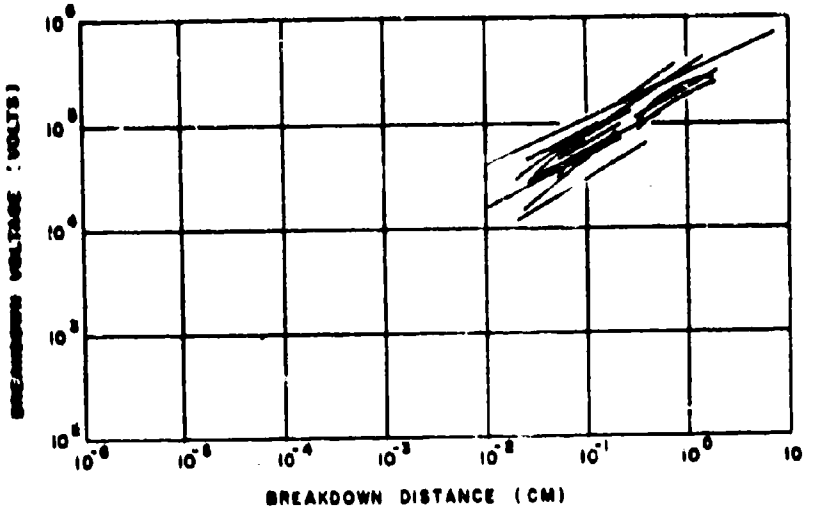

Fig. 1. Breakdown Data - Voltage versus Distance

*Sponsored by Advanced Research Projects Agency (ARPA Order No. 517), PROJECT DEFENDER, under ECOM Contract DA28-043 AMC-00394(E)

These curves are a few of the most closely grouped breakdown curves of those reported. For each curve a new theory was probably presented. Our own experiments with high-voltage breakdown showed that there is more than one breakdown mechanism; a break in the curve exists around 1.5 mm spacing with a slope of 0.75 below 1.5 mm and a slope of 0.5 above. These experiments were carried out in the traditional manner, varying the distance between electrodes and recording a breakdown voltage for that spacing. It is obvious that, after each breakdown, measurement conditions in the electrode system are changed; surfaces are pitted or melted, gas is liberated, and even the conductivity of the insulating vacuum envelope is changed. For ideal experimentation, therefore, a method of avoiding breakdown would be desirable.

FACTORS AFFECTING BREAKDOWN. In order to investigate the mechanism of breakdown, the 16 factors shown in Table I were considered as probably contributors to the breakdown process:

TABLE I

FACTORS AFFECTING BREAKDOWN

1. Cathode Material	9. Envelope Diameter
2. Anode Material	10. Electrode Shield Size
3. Cathode Finish	11. Electrode Shield Placement
4. Anode Finish	12. Residual Gas Pressure
5. Cathode Geometry	13. Energy of Supply
6. Anode Geometry	14. Contaminant
7. Vehicle Bakeout	15. Magnetic Field
8. Envelope Material	16. Electrode Spacing

Traditional experimentation varying a few of these factors for each experiment leads to the neglecting of joint effects of more than one factor and probably is responsible for some of the spread in data seen in Fig. 1. A full factorial experiment, on the other hand, would require a prohibitive amount of experiments and time even though tests were performed at only two levels of each factor. The initiation of such a massive experiment would only contribute to the already existing chaos in this field.

So as to bring order to this problem, a program of investigation of the breakdown process was initiated. The program is based on a statistical design plan that will consider all pertinent factors, without bias, so that the significance of the main effects and interaction effects can be analyzed.

It was recognized* that the list of 16 factors could be separated into two groups, as shown in Table II:

TABLE II

INFLEXIBLE AND FLEXIBLE FACTORS

Inflexible Factors	Flexible Factors
1. Cathode Material	12. Residual Gas Pressure
2. Anode Material	13. Energy of Supply
3. Cathode Finish	14. Contaminant
4. Anode Finish	15. Magnetic Field
5. Cathode Geometry	16. Electrode Spacing
6. Anode Geometry	
7. Vehicle Bakeout	
8. Envelope Material	
9. Envelope Diameter	
10. Electrode Shield Size	
11. Electrode Shield Placement	

The inflexible factors are those that are constructional. With the exception of factor 7 - Vehicle Bakeout - they cannot be varied without opening the vacuum test chamber. The flexible factors are all susceptible to being varied continuously without disturbing the test setup. It was also recognized that the last four of the inflexible factors were factors concerned with a particular application device design and they could be dropped at this time to reduce the complexity of the experiment and to accelerate the investigation. They will be introduced into future experiments.

*In discussions with C. Daniel.

The remaining factors will be investigated at the two levels shown in Table III, recognizing that we are assuming a linear model. Future experiments will allow us to build a prediction model from the results and to test at other levels in each factor space.

EXPERIMENTAL SETUP. The experiments will be run in the test vehicle shown in Fig. 2 at voltages up to 320 kilovolts. The chamber is equipped with access ports for electrode changes, optical viewing, X-ray detectors, and a mass spectrometer for monitoring the gap activity. For cleanliness, the whole chamber can be baked out by an oven assembly surrounding the chamber as well as the titanium sputter pump appended to the side, which controls the degree of vacuum. The power supply is a Van de Graaff generator that, for the high-energy level, charges up a bank of capacitors to 7000 joules. For the low level, the energy bank is not connected. The stored energy in this case is less than 1000 joules. The magnetic field is generated by two large field coils pivoted at the sides of the chamber so that they can generate perpendicular, parallel, and oblique fields. The chamber is constructed so that the factors that were dropped for the initial experiment can be included in future experiments by placing glass and ceramic envelopes at two levels (large and small) of diameters and electric shields could be placed around the electrodes at levels of interest. The length of the gap can be varied by a drive mechanism at the top of the chamber.

EXPERIMENTAL PROCEDURE. The first experiments will be conducted using a limited series of trials consisting of 32 runs as shown in Table IV. The table constitutes a quarter replicate of a seven-factor experiment taken at two levels of each factor. The seven factors used for this test plan will be the seven inflexible factors previously discussed. In each test run the flexible factors will be tested on a factorial basis at two or more levels for each treatment. Table IV was derived by using the five letters, A, B, D, E, and G, with defining relations, C + ABE, F + ABDG in Table M of Davies' "Design and Analysis of Industrial Experiments." [1]

The design shows the levels of each factor for each of the 32 runs. The minus sign in each run means that the factor is either at the low level or absent from the treatment; the plus sign means that the factor is at the high level or present in the treatment. The set is orthogonal; i.e., each level of any factor is tested equally against each of the other factor level combinations.

TABLE III - FACTOR LEVELS FOR INVESTIGATION

LEVELS OF INFLEXIBLE FACTORS		LEVELS OF FLEXIBLE FACTORS	
CATHODE MATERIAL	Ti-7Al-4Mo 304-SS OFHC Cu	PRESSURE	10^{-4} TORR 10^{-8} TORR
ANODE MATERIAL	Ti-7Al-4Mo 304-SS OFHC Cu	ENERGY	7K JOULE 1K JOULE
CATHODE FINISH	COARSE FINE	CONTAMINANT	ABSENT PRESENT
ANODE FINISH	COARSE FINE	MAGNETIC FIELD	PARALLEL OBLIQUE PERPENDICULAR
CATHODE GEOMETRY	SPHERE PLANE	ELECTRODE SPACING	SMALL LARGE
ANODE GEOMETRY	SPHERE PLANE		
VEHICLE BAKEOUT	ABSENT PRESENT		

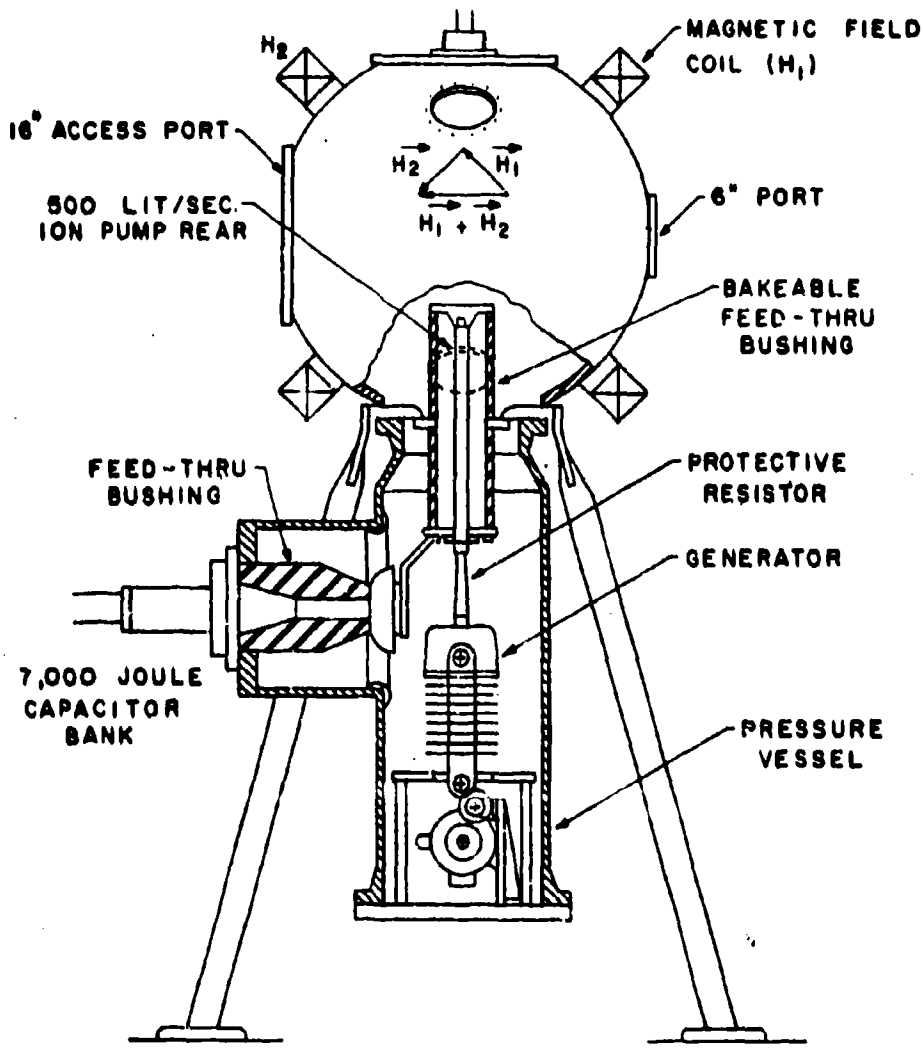

Fig. 2 Test Vehicle

TABLE IV - 2^{7-3} PLAN

TREATMENT	A	B	C	D	E	F	G
(1)	-	-	-	-	-	-	-
acf	+	-	+	-	-	+	-
bcf	-	+	+	-	-	+	-
ab	+	+	-	-	-	-	-
df	-	-	-	+	-	+	-
acd	+	-	+	+	-	-	-
bcd	-	+	+	+	-	-	-
abdf	+	+	-	+	-	+	-
ce	-	-	+	-	+	-	-
aef	+	-	-	-	+	+	-
bef	-	+	-	-	+	+	-
abce	+	+	+	-	+	-	-
cdef	-	-	+	+	+	+	-
ade	+	-	-	+	+	-	-
bde	-	+	-	+	+	-	-
abcdef	+	+	+	+	+	+	-
fg	-	-	-	-	-	+	+
acg	+	-	+	-	-	-	+
bcg	-	+	+	-	-	-	+
abfg	+	+	-	-	-	+	+
dg	-	-	-	+	-	-	+
acdfg	+	-	+	+	-	+	+
bcdfg	-	+	+	+	-	+	+
abdg	+	+	-	+	-	-	+
cefg	-	-	+	-	+	+	+
aeg	+	-	-	-	+	-	+
beg	-	+	-	-	+	-	+
abcefg	+	+	+	-	+	+	+
cdeg	-	-	+	+	+	-	+
adefg	+	-	-	+	+	+	+
bcefg	-	+	-	+	+	+	+
abcdeg	+	+	+	+	+	-	+

The following letter assignments were carefully chosen so that in the treatment and analysis of the results the effect of any two-factor interaction involving the Bakeout factor, D, would be clear of any other main effect or two-factor interaction of interest:

TABLE V

LETTER ASSIGNMENT

A - Anode Material

B - Cathode Shape

C - Cathode Material

D - Bakeout

E - Anode Shape

F - Anode Finish

G - Cathode Finish

The isolation of the bakeout main effect and all two-factor interactions involving bakeout was designed into the experiment with the objective of eliminating bakeout in future experiments. Since bakeout of the large mass of the test vehicle is a long time process of heating and cooling, it would be desirable to eliminate it if results indicate negligible main and two-factor effects. The absence of bakeout in the test run involves the use of inert gases during the time that the test vehicle is being modified and the testing of the electrodes, themselves, using built-in heaters. There is, therefore, a possibility that the lack of a bakeout of the entire structure will not influence the test results.

A, B, and C were assigned to factors whose interactions with each other could be assumed to be negligible.

The tabulation of minus and plus signs shown in Table IV not only gives the levels of the factors but indicates how the data collected from all of the test runs, or treatments, should be handled in order to determine each effect; i.e., to determine the A effect, the test results for tests 1 to 32 are added where a plus sign is present under column A and subtracted for the minus signs. For two-factor interactions, the two columns are first multiplied one by the other and then the data are treated

in accordance with the resulting column. The results can be obtained in a more systematic manner by using the Yates Algorithm, which consists of repeatedly adding and subtracting adjacent test results [2] until the results for mean, main effects, and two-factor interactions are obtained as shown in Table VI. All the two-factor interactions are measurable except AB, CE, AC, BE, AE, and BC. As can be seen, we can get seven main effects and six two-factor interactions with D (the bakeout) plus the mean, which allows eighteen degrees of freedom for estimating error. We expect that this analysis will tell us the significance of each main factor and two-factor interaction involving D and thus allow us to better design an experiment that includes only the important factors in a full factorial for a complete significant factor space investigation.

An investigation is now under way searching for a repeatable, non-destructive, performance criterion that can be obtained without taking the electrodes to breakdown. This criterion is necessary to make measurements for the values of voltage to be used for the analysis. The areas being investigated to find a breakdown criterion are: gap current; X-radiation; gas evolution and gas analysis; and the spectral response of visible radiation as a function of voltage. All of these characteristics will be continuously monitored with the hope that one or all will permit the onset of breakdown to be predicted. To prevent severe damage to the electrodes and the system in the event that breakdown does occur, an electronic energy diverter will be incorporated in the test setup. The diverter can be triggered by a chosen level of current, X-ray output, or the output of a photomultiplier, and can respond in a micro-second or less after a fault is sensed to remove the voltage from the gap.

Two or three runs per week will be carried out according to the dictate of the inflexible factors that require change. Changes of the inflexible factors will be made in an ultraclean, dry nitrogen, pressurized white-bench atmosphere. This atmosphere is monitored for dust particles and water vapor content. The materials for the electrodes will be certified from a single heat and will be chemically analyzed for record purposes. The electrode finishes will be obtained by precise polishing techniques, with prescribed abrasives down to 0.05 micron size particle finish for the "fine" level. The electrodes are being constructed with Bruce profiles so that the E field is maximum in the gap. The vacuum pumping system is an ultraclean, oil-free cryogenic and titanium ion sputter system.

TABLE VI - DEFINING RELATION

I = -ABDFG = -CDEFG = ABCE

YIELDS OF YATES ALGORITHM

1	mean	12	ABE + (C)	23	BDG - AF
2	(A)	13	[DE]	24	ABDG - (F)
3	(B)	14	ADE	25	EG
4	AB + CE	15	BDE	26	AEG
5	[(D)]	16	ABDE + [CD]	27	BEG
6	[AD]	17	(G)	28	A BEG + CG
7	[BD]	18	AG	29	DEG - CF
8	ABD - FG	19	BG	30	ADEG
9	(E)	20	ABG - [DF]	31	BDEG
10	AE + BC	21	[DG]	32	ABDEG - EF
11	BE + AC	22	ADG - BF		

CONCLUSIONS. It is expected that sufficient information will be collected during these pilot experiments to permit elimination of factors having minor effects and to permit a more comprehensive design for the final experiment. The initial 32 runs are specifically aimed at the bakeout factor, D; hopefully to eliminate this time-consuming process in subsequent experiments. The final experiment will be a full factorial using only those factors that are determined to be significant in this pilot experiment. Results from the pilot experiment are now being collected.

The techniques developed for this program are applicable to other studies in the physical sciences where large numbers of variables of both a qualitative and nonqualitative nature are involved.

REFERENCES

1. Owen L. Davies, Design and Analysis of Industrial Experiments (Hafner Publishing Company, New York, N.Y.) 1963.

2. For an exact description of the process see Davies, Ibid., pp 262-264.

SOME INFERENTIAL STATISTICS WHICH ARE RELATIVELY COMPATIBLE WITH AN INDIVIDUAL ORGANISM METHODOLOGY

Samuel H. Revusky
U. S. Army Medical Research Laboratory, Fort Knox, Kentucky

ABSTRACT. A number of new statistical techniques are described which are very sensitive to effects of an independent variable when a relatively small number of subjects are used and the effects of the independent variable are irreversible. The same notions are generalized to the case when the effects of the independent variable are reversible.

INTRODUCTION. Operant conditioning techniques are most useful when a number of experimental conditions are tested on a single animal. It is an empirical fact that within-subject comparisons are far more sensitive to small effects than between-subject comparisons. Furthermore, when within-subject experimental manipulations are not made, each S can only contribute one data item (strictly speaking) toward a valid statistical analysis because of the requirement, central to inferential statistics, of random sampling. The net result is that splitting a number of subjects into groups will yield evidence only of very pronounced effects unless a very large number of Ss are used. The establishment of a complex operant performance is usually too time consuming and difficult to permit use of a large number of Ss, so that statistical procedures in which each S supplies only one data item are usually not practical. Similar considerations are applicable to many subject matters in addition to operant conditioning. For these reasons, as well as some others, single organism methodologies with within-subject controls have been among the most prominent scientific techniques.

But the use of a number of scores from a single S as separate inputs into statistical tests does not rigorously adhere to the assumptions involved in inferential statistics when the independent variable (IV) has irreversible effects.[1] Examples of such IVs are x-irradiation and

[1]By irreversible effect we mean, in the present context, the case in which baseline data cannot readily be recovered after the IV is administered. It is possible to compare performance after the IV with baseline performance, but, for each S, only one statistically independent data item, such as a difference score, can be used rigorously as input into statistical tests of the type in general use. This is because the data obtained after introduction of the IV always follows the baseline data so that the sampling cannot be random. Of course, one may decide (legitimately, I think) that such violation of random sampling will be of little practical importance in some particular instance.

surgery; in certain contexts, drive operations and novel stimuli may also be considered irreversible. Thus, it would seem, at first glance, that the use of difficult individual organism techniques is usually impractical when irreversible IVs are studied and assessment of the results is by means of inferential statistics.[2] But due to a recent development in statistical methodology (Cronholm and Revusky, 1965), such assessment is not as impractical as it used to be. The reason is that statistically rigorous inference about irreversible IVs may be made with a smaller number of Ss then has hitherto been feasible. First, I will describe the basic idea underlying the Cronholm - Revusky paper in concrete and intuitive form, and then I will extend some of its notions to more complex experimental designs.

THE R_n METHOD. Suppose 6 Ss are trained to final performance on a complex schedule of reinforcement and we wish to assess the effects of a novel stimulus on this performance. Since exposure to a novel stimulus has irreversible effects, (in the weak sense that after the first exposure the stimulus no longer is novel), conventional experimental design requires that we randomly divide the 6 Ss into groups of 3 each, subject one group to the novel stimulus and the other group to a control procedure. For analytic purposes, we shall always refer to rank tests and in the present example, the rank test to be used would be the Mann-Whitney U Test (Siegel, 1956). With this test, the total number of possible (and equiprobable) outcomes is $6!/(3!\ 3!) = 20$ and the probability of the most extreme outcome is $3!\ 3!/6! = 1/20 = .05$. Thus, the maximum significance level obtainable with 6 Ss and a conventional experimental design is .05 (one-tailed). Only with extremely pronounced effects would it seem intuitively reasonable to study any hypothesis with less than 10 Ss, and for many operant conditioning procedures, this is an impracticably large number of Ss.

With the same 6 Ss a result significant beyond the one-tailed. .002 level is possible, if the following technique described by Cronholm and Revusky is used. First, administer the novel stimulus to one randomly selected S and the control procedure to the remaining 5 Ss. Rank the performance of the experimental S with respect to the 5 controls. Thus, the statistical outcome of this procedure (which may be called a sub-

[2] No claim is made here that all results must be assessed by means of inferential statistics.

experiment) is a rank from 1 to 6. We now have 5 Ss which have not been exposed to novelty. Randomly select one for exposure to the novel stimulus and rank it, as before with respect to the 4 controls. This rank will be between 1 and 5. Now continue this process until one S remains; this last S will receive a rank of 1 regardless of what it does. Table 1 is a precis of the procedure.

TABLE 1

Precis of the experimental design used with R_n. Each line contains the possible outcomes of one sub-experiment. The sub-experiments are numbered in chronological order.

Sub-experiment	Possible, equiprobable, ranks
1	1, 2, 3, 4, 5, 6
2	1, 2, 3, 4, 5
3	1, 2, 3, 4
4	1, 2, 3
5	1, 2
6	1

Since the total number of outcomes in each sub-experiment is equal to the number of possible ranks, the total number of outcomes over all 6 sub-experiments shown in Table 1 is equal to the product of the number of equiprobable outcomes for each sub-experiment; that is, $6x5x4x3x2x1 = 6! = 720$. It is this large number of outcomes, compared to the 20 possible outcomes of the Mann - Whitney U with 6 Ss, which is the secret of the remarkable sensitivity of the procedure we are describing.

Now we will determine the chance distribution of the results of the sub-experiments so that results obtained by this procedure can be subjected to inferential statistical analysis. Chance is defined to mean that the random selection of the experimental S in each sub-experiment alone determines the probability of any rank outcome; in

other words, the novel stimulus is assumed to have absolutely no effect on what is measured. Given this definition of chance, in each sub-experiment each of the possible outcomes is equally probable. Thus, in sub-experiment 1, each rank from 1 to 6 has a probability of 1/6. In sub-experiment 2, each possible rank has a probability of 1/5. And so on. A physical model of the chance distribution may make it clearer. Sub-experiment 1 is similar to the toss of a true die and the rank outcome is equivalent to the number of pips which appear. Sub-experiment 2 is the toss of a five-sided die, with a different number of pips (from 1 to 5) on each side. And so on.

Under this assumption, each sub-experiment may be said to have a probability generating function of its own, which is of no intrinsic interest, but is necessary for the understanding of the probability generating function of R_n, as well as the other statistics to be described in this paper. When k is the number of possible ranks, this function is

$$\frac{\sum_{i=1}^{k} s^i}{k} .$$

The coefficient of the ith power of s in this function is equal to the probability that the rank obtained in the sub-experiment will be equal to i; s has no numerical meaning and its only function is to supply a place for the exponent i, which indicates the outcome for which the coefficient of s^i is the probability. For instance if $k = 5$, the function is

$$\frac{\sum_{i=1}^{5} s^i}{5} = \frac{1}{5}s^1 + \frac{1}{5}s^2 + \frac{1}{5}s^3 + \frac{1}{5}s^4 + \frac{1}{5}s^5 .$$

This function means that each rank from 1 to 5 has a probability of 1/5.

The statistic to be used to evaluate the probability of the entire series of sub-experiments is simply the sum of the ranks obtained in each sub-experiment (called R_n). To find the generating function of

R_n, we multiply together the generating functions for each sub-experiment. For instance, when n = 6, we have

$$\left(\frac{\sum_{i=1}^{6} s^i}{6}\right)\left(\frac{\sum_{i=1}^{5} s^i}{5}\right)\left(\frac{\sum_{i=1}^{4} s^i}{4}\right)\left(\frac{\sum_{i=1}^{3} s^i}{3}\right)\left(\frac{\sum_{i=1}^{2} s^i}{2}\right)\left(\frac{\sum_{i=1}^{1} s^i}{1}\right) = \frac{\prod_{k=1}^{6}\left(\sum_{i=1}^{k} s^i\right)}{6!}$$

I will clarify the meaning of this generating function by multiplying it out and then explaining it; the more formally inclined reader may consult Cronholm and Revusky (1965), where an intuitively less understandable but easier to use version of this generating function is explained.

$$\frac{s^6}{720} + \frac{5s^7}{720} + \frac{14s^8}{720} + \frac{29s^9}{720} + \frac{49s^{10}}{720} + \frac{71s^{11}}{720}$$

$$+ \frac{90s^{12}}{720} + \frac{101s^{13}}{720} + \frac{101s^{14}}{720} + \frac{90s^{15}}{720} + \frac{71s^{16}}{720}$$

$$+ \frac{49s^{17}}{720} + \frac{29s^{18}}{720} + \frac{14s^{19}}{720} + \frac{5s^{20}}{720} + \frac{s^{21}}{720} .$$

In the above expansion, the coefficient of any power of s is equal to the chance probability that the value of R_n equal to that power will occur. More specifically, the coefficient is a fraction, the numerator of which is equal to the number of outcomes which result in the corresponding value of R_n and the denominator of which is equal to the total number of possible outcomes. The probabilities shown are not cumulative. To obtain the cumulative probability the probabilities of all more extreme events must be added to the probability of the event itself. For instance, the probability that $R_n = 8$ is 14/720; the probability that $R_n \leq 8$ is 1/720 + 5/720 + 14/720 = 20/720. It is apparent that the smallest possible value of R_n, 6, has a probability of 1/720, as against a smallest possible probability of 1/20 for a U test utilizing the same number of Ss.

Cronholm and Revusky (1965) have supplied a detailed description of the properties of R_n, a rigorous discussion of its sensitivity to small effects as compared with the Wilcoxon T (which is functionally identical to the U test), and a table suitable for practical use of the statistic with up to 12 Ss. They also discuss when the R_n procedure should and should not be used, as well as its use as a quasi-sequential test. One matter of particular importance to operant conditioners, is that one can use such measures as percentage change in each sub-experiment without affecting the chance distribution; this permits a correction for the base line of each S. This will be true of all the tests to be mentioned in this paper, as well as most common statistical tests.

PURPOSE OF EXTENSION OF THE R_n METHOD. The basic idea underlying R_n, the use of a number of sub-experiments each containing one experimental S and a number of controls, can generate a large number of statistical techniques more compatible with a single-organism methodology than conventional statistics. Unfortunately, in practice, the experimenter will have to supply his own probability generating function if he must depart from a straightforward use of R_n, because the number of possible variations on the basic procedure is huge. The tedium of computing generating functions is partially compensated for by the ease with which the statistics can be computed. The remainder of this paper will consist of examples of statistics tailored for particular experiments in the hope that they will be a guide for anybody who has special needs to be filled. The rationale for this unusual procedure is that it increases the flexibility of the experimenter's attack on the subject matter.

A VARIETY OF LEVELS OF THE IV; ONE LEVEL STUDIED IN EACH SUB-EXPERIMENT. Suppose we are studying the affects of a poison on stabilized performance and wish to use 3 dose levels. We are willing to assume that the direction of the effects does not change as a function of dose level; for example, if one dose level either improves or interferes with performance, any of the other dose levels to be used either will do the same or will have no effect. If it is reasonable to suppose that one dose level improves performance and a second dose level interferes with it, the present type of analysis makes no sense, although modifications, to be mentioned later, may be made for such situations.

We begin with 10 Ss under a modification of the R_n procedure described by Table 2. The change in our procedure is that for each sub-experiment one of the 3 dose levels is used for the experiment S.

TABLE 2

The experimental procedure by which the R_n statistic is used to study the effects of 3 levels of an IV.

Chronological order is from top to bottom.

Sub-experiment	Dose Level	Possible, equiprobable, ranks
1	A	1, 2, 3, 4, 5, 6, 7, 8, 9, 10
2	B	1, 2, 3, 4, 5, 6, 7, 8, 9
3	C	1, 2, 3, 4, 5, 6, 7, 8
4	A	1, 2, 3, 4, 5, 6, 7
5	B	1, 2, 3, 4, 5, 6
6	C	1, 2, 3, 4, 5
7	C	1, 2, 3, 4
8	B	1, 2, 3
9	A	1, 2

Thus, we select 3 sub-experiments to test each of the 3 dose levels; we do not use the last sub-experiment for purposes of statistical inference because its outcome is predetermined. To assess the probability of the overall effect, we simply use R_n, ignoring the individual dose levels. To obtain a separate statistic for each dose level, we add the ranks obtained in the sub-experiments in which that dose level was used. Thus for dose levels A, B and C, we have r_A, r_B and r_C. The generating functions for each of these 3 statistics are straightforward. Consider r_A and remember our physical analogy. Table 2

shows dose level A was used in sub-experiments 1, 4, and 9. The dice analogy for each of these sub-experiments, respectively is a ten-sided die, a seven-sided die, and a two-sided die. Thus, the probability generating function of r_A may be constructed much like the probability generating function for $\underline{R}_n$

$$\frac{\sum_{i=1}^{10} s^i \quad \sum_{i=1}^{7} s^i \quad \sum_{i=1}^{2} s^i}{10 \cdot 7 \cdot 2}$$

where, as before, the coefficient of any power of s corresponds to the probability that a sum of ranks equal to that power may be obtained. For similar reasons, the generating function for r_B is

$$\frac{\sum_{i=1}^{9} s^i \quad \sum_{i=1}^{6} s^i \quad \sum_{i=1}^{3} s^i}{9 \cdot 6 \cdot 3}$$

and the generating of r_C is

$$\frac{\sum_{i=1}^{8} s^i \quad \sum_{i=1}^{5} s^i \quad \sum_{i=1}^{4} s^i}{8 \cdot 5 \cdot 4} .$$

Inspection of the denominators of these 3 generating functions, shows 140 possible outcomes for dose level A, 162 outcomes for B and 160 outcomes for C. I contrived the sequence of administration of the dose levels, so that the number of outcomes for each dose level would be as nearly equal as I could make it in the hope that the statistical power at each dose level would then be similar. Of course, this may not be desirable in some cases.

The net result is that in the above example, the significance of an overall effect can be determined. Given a significant overall effect,

the significance of the effect at each dose level can be determined. Unfortunately, however, there is no reasonably powerful technique to assess differences between the effects of the different dose levels. The best that can be done is to use the Kruskall-Wallis one-way analysis of variance (Siegel, 1956) to compare the magnitude of the effects at different dose levels; the input into this test is all the experimental scores and none of the control scores; the assumption is made that the effects do not change over sub-experiments.

Still more statistical sensitivity may be obtained with the above procedure if some results may be discounted before the data are collected. An analogy from conventional statistics is the one-tailed test in which the experimenter is so certain that the results will occur in only one direction, that he is willing to state that any result in the opposite direction, no matter how extreme, is a sampling error. Similarly, in the present case, we may be entirely certain that if any effect exists, dose level A (the lowest level) will have the smallest effect and dose level C (the highest level) will have the largest effect. If we are willing to assert that any other result is due to chance, we may divide our obtained probability levels by 1/6 because there are 3! = 6 possible permutations of the results obtained for the 3 dose levels, and we are assuming only one of these 6 possible outcomes can be non-chance. Alternatively, we may also accept a significant result if A has the largest effect and C has the smallest effect, in which case the probability level may be divided by 3 since 2 of the 6 possible permutations are acceptable as not due to chance. Of course, if the data seem to clearly contradict one's preconceptions; one is in the unenviable position of discarding data not because of anything in nature but because of the foolishness of his a priori notions. On the other hand, if one does accept the unexpected result as not due to chance, the true probability of rejection of the null hypothesis at the chance .05 level will be .30 if only one permutation had been expected and .15 if one of two permutations had been expected. I think the best solution in event of an unexpected outcome is to repeat the experiment unless the unexpected result is entirely convincing without any formal statistical evidence in its favor.

A NUMBER OF LEVELS OF THE IV; ONE S IN EACH LEVEL TESTED IN EACH SUB-EXPERIMENT. The preceding application included 9 sub-experiments. A variant on this procedure, also utilizing

10 Ss, permits a reduction to 3 sub-experiments as follows: (a) Sub-experiment 1. Beginning with 10 Ss, randomly assign 1 S to each dose level and utilize 7 controls. (b) Sub-experiment 2. Of the 7 controls of sub-experiment 1, randomly assign 1 S to each of the dose levels and use the 4 remaining Ss as controls. (c) Sub-experiment 3. Repeat the procedure with 3 experimental Ss and 1 control. In this design, the probability generating function for each dose level is straightforward, but the assessment of whether an overall effect occurred is difficult. Therefore, we will begin backward with an assessment of the effects at the separate dose levels and then we will consider the overall effect.

Consider dose level A. A rank is obtained for each sub-experiment by ranking the subject receiving dose level with respect to the controls and ignoring the results obtained with levels B and C. These ranks are then summed over the 3 sub-experiments. The following probability generating function is applicable.

$$\frac{\sum_{i=1}^{8} s^i \quad \sum_{i=1}^{5} s^i \quad \sum_{i=1}^{2} s^i}{8 \cdot 5 \cdot 2}$$

A similar statistic is obtained for levels B and C; of course, their probability generating functions are the same as for level A. It should be noted that the denominator of the generating function shows 80 possible outcomes; when only one experimental S was run at a time in the otherwise similar design of the preceding section, the smallest number of outcomes was 140. Thus it is evident that this method reduces the number of sub-experiments needed in the preceding section at the price of some power. Whether this price is worth paying is up to the experimenter.

We are now faced with 3 statistics and the problem of deciding if the overall pattern is due to chance; obviously the probability that at least one of these statistics will be significant at the .05 level has a higher chance level than .05, which will be taken, in this discussion, to be the rejection level for the chance hypothesis. There are 3 ways of doing this and the experimeter must select the most reasonable way for his particular experiment before he has seen the data. The first 2 of these ways are also applicable to the method of the preceding

section in cases where one dose level may improve performance and a second level may interfere with it. Following are the 3 ways:

a. If the result is significant at the .05 level at the highest dose level, assume any other apparently significant results are real. If it is not, assume any other significant results are spurious.

b. If each of 3 statistical probabilities were independent, one or more of the 3 results would be significant at the .017 level with a probability of .05. Since the results are not entirely independent because they all depend on the same control scores, a conservative guess at the chance level is .02. If one of the 3 results has a chance probability below .02, regard any other results significant at the .05 level as non-chance.

c. Combine all 3 dose levels for each sub-experiment and regard it as the comparison of an experiment with a control group. Then, for each sub-experiment, obtain a probability level by some conventional test; the Mann-Whitney U test (Siegel, 1956) would be very consistent with our other tests because it is a rank test. Then combine the 3 obtained probabilities by means of the z-transformation (Mosteller and Bush, 1954). If, and only if, the combined probability level is below .05, there is a significant overall effect. If this method is to be sensitive, it must be reasonable to suppose that all dose levels act in the same direction on the performance.[3] Because U is a discrete distribution, the combined probability will be conservative.

THE CASE WHERE THE EFFECTS OF THE IV ARE REVERSIBLE. So far, we have dealt with cases in which the Ss are irreversibly affected by the IV, because this is the situation in which the new statistical method makes a unique contribution. Nevertheless, an extension in which a subject is used for control data after it has been subjected to the IV may be of interest to some experimenters, particularly psychopharmacologists.

Suppose there are n subjects. On each of k occasions, one S is randomly selected for the experimental treatment and the remaining

[3] It is cautioned that combination of the probabilities obtained for each dose level is not valid, strictly speaking, because the same control scores are used for each dose level.

Ss are used as controls. For the foregoing material to be rigorous, it is necessary that the selection be entirely at random, even if it results in the same S being administered the experimental treatment on each of the k occasions. The probability generating functions for the sum of the ranks obtained by the experimental Ss is

$$\frac{\left(\sum_{i=1}^{n} s^i\right)^k}{n^k}$$

Irreversible effects will not affect the statistical validity of any rejection of the null hypothesis, although the sensitivity of the test will be reduced, so that it is only necessary that the effects of the IV be reversible enough so that a significant result is conceivable and will make scientific sense.

Now consider a concrete example. There are 4 Ss, each trained to a high performance criterion. On each of the 8 occasions, one of these Ss is randomly selected for drug administration and the remaining 3 Ss act as controls. The probability generating function looks like this!

$$\frac{(S^1 + S^2 + S^3 + S^4)^8}{4^8}$$

The denominator of the above function, $4^8 = 65,536$, is the number of possible outcomes. I hope the reader shares my intuition that this huge number is indicative of remarkable sensitivity to small effects.

Because of this large number of outcomes, the probability generating function discussed in the preceding two paragraphs cannot usually be computed except by an electronic computer. Fortunately, both editions of Feller's (1950, 1957) textbook on probability theory include equations for the chance probability of any sum of ranks under this procedure. For the 1950 edition: examples 11 and 12 on page 236 with necessary background on pages 40-41. For the 1957 edition: examples 18 and 19 on page 266 with necessary background on pages 48-49.

As already mentioned, if the use of the statistic is to be mathematically rigorous, the experiment S to be used in each sub-experiment must be selected entirely at random so that some Ss may receive the experimental treatment more often than others. From an experimental viewpoint, however, it usually seems more desirable to administer the experimental treatment in a restricted random sequence in which no S receives the treatment a second time until all Ss have received it once. My preference is for use of restricted randomization and I expect, without solid proof, that its effects are to reduce the probability of a significant result due to chance. If the experimenter prefers statistical rigor and still wishes to use restricted randomization, he may use the R_n procedure. Of course, in this case, discarded Ss will simply be ignored for statistical purposes and may remain in training. After all Ss have received the experimental treatment, the group can be reinstated and another R_n procedure be administered. Cronholm and Revusky (1965) describe how a joint generating function can be obtained for a number of R_n experiments.

There are other usable statistical methods for reversible effects and I am not sure the present method is better. It has been mentioned with reference to the effects of drugs on behavior because it permits a great deal of sensitivity with a low frequency of drug injection. Furthermore, computation of the statistic is almost instantaneous. If it happens to be useful, it can be elaborated much as procedures for irreversible effects have been elaborated in this paper. For instance, in the case we used as an example, 4 sub-experiments can be administered at one dose level and 4 sub-experiments at a second level.

REFERENCES

Cronholm, J. N. and Revusky, S. H. A sensitive rank test for comparing the effects of two treatments on a single group. Psychometrika, 1965, 30.

Feller, William. An Introduction to Probability Theory and its Applications, Vol. 1, New York, John Wiley. First edition, 1950; Second edition, 1957.

Mosteller, F. and Bush, R. R. Selected quantitative techniques in G. Kindzey (Ed.), Handbook of Social Psychology. Reading, Mass. Addison-Wesley, 1954.

Siegel, S. Nonparametric Statistics for the Behavioral Sciences, New York: McGraw-Hill, 1956.

CONTROL OF DATA-SUPPORT QUALITY

Fred S. Hanson
Plans and Operations Directorate
White Sands Missile Range, New Mexico

ABSTRACT. The need for businesslike management of range-user support is a requirement for quality control. Required, or committed, levels of quality and reliability largely determine cost of support and value of the services. Measurement support is the best area to start a Range quality-control program. Evaluation support is an easier place to start formal control than real-time support. In this frame of reference, quality is the technical level -- accuracy and/or precision -- of data support. The problem of specifying data quality has been largely resolved. The statistical control chart for the standard deviation can be directly carried over to the flight-measurement operation. The Ranges have available a sufficient basis for operating control -- and for some of the user's needs -- in the precision of observations and of data. It appears that quality assurance for everything is not necessary, so far as data-support contractors are concerned. A single number (average precision) can serve as an index of technical level of support performance -- for control of resources and for long-term planning. An approach to technical validation of measurement requirements is proposed.

INTRODUCTION. By definition, some technical criteria are necessary to efficient management of technical operations. In the case of a missile range, the keys to some of these criteria lie in the discipline of data analysis -- which is the hardest place for Management to get them out.

BACKGROUND. Almost two years ago, White Sands' Range Operations Directorate appointed a Quality Assurance Committee -- because the formal organization had failed to develop adequate quality control. (The writer serves as Chairman.) The Committee engaged a consultant, thru ARO(D) -- Charles Bicking, who once worked with General L. E. Simon.

Figure 1 shows a (missile) range as a system. The input is from the range user. Support may be represented as a transfer function. The idealized diagram shows open two-way communication, within the support function. The output is to the user.

A need of this system is businesslike management of user support -- to make the output match the input -- and to minimize the cost of the transfer function, which includes management (plus a goodly share of the overhead). This paper shows the extent to which this need is a requirement for quality control.

DEFINITIONS. Quality is how well and how good. Broadly, quality is any desirable characteristic of process or product - other than sheer quantity or rate.

The viewpoint that a missile range need be concerned only with production; that exactly what it turns out is less important; and that how good this is is scarcely worth mentioning is, of course, not rational. However, pressures to meet deadlines - and limitations of resources of all kinds - tend to reduce a Range to this viewpoint.

Reliability is how often -- either within a test or among tests. It is % success.

Support reliability is - strictly speaking - a production characteristic. However, hardware reliability is sustained quality - of the hardware. So, as a discipline, reliability is found with quality. This paper considers reliability control common to production control and quality control, for missile ranges.

Required, or committed, levels of quality and reliability largely determine cost of support and value of the services. So, can a Range have an economical, consistently-valid support operation without (some form of) quality control?

This paper considers the distinction between quality assurance and quality control to be a matter of degree. Assurance is broader -- more staff like.

This paper defines statistical quality control - industrial quality control - as: closed-loop control of operations. It's emphasis is on formulative and evaluative control actions. As a separate discipline, or function, quality control is taken (in Figure 2) to comprise: specification, score-keeping, feedback, and followup. Let's explore quality control, itself, and each of these phases (in relation to a range).

QUALITY CONTROL. The (missile) Ranges tend to overemphasize measurement -- somewhat at the expense of other support. I think this (emphasis) is partly due to the cost. But, it's mostly that data support is a focus of confusion (and difficulty). Measurement is the best place to start a (support) quality-control program. Because it offers a big pay-off (thru more economic control of resources and of planning); because it is a key to the technical level of the missile effort; and because it lends itself directly to conventional (statistical) quality control -- as will be shown.

Evaluation support is an easier place than real-time support to start formal quality control. Because the data holds still - and sits around - during postflight reduction. And there's less sound and fury connected with it.

An overland missile range is ideal for (pioneering) statistical quality control of flight data -- because it has an unlimited number of possible locations for instruments.

In this frame of reference, quality is the technical level of a range's (daily-operating) data support -- evaluated against the corresponding requirement. Quality (level) is the percent to which a particular (quality) requirement is met.

A range may need other things as much - or more - than it needs quality control. For instance: standard operating procedures for instrumentation; reliability control; an integral production-control system. The National Ranges have to work on all of these.

SPECIFICATION. As this paper sees it, specification is the cornerstone of quality control. A spec. is a practically foolproof (and knave-proof) description of an item or service. It is the standard that tells what counts as a goal - in the particular game. It has to be definite, and quantitative.

In specifying measurement quality, one should ask the question: "What do we mean, 'accuracy'?"

Suppose a user has furnished the characteristics of his vehicle - and its proposed trajectories. Assume that a missile-performance variable (to be measured) has been identified; and the desired units,

and coordinate system, have been specified. It takes about nine more questions to "pin down" the user's "accuracy" requirement.

Figure 3 shows the elements - demonstrably - required to specify the "accuracy" of flight measurements:

1. What part of the trajectory? (trajectory phase)

2. At what intervals (do you want data)? (reporting interval)

3. Is this accuracy or precision? (quality characteristic)
The user could be stating the allowable discrete error (of the data) with respect to his (preferred) coordinate system. Or, he could be stating the allowable inconsistency of the data with itself.

4. Does this number apply to the vector or to a component? (mode or representation)
(If he says "component", there is a second question: Is the requirement the same for each component?)

5. What % (of the data) must be within this tolerance? (probability level -- % compliance)

6. Precision (or accuracy) or exactly what? (data phase)
i.e., What stage of the measurement-computation-analysis process is being characterized?

7. What is the "operational" basis of the quality characteristic? (quality criterion)
In other words, what sort of procedure is (to be) employed to obtain this precision (or accuracy) figure?

8. Over what interval do you want the precision (or accuracy) to average out to the requirement? (lot size)
Question 5 was: What % (of the time) do you want the data (to be) within the stated tolerance? If the user said "68% of the time", the present question is: 68% of what time -- what is the minimum lot size to which the spec. applies? (What constitutes an acceptance lot?)

9. How much variation is acceptable within a lot? (variability w/in lot)
Of course, this is already reflected in the lot-average tolerance.

10. Finally, what support-reliability (level) will you accept? (reliability) Or, (will you) find the Range sufficiently to assure? Actually, neither the users nor the Ranges are ready for quantitative specification of data-support reliability.

People go around saying "accuracy". Figure 3 shows the kinds of uncertainty implicit in that word - when applied to flight measurement. It turns out - if one says accuracy without further qualification - the uncertainty as to what is meant can be as large as 15 or 16 times the requirement. This was shown in the writer's paper (Ref. 1) at the 1963 Army Operations Research Symposium. People should be more scientific than being away from what they are dealing with by a factor of 15 or 16 - as a matter of pride. Also, the taxpayer can't afford to have the Ranges spend his dollars so vaguely.

These elements of a spec. apply to all performance variables. Actually, they cover any quantity -- no matter how obtained. Asking these questions, of the user was an expository device. They could, just as well, be asked of a range - regarding its capability. In practice, White Sands has built a sufficient basis, and a standard basis, for a measurement-quality spec. into its user-document formats -- with the door left open for (the user to state) a different basis.

WSMR's standard basis is:

Quality characteristic -- precision

Mode of representation -- component

Probability level -- 68%

Data phase -- a single value of the missile variable - at a given point in time - in component form

Quality criterion -- propagation of error (from the previous data phase)

Lot size -- the series of firings covered by the requirement (the average precision for that)
WSMR wants to be judged on the average quality of "the whole trainload of apples". First, it was necessary to state what constitutes an "apple" (data phase) in this case.

Reliability -- in the White Sands edition of the National Range Documentation, categorizing a requirement as "Mandatory", "Required", or "Desired" yields a qualitative judgment of the user's need for reliability of (obtaining this) support.

Because WSMR's standard basis is (rather) concisely stated, it's not foolproof - unless one (also) refers to the procedure for its calculation (stated) in Final Data Reports. It would improve communication if that were expressed in "English" - as well as matrix algebra. For instance, WSMR calculates the precision of a single value of a position component from the precision of observations of (physical) determinants of that position. In three dimensions, and matrix algebra, the square root of the sample size is replaced by the square root of: Δ_{11} over Δ. It would be desirable to spell out what that means in ordinary algebra - and ordinary English.

It is more in accord with a search for ultimate purity, and more convenient, to say that accuracy and precision should be left in the qualitative realm. But, the Ranges are in business. So, they have to go ahead as best they are able. The writer has collected many publications on measurement semantics. This paper's semantic criteria are:

First -- usefulness (for the particular purpose)

Second -- simplicity, clarity, ordinary logic

Third -- tradition, rigor, abstract symbolism

In the unsheltered world, communication between disciplines is more useful than purity of discipline. If it's authoritarian, it's not science - anyhow.

The writer's paper at the Tenth Conference (Ref. 2) may lead WSMR to (separately) specify the quality of measurement of the time dimension of missile-performance variables.

The economic goal is to give the range user exactly what he asks for -- and not one iota more. If the user finds he needs more, he has only to ask.

SCOREKEEPING. Standard statistical quality control can be directly carried over to data-support operation - as follows:

A manufacturer of "widgets" will inspect a sample of (several) widgets taken from production. The average caliper of the sample will become a dot on a control chart showing the level at which his operation is running. The average variation (standard deviation), from-widget-to-widget within the sample, may become a dot on a control chart showing the (current) variability of his process. Control of the level of a missile-performance variable is a (range-) user function. The Ranges can directly carry over the control chart for variability - of their measuring operation. The dot on a Range's chart can be a statistical average of the variability for an entire (phase of a) trajectory; because feedback control can only be from-firing-to-firing - of a given type. Variability of the measuring operation is, of course, precision of measurement. We are talking, here, about using a standard measure of final-data quality as an overall-performance index for a data-support operation -- besides using it as a consistent basis for user-range communication of (data-support) requirements.

Physical accuracy is important. But, the least we can be is consistent. The Ranges have available a sufficient basis for operating control -- and for some of the user's needs -- in the (internal) precision of their insufficiently-calibrated data-support systems. (Insufficiently-calibrated as systems.) White Sands' standard precision of position measures consistency between (observing) stations -- which contains a portion of physical truth.

A few samples of WSMR scorekeeping:

1. Our consultant, Mr. Bicking, developed a control chart for instrument and system support reliability. The number of unusable records, of a system, is plotted directly from Data Reduction's Field Record Quality Report - without (the necessity of) calculating (the) fraction defective. The horizontal scale is total number of instrument operations (in a week). This avoids fluctuating limits. So, the chart can be prepared in advance -- with (2-sigma) limits which increase smoothly with number operated.

2. Figure 4 is another control chart on an intermediate "product". This is from Data Reduction's monthly Data Quality Report

(Ref. 3). It shows the (rms-) average precision of azimuth-angle observations by each (Askania-) cinetheodolite station - identified by number. (Ordinate scale is minutes of arc.) The precisions for August are the plain bars. The shaded bars are cumulative-average precisions. The UCL is a 3-sigma control limit -- based on the fluctuations of the cumulative-average precisions (cumulative from 1 January) about their central value, during the March-April period. (It should be realized this is 3-sigma of sigma.)

3. Let's look at (an example of) overall data-support quality. Figure 5 is from Data Reduction's Data Quality Report for May (Ref. 4). It shows the (rms-) average precision of (cinetheodolite) position measurement, in feet, for (the) Little Joe (component of NASA's Apollo). The solid curve shows the average (data-point component) precision for each round. The dotted curve is the cumulative-average precision. For this Project, the requirement and the range commitment happen to be the same. In the beginning, Data Reduction didn't use statistical control limits; because WSMR's greatest need was to see where it stood -- and what sort of creature it was. There were better - and worse - charts than Figure 5. The main point is: the quality of WSMR data support can vary widely from-test-to-test. (Also, from-month-to-month - and from-project-to-project.)

The average precision of final data is a measure of support performance. When the user's requirement is valid, average precision is (also) a measure of Range effectiveness.

Two of WSMR's operating chiefs were displeased by the test-to-test precision charts. The bad data was too evident. Since the May Report, precisions for each test have been shown only in tables. Starting with the current Data Quality Report (Ref. 5), monthly and cumulative-average precisions for each project - along with the requirement and commitment - are shown on bar graphs.

One of WSMR's operating supervisors suggested (seriously) final-data charts could be improved by editing the input to the average precisions - at (about) 75% confidence. That's editing at 1.15 time sigma (the variable being plotted). It would do a great deal for the charts, but it would nullify their usefulness.

A comment on (the problem of) monitoring a range-support contractor:

MIL-Q-9858, etc. furnish guidelines for quality assurance - almost "from-womb-to-tomb". These are procurement-oriented regulations. When procurement requirements "cannot" be numerically specified; compliance "cannot" be demonstrated by test; or initial failure to meet "cannot" be tolerated; it is necessary to inspect a contractor for "everything". This paper has shown a basis for definite, numerical specification of flight measurement - and demonstration of compliance. The fact that, in the past, the Ranges have not had systems for reporting whether requirements were met (in a technical sense) is evidence that initial failure to meet can be tolerated. So, it appears that quality assurance for "everything" is not necessary - so far as data-support contractors are concerned. A single number - average precision of measurement - can serve as an index of variability of (a given data-support) process and product; and as an index of technical level of support performance (add effectiveness) -- for control of resources and for (long-term) planning.

FEEDBACK. Open-loop control gives good results only for very simple, easily-controlled processes. Flight measurement is not simple or easily-controlled.

In the past year, WSMR has increased feedback on field-record assessments; and on which stations are thrown out in data reduction. WSMR has also initiated feedback on average angular errors of each (optical) station (Fig. 4); and feedback on final-data quality (Fig. 5). Purposes of these feedbacks include: input to an "calibration" of station-selection (computer) programs (Ref. 6); and input to (the actual) instrumentation plans. Which feedbacks have the greatest "profit potential" - and what the optimum and achievable time frames are - remains to be determined.

Some range personnel, who are not quality-minded, make a counter-issue of "timeliness" (of data delivery). So, the (Plans & Operations Directorate's) Quality Assurance Committee has adopted that word. The Committee is stressing timeliness of feedback -- timeliness of quality reporting, as well as of data reporting.

It should be realized that final-data quality reports are (also) a formal system for knowing Range capabilities -- the beginning of such

a system. Copies of final-data quality reports now go to White Sands' (long-Term) planners. These reports also serve as feedup to top management. They put numbers on some of WSMR's technical, operating, and management problems.

FOLLOWUP. Assurance of followup, in a procedural sense, is a Quality Control responsibility. Actual followup is an operating responsibility.

When Data Reduction QC gets a very bad average precision of final data, they check to be sure the analyst is not including the poorest part of that trajectory in the formal report.

When an optical station has the same (major) deficiency in its field record for two consecutive tests, Data Reduction assessment personnel report this, by telephone, to Optical Division technical personnel. When this proves insufficient, Data Reduction will send a (written) memo to Data Collection - requesting a reply stating what corrective action has been taken, and what further action is planned.

The writer suggested Data Reduction look at average relative bias of each (cinetheodolite) station -- by taking algebraic means of angular residuals (from least-squares solutions). A good deal of what WSMR treats as random error is persistent bias. It turns out this step will not be practical until WSMR has quality control per segment of trajectory - so average relative bias (of a station) will be with respect to a single group of stations. The fact the reference changes with each station added (or subtracted) shows the extent of the station-bias problem.

Of course, White Sands is setting its sights on controlling (both) the level and the test-to-test consistency of average precision (of data). To do this, it needs to learn how to break down the firing-to-firing variability (for a given project) into that due to: project; weather; collection; reduction; other. Major factors are: number of stations; where the missile flies; reliability of stations; "visibility"; relative locations of stations; quality of stations.

WSMR won't have real control until it moves its feedback out of a management time frame into an operating time frame. It is also necessary to increase supervisory awareness of the quality feedback (and feedup) now available.

White Sands is slowly moving toward: reliability and precision standards for each type of instrument and system; clearly defined responsibilities (of Collection and Reduction) in relation to final-data quality; functional management of this shared responsibility.

Mr. Bicking essayed an analysis of variance of undesigned, operational precision data. He was able to test whether: stations, film-reading machines, (human) readers, etc. had significant effects on data precision. He was not able to determine the amount by which each affected precision. Further investigation (of this approach) is certain to be fruitful.

Range support is a hard place to carry out classical design of experiment. The missile Project does the test design. The Range has, occasionally, put two (similar) instruments at the same site. WSMR runs a range-calibration "test" (Ref. 7), at infrequent intervals. Instrumentation (support) planning is a statistical-design problem. However, current station-selection computer programs (Ref. 6) are a long step away from representing analyses of variance. P&O's Quality Assurance Committee aims to develop the Range's quality-control situation to the point where it will use Evolutionary Operation (EVOP) (Ref. 8). Presently, the Range needs to carry out (more) correlations - and analyses of variance - on undesigned, operational data. WSMR urgently needs a statistical-calculating service. It also needs better coordination of its applied-statistics efforts.

REAL TIME. Quality control applies - in its entirety - to real-time data support. Specification is exactly the same; but WSMR hasn't built this into its edition of the National Range Documentation (to the same extent) - yet. Realtime scorekeeping and feedback can be carried out on a firing-to-firing basis. To some degree, they can be included in the real-time computer program. Followup is the same (problem) as for evaluation support.

STATUS OF QUALITY CONTROL. The suggestion to use (a standardized) average precision as an index of overall data-support performance was made five years ago, by this writer (Ref. 9). It took four years, one Committee, and John Carrillo (of Data Reduction) to implement this.

In applying statistical quality control to data support, White Sands is running counter to Thurman Arnold's corollary (to Parkinson's law):

No new government activity can possibly be effectively carried out by any established government organization.

Only a little over a year ago, the most important product of P&O's Quality Assurance Committee was hope -- hope that data support could be put on a more objective basis.

The focus of Quality Control has caused White Sands to correct a few errors in its data-reduction methods.

P&O's Quality Assurance Committee is still selling quality control to operators -- as a tool for their use -- not as a club held by Management. Data Collection (people) recently asked that Data Reduction's Field Record Quality Report be discontinued -- on the ground that Data Reduction's assessments were not valid. Data Collection personnel have since been told to exchange assessment sheets with Data Reduction - both ways - to improve understanding. A Quality Assurance Subcommittee is developing a single set of standards, and a single SOP, for assessment of optical records. Data Reduction Groups on the Ranges are predominantly mathematicians. To this writer, they seem inclined toward monodisciplinary and laboratory viewpoints - and to favor a priori approaches. Resistance by data-reduction personnel to quality control may have been due to QC's management, and factory, and a posteriori connections. But, quality control is not the factory in science. It's science in the factory. (This is now recognized by White Sands data-reduction personnel.)

Data Collection Quality Control has been mainly concerned with solving the problems of station reliability.

There is still a need to sell quality control (of range support) to various echelons of Range Mangement -- as a tool for their use -- not as a constraint. The key to selling Management probably lies in the fact that - for data support - quality control is resource control. The prospect of better bridging the (communication) gulf between Management and data-analysis (personnel) may cause some discomfort on both sides. Of cource, at some date, White Sands will have to bring cost into its Quality Control picture. Specifically: precision/manhour, precision/dollar, and value of precision (as distinquished from cost).

PSYCHOLOGICAL IMPACT OF QUALITY CONTROL. It is this writer's observation that truth for the sake of the mission is psychologically

closer to truth for its own sake than it is to truth as an instrument of power.

Negative reactions to quality control appear to be due to resistance to change - and to dislike of the "criticism" inherent in scorekeeping (feeling threatened by any demand to be objective). Quality control is partly an educational - and re-educational - problem. AMETA gave a composite of its basic and advanced Statistical Quality Control courses at White Sands. This writer is working on an executive primer of flight-measurment quality (and specification). WSMR may bring in a quality-control speaker. The Chief of Data Collection Quality Control has written a memo to the individual (field) operators, and their supervisors, asking them to identify - verbally or in writing - existing or potential causes of error; and to grade these as critical, major, or minor. (This will also be an input to the work of the optical-assessment Subcommittee.)

On the positive side, keeping score adds meaning and significance to any game. Keeping score makes how-to-play (how-to-operate) more important - not less. It improves the motivation and morale of functionally-oriented people.

PHYSICAL ACCURACY. This paper defines accuracy as: the numerical difference between any value and the "true" value. It is further necessary to say that the "true" value must be a reference physically independent of the value characterized. Physically independent means: the errors of measurement (of the two) are uncorrelated. (Of course, accuracy is the inverse of the "absolute" error defined here as its measure.)

The development of the potential of its star-reference BC-4 camera system is White Sands' only real hope for an absolute-accuracy reference for flight data.

WSMR could derive accuracy (as well as precision) estimates for two kinds of data in its current operation. Besides star-referenced ballistic-camera data, it could do this for (launch and terminal) fixed-camera data - in which the reference-target poles are photographed in the same frame as the missile.

Of course, measurements cannot be consistently accurate unless they are also precise. Differences in the accuracies of stations affect system precision.

This writer holds that being more definite and quantitative about precision will increase (range and user) understanding of accuracy - and awareness of specific needs for it.

VALIDATION OF REQUIREMENTS. Range-support personnel are often asked "Why don't you tell them they don't need all this data?"

Of course, user requirements should be based on missile technology and missile-test design. Support personnel have no particular qualifications in those fields.

This writer has suggested an approach to deriving measurement requirements in which the Range can assist the user (Ref. 10).

The simplest way to derive estimates of required data quality is to convert missile-performance tolerances to measurement "tolerances" -- directly, when they are the same variable -- or by (complete) propagation of error (formulas) thru an equation relating the performance variable and the measured variable. As Figure 6 shows, the resulting "tolerance" must then be tightened -- on the basis that the actual uncertainty whether missile performance meets its specified tolerance is the sum of the uncertainty of the measured performance and the allowable uncertainty of the specified performance. The required measurement tolerance depends on the level of risk at which the missile-using agency is, practically, willing to operate. While a Range superiority of 10 times (in standard deviation - sacrificing elegance for clarity) would be ideal -- 2-2½ times is the necessary level; 5 times is certainly the sufficient level.

REFERENCES

1. Hanson. F. S. "An Operational Specification for Flight Measurement", Proceedings of the United States Army Operations Research Symposium - Part 1, 1963, pp. 307-314.

2. Hanson, F. S. "System Configuration Problems and Error Separation Problems", Proceedings of the Tenth Conference on the Design of Experiments in Army Research, Development, and Testing, 1964, pp. 119-143.

3. "Data Quality", 24 July - 31 August 1965, Data Analysis Directorate, White Sands Missile Range, New Mexico, p. 8.

4. Carrillo, J. V. "Cinetheodolite Statistical Data", 1 - 31 May 1965, Data Analysis Directorate, White Sands Missile Range, New Mexico, p. 12.

5. Carrillo, J. V. "Data Quality", 1 - 30 September 1965, Data Analysis Directorate, White Sands Missile Range, New Mexico, pp. 3-5.

6. Hall, C. A. "Deleting Observations from a Least Squares Solution", Paper presented at the Eleventh Conference on the Design of Experiments in Army Research, Development, and Testing, 1965.

7. Williams, B. L. "Precision and Bias Estimates for Data from Cinetheodolites and FPS-16 Radars", Paper presented at the Eleventh Conference on the Design of Experiments in Army Research, Development, and Testing, 1965.

8. Hunter, J. S. "Experimental Methods of Determining Optimum Conditions", Proceedings of the First Conference on the Design of Experiments in Army Research, Development, and Testing, 1955.

9. Hanson, F. S. "Quality Control", Memo to Deputy for Technical Operations, Integrated Range Mission, White Sands Missile Range, New Mexico, 21 November 1960.

10. Hanson, F. S. "Exploring the Need for Quality Control", WSMR Presentations at Inter-Range Conference on Performance Evaluation and Quality Assurance, May 1965, Section 4D.

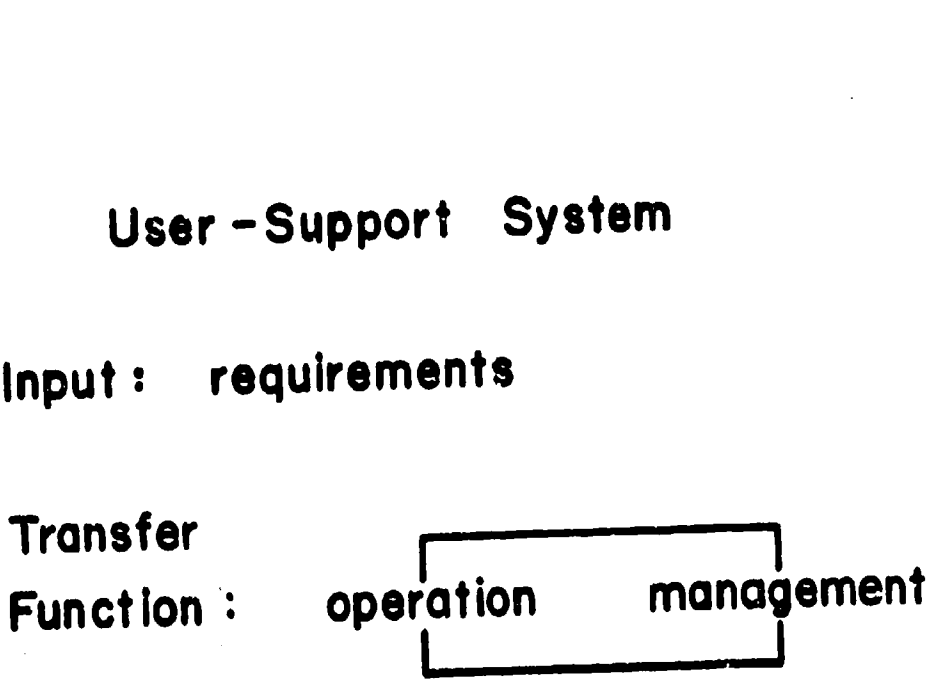
User-Support System
Input: requirements
Transfer Function: operation management
Output: services

Figure 1

Quality Control

Specification

Scorekeeping

Feedback

Followup

Figure 2

Elements of "Accuracy" Spec.

Trajectory Phase

Reporting Frequency

Quality Characteristic

Mode of Representation

Probability Level

Data Phase

Quality Criterion

Lot Size

~~Variability w/in Lot~~

Reliability

Figure 3

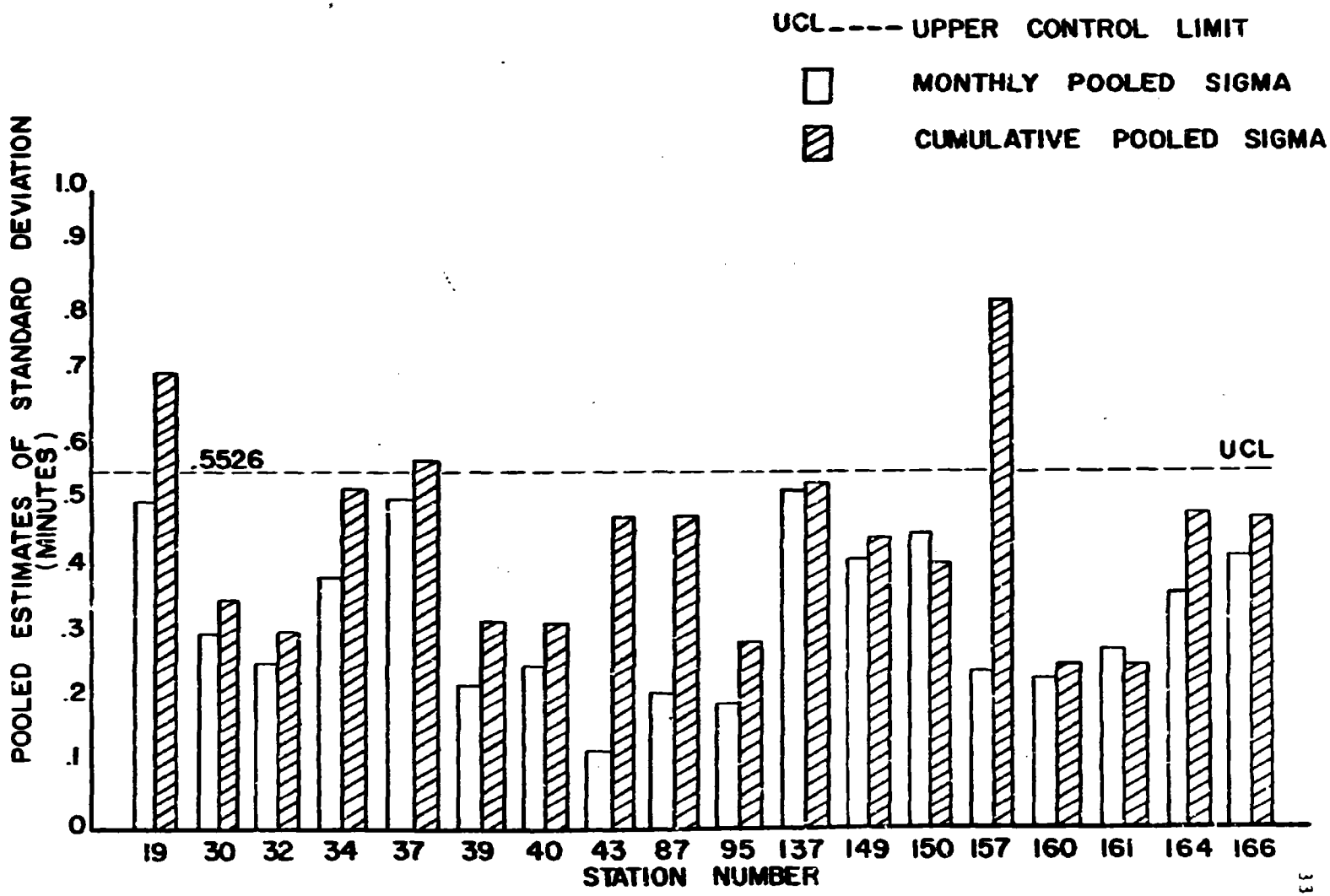

FIGURE 4 CONTROL CHART FOR ASKANIA (AZIMUTH)

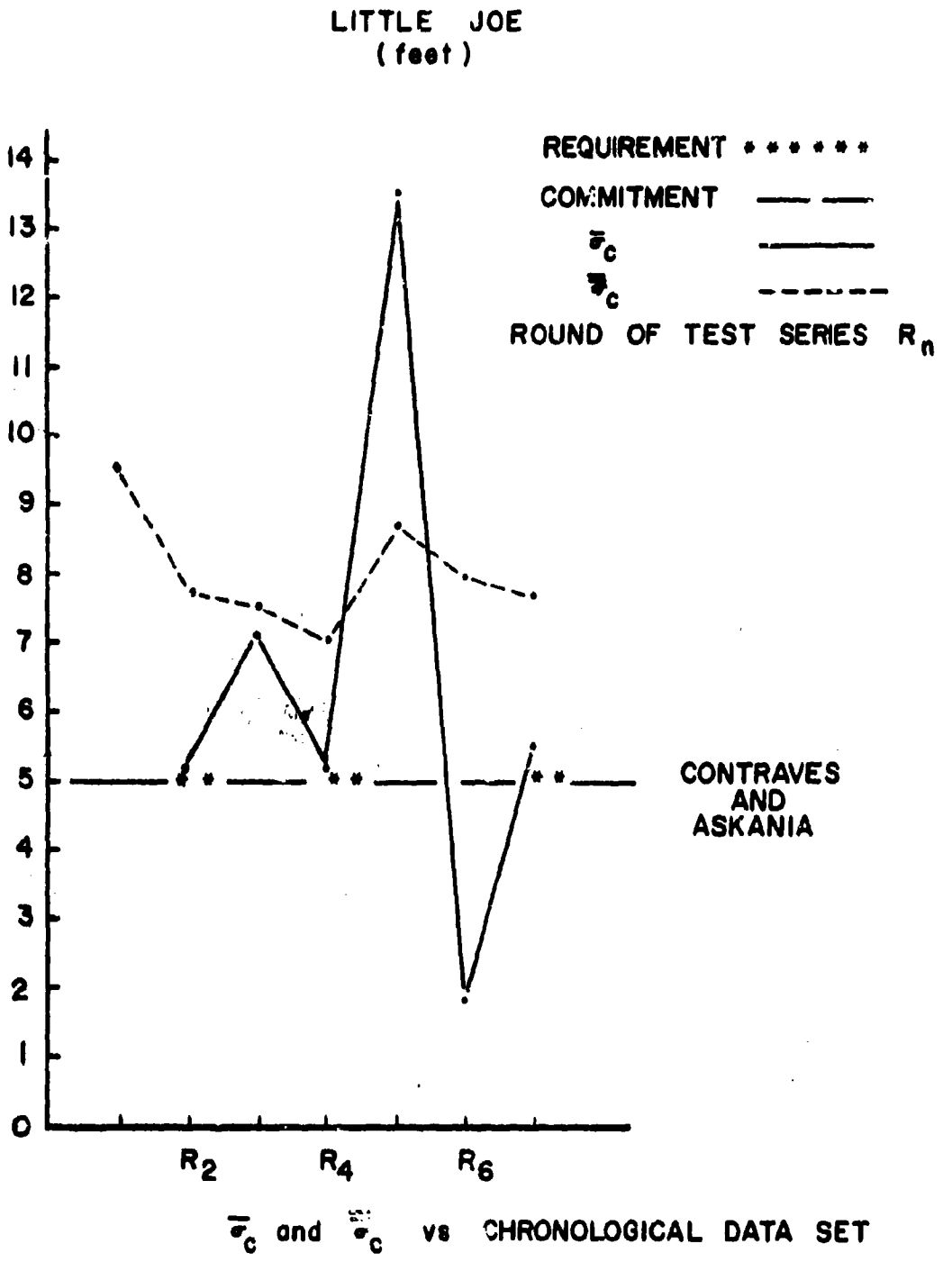
LITTLE JOE
(feet)
REQUIREMENT
COMMITMENT
$\bar{\sigma}_c$
$\tilde{\sigma}_c$
ROUND OF TEST SERIES R_n
14
13
12
11
10
9
8
7
6
5
4
3
2
1
0
CONTRAVES AND ASKANIA
R_2
R_4
R_6
$\bar{\sigma}_c$ and $\tilde{\sigma}_c$ vs CHRONOLOGICAL DATA SET

FIGURE 5

$$\text{EVALUATION VARIANCE} = \text{MEASURED VARIANCE} + \text{SPECIFIED VARIANCE}$$

FACTOR OF SUPERIORITY $\frac{\sigma_s}{\sigma_m}$	ERROR IN EVALUATION
1.7 X	36 %
2 X	25 %
2.5 X	16 %
3.3 X	9 %
5 X	4 %
10 X	1 %

$$\text{REQUIRED VARIANCE} = \text{SPECIFIED VARIANCE} \times \frac{1}{(\text{CHOSEN FACTOR})^2}$$

FIGURE 6

DESIGNS AND ANALYSES FOR INVERSE RESPONSE PROBLEMS IN SENSITIVITY TESTING*

M. J. Alexander and D. Rothman
Rocketdyne, A Division of North American Aviation, Inc.
Canoga Park, California

INTRODUCTION. Sensitivity testing is that area of experimentation in which each test is characterized by a quantal response. To some sample specimen or realization of a system one or more stimuli are applied and the result is either a "response" or a "nonresponse", depending on whether some critical physical threshold was or was not exceeded for that particular sample. The most commonly encountered type of sensitivity problem is that of finding at what level of the stimulus variable a given percent response will occur. For example, in biological assay it is often necessary to determine the dose (called LD 50 or ED 50) which is effective half the time, and in testing explosives, it is often of interest to find the stress that results in a detonation, say, 95% of the time. In each of these situations we are concerned with inverting the relationship which gives the probability of a response as a function of the stimulus; thus the terminology (probably due to J. W. Tukey) of the "Inverse Response Problem."

The general problem can be stated more precisely as follows: Suppose we have a stress variable x, and suppose that a test at this stress can result in a response which is either "1" or "0". This is the well known quantal response experiment. Let M(x) denote the mean or average response fraction at x. In this situation M(x) is called the response function. If M(x) is monotone nondecreasing, it may be thought of as representing a cumulative distribution function, as, for example, the cumulative normal distribution

$$\int_{-\infty}^{x} \frac{1}{\sqrt{2\pi}\,\sigma} \, e^{-(y-\mu)^2/2\sigma^2} \, dy.$$

In most cases, however, the explicit form of M(x) is not known.

*This work was supported by the George C. Marshall Space Flight Center, NASA, Huntsville, Alabama, under Contract No. NAS 8-11061.

For the inverse response problem the experimental objective is the estimation of that $x = x_\alpha$ (generally unique, but not necessarily so) at which $M(x) = \alpha$, for a given value of α. We shall be concerned here both with experimental designs for the inverse response problem and methods for analyzing the test results.

The first approach to this problem was based on the use of the probit design [1] which was originally formulated for biological applications. This design requires a fixed number of tests at each of a given set of stimulus levels, and thus a large number of tests is necessary. The analysis generally used with the probit design is based on assumptions concerning the response function $M(x)$ and the objective of the analysis is the determination of response function parameters. Once these have been estimated, the solution of the inverse response problem can be obtained for any α.

When cost of availability of materials is an important consideration, the probit design, because of the larger number of tests involved, becomes impractical. To obtain estimates of x_α, particularly for $\alpha = 0.5$, in fewer tests, a sequential design was introduced in 1943 at the Explosives Research Laboratory at Bruceton, Pa. [2]. The rules for the Bruceton or up-and-down design require increasing the stimulus by a fixed step-size after a nonresponse and decreasing the stimulus one step after a response. The up-and-down design is still the most widely known and most extensively used test procedure, particularly for explosive testing and other engineering applications. For $\alpha = 0.5$ it is used in conjunction with the Dixon-Mood [3] or more recently Dixon [4] analysis, both of which assume that the response function $M(x)$ is cumulative normal.

Other methods generally used with distributional assumptions are the Langlie [10] and rundown designs. When these procedures are used to estimate x_α for values of α near .5, inappropriate distributional assumptions do not have a critical effect on the efficiency of the design. However, for more extreme values of α the situation is more critical not only because the tails of the response distribution are more sensitive to inappropriate assumptions, but also the estimates of x_α in these cases are generally less robust.

In the absence of distributional assumptions on M(x) the inverse response problem was first attacked directly by Robbins and Monro [5] who employed a stochastic approximation design. In this procedure the step-size is no longer fixed, and the rules for determining successive test levels depend only on the last test (as in the up-and-down design). The levels converge to the desired critical level, x_α, not only in probability but with probability one. This design and its variations, Kesten [6], Odell [7], and delayed [8], particularly the latter, are slightly more efficient than the Bruceton or probit designs for $\alpha = 0.5$. However, for more extreme values of α (e.g., $\alpha = 0.05, 0.95$), simulations [9] indicate that the design seems to be much less efficient than expected.

For many years the major attention in the inverse response problem was focused on the case $\alpha = 0.5$. For this problem both the up-and-down and Robbins-Monro types of designs give reasonable answers in about 6-12 tests. However, reliability and safety problems require estimates of x_α for $\alpha \leq .05$ or $\alpha \geq .95$. For such extreme values of α, when prior knowledge of the response function M(x) is limited, it was necessary to consider new design and analysis procedures. In the Robbins-Monro design, successive test levels are determined from only the previous test results. One would expect that improved estimates of x_α could be obtained if all data were analyzed before the next test level was selected.

The two designs described in this paper were formulated from this point of view; they give good results with limited sample sizes for $\alpha \sim .05$ (.95) and are still useful in many applications for $\alpha \sim .02$ (.98). One design is appropriate when it is desired to continue testing on a set of discrete test levels until a specified precision in the estimate of x_α is attained. The other is appropriate when the sample size is fixed in advance and there are no restrictions on test levels. Both designs have been evaluated by simulation and it is shown that they compare favorably with existing procedures and with a conjectured asymptotic criterion for distribution-free inverse response problems.

ALEXANDER DESIGN

GENERAL DESCRIPTION. In sequential designs new levels for testing are determined from previous test results, and this may be accomplished in many different ways. In the Alexander design the step size is constant but (unlike the Bruceton and Robbins-Monro procedures) new test levels depend on all previous test results. It is assumed only that the response function $M(x)$ is monotone nondecreasing, so that the design is otherwise distribution-free. It uses alternately increasing and decreasing sequences to bound the sought-for stimulus level x_a. Testing ends when x_a is, with a specified probability, located within an interval of length not more than 2Δ, where Δ is the step size. From an estimate of this interval, an estimate of x_a can be found in turn by linear interpolation.

The initiation and termination rules for the sequences are defined in terms of monotone estimates of the response probabilities at the test levels. In one version of the design, which should be used for α near 0.5, maximum-likelihood estimates are used. However, for extreme values of α, it is more efficient to use both maximum-likelihood estimates and certain estimates based on confidence bounds which will be described subsequently.

Simulations of both 0.5 and 0.05 designs have been carried out. The design is generally quite efficient relative to other available distribution-free designs, and is roughly as efficient as the best parametric stochastic approximation when distributional assumptions on $M(x)$ can be made.

The general rules for the design may be described as follows:

1. The first test is at L_1, the a priori best guess of x_a.
2. By the method of reversals (Appendix I) monotone estimates are evaluated at all test levels after each test.
3. Testing will be performed by alternately increasing and decreasing sequences of test levels.
4. The first test of an increasing (decreasing) sequence is at

either the highest (lowest) level, strictly above (below) the last test level, at which the estimate is less (greater) than or equal to α or, if there is no such level, at the level above (below) the last test level.

5. An increasing (decreasing) sequence will be terminated at the first level at which the estimate after a test at that level is strictly greater (less) than α.

6. The rules for ending the design depend on the value of α and are given explicitly below.

THE DESIGN FOR $\alpha = 0.5$. For $\alpha = 0.5$ the estimates used in following the design rules are the maximum-likelihood estimates given by the method of reversals. When the testing is finished we wish to have an interval I such that $\text{Prob}(x_\alpha \in I) > P$, where P is some prescribed probability. The length of I depends on the particular experiment; it is never more than twice Δ, the step size, but in most cases it is Δ. The occurrence of an interval of length 2Δ corresponds to the situation when $\hat{x}_\alpha$ is at the center of I. Testing will be stopped when either of the following conditions is satisfied: (a) there are three adjacent test levels $L_0 < L_1 < L_2$ such that the response estimate at L_1 is .5 and the response estimates $\hat{p}_0$ and $\hat{p}_2$ at levels L_0 and L_2, respectively, lead to the confidence statements

$$\text{Prob}\{p_0 > .5\} < (1-P)/2$$

$$\text{Prob}\{p_2 < .5\} < (1-P)/2$$

or (b) there are two adjacent levels $L_0 < L_2$ for which the above confidence statements can be made.

When P is .5 then the conditions for L_1 and L_2 are given by the following table:

A	B
0	2
1	3
2	4
3	6
4	7
5	8
6	9
7	10
8	12
9	13
10	14

In this table, A denotes the number of responses at L_1 and B denotes the minimum number of nonresponses which must be observed at the level for the condition in (a) to be satisfied. Similarly, if A is the number of nonresponses at L_2 then at least B responses at L_2 are required for termination.

THE DESIGN FOR EXTREME VALUES OF α. In a desirable distribution-free design for the inverse response problem, most of the test levels are concentrated in a region around x_α. Therefore, when $\alpha \sim .05$ we would expect on the average 19 nonresponses for every response. Thus in this case a good design forces some testing in the stimulus region below the lowest level at which a response has been observed. Since the maximum-likelihood estimates of the response probabilities are all zero in such a region, a new kind of "estimate" will be introduced to insure a sufficient number of zero responses. This "estimate" is actually used only to determine when to terminate a decreasing sequence. The method is most easily introduced in terms of an example.

Suppose that after some testing the following responses have occurred

$$\underset{L_1}{0} \quad \underset{L_2}{0} \quad \underset{L_3}{0} \quad \underset{L_4}{1} \qquad (L_1 < L_2 < L_3 < L_4);$$

that is, one nonresponse at each of the levels L_1 and L_2, two nonresponses at L_3 and one response at L_4. At L_1, L_2 and L_3 we would like to obtain estimates which satisfy the monotonicity assumption on $M(x)$ and which indicate that it is likely that the actual response fractions at these levels are greater than zero. We will accomplish this by introducing an appropriate confidence bound. In the example being considered two nonresponses were observed at L_3 and either from binominal tables or the equation

$$(1) \qquad (1-\tilde{p}_3)^N = 1-P \qquad (N = 2)$$

one can obtain an estimate, $\tilde{p}_3$, for a given probability P (specified in advance) such that

$$\text{Prob}\{p_3 < \tilde{p}_3\} \geq P \ .$$

If the same criterion is used at L_2 a larger estimate than that at L_3 should result. To insure monotonicity an interval estimate will be used. This will be accomplished by introducing a "zero region" for each level defined as that level and all consecutive higher levels at which no responses have occurred. Thus the zero region Z_2 for L_2 is the interval (L_2, L_3) and similarly $Z_1 = (L_1, L_3)$. The estimate for L_2 can then be found from (1) with N = 3 (the number of zeros in Z_2).

The objective in using the new type of "estimate" is to be reasonably sure that decreasing sequences end below x_α. From the rules of the design, a decreasing sequence will terminate at level L_0 where $\tilde{p}_0 < \alpha$. Because of the way $\tilde{p}_0$ is defined the following confidence statement can be made:

$$\text{Prob}\{p_0 < \alpha \mid \text{observed responses}\} > P \ ;$$

i.e., on the basis of the observed responses the probability that L_0 is below x_α is greater than P. For each decreasing sequence, the same

total number of nonresponses in the appropriate zero region will be required for termination. Thus, it is not necessary to determine estimates at each level. Instead, from

$$(2) \qquad (1-\alpha)^n = 1-P \ , \qquad N = [n] + 1$$

one can determine the appropriate N for a given P and then it is only necessary to count zeros in the zero region.

A uniform set of rules for the design can now be given:

1. The first test of an increasing sequence is at the level below the lowest level at which a response has been observed. If the result of this test is a response the sequence ends; otherwise, one more test (at the next higher level) is performed.

2. The first test of a decreasing sequence is at the level below the lowest level at which a response has been observed. The sequence ends at level L_0 whose zero region contains at least N nonresponses. Values for N can be found from (2). The following table gives values of N for $P = .5$

α	N
.1	7
.09	8
.08	9
.07	10
.06	12
.05	14
.04	17
.03	23
.02	35
.01	69

3. Testing ends when there are three adjacent levels L_0, L_1, and L_2 such that at least one response has been observed at L_2 (and none at a lower level), and a total of at least N nonresponses has been observed at L_0 and L_1. The value of N is given in the preceding table.

4. An estimate $\hat{x}_\alpha$ can be found by linear interpolation between the response probabilities estimated at L_1 and L_2.

The Alexander designs have the virtue that once the rules are understood, the actual procedure is fairly straightforward and the calculations required between tests are extremely simple. Of course, as with any distribution-free design, distribution assumptions can always be adopted after testing is complete. If,for example, it is desired to find $x_{.01}$ under the assumption of an underlying cumulative normal distribution, the estimates determined from the data generated by this design are somewhat better than those based on the data obtained from an up-and-down design, and are in fact almost as good asymptotically as the optimum for the 1% cumulative normal inverse response problem. Furthermore, any departure from normality will probably affect the estimates obtained from these data much less than the (extrapolated) estimates gotten from up-and-down data. One of the advantages of these designs is the small number of tests required. An estimate of the expected upper bound $\overline{N}$ is given by

$$\overline{N} = 2N(1 + \tfrac{1}{2} + \ldots + \frac{1}{N/2})$$

$$N = \begin{cases} N_0 & , \ N_0 \text{ an integer} \\ [N_0] + 1 & , \ \text{otherwise} \end{cases} .$$

When $P_0 = .5$ this gives an expected upper bound of 76 tests for $\alpha = .05$.

The design has been simulated for $\alpha = .5$ and $.05$. It appears that this design, particularly for extreme values of α, is more efficient than other nonparametric designs which are not based on analysis of all previous results at each stage. In our simulations, the median number of tests was about 64 for $\alpha = .05$; for $\alpha = .5$ the median number of tests was about 16.

EXAMPLES:

1. In the following simulated example, the Alexander design is used for $\alpha = .5$, $\Delta = .5$, with a cumulative normal response function, $\mu = 0$, $\sigma = 1$:

Test Number	Stress	Response
1	1.3	1
2	.8	1
3	.3	0
4	.8	1
5	.3	1
6	-.2	1
7	-.7	0
8	-.2	0
9	.3	1
10	-.2	1
11	-.7	0
12	-.2	1

Since the response fraction at -.2 is 3/4, while at .3 it is 2/3, the method of reversals must be used, giving 5/7 at -.2 and at .3. Linear interpolation between 5/7 at -.2 and 0/2 at -.7 gives as final estimate $\hat{x}_{.5} = -.35$.

2. The following data were simulated using a normal response function with $\mu = 0$, $\sigma = 1$, so that for $\alpha = .05$, $x_\alpha = -1.645$.

The first test was at -3σ and the step size chosen was $.25\sigma$. (The X's and O's indicate responses and nonresponses, respectively.)

Stimulus Level	Test Results									
-3.00	0									
-2.75	0									
-2.50	0	0				0				
-2.25	0	0				0		0		
-2.00	0	0		0		0		0		0
-1.75	0	0		0		0	0	0	0	0
-1.50	0	0		0		X	0		0	
-1.25	0	0		0		0				
-1.00	0	0	0	0	0	0				
-.75	0	X	0		0					
-.50	X									
	I_1	D_1	I_2	D_2	I_3	D_3	I_4	D_4	I_5	D_5 .

In the above table, the columns indicate sequences (I for increasing, D for decreasing). The final estimate is obtained by linear interpolation which yields $\hat{x}_{.5} = -1.675$. Note that a total of 44 tests was required.

ROTHMAN DESIGN

BACKGROUND. The second new design for the inverse response problem is built on a design by Marks [11] for locating the step in a step response function. Thus we shall begin with a brief review of that design in the case of infinite sample size (the same design is very nearly optimum even for small samples).

Let the step response function $M(x)$ be such that

$$M(x) = \begin{cases} 0 & , \ x < x_s \\ M_0 & , \ x = x_s \\ 1 & , \ x > x_s \end{cases} \qquad \text{and } 0 \leq M_0 \leq 1.$$

Suppose we have some previous estimate of the step location x_s which we denote by $\hat{x}_s$ and which we assume is normally distributed with unknown mean, x_s, and known standard deviation, w. Let the successive test levels be L_i $(i = 1, 2, \ldots)$ and the response at L_i be R_i. The first test is at that stress, $L_1 = \hat{x}_s$, which is the best prior guess of x_s. Then

$$L_2 = \begin{cases} L_1 - 1.17w & \text{if } R_1 = 1 \\ L_1 + 1.17w & \text{if } R_1 = 0 \end{cases} .$$

Since the design is symmetric about L_1, we shall give the next two test levels only for $R_1 = 0$; these are

$$L_3 = \begin{cases} L_1 + .55w & R_1 = 0, \ R_2 = 1 \\ L_1 + 1.99w & R_1 = 0, \ R_2 = 0 \end{cases}$$

and

$$L_4 = \begin{cases} L_1 + .273w & R_1 = 0,\ R_2 = 1,\ R_3 = 1 \\ L_1 + .847w & R_1 = 0,\ R_2 = 1,\ R_3 = 0 \\ L_1 + 1.537w & R_1 = 0,\ R_2 = 0,\ R_3 = 1 \\ L_1 + 2.657w & R_1 = 0,\ R_2 = 0,\ R_3 = 0 \end{cases} .$$

In order to simplify the computations, the following approximation, which only slightly affects the efficiency of the Marks design, will be used:

1. If $R_1 = R_2 = \cdots = R_i$, then $L_{i+1} = L_i \pm 1.167w/\sqrt{i}$, $i = 1, 2, \cdots$.
2. For all other cases the successive test levels are determined by "splitting the difference" between the lowest 1 and the highest 0.

For the fourth test, for example, this approximation gives (for the same result situation as above)

$$L_4 \tilde{=} L_1 + \begin{cases} .292w \\ .875w \\ 1.580w \\ 2.666w \end{cases} .$$

The effect of these small changes from the Marks values on the efficiency of the design is negligible. In fact Marks has shown [11] that even larger changes do not have a significant effect.

It is interesting to note that the factor $1/\sqrt{i}$ can be thought of as a compromise between the term $1/i$ in the original Robbins-Monro process and the constant step used to start the delayed R-M process.

RULES FOR ROTHMAN DESIGN. If it is known that w is very large compared to the distance of the interval in which the response function essentially goes from 0 to 1, then it is obvious that the Marks design could very profitably be used for the first few tests. Thus we propose the following design:

$$L_1 = y_o + 1.167w(a - .5)$$

where y_o denotes the experimenter's initial estimate of x_a. The second test is at

$$L_2 = L_1 + 1.167w$$

if the first result is a 0, and at

$$L_2 = L_1 - 1.167w$$

if it is a 1. The general rules for planning the $(r+1)^{st}$ test are:

1. After the r^{th} test, all of the data are analyzed by the method of reversals (Appendix I).

2. Compute

$$Y_r = \sum_{i=1}^{r} (1/i) \tilde{=} \gamma + \ell n(r+.5) + 1/24(r+.5)^2 - \cdots$$

where γ is Euler's constant $\gamma = .5772\cdots$. This quantity is asymptotic to the expected number of plateaus given by the method of reversals. Thus r/Y_r is roughly the average number of points which have gone into each response estimate.

3. Compute

$$\Delta = .6745 \sqrt{a(1-a)\, Y_r/r} \quad .$$

4. If there are any stress levels at which the estimated response is greater than or equal to $\min(a + \Delta, 1)$, let S_1 denote the lowest of these. If there are any stress levels at which the estimated response is less than or equal to $\max(a - \Delta, 0)$, let S_2 denote the highest of these.

5. If neither S_1 nor S_2 exists, let

$$L_{r+1} = L_1 \quad .$$

If S_1 exists, but not S_2, let

$$L_{r+1} = (S_1+L_r)/2 - 1.167w/\sqrt{r} \quad .$$

If S_2 exists, but not S_1, let

$$L_{r+1} = (L_r + S_2)/2 + 1.167w/\sqrt{r} \quad .$$

If both S_1 and S_2 exist, as is generally the case for large sample sizes, let

$$L_{r+1} = (S_1+S_2)/2 + 1.167w(\alpha-a_r) \quad ,$$

where a_r is the fraction of responses in the first r tests:

$$a_r = \sum_{i=1}^{r} R_r/r \quad .$$

For large sample sizes, the second term should be replaced by $(\alpha-a_r)/d_r$, where d_r is an estimate of $M'(x_\alpha)$ based on the sample. For example, $d_r = 2\Delta/(S_1-S_2)$ could be used, but only if there is some data in the interval (S_2, S_1). (Note that this interval is also an approximate 50% confidence interval on $\hat{x}_\alpha$.)

SIMULATED EXAMPLE OF DESIGN. Let $\alpha = .05$, $w = 5$, and the true response function be cumulative normal with $\mu = 0$, $\sigma = 1$. Then $x_\alpha = -1.645$. Suppose $y = -.2$. Then

$$L_1 = -.2 + (1.167)(5)(.05-.5) = -.2 - 2.626 = -2.826 .$$

Now suppose $R_1 = 0$ ($\bar{R}_r$ denotes the response to the r^{th} stress). At this point $Y_1 = 1$, $\Delta = .6745 \cdot \sqrt{.05 \times .95} \tilde{=} .15$.

Since the estimated response at -2.826 is 0, and since this is the highest level at which the estimate is less than or equal to max(.05-.15, 0) = 0, we have $S_2 = 0$. Since there are no test levels at which the estimated response exceeds min(.05+.15, 1) = .20, S_1 does not exist. Then

$$L_2 = (L_1+S_2)/2 + (1.167)5/\sqrt{1}$$

$$= -2.826 + 5.835$$

$$= 3.009 .$$

Suppose now $R_2 = 1$. Now we have $S_1 = 3.009$, $S_2 = -2.826$,

$$L_3 = (.183)/2 + 1.167(5)(.05-.50)$$

$$= -2.534 .$$

Suppose now $R_3 = 0$. Then $S_1 = 3.009$, $S_2 = -2.534$,

$$L_4 = (.575)/2 + 1.167(5)(.05-.3333)$$

$$= -1.366 .$$

Suppose now $R_4 = 0$. Then $S_1 = 3.009$, $S_2 = -1.366$,

$$L_5 = (1.643)/2 + 1.167(5)\,(.05-.25)$$

$$= -.345 \quad .$$

If $R_5 = 1$, then $S_1 = -.345$, $S_2 = -1.366$,

$$L_6 = (-1.711)/2 + 1.167(5)\,(.05-.4)$$

$$= -2.898 \quad .$$

The design might continue as follows:

r	L_r	R_r	r	L_r	R_r	r	L_r	R_r
6	-2.898	0	16	-1.342	0	26	-1.505	0
7	-2.509	0	17	-1.281	0	27	-1.478	0
8	-2.231	0	18	-1.208	0	28	-1.454	0
9	-2.023	0	19	-1.133	0	29	-1.430	0
10	-1.860	0	20	-1.061	1	30	-1.409	0
11	-1.731	0	21	-1.681	0	31	-1.389	0
12	-1.625	0	22	-1.639	0	32	-1.370	0
13	-1.536	0	23	-1.601	0	33	-1.352	1
14	-1.461	0	24	-1.566	0			
15	-1.398	0	25	-1.535	0			

At this point the analysis of results by means of the method of reversals becomes nontrivial. The estimate is $1/5 = .2$ at -1.352. It turns out that $S_1 = -1.352$, $S_2 = -1.366$,

$$L_{34} = -1.359 + 1.167(5)(.05-4/33)$$

$$= -1.774 \quad .$$

We continue:

r	L_r	R_r
34	-1.774	0
35	-1.754	0
36	-1.734	0
37	-1.716	0
38	-1.698	1

Let us present the entire analysis at this step, for this is the first time it is possible to get a decent estimate of $M'(x_0')$.

Stress	Responses/Trials		Estimates
3.009	1/1		1.00
- .345	1/1		1.00
-1.061	1/1		1.00
-1.133	0/1		.20
-1.208	0/1		.20
-1.281	0/1	1/5	.20
-1.342	0/1		.20
-1.352	1/1		.20
-1.366	0/1		.056
-1.370	0/1		.056
-1.389	0/1		.056
-1.398	0/1		.056
-1.409	0/1		.056
-1.430	0/1		.056
-1.454	0/1		.056
-1.461	0/1		.056
-1.478	0/1	1/18	.056
-1.505	0/1		.056
-1.535	0/1		.056
-1.536	0/1		.056
-1.566	0/1		.056
-1.601	0/1		.056
-1.625	0/1		.056
-1.639	0/1		.056
-1.681	0/1		.056
-1.698	1/1		.056
-1.716	0/1		.0
-1.731	0/1		.0

Stress	Responses/Trials	Estimates (continued)
-1.734	0/1	.0
-1.754	0/1	.0
-1.774	0/1	.0
-1.860	0/1	.0
-2.023	0/1	.0
-2.231	0/1	.0
-2.509	0/1	.0
-2.534	0/1	.0
-2.826	0/1	.0
-2.898	0/1	.0

Now we have $r = 38$, $Y_r \tilde{=} .5772 + \ell n(38.5) \tilde{=} 4.228$,

$$\Delta \tilde{=} .6745 \sqrt{(.05)(.95)(4.228)/38}$$

$$\tilde{=} .049 \quad .$$

Since $\min(a + \Delta, 1) = .099$, we have $S_1 = -1.352$. Since $\max(a - \Delta, 0) = .001$, we have $S_2 = -1.716$. Furthermore, (S_2, S_1) is not empty, so we may replace $1.167w = 5.835$ by our estimate of $1/M'(x_a)$, which is

$$\frac{S_1 - S_2}{2\Delta} = \frac{.364}{.098} = 3.71 \quad .$$

(The true value is actually $1/M'(x_a) = 9.7$, so we have accidentally adjusted the coefficient in the wrong direction.) Then L

$$L_{39} = (-1.352 - 1.716)/2 + 3.71\,(.05 - 5/38)$$

$$= -1.837 \quad .$$

The analysis again becomes routine until the next 1 occurs.

SIMULATION RESULTS FOR ALEXANDER AND ROTHMAN DESIGNS. The new designs for the inverse response problem have been simulated on a digital computer for a wide variety of response functions and (in each case) for two different values of w, the standard deviation of the density of the prior estimate of x_a. The response functions used were

1. Cumulative normal: $\mu = 0$, $\sigma = 1$

2. Cumulative uniform: x, $0 \leq x \leq 1$

3. The five functions given by Odell [7]

   (a) $x^{.25}$, $0 \leq x \leq 1$

   (b) $\begin{cases} 4x^2, & 0 \leq x \leq .25 \\ 1-4(1-x)^2/3, & .25 \leq x \leq 1 \end{cases}$

   (c) $\begin{cases} 2x^2, & 0 \leq x \leq .5 \\ 1-2(1-x)^2, & .5 \leq x \leq 1 \end{cases}$

   (d) $\begin{cases} 4x^2/3, & 0 \leq x \leq .75 \\ 1-4(1-x)^2, & .75 \leq x \leq 1 \end{cases}$

   (e) x^4, $0 \leq x \leq 1$.

4. Two functions with pathologies at $x_{.5} = 0$

   (a) $.5 + x^5$, $-.87056 \leq x \leq .87056$

   Here $M'(x_{.5}) = 0$.

   (b) $\begin{cases} .5 - \dfrac{1}{2+|x|^{-.2}}, & x < 0 \\ .5, & x = 0 \\ .5 + \dfrac{1}{2+|x|^{-.2}}, & x > 0 \end{cases}$

Here $M'(x_{.5}) = \infty$.

Since the results of all these simulations do not differ very much, we shall report here only the results for the cumulative normal response function. These results are tabulated below:

Design	w	Sample Size (N)	Asymptotic Minimum Variance for	Variance of Estimator in 100 Simulations
$\alpha = .5$				
Alexander ($\Delta = .1$)	1	4 8 17*	.39 .20 .092	.60 .40 .14
Rothman**	1	8 16 32 64	.20 .098 .049 .025	.36 .15 .10 .041
Alexander ($\Delta = 1$)	10	4 8 14*	.39 .20 .11	45.6 1.98 .39
Rothman	10	8 16 32 64	.20 .098 .049 .025	1.10 .38 .12 .061
$\alpha = .05$			Asymptotic Minimum Variance for $\alpha = .05$ $(4.46\sigma^2/N)$	Variance of Estimator in 100 Simulations
Alexander ($\Delta = .025$)	1	16 32 62*	.28 .14 .072	1.59 .75 .10
Rothman	1	16 32 64	.28 .14 .070	.60 .24 .092
Alexander ($\Delta = .25$)	10	16 32 65*	.28 .14 .069	17.5 5.88 .23
Rothman	10	16 32 64	.28 .14 .070	1.04 .31 .14
$\alpha = .01$			Asymptotic Minimum Variance for $\alpha = .01$ $(13.91\sigma^2/N)$	Variance of Estimator in 25 Simulations
Rothman	1	64 128 256	.22 .11 .054	.64*** .39*** .17***
Rothman	10	64 128 256	.22 .11 .054	.33 .11 .072

* Median sample size required to complete design
** Without altering design to incorporate estimates of the derivative
*** Unsatisfactory because 1.167w was much smaller than $1/M'(x_{.01})$

From this table we may draw certain conclusions:

1. The Alexander designs are excellent if completed or if carried out to at least 16 tests for $\alpha = .5$ and 64 tests for $\alpha = .05$.

2. The Rothman designs are excellent for smaller sample sizes. However, if large samples are intended, the experimenter should utilize the more complicated version of the design (not yet simulated) in which $M'(x_\alpha)$ is eventually estimated from the sample and then used to modify the spacing of the subsequent test levels. Otherwise, as in the anomalous result for $\alpha = .01$, $w = 1$, we may find that the initial spacing (based on $1.167w$ rather than on an estimate of $1/M'(x_\alpha)$) is completely inappropriate.

A comparison of all simulations reported in [15] indicates that the Rothman method is slightly better for poor prior information, and the Alexander design is slightly better for small w, for most response functions included in our simulations.

Simulations of other 50% designs have appeared in the literature. Wetherill [9] has shown that for the 50% logit problem, the Robbins-Monro process gives an estimator with variance very close to the asymptotic minimum. However, his initial test level is very close to the level sought, which corresponds to a small value of w (i.e., a great deal of prior information). But the R-M process would be very poor for small samples if w is very large. Our designs are intended to cover both cases, and it follows that their efficiencies at small values of w are therefore somewhat impaired.

Wetherill claims that small sample inefficiency is due to lack of linearity in the neighborhood of x_α. However, there is a "growth of information" (growth of efficiency per test) aspect of small sample work for any response problem (cf [15], pp. 212-220) even for the homoscedastic problem on a straight line (non-quantal response).

Wetherill apparently found unsatisfactory the performance of all known designs for the inverse response problem when α is not near 50%. This seems to have been due to the bias of the estimators in the small-sample situation, which we believe is due in turn to increased

nonlinearity of conventionally used types of response functions as one leaves the neighborhood of $\alpha = .5$. For example, $|M''(x)|$ for the cumulative normal response function is maximized at $\mu \pm \sigma$. For values even further out, it might be imagined that heteroscedasticity would have an effect.

Our designs for $\alpha = .05$ show the same small-sample inefficiency, but we do not conclude that this necessarily implies that the designs are unsatisfactory. More work is needed on the effect of (1) $M''(x_\alpha)$, (2) heteroscedasticity, and (3) prior information on the minimum variance which can be reached for a particular sample size.

REFERENCES

[1] Finney, D. J. (1952). Probit Analysis. Cambridge University Press, Cambridge, second edition.

[2] _____ (1944). Statistical analysis for a new procedure in sensitivity experiments. Statistical Research Group, Princeton, No. 40 (Applied Mathematics Panel Report No. 101.1R) 58 pp.

[3] Dixon, W. J. and F. J. Massey. (1957). Introduction to Statistical Analysis. McGraw-Hill, New York, second edition, 318-327.

[4] Dixon, W. J. (1965). The up-and-down method for small samples. To be published in the J. Amer. Statist. Assoc.

[5] Robbins, H. and S. Monro. (1951). A stochastic approximation method. Ann. Math. Statist., 22, 400-407.

[6] Kesten, H. (1958). Accelerated stochastic approximation. Ann. Math. Statist., 29, 41-59.

[7] Odell, P. L. (1962) Stochastic approximation and nonparametric interval estimation in sensitivity testing which involves quantal response data. Oklahoma State University, Ph.D. Thesis.

[8] Cochran, W. G. and Miles Davis. (1964). Stochastic approximation to the median effective dose in bioassay. Stochastic Models in Medicine and Biology. University of Wisconsin Press, Madison.

[9] Wetherill, G. B. (1963). Sequential estimation of quantal response curves. J. Roy. Statist. Soc. Ser. B, 25, 1-48.

[10] Langlie, H. J. (1962). A reliability test method for "one-shot" items. Aeronutronic Publication No. U-1792.

[11] Marks, B. L. (1962). Some optimal sequential schemes for estimating the mean of a cumulative normal quantal response curve. J. Roy. Statist. Soc. Ser. B (Method.), 24, 393-400.

[12] Ayer, M., H. D. Brunk, G. M. Ewing, W. T. Reid, and E. Silverman. (1955). An empirical distribution function for sampling with incomplete information. Ann. Math. Statist., 26, 641-647.

[13] Van Eeden, C. (1958). Testing and estimating ordered parameters of probability distributions. Studentendrukkerij Pootpers N. V.

[14] Chernoff, H. (1962). Optimal design of experiments. Technical Report No. 82, Applied Mathematics and Statistics Laboratories, Stanford University.

[15] Rothman, D., M. J. Alexander, and J. M. Zimmerman. (1965). The design and analysis of sensitivity experiments, Rocketdyne Report R-6152, 438 pp. (two volumes).

APPENDIX I

METHOD OF REVERSALS

The method of reversals was first proposed by Brunk, Ayers, Van Eeden and others [12, 13]. The method is based only on the assumption that the response function is nondecreasing with increasing stimulus level. This method is best demonstrated by an example (see [15] for examples and uses of this method):

Stress	Responses/Trials	First Attempt	Second Attempt	Response Probability Estimates
5.0	2/3	2/3	2/3	2/3
3.7	0/1	2/5		5/12
3.2	2/4		5/12	5/12
1.9	3/7	3/7		5/12

The sample response fractions are first arranged in order of increasing stress. Since the response function is assumed to be nondecreasing with increasing stress, the sample response fractions may be used as estimates unless they violate this rule. Whenever such a violation occurs on consecutive stress levels, an attempt is made to correct the situation by merging the two response fractions. In the example, the fractions 0/1 and 2/4 violate this rule, and are therefore merged to give 2/5. The other response fractions remain the same. At this point 3/7 and 2/5 are a violation, and are merged to get 5/12. The result is now satisfactory. No matter what order the violations are corrected, it can be shown that the final estimates are the unique maximum likelihood estimates.

Since we need it in the test, let us define a "plateau" as an ordinate on the partially estimated response function. In the above example there are two plateaus.

APPENDIX II

GENERAL CRITERIA FOR EVALUATING DESIGNS FOR THE INVERSE RESPONSE PROBLEM

D. Rothman

The estimation of the abscissa x_α at which a nondecreasing mean response function $M(x)$ takes on a specified ordinate α may be called the distribution-free inverse response problem. A judiciously chosen experimental design for this problem would very likely enjoy certain common properties independent of considerations due to the intended sample size, the domain of allowable test levels, the desired response fraction, the technique of analyzing the data, and the extent to which blocking is required. One would also expect that designs which lacked some of these characteristics, but were otherwise excellent, could be easily modified to conform, and would thereby be slightly improved. The properties are:

1. The design is as sequential as possible, in that as much as possible of the past data is utilized at each step to plan the next test level, or block of test levels,

2. The stress levels in a test block average the same or less (more) than the stress levels in the previous block if the average response in that previous block was greater (less) than the desired response fraction,

3. The test levels converge as rapidly as possible to x_α or to some minimal set in the test level domain spanning x_α,

4. The sample response fraction converges to α, and

5. The spacing of the early test levels takes into consideration the prior density on x_α.

Let us discuss these characteristics in detail.

1. The design should be as sequential as possible. A purely sequential design would be one in which each test level is not chosen until all previous data have been carefully analyzed. The reason for this is that

the design must be able to correct itself if it has been testing in the wrong region due to a poorly chosen initial test level. For example, a Robbins-Monro process which starts out with too small a step size and a bad first guess is very poor for small samples, and there is no mechanism for altering the design after a few results have been observed.

A maximum likelihood technique for such data analysis in the distribution-free case which can be used with any sequential design is the "method of reversals" discussed in Appendix I.

In practice such an analysis may not be feasible, since the results of all previous tests may not be available when the new test is planned, or there may not be time for the calculations. Nevertheless, as much data as are available should be analyzed, and it would be hard to beat the method of reversals for simplicity. We know of no design presently used which obeys this precept, and we feel that this is really a serious defect. Both of our new designs were conceived to meet this need.

2. The stress levels in a test block should average the same or less (more) than the stress levels in the previous block if the average response in that previous block was greater (less) than the desired response fraction, α.

For purely sequential designs this condition implies that the test level after a "1" will be at an equal or lower level, and the test level after a "0" will be at an equal or higher level. The up-and-down design and the stochastic approximations all follow this rule, whereas the Derman design does not.

For extremely small values of α one would not be too fussy in demanding that the test after a "0" be at a higher level. In practice the test efficiency is relatively insensitive to the location of the test following a "0". This is why it is possible to violate this rule in the Alexander design for $\alpha = 5\%$. A similar observation could be made for high values of α.

3. The test levels should converge as rapidly as possible to x_α or to some minimal set in the test level domain spanning x_α.

If the allowable test levels are discrete, then the design should converge to the two levels bounding x_α. If the allowable test levels are

dense in a neighborhood of x_α, the design should actually converge to x_α. Such a design is called a stochastic approximation (of x_α), and an example is given by the Robbins-Monro process,

$$L_{n+1} = L_n + c_n(\alpha - R_n)$$

where L_n denotes the n^{th} test level, R_n denotes the n^{th} test result, and c_n is generally of the form $c/(n+n_o)$. It has been conjectured that the minimum asymptotic variance for such designs, and for the general nonparametric inverse response problem for quantal data, is given by

$$V_{min}(\hat{x}_\alpha) \sim \alpha(1-\alpha)/N[M'(x_\alpha)]^2 \quad ,$$

where $M'(x)$ denotes the derivative of the response function, and N denotes sample size. $M'(x)$ should be continuous at x_α, and $0 < M'(x_\alpha) < \infty$. For example, if $\alpha = .5$ and $M(x)$ is cumulative normal, then

$$V_{min}(\hat{x}_{.5}) \sim (\pi/2)\sigma^2/N \quad .$$

Based on this conjecture, a relative asymptotic efficiency may be defined as follows:

$$e \sim V_{min}(\hat{x}_\alpha)/V(\hat{x}_\alpha) \quad .$$

To our knowledge this conjecture at present lacks proof, but may be justified as follows:

a. The R-M process can match this asymptotic variance for the right choice of c_n, namely, $c_n = 1/nM'(x_\alpha)$.

b. When the response function is known to be cumulative normal and when the optimal design still turns out to be a stochastic approximation of x_α (as in Chernoff [14]), the variance is

equal to the expression above, thus making it plausible to conclude that we can generally do no better.

It is intended that the new designs satisfy this rule. The up-and-down, Langlie, and Derman designs do not. It should be pointed out however that the first two of these were intended only for the cumulative normal inverse response problem.

4. The sample response fraction a_r should converge to a.

If the design is a stochastic approximation, and if $M(x)$ is continuous at x_a, then this property will hold. Of the allowable test levels are discrete, then this rule gives the asymptotic percentage at each of the two levels that the design converges to.

One might deduce from this a principle of "compensation": If $a_r > a$, take the next test at a level under the latest estimate, to compensate for the lack of 0's. A similar statement could be made for $a_r < a$. The Rothman design does this explicitly.

5. The spacing of the early test levels should take into consideration the prior density on x_a.

Let w denote the known standard deviation of the (normal) prior density on x_a, L_i denote the i^{th} test level, R_i denote the i^{th} response, and let $g = wM'(x_a)/\sqrt{a(1-a)}$. Then the situation $g >> 1$ corresponds to the Marks problem of locating a step; the situation $g << 1$ would permit us to imagine that we are merely continuing a design which had already gone quite far.

Then the above property has the following ramifications:

a. The quantity $|L_2-L_1|$ should be close to $1.17w$ (as in the Marks design) for $g >> 1$, and close to $g^2|a-R_1|/M'(x_a)$ for $g << 1$ (c.f. $L_2-L_1 = (a-R_1)/M'(x_a)$ for the Robbins-Monro process).

b. If $R_2 = R_1$, then

$$|L_2-L_1|/\sqrt{2} \leq |L_3-L_2| \leq |L_2-L_1| .$$

If $g >> 1$, the lower bound is more useful, as in the Marks design. If $g << 1$, the upper bound is more appropriate, as in the delayed R-M process. The conventional R-M process,

$$L_{n+1} = L_n + (a-R_n)c/n \quad ,$$

violates this precept.

c. If $R_2 \neq R_1$, then $|L_3-L_2|/|L_2-L_1|$ should be close to 1/2 (as in the Marks design) for $g >> 1$, and close to $|a-R_2|/|a-R_1|$ for $g << 1$.

The big question here is the quantity w. If the prior density is uniform with range D, then the Marks design would change. Nevertheless, the above rules with

$$w = D/\sqrt{12}$$

should still be useful guidelines.

Often one is testing a population similar to populations previously tested in the past, differing perhaps only because of small changes in chemical formulation or test equipment. In this case the distribution of past estimates of x_a is just the "prior density" we are using.

If w itself is extremely uncertain, the experimenter should use a high value as a precautionary measure.

ACKNOWLEDGEMENTS

The authors would like to acknowledge the encouragement and support of Dr. J. M. Zimmerman, formerly of Rocketdyne, and Dr. J. B. Gayle, formerly of NASA, Marshall Space Flight Center, Huntsville, in developing the techniques described above.

MONTE CARLO INVESTIGATION OF THE PROBABILITY DISTRIBUTIONS OF DIXON'S CRITERIA FOR TESTING OUTLYING OBSERVATIONS

Walter L. Mowchan
Surveillance Branch, Ballistic Research Laboratories,
Aberdeen Proving Ground, Maryland

ABSTRACT. An empirical or Monte Carlo method for determining the distribution of Dixon-type sample statistics for testing outlying observations is presented. Results are presented for samples generated from a normal distribution and for samples generated from a uniform distribution. The method employed was to select random samples of sizes n = 5, 10, 15, and 20 from each of the aforementioned distributions. After ordering the sample values such that $X_1 \leq X_2 \ldots \leq X_n$, the six different statistics (defined later) for each sample size were computed for each distribution. A sampling distribution was therefore obtained empirically for each sample size for each distribution after 500 such sample trials. The cumulative frequency functions were then plotted for both the normal and the uniform distributions. With respect to the normal distribution, these results can be compared with theoretical values which are published in tabular form by W. J. Dixon [1] With respect to the uniform distribution, two contributions are made to the statistical literature:

1. A procedure for detecting outlying observations in samples from a uniform distribution is presented.

2. A comparison of the cumulative frequency functions indicates that all extreme values, except for sample size n = 5, rejected under the assumption of normality would also be rejected if the actual data were in fact selected from a uniform distribution, since the upper percentage points for the normal distribution are higher than for the uniform distribution.

Finally, a comparison of the two cumulative distribution functions indicates which statistics of the six presented are best suitable for checking an extreme value given a certain sample size.

1. INTRODUCTION.

1.1 Definitions of Statistics to be Investigated

Six statistics proposed by Dixon [9] for testing the significance of outliers are presented. The author has attempted to obtain the probability distributions of these statistics by the Monte Carlo method of sampling on an electronic computer. Let us consider n observations of a sample from Normal and Uniform distributions such that $X_1 \leq X_2 \leq \ldots \leq X_n$, where X_1 is the suspect outlier. Since both the normal and the uniform distribution are symmetric, we could also have considered the largest observation, X_n, to be a suspected outlier. Of course, it is easy to observe that for any of the six statistics the sampling distribution of the smallest value, X_1, would be equivalent to the sampling distribution of the largest value, X_n, except for location or mean.

For definition purposes, let us consider the following six statistics which will be investigated in detail:

1. For a single outlier, X_1

$$r_{10} = \frac{X_2 - X_1}{X_n - X_1}$$

2. For a single outlier X_1 avoiding X_n

$$r_{11} = \frac{X_2 - X_1}{X_{n-1} - X_1}$$

3. For a single outlier X_1 avoiding X_n, X_{n-1}

$$r_{12} = \frac{X_2 - X_1}{X_{n-2} - X_1}$$

4. For outlier X_1 avoiding X_2

$$r_{20} = \frac{X_3 - X_1}{X_n - X_1}$$

5. For outlier X_1 avoiding X_2 and X_n

$$r_{21} = \frac{X_3 - X_1}{X_{n-1} - X_1}$$

6. For outlier X_1 avoiding X_2 and X_n, X_{n-1}

$$r_{22} = \frac{X_3 - X_1}{X_{n-2} - X_1}$$

12. Brief Historical Background

The testing of extreme values is a very old problem in applied statistics. The data obtained in experimentation must be carefully examined so that one can be reasonably certain that the results of sampling are representative of the process. It is quite obvious that rejection (or acceptance) of outliers could lead to a much different course of action than otherwise taken. It should be noted that in some cases the problem of outliers may depend on common sense and hence may be a practical problem as well as a statistical problem. A review of the literature indicates that the problem of outliers received much attention prior to 1940. In fact explanations concerning outliers were presented as early as 1850 by W. Chauvenet [2]. His hypothesis basically stated that some samples contained a very small portion of observations from a population with a different mean value. P. R. Rider [3], for example, proposed a solution based on the assumption that the population standard deviation, σ, be accurately known. In a similar manner, J. O. Irwin [4] published in 1925 criteria based on the difference of the first and second (ranked) observations and on the difference of the second and third (ranked)

observations in a random sample from a normal population. Another very practical approach was presented in 1935 by McKay [5] who published a paper on the difference between an extreme observation and the sample mean. In conjunction with his work, K. R. Nair [6] in 1948 tabulated the distribution of the difference between an extreme observation and the sample mean for small sample sizes. W. R. Thompson [7] in 1935 working on the assumption that the standard deviation was not known presented a paper, "On a Criterion for the Rejection of Observations and the Distribution of the Ratio of the Deviation to the Sample Standard Deviation." One interesting fact concerning Thompson's work is that he presented an exact test for the hypothesis that all sample observations were from the same normal population. Another significant contribution is presented by Grubbs [8] whose criteria are based on the sample sum of squared deviations from the mean for all observations as compared to the sum of the squared deviations omitting the "outlier". W. J. Dixon [9] in 1950 presented a paper based on sample ranges and subranges. His paper assumes that the random samples are drawn from a normal population. In connection with this, Dixon and Massey [10] proposed a method for estimating the mean and standard deviation when the effect of outliers (light, medium or heavy) is known. This paper is concerned primarily with the statistics presented by Dixon [9] in 1950 since for practical purposes they are very easy to compute. In addition, one would like to know how much non-normality would affect the tests and this is also studied. As an example, this paper attempts to develop empirically how sample criteria for non-normal distribution (the uniform) compares to that for the normal distribution when various tests for suspected outliers are performed. As already mentioned, one of the primary reasons for selecting Dixon's criteria is that the statistics presented are very easy to compute.

1.3 Monte Carlo Method

With the aid of high speed electronic computers such as BRLESC (Ballistic Research Laboratories Electronic Scientific Computer) at Aberdeen Proving Ground, Maryland, a program was available to obtain random numbers with frequencies equal to those of the uniform or normal distribution. In order to generate random numbers for both the uniform and the normal distributions, it was necessary therefore only to enter a subroutine already on tape. Basically, the subroutine works as follows for the uniform distribution. An initial value, X_o, (.547812619135913)

is selected and multiplied by a "K" factor which is always $5^{25} \times 2^{-60}$. The last fourteen digits are then preceeded by a decimal point so that the number X_1 lies between 0 and 1. The X_1 is then used to generate X_2 in an identical manner and the process is continued until the n random numbers desired are generated.

In order to generate numbers which follow the normal distribution, i.e., N(0, 1) a very similar procedure is employed. The computer first selects 64 random numbers from the uniform distribution and computes the mean, $\bar{X}_1$. One-half is then subtracted from the mean $\bar{X}_1$ and the whole quantity is multiplied by $16\sqrt{3}$. Therefore the first random normal observation X_1 would be $16\sqrt{3}(\bar{X}_1 - .5)$. For the second random normal number, the computer again selects 64 random uniform numbers and follows exactly the same process until n observations are generated. Since the $\bar{X}_i$ (i = 1, 2, 3, . . . n) are obtained from a uniform distribution, it can easily be shown by use of the well known central limit theorum [11] that $\bar{X}$ is approximately N (1/2, 1/768). Therefore, it is obvious that $(\bar{X} - .5) / 1/16\sqrt{3}$ is approximately normally distributed with mean 0 and variance 1. These routines have been checked by χ^2 for Normality and Uniformity and the results are contained in BRL Report No. 855 dated May 1953 [12]. Incidentally, the periodicity of the subroutine is one in every four million computing years.

In order to obtain a sampling distribution for each of the previously mentioned six statistics for each distribution, it was decided that 500 trials might be acceptable. For example, for sample size n = 5 from the uniform distribution, $r_{10} = (X_2 - X_1)/(X_5 - X_1)$ was computed from 500 trials and the observed cumulative distribution was plotted. Likewise, this same general procedure was used to obtain r_{10} for the normal distribution. Since Dixon [1] has already published tabular results based on an analytical function of the distribution for r_{10} for the normal universe, it is of primary interest to compare his analytical function with both the uniform and normal distributions which were derived in this work empirically by Monte Carlo techniques. These results (see Appendices I and II) are tabulated and plotted for each of the six statistics for each of the sample sizes n = 5, 10, 15 and 20.

2. MONTE CARLO NORMAL VERSUS THEORETICAL NORMAL. The general contribution of Dixon [1] was to obtain analytical results based on small sample sizes for the distributions of the six previously mentioned statistics. Percentage points were then obtained by numerical integration for various sample sizes from $n = 5$ to $n = 30$.

As an example let us consider $r_{10} = (X_n - X_{n-1})/(X_n - X_1)$ where the subscripts on the X's indicate ordered values such that $X_1 \leq X_2 \leq \cdots \leq X_n$. Dixon [1] indicates the density function for X_1, X_{n-1}, X_n to be

$$(a)\quad \frac{n!}{(n-3)!}\, f(x_1)\, dx_1 \left(\int_{x_1}^{x_{n-1}} f(t)dt\right)^{n-3} f(x_{n-1})\, dx_{n-1}\, f(x_n)\, dx_n \quad .$$

If we let $v = x_n - x_1$, $rv = x_n - x_{n-1}$, $x = x_n$ and integrate x and v over their range of definition we get the density of (v, r, x) to be

$$(b)\quad \frac{n!}{(n-3)!} \int_{-\infty}^{\infty}\int_{0}^{\infty} \left[\int_{x-v}^{x-rv} f(t)dt\right]^{n-3} f(x-v)\, f(x-rv)\, f(x)\, v\, dv\, dx$$

where $-\infty < x < \infty$ and $0 < v < \infty$. Also let $f(t) = (1/\sqrt{2\pi})\, e^{-t^2/2}$.

Let us now consider a specific case where $n = 3$. Formula (b) now appears as

$$(c)\quad \frac{3!}{0!} \int_{-\infty}^{\infty} \int_{0}^{\infty} \left(\int_{x-v}^{x-rv} f(t)dt\right)^{3-3} \frac{1}{(2\pi)^{3/2}}\, e^{-\left[\frac{(x-v)^2}{2} + \frac{(x-rv)^2}{2} + \frac{x^2}{2}\right]}\, v\, dv\, dx$$

and collecting terms we get the density function to be

$$(d)\quad \frac{6}{(2\pi)^{3/2}} \int_{0}^{\infty} e^{-\left[\frac{v^2(1+r^2)}{2}\right]}\, v \int_{-\infty}^{\infty} e^{-\left[\frac{3x^2 - 2xv(1+r)}{2}\right]}\, dx\, dv \quad .$$

Upon completing the square we get

$$(e)\quad \frac{3}{\pi}\int_0^{\infty} e^{-\left[\frac{v^2}{2}\left\{(1+r^2)-1/3\,(1+2r+r^2)\right\}\right]} v\,\frac{1}{\sqrt{3}}\int_{-\infty}^{\infty}\frac{1}{\sqrt{2\pi}\,(1/\sqrt{3})} \cdot e^{-1/2\left[\frac{x-1/3v(1+r)}{1/\sqrt{3}}\right]^2} dx\,dv$$

which can easily be integrated to obtain

$$(f)\quad f(r) = \frac{3\sqrt{3}}{2\pi(1-r+r^2)} \quad .$$

Integration of the density function results in the cumulative density function (cdf) which is expressed as

$$(g)\quad F(R) = \frac{3}{\pi}\ \text{arc tan}\ \left[\frac{2}{\sqrt{3}}(R_{10}-1/2)\right] + 1/2$$

and upon setting (g) equal to 1 - α, we can easily obtain

(h) $R_{10_\alpha} = \frac{\sqrt{3}}{2}\tan \pi/3\ (1/2 - \alpha) + 1/2$ where R_{10_α} is the upper α probability level or percentage point.

In comparison, the Monte Carlo distribution (based on a sample of 500 trials) for r_{10} for sample size n = 5 agrees very well with the analytical function derived by Dixon for n = 5. In general, the six statistics for sample sizes n = 5, 10, 15, and 20 agree quite well with Dixon's results - particularly for the upper percentage points. A χ^2 goodness of fit test indicated that the percentage points for the Monte Carlo method of sampling did not differ significantly (.05 level

of significance) from those derived theoretically by Dixon; however, it is strongly recommended that in future work more than 500 trials be utilized in order that more accuracy may be obtained by Monte Carlo methods.

Let us derive the density function, the cdf and the upper α probability level for the uniform distribution for the statistic, r_{10}. As indicated in (a) and (b) earlier, we can write the density of (v, r, x) to be

$$(i)\quad \frac{n!}{(n-3)!} \int_{-\infty}^{\infty}\int_{0}^{\infty} \left(\int_{x-v}^{x-rv} f(t)dt\right)^{n-3} f(x-v)\ f(x-rv)\ f(x)\ v\ dv\ dx$$

and let $f(t) = 1/b-a$ where $a < x < b$ which readily gives us

$$(j)\quad \frac{n!}{(n-3)!} \int_{a}^{b} \int_{0}^{x-a} \left(\frac{v(1-r)}{b-a}\right)^{n-3} \cdot \frac{v}{(b-a)^3}\ dv\ dx \quad .$$

Upon performing the integration in (j) we get the density function

$$(k)\quad f(r) = (n-2)(1-r)^{n-3} \quad \text{where} \quad \begin{matrix} 0 < r_{10} < 1 \\ n > 3 \end{matrix} \quad .$$

Integration of the density function results in the cdf which is expressed as

(l) $F(R) = 1 - (1 - R_{10})^{n-2}$ and upon setting (l) equal to $1-\alpha$ we obtain

$$(m)\quad R_{10_\alpha} = 1 - \alpha^{1/n-2}$$ where R_{10_α} is the upper α probability level or percentage point. These theoretical results are compared with the Monte Carlo results and are contained in Appendix No. I.

Another point of interest is that the Monte Carlo results for the uniform distribution were significantly different from the (theoretical)

normal when the χ^2 goodness of fit test was applied at the .05 level of significance as might have been suspected. This would indicate that Dixon's criteria are rather sensitive to departures from a normal universe.

3. COMPARISON OF NORMAL AND UNIFORM DISTRIBUTION.

3.1 Sampling from a Normal Distribution.

As previously mentioned, the Monte Carlo method based on a sample of 500 trails did not differ significantly from the analytical method developed by Dixon for Normal distributions. If one assumed that he were sampling from a normal distribution, it can be seen that all extreme values rejected under the assumption of normality (with the exception of n = 5) would also be rejected if in fact the actual distribution sampled were uniform. (See Appendix No. I)

3.2 Sampling from a Uniform Distribution.

If one assumed that he were sampling from a uniform distribution, then many extreme values rejected values under the assumption of sampling a uniform distribution would be wrongly rejected if in fact the actual distribution sampled were normal. (See Appendix No. I) Hence, the error involved in 3.1 would probably be less serious than the error involved in 3.2.

4. AN EXAMPLE.

This section will serve to illustrate the use of Dixon's criteria for determining whether a doubtful observation is to be retained or rejected. One of the classic examples consists of a sample of fifteen observations of the vertical semi-diameters of Venus made by a Lieutenant Herndon in 1846 and presented by Chauvenet (2). In the analysis of the data which followed the following fifteen residuals were obtained and have been arranged in ascending order of magnitude

-1.40"	-0.24	-0.05	0.18	0.48
-0.44	-0.22	0.06	0.20	0.63
-0.30	-0.13	0.10	0.39	1.01

The residuals -1.40 (X_1) and 1.01 (X_{15}) appear to be questionable. Here the suspect outliers lie at each end of the sample. Since no optimum procedure for testing outliers at both ends of the sample is currently available unless the population variance, σ^2, is known, we shall now illustrate the simplicity or ease at which Dixon's statistics may be computed. Let us first test the observation -1.40 since it is most distant from the mean of the sample. Also, we shall select $\alpha = .05$ which means that $Pr(r_{22} > R) = .05$. For sample size n = 15, we get:

$$r_{22} = \frac{X_3 - X_1}{X_{13} - X_1} = \frac{-.30 + 1.40}{.48 + 1.40} = \frac{1.10}{1.88} = .585 \quad .$$

Since the calculated value of .585 is greater than the critical value of .525, we reject the observation -1.40 by Dixon's test and now proceed to check the observation 1.01 for sample size n = 14.

$$r_{22} = \frac{X_{14} - X_{12}}{X_{14} - X_3} = \frac{1.01 - .48}{1.01 + .24} = \frac{.53}{1.25} = .425 \quad .$$

Since the calculated value of .425 is less than the critical value of .546, we accept the observation 1.01 by Dixon's test and no other values would be tested in this sample.

5. CONCLUSIONS.

5.1 Extension of Tables Based on the Normal Distribution

Since the Monte Carlo Normal Distribution can be used to represent the analytical solution presented by W. J. Dixon, it is therefore possible to extend these tables (See Appendix I) to sample sizes for larger values of n, which in many cases would be of considerable interest in applied statistics.

5.2 Development of Criteria Based on the Uniform Distribution

The Monte Carlo uniform distribution can be employed to develop a criteria for the rejection of extreme values based on the assumption

of sampling a uniform distribution. Thus, the tables and figures presented in Appendices I and II may be of significant importance in many practical situations where the actual distribution is in fact uniform.

5.3 Choice of Statistics

The cumulative distribution functions plotted in Appendix II provide very helpful information regarding which statistic should or should not be used given a certain distribution and a certain sample size. For example, if given the normal distribution, the statistic r_{10} appears to perform very well for small sample sizes such as $n = 5$ while it is obvious that the statistics r_{12} and r_{21} would not provide a good test for these small samples because of the slope of the curves.

5.4 Additional Comments

In this paper, I have attempted to show that Dixon's [1] criteria for testing of extreme values based on the assumption of normality can be established empirically. Also, I have attempted to show what would happen if the distribution sampled were in fact uniformly distributed.

Since analytical or theoretical functions for testing outlying observations generally become quite involved, further work involving the effect of skewed distributions such as some of the Pearson Type curves [11] could be accomplished by Monte Carlo methods on a high speed computer.

It would also be of interest to develop a two sided test for examining extreme values from a sample. In this connection it is suggested that the sample observations be arranged such that $X_1 \leq X_2 \leq \ldots \leq X_n$. A proposal for the two sided test would be to first let X_1 be the suspected outlier (Dixon's approach) and then to compute the desired statistic. Next, from the same sample, let X_n be the suspected outlier and again compute the statistic. The higher of the two values obtained would then be chosen. If this procedure were repeated at least 500 times, then a two sided test could be developed empirically for testing extreme values and this might have rather wide application. Again, it is once more repeated that at least 500 trials should be used.

Finally, Appendices III and IV contain machine programming data which could easily be used for obtaining Monte Carlo distributions of Dixon's statistics [1] based on the assumption of uniformity or normality, if sample sizes of greater than 20 are desired.

BIBLIOGRAPHY

[1] Dixon, W. J., Ratios Involving Extreme Values, Annals of Math. Stat., Vol. 22 (1951), pp 68-78.

[2] Chauvenet, William, Sperical and Practical Astronomy, J. B. Lippincott Co., Philadelphia, 1863.

[3] Rider, P. R., Criteria for Rejection of Observations, Washington University Studies - New Series, Science and Technology - No. 8, St. Louis (1933).

[4] Irwin, J. O., On a Criterion for the Rejection of Outlying Observations, Biometrika, Vol. 17 (1925), pp 238-250.

[5] McKay, A. T., The Distribution of the Difference Between the Extreme and the Sample Mean in Samples of n from a Normal Universe, Biometrika, Vol. 27 (1935), pp 466-471.

[6] Nair, K. R., The Distribution of the Extreme Deviate from the Sample Mean and its Studentized Form, Biometrika, Vol. 35 (1948), pp. 118-144.

[7] Thompson, W. R., On a Criterion for the Rejection of Observations and the Distribution of the Ratio of the Deviation to the Sample Standard Deviation, Annals of Math. Stat., Vol. 6 (1935), pp 214-219.

[8] Grubbs, F. E., Sample Criteria for Testing Outlying Observations, Annals of Math. Stat., Vol. 21 (1950), pp 27-58.

[9] Dixon, W. J., Analysis of Extreme Values, Annals of Math. Stat., Vol. 21 (1950), pp 488-506.

[10] Dixon, W. J., and Massey, F. J., Jr., Introduction to Statistical Analysis, McGraw Hill Book Co., Inc., New York, 1957.

[11] Mood, A. M., Introduction to the Theory of Statistics, McGraw Hill Book Co., Inc., New York, 1950.

[12] Juncosa, M. L., Random Number Generation of the BRL High-speed Computing Machines, BRL, Report No. 855, Aberdeen Proving Ground, Maryland, May 1953.

APPENDIX I

Tables of Upper Percentage Points for the Uniform and the Normal Distribution

Table of the Upper Percentage Points for the Uniform Distribution

$$Pr(r_{1j} > R) = \alpha \text{ where } j = 0,1,2$$

Sample Size	Statistic	α = .005		α = .01		α = .02		α = .05	
		T*	U**	T*	U**	T*	U**	T*	U**
n=5	r_{10}	.829	.833	.785	.775	.729	.716	.631	.626
	r_{11}	.928	.918	.900	.886	.859	.831	.776	.736
	r_{12}	.995	.996	.990	.990	.980	.980	.950	.946
n=10	r_{10}	.484	.490	.438	.440	.387	.391	.312	.313
	r_{11}	.531	.534	.482	.484	.428	.427	.347	.349
	r_{12}	.586	.588	.536	.541	.479	.476	.393	.391
n=15	r_{10}	.335	.333	.298	.300	.260	.262	.206	.209
	r_{11}	.357	.356	.319	.323	.278	.279	.221	.221
	r_{12}	.382	.381	.342	.345	.299	.298	.238	.235
n=20	r_{10}	.255	.250	.226	.221	.195	.193	.153	.145
	r_{11}	.268	.264	.237	.231	.206	.197	.162	.153
	r_{12}	.282	.281	.250	.253	.235	.230	.171	.166

*Upper percentage points based on Dixon's Uniform (theoretical).
**Upper percentage points based on Monte Carlo Uniform.

Table of Upper Percentage Points for the Normal Distribution

$\Pr(r_{ij} > R) = \alpha$ where i = 1, 2 and j = 0, 1, 2

Sample Size	Statistic	α = .005		α = .01		α = .02		α = .05	
		T*	N**	T*	N**	T*	N**	T*	N**
n=5	r_{10}	.821	.822	.780	.790	.729	.715	.642	.642
	r_{11}	.93	.939	916	.916	.876	.882	807	.812
	r_{12}	.996	.996	.992	993	984	.985	.960	.963
	r_{20}	.950	.952	.929	.927	.901	.901	.845	.834
	r_{21}	.998	.998	.995	.996	.990	.992	.976	.979
n=10	r_{10}	.568	.542	.527	.521	.483	.478	.412	.416
	r_{11}	.639	.626	.597	.579	.551	.541	.477	.470
	r_{12}	.694	.682	.655	.652	.610	.600	.537	.535
	r_{20}	.664	.663	.632	.631	.592	.599	.531	.539
	r_{21}	.760	.749	.726	.707	.678	.671	.612	.606
	r_{22}	.826	.815	.791	.802	.749	.742	.682	.679
n=15	r_{10}	.475	.470	.438	.443	.399	.414	.338	.351
	r_{11}	.522	.527	.486	.493	.445	.460	.381	.402
	r_{12}	.560	.564	.523	.526	.482	.488	.416	.437
	r_{20}	.554	.556	.522	.515	.486	.489	.430	.438
	r_{21}	.607	.605	.574	.575	.537	.540	.483	.494
	r_{22}	.647	.645	.616	.615	.579	.582	.525	.529
n=20	r_{10}	.425	.422	.391	.390	.356	351	.300	.295
	r_{11}	.464	.456	.430	.434	.392	.387	.334	.338
	r_{12}	.493	.482	.458	.443	.419	.411	.358	.358
	r_{20}	.494	.487	.464	.452	.430	.427	.372	.375
	r_{21}	.536	.529	.506	.507	.472	.471	.419	.421
	r_{22}	.562	.556	.535	.530	.502	503	.450	.451

*Upper percentage points based on Dixon's Normal (theoretical).
**Upper percentage points based on Monte Carlo Normal.

APPENDIX II

Figures of Cumulative Distributions

Figure 1 - Graph of r_{10} for sample size n=5

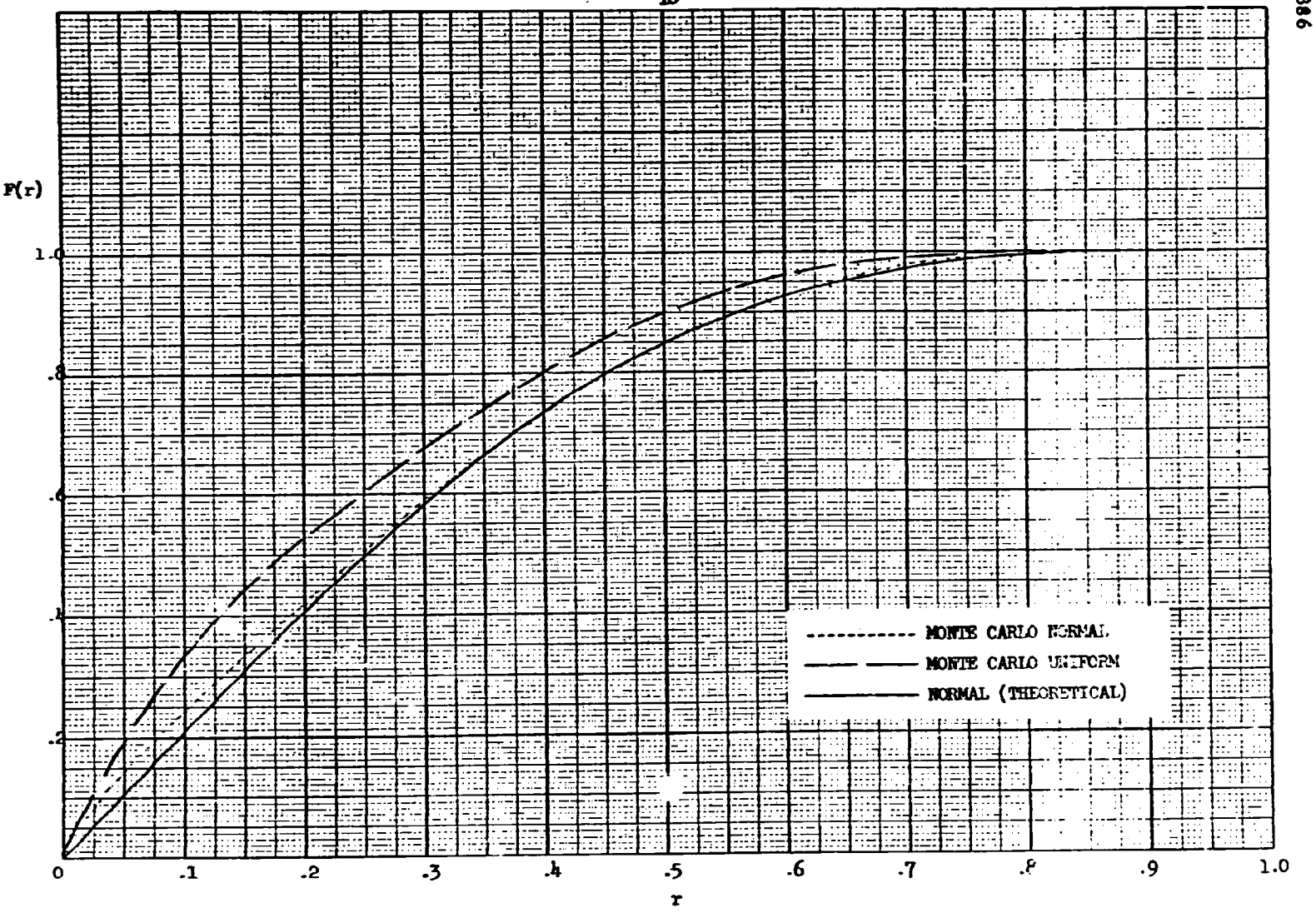

Figure 2 - Graph of r_{11} for sample size n=5

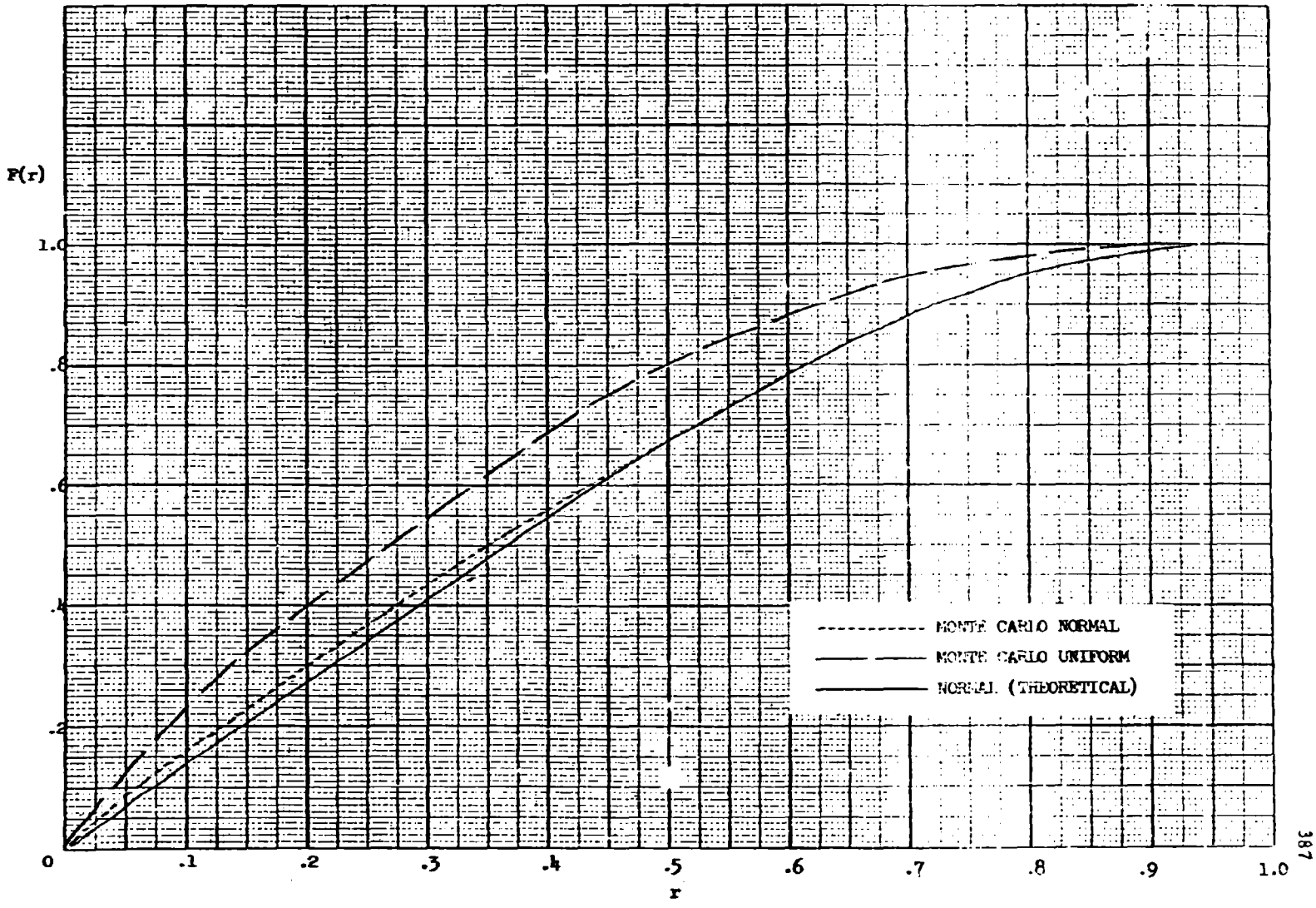

Figure 3 - Graph of r_{12} for sample size n=5

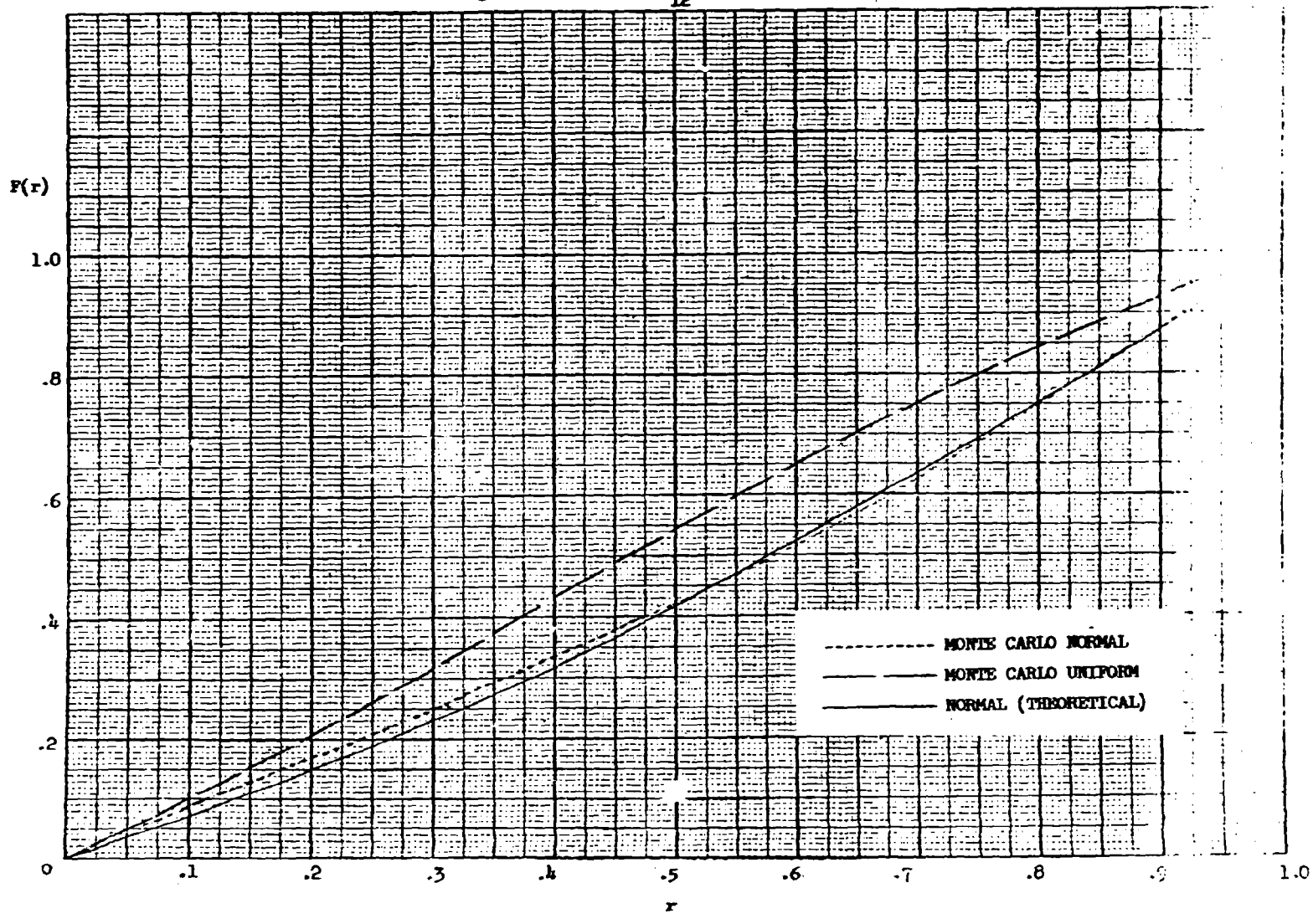

Figure 4 - Graph of r_{20} for sample size n=5

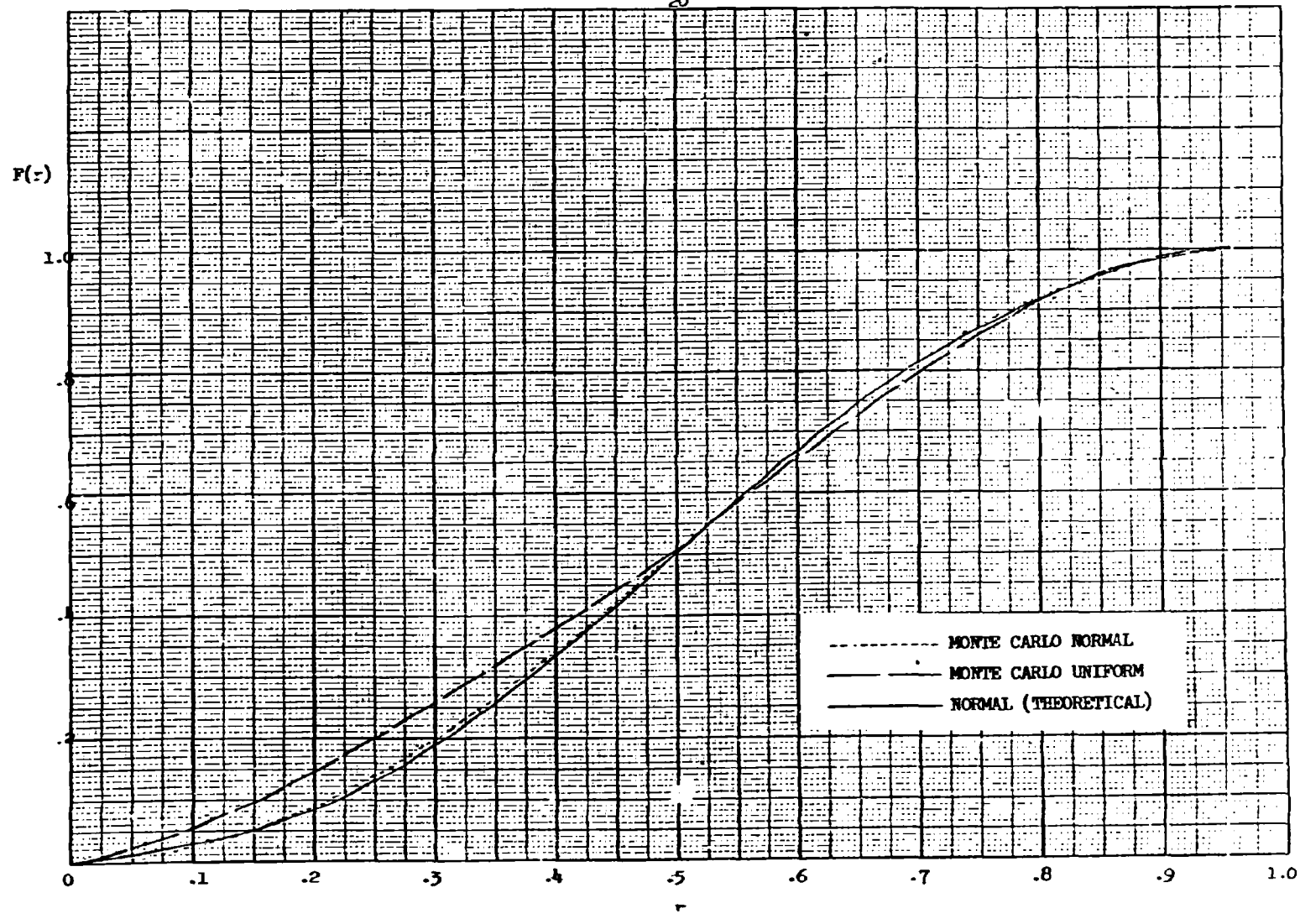

Figure 5 - Graph of r_{21} for sample size n=5

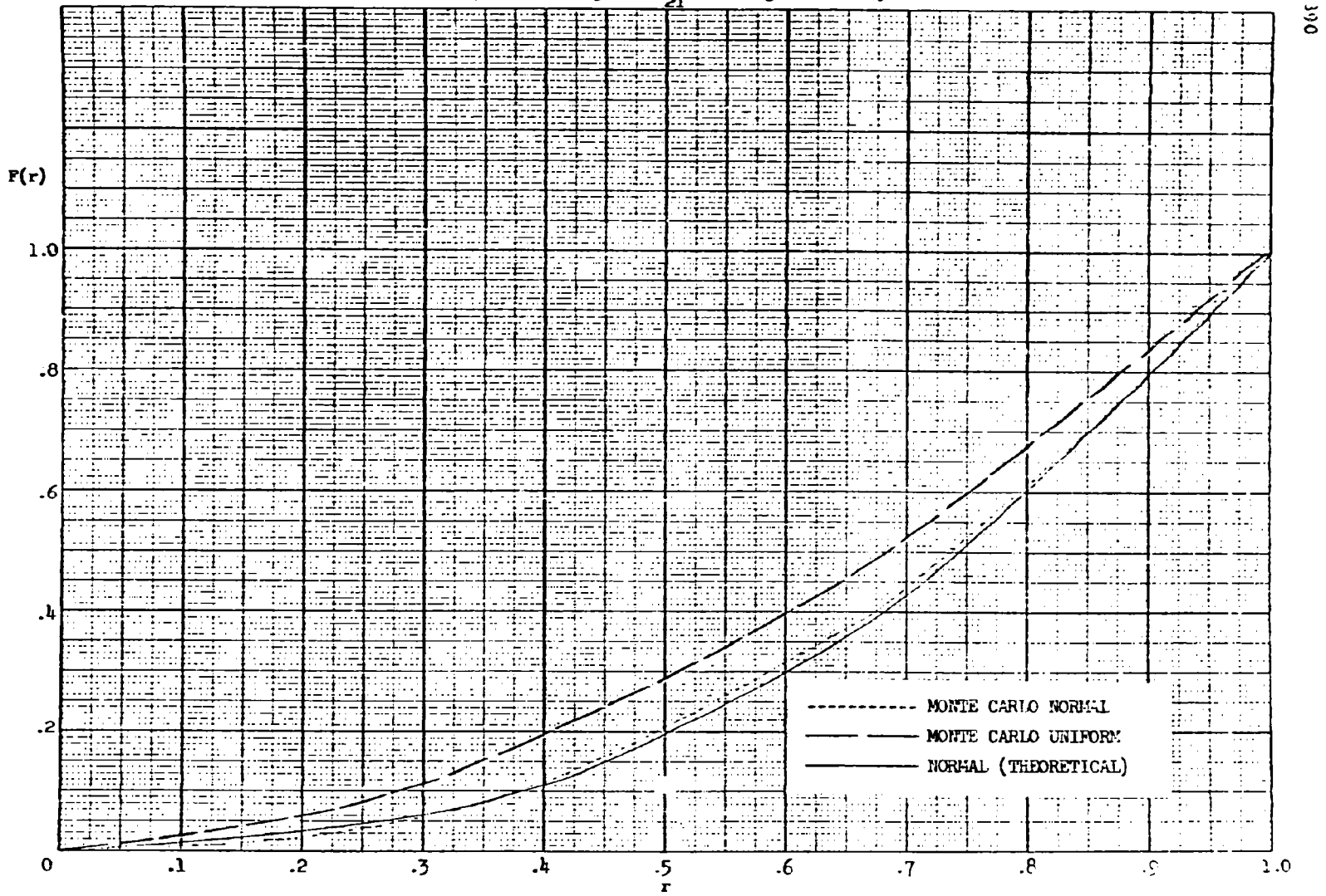

Figure 6 - Graph of r_{10} for sample size n=10

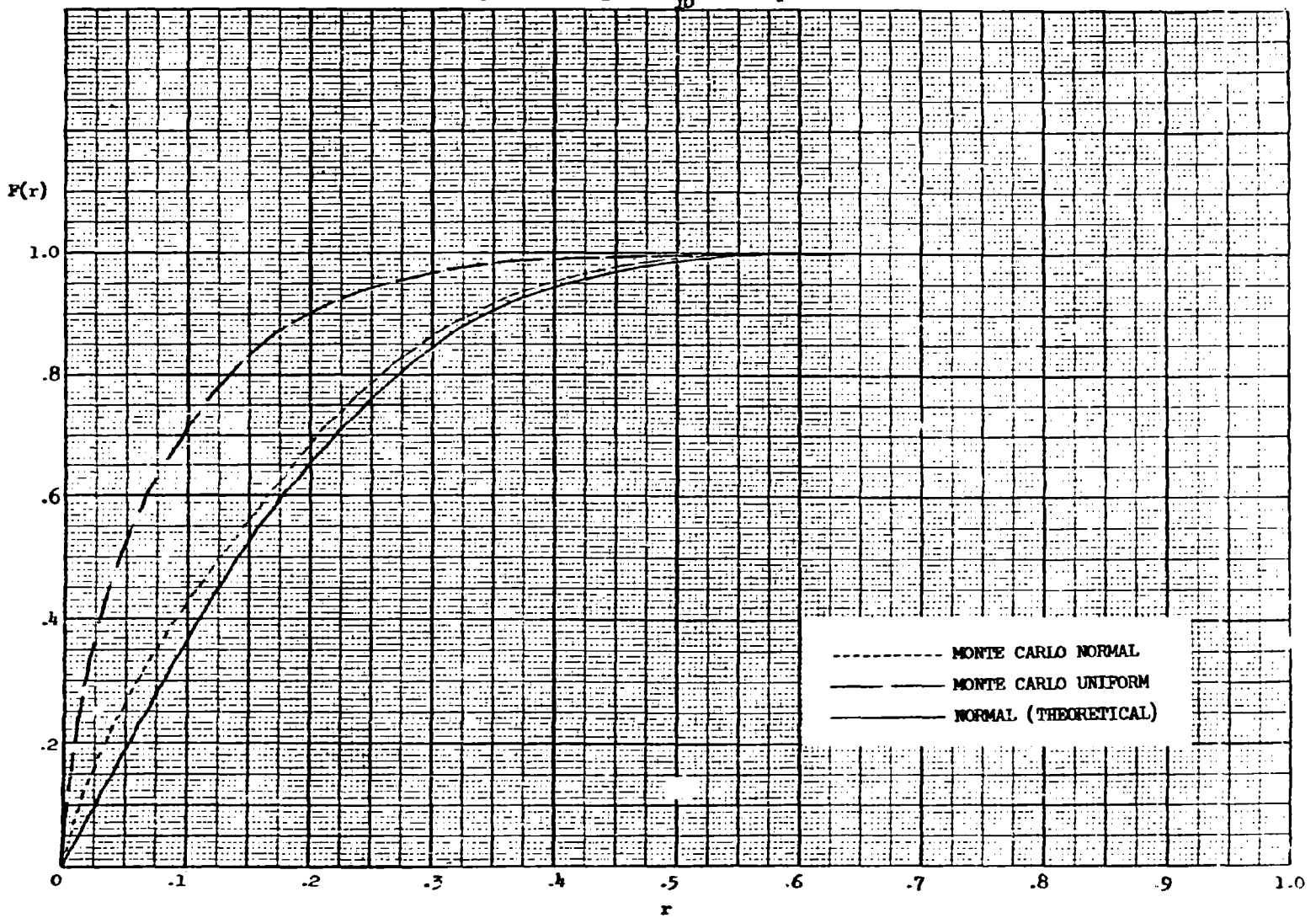

Figure 7 - Graph of r_{11} for sample size n=10

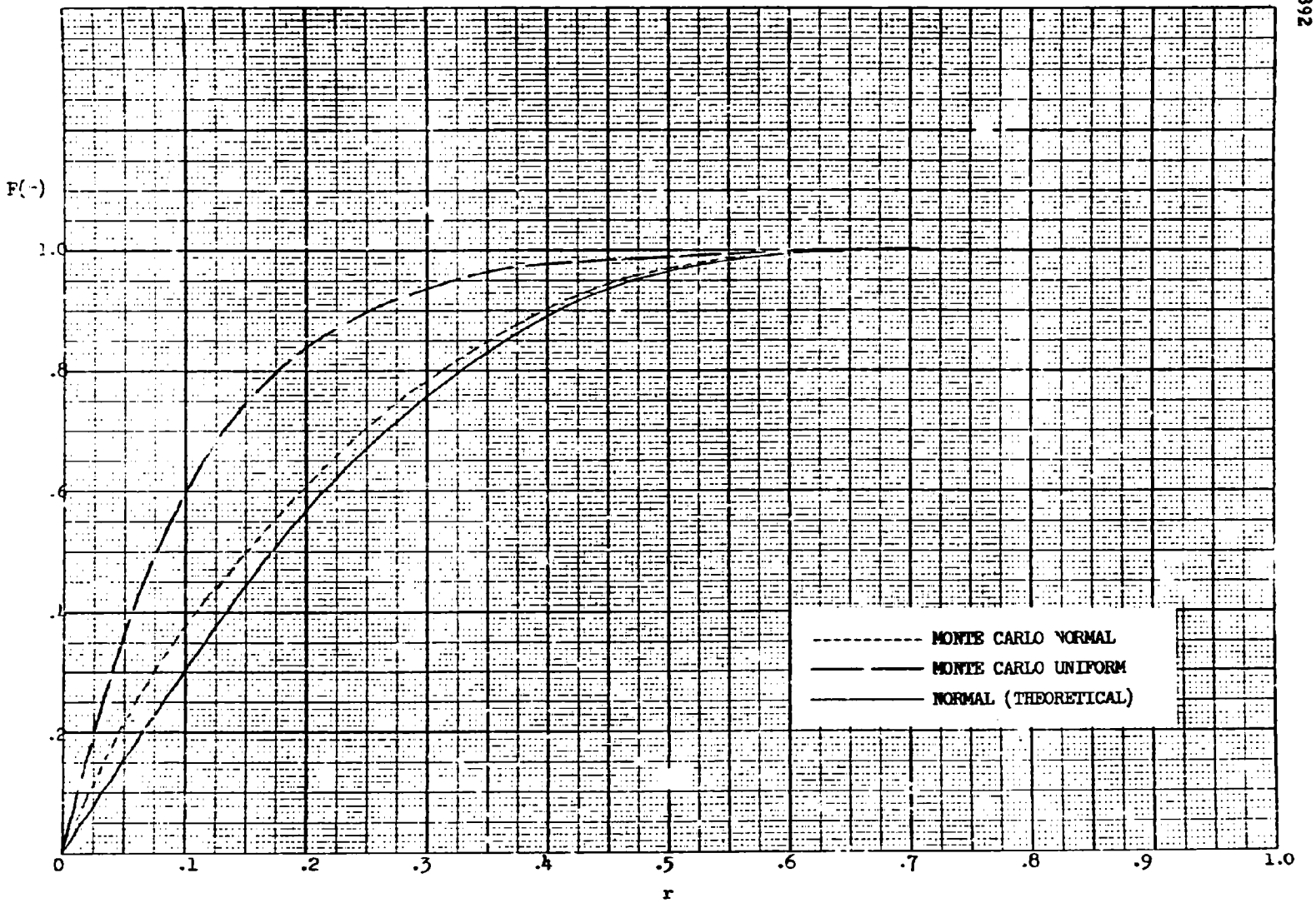

Figure 8 - Graph of r_{12} for sample size n=10

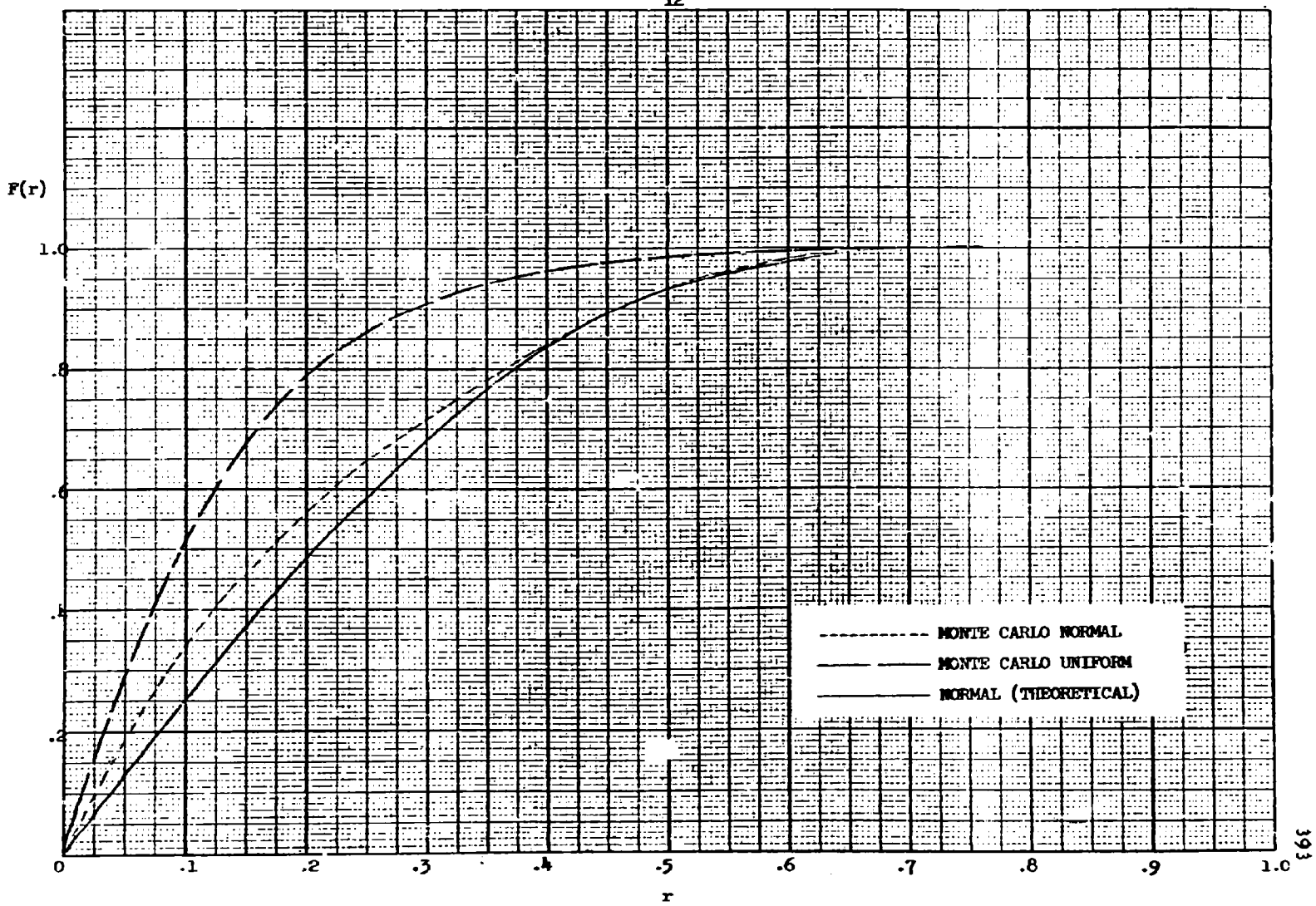

Figure 9 - Graph of r_{20} for sample size n=10

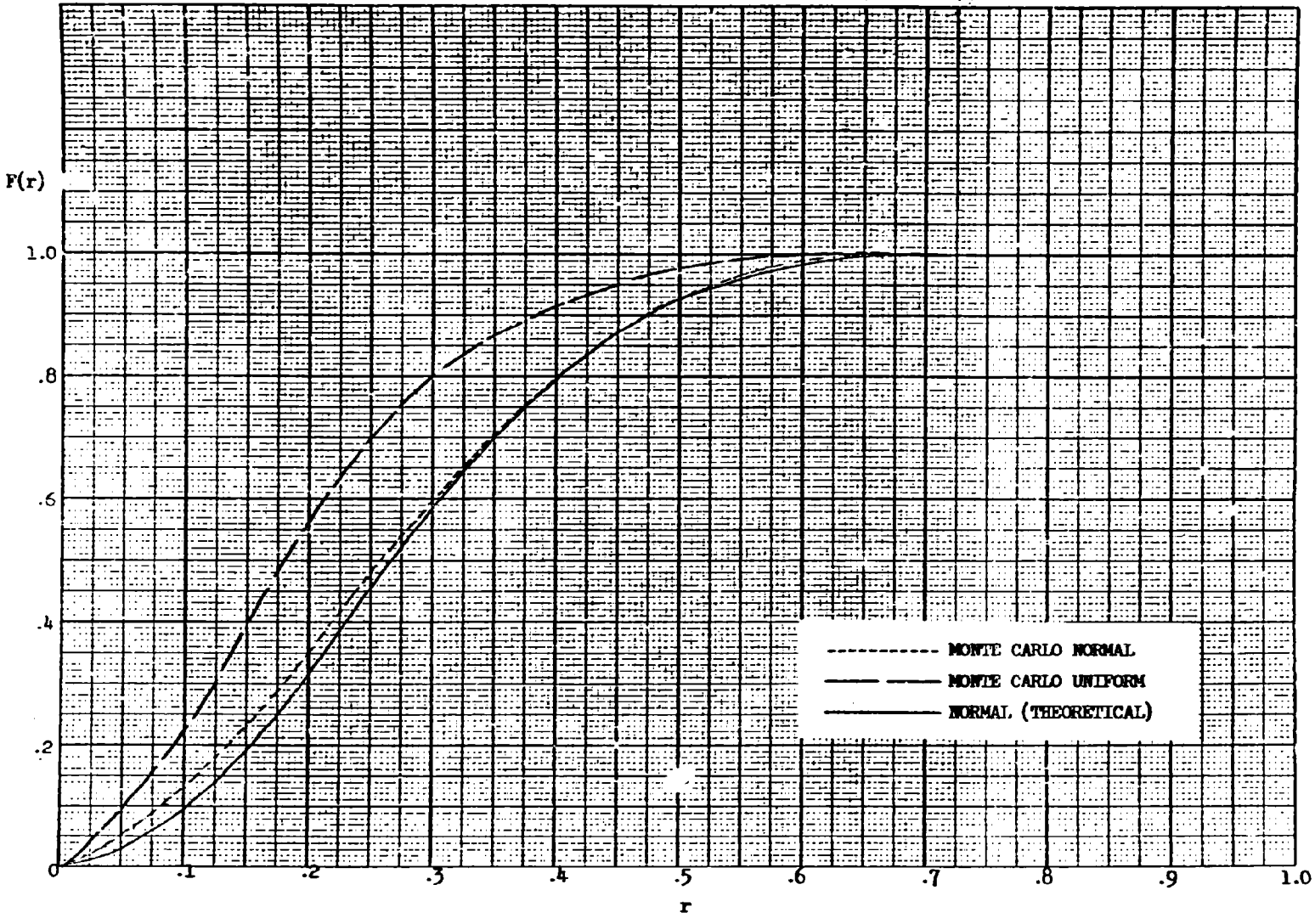

Figure 10 - Graph of r_{21} for sample size n=10

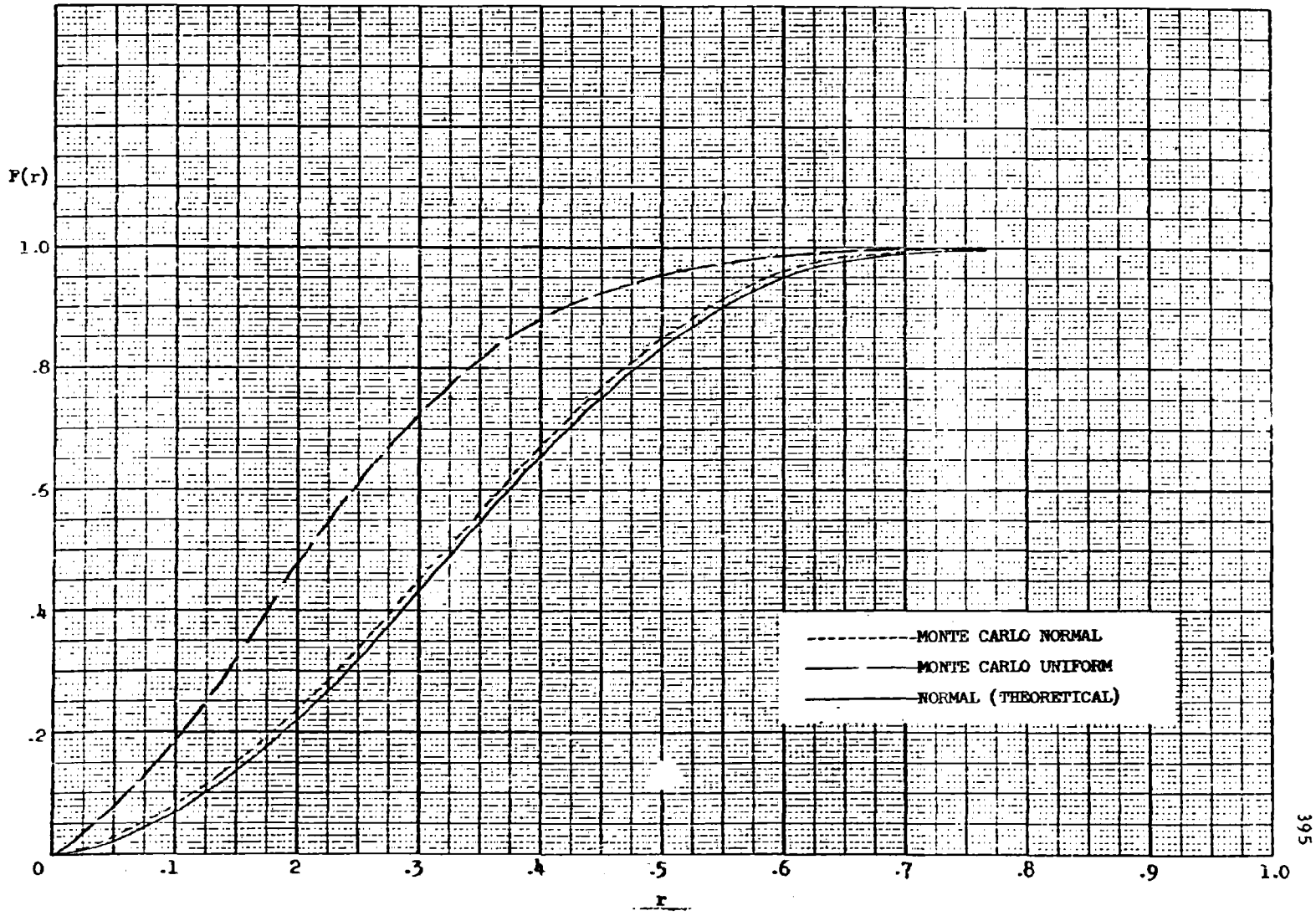

Figure 11 - Graph of r_{22} for sample size n=10

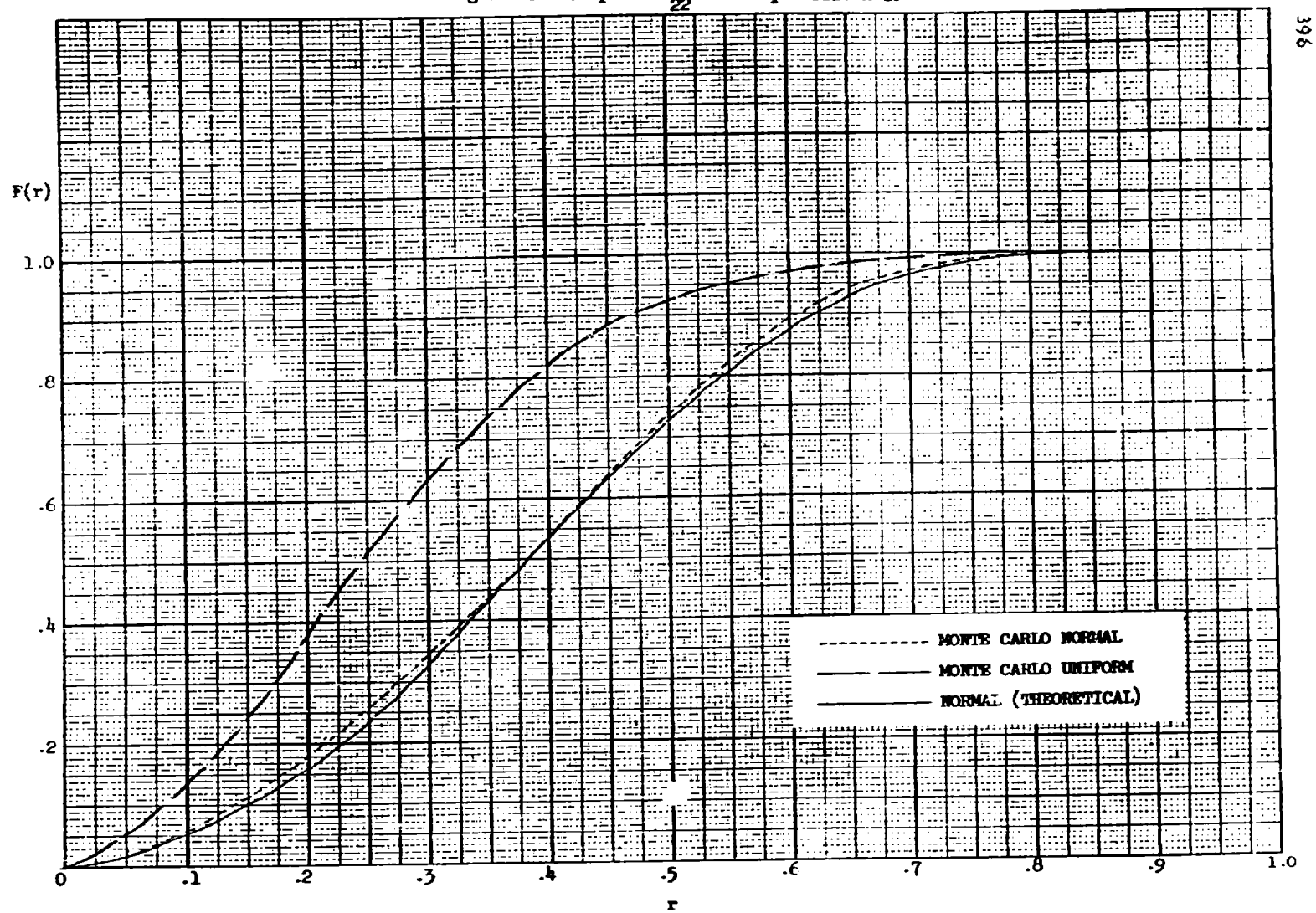

Figure 12 - Graph of r_{10} for sample size n=15

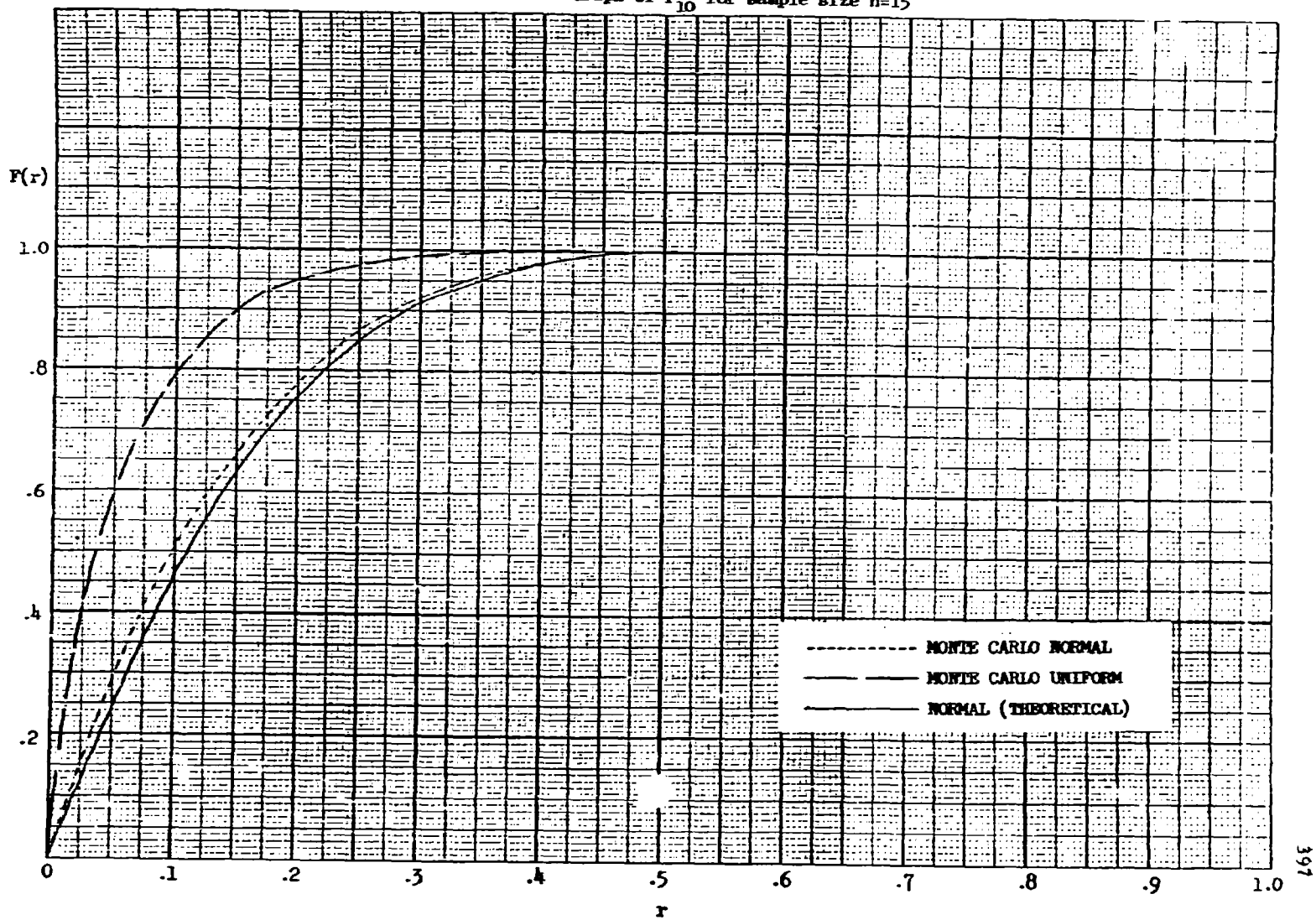

Figure 13 - Graph of r_{11} for sample size n=15

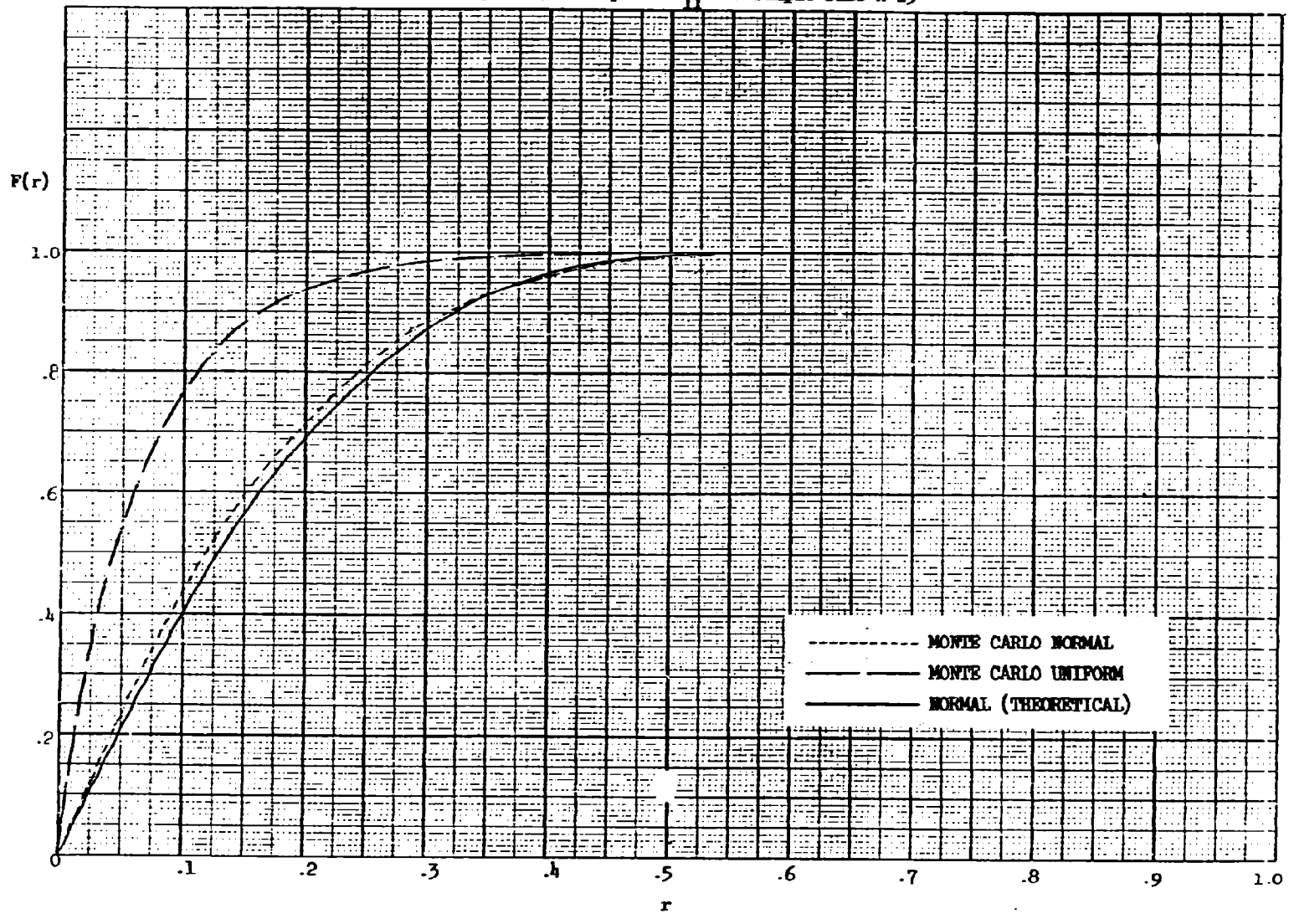

Figure 14 - Graph of r_{12} for sample size n=15

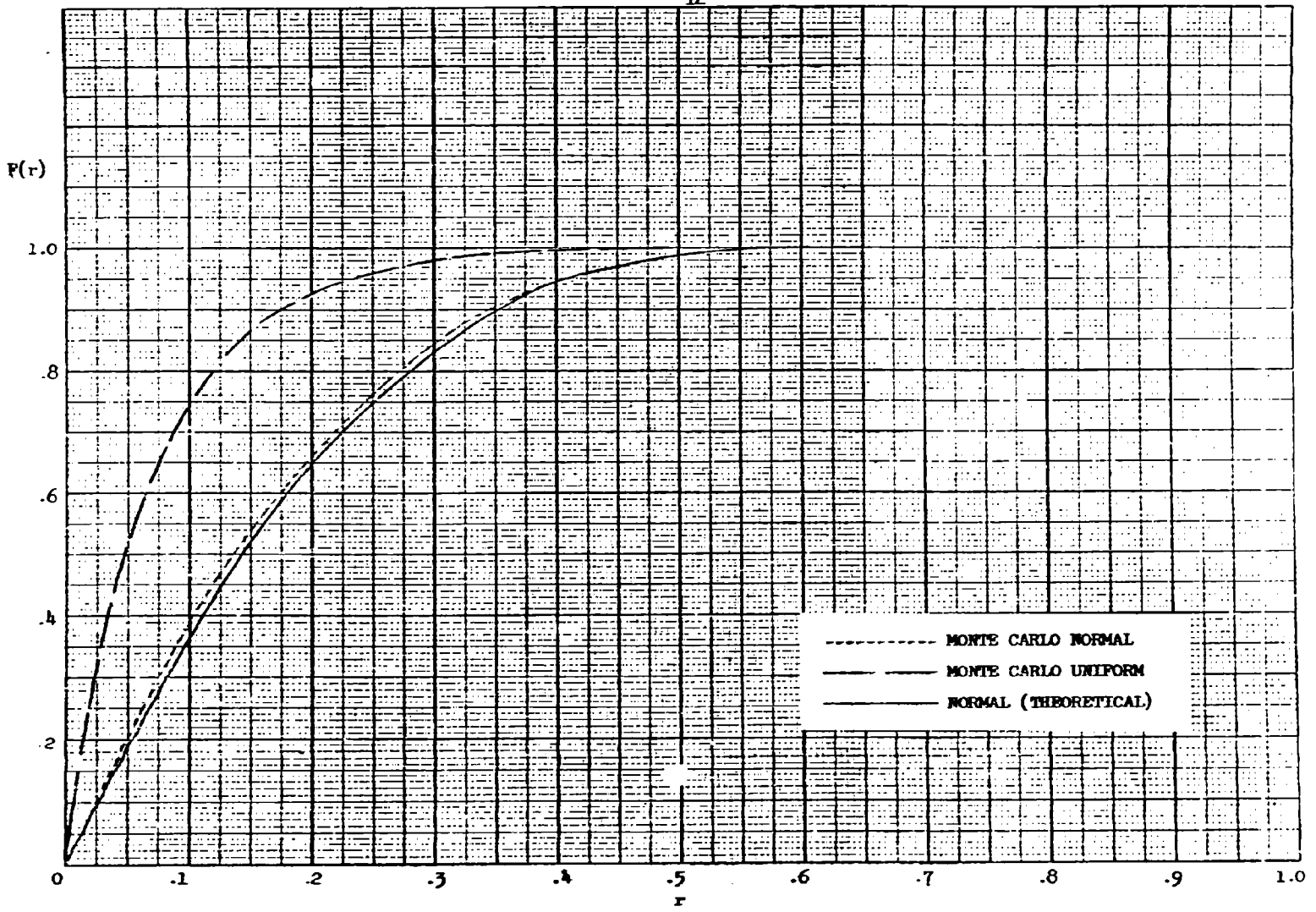

Figure 15 - Graph of r_{20} for sample size n=15

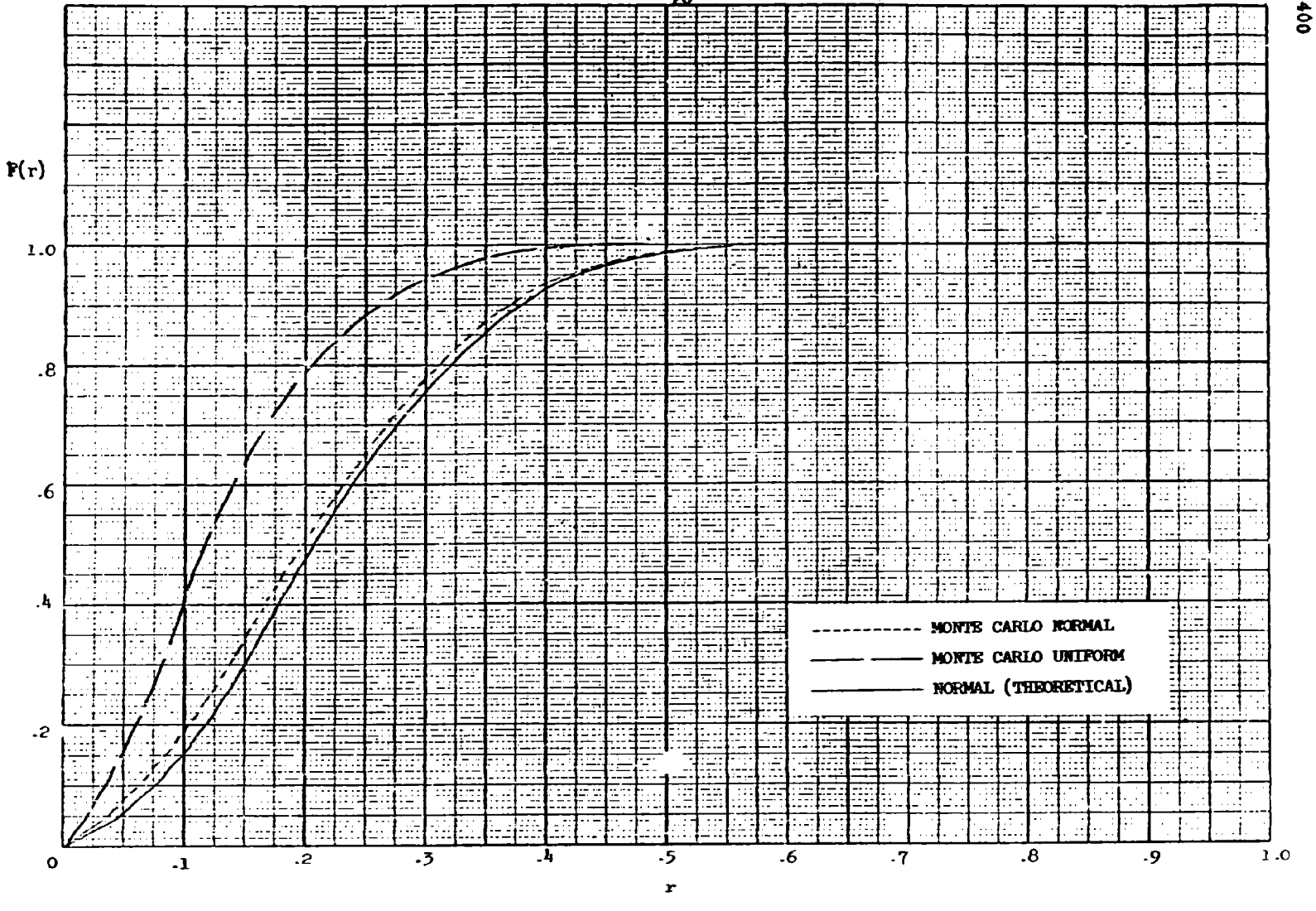

Figure 16 - Graph of r_{21} for sample size n=15

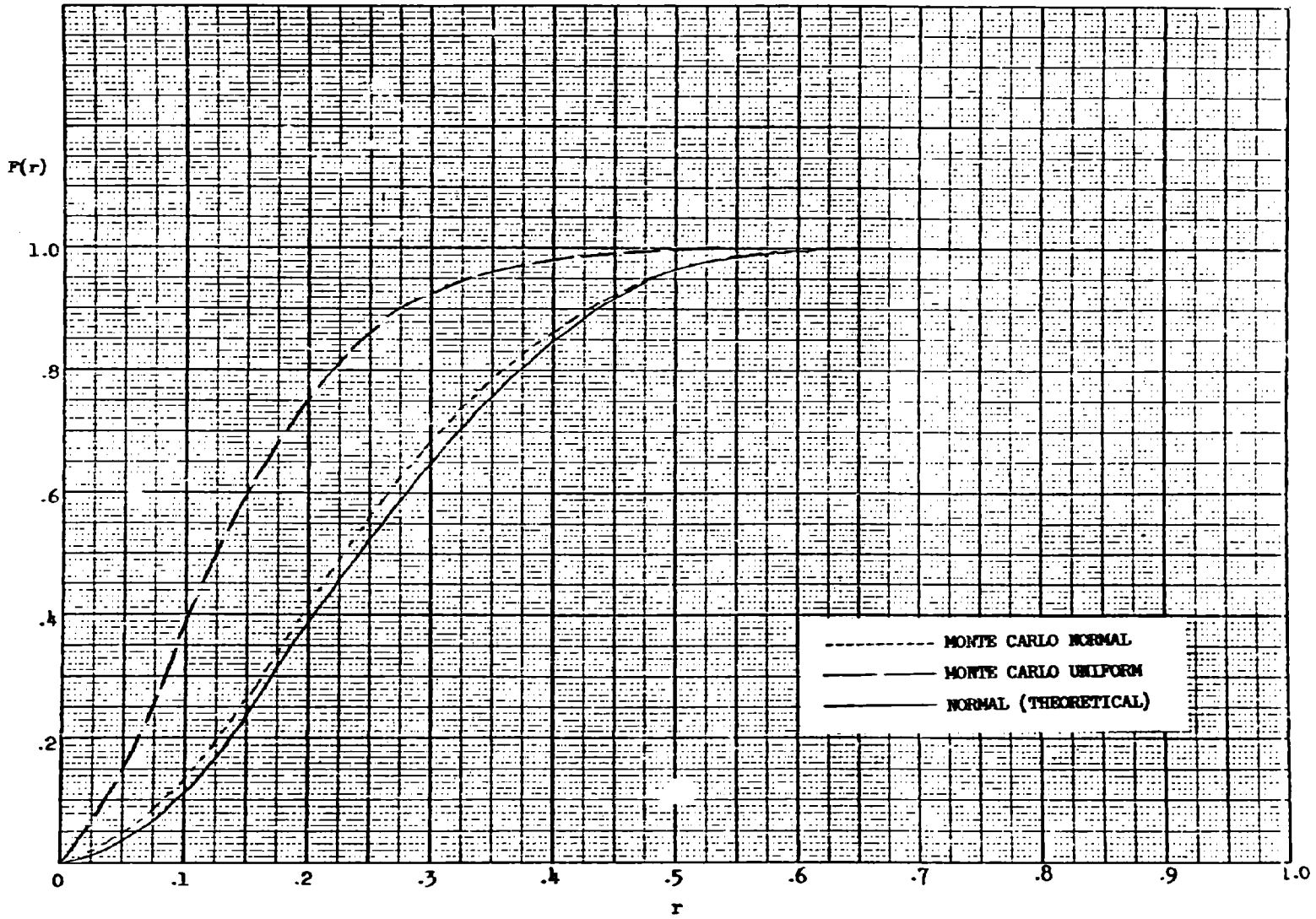

Figure 17 - Graph of r_{22} for sample size n=15

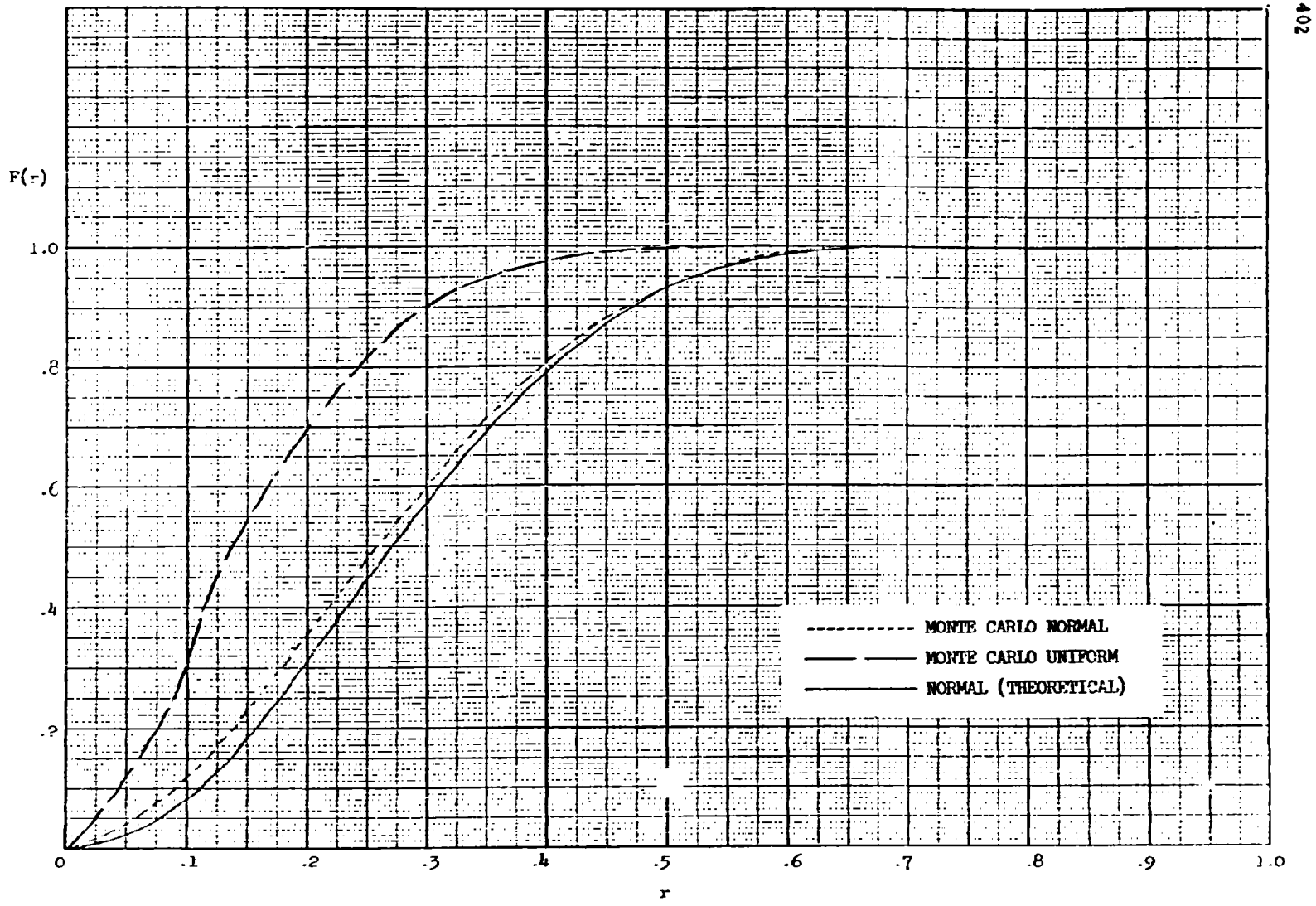

Figure 18 - Graph of r_{10} for sample size n=20

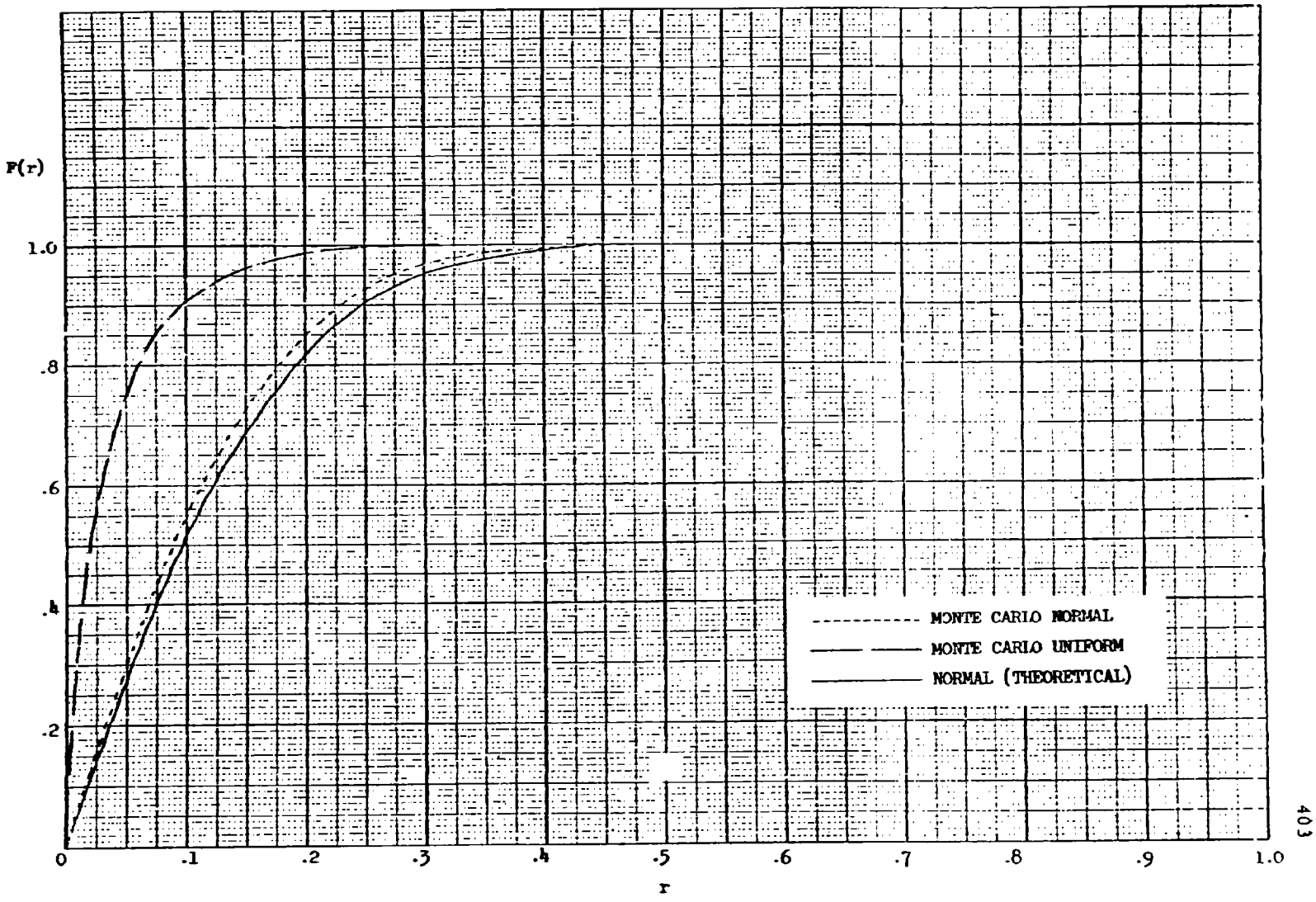

Figure 19 - Graph of r_{11} for sample size n=20

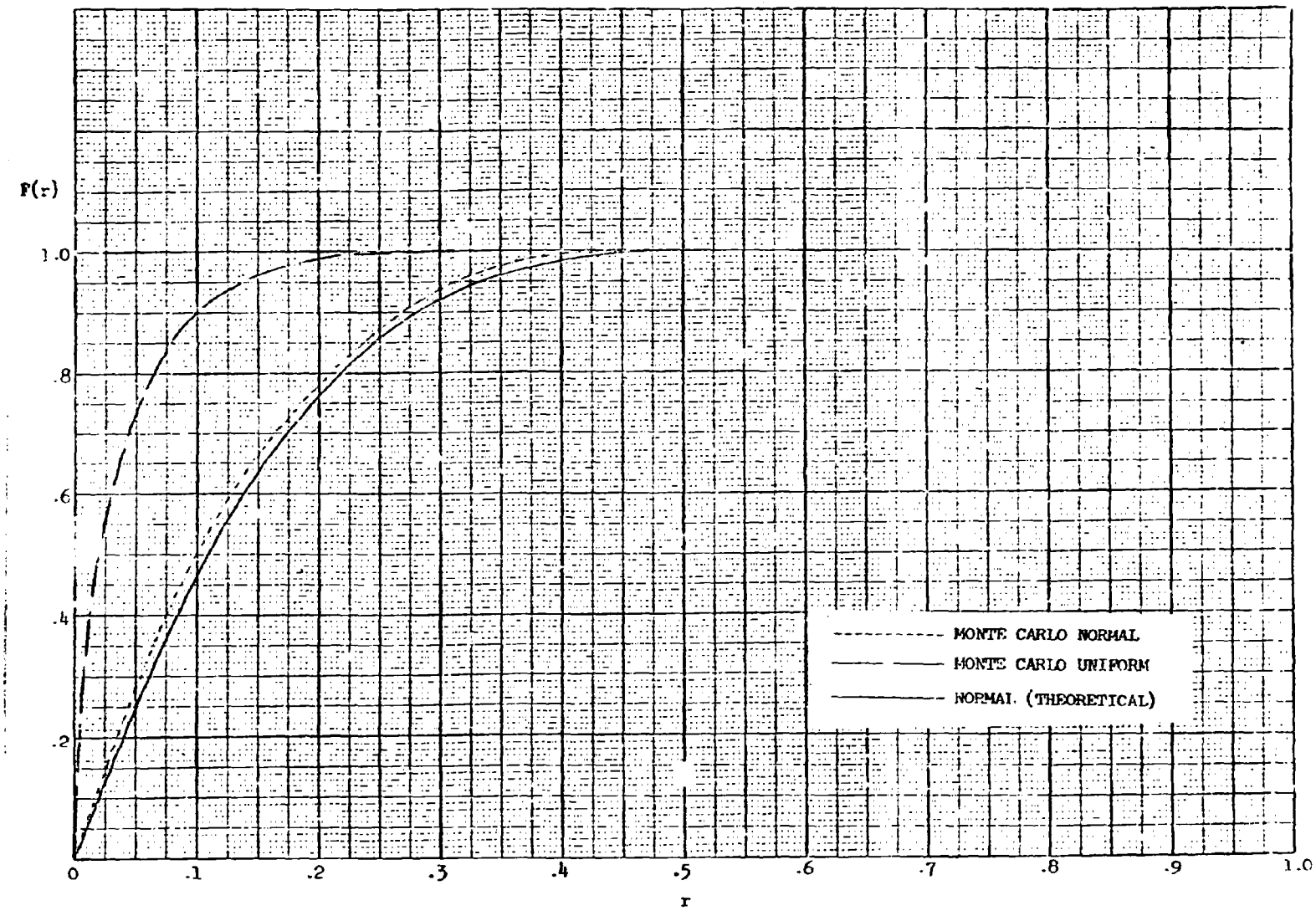

Figure 20 - Graph of r_{12} for sample size n=20

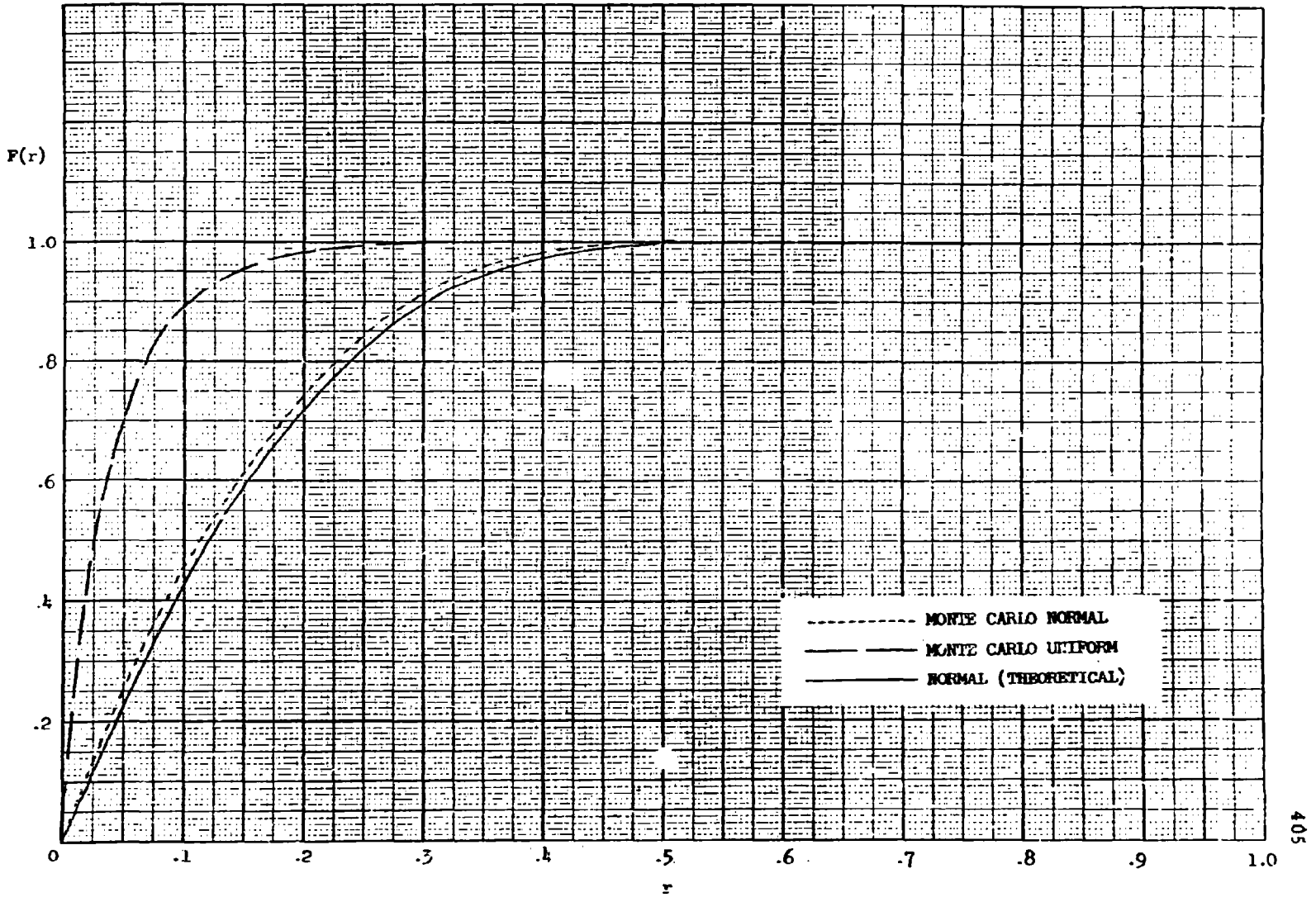

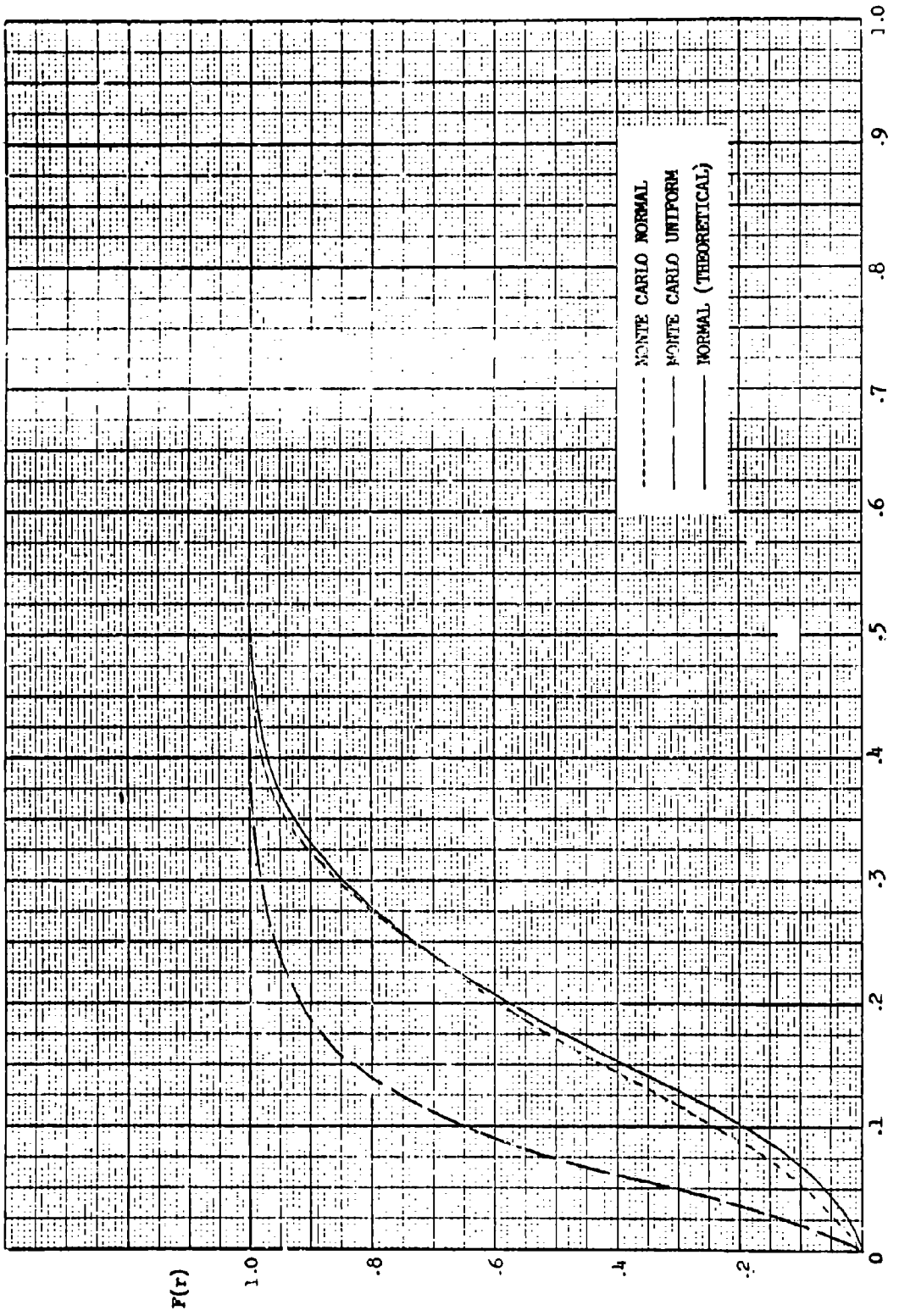

Figure 21 - Graph of r_{20} for sample size n=20

Figure 22 - Graph of r_{21} for sample size n=20

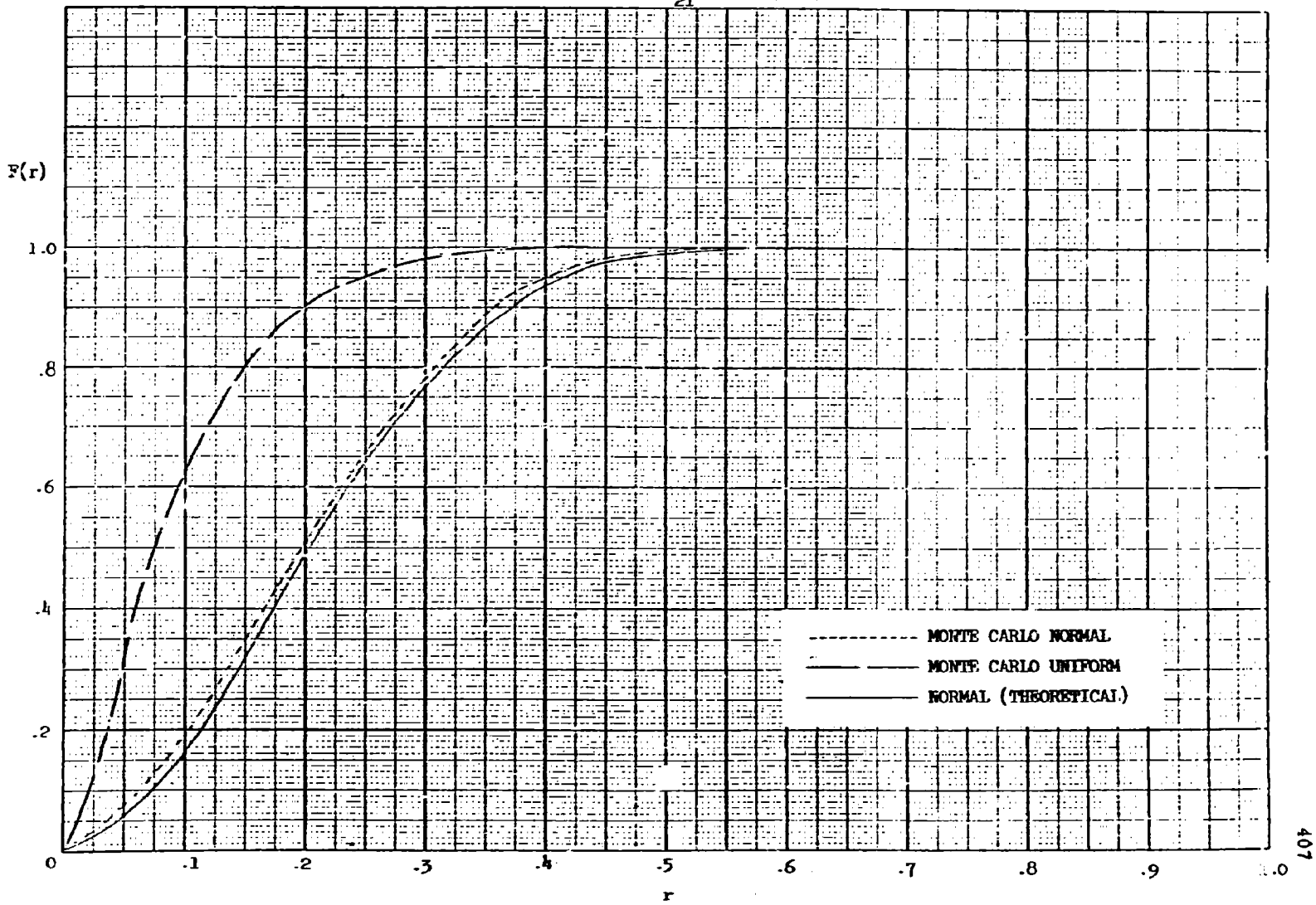

Figure 23 - Graph of r_{22} for sample size n=20

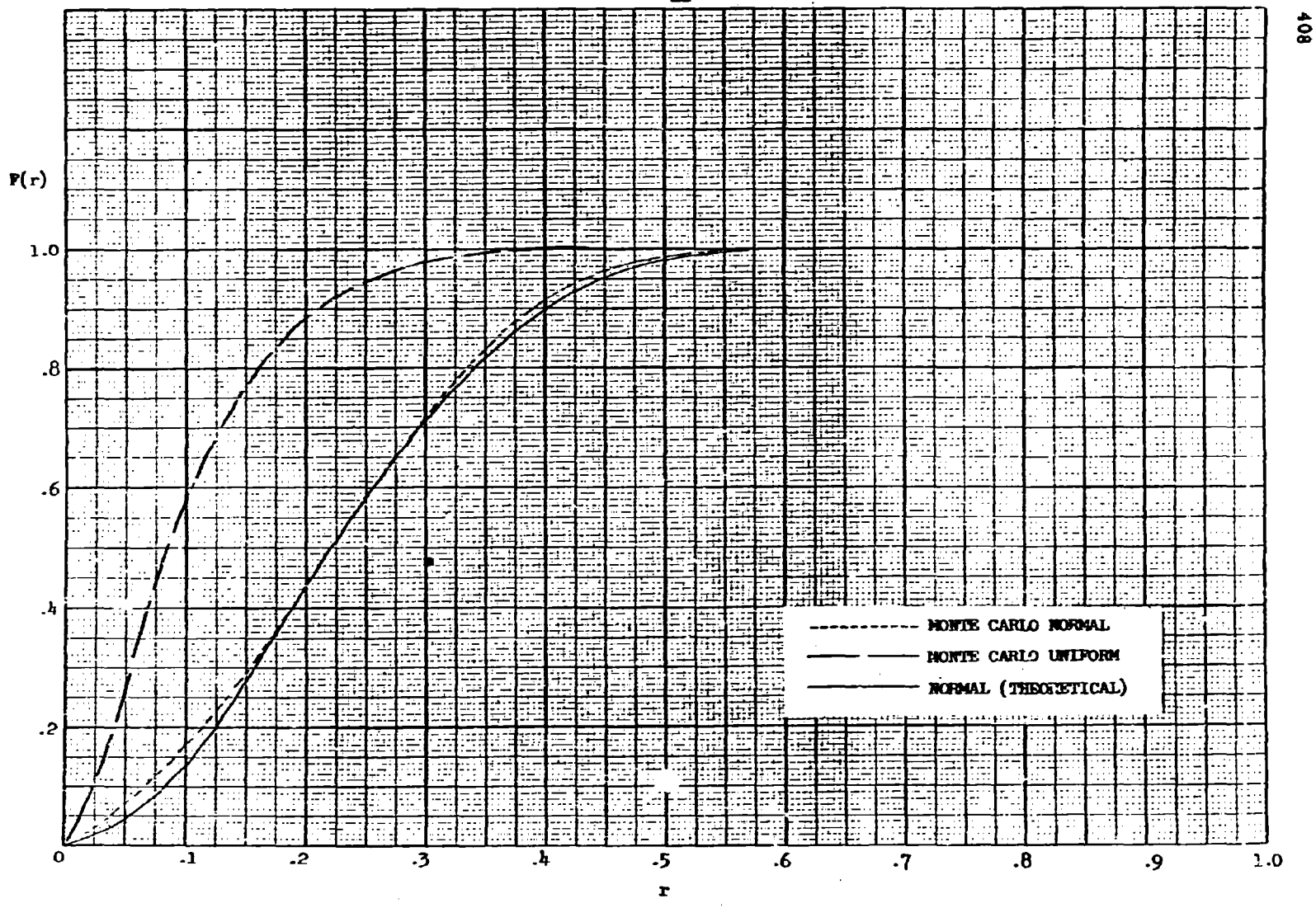

APPENDIX III

Machine Programming of Distributions

410 PROBW-069 DISTRIBUTION SKEET W. MOWCHAN

```
      BLOC(N1-N30)U1-U30)
      BLOC(DIS1-DIS18)D1-D1440)
      BLOC(T1-T30)S1-S30)SUM1-SUM5)
F2    FORM(9-10)9-10)4-10)4-10)4-5)5-1-5)
START     Y0=.0249284555% Z0=-.0002134656l%
          CLEAR(1440)NOS.AT(D1)%
          SET(SS=5)N=500)% FSS=5% DES=0% SET(MAX=0)%
3.0       SET(I=0)%
3.1       S1,I=1%
          COUNT(30)IN(I)GOTO(3.1)%
1.0       SET(I=0)% ENTER(ZEROCC)%
          SET(M1=0)PQ=0)%
          IF(DES=0)GOTO(1.2)%
1.1       ENTER(URNOS2)URN)% GOTO(1.3)%
1.2       ENTER(URNOS1)URN)%
1.3       U1,I=URN% T1,I=14.5*URN-4.5%
          COUNT(SS)IN(I)GOTO(1.1)%
4.0       SET(I=0)%
          IF(DES=0)GOTO(4.1)%    GOTO(4.2)%
4.1       ENTER(NRNOS1)S1,I))1)N1,I)% DES=1% GOTO(4.3)%
4.2       ENTER(NRNOS2)S1,I))1)N1,I)%
4.3       COUNT(SS)IN(I)GOTO(4.2)%
9.0       SET(CT=0)%
          SET(M=N1)%
10.0      INT(I=M+1)% INT(K=M)% SET(X=0)Z=0)%
11.0      IF(,K<,I)GOTO(12.0)%
          T1=,K% ,K=,I% ,I=T1%
12.0      COUNT(SS-1)IN(X)GOTO(13.0)% GOTO(14.0)%
13.0      INC(I=I+1)% GOTO(11.0)%
14.0      COUNT(SS-1)IN(Z)GOTO(15.0)% GOTO(16.0)%
15.0      INT(K=M+Z)% INT(I=K+1)% INT(X=Z)%
          GOTO(11.0)%
16.0      INC(CT=CT+1)%
          IF-INT(CT=1)GOTO(16.1)%
          GOTO(17.0)%
16.1      SET(M=U1)% GOTO(10.0)%
17.0      SET(CT=1)% SET(M=N1)% ENTER(ZEROCC)%
17.1      INT(I=M+SS-1)%
18.0      T1=,(M+1)-,M% T2=,(M+2)-,M%
          T3=,I-,M% T4=,(I-1)-,M% T5=,(I-2)-,M%
18.1      DIS1=T1/T3% DIS2=T1/T4% DIS3=T1/T5%
          DIS4=T2/T3% DIS5=T2/T4% DIS6=T2/T5%
          INC(CT=CT+1)%
          T1=,I-,(I-1)% T2=,I-,(I-2)% T4=,I-,(M+1)% T5=,I-,(M+2)%
          DIS7=T1/T3% DIS8=T1/T4% DIS9=T1/T5%
          DIS10=T2/T3% DIS11=T2/T4% DIS12=T2/T5%
          IF(DIS1>DIS7)GOTO(25.0)% DIS13=DIS7%
24.0      IF(DIS2>DIS8)GOTO(25.1)% DIS14=DIS8%
24.1      IF(DIS3>DIS9)GOTO(25.2)% DIS15=DIS9%
24.2      IF(DIS4>DIS10)GOTO(25.3)% DIS16=DIS10%
24.3      IF(DIS5>DIS11)GOTO(25.4)% DIS17=DIS11%
24.4      IF(DIS6>DIS12)GOTO(25.5)% DIS18=DIS12%
24.5      GOTO(TALLY1)%
25.0      DIS13=DIS1% GOTO(24.0)%
25.1      DIS14=DIS2% GOTO(24.1)%
25.2      DIS15=DIS3% GOTO(24.2)%
25.3      DIS16=DIS4% GOTO(24.3)%
25.4      DIS17=DIS5% GOTO(24.4)%
25.5      DIS18=DIS6% GOTO(24.5)%
TALLY1    SET(G=0)% SET(Q=D1)%
```

```
LL1         T1=DIST.6% INT(M1=0+PQ)%
            IF(T1=>.5)GOTO(LL2)%
            IF(T1=>.25)GOTO(LL3)%
            IF(T1=>.125)GOTO(LL4)%
            T2=0% T3=.025% GOTO(OPEN)%
LL2         IF(T1=>.75)GOTO(LL5)%
            INT(M1=M1+20)% T2=.5% T3=.525% GOTO(OPEN)%
LL3         INT(M1=M1+10)% T2=.25% T3=.275% GOTO(OPEN)%
LL4         INT(M1=M1+5)% T2=.125% T3=.15% GOTO(OPEN)%
LL5         IF(T1=>.875)GOTO(LL6)%
            INT(M1=M1+30)% T2=.75% T3=.775% GOTO(OPEN)%
LL6         INT(M1=M1+35)% T2=.875% T3=.9%
OPEN        IF(T2=<T1<T3)GOTO(TALLY2)%
            T2=T2+.025% T3=T3+.025% IF(T2=1)WITHIN(.001)GOTO(TALLY2)%
            INT(M1=M1+1)% GOTO(OPEN)%
TALLY2      INT(,M1=,M1+1)%
            COUNT(18)IN(G)GOTO(ZIP)% GOTO(19.0)%
ZIP         INT(PQ=PQ+40)%GOTO(LL1)%
19.0        INT(PQ=PQ+40)%
            IF-INT(CT=2)GOTO(19.2)%
            GOTO(20.0)%
19.2        SET(M=U1)% GOTO(17.1)%
20.0        COUNT(N)IN(MAX)GOTO(1.0)%
26.0        ENTER(ZEROCC)% SET(Z=0)
26.1        T1=0% T2=.025% SET(I=0)% INT(SUM=0)%
26.2        INT(SUM=SUM+D1,Z)%
            PRINT-FORMAT(F2)~(T1)(T2)D1,Z)SUM  )SS)
            T1=T1+.025% T2=T2+.025% INC(Z=Z+1)%
            COUNT(40)IN(I)GOTO(26.2)%
            IF-INT(Z=1440)GOTO(21.0)% GOTO(26.1)%
21.0        INC(SS=SS+5)% FSS=FSS+5
            CLEAR(1440)NOS.AT(D1)%
            SET(MAX=0)%
22.0        IF-INT(SS>30)GOTO(N.PROB)%
            GOTO(1.0)%
            LIST
        END GOTO(START)%
```

APPENDIX IV

Machine Programming for Cumulative Frequency Distribution

```
414     PROG W-089  DISTRIBUTION  SHEET FOR W.MOWCHAN

        BLOC(X1:X500)C1:C40)TAL1:TAL40)
F1      FORM(4-5)8-5)8-5)
F2      FORM(9-10)3-70)
F3      FORM(9-10)9-10)4-10)4-10)4-5)8-5)8-5)
START       READ-FOR.  (F1)-(SS)R)D)
            READ-FORMAT(F2)-(500)NOS.AT(X1)%
            CLEAR(40)NOS.AT(C1)%
            CLEAR(40)NOS.AT(TAL1)%
1.0         SET(I=0)%
1.1         T1=0% T2=.025% SET(Z=0)%
2.0         IF(T1=<X1,I<T2)GOTO(3.0)%
2.1         T1=T1+.025% T2=T2+.025%
            IF(T1=1.0)WITHIN(.001)GOTO(3.0),
            INC(Z=Z+1)% GOTO(2.0)%
3.0         INT(C1,Z=C1,Z+1)
4.0         COUNT(5.0)I,(I)=TO(1.1)%
5.0         SUM=0% SET(Z=0)%
6.0         INT(SUM=SUM+C1,Z)  INT(TAL1,Z=SUM)%
            COUNT(40)IN(Z)GOTO(6.0)%
7.0         T1=0% T2=.025% SET(I=0)%
8.0         PRINT-FORMAT(F3)-(T1)T2)C1,I)TAL1,I)SS)R)D)%
            T1=T1+.025% T2=T2+.025%
            COUNT(40)IN(I)GOTO(8.0)% GOTO(START)%
        END GOTO(START)%
```

A SIMPLIFIED TECHNIQUE FOR ESTIMATING DEGREES OF FREEDOM FOR A TWO POPULATION T TEST WHEN THE STANDARD DEVIATIONS ARE UNKNOWN AND NOT NECESSARILY EQUAL

Eugene Dutoit and Robert Webster
Quality Assurance Directorate, Ammunition Reliability Division
Mathematics and Statistics Branch,
Picatinny Arsenal, Dover, New Jersey

The purpose of this paper is to develop a practical aid for the descriptive statistician performing tests of statistical significance who must do most of his computing at a desk using an ordinary "desk-top" calculator.

The t statistic is used to test for significant differences between two sample means when samples are randomly selected from two normally distributed populations. If samples are drawn from two normal populations and the standard deviations of these populations are unknown and their computed estimates indicate they are not necessarily equal, then the t test statistic is computed by:

$$(1) \qquad t' = \frac{\bar{X}_1 - \bar{X}_2}{(S_1^2/n_1 + S_2^2/n_2)^{1/2}}$$

where this random variable follows a t-distribution with degrees of freedom (d.f.) equal to:

$$(2) \qquad \text{d.f.} = \frac{\left(\frac{S_1^2}{n_1} + \frac{S_2^2}{n_2}\right)^2}{\frac{\left(S_1^2/n_1\right)^2}{n_1 - 1} + \frac{\left(S_2^2/n_2\right)^2}{n_2 - 1}}$$

where S_1^2 and S_2^2 are estimates of σ_1^2 and σ_2^2 respectively and n_1 and n_2 are the sample sizes. Since equation (2) is a cumbersome expression to work with, an alternate form of this expression would be desirable for analysis performed on a desk calculator or a slide rule.

In order to determine whether or not the standard deviations are equal the F ratio test is used:

$$F = S_2^2 / S_1^2 \tag{3}$$

where S_2^2 is denoted such that $S_2^2 \geq S_1^2$. This guarantees that $F \geq 1$. If the computed F ratio is larger than the tabulated critical values of F ratios, the two standard deviations are unequal. Equation (2) can be manipulated so that the d.f. can be expressed as a function of the ratios of the variances and the values n_1 and n_2. Since the ratio of the variances has already been computed as the F test statistic, equation (2) can be generalized as:

$$\text{d.f.} = f(F = S_2^2 / S_1^2 \ , \ n_1, n_2) \ . \tag{4}$$

If $n_1 \neq n_2$ then equation (2) can be rewritten as:

$$\text{d.f.} = \frac{(n_1 - 1)(n_2 - 1)(n_2 + n_1 F)^2}{n_2^2 (n_2 - 1) + F^2 n_1^2 (n_1 - 1)} \tag{5}$$

or alternatively:

$$\text{d.f.} = \frac{(n_2 + n_1 F)^2}{\frac{n_2^2}{n_1 - 1} + \frac{n_1^2 F^2}{n_2 - 1}} \ . \tag{6}$$

Equation (6) is more efficient because twelve operations are needed to calculate the d.f. whereas equation (5) requires 17 separate operations. Equation (5) however, has eliminated the "complex function" appearance and might be more palatable to the statistical employee who would have to compute the value.

If $n_1 = n_2 = n$, then equations (5) and (6) reduce to:

$$(7) \qquad d.f. = \frac{(1 + F)^2 (n - 1)}{1 + F^2} \quad .$$

The derivation of equations (5), (6) and (7) will be presented in Appendix A. These equations lend to computer applications for selected values of n_1, n_2 and F. The number of degrees of freedom can then be calculated and presented as tables or graphs. The output format used for the initial computer run was of the type:

Figure 1

$F = F_k$

n_2 \ n_1	10	15	. . .		. . . .	180
10	$d.f._{11}$	$d.f._{12}$	. . .	$d.f._{1j}$	. . . .	$d.f._{1m}$
15	$d.f._{21}$	$d.f._{22}$	. . .	$d.f._{2j}$	. . . .	$d.f._{2m}$
.	.	.		.		.
.	.	.		.		.
.	.	.		.		.
	$d.f._{i1}$	$d.f._{i2}$	. . .	$d.f._{ij}$	. . . .	$d.f._{im}$
.	.	.		.		.
.	.	.		.		.
.	.	.		.		.
.	.	.		.		.
180	$d.f._{m1}$	$d.f._{m2}$	. . .	$d.f._{mj}$	. . . .	$d.f._{mm}$

Twenty values of F were chosen so that twenty tables (see Figure 1) were generated. These tables were then used to generate sets of curves as per Figure 2 below:

Figure 2

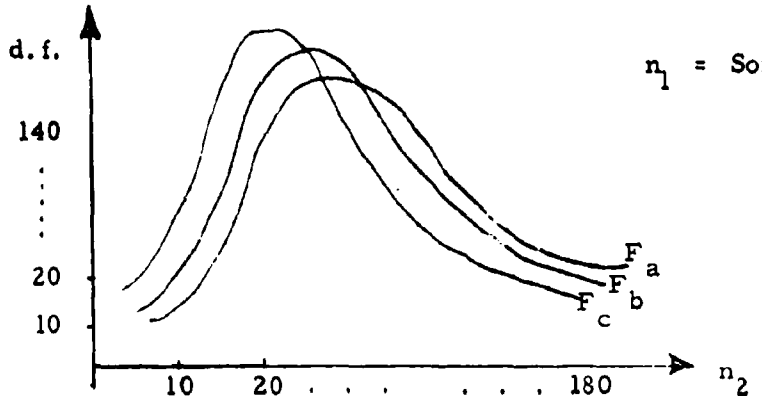

A fixed value for n_1 and F produces a set of smooth curves for various values of n_2. The first attempt at plotting curves proved to be a bit impractical for larger values of n_1, n_2 because the curves become highly confounded. A more realistic plot can be made (for Ordnance purposes) by using values of n_1, $n_2 \leq 50$.

Example: Suppose we should like to compare the test scores of two high school science classes. We wish to detect a significant difference in the dispersion of scores within each class and, in addition, we should like to detect whether or not the average score of one class is significantly greater than the other.

We consider the following data:

Class a.		Class b.	
95	81	69	80
83	67	74	77
46	81	91	92
71	85	90	86
76	52	82	78
64	86	71	82
82	79	72	
84	80	80	
84	88	91	
56	64	83	
n_2 =	20	n_b =	16
$\bar{X}_a$ =	75.2	$\bar{X}_b$ =	81.3
s_a^2 =	170.06	s_b^2 =	60.10
s_a =	13.04	s_b =	7.75

Using the F-ratio test for equality of variances (dispersions),

$$F_o = \frac{s_a^2}{s_b^2} = 2.83 > 2.77 = F_{\alpha/2,\, n_a-1,\, n_b-1}$$

when $\alpha = 0.05$. We conclude that a significant difference between the variability (or dispersion) of test scores is detected.

Since we only have estimates of the true variance of the data and have shown these estimates to be unequal, we should employ the two population t-test for data with unknown and unequal variances to determine whether the average score of Class b significantly exceed that of Class a. We must, therefore, compute

$$t_o = \frac{\bar{X}_b - \bar{X}_a}{\sqrt{\frac{s_b^2}{n_b} + \frac{s_a^2}{n_a}}}$$

$$\text{and d. f.} = \frac{\left(\frac{s_b^2}{n_b} + \frac{s_a^2}{n_a}\right)^2}{\frac{\left(\frac{s_b^2}{n_b}\right)^2}{n_b - 1} + \frac{\left(\frac{s_a^2}{n_2}\right)^2}{n_a - 1}}$$

$$\text{Then, } t_o = \frac{81.3 - 75.2}{\sqrt{\frac{170.06}{20} + \frac{60.10}{16}}}$$

$$= \frac{6.1}{\sqrt{12.26}}$$

$$= 1.73$$

$$\text{and d. f.} = \frac{\left(\frac{170.06}{20} + \frac{60.10}{16}\right)^2}{\frac{\left(\frac{170.06}{20}\right)^2}{19} + \frac{\left(\frac{60.10}{16}\right)^2}{15}}$$

$$= \frac{(12.26)^2}{3.81 + 0.94}$$

$$= \frac{150.31}{4.75}$$

$$= 31.6 \sim 32 \quad .$$

As might be expected, these calculations are lengthy, time-comsuming and error prone. An alternate method to determine d.f. would be to consult the graphs which have been prepared to yield values of d.f. when the sample sizes and F-ratio are known.

The graphs plot d.f. vs N_2 for a specified value of N_1 and for certain values of F_o. In this case $N_2 = 20$ and $N_1 = 16$ since the variance of $n_a >$ variance of n_b. The simple steps to determine d.f. are as follows:

1. Find the graph corresponding to $N_1 = 16$
2. On this graph find $N_2 = 20$.
3. On the vertical line corresponding to $N_2 = 20$ find the points of intersection corresponding to F-ratio's of 2.00 and 3.00 (only values of $F_o = 1.50, 2.00, 3.00, 4.00, 5.00, 8.00$ and 14.00 are plotted).
4. From these points read d.f. (F=2.00) and d.f. (F = 3.00) off the ordinate

   d.f. (F=2.00) = 33.5
   d.f. (F=3.00) = 31.3

5. Interpolate to determine d.f. (F = 2.83)

   33.5 - 31.3 = 2.2
   (.83) (2.2) = 1.8
   33.5 - 1.8 = 31.7 $\sim$ d.f. (F = 2.83) .

Thus d.f. = 31.7 $\sim$ 32 - which is compatible with the calculated value of 31.6 $\approx$ 32.

REFERENCES

[1] Li, J: Introduction to Statistical Inference, Distributed by Edwards Bros. Inc., Ann Arbor, Michigan, 1957.

[2] E. L. Bombara: Probability That Stress is Less Than Strength at Prescribed Confidence Levels, For Normally Distributed Data, Proceedings of the Ninth Conference on the Design of Experiments in Army Research Development and Testing, October 1963.

ACKNOWLEDGEMENT. A special acknowledgement is extended to Mr. Stuart Ritter who developed the computer program for this work.

APPENDIX A

Derivative of equation (6):

$$\text{d.f.} = \frac{\left(\frac{s_1^2}{n_1} + \frac{s_2^2}{n_2}\right)^2}{\frac{\left(s_1^2/n_1\right)^2}{n_1 - 1} + \frac{\left(s_2^2/n_2\right)^2}{n_2 - 1}}$$

multiplying by $\frac{1/s_1^4}{1/s_1^4}$ and letting the

ratio $\frac{s_2^2}{s_1^2} = F \geq 1$

$$\text{d.f.} = \frac{\left(\frac{1}{n_1} + \frac{F}{n_2}\right)^2}{\frac{(1/n_1)^2}{n_1 - 1} + \frac{(F/n_2)^2}{n_2 - 1}}$$

multiplying by $(n_1 n_2)^2 / (n_1 n_2)^2$ gives equation (5):

$$\text{d.f.} = \frac{(n_2 + n_1 F)^2}{\frac{n_2^2}{n_1 - 1} + \frac{n_1^2 F^2}{n_2 - 1}}$$

Equation (5) follows by multiplying by $\frac{(n_1-1)(n_2-1)}{(n_1-1)(n_2-1)}$

$$\text{d.f.} = \frac{(n_1 - 1)(n_2 - 1)(n_2 + n_1 F)^2}{n_2^2 (n_2 - 1) + n_1^2 (n_1 - 1) F^2}$$

when $n_1 = n_2 = n$

$$\text{d.f.} = \frac{(1 + F)^2 (n - 1)}{1 + F^2}$$

which is a linear function for d.f. with "n" intercept n = 1 and slope $= \frac{(1 + F)^2}{1 + F^2}$.

APPENDIX B

Logic diagram of computer program:

Figure 3

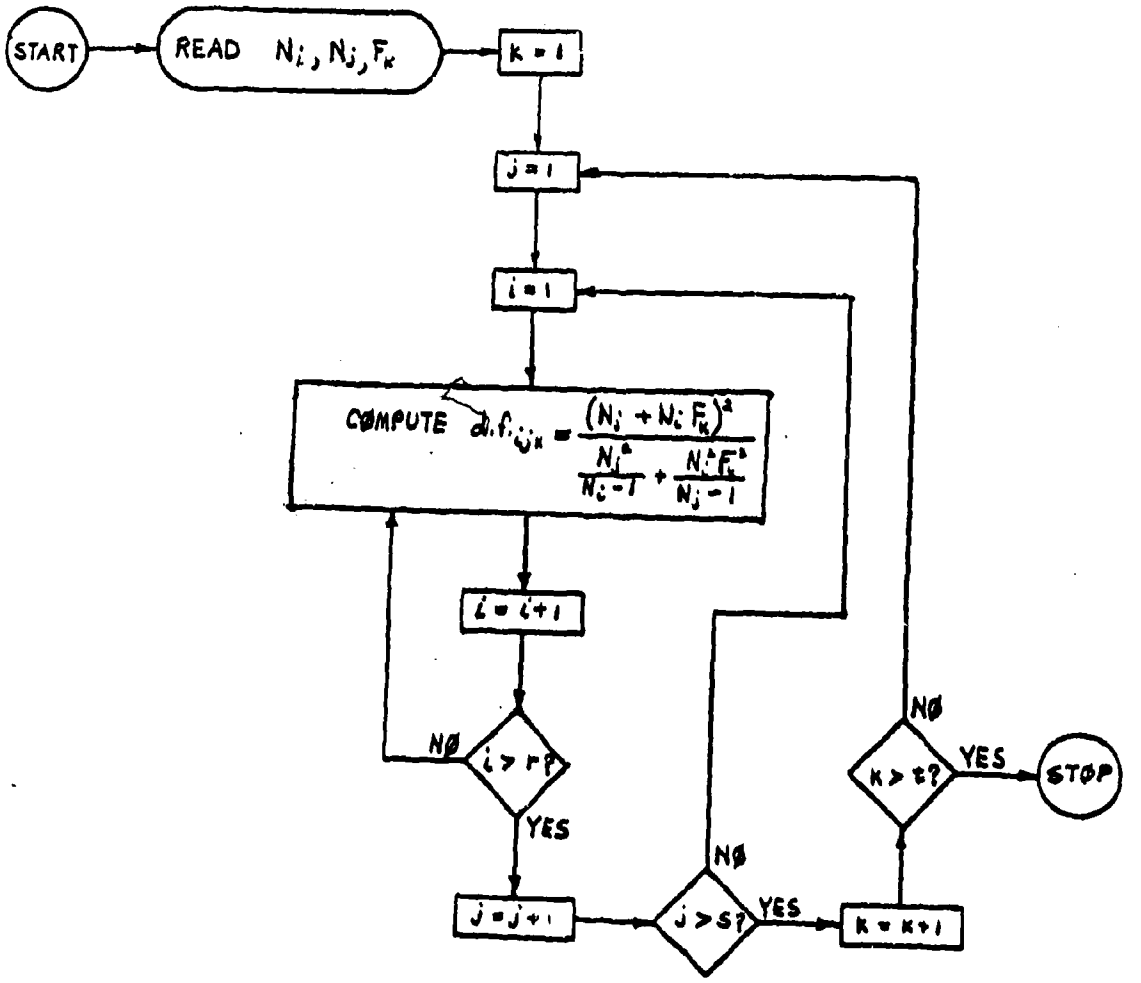

The Fortran statement for the above logic diagram is presented below as Figure 4.

Figure 4

```
      DEGREES ØF FREEDØM FØR UNEQUAL VARIANCE T-TEST
      DIMENSIØN SIZES(20),SIZEL(20),F(20),DF(20,20,20)
   99 READ INPUT TAPE 2,100,N1,N2,N3
  100 FØRMAT(3I2)
      READ INPUT TAPE 2,101,(SIZES(I),I=1,N1)
      READ INPUT TAPE 2,101,(SIZEL(J),J=1,N2)
      READ INPUT TAPE 2,101,(F(K),K=1,N3)
  101 FØRMAT(12F6.0)
      DØ 1000 K=1,N3
      DØ 1000 J=1,N2
      DØ 1000 I=1,N1
      UPPER=(SIZEL(J)+SIZES(I)*F(K))**2
      DENØM=(SIZEL(J)*SIZEL(J))/(SIZES(I)-1.)+(F(K)*SIZES(I))**2/
     1(SIZEL(J)-1.)
 1000 DF(K,J,I)=UPPER/DENØM
      DØ 400 K=1,N3
      WRITE ØUTPUT TAPE 3,301,F(K),(SIZES(I),I=1,N1)
  301 FØRMAT(1H1,7X,98HDEGREES ØF FREEDØM FØR TWØ PØPULATIØN T-TEST WITH
     1 UNEQUAL VARIANCES WHERE VAR(N2) EXCEEDS VAR(N1).,//10X,3HF =,F6.2
     2,//8H X      X,/8H  X N1 X,/8H    X    X,/8H     X  X,1X,18(F4.0,2X))
      WRITE ØUTPUT TAPE 3,3011
 3011 FØRMAT(8H  N2 X X,/6X,2HXX,/1X,115(1HX),/7X,1HX)
      DØ 400 J=1,N2
      WRITE ØUTPUT TAPE 3,302,SIZEL(J),(DF(K,J,I),I=1,N1)
  302 FØRMAT(2X,F4.0,1X,1HX,18(1X,F5.1))
      WRITE ØUTPUT TAPE 3,3022
 3022 FØRMAT(7X,1HX)
  400 CØNTINUE
      GØ TØ 99
      ENU(1,0,0,0,0,0,1,0,0,1.0,0,0,0,0)
```

The computed output follows the format as given in Figure 5

Example of the cutoffs for F = 3.50 and n_1, n_2 are 10, 12 ..... 44 in increments of 2

Cutoffs for the POPULATION T-TEST with UNEQUAL VARIANCES where VARIANCE EXCEEDS VARIANCE.

	10.	12.	14.	16.	18.	20.	22.	24.	26.	28.	30.	32.	34.	36.	38.	40.	42.
10.	11.8	13.2	12.7	12.3	11.9	11.6	11.4	11.2	11.0	10.9	10.8	10.7	10.6	10.5	10.4	10.3	10
12.	17.3	16.8	16.2	15.7	15.2	14.8	14.5	14.2	14.0	13.8	13.6	13.4	13.3	13.2	13.0	12.9	12.
14.	22.7	20.4	19.9	19.3	18.7	18.2	17.8	17.4	17.1	16.8	16.6	16.3	16.2	16.0	15.8	15.7	15.
16.	25.6	23.9	23.5	22.9	22.3	21.7	21.2	20.8	20.4	20.0	19.7	19.4	19.1	18.9	18.7	18.5	18.
18.	25.3	27.0	27.0	26.6	26.0	25.4	24.8	24.2	23.8	23.3	22.9	22.6	22.3	22.0	21.7	21.5	21.
20.	27.8	27.6	30.3	30.1	29.6	29.0	28.4	27.8	27.3	26.8	26.3	25.9	25.5	25.2	24.9	24.6	24.
22.	29.0	32.0	33.8	33.5	33.2	32.7	32.1	31.5	30.9	30.3	29.8	29.3	28.9	28.5	28.1	27.7	27.
24.	29.7	33.8	35.8	36.6	36.7	36.3	35.8	35.2	34.5	33.9	33.3	32.8	32.3	31.8	31.4	31.0	30.
26.	30.0	35.0	38.0	39.4	39.9	39.8	39.4	38.8	38.2	37.6	37.0	36.4	35.8	35.3	34.8	34.4	34.
28.	30.0	35.9	39.7	41.9	42.9	43.1	42.9	42.5	41.9	41.3	40.6	40.0	39.4	38.9	38.3	37.8	37.
30.	29.7	36.1	41.1	44.0	45.6	46.2	46.3	46.0	45.5	44.9	44.3	43.7	43.1	42.5	41.9	41.3	40.
32.	29.3	36.5	42.0	45.7	47.9	49.1	49.5	49.4	49.1	48.6	48.0	47.4	46.7	46.1	45.5	44.9	44.
34.	28.8	36.4	42.6	47.1	50.0	51.7	52.5	52.7	52.6	52.2	51.7	51.1	50.4	49.8	49.2	48.6	48.
36.	28.2	36.2	42.9	48.1	51.7	54.0	55.2	55.8	55.9	55.7	55.3	54.7	54.1	53.5	52.8	52.2	51.
38.	27.5	35.8	43.0	48.8	53.1	56.0	57.7	58.7	59.1	59.1	58.8	58.3	57.8	57.2	56.5	55.9	55.
40.	26.9	35.3	42.9	49.3	54.2	57.7	60.0	61.4	62.1	62.3	62.2	61.9	61.4	60.9	60.2	59.6	59.
[illegible]																	
[illegible]																	

APPENDIX C

1. Charts for n_1, n_2, F

   n_1, n_2 = 10, 12, 14 ....., 44

2. Chart for $n_1 = n_2 = n$, F

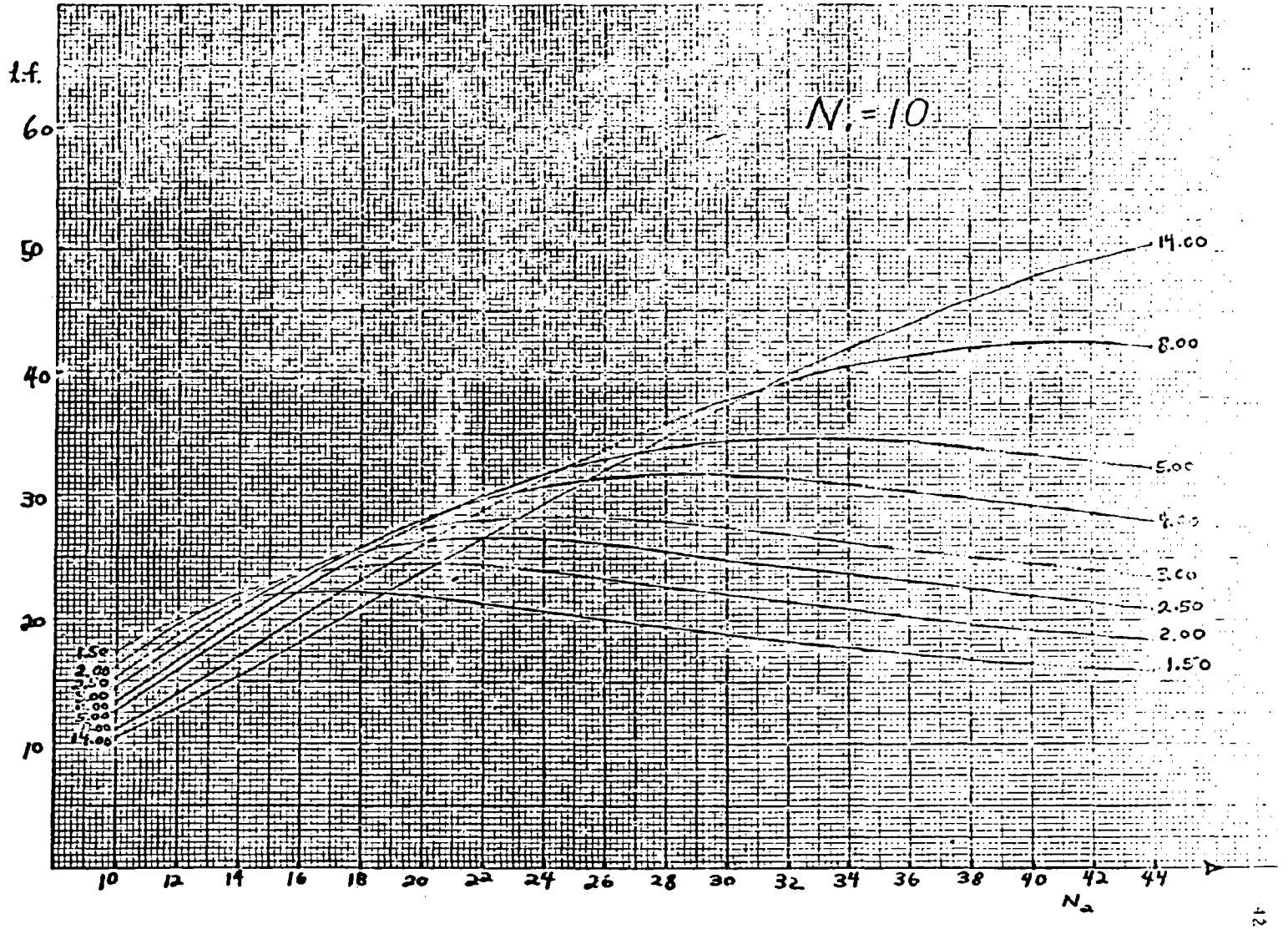
l.f.
60
50
40
30
20
10
$N_1 = 10$
14.00
8.00
5.00
4.00
3.00
2.50
2.00
1.50
1.50
2.00
2.50
3.00
4.00
5.00
6.00
8.00
14.00
10 12 14 16 18 20 22 24 26 28 30 32 34 36 38 40 42 44
N_2

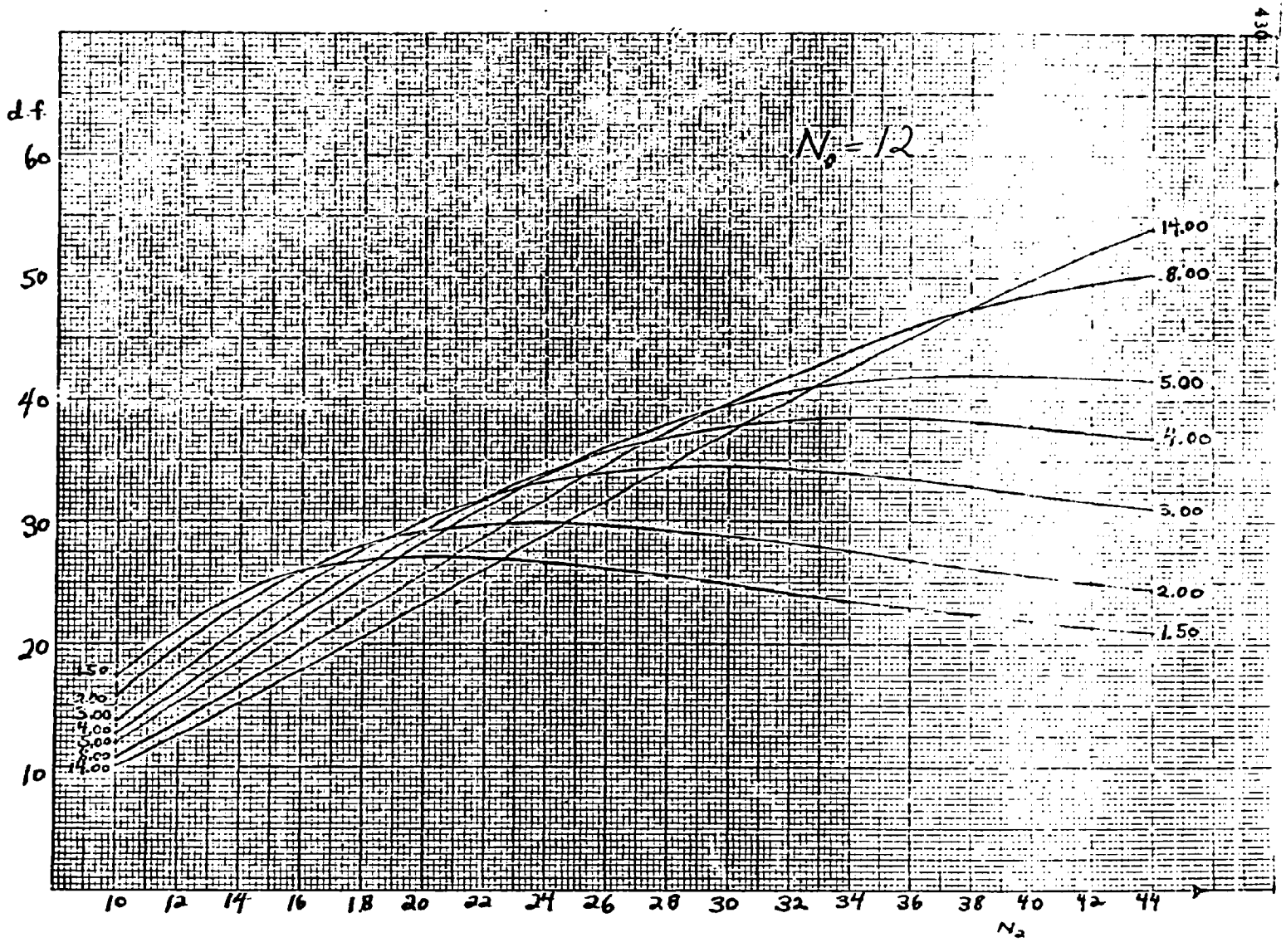
430
df
60
50
40
30
20
10
$N_0 = 12$
14.00
8.00
5.00
4.00
3.00
2.00
1.50
10 12 14 16 18 20 22 24 26 28 30 32 34 36 38 40 42 44
N_2

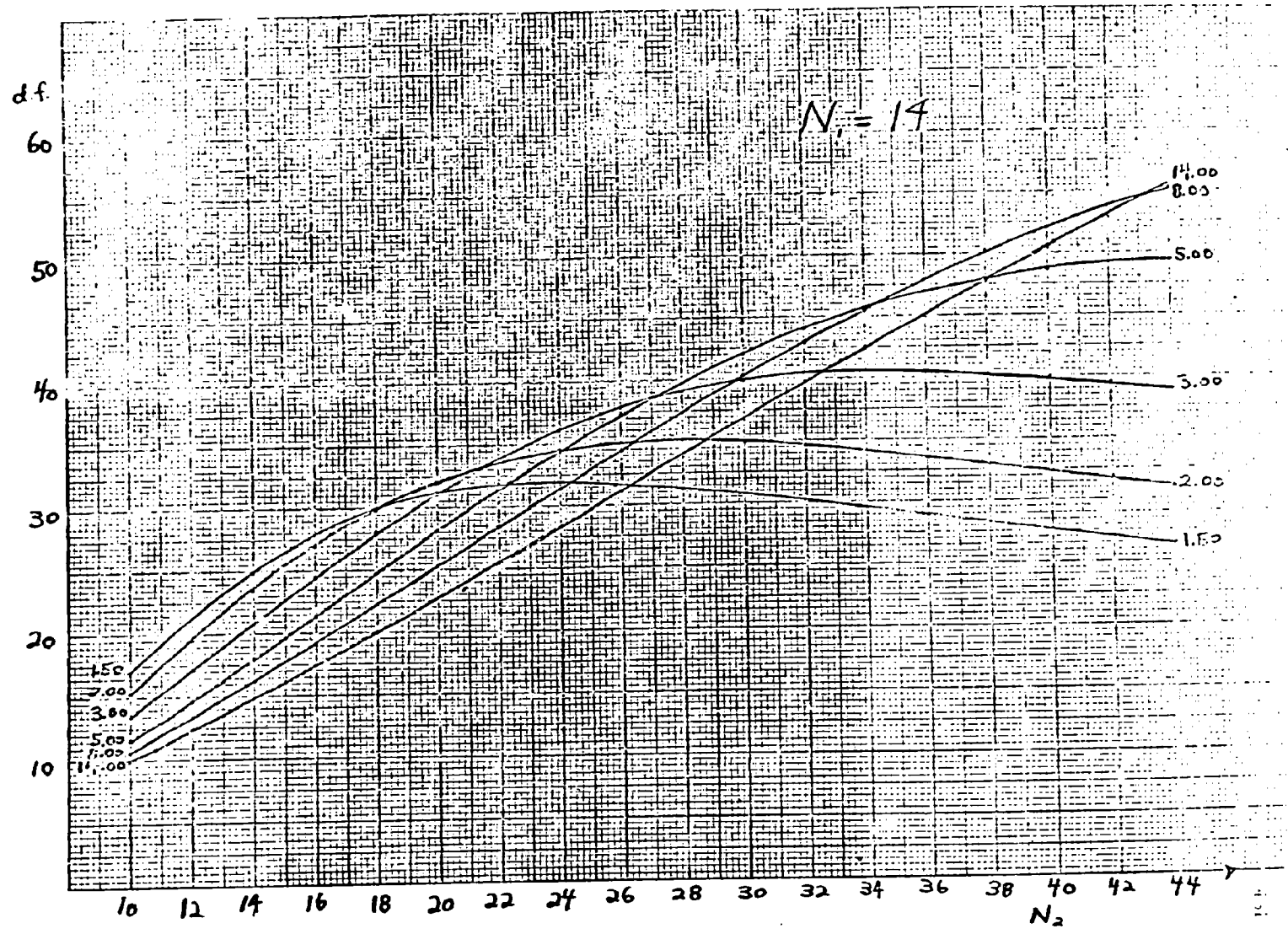
$N_1 = 14$
d.f.
60
50
40
30
20
10
14.00
8.00
5.00
3.00
2.00
1.50
1.50
2.00
3.00
5.00
8.00
14.00
10
12
14
16
18
20
22
24
26
28
30
32
34
36
38
40
42
44
N_2

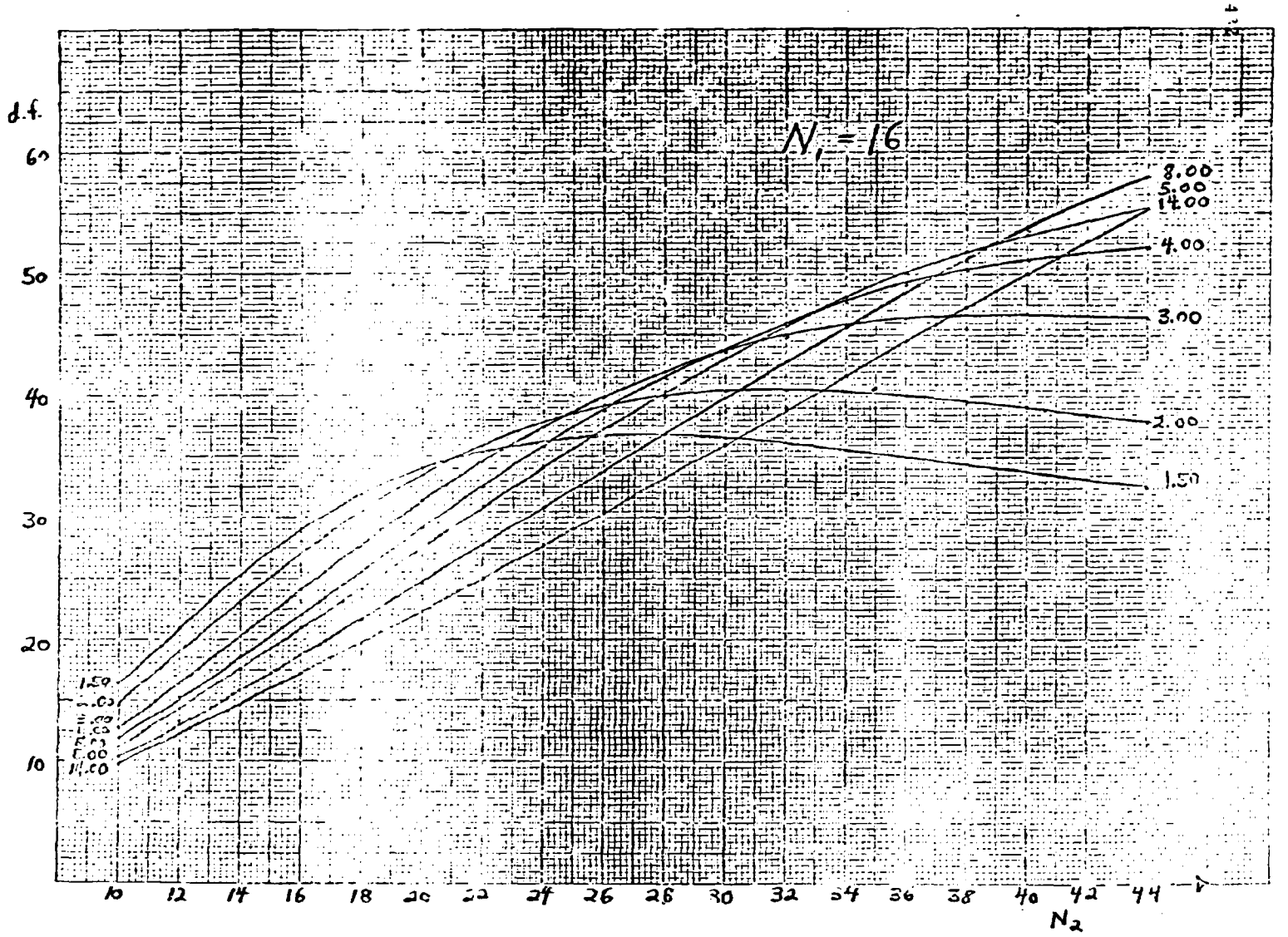
d.f.
60
50
40
30
20
10
$N_1 = 16$
8.00
5.00
14.00
4.00
3.00
2.00
1.50
10
12
14
16
18
20
22
24
26
28
30
32
34
36
38
40
42
44
N_2

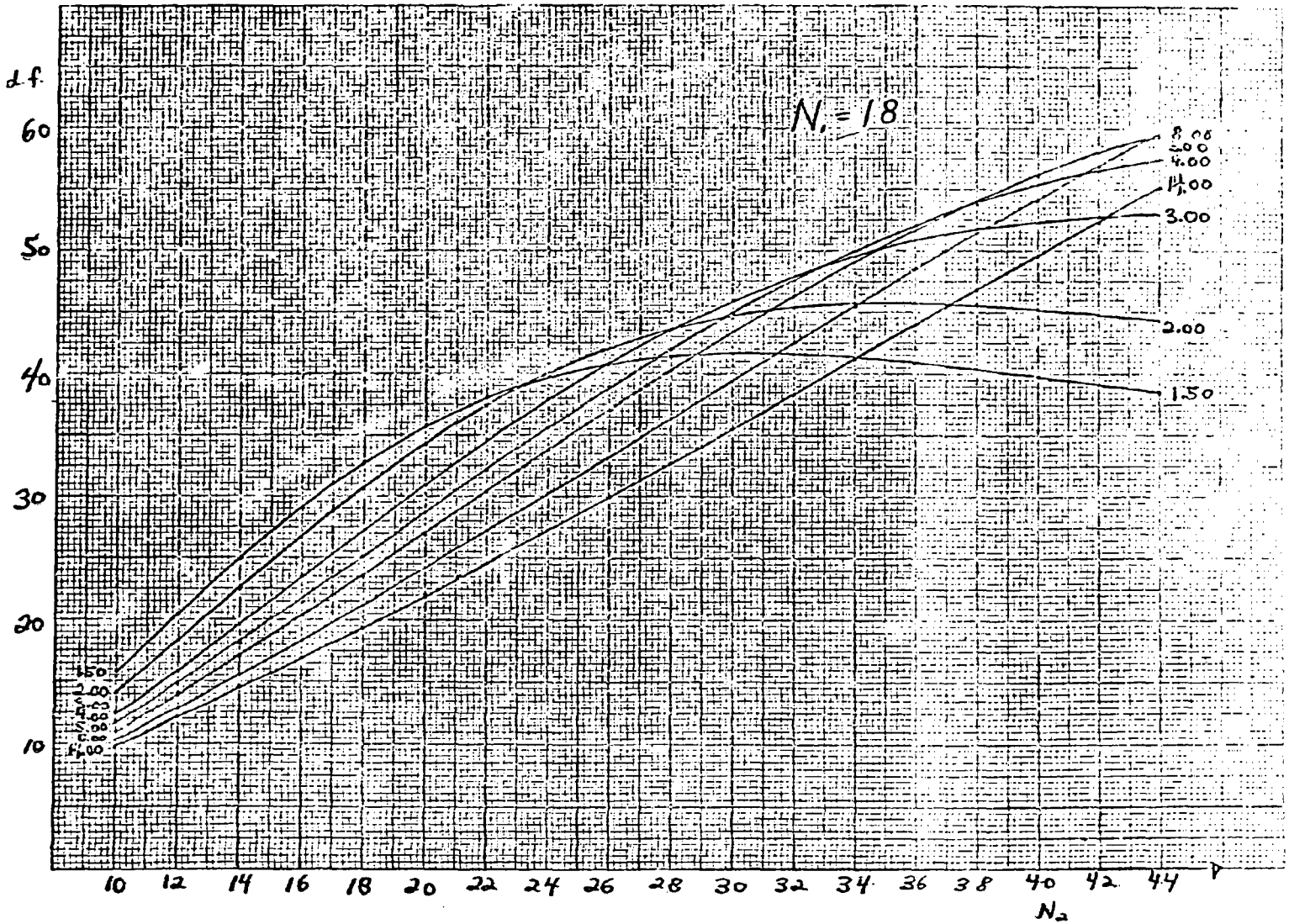
$N_1 = 18$
d.f.
60
50
40
30
20
10
8.00
4.00
3.00
2.00
1.50
10 12 14 16 18 20 22 24 26 28 30 32 34 36 38 40 42 44
N_2

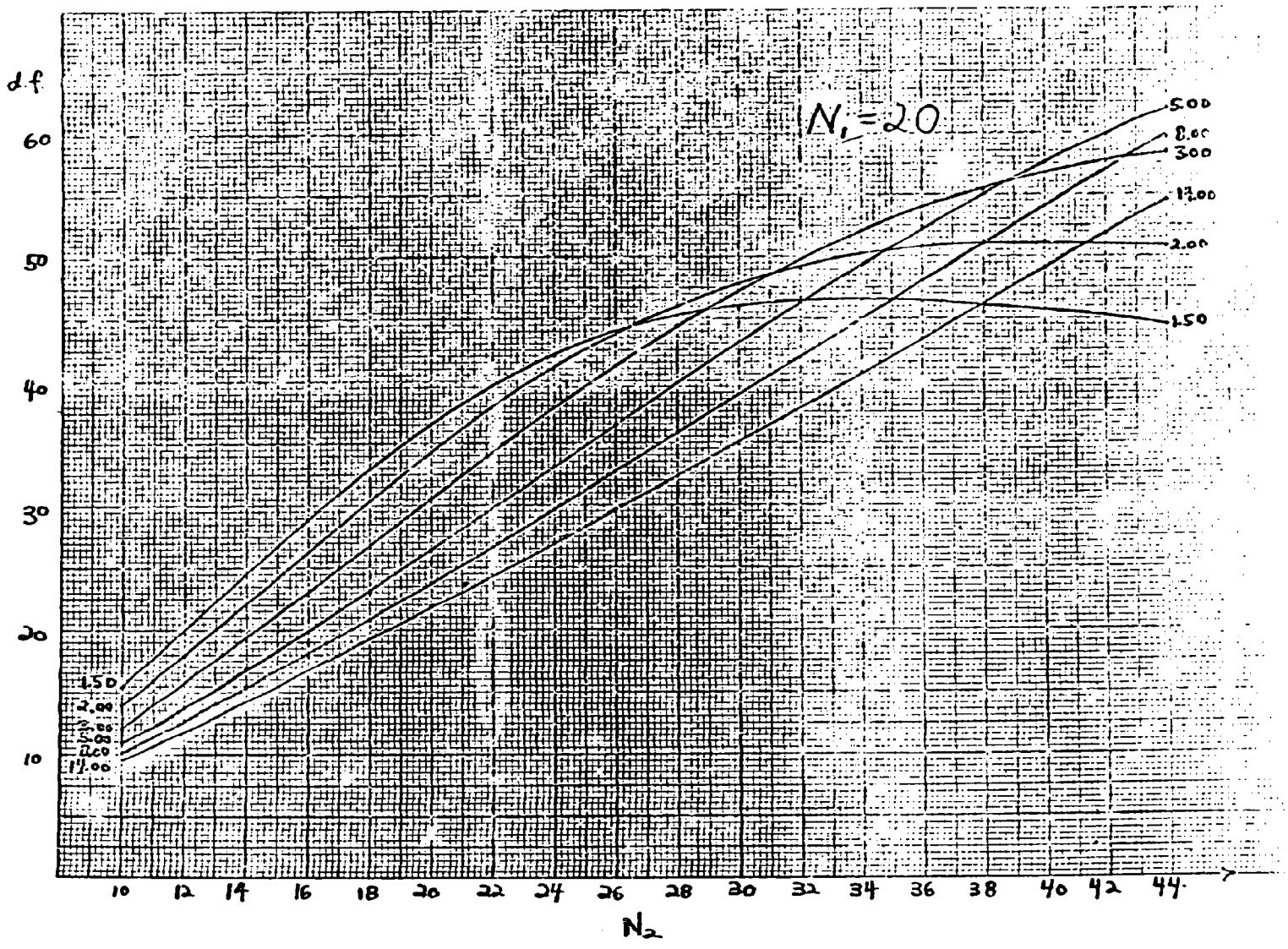
d.f
60
50
40
30
20
10
$N_1 = 20$
5.00
8.00
3.00
17.00
2.00
1.50
1.50
2.00
3.00
8.00
17.00
10
12
14
16
18
20
22
24
26
28
30
32
34
36
38
40
42
44
N_2

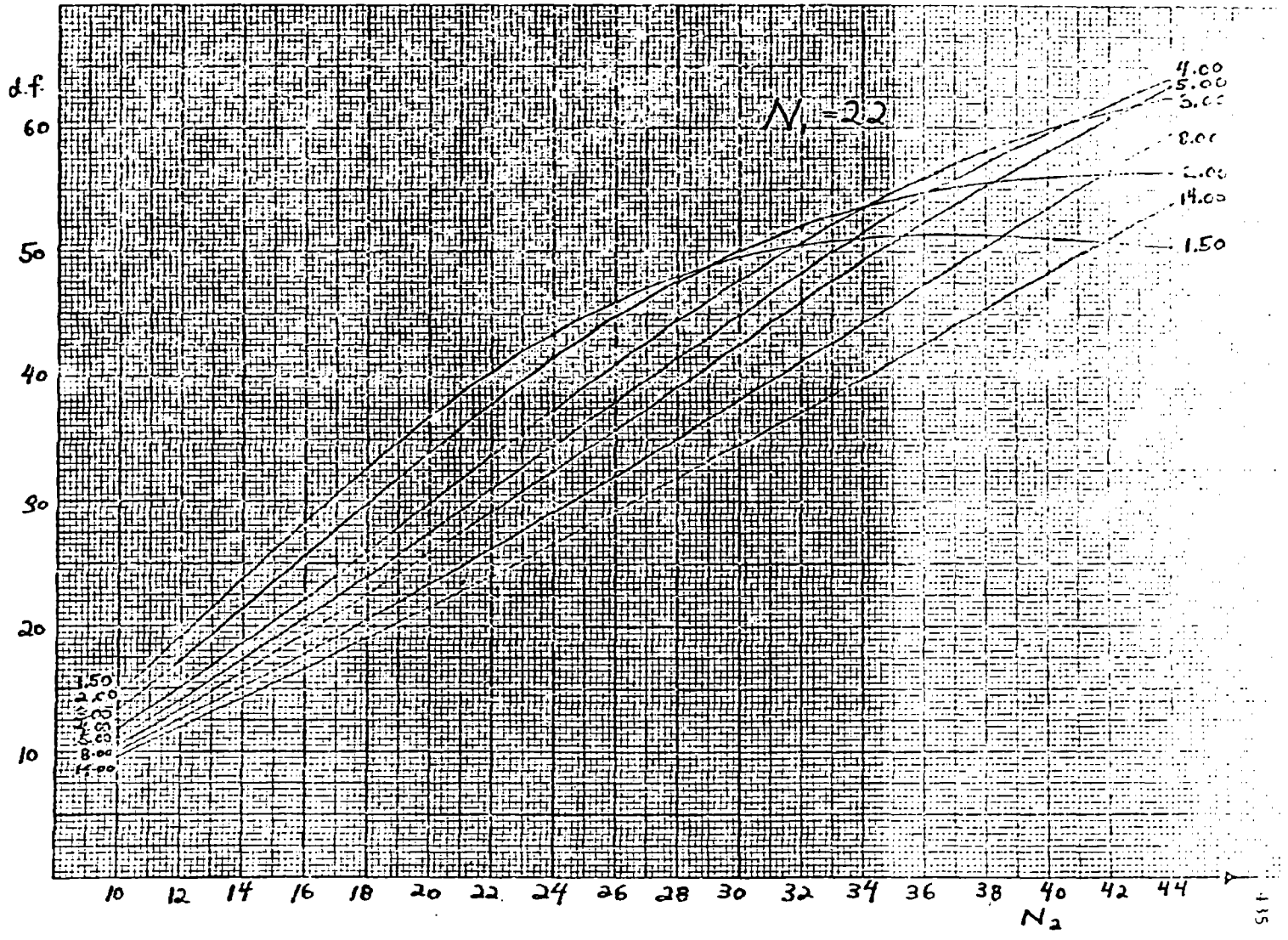
d.f.
60
50
40
30
20
10
$N_1 = 22$
4.00
5.00
8.00
2.00
14.00
1.50
3.50
2.00
4.00
5.00
8.00
14.00
10 12 14 16 18 20 22 24 26 28 30 32 34 36 38 40 42 44
N_2

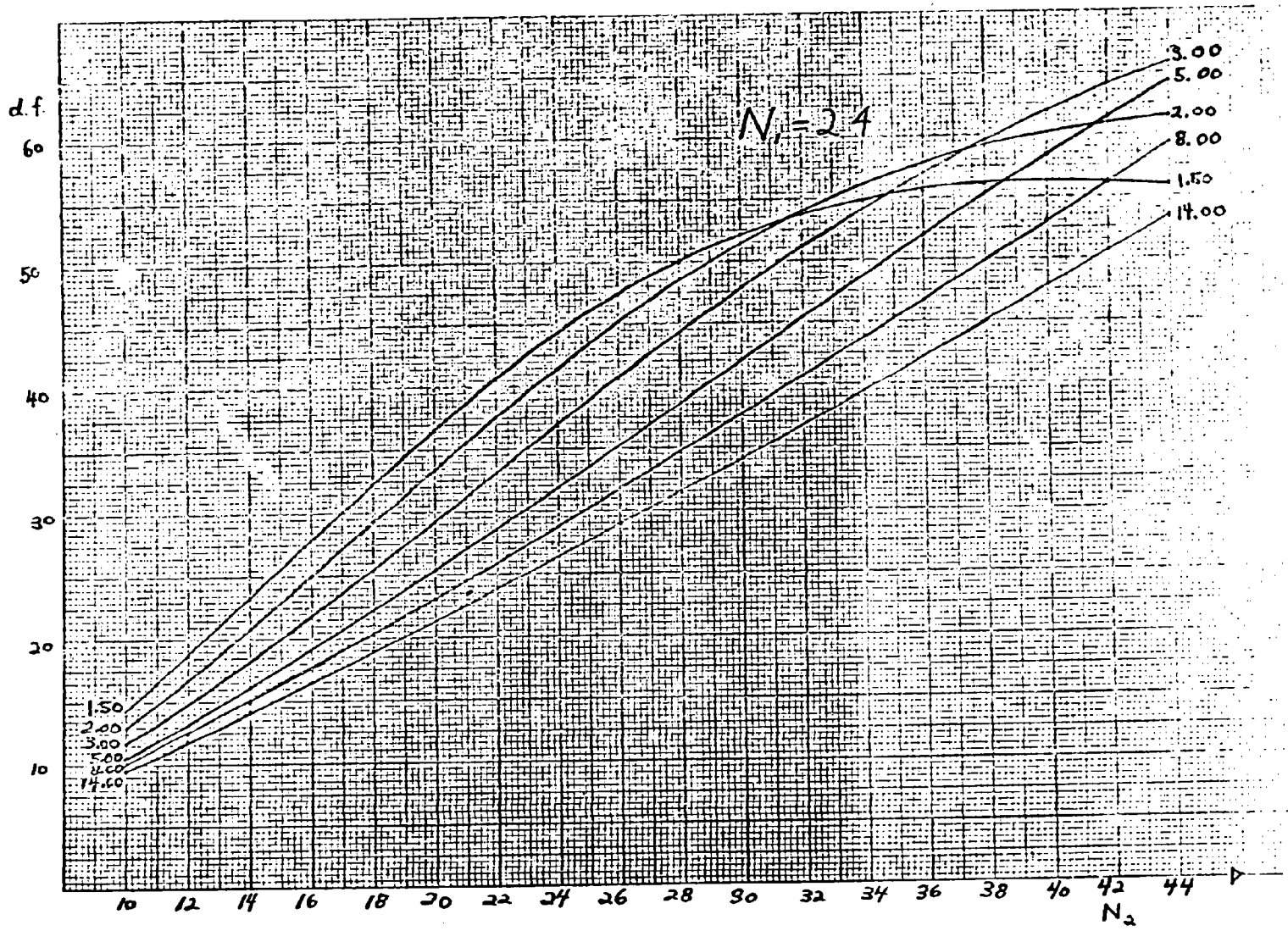
d.f.
$N_1 = 24$
3.00
5.00
2.00
8.00
1.50
14.00
60
50
40
30
20
10
1.50
2.00
3.00
5.00
8.00
14.00
10 12 14 16 18 20 22 24 26 28 30 32 34 36 38 40 42 44
N_2

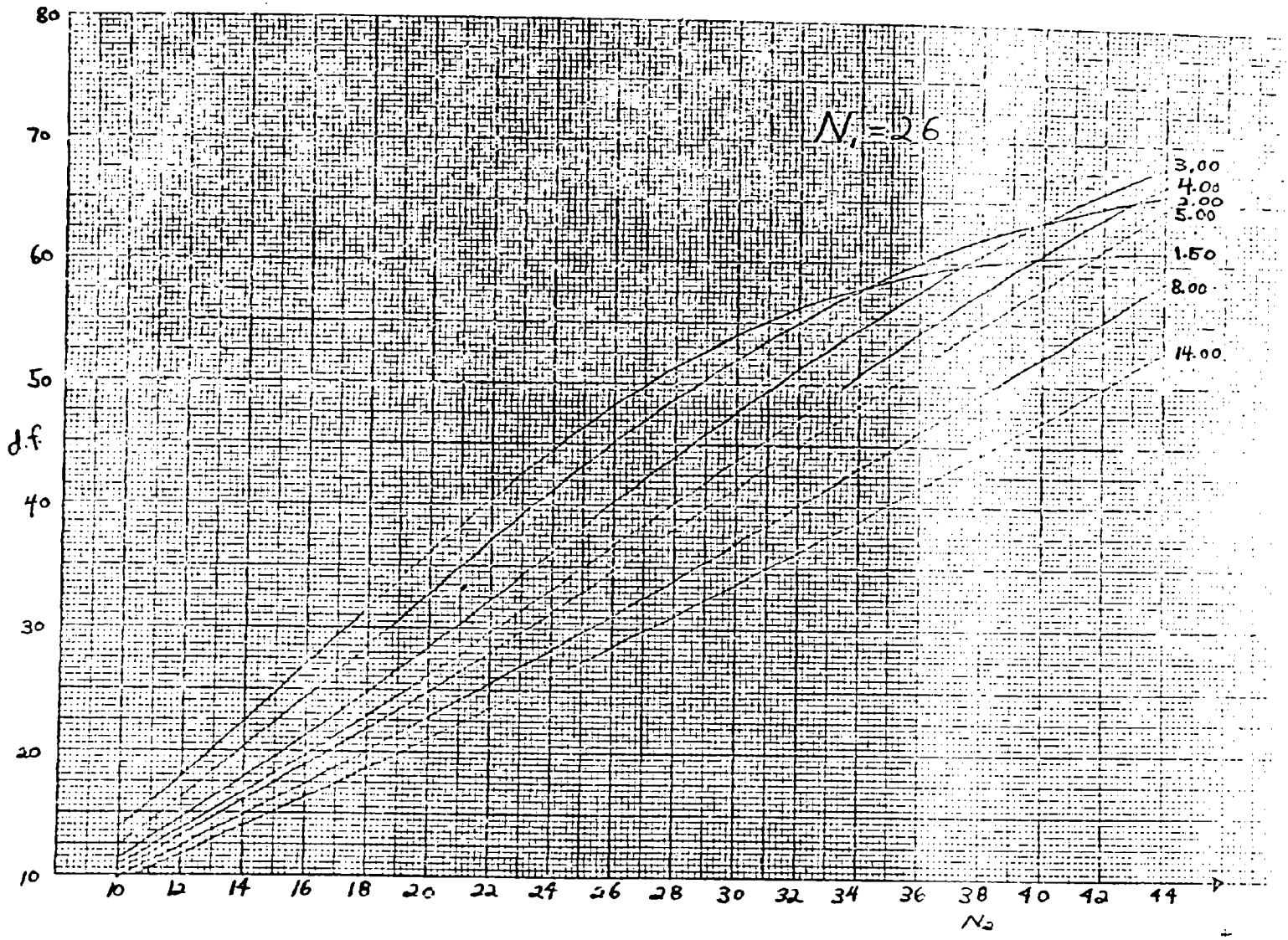
80
70
60
50
d.f.
40
30
20
10
$N_1 = 26$
3.00
4.00
2.00
5.00
1.50
8.00
14.00
10 12 14 16 18 20 22 24 26 28 30 32 34 36 38 40 42 44
N_2

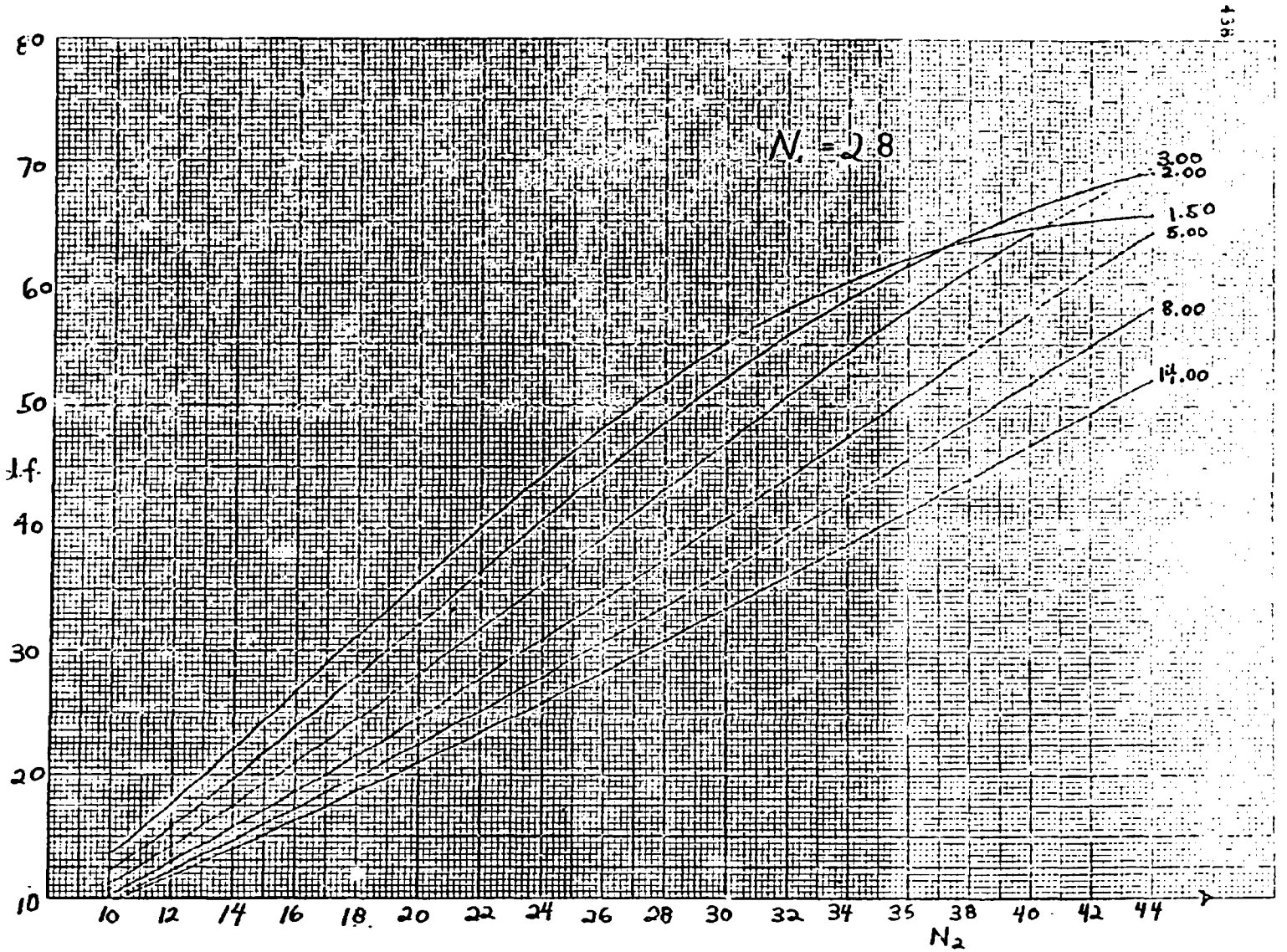
438
80
70
60
50
1.f.
40
30
20
10
N_2 = 28
3.00
2.00
1.50
5.00
8.00
14.00
10 12 14 16 18 20 22 24 26 28 30 32 34 35 38 40 42 44
N_2

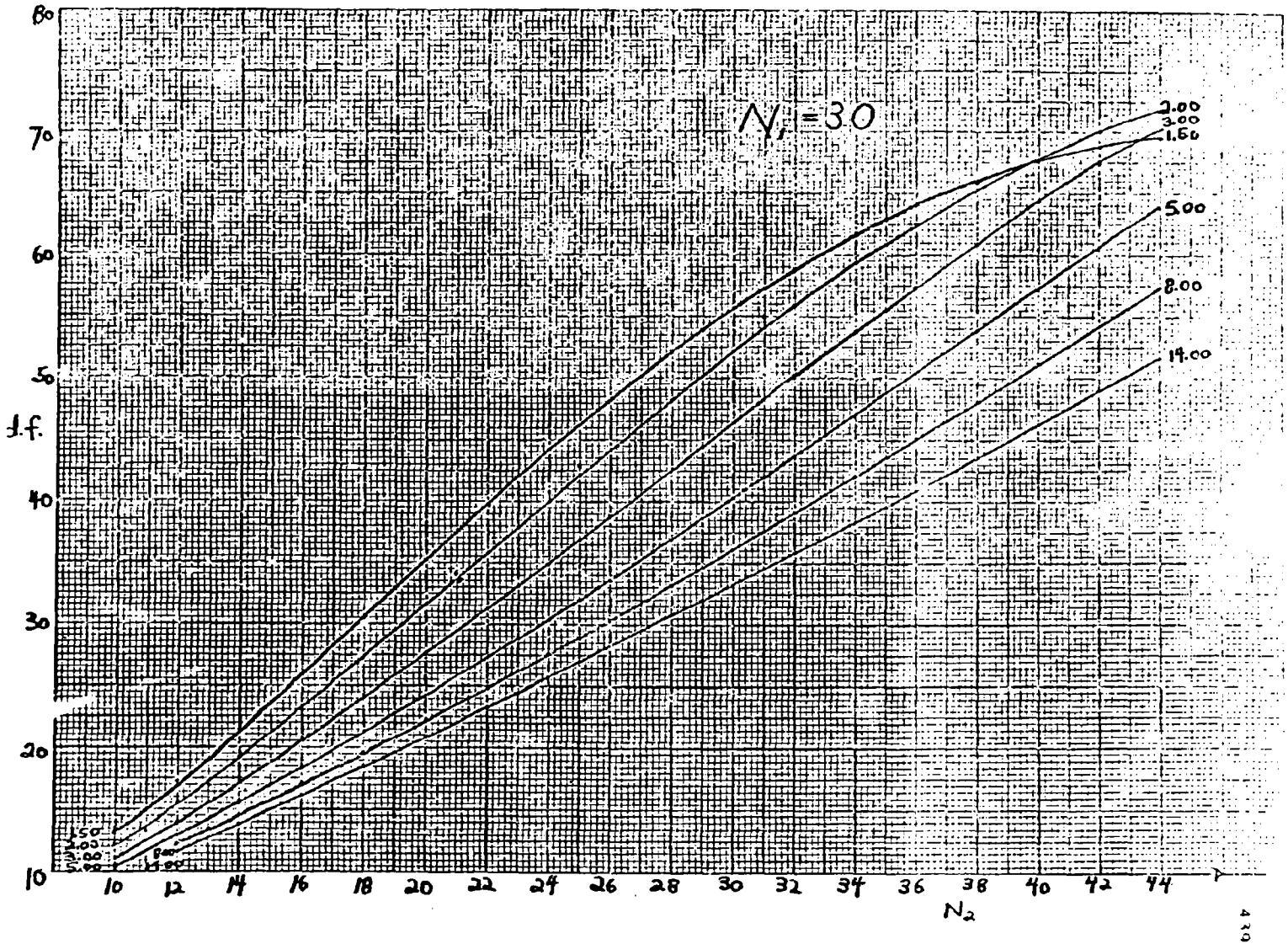
$N_f = 30$
2.00
3.00
1.60
5.00
8.00
14.00
1.50
2.00
3.00
5.00
8.00
14.00
80
70
60
50
40
30
20
10
l.f.
10
12
14
16
18
20
22
24
26
28
30
32
34
36
38
40
42
44
N_2
420

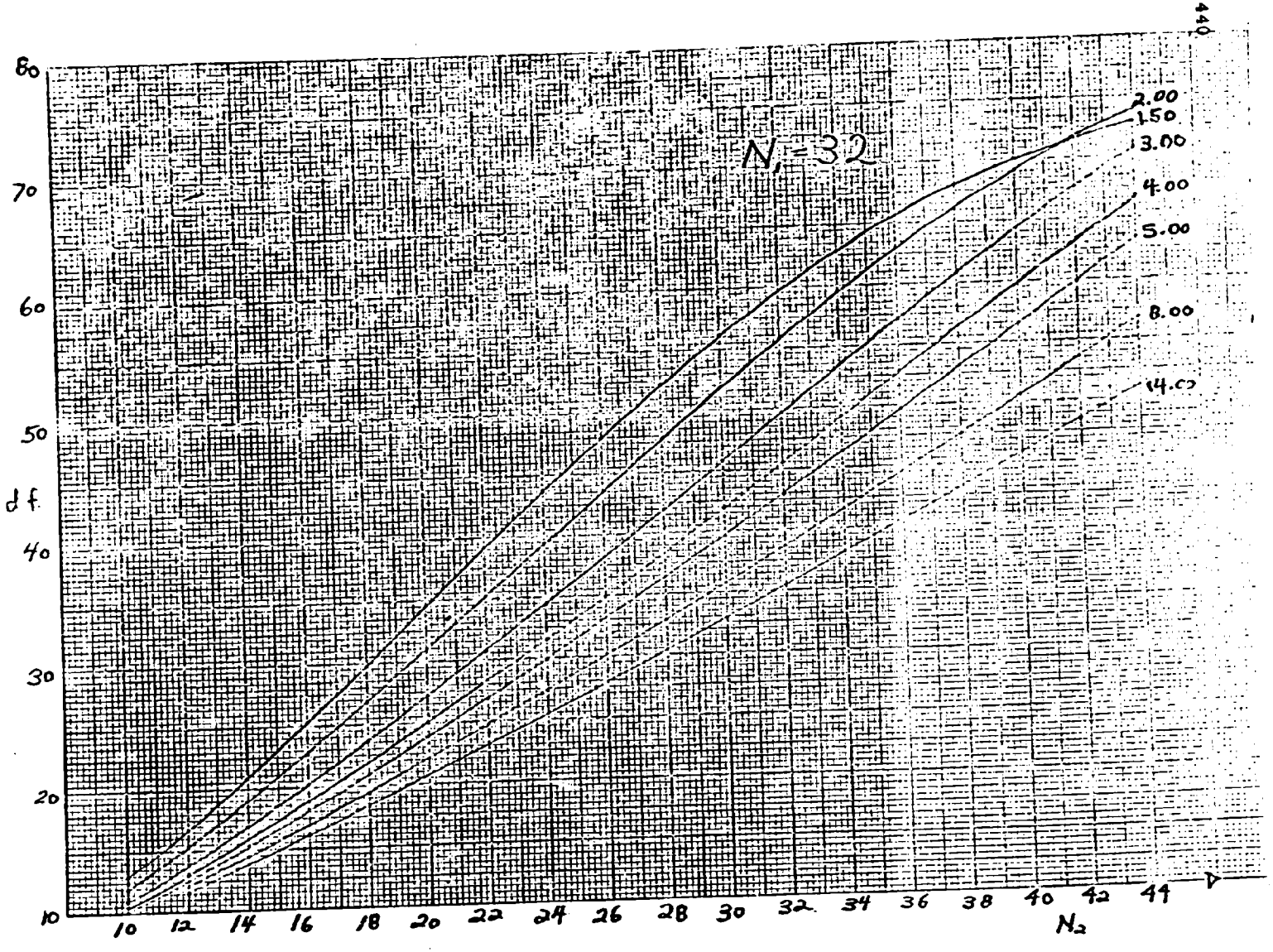
N₁ = 32
2.00
1.50
3.00
4.00
5.00
8.00
14.00
df
80
70
60
50
40
30
20
10
10 12 14 16 18 20 22 24 26 28 30 32 34 36 38 40 42 44
N₂

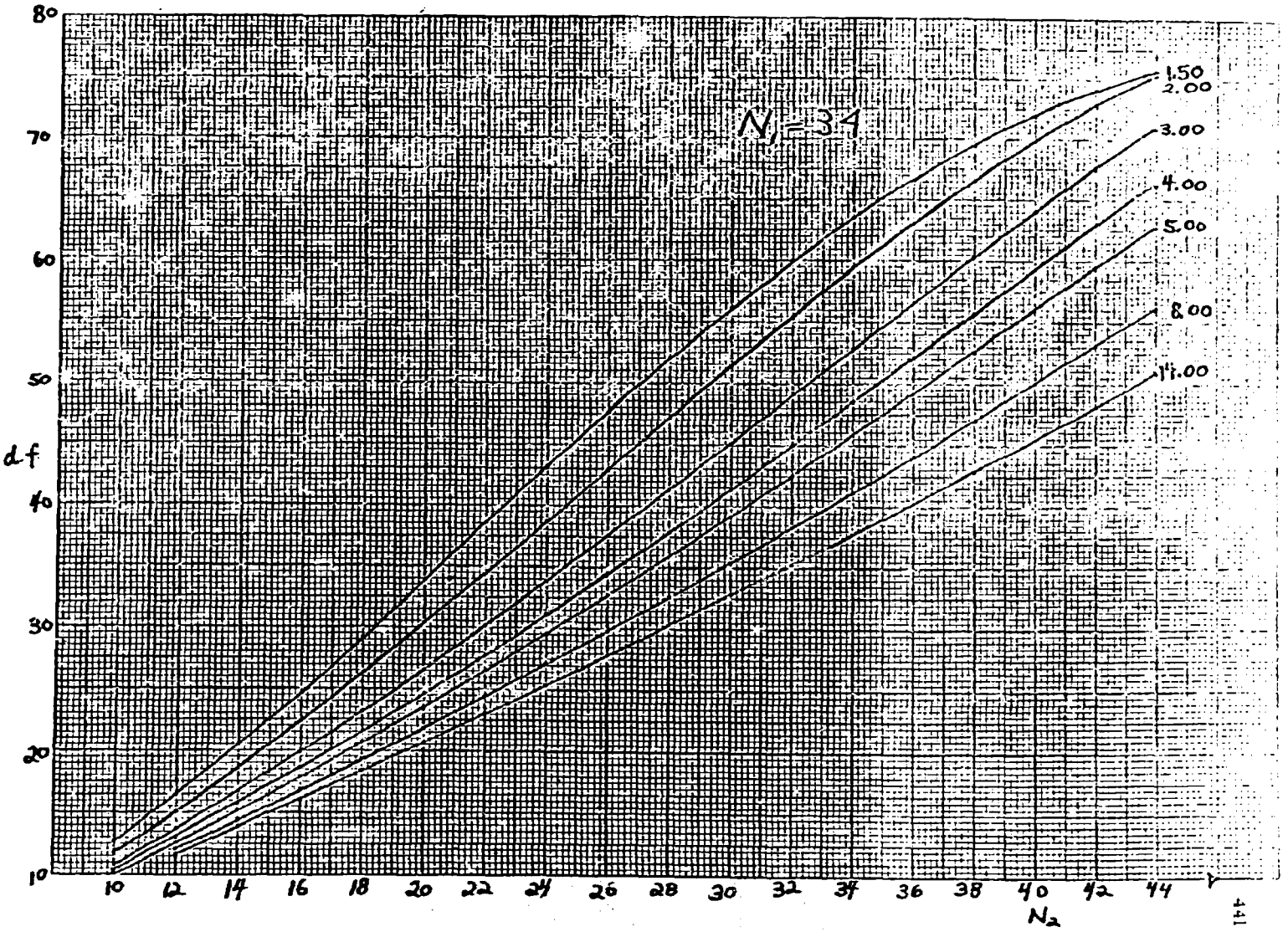
80
70
60
50
df
40
30
20
10
$N_1 = 34$
1.50
2.00
3.00
4.00
5.00
8.00
11.00
10 12 14 16 18 20 22 24 26 28 30 32 34 36 38 40 42 44
N_2
441

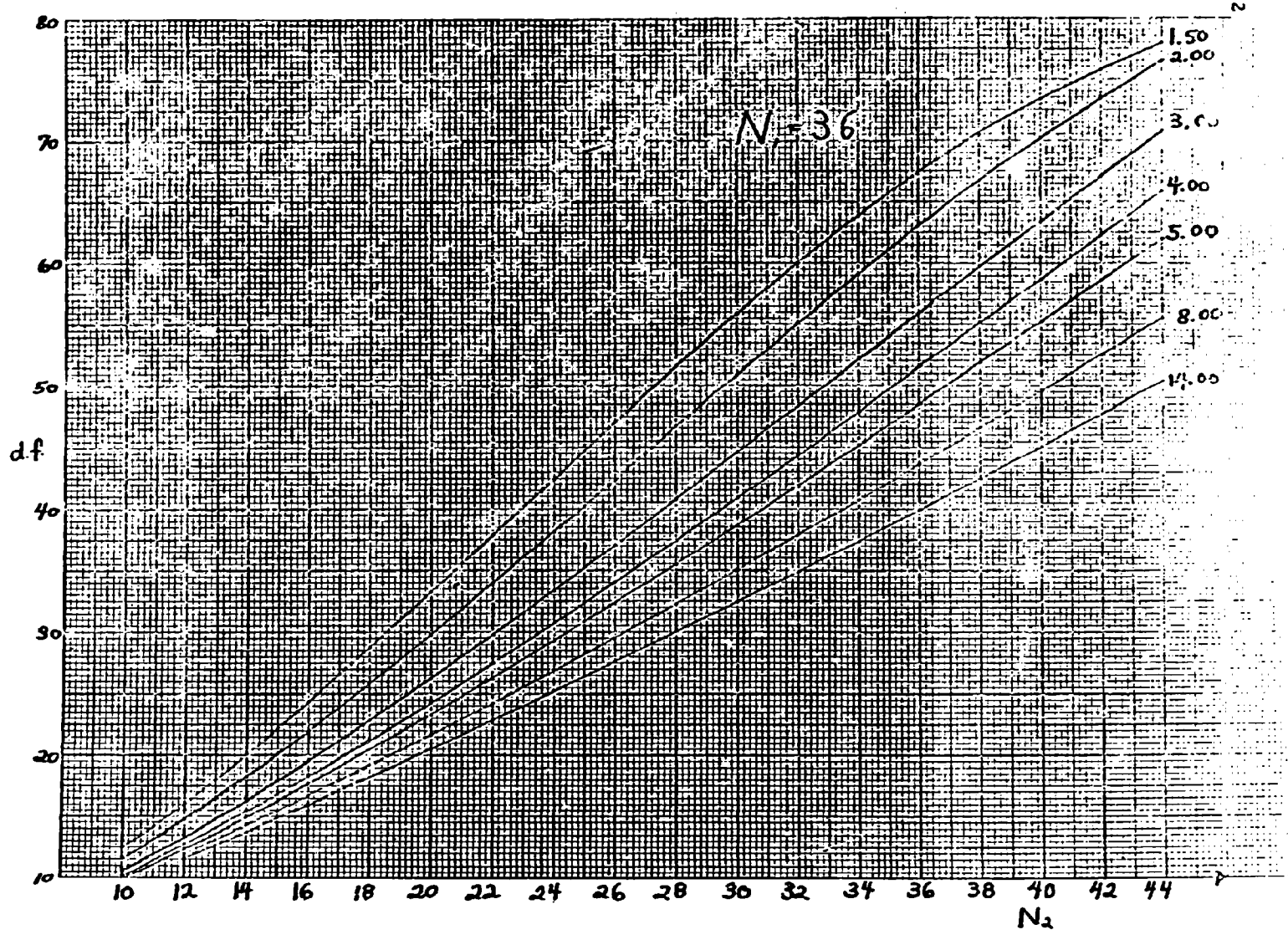
N=36
1.50
2.00
3.00
4.00
5.00
8.00
14.00
d.f.
80
70
60
50
40
30
20
10
10 12 14 16 18 20 22 24 26 28 30 32 34 36 38 40 42 44
N₂
P

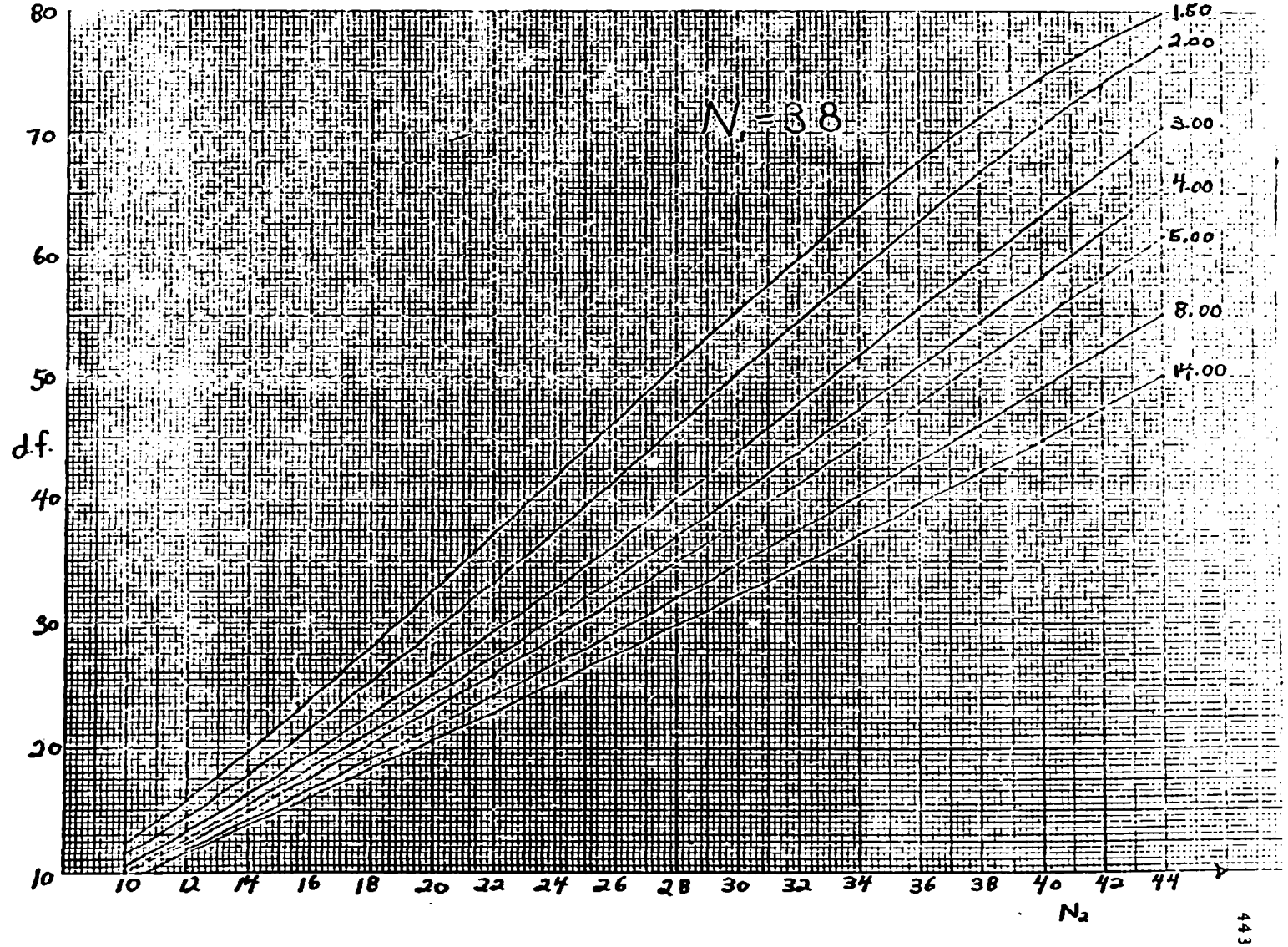
N₁=38
1.50
2.00
3.00
4.00
5.00
8.00
14.00
80
70
60
50
d.f.
40
30
20
10
10 12 14 16 18 20 22 24 26 28 30 32 34 36 38 40 42 44
N₂

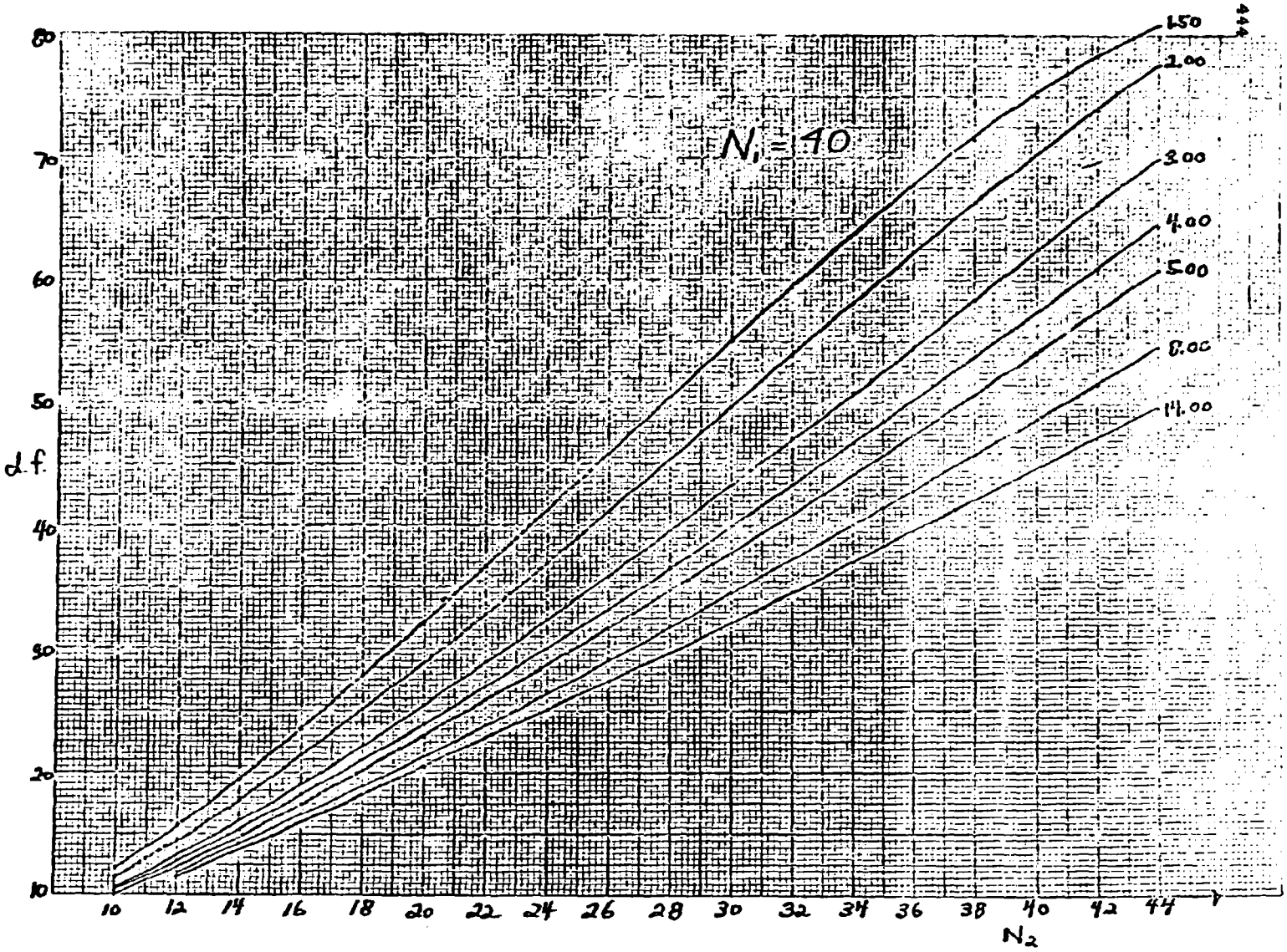
$N_1 = 40$
1.50
2.00
3.00
4.00
5.00
8.00
14.00
d.f.
80
70
60
50
40
30
20
10
10 12 14 16 18 20 22 24 26 28 30 32 34 36 38 40 42 44
N_2

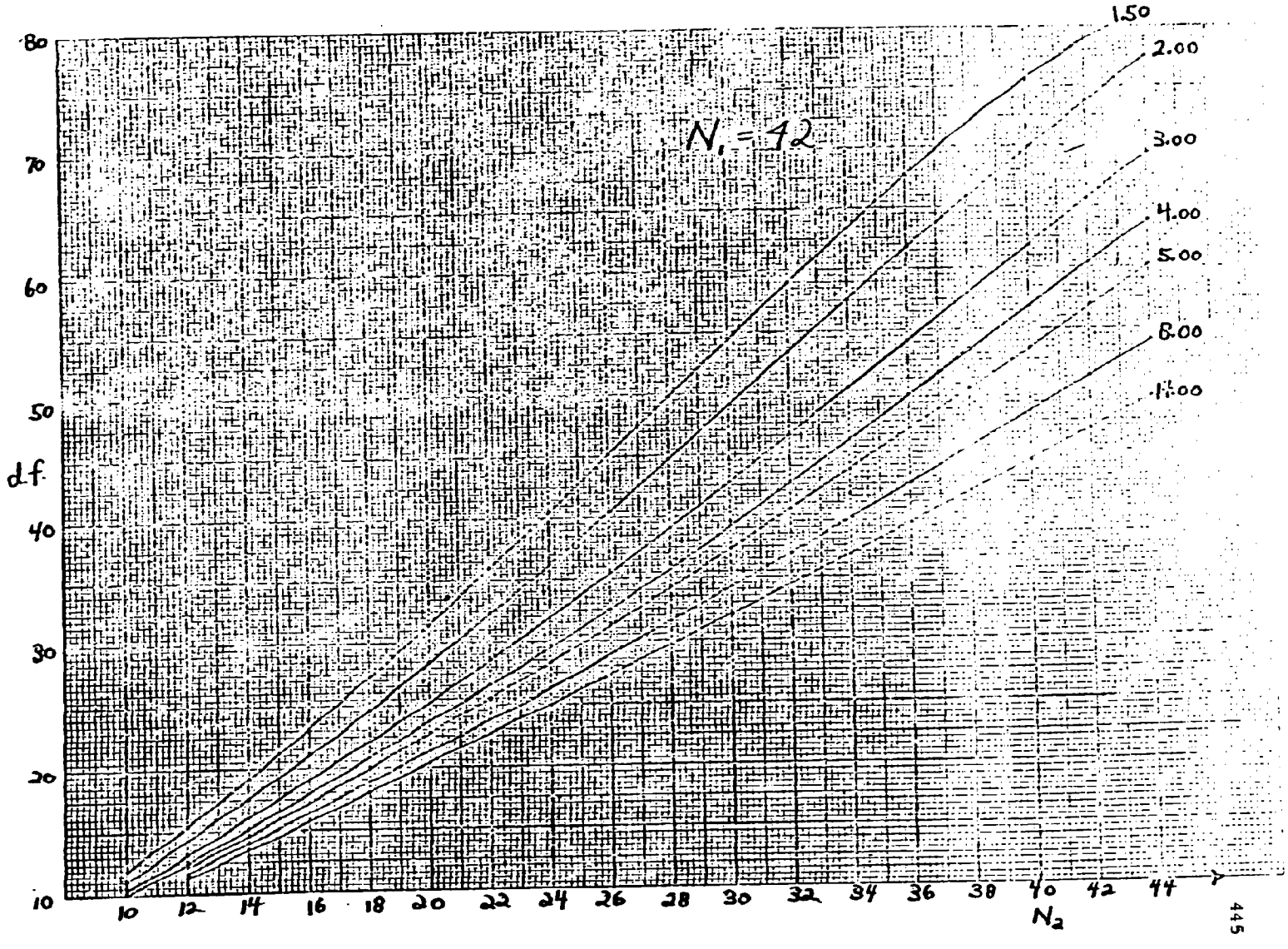
$N_1 = 12$
1.50
2.00
3.00
4.00
5.00
8.00
11.00
d.f.
80
70
60
50
40
30
20
10
10 12 14 16 18 20 22 24 26 28 30 32 34 36 38 40 42 44
N_2

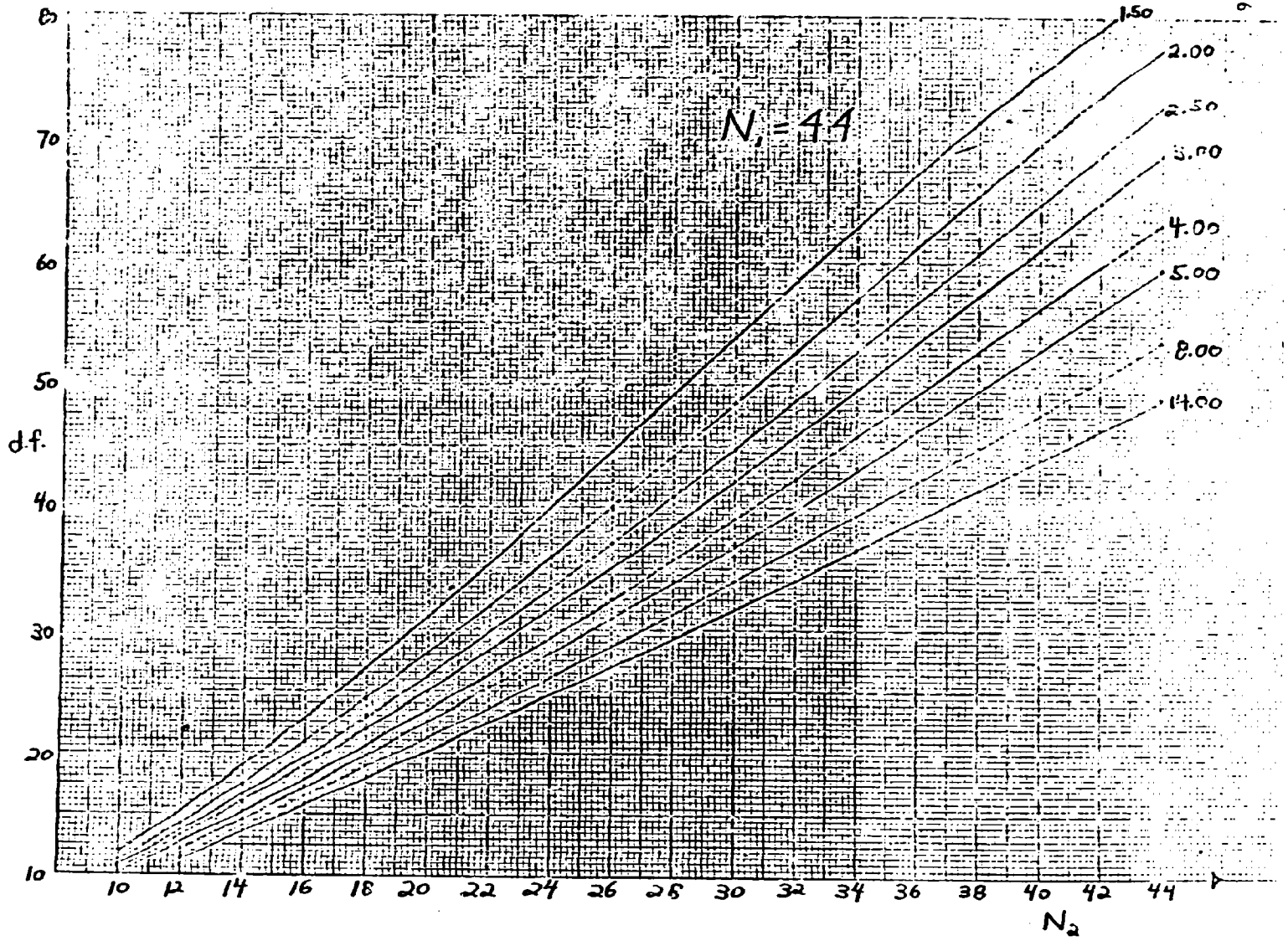
80
70
60
50
d.f.
40
30
20
10
$N_1 = 44$
1.50
2.00
2.50
3.00
4.00
5.00
8.00
14.00
10 12 14 16 18 20 22 24 26 28 30 32 34 36 38 40 42 44
N_2

Degrees of Freedom (d.f.) for Two Population t-Test when $n_1 = n_2 = n$ and $\sigma_1 \neq \sigma_2$

DELETING OBSERVATIONS FROM A LEAST SQUARES SOLUTION

Charles A. Hall
Technical Services Division, Data Analysis Directorate,
White Sands Missile Range, New Mexico

ABSTRACT. In this paper we give a matrix treatment of the classical least squares theory and determine each observation's contribution to the least squares solution. If each observation's (or observer's) contribution is known, then it may be possible to delete certain observations (or observers), (1) to improve the least squares solution or (2) to minimize the number of observations (or observers) entering the least squares solution. It should be emphasized that redundancy is necessary to obtain a statistically sound least squares solution, however it may be advantageously limited without significantly changing the solution.

Although we present a general least squares theory for uncorrelated observations, special emphasis is given to the least squares missile position problem generated by a set of observed azimuths, elevations and slant ranges from a system of missile tracking systems such as Radar. The above treatment is used to develope a geometric ordering of available tracking stations, which is then combined with station ability and reliability to determine pre-flight minimal station participation. That is, given an approximate trajectory and n available tracking stations we predict the minimum station combination for an adequate coverage of a flight along this trajectory.

1.0 INTRODUCTION. In this paper we give a matrix treatment of the classical least squares theory and determine each observation's contribution to the least squares solution. If each observation's (or observer's) contribution is known, then it may be possible to delete certain observations (or observers), (1) to improve the least squares solution or (2) to minimize the number of observations (or observers) entering a least squares solution. It should be emphasized that redundancy is necessary to obtain a statistically sound least squares solution, however it may be advantageously limited.

The following procedure has been applied successfully in [4, 5, 6] to the following problem:

GIVEN: An approximate missile trajectory and the co-ordinates of n tracking stations (Cinetheodolite, Radars or Dovap receivers) along with various other pre-flight data;

DETERMINE: The best minimal station combination (how many? and which ones?) for an adequate coverage of a flight along this trajectory.

We will use the n-station radar position solution presented in [5] as an example of the general theory which follows.

2.0 LEAST SQUARES THEORY. A brief outline of a least squares method following the notation of D. Brown [1] will now be given. The model under consideration is assumed to be non-linear. There are obvious simplifications if the model is linear.

Let $\{X_i\}$ be a set of random variates ($i = 1, 2, \ldots, q$)

$\{X_i^o\}$ be a set of uncorrelated observations of the set $\{X_i\}$,

For example: $\{A_i^o, E_i^o, R_i^o\}$, the set of azimuth, elevation and range readings from a system of n radar stations to a missile ($i = 1, 2, \ldots, n$).

Let $\{Y_j\}$ be a set of variates (parameters) dependent on the X_i,

$$Y_j = Y_j(X_1, X_2, \ldots, X_q) , \quad (j = 1, 2, \ldots, p) .$$

We note that the explicit form the for Y_j as functions of the X_i may not exist, in which case only an implicit form for this dependence is available.

For example: (x, y, z), the missile co-ordinates are dependent on A_i, E_i, R_i.

If the set $\{X_i\}$ is such that not all the X_i are necessary to determine the entire set of $\{X_i\}$, or what is of more importance here and in [5] , to determine the derived set $\{Y_j\}$, then the set $\{X_i\}$ is said to be over-determined. A least squares solution is in order. We need to find $\{Y_j'\}$ a set of approximations to $\{Y_j\}$ such that the sum of the squares of the residuals of the observed set $\{X_i^o\}$ is a minimum.

For example: In the n-station radar case [5] , each radar determines a missile position $(x(j), y(j), z(j))$, $(j = 1, 2, \ldots, n)$. These points will coincide with probability zero. We use the least squares method below to determine the "true" missile position.

We have $$X_i' = X_i^o + \gamma_i \quad (i = 1, 2, \ldots, q)$$

$$Y_j' = Y_j^o + \delta_j \quad (j = 1, 2, \ldots, p)$$

where $\{Y_j^o\}$ is a first approximation to $\{Y_j\}$, $\{X_i'\}$ and $\{Y_j'\}$ are least squares approximations and the γ_i and δ_j are undetermined residuals.

Suppose the minimum number of $\{X_i\}$ required to determine the entire set of $\{X_i\}$ is q_o, then the number of independent conditional equations relating the $\{X_i\}$ and $\{Y_j\}$ is $m = (q - q_o) + p$. Let these m equations be given by

$$(2.1) \qquad f_i(X_1, \ldots X_q, Y_1, \ldots, Y_p) = 0 \quad (i = 1, 2, \ldots, m).$$

For example: In the radar case if 3 observations are known (azimuth, elevation and range readings from one station) then the others can be determined, thus $m = (3m - 3) + 3 = 3m$. In this example

$$f_{3i-2} = A_i - \mathrm{Tan}^{-1}\left[\frac{y - y_i}{x - x_i}\right] = 0$$

$$f_{3i-1} = E_i - \mathrm{Tan}^{-1}\left[\frac{z - z_i}{[(x-x_i)^2 + (y-y_i)^2]^{1/2}}\right] = 0$$

$$f_{3i} = R_i - \sqrt{(x-x_i)^2 + (y-y_i)^2 + (z-z_i)^2} = 0$$

$(i = 1, 2, \ldots, n)$. Note that here (x_i, y_i, z_i) are the co-ordinates of of the i^{th} radar station.

Assume that the f_i can be expanded in a Taylor series about the point $t = (X_1^o, X_2^o, \ldots, X_n^o, Y_1^o, \ldots, Y_p^o)$. Approximate the f_i by the constant and linear terms of these Taylor expansions and replace X_i by $X_i^o + \gamma_i$. Equation (2.1) becomes (in matrix notation)

(2.2) $$AV + BD + E = 0 \quad \text{where}$$

A is the m by q matrix (A_{ij}) with $A_{ij} = [\partial f_i/\partial X_j]\ (t)$,
B is the m by p matrix (B_{ik}) with $B_{ik} = [\partial f_i/\partial Y_k]\ (t)$,
E is the m by 1 matrix E_i with $E_i = f_i(t)$

$$V = (\gamma_1, \gamma_2, \ldots, \gamma_q)^t \text{ and } D = (\delta_1, \delta_2, \ldots, \delta_p)^t.$$

For example: Note that A = I in the Radar and Cinetheodolite cases, and A is a scalar matrix in the Dovap case.

Assuming uncorrelated observations, the least squares solution is that which results in minimizing the weighted sum of the squares of the residuals

(2.3) $$S = V^t(\sigma)^{-1}V \qquad \text{where}$$

(σ) is the relative variance matrix of the observations $\{X_i^o\}$. The element $(\sigma)_{ii}^{-1} = W_i$ is the weight of the i^{th} observation.

For example: In the radar case the weight $(\sigma)_{jj}^{-1} = W_j$ can be determined as follows. Compute

$$\bar{x}_j = \frac{\sum_{i \neq j} x(i)}{n-1}$$

$$\bar{y}_j = \frac{\sum_{i \neq j} y(i)}{n-1}$$

$$\bar{z}_j = \frac{\sum_{i \neq j} z(i)}{n-1} \qquad (j = 1, 2, \ldots, n),$$

Compute the back azimuth: $\overline{A}_j = \mathrm{Tan}^{-1}\left[\dfrac{\overline{y}_j - y_j}{\overline{x}_j - x_j}\right]$

the back elevation: $\overline{E}_j = \mathrm{Tan}^{-1}\left[\dfrac{\overline{z}_j - z_j}{[(\overline{x}_j - x_j)^2 + (\overline{y}_j - y_j)^2]^{1/2}}\right]$

the back range: $\overline{R}_j = \sqrt{(\overline{x}_j - x_j)^2 + (\overline{y}_j - y_j)^2 + (\overline{z}_j - z_j)^2}$.

Let: $W_{3j-2} = 1 / (\overline{A}_j - A_j^o)^2$

$W_{3j-1} = 1 / (\overline{E}_j - E_j^o)^2$

$W_{3j} = 1 / (\overline{R}_j - R_j^o)^2$, $(j = 1, 2, \ldots, n)$.

In the terminology of matrix algebra the problem of least squares as considered by Brown [1, 2] and Hall [4, 5, 6] consists of determining of all possible vectors V and D satisfying (2. 2), those which minimize (2. 3).

We solve the constrained minima problem with the aid of Lagrange multipliers. Let $\lambda = (\lambda_1, \lambda_2, \ldots, \lambda_q)^t$, from (2. 2) and (2. 3) we have

(2.4) $$S = V^t (\sigma)^{-1} V - 2\lambda^t (AV + BD + E).$$

To determine the minimum value of S, equate to zero the partial derivatives of S with respect to the γ_i and δ_i.

Differentiation of S with respect to the residuals γ_i yields

(2.5) $$(\sigma)^{-1} V - A^t\lambda = 0 \quad \text{or} \quad V = (\sigma) A^t\lambda .$$

Differentiation of S with respect to the residuals δ_i yields

$$B^t\lambda = 0 . \tag{2.6}$$

Substitution of (2.5) into (2.2) yields

$$(A(\sigma)\, A^t)\lambda + BD + E = 0 . \tag{2.7}$$

If $(A(\sigma)\, A^t)$ is nonsingular then the least squares solution results from (1.) Solve (2.7) for $\lambda = -(A(\sigma)\, A^t)^{-1}(BD + E)$

(2.) Substitute λ into (2.6) and derive the Reduced Normal Equation

$$ND + C = 0 \quad \text{where} \tag{2.8}$$

$N = B^t(A(\sigma)\, A^t)^{-1} B$ and $C = B^t(A(\sigma)\, A^t)^{-1} E$.

(3.) Solve (2.8) for D.

(4.) Solve (2.5) for V.

In most cases the matrix $A(\sigma)\, A^t$ is nonsingular and (2.8) is valid. In the few cases where this is not true, it is possible to remove the difficulty by manipulating the conditional equations, [2].

We have computed a least squares approximation to the parameters $\{Y_i\}$ using an initial approximation. We now repeat this procedure using $\{Y_i'\}$ instead of $\{Y_i^o\}$ as an approximation and compute a new residual matrix D. The iteration continues until $||D||$ is sufficiently small.

Since we want to delete observations (or observers), we need some basis for determining which observations are the most likely candidates for deletion. We use the partial derivatives $\dfrac{\partial(\delta_1, \delta_2, \ldots, \delta_q)}{\partial(X_1, X_2, \ldots, X_p)}$ evaluated at t to aid in this determination.

3.0 DERIVATION OF D_U. As pointed out in the introduction there are two distinct motives for deleting observations. In general if we are trying

(a.) TO IMPROVE THE SOLUTION

WANT: $\partial\delta_j / \partial X_i^o$ small, so that errors in X_i^o will have little effect on δ_j.

DELETE: $\partial\delta_j / \partial X_i^o$ large, since a small error in X_i^o will result in a large error in the δ_j.

(b.) TO MINIMIZE PARTICIPATION

WANT: $\partial\delta_j / \partial X_i^o$ large, since this observation (X_i^o) has a great effect on the solution.

DELETE: $\partial\delta_j / \partial X_i^o$ small, since this observation (X_i^o) has little effect on the solution.

Let $U = (X_1, \ldots, X_q)$ and define the p by q matrix

$$D_U = [\partial/\partial U]\,[D] = \left[\begin{bmatrix} \frac{\partial}{\partial X_1^o} \\ \cdot \\ \cdot \\ \cdot \\ \frac{\partial}{\partial X_q^o} \end{bmatrix} [\delta_1, \delta_2, \ldots, \delta_p]\right]^t = \begin{bmatrix} \frac{\partial\delta_1}{\partial X_1^o} & \cdots & \frac{\partial\delta_1}{\partial X_q^o} \\ \cdot & \cdots & \cdot \\ \frac{\partial\delta_p}{\partial X_1^o} & \cdots & \frac{\partial\delta_p}{\partial X_q^o} \end{bmatrix}$$

where $\dfrac{\partial\delta_i}{\partial X_j^o} = \dfrac{\partial\delta_i}{\partial X_j}\,(t)$.

One of the objectives of this paper is the derivation of D_U. Note that $(D_U)_{ji}$ is the rate of change of δ_j (the correction in the dependent variable Y_j) with respect to the observation X_i^o.

For example: In the radar case $(D_U)_{ij}$ is the rate of change of the correction in one of the missile position co-ordinates with respect to a change in azimuth, elevation or range at the j^{th} station.

From (2.8) we have

$$D = -N^{-1} C = - [B^t(A(\sigma) A^t)^{-1} B]^{-1} [B (A (\sigma) A^t)^{-1}] E.$$

Since observational errors have no significant effect on the matrices A, B and (σ), they may be regarded as constants in the propagation of error under consideration. The vector E however is affected by the observational errors. Thus the error in D arises primarily from errors in E, which in turn are caused by errors in the observational vector U. Therefore

$$D_U = - N^{-1} R E_U \text{ where } R = B^t (A (\sigma) A^t)^{-1} \text{ and } E_U = [\frac{\partial}{\partial U}] [E] .$$

But $E_U = A$ and thus

$$D_U = - N^{-1} R A. \tag{3.1}$$

Note the simplification if A = I, as is the case in [4, 5].

4.0 VARIANCE - COVARIANCE MATRIX. A well known, [2.7], generalized law of covariance (in matrix notation) states that if $D = (\delta_1, \ldots, \delta_p)$ is a vector of functions of the elements of the vector $U = (X_1^o, X_2^o, \ldots, X_q^o)$ which has the variance matrix $\sigma_o^2 (\sigma)$, then the variance-covariance matrix of the vector D is given by

$$(\sigma_D) = \sigma_o^2 D_U (\sigma) D_U^t .$$

In our discussion this reduces to

$$(4.1) \qquad (\sigma_D) = \sigma_o^2 \, N^{-1} \ .$$

Note that σ_o^2 is the population variance and (σ) is a relative variance matrix of the observations.

In the radar case $\sigma_o^2 = \dfrac{\sum_{i=1}^{n} (\gamma_{i1}^2 w_{i1} + \gamma_{i2}^2 w_{i2} + \gamma_{i3}^2 w_{i3})}{3n - 3}$.

5.0 VARIABILITY ESTIMATE. For each correction δ_i of the derived quantities Y_i, a "variability estimate" will now be associated with each observation.

In the radar case, for each co-ordinate residual a variability estimate is associated with each tracking station.

Consider the matrix $H = \sigma_o \, D_U \, (\sigma)^{1/2}$. Note that

$$H_{ij} = \frac{\sigma_o}{w_j} \frac{\partial \delta_i}{\partial X_j^o} \ , \quad (i = 1, 2, \ldots , p; \ j = 1, 2, \ldots , q) \ ,$$

and

$$HH^t = (\sigma_D) \ .$$

It follows that the variance in the derived quantity Y_i

$$(5.1) \qquad \sigma_{Y_i}^2 = \sum_{j=1}^{q} H_{ij}^2 = \sum_{j=1}^{q} \frac{\sigma_o^2}{w_j^2} \left[\frac{\partial \delta_i}{\partial X_j^o} \right]^2 , \quad (i = 1, 2, \ldots , p).$$

Since H_{ij}^2 is the j^{th} observation's contribution to the variance in Y_i, we will refer to H_{ij}^2 as the "avriability estimate" in δ_i for the j^{th} observation, $(i = 1, 2, \ldots , p \ ; \ j = 1, 2, \ldots , q)$.

In the radar case there are three observations per station (azimuth, elevation and range) and thus the variability estimate "for the j^{th} station" is defined as the sum of the variability estimates (as defined above) for the azimuth, elevation and range readings at the j^{th} station. We are interested in eliminating stations and thus observations three at a time.

$$C_{ij}^2 = H_{i,3j-2}^2 + H_{i,3j-1}^2 + H_{i,3j}^2$$

is the variability estimate for the j^{th} station, where

$$X_{3j-2} = A_j,\ X_{3j-1} = E_j \text{ and } X_{3j} = R_j \quad (j = 1, 2, \ldots, 3n).$$

6.0 MOTIVES FOR DELETING OBSERVATIONS. We will now discuss motives or reasons why one might want to delete observations before computing a least squares solution.

6.1 TO IMPROVE LEAST SQUARES SOLUTION. In this case we are interested in deleting observations which are "extremely" poor, that is, observations which contribute greatly to the variances. Certainly if all of the H_{ij}^2 $(j = 1, 2, \ldots, q)$ are relatively close to being equal then no observation is predominately worse than the others and no observation should be deleted as a result of investigating the variability estimates. One should remember that usually the variances increase with a decrease in observations. However, if one (or more) observation's variability estimate is quite large in comparison to the others, then this observation would be considered a predominate contributor to the variances σ_{Yi}^2 (or least squares solution) and would definitely be a candidate for deletion. One must consider an observation's contribution to each variance σ_{Yi}^2 $(i = 1, 2, \ldots, p)$ when deciding if an observation should be deleted. There are various ways one might want to combine these contributions to the variances σ_{Yi}^2 so as to be able to order the observations (or observers). In the radar case we have three variances σ_x^2, σ_y^2, σ_z^2 $(p=3)$ to consider and define station constants

$$D_j = \sqrt{C_{1j}^2 + C_{2j}^2 + C_{3j}^2} \qquad (j = 1, 2, \ldots, n) \ .$$

The stations are then ordered according to the magnitude of their station constants. $(D_{i_1} \geq D_{i_2} \geq \ldots \geq D_{i_n})$.

To improve a least squares solution the station corresponding to the largest station constant is designated the most likely to be deleted.

This case of improving solution, not being our main motive for the study, has not yet been thoroughly investigated.

6.2 TO MINIMIZE THE NUMBER OF OBSERVATIONS. In this case we are not primarily interested in an improved solution, but rather deleting observations which contribute "very little" to the solution, so as to minimize the data that we must consider for a solution. The observations (or observers) that contribute least to the variances of those with the smallest variability estimates are the most likely candidates for deletion. Our motive here might be completely logistical.

In the radar case, it should be pointed out that the matrices needed to obtain the ordering of stations given above $(D_{i_1} \geq D_{i_2} \geq \ldots \geq D_{i_n})$ can be determined (or at least approximated) before flight. To find the variability estimates we need to know:

(1) $B = (b_{ij}) = \dfrac{\partial(X, Y, Z)}{\partial(A_j, E_j, R_j)}(t)$. This matrix is readily computed given station co-ordinates and an approximate missile position.

(2) $(\sigma) = dg\,(\sigma_{11}, \sigma_{22}, \ldots, \sigma_{3n,\,3n})$ = variance-covariance matrix of the observation variables. If the standard deviations $\sigma_{Aj}, \sigma_{Ej}, \sigma_{Rj}$ $(j = 1, 2, \ldots, n)$ are known from past histories then set:

$$(\sigma)_{3j-2,\,3j-2} = \sigma^2_{Aj} / \mathrm{Cos}^2 E_j / \sigma^2_o$$

$$(\sigma)_{3j-1,\,3j-1} = \sigma^2_{Ej} / \sigma^2_o$$

$$(\sigma)_{3j,\,3j} = \sigma^2_{Rj} / \sigma^2_o \qquad (j = 1, 2, \ldots, n)$$

where $\sigma^2_o = \dfrac{\sum_{j=1}^{n} (\sigma^2_{Aj} + \sigma^2_{Ej} + \sigma^2_{Rj} / R^2_j)}{3n}$.

In the Cinetheodolite Study, DR-Q has estimates of σ_{Aj} and σ_{Ej} and plans are being made to keep records for the Radar and Dovap systems.

If the standard deviations are not available, then the present weighting scheme at WSMR may be used setting

$$(\sigma)_{3j-2,\,3j-2} = 1/R^2_j \,\mathrm{Cos}^2 E_j$$

$$(\sigma)_{3j-1,\,3j-1} = 1/R^2_j$$

$$(\sigma)_{3j,\,3j} = 1 \qquad (j = 1, 2, \ldots, n).$$

In this latter case an approximation of σ^2_o is used instead of the above calculated values. (If neither of these weighting schemes are acceptable, then one can simply set $(\sigma) = I$.)

(3.) $D_U = -[B^t (\sigma)^{-1} B]^{-1} [B^t (\sigma)^{-1}]$ since $A = I$.

(4.) $H = \sigma_o D_U (\sigma)^{1/2}$, and thus the variability estimates and station constants are available before flight.

Thus before flight we can order the stations geometrically by inducing "observational" errors, with the standard deviations σ_{Aj}, σ_{Ej} and σ_{Rj}, in a simulated least squares solution.

It should be pointed out here that this ordering determines the best k station combination ($k \leq n$) as the stations $(i_1, i_2, \ldots, i_k)$. Otherwise one would have to consider $_nC_k = \frac{n!}{k!(n-k)!}$ possible combinations of k station solutions to arrive at this stage.

In the final stage the Minimal Station Participation problem [4, 5, 6] takes the form:

GIVEN: (1) A geometric ordering of n stations $(D_{i_1} \geq \ldots \geq D_{i_n})$,

(2) A reliability factor P_j for each station - the probability of successful operation if scheduled,

(3) Data precision factors for each variable (A, E, R) per station - σ_{Aj}, σ_{Ej}, σ_{Rj},

(4) Necessary data to determine tracking capabilities such as tracking rates (focal lengths and object size in the case of Cinetheodolite), etc.

FIND: A subsystem of k stations ($k \leq n$), k a minimum, such that for this particular point and missile we have:

(1.) Each station in the subsystem is able to track,

(2.) The probability of two or more (three or more in Cinetheodolite case) of the k stations will operate successfully is greater than P,

(3.) The geometric ordering given above is such that the stations deleted are insignificant contributors to the solution.

Thus we consider station ability, reliability and geometry in determining the Minimal Station Participation Before Flight (MSPARB) System.

The RADAR and DOVAP programs are in the process of being written. Consider the following SLIDE of the MSPARB Cinetheodolite program [4], as of 13 August 1965.

The input includes

(1) (x_j, y_j, z_j) ------- $(j = 1, 2, \ldots, n)$, WSCS co-ordinates of the j^{th} station,

(2) (x, y, z) --------- an approximate missile position,

(3) $(\dot{x}, \dot{y}, \dot{z})$ --------- approximate velocity components,

(4) $(\ddot{x}, \ddot{y}, \ddot{z})$ --------- approximate acceleration components,

(5) σ_{A_j} ---------- $(j = 1, 2, \ldots, n)$, the standard deviation in azimuth readings at the j^{th} station,

(6) σ_{E_j} ---------- $(j = 1, 2, \ldots, n)$, the standard deviation in elevation readings at the j^{th} station,

(7) k_{1j} ---------- $(j = 1, 2, \ldots, n)$, the angular velocity limit in azimuth for the j^{th} station,

(8) k_{2j} ---------- $(j = 1, 2, \ldots, n)$, the angular acceleration limit in azimuth for the j^{th} station,

(9) k_{3j} ---------- $(j = 1, 2, \ldots, n)$, the angular velocity limit in elevation for the j^{th} station,

(10) k_{4j} ---------- $(j = 1, 2, \ldots, n)$, the angular acceleration limit in elevation for the j^{th} station,

(11) F_j ---------- $(j = 1, 2, \ldots, n)$, effective focal length of the j^{th} camera,

(12) 0 ---------- object size

(13) P_j ---------- $(j = 1, 2, \ldots, n)$, the probability that station j will operate successfully if scheduled.

Notice that the criterion for deletion of stations contains three main considerations:

I. STATION ABILITY. All stations considered will first be tested as to inability to track for a certain interval for one or all of the following reasons:

(1) Image size too small,

(2) Tracking rates too large,

(3) Elevation angle too small.

II. STATION RELIABILITY. The minimum number of stations is chosen so that the probability of three or more stations operating successfully at any one time is greater than a pre-determined number.

III. STATION GEOMETRY. The stations are ordered according to station geometry. Stations are deleted if their geometric contributions are "insignificant".

Program output includes:

(1) Print out of all or part of input to program,

(2) Computed azimuth and elevation angles from each station to the point under consideration,

(3) Computed approximations to expected standard deviations in missile co-ordinates and angular standard deviation,

(4) Geometric ordering of stations to include station numbers and geometric factors,

(5) The probability that three or more of the stations in MSPARB will operate successfully if scheduled.

Modifications of the above MSPARB Cinetheodolite program since 13 Aug 65 include (1) a print out of error estimates for the system of the worst three stations in MSPARB as well as error estimates for MSPARB, (2) a print out of cumulative error estimates over the entire trajectory. (3) a print out

of how many times a station was used over the entire trajectory. (I have available here sample print outs for a few trajectories if anyone is interested.)

Areas where MSPARB can be used include:

(1) Schedule determination.

(2) Minimizing the current scheduling efforts.

(3) Determination of best launch point (balloons).

(4) Determination of best positioning of mobile units.

(5) Determination of best positioning of future station sites.

(6) Statement of expected system (MSPARB) errors - (confidence interval) - pre-flight.

(7) Determination of which system (Cinetheodolites, Radar, or Dovap) or combination of systems will yield the best trajectory coverage-BET.

(8) Pure error studies concerning geometry versus data precision.

Let us close by stating again that redundancy is necessary to obtain a statistically sound least squares solution, however, through the methods outlined here it can very definitely be advantageously limited.

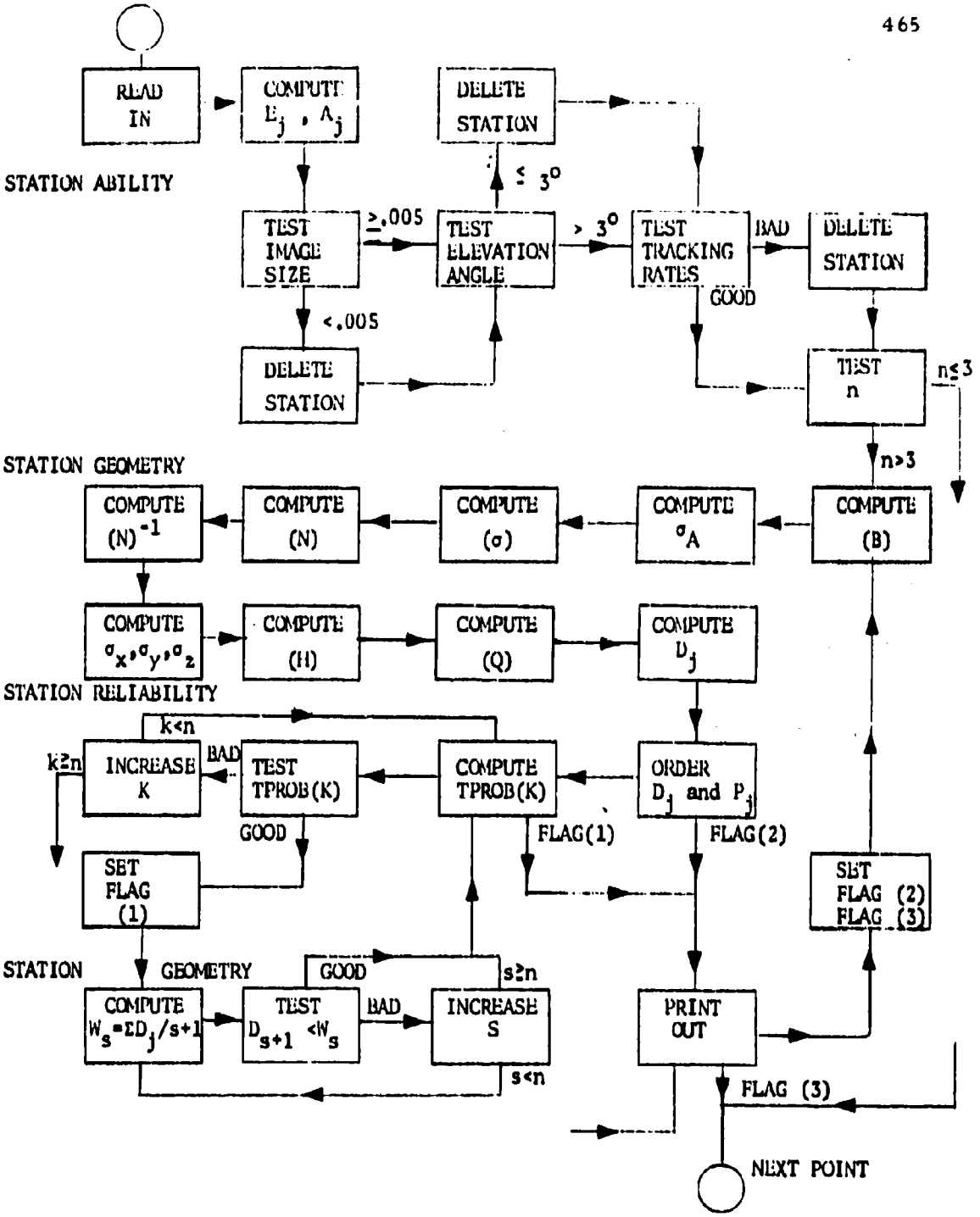

MSPARB
CINETHEODOLITES
as of 13 Aug 65

BIBLIOGRAPHY

1. BROWN, D. C., A Treatment of Analytical Photogrammetry, RCA Data Reduction Tech. Report No. 39, 1957.

2. BROWN, D. C., A Matrix Treatment of the General Problem of Least Squares Considering Correlated Observations, BRL Report No. 937, 1955.

3. COMSTOCK, WRIGHT, TIPTON, Handbook of Data Reduction Methods, Data Analysis Directorate (DR-T) Tech. Report, WSMR, 1964.

4. HALL, C. A., Minimal Station Participation Before Flight (MSPARB): Cinetheodolite Case, Data Analysis Directorate (DR-T) Tech. Report, WSMR, 1965.

5. HALL, C. A., Minimal Station Participation: Radar Case, DR-T Tech. Report, WSMR, 1965.

6. HALL, C. A., Minimal Station Participation: Dovap Case, DR-T Tech. Report, WSMR, 1965.

7. WORTHING and GEFFNER, Treatment of Experimental Data, New York, John Wiley and Son, 1948.

PRECISION AND BIAS ESTIMATES FOR DATA FROM CINETHEODOLITE AND AN/FPS-16 RADAR TRAJECTORY MEASURING SYSTEMS

Oliver L. Kingsley and Burton L. Williams
Range Instrumentation Systems Office
White Sands Missile Range, New Mexico

INTRODUCTION. A series of flight tests have been conducted at White Sands Missile Range in an effort to obtain a comparison of trajectory data derived from the measurements produced by different instrumentation systems. The instrumentation systems that have been used in some of these tests are Ballistic Camera, DOVAP, Cinetheodolite, and FPS-16 Radars. Interim reports were prepared, based on the data from the three earlier flights conducted on March 29, 1960, September 19, 1960, and January 29, 1962. Mr. Kingsley and Mr. Free presented a summary of the analysis and results of these earlier flights at the sixth, seventh and ninth annual meetings of this conference.

Purpose of Report

The fourth flight test was conducted on October 1, 1962 using a modified Nike Hercules Missile. The purpose of this report is to present an analysis of the bias and random error associated with some of the major range instrumentation systems used for this flight and to compare this data with the data from the earlier flight tests.

Comparability of Results and Earlier Flight Tests

The precision estimates are directly comparable but the bias estimates are not, because the comparison with trajectory data from the Ballistic Camera System was not available.

The earlier three flight tests were conducted at night so the Ballistic Camera System could be utilized to obtain trajectory data to be used as a standard for position bias error estimation. The Ballistic Camera, used on earlier tests, photographed a flashing light beacon on-board the missile against a star trail background. The light beacon flashes were controlled from the ground by a trasponder aboard the missile.

Fourth Flight Test

The fourth flight test was conducted during the daylight hours utilizing two cinetheodolite systems and seven AN/FPS-16 radar systems, though only two of the radar systems are analyzed here. The Askania Cinetheodolite System was used as the reference standard for system position bias error estimation for the Contraves cinetheodolite and FPS-16 radar systems. No DOVAP or Ballistic Camera systems were used for this fourth flight test. The AN/FPS-16 radar systems were operated successfully in the beacon tracking mode for the first time during this fourth test of the series. Attempts were made to use the FPS-16 radar systems in the beacon tracking mode for the three earlier flight tests, but the on-board beacon did not operate properly.

Position, Velocity and Acceleration, Precision and Bias

In addition to the estimates of bias and precision for the position data as given in the earlier reports, estimates of the bias and precision given for the derived velocity, acceleration and smoothed trajectory position data are presented. These fourth flight test estimates of bias for position, velocity and acceleration are based on data taken from the Askania cinetheodolite system.

PRECISION ESTIMATES FOR TRAJECTORY DATA.

Standard Deviation Estimate

Precision estimates were derived from trajectory data obtained from two cinetheodolite systems and two AN/FPS-16 radar systems in terms of standard deviations for the Cartesian component trajectory data. The standard deviation estimates were derived by the multi-instrument components of variance technique as given by Simon and Grubbs. [1,2]

Instrument Reduction for Position

The cinetheodolite trajectory position data were derived from a least squares reduction of angular measurements [3] . The Askania cinetheodolite system was a five instrument system making ten angular observations for each trajectory space point; the Contraves cinetheodolite system was a three instrument system for trajectory section one and a two instrument

system for trajectory section two, making six and four angular observations respectively for each trajectory space point. The radar trajectory position data were derived from the range, azimuth, and elevation observations that were reduced to the Cartesian coordinate system.

Mathematical Model

A mathematical model for the trajectory position data from the jth instrument system at the ith time may be written: $X_{ij} = X_i\,(\text{true}) + e_{ij}$, where e_{ij} represents a composite random error for the jth instrument system at the ith time. Standard deviation estimates were determined for these position data, and also for sets of smoothed position, velocity, and acceleration data that were derived by fitting a set of component position data to an eleven point second degree polynomial in time, and evaluating at the midpoint for successive trajectory space points (50 per trajectory section). The polynomial equation for the smoothed X-component data for the ith time would be of the form:

$$X_{ij}\,(\text{smoothed}) = a_{oj} + a_{1j}t_i + a_{2j}t_i^2 \tag{1}$$

for the jth instrumentation system. An error would generally be associated with each of the coefficients for the jth instrumentation system. A composite random error for the jth system can be expressed in the mathematical model:

$$X_{ij}\,(\text{smoothed}) = X_i\,(\text{true}) + \bar{e}_{ij} \tag{2}$$

where $\bar{e}_{ij}$ is the composite random error for the jth system at the ith time. The velocity equation is written:

$$\dot{X}_{ij} = a_{1j} + 2a_{2j}t_i \tag{3}$$

The composite random error for the velocity data can be expressed by the velocity equation:

$$\dot{X}_{ij} = \dot{X}_i\,(\text{true}) + \dot{e}_{ij} \tag{4}$$

where the composite random error in velocity ($\dot{e}_{ij}$) arises in the two of the terms of the velocity equation. A similar pair of equations could be written for the derived acceleration data.

Discussion of Precision Estimates

The position standard deviation estimates presented in Table I represent essentially random error in position data from the particular system. The standard deviation estimates range from two to twenty-two feet with the exception of trajectory section two for the Contraves system where the system geometry is very poor. Generally, this would not be considered satisfactory coverage; it is included for the sake of continuity.

The position, velocity, and acceleration standard deviation estimates presented in Tables II, III, IV, and V represent the residual random error in the derived (or smoothed) position, derived velocity, and derived acceleration data respectively. The velocity standard deviations for the cinetheodolite data ranged from two feet per second to eleven feet per second except for the second trajectory section for the Contraves cinetheodolite. The velocity standard deviations for the radar data ranged from three feet per second to sixteen feet per second. Velocity data derived from the radar observations is as good as the velocity data derived from the cinetheodolites with respect to variability. The cinetheodolite systems and the radar systems are essentially equivalent in variability with respect to the acceleration data; the only exceptional values are the two large acceleration standard deviations due to the poor system geometry for the Contraves system.

BIAS ESTIMATES FOR TRAJECTORY DATA.

Standards Used In Computation.

All of the bias estimates for Flight Test Nr. 4 of the Operation Precise Program are based on trajectory data from the Askania cinetheodolite system with a mode of ten angular measurements. Earlier flight tests have used trajectory data from the Ballistic Camera System which was based on star trail background for calibration. The Askania system does very well in the determination of the horizontal trajectory position points but has some bias in the vertical determination as indicated by earlier flight tests [9, 11, 12].

Definition of Bias Errors and Discussion

The average bias estimates for position, velocity and acceleration are presented in Tables VI, VII, and VIII for the respective Contraves, Radar 112 and Radar 122 systems. A positive average bias means that the particular system trajectory data was on the average greater than that corresponding data from the Askania system.

The average absolute component position bias estimates ranged from a low of six feet to a high eighty-two feet. The velocity and acceleration average bias estimates were low. The largest velocity component bias was four feet per second; the largest acceleration component bias was only seven feet per second squared. The explanation for the large average position bias error and the much smaller average velocity and acceleration bias error is that the trajectories as determined by the instrumentation systems are parallel but differ by a constant amount in position. This means that the least squares fitting differ by essentially the constant term of the second degree polynomial in time.

A comparison of the unsmoothed position data from the Contraves and radar systems with the corresponding data from the Askania system reveals that the average bias does not differ from the corresponding bias estimates shown in Tables VI, VII, and VIII by more than one foot. This indicates that the smoothing process either moves the average bias estimate the same amount for all systems or that smoothing does not change the bias. A further study of the smoothed and unsmoothed trajectory data from the Askania system reveals that the smoothing process leaves the Askania trajectory data essentially unchanged.

SOME COMPARISONS OF PRECISION ESTIMATES WITH EARLIER FLIGHT TESTS. Comparison of earlier flight tests were possible for the Askania System and the two FPS-16 Radar Systems. The Contraves System was not operated on the earlier tests. Table IX shows the mode number of instruments that make up the Askania System for each flight test. Data from the first trajectory section were selected from the third flight test so as to approximate more closely the other tests. The standard deviation estimates for the Askania system are smaller for the X and Y component data for the later two flight tests.

Precision estimates for data from the earlier flight tests for radar systems 112 and 122 are shown in Table X. These standard deviation

estimates indicate that the best performance for the radar systems was during the fourth flight test. The FPS-16 radars were operated in the beacon tracking mode with a radar beacon aboard the tracked missile.

SUMMARY AND CONCLUSIONS. The standard deviation estimates for the position data ranged from two to nineteen feet for the cinetheodolite systems and ranged from five to twenty-two feet for the FPS-16 radar systems. This indicates that the radar system position data precision are as good as the cinetheodolite system position data precision for these flight test data. The velocity standard deviation estimates ranged from two to eleven feet per second for the cinetheodolite systems (exception Contraves section 2 data) and ranged from three to sixteen feet per second for the FPS-16 radar systems. Again, a precision equivalence for velocity data from these systems can be stated. The acceleration standard deviation estimates for all four tracking systems ranged from eight to forty feet per second squared (with the exception of Contraves section 2 data). Again an equivalence can be stated for precision of the acceleration data from these systems.

The position component average bias were based on the trajectory data from the Askania cinetheodolite system. The average bias for position data from the Contraves cinetheodolite ranged in absolute (component) value from six to seventeen feet (except for section 2 data). The average bias for position data from radar 122 ranged in absolute (component) value from eight to thirty-eight feet and from radar 112, the average bias range in absolute value from a low of 23 to 73 feet. Based on the Askania cinetheodolite position data, the radar systems did not do as well as the Contraves systems, with respect to bias error estimates. The average component bias for the derived velocity data ranged in absolute value from zero to four feet per second for the Contraves system and ranged in absolute value from zero to three feet per second for the FPS-16 radar systems. Essentially the average velocity bias errors are equal.

The acceleration component bias ranged in absolute value from zero to six feet per second squared for Contraves system and from zero to seven feet per second squared for the FPS-16 radar systems. These derived acceleration data for eleven point (two second) smoothed data are essentially equal in average component bias error.

TABLE I

PRECISION ESTIMATES FOR TRAJECTORY POSITION DATA

FROM FLIGHT TEST NUMBER FOUR

Instrumentation System	Trajectory System	Component Standard Deviation Estimate in Feet		
		North (X)	East (Y)	Up (Z)
Askania	1	5	8	10
Askania	2	7	3	17
Contraves	1	10	2	19
Contraves	2	45*	2	67*
Radar 112	1	12	8	16
Radar 112	2	12	5	7
Radar 122	1	9	5	22
Radar 122	2	9	8	22

*Very poor geometry for a two instrument (theodolite) system.

TABLE II

STANDARD DEVIATION ESTIMATES FOR DERIVED (SMOOTHED) TRAJECTORY DATA FROM ASKANIA CINETHEODOLITE SYSTEM FOR FLIGHT TEST NUMBER FOUR

Trajectory Section	Derived Trajectory Element*	Dimensions	Component Estimates of Standard Deviation		
			North (X)	East (Y)	Up (Z)
1	position	feet	5	8	6
2	position	feet	5	2	13
1	velocity	ft/sec.	5	4	5
2	velocity	ft/sec.	6	3	11
1	acceleration	$ft/sec.^2$	11	8	25
2	acceleration	$ft/sec.^2$	15	8	40

*All data were derived from mid-point evaluation of a second degree least square polynomial fitted over a two second interval (11 points) with time as the independent variable.

TABLE III

STANDARD DEVIATION ESTIMATES

FOR DERIVED (SMOOTHED) TRAJECTORY DATA

FROM CONTRAVES CINETHEODOLITE SYSTEM

FOR FLIGHT TEST NUMBER FOUR

Trajectory Section	Derived Trajectory Element*	Dimensions	Component Estimates of Standard Deviation		
			North (X)	East (Y)	Up (Z)
1	position	feet	5	2	10
2**	position	feet	19	1	34
1	velocity	ft/sec.	5	2	4
2**	velocity	ft/sec.	25	4	43
1	acceleration	$ft/sec.^2$	16	3	38
2**	acceleration	$ft/sec.^2$	87	12	148

*All data were derived from mid-point evaluation of a second degree least squares polynomial fitted over a two second interval (11 points) with time as the independent variable.

**Poor geometry for a two cinetheodolite instrumentation system.

TABLE IV

STANDARD DEVIATION ESTIMATES

FOR DERIVED (SMOOTHED) TRAJECTORY DATA

FROM RADAR (112) SYSTEM

FOR FLIGHT TEST NUMBER FOUR

Trajectory Section	Derived Trajectory Element*	Dimensions	Component Estimates of Standard Deviation		
			North (X)	East (Y)	Up (Z)
1	position	feet	10	7	13
2	position	feet	12	4	7
1	velocity	ft/sec.	10	10	10
2	velocity	ft/sec.	6	4	6
1	acceleration	$ft/sec.^2$	32	26	40
2	acceleration	$ft/sec.^2$	30	8	20

*All data were derived from mid-point evaluation of a second degree least square polynomial fitted over two second interval (11 points) with time as the independent variable. The standard deviation estimates are based on a sample of fifty (50) trajectory points for each trajectory section.

TABLE V

STANDARD DEVIATION ESTIMATES

FOR DERIVED (SMOOTHED) TRAJECTORY DATA

FROM RADAR (122) SYSTEM

FOR FLIGHT TEST NUMBER FOUR

Trajectory Section	Derived Trajectory Element*	Dimensions	Component Estimates of Standard Deviation		
			North (X)	East (Y)	Up (Z)
1	position	feet	7	4	10
2	position	feet	6	2	9
1	velocity	ft/sec.	6	4	16
2	velocity	ft/sec.	4	3	9
1	acceleration	$ft/sec.^2$	10	16	44
2	acceleration	$ft/sec.^2$	10	12	30

*All data were derived from mid-point evaluation of a second degree least squares polynomial fitted over a two second interval (11 points) with time as the independent variable.

TABLE VI

BIAS ESTIMATES FOR DERIVED (ELEVEN POINT SMOOTHING) DATA FROM CONTRAVES SYSTEM FOR FLIGHT TEST NUMBER FOUR

Trajectory Section	Derived Trajectory Element*	Bias Dimensions	Component Estimates of Average Bias**		
			North (X)	East (Y)	Up (Z)
1	position	feet	- 6	9	-17
2	position	feet	-28	13	-82
1	velocity	ft/sec.	- 2	1	- 4
2	velocity	ft/sec.	0	0	- 2
1	acceleration	$ft/sec.^2$	0	- 1	1
2	acceleration	$ft/sec.^2$	- 4	0	- 6

*See note in Table II.

**The trajectory data at simultaneous times from the Askania System (chosen standard) were subtracted from corresponding data from the Contraves System to form an error set of data which were averaged for each trajectory section.

TABLE VII

BIAS ESTIMATES FOR DERIVED (ELEVEN POINT SMOOTHING) DATA FROM RADAR 112 SYSTEM FOR FLIGHT TEST NUMBER FOUR

Trajectory Section	Derived Trajectory Element*	Bias Dimensions	Component Estimates of Average Bias**		
			North (X)	East (Y)	Up (Z)
1	position	feet	-55	-23	-52
2	position	feet	-73	-27	-41
1	velocity	ft/sec.	- 2	1	1
2	velocity	ft/sec.	- 2	- 1	0
1	acceleration	$ft/sec.^2$	- 1	0	2
2	acceleration	$ft/sec.^2$	- 1	- 1	- 3

*See note in Table II.

**The trajectory data at simultaneous times from the Askania System (chosen standard) were subtracted from corresponding data from Radar 112 System to form an error set of data which were averaged for each trajectory section.

TABLE VIII

BIAS ESTIMATES FOR DERIVED (ELEVEN POINT SMOOTHING) DATA FROM RADAR 122 SYSTEM FOR FLIGHT TEST NUMBER FOUR

Trajectory Section	Derived Trajectory Element*	Bias Dimensions	Component Estimates of Average Bias**		
			North (X)	East (Y)	Up (Z)
1	position	feet	-38	-11	31
2	position	feet	-28	- 8	26
1	velocity	ft/sec.	0	1	0
2	velocity	ft/sec.	3	0	- 2
1	acceleration	$ft/sec.^2$	1	1	7
2	acceleration	$ft/sec.^2$	0	0	- 2

*See note in Table II.

**The trajectory data at simultaneous times from the Askania System (chosen standard) were subtracted from corresponding data from Radar 122 System to form an error set of data which were averaged for each trajectory section.

TABLE IX

COMPARISON OF ASKANIA CINETHEODOLITE SYSTEM

BY FLIGHT TEST PERFORMANCE

Flight Test Number	Mode Number of Cinetheodolite	Component Standard Deviation Estimate in Feet		
		North (X)	East (Y)	Up (Z)
1	6	11	11	8
2	7	10	15	12
3*	7	7	4	10
4**	5	6	6	14

*Trajectory section one and mode number of instruments corresponding more closely to earlier tests. Average set for the three trajectory sections is 8, 8 and 12 respectively for Flight Test three.

**The first three flight tests were night tests with a point source of light for optical system tracking; whereas, the fourth flight test was conducted during daylight hours.

TABLE X

COMPARISON OF RADAR SYSTEMS

BY FLIGHT TEST PERFORMANCE

Flight Test Number	Radar Designation	Component Standard Deviation Estimation in Feet		
		North (X)	East (Y)	Up (Z)
1	R-112	18	46	34
2	R-112	25	68	92
3	R-112*	19	39	16
4	R-112**	12	7	12
1	R-122	29	29	21
2	R-122	21	18	20
3	R-122	26	34	31
4	R-122*	9	8	22

*Variate difference estimates for trajectory section 1; data sampled at 2 per second.

**These radars were operated in the beacon tracking mode; whereas, prior tests have utilized the skin tracking mode.

REFERENCES

[1]. Simmon, L. E., "On the Relation of Instrumentation of Quality Control, "Instruments, Vol. 19, November 1946.

[2] Grubbs, F. E., "On Estimating Precision of Measuring Instruments and Product Variability", American Statistical Assn. Vol. 43, pp 243-264.

[3] Davis, R. C., "Techniques for the Statistical Analysis of Cinetheodolite Data, "NAVORAD Report 1299, China Lake, Calif. (March 22, 1951).

[4] Pearson, K. E., "Evaluation of the AN/FPS-16 (System No. 1) at White Sands Missile Range," WSMR Technical Memorandum No. 606, February 1959.

[5] Dibble, H. L., Carroll, C. L. Jr., "A Best Estimate of Trajectory using Reduced Data from Various Instruments at a Single Point in Time," AFMTC-TR-60-12, May 1960, Patrick Air Force Base, Florida.

[6] Wine, L. R., "Statistics for Scientists and Engineers," Prentice-Hall Inc., Englewood Cliffs, N. J., 1964.

[7] Duncan, David B., "On the Optimum Estimation of a Missile Trajectory from Several Tracking Systems", AMFTC-TR-60-16, 24 August 1960, Patrick Air Force Missile Test Center, Florida.

[8] Kendall, M. G., "The Advanced Theory of Statistics," Vol. II, 3rd Ed. C. Griffin and Co. Ltd. London, 1951.

[9] Kingsley, O. L., "Analysis of Some Trajectory Measuring Instrumentation Systems," Paper presented at the Sixth Conference on the Design of Experiments in Army Research, Development and Testing, October 1960, Aberdeen Proving Ground, Aberdeen, Maryland.

[10] Weiss, J. E., Kingsley, O. L., "Study of Accuracy and Precision of Trajectory Measuring Systems," 30 June 1961 (U) ORDBS-IRM Task 5-4-2. WSMR, New Mexico.

[11] Kingsley, O. L., "A Further Analysis of Missile Range Tracking Systems." Paper presented at the Seventh Conference on the Design of Experiments in Army Research, Development, and Testing, October 1961, Fort Monmouth, N. J.

[12] Kingsley, O. L., Free, B. R., "Additional Analysis of Missile Trajectory Measuring Systems." Paper presented at the Ninth Conference on the Design of Experiments in Army Research, Development and Testing, October 1963, Redstone Arsenal, Alabama.

[13] "Final Data Report No. 14775. AN/FPS-16 Radar R-112 for Nike Hercules RT-2 in Support of Accuracy and Precision of Trajectory Measuring System Launched 1 October 1962." (U) IRM-DRD WSMR, N. Mex. (16 November 1962) Classified Confidential.

[14] "Final Data Report No. 14777. AN/FPS-16A Radar R-122 for Nike Hercules RT-2 In Support of Accuracy and Precision of Trajectory Measuring System Launched 1 October 1962" (U) IRM-DRD, WSMR, N. Mex. (16 November 1962) Classified Confidential.

[15] "Final Data Report No. 14847. Contraves Trajectory Data for Nike Hercules RT-2 In Support of Accuracy and Precision of Trajectory Measuring Systems. Launched 1 October 1962." (U) IRM-DRD, WSMR, N. Mex. (3 December 1962) Classified Confidential.

[16] "Final Data Report No. 14829. Askania Trajectory Data for Nike Hercules RT-2 In Support of Accuracy and Precision of Trajectory Measuring Systems." (U) IRM-DRD, WSMR, N. Mex. (28 November 1962) Classified Confidential.

THERMAL CYCLES IN WELDING

Mark M. D'Andrea, Jr.
U. S. Army Materials Research Agency
Watertown, Massachusetts

INTRODUCTION: The mechanical property integrity of weld heat-affected zones is an inherent and vital consideration in arc welding applications. A weld heat-affected zone, hereinafter termed "weld-HAZ", is defined as that volume of base material in a weldment that has been heated, as a result of welding, to a range of peak temperatures between the pre-heat temperature and the materials melting point.

Previous work conducted at the U. S. Army Materials Research Agency, concerning the welding of fully heat-treated high-strength steels for service in the as-welded condition, demonstrated that weld-HAZ areas characterized by peak temperatures at or about the lower critical temperature, suffered a marked loss of strength, thus reducing weld-joint efficiencies considerably. Other studies with high-strength and maraging steels have revealed deleterious mechanical property effects resulting from thermal cycles characterized by peak temperatures above the upper critical temperature. In addition, it is well known that an embrittling effect in alloy steels is generally associated with weld-HAZ structures characterized by peak temperatures between the lower and upper critical temperatures.

Recent work conducted at AMRA, established the general parameters necessary to define and reproduce the transformational behavior of weld-HAZ microstructures. These parameters included (but are not necessarily limited to) the following; (1) The time-temperature shape of a weld-HAZ thermal cycle, (2) the peak temperature of a thermal cycle, (3) the microstructure of the base material (defined by heat treatment, chemistry, working, etc.), prior to the imposition of a thermal cycle, and (4) factors affecting restraining stresses and strains produced in the base material as a result of the overall welding operation.

The gamut of microstructures produced in a weld-HAZ is the end result of the complex and varied transformations caused by welding thermal cycles. An important consideration which has been a pertinent reference point in the present investigation, was the fact that in any arc weld in a given material there will always be thermal cycles that have the same peak

temperature; these thermal cycles will differ only in that the shape and position of associated heating and cooling curves will be displaced somewhat in time and temperature. It is a well established metallurgical fact that the mechanical properties of a material depend primarily upon microstructure. In order to predict and perhaps control weld-HAZ microstructures resulting from welding thermal cycles, it is necessary first to investigate the effects of basic parameters of such structures.

OBJECT AND SCOPE:

Welding Metallurgy

The overall objective is to investigate and to establish basic metallurgical concepts to account for the phenomena of the attendant transformation behavior of weld-HAZ microstructures produced in 4340, H-11, and 18 1/2% Ni (300) maraging steels. The work is limited to a study of the effects of fundamental material and welding time-temperature parameters pertaining to single pass, arc welding situations. Realizing the potentially staggering number of general and sub-parameters that may significantly affect resultant microstructure, it was deemed advisable to initiate the investigation by studying only the effects of some of the general parameters, viz; the prior base material microstructure, the peak temperature of a thermal cycle, and the time-temperature shape of thermal cycles imposed by welding. The number and kind of stress-strain conditions that are applicable to welding were initially considered to be overwhelming; consequently the utilization of this general parameter in this initial investigation was abandoned in the sense that such conditions were kept constant.

Statistical Inference

The overall objective of the utilization of statistical inference techniques is to assist the metallurgical investigation by determining the significant factors (i.e., the more critical variables), affecting this phenomena. and to detect the specific significant differences that may exist among each set of significant factors. The transformational behavior and the resultant heat-affected zone microstructures produced will be evaluated metallurgically in terms of such specific significant differences obtained.

THE EXPERIMENT. A high-speed time-temperature controller is being used in this investigation to produce weld-HAZ synthetically.

The controller essentially is a simulating device which permits the duplication of welding thermal cycles experienced in weld-heat-affected zones. Each specimen is heated by its resistance to the passage of an A-C electric current furnished from a transformer, and is cooled by the removal of heat from the specimen by conduction through water-cooled copper clamps. A thermocouple percussion welded to the surface of the specimen, provides a signal which is balanced against a reference control signal designed to reproduce the desired thermal cycle. The resultant error signal is amplified and utilized by the controller to maintain temperature control during the cycle to within $\pm$ 5°F.

The basic experiment involves two of the general parameters as variables, viz., the prior base material microstructure (defined by various heat treated conditions of a given single heat of steel) and the time-temperature shape of various welding thermal cycles. The thermal cycle peak temperature parameter is a constant in each basic experiment, i.e., each basic experiment is conducted utilizing thermal cycles having the same peak temperature.

In each basic experiment, it is desired to determine the effects of prior base material microstructure (denoted factor code "H"), and the time-temperature shape of thermal cycles (denoted factor code "C"), on the notch toughness (quantitative response variable, measured in in.-lb/in.^{2}, indicative of microstructural change) of the resultant weld-HAZ microstructures.

In a given heat of steel, the interest lies in the effects of five particular prior base material microstructures and seven particular thermal cycles, i.e., factor "H" is a fixed factor at five fixed levels and factor "C" is a fixed factor at seven fixed levels.

There are three steels (one heat of each) involved in the investigation along with seven different peak temperatures per heat; therefore, there are three times seven or twenty-one basic experiments to be evaluated independently. Metallurgical considerations preclude statistical correlations between steel types and between peak temperatures per heat of steel.

THE DESIGN AND ANALYSIS: The number of observations (notch toughness values) to be taken is initially unknown; however it is desired

to design the statistical analysis to allow for the general situation of dealing with an uneven number of replications per cell, since some experimental observations are lost occasionally. A basic model appears to be a fixed, two-way analysis of variance; the suggested mathematical model for the sum of squares is:

$$\underline{\text{Total}} \qquad\qquad \underline{\text{H}} \qquad\qquad \underline{\text{C}}$$

$$\left(\Sigma\Sigma_{ijk}{}^{2} - \frac{T...^{2}}{npq}\right) - \left(\frac{T._{j}.^{2}}{nq} - \frac{T...^{2}}{npq}\right) + \left(\frac{T..k^{2}}{np} - \frac{T...^{2}}{npq}\right) +$$

$$\underline{\text{Interaction}} \qquad\qquad \underline{\text{Residual}}$$

$$\left(\frac{T._{j}k^{2}}{n} - \frac{T._{j}.^{2}}{nq} - \frac{T..k^{2}}{np} + \frac{T...^{2}}{npq}\right) + \left(\Sigma\Sigma_{ijk}{}^{2} - \frac{T._{j}k^{2}}{n}\right).$$

Once the individual ANOVA's are run for each basic experiment, one of the following techniques could be used to detect specific significant differences that may exist among each set of significant factors obtained.

(1) Use Duncan's Test of the means if, and only if, the cells have the same number of replications. The means used here are those of the columns, or rows as the case may be, of the cells pertaining to the significant factor; if both factors are significant, two such tests are made regardless of interaction effects. Perhaps this is not a proper technique, in that only the individual cell averages should be tested by Duncan's method.

(2) Use the following relationship to test the means of each cell if there are minor variations in the number of observations per cell.

$$\frac{S_{\chi}(\text{entry from studentized range})}{\sqrt{\text{no. observations/cell}}}$$

(3) Use the following relationship to test the means of each cell, if there are major variations in the number of observations per cell.

$$S\sqrt{\frac{1}{n_1} + \frac{1}{n_2}} \quad x \quad \sqrt{(k-1)\, F\,(k-1, \gamma)} \quad .$$

The foregoing is the author's suggested method of analysis. It is important to note that the author is merely a novice at this business of statistical analysis.

It has been suggested since the presentation of this paper that the use of regression analysis techniques may be a better approach to solving this statistical problem. Unfortunately, circumstances to date have not yet permitted a further investigation into the most efficient statistical procedures to be used in this problem.

STATISTICAL ANALYSIS OF TENSILE STRENGTH-HARDNESS RELATIONSHIPS IN THERMOMECHANICALLY TREATED STEELS*

Albert A. Anctil
U. S. Army Materials Research Agency
Watertown, Massachusetts 02172

INTRODUCTION. Generally speaking, statistical analysis finds limited applications in metallurgical problems. This is true because the sample size is usually quite small and in most cases, the variables are known and can be controlled. The clinical (statistical) problem described here is a segment of an investigation entitled, "Tensile Strength-Hardness Relationships in Thermomechanically Treated Steels." [1] The objective of the study was to determine metallurgically and statistically how well thermomechanically treated steels followed established tensile strength-hardness correlations.

The generally accepted tensile strength-hardness correlations are published by the American Society for Testing and Materials (ASTM) [2] and the Society of Automotive Engineers (SAE) [3]. These correlations specifically excluded cold worked, stainless steels and other thermomechanically treated steels. The ASTM and SAE correlations have been obtained from a particular steel quenched and tempered to various strength levels. Tensile specimens which contain hardness coupons were machined from each strength level condition. These specimens were distributed randomly to several laboratories participating in a standardized testing program. The assembled data were treated statistically to obtain a tensile strength-hardness correlation.

Thermomechanical treatments which are under consideration here, involve the introduction of cold work into the heat treatment cycle of steel to obtain higher strengths. There are three types of thermomechanical treatments based upon when in the heat treatment cycle the working cycle is performed. [4]

Type I - Deformation of austenite followed by transformation
Type II - Deformation of austenite during transformation
Type III - Deformation after transformation of austenite

*Comments on this paper by one of the panelists can be found at the end of this article.

EXPERIMENTAL PROCEDURE. The experimental tensile strength-hardness data came from a literature survey of thermomechanically treated steels. Refer to Reference 1 for a more detailed explanation and data references for this presentation.

Figure 1 shows the ASTM (solid curve) and SAE (dashed curve) tensile strength-hardness correlations. There is some difference of opinion as to which is the better curve. A joint ASTM-SAE committee is presently working out a compromise curve. The ASTM curve has been extended beyond Rockwell C hardness 58 to encompass the very high strength steels. The data points are from Reference 1 and represent various steels having a quenched and tempered heat treatment. Such data could have been used to obtain these correlations. These same steels were then processed thermomechanically with Type I (open symbols) and Type III (closed symbols) treatments. Statistically the quenched and tempered data fits the ASTM correlation better than the SAE correlation. Accordingly, the ASTM correlation will be used for comparative purposes.

Tensile strength-hardness data for the Type I thermomechanical treatment are shown in Figure 2. The thermomechanical heat treatment cycle is shown schematically. The data follow the ASTM correlation (solid curve) reasonably well. Figure 3 illustrates Type II data. This thermomechanical treatment is usually performed on austenitic stainless steels at subzero temperatures. Meaningful comparisons of this data are difficult with such a small sample size. Type III data are shown in Figure 4. The cold work may be performed upon the asquenched martensite or upon tempered martensite that is subsequently aged. A positive deviation from the ASTM correlation is immediately apparent over the major portion of the hardness range for Type III data.

Selected data for Type III treatments where the percent reduction has been varied are shown in Figure 5. Consider the 5Cr-Mo steel where the lowest tensile strength plotted represents the quenched and tempered condition. Note, that as the amount of cold work is increased, the tensile strength increases at a faster rate than that shown by the ASTM correlation. This same trend can be seen for the majority of these steels. It is for this reason that a regression line was not drawn for this data. A tensile strength-hardness correlation for these steels would be dependent upon the amount of cold work.

DISCUSSION. Metallurgically the behavior was explained using Tabor's analysis [5] which relates hardness and tensile strength through an additional parameter, the strain hardening exponent n. The analysis is summarized in Figure 6. Quenched and tempered steels have strain hardening exponents in the range from 0.04 to 0.12. In this range the tensile strength-hardness ratio is nearly constant. It is for this reason that a unique tensile strength-hardness correlation exists. For Type I treatments the strain hardening exponents fall in the same range, therefore, the data fit the ASTM correlation. With Type III treatments the ratio starts at the minimum and increases as the exponent decreases to nearly zero with increasing amounts of cold work. This results in positive deviations from the ASTM correlation. Type II treatments are usually performed on austenitic stainless steels at subzero temperatures. These steels have very high exponents (0.3) in the annealed condition which decrease to nearly zero with increasing amounts of deformation. One would expect positive deviations from the high and low exponents and adherence to the correlation as the ratio passes through its minimum value. Cold-worked steel (Type III) and stainless steels (Type II) have been excluded from the ASTM correlation because of these drastic changes in strain hardening characteristics.

Statistical analysis of the data is summarized in Table I. The deviation d refers to the experimental tensile strength σ, minus the corresponding tensile strength σ_{ASTM}, from the ASTM correlation at a particular hardness. This deviation was determined for every data point. The arithmetic mean of the deviations $\overline{\Delta\sigma}$ was taken as the sum of the deviations divided by the sample size. It serves as an indication of how well the data for thermomechanically treated steels fit the ASTM correlation. This value would be zero for a regression line of the data. The absolute deviation $|\overline{\Delta\sigma}|$ and the standard error of estimate Sy* were calculated as measures of the dispersion of the data about the ASTM curve. These differ from the usually defined mean absolute deviation and standard error of estimate which measure the dispersion around a regression line.

Statistical results are shown in Table II. The mean of the deviations $\overline{\Delta\sigma}$, shows a better fit of the quenched and tempered data about the ASTM rather than the SAE correlation. Further, the data for the Type I treatment fit the ASTM correlation better than the Type III treatments.

Also, the predominantly positive deviation of the Type III data from the ASTM curve is obvious. Both measures of dispersion about the ASTM curve yield approximately the same results. They do not, however, reflect the positive deviation of data for the Type III treatments.

The problem before the panel is that of offering more descriptive statistical alternatives for comparing several populations of data (tensile strength-hardness values for thermomechanically treated steels) to a given regression line (the standard ASTM tensile strength-hardness correlation). Consider further that it may not be possible or meaningful to draw a regression line through each population of data.

REFERENCES

1. E. B. Kula and A. A. Anctil, Tensile Strength-Hardness Relationships in Thermomechanically Treated Steels, Proceedings, Am. Soc. Testing Mat'ls, Vol. 64, 1964, p. 719

2. Methods and Definitions for Mechanical Testing of Steel Products, 1965 Book of ASTM Standards, Part 1 (currently available as a separate reprint)

3. Hardness Tests and Hardness Number Conversions - SAE J417, SAE Handbook, 1964, p. 94

4. S. V. Radcliffe and E. B. Kula, Deformation, Transformation and Strength, Fundamentals of Deformation Processing, Syracuse University Press, Syracuse, N. Y., 1964, p. 321; also, E. B. Kula and S. V. Radcliffe, Thermomechanical Treatment of Steel, Journal of Metals, Vol. 16, 1963, p. 755.

5. D. Tabor, The Hardness of Metals, Oxford University Press, London, 1951

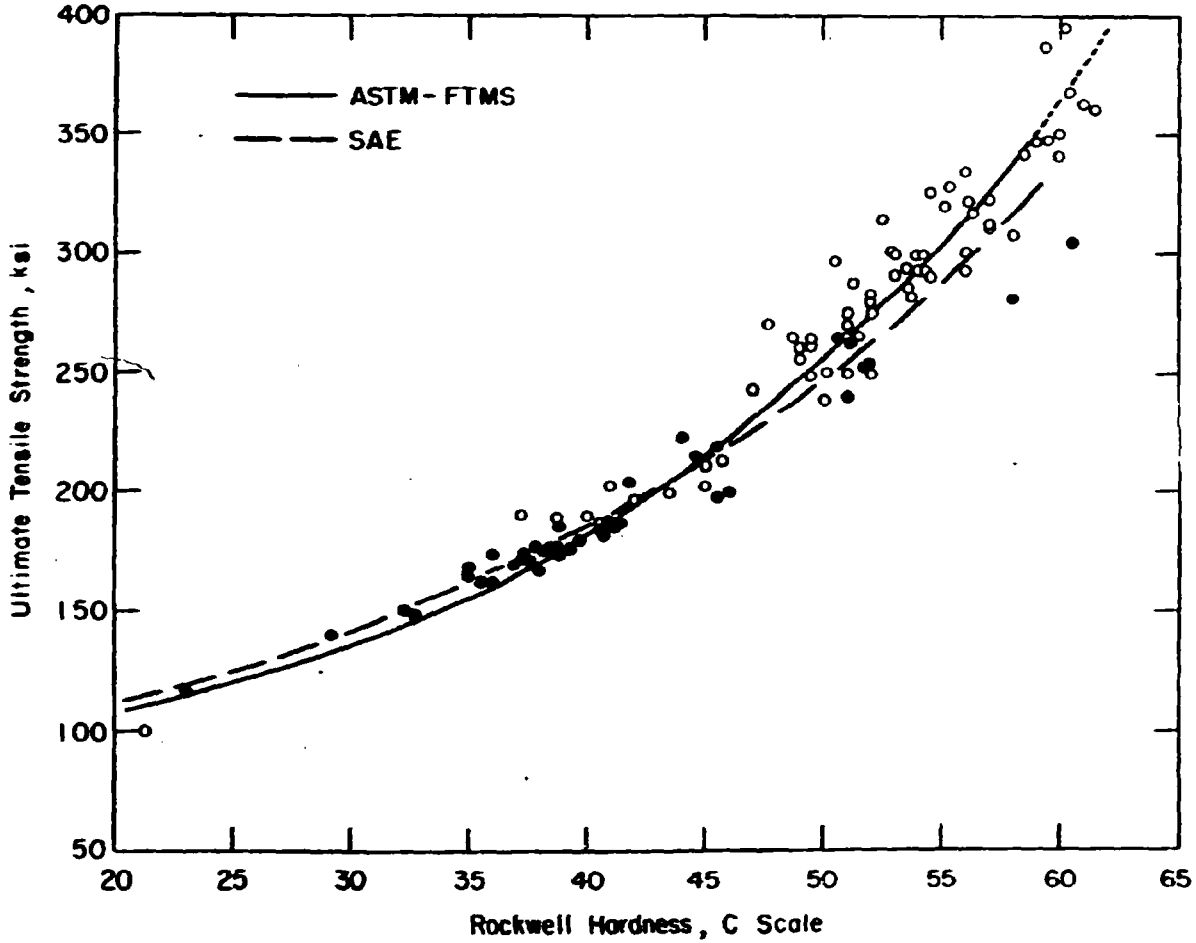

Figure 1. ULTIMATE TENSILE STRENGTH VERSUS ROCKWELL C HARDNESS FOR STEELS HAVING A CONVENTIONAL HEAT TREATMENT (QUENCHED AND TEMPERED). STEELS, ○ USED IN TYPE I, AND ● USED IN TYPE III THERMOMECHANICAL TREATMENT.

U. S. ARMY MATERIALS RESEARCH AGENCY

19-066 525/AMC-68

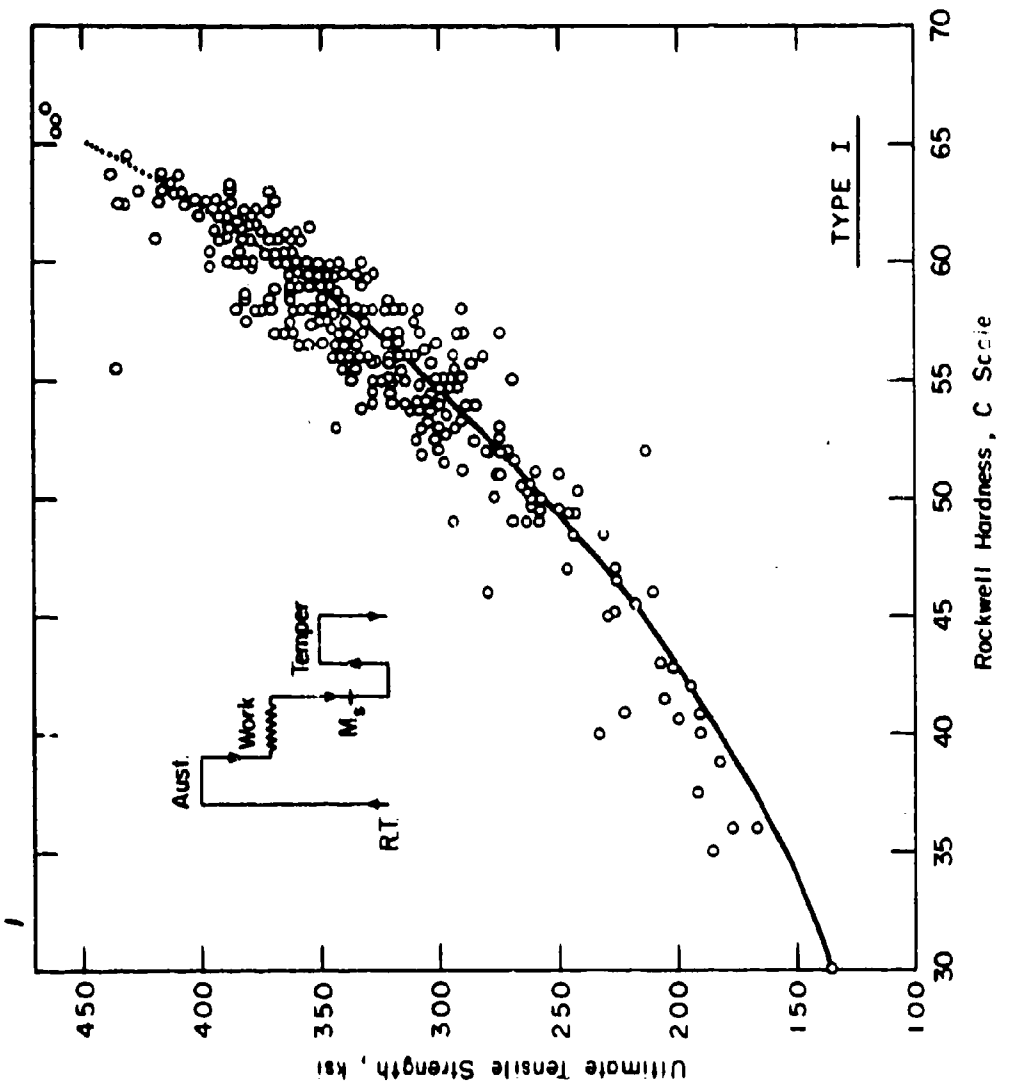

Figure 2. ULTIMATE TENSILE STRENGTH VERSUS ROCKWELL C HARDNESS FOR TYPE I THERMOMECHANICALLY TREATED STEELS.

U. S. ARMY MATERIALS RESEARCH AGENCY

19-066-526/AMC-64

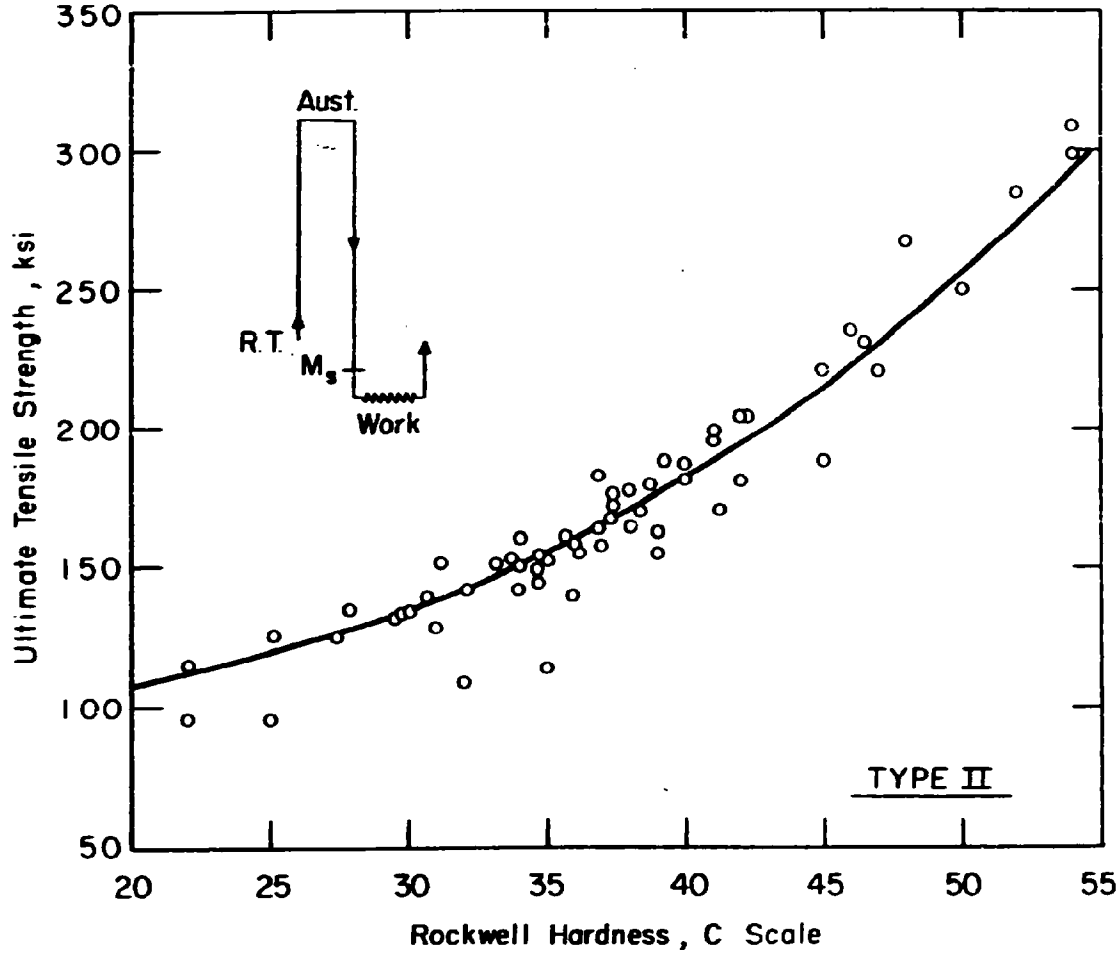

Figure 3. ULTIMATE TENSILE STRENGTH VERSUS ROCKWELL C HARDNESS FOR TYPE II THERMOMECHANICALLY TREATED STEELS.

U. S. ARMY MATERIALS RESEARCH AGENCY

19-066-529/AMC-68

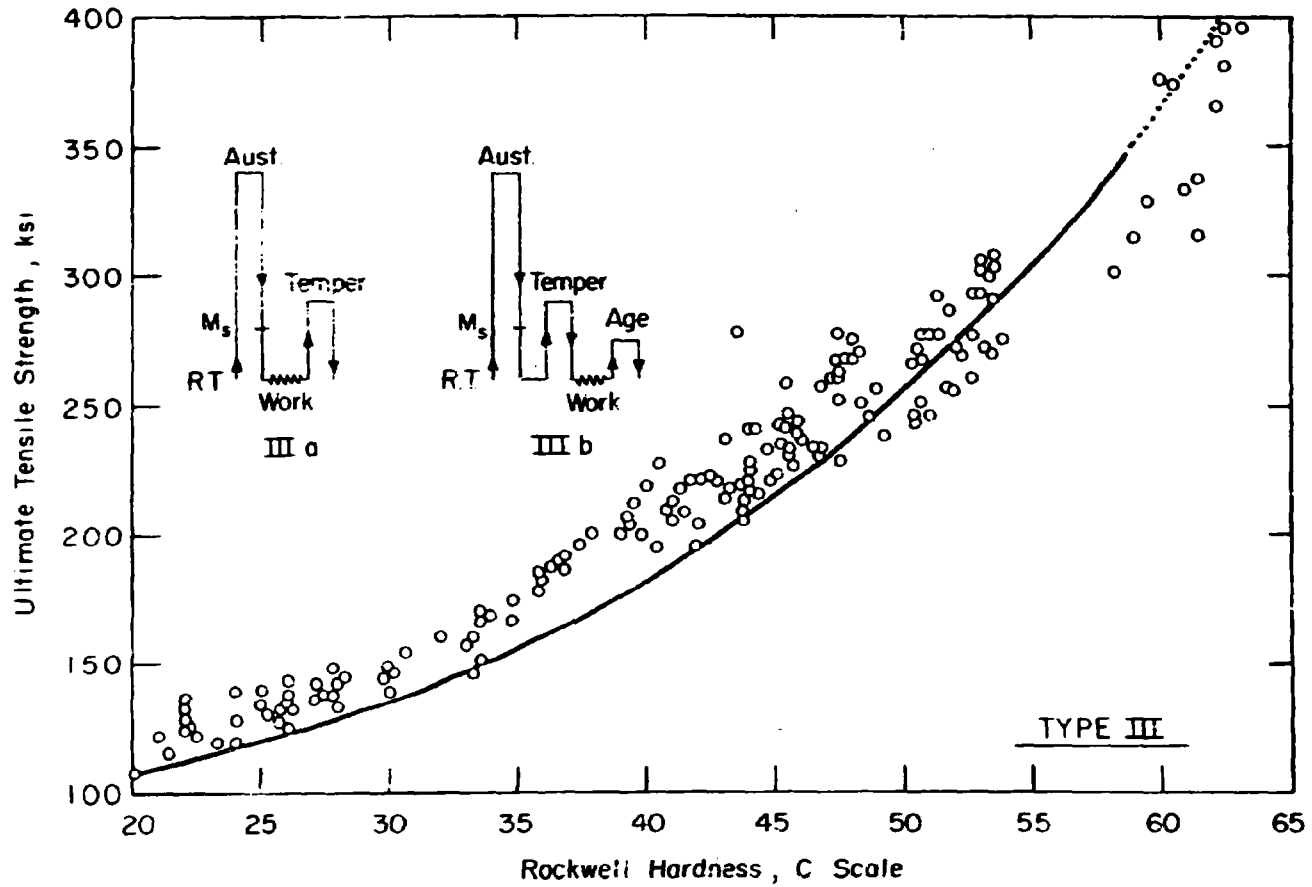

Figure 4 ULTIMATE TENSILE STRENGTH VERSUS ROCKWELL C HARDNESS FOR TYPE III THERMOMECHANICALLY TREATED STEELS.

U. S. ARMY MATERIALS RESEARCH AGENCY

19-066 531/AMC-68

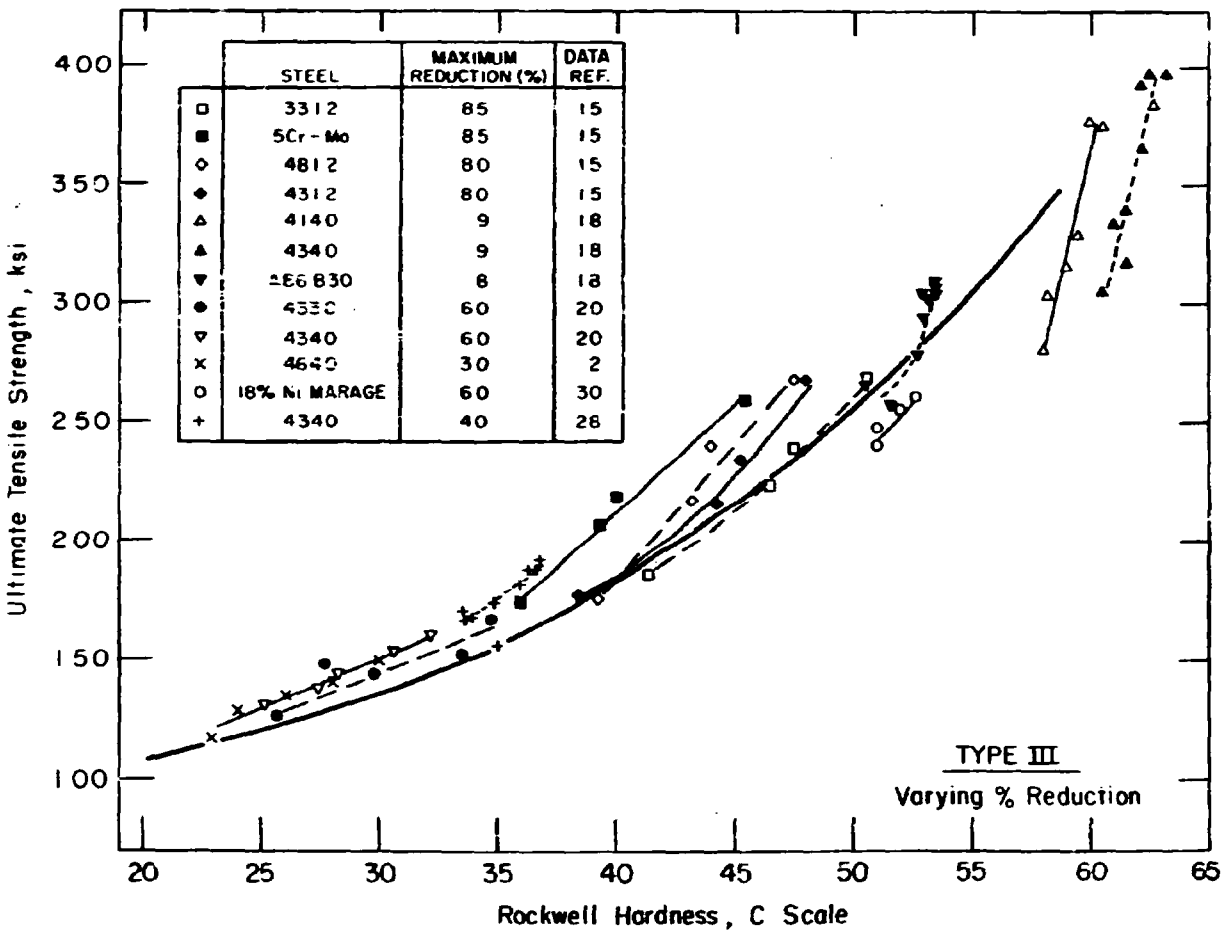

Figure 5 ULTIMATE TENSILE STRENGTH VERSUS ROCKWELL C HARDNESS FOR TYPE III TREATMENTS WITH VARYING AMOUNTS OF REDUCTION AND CONSTANT TEMPERING TEMPERATURE.

U. S. ARMY MATERIALS RESEARCH AGENCY

19-066-533/AMC-68

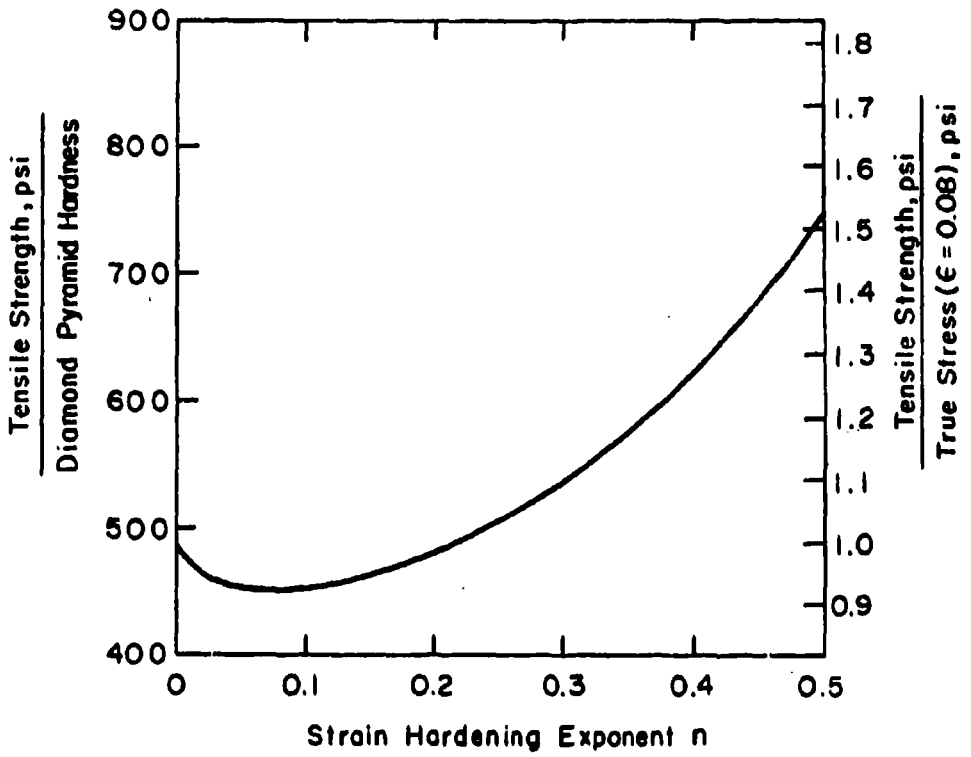

Figure 6. RATIO OF TENSILE STRENGTH TO DIAMOND PYRAMID HARDNESS AND TO TRUE STRESS (ϵ = 0.08) AS A FUNCTION OF THE STRAIN-HARDENING EXPONENT

U. S. ARMY MATERIALS RESEARCH AGENCY

19-066-659/AMC-64

Table I. STATISTICAL ANALYSIS

$$d = \sigma - \sigma_{ASTM}$$

$$\overline{\Delta\sigma} = \frac{1}{n}\Sigma d$$

$$\overline{|\Delta\sigma|} = \frac{1}{n}\Sigma |d|$$

$$Sy^* = \left(\frac{\Sigma d^2}{n}\right)^{\frac{1}{2}}$$

Table II. STATISTICAL RESULTS FOR QUENCHED AND TEMPERED AND THERMOMECHANICALLY TREATED STEELS

Condition	$\overline{\Delta\sigma}$, ksi	$\overline{\lvert\Delta\sigma\rvert}$, ksi	Sy^*, ksi	n
Quenched and Tempered				
ASTM curve	0.23	11.7	17.7	112
SAE curve	7.33	14.1	19.4	112
Thermomechanically Treated				
Type I	3.70	15.4	20.6	319
Type II	1.45	9.3	12.8	60
Type III	11.00	17.2	20.8	176

COMMENTS ON PRESENTATION BY ALBERT A. ANCTIL

Joan Raup Rosenblatt
Statistical Engineering Laboratory
National Bureau of Standards, Gaithersburg, Maryland

The evaluation of empirical relations of the kind you discussed is a difficult problem. The various functions of deviations from the ASTM curve that are presented in your Table II are extremely difficult to interpret: By themselves, they are nearly meaningless. Taken together with the data, as exhibited in your figures, they add very little and may be misleading.

For example, looking at Figure 1, I notice that the steels used in Type I and Type III thermomechanical treatments respectively seem to be grouped preponderantly in different hardness ranges. Is it possible that the ASTM curve fits better for Type I and the SAE curve for Type III? If this were so, an explanation would have to be sought in the metallurgical facts about the data used, and in the history of the two standard curves.

Table II gives overall measures of goodness-of-fit. Since these are well-defined functions of the data, they cannot be "wrong" in themselves. But if the deviations from the standard curves occur for different reasons if different types of steels and in different hardness ranges, the overall measures cannot be relied upon to describe the uncertainty of tensile strength estimates derived (using the curves) from hardness measurements. Furthermore, if the overall measures are used to select the "best-fitted" curve, there is great danger that the resulting curve will have systematic errors arising from the particular choice of data.

Of course, for many purposes a standard curve is entirely adequate. But your data seem to make it clear that one possible long-run goal would be the development of a collection of curves each applicable to specific circumstances. This development would probably require the performance of many new experiments. It could lead to the evolution of your qualitative explanation of the behavior of thermomechanically treated steels into a quantitative explanation.

The statistical measures quite properly play a very small role in your valuable summary of the published evidence on tensile-strength/

hardness relationships. I am sure that in future studies you will continue to be guided by the totality of scientific information available to you, and I hope you will often find that statistical techniques are helpful in data analysis.

SOME PROBLEMS IN STATISTICAL INFERENCE FOR GENERALIZED MULTINOMIAL POPULATIONS

Bernard Harris
Mathematics Research Center, U. S. Army
University of Wisconsin, Madison, Wisconsin

INTRODUCTION. Assume that a random sample of size N has been drawn from a "multinomial population" with an unknown and possibly countable infinite number of classes. That is, if X_i is the ith observation and M_j the jth class, then

$$P\{X_i \in M_j\} = p_j \geq 0, \quad j = 1, 2, \ldots ; \quad i = 1, 2, \ldots, N ,$$

and $\sum_{i=1}^{\infty} p_i = 1$. The classes are not assumed to have a natural ordering. Let n_r be the number of classes occurring exactly r times in the sample. Then, we clearly have

$$\sum_{r=0}^{\infty} r\, n_r = N .$$

We will be concerned with estimating the following two quantities which are generally of interest to experimenters.

(1) The sample coverage, defined by

$$C = \Sigma p_i , \tag{1}$$

where the sum runs over all classes which have occurred at least once in the sample.

(2) The population entropy, defined by

$$H = - \sum_{i=1}^{\infty} p_i \log p_i . \tag{2}$$

It will be convenient in our definition of entropy to violate the usual conventions and use natural logarithms rather than logarithms to base 2. This is equivalent to a scale change in units of measurement and will have no essential effect on any uses for which the entropy might be employed. Of course, we will assume throughout, that the series (2) converges, since otherwise the discussion will not be relevant.

In those problems which present difficulty, namely where too many of the p_i's are too small, small sample inference appears to be virtually hopeless, hence, all results described herein will be asymptotic results, i.e. for large N.

Estimation of H and C. For the moment, we will restrict to the case of an ordinary multinomial population, that is, one with a finite number, k, of classes. Then the "natural estimator" of entropy $\hat{H}$ is defined by

$$\hat{H} = -\sum_{i=1}^{N} \frac{in_i}{N} \log \frac{n_i}{N} = -\sum_{i=1}^{k} \hat{p}_i \log \hat{p}_i \tag{3}$$

where $\hat{p}_i$ is the maximum likelihood estimator of p_i.

Its properties has been discussed by G. P. Basharin [1] and we note them briefly. Basharin showed that

$$E(\hat{H}) = H - \frac{k-1}{2N} + O(N^{-2}) \tag{4}$$

and

$$\sigma^2_{\hat{H}} = \frac{1}{N} \sum_{i=1}^{k} [p_i \log^2 p_i - H^2] + O(N^{-2}) \tag{5}$$

and $\sqrt{N}(\hat{H} - H)$ is asymptotically normally distributed. If we attempt to apply Basharin's results to the more general case described earlier, it is easily seen that the naive replacement of p_i by $\hat{p}_i$ in (2) may not be successful. Essentially, Basharin's technique depends on the following sort of asymptotic behaviour,

as $N \to \infty$, $Np_i \to \alpha$, $i = 1, 2, \ldots, k$.

Consequently, if we have zero as a limit point of the p_i's, or even, if we have the limiting behaviour associated with the Poisson approximation,

as $N \to \infty$, $p_i \to 0$, $Np_i \to \lambda_i$, $0 < \lambda_i < \infty$,

for a sufficiently large number of classes, then Basharin's estimator, $\hat{H}$, may be quite poor. The following illustration will exhibit this. Let $p_i = \frac{1}{N^2}$, $i = 1, 2, \ldots, N^2$. Then $H = 2 \log N$. However, since the maximum of H occurs for $p_i = \frac{1}{k}$, when there are k classes, we have that $\hat{H} \leq \log N$. Hence, it is quite clear, that if there are "too many classes whose probabilities are too small", $\hat{H}$ will not be a satisfactory estimator. One of the causes of the difficulty is that $\hat{H}$ gives no weight to unobserved cells, so that if the total probability in unobserved cells is large, $\hat{H}$ will not perform too well.

We can gain some insight in dealing with this, if we examine the second question we advanced, the estimation of the sample coverage. This problem is discussed in greater detail in B. Harris [3] , but it is convenient at this time to make some intuitive observations concerning the estimation of C, so that we can resolve the difficulties noted above in the estimation of H.

First, note that if we were to proceed as Basharin did and set

$$\hat{C} = \Sigma \hat{p}_i$$

then we have that $\hat{C} = 1$ for all samples, which is clearly inappropriate. We can guide our intuition by first examining some extreme cases.

(1) If $n_1 = N$, then we readily reach the conclusion that C must be small. We can see this as follows. If we now take another observation, inasmuch as every past observation resulted in a new class being observed, it is apparent that with probability quite close to unity, the N+1th observation will also result in a new class. In fact, the probability that the N+1th observation will not result in a new class is C, which of course should be near 0, as noted.

(2) If, on the other hand, there is an integer t, substantially larger than one, such that $n_1 = n_2 = \ldots = n_{t-1} = 0$, $n_t > 0$. Then, similar reasoning would lead us to conclude that most of the probability is concentrated in classes with high probability, and therefore C should be near unity.

(3) Let $p_i = \frac{1}{N}$, $i = 1, 2, \ldots, N$. Then $E(n_1) \sim Ne^{-1}$ and $E(n_0) \sim Ne^{-1}$. Thus, we should have $C \sim 1 - e^{-1}$.

In short, as is shown in B. Harris [3], it is the low order occupancy numbers, such as n_1, n_2, and n_3, which contain the principal information concerning the probability content of unobserved classes. A cursory examination of the three examples cited above suggest that an appropriate estimator for C is given by

$$\hat{C} = 1 - \frac{n_1}{N} \quad . \tag{6}$$

In Harris [3], it is shown that $\hat{C}$ is in fact an suitable estimator, in that it has good asymptotic properties.

In E. B. Cobb and B. Harris [2], a method for estimating entropy, when "all the sample information is contained in the low order occupancy numbers" was exhibited. In order to do this, we will show that we can represent entropy asymptotically by

$$H = \frac{1}{N} E(n_1) \int_{-\infty}^{\infty} e^{x} \log \left(\frac{N}{x}\right) dF^{*}(x) \tag{7}$$

where

$$F^{*}(x) = \sum_{Np_j \leq x} Np_j e^{-Np_j} \Big/ \sum_{j=1}^{\infty} Np_j e^{-Np_j} \quad . \tag{8}$$

It is easily verified that $F^{*}(x)$ is a cumulative distribution function. Since

$$E(n_1) \sim \sum_{j=1}^{\infty} Np_j e^{-Np_j} \tag{9}$$

substitution of (8) and (9) into (7) produces

$$\frac{1}{N} \sum_{j=1}^{\infty} e^{Np_j} \log \left(\frac{1}{p_j}\right) Np_j e^{-Np_j} = -\sum_{j=1}^{\infty} p_j \log p_j = H$$

which verifies (7).

Under the assumptions stated above Cobb and Harris [3] suggested that the entropy be estimated by

$$\breve{H} = \frac{n_1}{N} \frac{(N-m_1)^2}{(N-m_1)^2 + (m_2 - m_1^2)} e^{(Nm_1 - m_2)/(N-m_1) \log\left[\frac{N(N-m_1)}{Nm_1 - m_2}\right]} \tag{10}$$

where $m_1 = 2n_2/n_1$ and $m_2 = \max(m_1^2, 6n_3/n_1)$.

At this point it is worthwhile to present a numerical example, which will illustrate the behavior of $\breve{H}$.

Example $p_i = \frac{1}{N}$, $i = 1, 2, \ldots, N$. Then $n_1 \sim Ne^{-1}$, $n_2 \sim \frac{N}{2} e^{-1}$, and $n_3 \sim \frac{N}{6} e^{-1}$. Thus, $m_1 \sim 1$, $m_2 \sim 1$ and

$$F^*(x) = \begin{cases} 0 & x < 1 \\ 1 & x \geq 1 \end{cases}.$$

Then

$$\breve{H} \sim \frac{Ne^{-1}}{N} \frac{(N-1)^2}{(N-1)^2} e^{(N-1)/(N-1) \log\left[\frac{N(N-1)}{N-1}\right]} = \log N$$

and $H = \log N$, which is as it should be.

Clearly, it is principally the classes with small probabilities that contribute to n_0, n_1, n_2, and n_3. For those classes with large probabilities, we can estimate p_i by $\hat{p}_i$.

Then, the natural way of proceeding is to estimate the contribution to entropy from large classes by means of Basharin's method and the contribution of small classes by $\overset{\smile}{H}$, and we denote the final estimator by H^*. Recall that in order to use $\overset{\smile}{H}$, we have taken n_1, n_2, and n_3 to determine $\overset{\smile}{H}$.

There is one last detail which must be taken into account. Part of the contribution to moderate order occupancy numbers, such as n_4, n_5, and some of the succeeding occupancy numbers, will be due to classes with small probabilities and the effect of sample fluctuations. Therefore, we need to examine the following. What proportion of each n_j, $j = 4, 5, \ldots, s$, s some sufficiently large integer, is due to a large deviation from a class with small probability? We can adopt a Theorem due to A. Wald [4] obtaining the following inequalities.

$$(11) \quad \text{if} \quad m_2 > m_1^2, \quad E(n_{k+1}) \geq \frac{6(3^{k-2})n_3^{k-1}}{(k+1)!\, n_2^{k-2}}, \quad k = 3, 4, \ldots,$$

$$(12) \quad \text{if} \quad m_2 = m_1^2, \quad E(n_{k+1}) \geq \frac{2^k n_2^k}{n_1^{k-1}(k+1)!}, \quad k = 3, 4, \ldots.$$

The right hand side of each inequality gives the expected values of n_{k+1}, if "the sample information is contained in n_1, n_2, and n_3". Thus the difference between the left and right hand sides of (11) and (12) gives an estimate of the contribution to n_{k+1} which is due to classes with larger probabilities. We apply Basharin's estimator (3) to these, upon replacing the expected values in the left hand sides of (11) and (12) by the observed values.

Thus, we finally write

$$H^{*} = \lambda \hat{H} + (1-\lambda) \breve{H} \tag{13}$$

where $0 \leq \lambda \leq 1$ is the proportion of the observations in n_1, n_2, and n_3 and the parts of $n_4, n_5, \ldots, n_s$ determined by (11) and (12). For the parts of the sample allocated to small classes as noted above we use $\breve{H}$, and use $\hat{H}$ on the part allocated to large classes.

The mathematical details will be given in a later publication.

REFERENCES

[1] Basharin, G.P., (1959) On a statistical estimate for the entropy of a sequence of independent random variables. Teorija Verojatnostei i ee Primenija, 333-336.

[2] Cobb, E.B. and Harris, B. An asymptotic lower bound for the entropy of discrete populations with application to the estimation of the entropy of almost uniform populations. (Submitted for publication).

[3] Harris, B. (1959) Determining bounds on integrals with applications to cataloging problems. Annals of Mathematical Statistics, 30, 521-548.

[4] Wald, A. (1939) Limits of a distribution function determined by absolute moments and inequalities satisfied by absolute moments. Transactions of the American Mathematical Society, 46, 280-306.

APPLICATION OF NUMERICAL TECHNIQUES TO EXPERIMENTALLY MODEL AN AERODYNAMIC FUNCTION*

Andrew H. Jenkins
Physical Sciences Laboratory, Directorate of Research and Development
U. S. Army Missile Command, Redstone Arsenal, Alabama

ABSTRACT. This report describes the use of an aeroballistic range in the design and execution of an aerodynamic experiment, the analysis of the experimental data by numerical techniques to develop a model of a physical function, and the statistical testing of the data and the model. The report discusses the approach, the experimental design, and the testing of the data using several frequency distributions. It presents and describes a multivariate nonlinear regression analysis performed on the data, the physical model developed by the regression analysis, and the testing of the model. It also lists and presents the tests of hypotheses made and discusses the results of the tests.

SYMBOLS

a	Acoustic velocity in air
A	Pure constant of regression equation
b	First coefficient of regression equation
C	Counts per inch of photoreader = 3502
c	Second coefficient of regression equation
c_p	Coefficient of specific heat at constant pressure
c_v	Coefficient of specific heat at constant volume
d. f.	Statistical degrees of freedom
F	Frequency distribution
F_{sh}	Magnification factor of shadowgraph = 1.009
F_{sc}	Magnification factor of Schlieren = 0.855
K	Ratio of shock density ρ_s to free stream density ρ^∞
ln	Natural logarithm (base e)

*This article was initially issued as U. S. Army Missile Command Report No. RR-TR-65-11.

SYMBOLS (continued)

M	Mach number = V/a
M_1	Mach factor level = 1.1 to 1.5
M_2	Mach factor level = 2.5 to 2.9
M_3	Mach factor level = 3.9 to 4.3
M_i	Mach factor effect in statistical equation
M_ℓ	Mach factor linear effect
M_q	Mach factor quadratic effect
MR_{ij}	Main factor interaction effect
N	Total observation
P	Statistical probability
r	Regression correlation coefficient
R_o	Universal gas constant. = 1715 sq. ft/sq. sec./°R.
R	Radius
R_1	Model nose/base radius ratio = 1.0
R_2	Model nose/base radius ratio = 0.7
R_3	Model nose/base radius ratio = 0.4
R_b	Model base radius = 0.112 inch
R_j	Radius factor effect in statistical equation
R_n	Nose radius of model
R_r	Model nose to base radius ratio
R_ℓ	Radius factor linear effect
R_q	Radius factor quadratic effect
S	Surface roughness of model
S_e^2	Experimental sample variance
S_e	Experimental sample standard deviation

SYMBOLS (continued)

SS	Sum of squares
t	Value of students frequency distribution
T	Absolute temperature (°Rankine)
V	Flight model velocity
$\overline{X}$	Mean
$\overline{X}_{aw}$	Mean of Ambrosio-Wortman model
$\overline{X}_{e}$	Mean of experimental responses
X_{i}	ith response
$\overline{X}_{r}$	Mean of regression model responses
$X_{2,\ 3}$	Dependent variable of regression equation (computer language)
Y	Independent variable of regression equation (computer language)
Z	Normal frequency distribution
α	Type I error risk level
β	Type II error risk level
γ	Ratio of specific heats = c_p/c_v
δ_{sh}	Shock detachment distance from shadowgraph optical system
δ_{sc}	Shock detachment distance from Schlieren optical system
Δ	Shock detachment distance in photoreader counts (corrected)
$\epsilon_{k(ij)}$	Experimental error
σ_e^2	Variance of experimental responses
σ_r^2	Variance of regression model
σ_{aw}^2	Variance of Ambrosio-Wortman model
μ	Universal means
χ^2	Frequency distribution
ρ	Density

1. INTRODUCTION. A number of new aerodynamic problems have come into prominence in recent years. The source of the problems has been the very high flight velocities achieved by use of rockets. The characteristics of the problems of the very high flight velocities, referred to as supersonic or hypersonic flight, are those of a hydrodynamic nature. The Mach numbers are high and problems of a physical and chemical nature also exist because the energy of the flow is large. The gases are rarefied so that the mean free path is not negligibly small compared with an appropriate macroscopic scale of the flow field. Under such conditions, kinetic thoery is included with the hydrodynamics.

The new features of a hydrodynamic nature allow the use of certain simplifying assumptions in developing theories for hypersonic flow. On the other hand, certain important features which appear introduce additional complications over those met within gas dynamics at more moderate speeds. The techniques of linearization of the flow equations and the use of mean-surface approximation for boundary conditions have a diminishing range of applicability. Also, entropy gradients produced by curved shock waves make the classical isentropic irrotational approach inapplicable.

The additional problems of a physical and/or chemical nature are associated with the high temperatures of the flow as the gases traverse the strong bow shock wave. The sudden shock heating of the gases excites the vibrational degrees of freedom of the molecules resulting in dissociation of the species into atoms, electrons, and ions which do not require treatment at lower velocities. Therefore, it must be recognized that physical phenomena rather than hydrodynamic phenomena may not only influence the flow but in many cases control it. In view of the complexities of the flow at high Mach numbers and the number of technical disciplines involved, many have resorted to experimental or empirical development of functional relationships.

The flow field originates at the bow shock. The shock wave characteristics are very important to the stagnation region characteristics. The volume of the stagnation region is dependent on the shock detachment distance. Therefore, much of the knowledge of the flow characteristics is dependent on the knowledge of the shock location. Experiments have been performed on wind tunnels to study the shock location. However, few experiments have been made to study this problem under free flight

conditions. Also, the studies which have been made and the derived relationships are lacking as tests have not been attempted to determine their reliability.

It is apparent that the community recognizes the need for improved hypersonic design theory. One of the important areas is the prediction of shock detachment distance. It is important to the computation of not only heat transfer but also pressure distributions and drag on the forepart of the vehicle. This has been pointed out by Serbin [1], Ambrosio and Wortman [2], DiDonato and Zondek [3], Heberle, Wood, and Gooderum [4], and Love [5].

The lack of purely theoretical models for the prediction of shock detachment distance at transonic and supersonic velocities has led to the natural consequence of an experimental approach. This is to be expected and in addition the theoretical hypothesis is inevitable subject to experimental verification. For this reason, one can also expect to contribute to scientific progress by the inverted approach of formulating models of the mathematical relationships between physical variables by experimentation. However, the relationships derived are subject to experimental control, measurement accuracy, human error, and many other sources of unexplained or unaccounted for deviations from the true universal relationships.

In the direct approach (i.e., the a priori derivation of a mathematical model) quite often ideal physical conditions are assumed and simplifying mathematical assumptions are made which depart from the real case. Therefore, one cannot be sure of the theory nor can one be certain of the experimental data. Yet, in scientific endeavor, exacting conclusions are often drawn by the comparison of an idealized hypothesis and real case data. That is, both quantities are coupled to each other and not to an independent estimate of the deviation present.

Empirical models of the shock detachment distance for blunt bodies of revolution have been made by Serbin [1], Ambrosio and Wortman [2], and Heberle, Wood, and Gooderum [4]. The data were obtained by these authors using moving streams of air surrounding stationary spheres (i.e., radius nosed bodies) in such experimental devices as wind tunnels and jet nozzles. Both of these devices have two common disadvantages. The gaseous medium is in a state of expansion just prior to the shock

compression. Also, holding devices are present in the flow around the body which cause perturbations in the flow. The flow is often not uniform in cross section. The measurements, therefore, include these perturbations and do not represent the real case of a vehicle in free flight.

Serbin [1] derived the following relationship for a sphere:

$$\frac{\Delta}{R} = 2/3\,(K - 1)^{-1}, \tag{1}$$

Ambrosio and Wortman[2] derived the following relationship:

$$\frac{\Delta}{R} = 0.143e^{3.24/M^2}, \tag{2}$$

and Heberle, Wood, and Gooderum[4] derived this relationship:

$$\frac{\Delta}{R} = 4/3\,(M - 1)^{-1/3}. \tag{3}$$

Each author stated that agreement between the model and the data was very satisfactory. However, the standard by which this was determine was not stated or explained. This type of unexplained, seemingly arbitrary, acceptance of a model and data appeared to be typical.

A machine literature search was made. In this search, over 100,000 documents were screened and matched by computer on the basis of key words and terms in aerodynamics and statistics. This was done to determine if, in the past, any use of statistics in testing aerodynamic experimental data had been done. Not one document was found during the search. However, this is not to imply that statistics have not been used. Apparently, it is either not a prevalent or accepted practice or possibly has not been reported.

Ambrosio and Wortman [6] did attempt the use of some simple statistical methods. This was done to the extent of computing the mean, the absolute mean, and the standard deviation. However, it was not for the purpose of testing the reliability of their data and model but to objectively establish the relative worth of their model as compared to Serbin[1].

This work has two objectives as follows:

1) To develop an empirical model of shock detachment distance as a function of Mach number and vehicle nose radius with experimental data obtained under free flight conditions

2) To subject this model and data to analysis by statistical methods to objectively define the level of confidence of such a model.

II. EXPERIMENTAL PROCEDURES.

1. Design

The shock detachment distance can be described aerodynamically for radius nosed bodies of revolution as:

$$\Delta = f(M, R). \tag{4}$$

Explicit models of several investigators were mentioned in the introduction.

Statistically, the model can be expressed as:

$$\Delta = \mu + M_i + R_j + MR_{ij} + \epsilon_{k(ij)}. \tag{5}$$

The model contains two independent factors, Mach number (M_i) and body radius (R_j). It also contains a second order effect, the MR_{ij} interaction.

The design of the experiment required consideration of both the aerodynamic and the statistical aspects. Past experience indicated that the shock detachment distance was a nonlinear function of Mach number (M) and a linear function of radius (R) The objectives of the experiment are to determine if the linear and quadratic effects of Mach number and radius contribute significantly to the shock detachment distance. Also, it was desired to determine if a second order or interaction effect between radius and Mach number contributes significantly to the shock location. The analysis of variance is a useful tool for this. In addition, it was also desired to develop an empirical model of the functional relationships between the independent and dependent variables. A regression analysis was planned for this.

The analysis of data by regression calculation can be simplified by the equal spacing of the independent variables which permits the use of orthogonal polynomials. This helps also in the subsequent adjustment arising from the discarding of insignificant variables or the addition of new terms. One objective of the experiment is to estimate the slope of the regression. The slope of a regression is estimated more precisely if the values of the independent variables are selected with equal spacing at the extremes of the quantified ranges of the variable. This is because interpolation is more reliable than extrapolation and the computations are simplified.

The effects of the main factors in this experiment could not be considered theoretically independent. Therefore, it is necessary to replicate the experiment within cells of all factor levels in order to test for interactions between factors and to estimate the experimental error. Since one objective is to statistically test for interaction, the analysis of variance will enable the test of interaction and estimates of error variance. The two best tests for statistical analysis of the aerodynamic experiment are the analysis of variance and the multivariate regression analysis. The experimental design most efficient for these methods is the factorial experiment with replication.

The factorial experiment enables one to test the effects of Mach number (M) and radius (R) on the shock location (Δ) over the ranges of interest of M and R at each factor level. It also promotes testing for the existence of interaction between M and R and the effect of interaction on Δ. One is also able to differentiate interaction effects from main effects. In addition, it allows the determination of confidence limits for the estimates of main and interaction effects based on the estimate of experimental error derived from replication.

Therefore, the experiment was designed as a fixed model 3^2 factorial. Both the radius and Mach number factors are equispaced three level, fixed and quantitative. The Mach number range of interest was 1.0 to 4.5. The levels selected were M_1 = 1.1 to 1.5, M_2 = 2.5 to 2.9, and M_3 = 3.9 to 4.3. The radii selected were nose to base radius ratios of R_1 = 1.0, R_2 = 0.7, and R_3 = 0.4. The experiment was replicated three times in each factor cell; therefore, a total of 27 observations was recorded (N = 3 x 3 x 3 = 27).

All 27 responses could not be obtained in 1 day. Therefore, to compensate for day-to-day variations in personnel, voltages, developing solutions, film batches, and printing, the firing sequence was randomized. All combinations of factors and replicates were listed and the experimental sequence was randomized by use of a random number generator [7] which was entered in a random manner. The results of the randomization are shown in Table I. The numbers shown without parentheses are the sequence of firing while the numbers in parentheses are the corresponding round identification numbers. Table I also shows the factor levels selected for the experiment.

Table I. Randomized Experimental Sequence

		Mach Number Levels		
Nose/Base Radius Ratio	Replicate	M_1 1.1 to 1.5	M_2 2.5 to 2.9	M_3 3.9 to 4.3
$R_1 = 1.0$	1	26 (75)	7 (56)	11 (60)
	2	22 (71)	8 (57)	6 (54)
	3	2 (49)	14 (63)	10 (59)
$R_2 = 0.7$	1	12 (61)	13 (62)	9 (58)
	2	23 (72)	27 (76)	25 (44)
	3	24 (73)	18 (67)	15 (64)
$R_3 = 0.4$	1	16 (65)	3 (50)	19 (68)
	2	1 (48)	17 (66)	5 (53)
	3	4 (52)	20 (69)	21 (70)

Notes:

1. Numbers without parentheses are randomly determined program firing sequence.

2. Numbers with parentheses are for experiment identification.

The radii of the models are discrete levels. The Mach number levels are discrete intervals as it is almost impossible to duplicate exact velocities by this method of experiment. This is due to variations in propellants, model material homogeneity, and model-launch tube interference. The Mach number levels chosen were fixed in selected ranges between Mach 1.0 and 4.5 which is the velocity regime of interest in this aerodynamic study. As a two factor fixed model experiment, it is assumed that μ is a fixed constant and the $\epsilon_{k(ij)}$'s are normally and independently distributed with a zero mean.

2. Procedure

The experimental data were obtained on the Physical Sciences Laboratory's free flight aeroballistic range. Figure 1 shows the experimental apparatus. It consists of a light gas gun for launching the models, and altitude simulation chamber, a shadowgraph and a Schlieren system for photographing the model and the flow around the model. Also, submicrosecond electronic counters to determine the model's time of flight are included.

The aerodynamic data required from this experiment are the radius of the model, the Mach number of the model, and the detachment distance of the shock. The radius of each model was known as the models were formed in accurately machined dies. Their geometries are shown in Figure 2. The models were made of copper coated lead. The Mach number is determined by taking the ratio of the model velocity to the acoustic velocity when the photographs are made. The acoustic velocity is computed as shown in Appendix A. It is seen that the acoustic velocity varies as the square root of the temperature and specific heat ratio. The temperature was recorded at the time of launching each model. The specific heat ratio was taken as 1.4. The model velocity was computed by taking the ratio of the distance between the shadowgraph and Schlieren stations to the time recorded on the counter. The distance between the shadowgraph and Schlieren stations is a constant of 5 feet. It was assumed that the deceleration of the model over 5 feet was linear; therefore, the velocity computed was the velocity of the model midpoint between the two stations.

Photographs of the model showing the shock detachment distance were taken by both the shadowgraph and Schlieren systems The measure of the shock detachment distance from either one of these photos

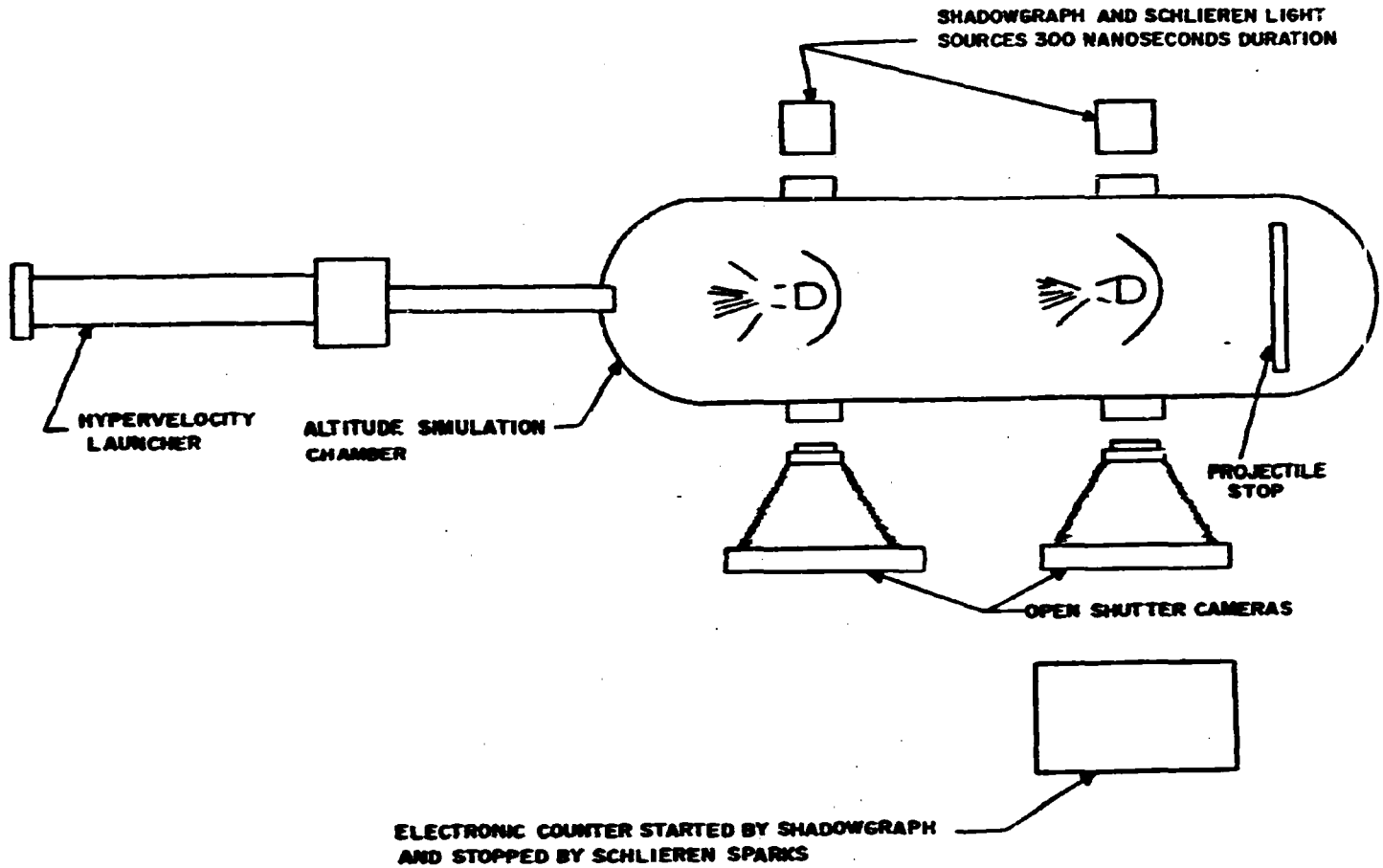

Figure 1. Arrangement of Experimental Apparatus

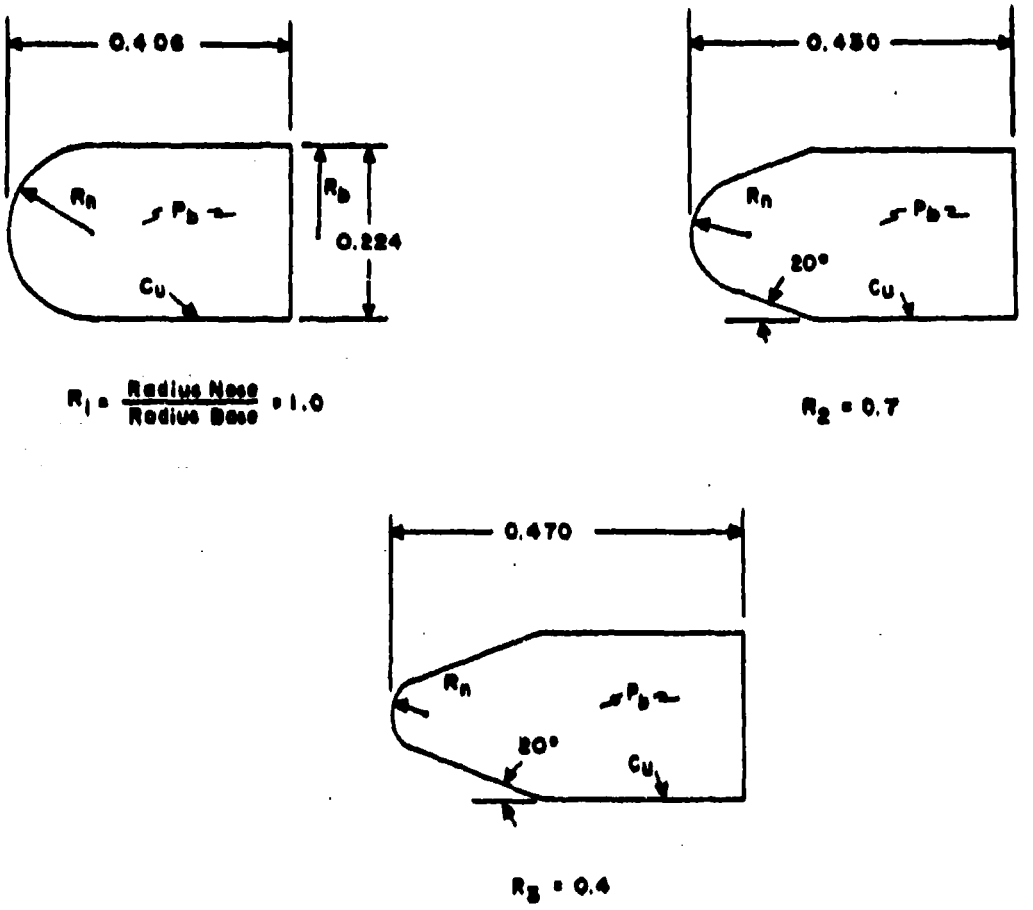

Figure 2. Sketch of Experimental Flight Models

would not coincide with the velocity of the model. Therefore, with the assumption of linearity, the shock detachment distance was corrected to the velocity computation. The correction of the detachment distance required the consideration of the magnification factors for the photographs. The magnification factor for the shadowgraph camera was 1.009 and the Schlieren camera was 0.855. The photo reader upon which the negatives were read was calibrated at 3502 electronic counts per inch in the plane of the negative on the photo reader. The shock detachment distance was read in counts from both the shadowgraph and Schlieren negatives. The detachment distance and radius of each type model was corrected to counts as follows:

$$\Delta = \delta_{sh} F_{sc} + \delta_{sc} F_{sh} \tag{6}$$

and

$$R = 2 \times C \times R_b \times F_{sh} \times F_{sc} \times R_r \ . \tag{7}$$

The values of Δ and R computed for each round are shown in Table II. A sketch of a typical shock detachment distance as taken by the shadowgraph and Schlieren is shown in Figure 3.

The experimental data obtained from the experimental program are compiled in Table II. The data are tabulated and identified by the round number assigned on the aeroballistic range. Computations of certain data presented in Table II are shown in Appendix A. The data from round number 75 were used to show a typical example of the computational procedures.

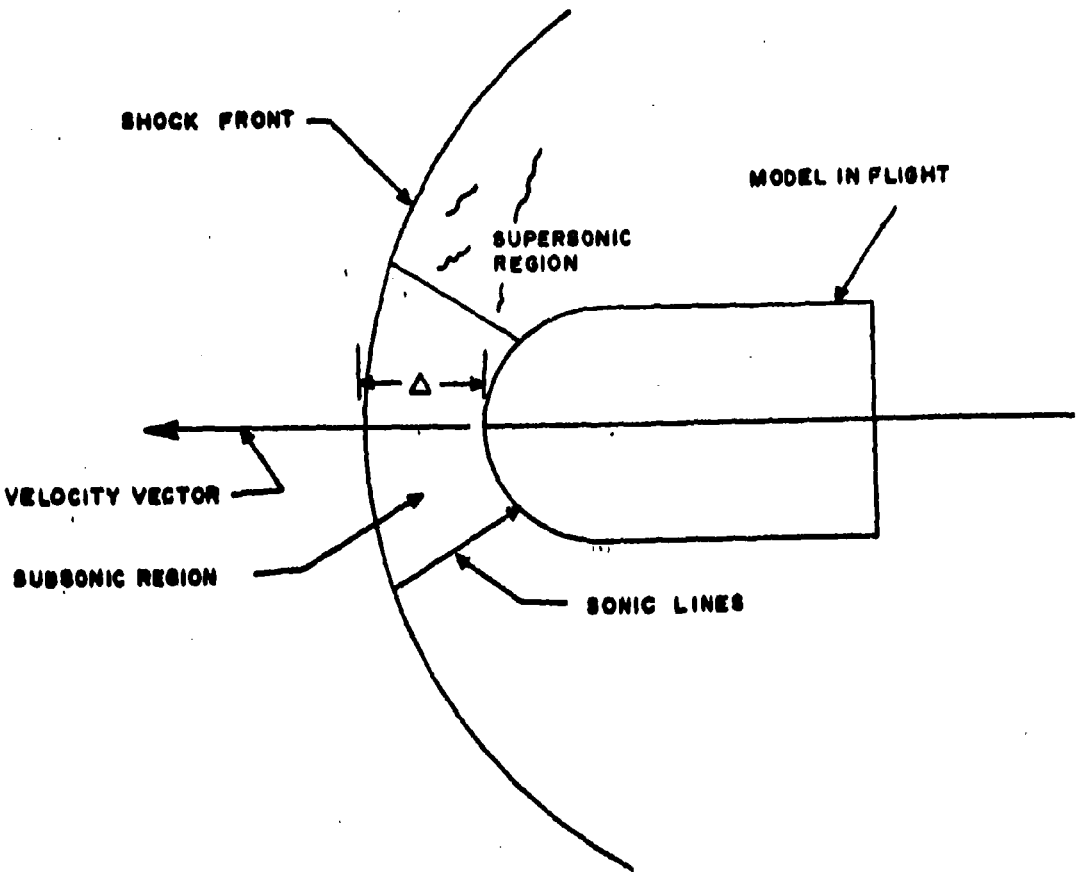

Figure 3. Sketch of Typical Shock Detachment

Table II. Compilation of Experimental Data

Round No.	Radius Ratio R_a/R_b	Nose Radius (Counts)	Mach Range	Temp. (°F)	Sonic Vel. (fps)	Model Vel. (fps)	Mach No. V/a	Shadowgraph (Counts)	Schlieren (Counts)	Δ (Counts)	$\frac{\Delta}{R}$
75	$R_1 = 1.0$	676.74	M_1 1.1 - 1.5	71	1131	1416	1.252	390	373	710	1.049
71				71	1131	1303	1.152	540	543	1010	1.492
69				73	1133	1342	1.184	487	450	870	1.286
56	$R_1 = 1.0$	676.74	M_2 2.5 - 2.9	75	1135	3142	2.768	73	36	99	0.146
57				73	1133	2969	2.620	78	32	99	0.146
63				72	1132	3215	2.840	92	49	128	0.189
60	$R_1 = 1.0$	676.74	M_3 3.9 - 4.3	72	1132	4541	4.011	102	63	151	0.223
54				72	1132	4474	3.952	66	37	94	0.139
59				72	1132	4500	3.975	69	36	95	0.140
61	$R_2 = 0.7$	473.72	M_1 1.1 - 1.5	71	1131	1329	1.175	342	396	692	1.461
72				71	1131	1156	1.022	1340	1438	2595	5.478
73				71	1131	1264	1.118	488	488	910	1.921
62	$R_2 = 0.7$	473.72	M_2 2.5 - 2.9	71	1131	3142	2.778	106	36	127	0.268
76				71	1131	3069	2.714	56	41	89	0.188
67				74	1134	3259	2.874	91	42	120	0.253
58	$R_2 = 0.7$	473.72	M_3 3.9 -4.3	72	1132	4464	3.943	61	34	86	0.182
74				71	1131	4516	3.993	67	27	85	0.179
64				71	1131	4500	3.979	75	33	97	0.235
65	$R_3 = 0.4$	270.70	M_1 1.1 - 1.5	71	1131	1478	1.307	142	157	280	1.034
48				73	1133	1284	1.133	332	320	607	2.243
52				72	1132	1326	1.171	257	248	470	1.736
50	$R_3 = 0.4$	270.70	M_2 2.5 - 2.9	73	1133	3306	2.908	50	18	61	0.226
66				71	1131	3242	2.866	64	21	76	0.280
69				70	1129	3589	3.179	72	25	87	0.321
68	$R_3 = 0.4$	270.70	M_3 3.9 - 4.3	70	1129	4730	4.190	33	27	55	0.203
53				72	1132	4288	3.788	43	20	57	0.210
70				70	1129	4662	4.112	64	21	59	0.217

III. ANALYSES. The data obtained from the experiment are presented in Table II. The observations taken as the dimensionless ratio of the standoff distance divided by the model radius are presented in the factorial design layout in Table III along with some computations in preparation for performing an analysis of variance. The statistical computations are presented in Appendix B.

The gathering of the data, the analysis, and derivation of the model of the functional relationships from the experimental observations are based on certain aerodynamic and statistical assumptions. These assumptions are:

1) Small angles of attack of the models (i.e., less than 2°) do not significantly effect the detachment distance.

2) The models were free from ablation products in the stagnation region.

3) The effects of gas constituent dissociation on the dynamics of flow was insignificant.

4) The effects of spin stabilization on the dynamics of flow was insignificant.

5) The effect of the conical section of two of the models on the dynamics of the flow was insignificant (i.e., all projectiles were hemispheres of various radii).

6) The experimental error is normally and independently distributed.

7) The experimental precision is essentially the same for all factor combinations.

8) The factors were fixed at discrete levels so, therefore, are not independent of each other.

Assumptions 1 through 5 are made concerning the aerodynamics of the experiment. These represent sources of variation which are considered negligible. They cannot be separated explicitly from the main

Table III. Data Layout for Shock Detachment Experiment

Body Radius Ratio		Mach Number Region M_1	Mach Number Region M_2	Mach Number Region M_3	$\Sigma X_{j\cdot}$	$\bar{X}_{j\cdot}$
	$R_1 = 1.0$	1.049	0.146	0.223		
		1.492	0.146	0.139	4.810	0.5344
		1.286	0.189	0.140		
		3.827	0.481	0.502		
	$R_2 = 0.7$	1.461	0.268	0.182		
		5.478	0.188	0.179	10.135	1.126
		1.921	0.253	0.205		
		8.860	0.709	0.566		
	$R_3 = 0.4$	1.034	0.225	0.203		
		2.243	0.280	0.210	6.469	0.719
		1.736	0.321	0.217		
		5.013	0.826	0.630		
$\Sigma X_{\cdot i}$		17.700	2.016	1.698	$\Sigma X_{\cdot\cdot} = 21.414$	
$\bar{X}_{\cdot i}$		1.967	0.244	0.189	$\bar{X}_{\cdot\cdot} = 0.793$	
					$\Sigma\Sigma X^2_{ij} = 50.7464$	

and interaction effects. It is important to note that, even though considered negligible, these variations are present and are statistically accounted for by summation into experimental error. The statistical assumptions 6 through 8 allude to these conditions.

1. Analysis of Variance

The experiment was described in Section II by the statistical model

$$\Delta = \mu + M_i + R_j + MR_{ij} + \epsilon_{k(ij)}. \tag{8}$$

The theoretical model underlying the analysis of variance assumes that each experimental response of the shock detachment distance (Δ) is the algebraic sum of:

1) An overall mean of the detachment distance, μ (i.e. true standoff distance)

2) A Mach number effect on the standoff distance, M_i

3) A radius effect on the standoff distance, R_j

4) An interaction effect on the standoff distance, MR_{ij}

5) A random residual error (experimental), $\epsilon_{k(ij)}$.

Since the model is a fixed model, none of the effects can be measured absolutely. They can be measured only as differential deviations, i.e., the M_i as deviations from μ, the R_j as deviations from μ, and the MR_{ij} as deviations from $M_i + R_j$.

The results of the analysis of variance are shown in Table IV. The computations are presented in Appendix B.

From Table IV, it can be seen that the main effects of radius have apparently no significant effect on the shock detachment distance at the 95 percent level of confidence. The linear and quadratic effects are also insignificant. The quadratic effects of radius seem to have the most effect on the standoff distance. They would be significant at the 80 percent level of confidence though still not significant at the 95 percent level.

Table IV. Analysis of Variance

Source of Variation	Degrees of Freedom (d. f.)	Sum of Squares (SS)	Mean Square (MS)	F Value (Computed)	F Value (Tables) $\alpha = 0.05$ $\frac{\text{df source}}{\text{df error}}$	Expected Mean Square	
						EMS	% Total
Radius (R_j)	2	1.6499	0.8249	1.410	3.55	$\sigma_e^2 + 9\sigma_R^2$	
R_l	1	0.1529	0.1529	0.261	4.41	$\sigma_R^2 = 0.027$	1.05
R_q	1	1.4970	1.4970	2.560	4.41		
Mach No. (M_i)	2	18.5583	9.2991	15.904	3.55*	$\sigma_e^2 + 9\sigma_M^2$	
M_l	1	14.3146	14.3146	24.481	4.41*	$\sigma_M^2 = 0.967$	59.15
M_q	1	4.2837	4.2837	7.478	4.41*		
Interaction (MR_{ij})	4	2.9885	0.7471	1.277	2.93	$\sigma_e^2 + 3\sigma_{MR}^2$	3.10
$R_l M_l$	1	0.0855	0.0855	0.146	4.41	$\sigma_{MR}^2 = 0.054$	
$R_q M_l$	1	2.1980	2.1980	3.759	4.41		
$R_l M_q$	1	0.0108	0.0108	0.018	4.41		
$R_q M_q$	1	0.6942	0.6942	1.187	4.41		
Error $e_{k(ij)}$	18	10.5261	0.5847			σ_e^2	
						$\sigma_e^2 = 0.585$	35.80
Total	26	33.7628					

*Significant

The Mach number is significant at the 95 percent level of confidence. The computed value in the F test is greater than the F distribution table value by a factor of about 5. The linear and quadratic effects are also significant. The linear effect of the Mach number factor was found to be more significant than the quadratic effect.

The analysis of variance also shows that there is apparently no significant effect of the MR_{ij} interaction on the standoff distance. It is interesting to note, however, that of all the combinations of linear and quadratic interactions between Mach numbers and radii, the quadratic radius and linear Mach number were most nearly significant at the 95 percent level of confidence. This is congruent with the fact that the test of the quadratic effects of radius and the linear effects of Mach number was highest in the main effects tests. Under the interaction effects tests, the computed value of 3.759 for the R_qM_1 combination would be significant at the 92 percent level as compared to 4.41 for the F value at the 95 percent level.

It is also noted in Table IV that the mean square for radius and radius-Mach number interactions were only slightly higher than the mean square for error. On the basis of the assumption that the experimental error is normally distributed between all factors and all levels, then radius and interaction effects do not significantly contribute to shock detachment distance within the limits of this experiment.

The results of the analysis of variance, as shown in Table IV, is further analyzed as shown in Figure 4. Figure 4 is the graphic display of the results of the Duncan range tests as computed in Appendix B. Figure 4(a), for the Mach number range significance test, shows that the M_1 level (1.1 to 1.5) is significantly different from the M_2 and M_3 levels of 2.5 to 2.9 and 3.9 to 4.3, respectively. The M_2 and M_3 levels were not found to be significantly different from each other. The radius factor range test as shown in Figure 4(b) shows the radius factor levels not significantly different from each other. The fact that the M_2 and M_3 levels are not significantly different from each other will be discussed later in this section.

2. Regression Analysis

The analysis of variance can be performed whether the factors are quantitative or qualitative. When the factors are quantitative, then

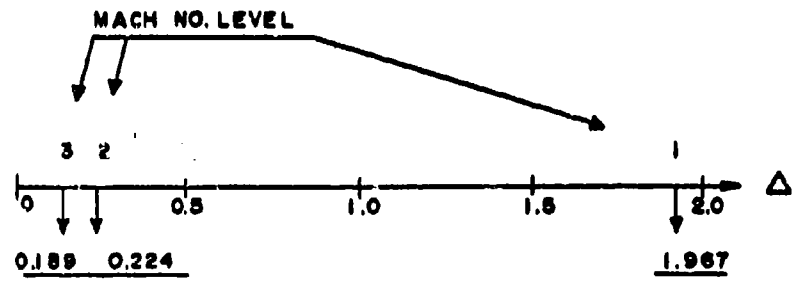

(a) MACH NUMBER RANGE SIGNIFICANCE TEST

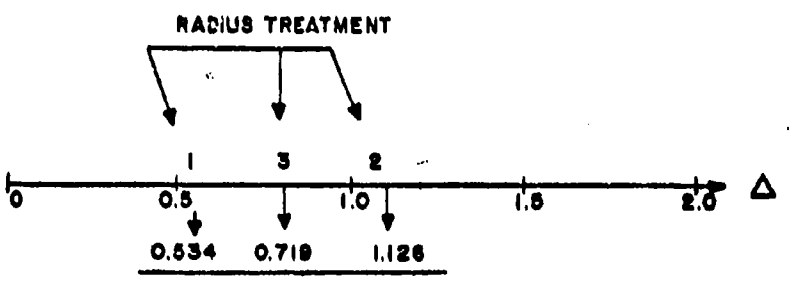

(b) RADIUS RANGE SIGNIFICANCE TEST

(COMMONLY UNDERLINED MEANS ARE NOT SIGNIFICANTLY DIFFERENT AND COULD HAVE COME FROM A COMMON POPULATION)

Figure 4. Graphic Display of Duncan Range Tests

a regression analysis can be performed on the data. This analysis is especially useful in the determination of the general functional relationships of the factors at other than the experimentally assigned levels. The analysis of variance has led to knowledge of the important factor considered in this experiment which contributes to the shock detachment distance. This was found to be the linear and quadratic effects of Mach number. This led to a bivariate regression analysis. The regression analysis used was the SNAP Multiple Regression Analysis for the IBM 7090 computer. It was the Army Missile Command SHARE 183 program.

As pointed out, it is realized that the shock detachment distance is not singularly a function of Mach number. There are other factors which were not included in this experiment. For the factors considered by the analysis of variance, some knowledge of the main significant factor (Mach number) is now available.

Before progressing with the regression analysis, the physical aspects of the shock detachment distance must be considered. The functional relationship must be consistent with the aerodynamic concepts of the detachment distance. The detachment distance is inversely proportional to Mach number. That is:

$$\Delta = \frac{1}{f(M)} = f\left(\frac{a}{V}\right) . \tag{9}$$

The limits of the functional relationships are then

$$\lim_{\substack{a \to o \\ M \to o}} f\left(\frac{a}{V}\right) = \lim \frac{1}{f(M)} = \lim \Delta = \infty$$

$$\lim_{\substack{a \to \infty \\ M \to \infty}} f\left(\frac{a}{V}\right) = \lim \frac{1}{f(M)} = \lim \Delta = 0$$

$$\lim_{\substack{V \to o \\ M \to \infty}} f\left(\frac{a}{V}\right) = \lim \frac{1}{f(M)} = \lim \Delta = 0$$

$$\lim_{V \to \infty} f\left(\frac{a}{V}\right) = \lim_{M \to o} \frac{\cdot}{f(M)} = \lim \Delta = \infty$$

$$\lim_{V \to a} f\left(\frac{a}{V}\right) = \lim_{M \to 1} \frac{1}{f(M)} = \lim \Delta = \text{constant.} \tag{10}$$

The functional relationship as determined by the regression analysis should be compatible with these bounds and pass the limit tests.

The computer program is a linear multiple regression analysis. However, the analysis of variance indicated that the linear and quadratic effects of Mach number are significant. Therefore, a transformation was required to make the computer program applicable to the hypothesized relationship. The relationship is hypothesized as

$$\Delta = AM^{b}M^{c}. \tag{11}$$

A physical limitation of the functional aspect of Δ is that

$$\frac{\Delta + R_n}{R_n} \geq 1 \tag{12}$$

because as the free stream Mach number goes to infinity, the shock is no longer detached but attached and the standoff distance is zero. Therefore, the desired functional form of the equation is

$$\frac{\Delta}{R_n} = AM^{b}M^{c}, \tag{13}$$

which presents the detachment distance as a dimensionless ratio, which is a more usable form for design engineering purposes.

This is not to indicate the dependence of detachment distance on body nose radius but to account for differences in body geometry. That is, the equations of detachment distance for bodies with radius noses cannot be used for sharp pointed bodies such as cones or purely blunt bodies such as right circular cylinders. Therefore, this functional relationship is for a geometric class of bodies, i.e., radius nosed bodies.

Equation (11) was programmed for the regression analysis by using the natural logarithm transformation. The equation programmed was

$$\ln \frac{\Delta}{R} = \ln A + b \ln M + c \ln M. \tag{14}$$

In computer language, the equation was

$$\ln Y = \ln A + b \ln X_1 + c \ln X_2 . \tag{15}$$

The values of Δ/R and M were taken from Table II and programmed into the computer, where

$$\begin{aligned} Y &= \frac{\Delta}{R} \\ X_1 &= M \\ X_2 &= M^2 . \end{aligned} \tag{16}$$

The computer transformed the experimental data to the natural logarithm form.

The results of the computer regression analysis are shown in Table V. The computer made two runs. After the first run, the results are automatically tested for significance ($\alpha = 0.05$) and the insignificant variables are dropped. It can be seen that the X_2 term was dropped by the computer. The data for run 2 were taken as the final regression analysis values. The pure constant (A), the first coefficient (b), and the regression coefficient (r) were tested and found significant as shown in Table V and Table VI. The regression equation is therefore:

$$\begin{aligned} \ln Y &= \ln A + b \ln X_1 \\ \ln Y &= \ln 0.7512 - 1.911 \ln X_1 . \end{aligned} \tag{17}$$

Taking the antilog the equation becomes

$$Y = 2.12\, X_1^{-1.911}$$

(18)

$$Y = \frac{2.12}{X^{1.911}}$$

or

(19) $$\frac{\Delta}{R} = \frac{2.12}{(M)^{1.911}}$$

with a standard error of estimate of 0.3933.

3. Testing the Model

Through the use of the analysis of variance, the effect of Mach number on the detachment distance was determined to be significant both linearly and quadratically. Based on this, a regression analysis was used to derive a general mathematical relationship between detachment distance and Mach number. Certain physical limits were prescribed for the form of the equation. These physical limits are tested as follows:

(20) $$\text{if } M = 0, \quad \frac{\Delta}{R} = \frac{2.12}{(0)^{1.911}} = \frac{2.12}{0} = \infty .$$

Test of Significance of Regression Coefficients A, b hypothesis A = 0
b = 0

$t(\frac{a}{2} = 0.025, \text{df} = 25) = \pm 2.06$

$t = \frac{0.751177 - 0}{0.39033/\sqrt{27}} = 10.002 > 2.06$ Test significant, reject hypothesis

$t = \frac{1.910723 - 0}{0.144127} = 13.25 > 2.06$ Test significant, reject hypothesis

Table V. Compilation of Regression Analysis Data

Model: $\ln Y = \ln A + b\ln X^1 + c\ln X^2$			
Type of Data		Run 1	Run 2
Pure Constant	(A)	0.748900	0.751177
First Coefficient	(b)	-27.610352	-1.910723
Second Coefficient	(c)	12.842773	(dropped)
Standard Deviation Y from Mean		1.084638	1.084638
Coefficient of Determination	(r^2)	0.878570	0.875469
Multiple Correlation Coefficient	(r)	-0.937321	-0.935665
Variance	$\sigma_{1.2}^2$	0.154759	0.152363
Standard Error of Estimate	$\sigma_{1.2}$	0.393394	0.390337
Standard Deviation of First Coefficient	σ_b	31.500086	0.144127
Standard Deviation of Second Coefficient	σ_c	15.740889	(dropped)
T Value for Coefficient Check after First Run ($\alpha = 0.05$)		2.60	--------

Test of Significance of Simple Correlation Coefficient r
hypothesis $r = 0$

$$t = \frac{0.935665-0}{0.152363} = 6.14 > 2.06$$ Test significant, reject hypothesis

(21)
$$\text{if } M = 1, \quad \frac{\Delta}{R} = \frac{2.12}{(1)^{1.911}}$$

$$= 2.12$$

$$\text{if } M = \infty, \frac{\Delta}{R} = \frac{2.12}{(\infty)^{1.911}} = \frac{2.12}{\infty} = 0. \tag{22}$$

Therefore, the regression equation has the correct form for the physical limitations. Since Mach number is dimensionless, the inclusion of R gives dimension to Δ. R is not tested for limits of 0 and ∞, as R = 0 implies a pointed body and R = ∞ a flat plate.

Table VI. Compilation of Test Hypotheses

Hypothesis	df	Frequency Distribution	α	Type Test	Significant	Hypothesis
$R = 0$	2, 18	F	0.05	1 Tail	No	Accept
$M = 0$	2, 18	F	0.05	1 Tail	Yes	Reject
$MR = 0$	4, 18	F	0.05	1 Tail	No	Accept
$\bar{X}_e = \bar{X}_r$	26	t	0.05	2 Tail	No	Accept
$\varepsilon_e^2 = \sigma_r^2$	26	X^2	0.05	2 Tail	Yes	Reject
$\bar{X}_r = \bar{X}_{aw}$		Z	0.05	2 Tail	No	Accept
$\sigma_r^2 = \sigma_{aw}^2$	26	X^2	0.05	2 Tail	No	Accept
$A = 0$	25	t	0.05	2 Tail	Yes	Reject
$b = 0$	25	t	0.05	2 Tail	Yes	Reject
$r = 0$	25	t	0.05	2 Tail	Yes	Reject

Next, the regression model was statistically tested against the experimental data and the Ambrosio-Wortman model mentioned in Section II. These computations are shown in Appendix B. The means and variances for the experimental data, the regression model, and the Ambrosio-Wortman model were computed based on responses computed for the experimental Mach numbers. Table VI shows a compilation of the hypotheses for testing the regression model means and variances. Table VII shows the computed 95 percent confidence limits of the means for the experiment, the regression model, and the Ambrosio-Wortman model. The hypothesis that there is no difference between the variance as experimentally determined and as determined by the regression model is the only hypotheses rejected. The hypothesis that there is no significant difference between the experimental mean and the regression model mean or between the regression model mean and the Ambrosio-Wortman model mean are accepted. The test of no significant difference between the regression model variance and the Ambrosio-Wortman model variance is also accepted.

Table VII. Compilation of 95 Percent Confidence Limits on Means

Type Mean	Mean Δ/R	Increment	Limits
Experiment	0.793	$\pm$ 0.451	1.244 to 0.342
Regression Model	0.726	$\pm$ 0.249	0.975 to 0.477
Ambrosio-Wortman	0.687	$\pm$ 0.293	0.981 to 0.395

The computation for the 95 percent confidence limits for the experimental responses, the regression model, and the Ambrosio-Wortman model are shown in Table VII. The regression model has the narrowest range of values for this level of confidence. However, the χ^2 test of the difference between the variances (the second statistical moment) is not significant nor is the difference in their means (the first statistical moment). Therefore, even though the limits of the regression model are narrower than the Ambrosio-Wortman model, they are not significantly different.

The fact that there is a significant difference between the variances of the regression model and the experimental responses is indicative of the insight into the functional relationship between detachment distance and Mach number obtained by the analysis of variance performed prior to the regression analysis. The fit of the equation by the method of least squares is approaching the true mean as evidenced by the high and significant correlation coefficient (r) of 0.94 (Table V).

In order to determine the power of the tests between the means of the two models (regression model and Ambrosio-Wortman model), an operating characteristics curve was computed. The calculations are in Appendix B and the plotted values are shown in Figure 5. From this plot, the probabilities of an acceptance of the hypothesis when it is actually false (type II error) can be determined for selected differences in the means of the two models. For example, the probability of acceptance when the difference between X_r and X_{aw} is ± 0.30 is about 65 percent, and the probability of rejecting the hypothesis is 35 percent.

Plots of the values of Δ/R computed for Mach numbers from 1 to 8 for the regression model and the Ambrosio-Wortman model are shown in Figure 6. The locus of the points for the regression model and the Ambrosio-Wortman model are shown for comparison. There is a region of high curvature or nonlinearity between Mach 1.5 and about Mach 2.5 with the curves becoming asymptotic beyond 2.5. The Ambrosio-Wortman model becomes asymptotic to a Δ/R value of 0.143, whereas the regression model has a zero asymptote, the ultimate physical limit. As mentioned earlier in this section, the Duncan range test indicated that the M_1 level was significantly different from the M_2 and M_3 level. Figure 6 shows the curve becoming essentially asymptotic at about Mach 2.5 or at about the beginning of the M_2 factor level.

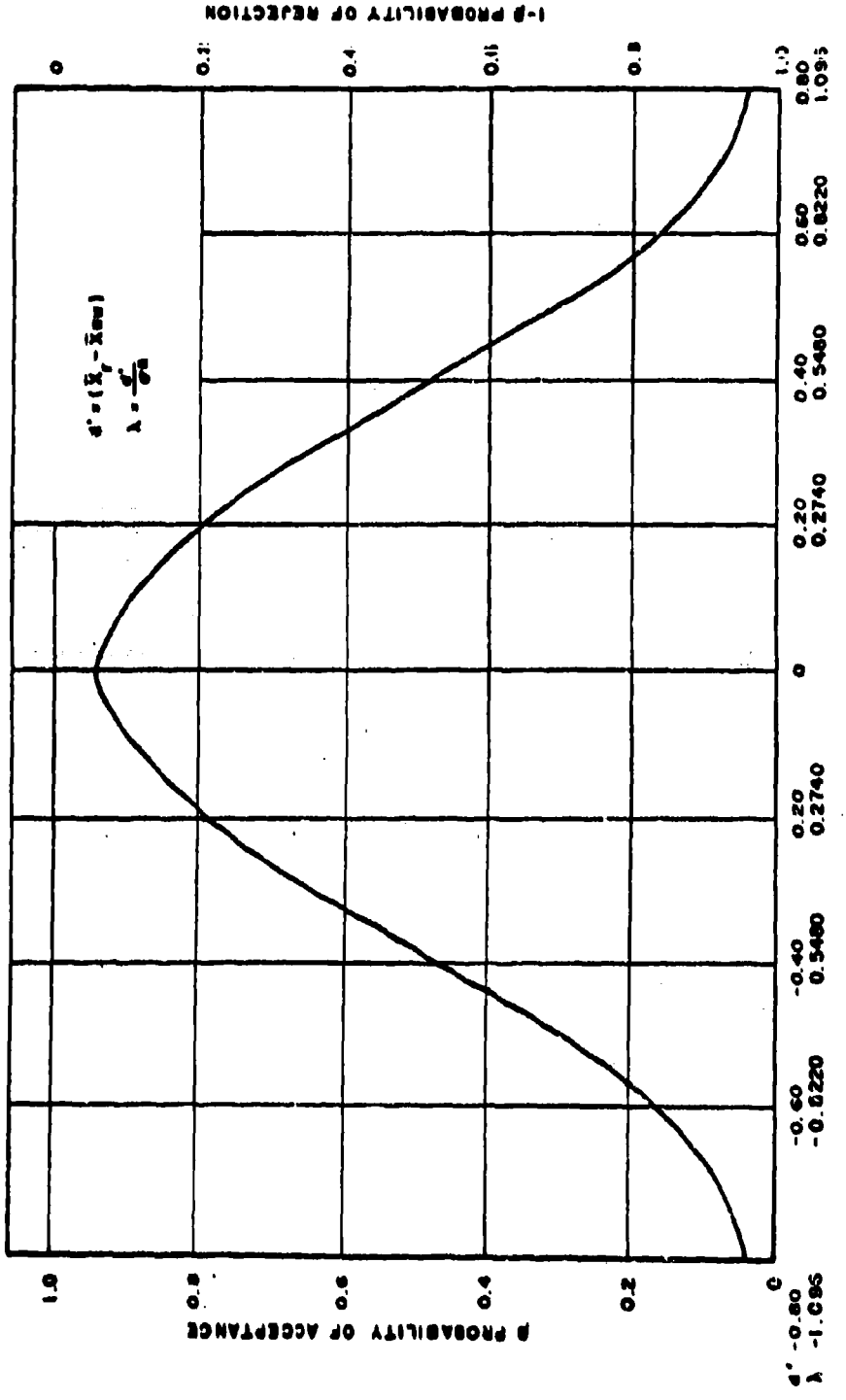

Figure 5. Operating Characteristics Curve for Two Tail Test of Differences Between $\overline{X}_T$ and $\overline{X}_{aw}$

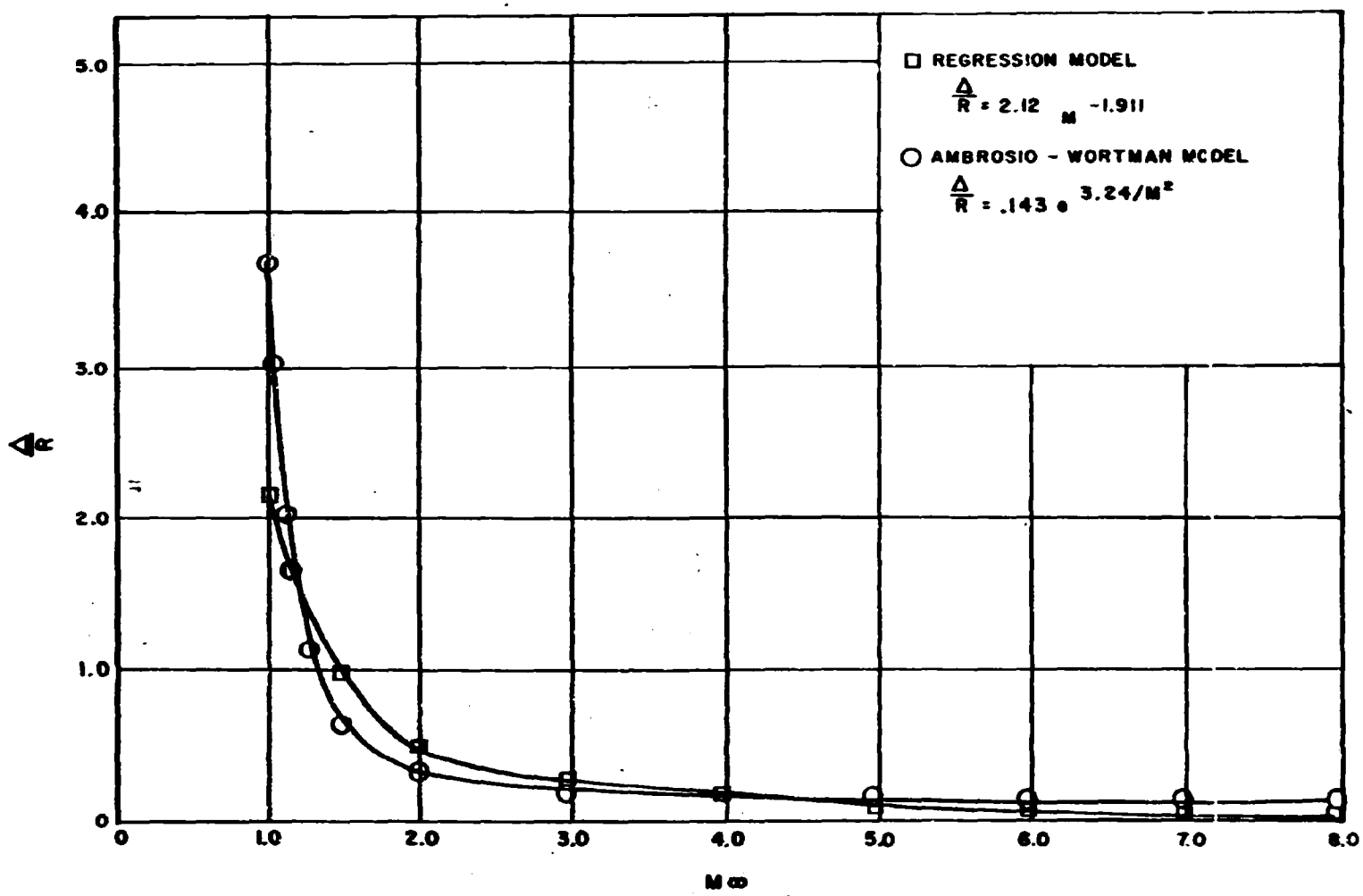

Figure 6. Plot of Δ/R Versus M for Derived Mathematical Model and Ambrosio-Wortman Model

IV. SUMMARY. This experimental and analytical exercise has led to the development of a mathematical model of shock detachment distance. This model has been statistically tested for significance on the basis of comparison with several universal frequency distributions. The hypotheses made and tested are compiled in Table VI.

The hypothesis that the radius has no effect on the detachment distance was accepted. This does not mean that radius has no effect on the shock detachment distance but that, within the limits of the tests, a significant effect cannot be detected. That is, one cannot reject the hypothesis.

The hypothesis that the Mach number has no effect on the detachment distance was rejected. Mach number is apparently a significant contributor to shock location. This means that within the limits of the test a significant variance associated with Mach number is detectable and cannot be attributed to experimental error.

The hypothesis that the MR interaction has no effect on detachment distance was also accepted. This hypothesis is accepted for similar reasons as the hypothesis on radius effects. From Table IV, the ANOVA table, it can be seen that the radius effect accounts for only 1.65 percent of the total expected mean square of the experiment. Mach number accounts for 59.25 percent, MR interaction accounts for 3.30 percent, and error accounts for 35.80 percent. It is pointed out that the variance attributable to variables not included in the experiment could be summed in the Mach number factor, which if separated would reduce the detectable effects of Mach number. For example, body surface roughness, free stream density, and humidity, possible sources not included in the experiment, may significantly effect shock location.

The hypothesis on the derived regression constants, coefficient, correlation coefficient were all rejected. This implies that these values were significantly different from the values one would derive from data where there was no correlation between the variables included in the analysis. The standard error of estimate of 0.390337 shows that the fit for the universe line of regression is good but not perfect. For a perfect fit, the standard error of estimate would be zero and the correlation coefficient 1.0 instead of 0.935665. This emphasizes the fact that all variables which affect the shock location are not included and all

variances present have not been accounted for. However, the model does account for the relative amount of variation in the dependent variable (Δ) that is "explained" by the independent variable (M).

The mean of the experimental data was not found to be significantly different from the mean of the regression model, whereas the variances were significantly different. However, since the variance test is a more sensitive test (i.e., the second statistical moments as compared to the first statistical moment), it is believed that this also attributes to the reliability of the model. The mean of the regression model was not found to be significantly different from the mean of the Ambrosio-Wortman model. This was also true for the variances of the two models. This indicates that within the limits of this investigation there is no significant difference between the model derived from wind tunnel data and free flight data. That is, the hypothesis that the perturbations of holding devices and expanding flow in wind tunnel tests increase the variance of main effects or experimental effects cannot be detected. This is not to say that they do not. It is indicated in Table VII that the regression model is to some degree more accurate than the Ambrosio-Wortman model as the 95 percent confidence limits on the means are more narrow but not significantly so.

Therefore, within the limits of the aerodynamic and statistical assumptions of this investigation, the following general observations are made:

1) The model derived is a reliable model for the prediction of shock detachment distance as a function of Mach number.

2) The model derived with free flight data is apparently not significantly better than models derived by data from wind tunnels.

3) The use of the statistical methods for the analysis of data can lead to increased knowledge of the functional relationships of physical variables.

4) The inferences that can be made through the analysis of data by statistical methods are more objective inferences than could otherwise be made.

5) The use of statistics is an extremely useful tool for the analysis of data which are functions of physical relationships and in many cases lead to increased confidence in the results of the analysis over mere visual inspection of experimental responses.

V. SUGGESTED FUTURE STUDIES. The results of this study indicate that the shock detachment distance for radius nosed bodies is strongly a function of Mach number between 1.0 and about 2.5. After 2.5, the detachment distance is practically independent of Mach number. This was established by the Duncan range test which shows that there is apparently no significant difference between the responses obtained at the M_2 (2.5 to 2.9) and the M_3 level (3.9 to 4.3). Therefore, it seems appropriate to perform future studies in the Mach range of 1.0 to 2.5 to obtain a better understanding of the function where the variation is most sensitive. This will provide a better estimate of the universe regression line of the shock detachment distance in this velocity range.

Another important point to consider for future experimental studies is to confound the daily variation with a selected interaction, since this study shows that there is apparently no significant effect of interaction on the shock detachment distance. In this study, the day effect was confounded with the experimental error and main effects through randomization of all factor levels and combinations with days. Another approach would be through design, to confound a priori the day effects with the interaction. This would separate the variance due to day effects from the experimental error and main effects and may result in a more sensitive test for main effects. However, this does not necessarily follow because the degrees of freedom for error would be reduced for the same number of responses. If the day effects are not large, the separation of the day effects may not be sufficient to offset the reduction in error degrees of freedom. This would require judgment in future designs. In this study, it is believed that it was advantageous to randomly distribute the day effects rather than confounding them with the main or secondary effects since one objective was to test for significance of interaction.

The very high significance of the Mach number factor indicated that further test should be initiated to include other factors as free stream density and some discrete levels of body surface roughness (density and body surface roughness effects were summed as experimental error in this study).

A suggested experiment of academic interest would be a 4^3 factorial with day effects confounded with the highest order interaction. The three factor, four level experiment is suggested in order to test for one degree higher order (cubic) effects. Models of constant radius, but with four levels of surface roughness, at four levels of free stream density and four levels of velocity would be flown in free flight.

This experiment would enable, through the analysis of variance the determination of cubic, surface roughness (S) and density (ρ) effects in addition to velocity effects. Since the first order interaction in this study $(MR)_{ij}$ was not significant, the day effects could be confounded with the second order interaction $(MS\rho)_{ijk}$.

LITERATURE CITED

1. H. Serbin, SUPERSONIC FLOW AROUND BLUNT BODIES, Journal of the Aeronautical Sciences, Vol 25, No. 1, January 1958.
2. A. Ambrosio, and A. Wortman, STAGNATION POINT SHOCK DETACHMENT DISTANCE FOR FLOW AROUND SPHERES AND CYLINDERS, ARS Journal, Vol 32, No. 2, February 1962.
3. DiDonato, and B. Zondek, CALCULATION OF THE TRANSONIC FLOW ABOUT A BLUNT-NOSED BODY WITH A REAR SKIRT, U. S. Naval Weapons Laboratory Unclassified Report (undated).
4. National Advisory Committee on Aeronautics, DATA ON SHAPE AND LOCATION OF DETACHED SHOCK WAVES ON CONES AND SPHERES by J. W. Heberle, G. P. Wood, and P. B. Gooderum, January 1950, TN 2000.
5. National Advisory Committee on Aeronautics, A RE-EXAMINATION OF THE USE OF SIMPLE CONCEPTS FOR PREDICTING THE SHAPE AND LOCATION OF DETACHED SHOCK WAVES by E. S. Love, December 1957, TN 4170.
6. A. Ambrosio, and A. Wortman, STAGNATION-POINT SHOCK-DETACHMENT DISTANCE FOR FLOW AROUND SPHERES AND CYLINDERS IN AIR, Journal of the Aerospace Sciences, Vol 29, No. 7, July 1962.
7. A. J. Duncan, QUALITY CONTROL AND INDUSTRIAL STATISTICS, Homewood, Illinois, Richard D. Irwin, Inc., 1959.

Appendix A
EXPERIMENTAL COMPUTATIONS

Sonic velocity was computed for each round from the following equation:

$$a = \sqrt{\gamma R_o T}. \tag{A-1}$$

Model velocity was computed for each round from the following equation:

$$V = \frac{5 \text{ feet}}{t}. \tag{A-2}$$

Mach number was computed for each round from the following equation:

$$M = \frac{V}{a}. \tag{A-3}$$

The magnification factors for the shadowgraph (F_{sh}) and Schlieren (F_{sc}) systems were computed for all rounds from the following equation:

$$F_{sh} \text{ and } F_{sc} = \frac{\sum_{N=1}^{8} \text{Film Model Diameter}/N}{\sum_{N=1}^{8} \text{Model Diameter}/N}. \tag{A-4}$$

The computed values are:

$$F_{sh} = \frac{0.226}{0.224} = 1.009$$

$$F_{sh} = \frac{0.1915}{0.224} = 0.855. \tag{A-5}$$

Shock detachment distance and model radius correcting for magnification and location was computed as follows:

$$\frac{\Delta}{R} = \frac{\frac{\delta_{sc}}{R_{sc}} + \frac{\delta_{sh}}{R_{sh}}}{2} \tag{A-6}$$

but

$$\begin{aligned} R_{sc(counts)} &= C \times R_b \times F_{sc} \times R_r \\ R_{sh(counts)} &= C \times R_b \times F_{sh} \times R_r , \end{aligned} \tag{A-7}$$

therefore

$$\begin{aligned} \frac{\Delta}{R}(counts) &= \frac{\frac{\delta_{sc}}{C \times R_b \times F_{sc} \times R_r} + \frac{\delta_{sc}}{C \times R_b \times F_{sh} \times R_r}}{2} \\ &= \frac{\delta_{sc}F_{sh} + \delta_{sh}F_{sc}}{2(C \times R_b \times F_{sc} \times F_{sh} \times R_r)} . \end{aligned} \tag{A-8}$$

Therefore,

$$\Delta(counts\ corrected) = \delta_{sc}F_{sh}\ \delta_{sh}F_{sc} \tag{A-9}$$

and

$$R(counts\ corrected) = 2(C \times R_b \times F_{sc} \times F_{sh} \times R_r). \tag{A-9}$$

Example computations for round 75 as shown in Table II.

$$a = \sqrt{1.4 \times 1715 \times (460 + 71)}$$
$$= 1131$$

$$V = \frac{5\ ft}{0.003531\ sec^*} = 1416$$

*This value for round 75 and all other rounds obtained from submicrosecond electronic counters as recorded in aeroballistic data log.

(A-10) $M = \frac{1416}{1131} = 1.252$

$\Delta = 373(0.855) + 390(1.009) = 710.46(\text{counts})$

$R_1 = 2(3502 \times 0.112 \times 1.009 \times 0.855 \times 1.0)$

$= 676.74(\text{counts})$

$\frac{\Delta}{R} \quad \frac{710.46}{676.74} = 1.049.$

Appendix B
STATISTICAL COMPUTATIONS

1. Analysis of Variance

The computations for the analysis of variance was made from the data shown in Table III.

Sums of squares are listed below.

Total sum of squares

$$SS_t = \sum_{ijk}^{abr} \Sigma\Sigma\Sigma\ X^2 \ldots - \frac{(\Sigma X..)^2}{rab} \tag{B-1}$$

$$= 50.746 - \frac{(21.414)^2}{3.3.3}$$

$$= 33.7628.$$

Sum of squares due to radius

$$SS_R = \frac{\sum_{j}^{b} X_{j..}^{\ 2}}{jra} - \frac{\Sigma X..^{\ 2}}{rab} \tag{B-2}$$

$$= \frac{(4.810)^2 + (10.135)^2 + (6.469)^2}{9} - \frac{(21.414)^2}{27}$$

$$= 18.6335 - 16.9836$$

$$= 1.6499.$$

Sum of squares due to Mach number.

$$SS_M = \frac{\Sigma X1_i^2}{irb} - \frac{\Sigma X_{..}^2}{rab}$$

(B-3)
$$= \frac{(17.700)^2 + (0.481)^2 + (0.502)^2}{9} - \frac{(21.414)^2}{27}$$

$$= 35.5819 - 16.9836$$

$$= 18.5983.$$

Sum of squares due to MR interaction

(B-4)
$$SS_{MR} = \frac{\Sigma\Sigma X^2_{..}}{r} - \sum_i^a \frac{X_{i.}}{rb} - \sum_j^b \frac{X_{.j}}{ra} + \frac{X^2_{..}}{rab}$$

$$= \frac{(3.87)^2 + (0.481)^2 + (0.502)^2 + (8.860)^2 + (0.799)^2 + (0.566)^2 + (5.013)^2 + (0.826)^2 + (9.630)^2}{3} - 1.6499 - 18.5989 - 16.9836$$

$$= 2.9885.$$

Sum of squares due to error

$$SS_\epsilon = SS_t - SS_R - SS_M - SS_{MR}$$

(B-5)
$$= 33.7628 - 1.6499 - 18.5983 - 2.9885$$

$$= 10.5261.$$

Sum of squares due to linear and quadratic effects within main and interaction effects. (Coefficients of orthogonal polynomials)[1]

---

[1] C. R. Hicks, Fundamental Concepts in the Design of Experiments, New York, New York, Holt, Rinehart and Winston, 1964

$$SS_{R\ell} = \frac{[-1(4.810) + 0(10.135) + 1(6.469)]^2}{3.3.2} - 0.1529$$

$$SS_{Rq} = \frac{[1(4.810) + -2(10.135) + 1(6.469)]^2}{3.3.6} = 1.4970$$

$$SS_{M\ell} = \frac{[-1(17.70) + 0(2.016)^2 + 1(1.698)]^2}{3.3.2} = 14.3146$$

(B-6)
$$SS_{Mq} = \frac{[1(17.70) + -2(2.016) + 1(1.698)]^2}{3.3.6} = 4.2837$$

$$SS_{R\ell\ M\ell} = \frac{[1(3.827) + -1(0.502) + -1(5.013) + 1(0.630)]^2}{3.} = 0.08551$$

$$SS_{RqM\ell} = \frac{[-1(3.627) + 1(0.502) + 2(8.860) + -2(0.566) + -1(5.013) + 1(0.630)]^2}{3.12}$$

$$= 2.198$$

$$SS_{R\ell\ Mq} = \frac{[-1(3.827) + 2(0.481) + -1(0.502) + 1(5.013) + -2(0.826) + 1(0.630)]^2}{3.12}$$

$$= 0.0108$$

$$SS_{RqMq} = \frac{[+1(3.827) + -2(0.481) + 1(0.502) + -2(8.860) + 4(0.709) \\ -2(0.566) + +1(5.013) + -2(0.826) + 1(0.630)]^2}{3.36}$$

$$= 0.6940.$$

2. **Multiple Range Tests**

Multiple range tests are listed below.

a. **Mach Number Effects**

(B-7)
$$\bar{X}_i \text{. treatments} \quad \underset{1}{1.967} \quad \underset{2}{0.224} \quad \underset{3}{0.188}$$

Error mean square = 0.5847 with 18 d.f.

Standard error of mean is

$$(B\text{-}8) \qquad S_{\overline{X}i.} = \sqrt{\frac{\text{Error MS}}{\text{No. of Obs.}}} = \sqrt{\frac{0.5847}{9}} = 0.2545 .$$

From Table E,[1] ($\alpha = 0.05$ $n_2 = 18$) the significant ranges are

$$(B\text{-}9) \qquad \begin{array}{lccc} p & = & 2 & 3 \\ \text{ranges} & = & 2.97 & 3.12 \end{array} .$$

Multiplying p values by $S_{\overline{X}i.}$, the least significant ranges are

$$(B\text{-}10) \qquad \begin{array}{lccc} p & = & 2 & 3 \\ \text{LSR} & = & 0.756 & 0.796 \end{array} .$$

Largest versus smallest:

$$(B\text{-}11) \qquad 1.967 - 0.224 = 1.743 > 0.796^{*} \text{(significant)}$$

Largest versus second smallest:

$$(B\text{-}12) \qquad 1.967 - 0.189 = 1.778 > 0.756^{*} \text{ (significant)}$$

Second largest versus smallest:

$$(B\text{-}13) \qquad 0.224 - 0.189 = 0.035 < 0.756$$

(See Figure 4 for display of results).

b. Radius Effects

$$(B\text{-}14) \qquad \begin{array}{lccc} \overline{X}_{.j} \text{ treatments} & \frac{1.126}{2} & \frac{0.719}{3} & \frac{0.534}{1} \end{array}$$

Standard error of mean is

[1] Hicks, loc. cit.

(B-15) $$S_{\bar{X}_{\cdot j}} = \sqrt{\frac{\text{Error MS}}{\text{No. of Obs.}}} = \sqrt{\frac{0.5847}{9}} = 0.2545$$

From Table E,[1] ($\alpha = 0.05$ $n_2 = 18$) the significant ranges are

(B-16) $$\begin{array}{lccc} p & = & 2 & 3 \\ \text{ranges} & = & 2.97 & 3.12 \end{array}.$$

Multiplying p values by $S_{\bar{X}_{\cdot j}}$, the least significant ranges are

(B-17) $$\begin{array}{lccc} p & = & 2 & 3 \\ \text{LSR} & = & 0.756 & 0.796 \end{array}.$$

Largest versus smallest:

$$1.126 - 0.5344 = 0.5916 < 0.796.$$

Largest versus second smallest:

$$1.126 - 0.719 = 0.407 < 0.756.$$

Second largest versus smallest:

$$0.719 - 0.534 = 0.184 < 0.756.$$

(See Figure 4 for display of results).

3. Computations for Testing the Model

a. Computation of Experiment Mean and Variance

[1] Hicks, loc. cit.

X_i	$\bar{X}_e$	$(X_i - X_e)^2$	$\bar{X}_i$	$\bar{X}_e$	$(X_i - X_e)^2$
1.049	0.793	0.0655	0.188		0.3660
1.492		0.4886	0.253		0.2916
1.286		0.2430	0.182		0.3732
0.146		0.4186	0.179		0.3769
0.146		0.4186	0.205		0.3457
0.189		0.3648	1.034		0.0580
0.223		0.3249	2.243		2.1025
0.139		0.4277	1.736		0.8892
0.140		0.4264	0.226		0.3226
1.461		0.4462	0.280		0.2631
5.478		21.9492	0.321		0.2227
1.921		1.2723	0.203		0.3481
0.268		0.2756	0.210		0.3398
			0.217		0.3317
			Σ 21.414		

$$\bar{X}_e = 21.414/27 = 0.793$$

$$s_e^2 = 33.752/27\text{-}1 = 1.298$$

$$s_e = \sqrt{1.298} = 1.139$$

b. Computation of Regression Model Mean and Variance

X_i	$\bar{X}_r$	$(\bar{X}_i - X_r)^2$	X_i	$\bar{X}_r$	$(X_i - \bar{X}_r)^2$
1.382	0.726	0.4303	0.314		0.1697
1.618		0.7956	0.282		0.1971
1.535		0.6544	0.154		0.3271
0.303		0.1789	0.151		0.3306
0.336		0.1521	0.152		0.3294
0.288		0.1918	1.271		0.2970
0.149		0.3329	1.668		0.8873
0.154		0.3271	1.568		0.7089
0.152		0.3294	0.276		0.2025
1.557		0.6905	0.283		0.1962
2.035		1.7134	0.232		0.2440
1.714		0.9761	0.137		0.3469
0.299		0.1823	0.167		0.3124
			0.142		0.3410
			Σ 19.597		Σ 11.8449

$$\overline{X}_r = 19.597/27 = 0.726$$

$$\sigma_r^2 = 11.8449/27 = 0.4387$$

$$\sigma_r = \sqrt{0.4387} = 0.6623$$

c. Computation of Mean and Variance of Ambrosio and Wortman's Model (Z) for the Experimental Conditions of this Study

$$\text{Model } \frac{\Delta}{R} = 0.143e^{3.24/M^2}$$

X_i	$\overline{X}_{aw}$	$(X_i - \overline{X}_{aw})^2$	X_i	$\overline{X}_{aw}$	$(X_i - \overline{X}_{aw})^2$
1.133	0.6875	0.1984	0.176		0.2616
1.642		0.9110	0.176		0.2616
1.444		0.5722	1.493		0.6568
0.218		0.2199	3.180		6.2125
0.229		0.2097	1.910		1.4945
0.214		0.2237	0.218		0.2204
0.175		0.2626	0.222		0.2166

X_i	$\overline{X}_{aw}$	$(X_i - \overline{X}_r')^2$	X_i	$\overline{X}_{aw}$	$(X_i - \overline{X}_r)^2$
0.212		0.2261	0.209		0.2289
0.176		0.2616	0.212		0.2261
0.175		0.2626	0.197		0.2411
0.176		0.2616	0.172		0.2657
0.951		0.0694	0.179		0.2636
1.783		1.2096	0.173		0.2647
1.519		0.6914	Σ18.564		Σ16.3939

$$\overline{X}_{aw} = 18.564/27 = 0.6875$$

(B-18)

$$\sigma_{aw}^2 = 16.3939/27 = 0.6072$$

$$\sigma_{aw} = \sqrt{0.6072} = 0.7792$$

95 percent confidence limits on experiment mean

(B-19) $$\bar{X}_{e(0.95)} = 0.793 \pm \frac{1.139}{\sqrt{n}}(2.06) = 0.793 \pm 0.451 = 1.244 \text{ to } 0.342$$

95 percent confidence limits on regression mean

(B-20) $$\bar{X}_{r(0.95)} = 0.726 \pm \frac{0.6623}{\sqrt{n}}(1.96) = 1726 \pm 0.249 = 0.975 \text{ to } 0.477$$

95 percent confidence limits on Ambrosio-Wortman Model mean

(B-21)

$$X_{aw(0.95)} = 0.6875 \pm \frac{0.7792}{\sqrt{27}}(1.96) = 0.6875 \pm 0.293 = 0.981 \text{ to } 0.395.$$

d. **Tests of Means and Variances**

Hypothesis: $\bar{X}_e = \bar{X}_r$

$$t\left(\frac{a}{2} = 0.025 \text{ d.f.} + 26\right) = \pm 2.06$$

(B-22)

$$t = \frac{\bar{X} - \bar{X}'}{S_e/\sqrt{n}} = \frac{0.793 - 0.726}{1.139/\sqrt{27}} = \frac{0.067}{1.139/5.196} = 0.305.$$

Computed value less than table value. Test not significant. Accept hypothesis.

Hypothesis: $S_e^2 = \sigma_r^2$

(B-23) $$\chi^2\left(\frac{a}{2} = 0.025 \text{ d.f.} = 26\right) + 13.8 \text{ to } 41.9$$

$$X^2 = n\frac{S_e^2}{\sigma_r^2} = 27\left(\frac{1.298}{0.4387}\right) = 79.885.$$

Computed value exceeds table value. Test is significantly higher. Reject hypothesis.

$$\text{Hypothesis: } \bar{X}_r = \bar{X}_{aw}$$

(B-24) $$Z\left(\frac{\alpha}{2} = 0.025\right) = \pm 1.960$$

$$\sigma_{r\text{-}aw} = \sqrt{\frac{0.4387}{27} + \frac{0.6072}{27}} = \sqrt{0.01624 + 0.02248} = \sqrt{0.03872} = 0.1968$$

$$Z = \frac{0.726 - 0.687}{0.1968} = +0.1981.$$

Computed value less than table value. Test not significant. Accept hypothesis.

$$\text{Hypothesis: } \sigma_r^2 = \sigma_{aw}^2$$

(B-25) $$\chi\left(\frac{\alpha}{2} = 0.025 \text{ d.f.} = 26\right) = 13.8 \text{ to } 41.9$$

$$\chi^2 = \frac{N\sigma_r^2}{\sigma_{aw}^2} = 27\left(\frac{0.4387}{0.6072}\right) = 19.510.$$

Computed value between table values. Test not significant. Accept hypothesis.

e. Computations for Operating Characteristics Curve for Two-Tail Test of Differences Between the Mean of the Regression Model ($\bar{X}_r$) and the Mean of the Ambrosio-Wortman Model ($\bar{X}_{aw}$)

Assumption - the variances are known for both models.

$$\sigma^* = \sqrt{\frac{N_{aw}\sigma_r^2 + N_r\sigma^2_{aw}}{N_{aw} + N_r}} = \sqrt{\frac{27(0.4387) + 27(0.6072)}{27 + 27}}$$

(B-26)

$$= \sqrt{0.52277} = 0.7299$$

These data are plotted in Figure 5.

$\frac{d'}{(\bar{X}_r - \bar{X}_{aw})}$	λ (d'/σ^*)	$\frac{d'}{\sigma_{r-aw}}$	Z 0.95 - d'/σ_{r-aw} = 1.96 - d'/σ_{r-aw}	Probability of Acceptance β	Probability of Rejection $1-\beta$
0	0	0	1.96	0.95	0.05
0.0492	0.0680	0.25	1.71	0.93	0.07
0.0984	0.1360	0.50	1.46	0.90	0.10
0.1476	0.2040	0.75	1.21	0.86	0.14
0.1968	0.2720	1.00	0.96	0.81	0.19
0.2460	0.3400	1.25	0.71	0.74	0.26
0.2952	0.4080	1.50	0.46	0.65	0.35
0.3936	0.5440	2.00	-0.04	0.50	0.50
0.4920	0.6800	2.50	-0.54	0.32	0.68
0.5904	0.8160	3.00	-1.04	0.17	0.83
0.6888	0.5520	3.50	-1.54	0.09	0.91
0.7872	1.0880	4.00	-2.04	0.05	0.95

PRESENTATION OF THE FIRST SAMUEL S. WILKS MEMORIAL MEDAL*

Frank E. Grubbs

ACCEPTANCE OF THE FIRST WILKS MEMORIAL AWARD

John W. Tukey

It is indeed a pleasure to have Mrs. Samuel S. Wilks with us this evening for the presentation of the first Samuel S. Wilks Memorial Medal Award.

The Samuel S. Wilks Memorial Award for statisticians was established and announced a year ago at the Tenth Conference on Design of Experiments in Army Research, Development and Testing. An account of the announcement of the Wilks Award is given in the American Statistician for December, 1964. The idea for the Award was due to Major General Leslie E. Simon (Ret.), who gave the opening paper at the Tenth Design of Experiments Conference entitled "The Stimulus of S. S. Wilks to Army Statistics". The Wilks Memorial Award is sponsored by the American Statistical Association through the generosity of Mr. Philip G. Rust, retired industrialist of the Winnstead Plantation, Thomasville, Georgia. The American Statistical Association accepted the obligation of administering the Award and funds in accordance with guidance and criteria which are consonant with law and with the wishes of the Army representatives, Mr. Rust, and the American Statistical Association. The name of the recipient of the Wilks Award is announced each year during the annual Conference on Design of Experiments in Army Research, Development and Testing.

With the approval of the President of the American Statistical Association the Wilks Award Committee for 1965 consisted of:

Dr. Francis G. Dressel, Duke University and the Army Research Office-Durham

Dr. Churchill Eisenhart, National Bureau of Standards

*After the dinner meeting at the Eleventh Conference on Design of Experiments in Army Research, Development and Testing, the chairman of the conference, Dr. Frank E. Grubbs, gave the above address. Professor John W. Tukey was presented the first Wilks Memorial Award. Following his acceptance of this honor he spoke to the group about his friend Sam Wilks.

Professor Oscar Kempthorne, Iowa State University
Dr. Alexander M. Mood, U. S. Office of Education
Major General Leslie E. Simon (Ret.), Winter Park, Florida
Dr. Frank E. Grubbs, Ballistic Research Laboratories, Aberdeen Proving Ground, Maryland - Chairman

The Wilks Award Committee met during the annual meeting of the American Statistical Association in Philadelphia on 8-10 September 1965. Many candidates for the 1965 Wilks Award were considered based on nominations from individuals and also statisticians thought worthy of consideration by the committee.

The Wilks Award is not limited to contributors to design of experiments activities in connection with Army research, development and testing, but rather all statisticians who have made significant contributions to the general field of Army statistical endeavors, whether theoretical or applied, are eligible. Moreover, persons eligible for the award include not only government statisticians but also those from universities and industry. The annual programs of the Conference on Design of Experiments in Army Research, Development and Testing indicate rather broadly the nature of statistical endeavors of interest to the Army, but the achievements of those being considered for the award need not be restricted to these areas. Rather, as indicated earlier, the awardee is selected for the advancement of scientific or technical knowledge in statistical efforts which co-incidentally will have benefited the Army and government in one way or another.

As a result of the committee meeting, it is a great pleasure to announce that Professor John W. Tukey of Princeton University has been selected to receive the first Samuel S. Wilks Memorial Medal Award.

Professor Tukey has long been an authority on the statistical analysis of data and has received wide recognition for his many contributions to mathematical statistics and applied statistics in many different fields. Professor Tukey has contributed to the Army Design of Experiments Conferences from the beginning and gave freely of his time to promulgating the uses of statistics in Army applications, DOD applications, Government and industrial applications. The citation for the first Wilks medalist reads as follows:

> To John W. Tukey for his contributions to the theory of statistical inference, his development of procedures for analyzing data, and his influence on applications of statistics in many fields.

Upon receiving the Wilks Medal, Professor Tukey responded as follows:

We are met to honor Sam Wilks' memory. All of us would have so much preferred to have had him here instead. Many of us knew him for ten or twenty years, some for thirty. No matter whether we knew him initimately as a close colleague and friend or only as someone met once a year at such a recurring event as this, we all respected him and all he stood for. In this we are but a small sample.

The memorial minute of the Princeton University faculty begins thus: "Samuel Stanley Wilks died in his sleep on March 7, 1964 at the peak of a distinguished career in teaching, research, and public service. His sudden death, without any warning leaves many friends and associates stunned by a sudden loss of a man upon whom they depended for advice on problems large and small, for a wise appraisal of proposals under consideration, for getting many jobs done---a man instinctively so friendly and fair that everyone responded to him with great affection. His death terminates a quiet, penetrating, and influential leadership in the work of many organizations---especially in mathematics, statistics, and social science---to which he brought wisdom, commitment, persistence, and a remarkable sense of the importance of new developments. His passing leaves an emptiness in so many plans, that one wonders how one man was so versatile and did so much".

The memorial notice of the American Philosophical Society approaches its end thus [1]: "In his service to our Society, Sam showed all the wonderful characteristics we have noticed elsewhere: quiet, modest diligence, deep wisdom, a technical skill that was always adequate to any demand; the ability to comprehend, and bring others to comprehend, the broader issues." The notice then ends: "Mosteller's memoir, written for statisticians, was fittingly entitled: "Samuel S. Wilks: Statesman of Statistics". As members of Benjamin Franklin's own society it is only right that we salute our departed colleague and friend as "Sam: A Quiet Contributor to Mankind".

On the afternoon of his death Sam told my wife: "Now that so many of our former graduate students are leading statistics departments of their own, it's time that John and I worked out something new to do." I never saw Sam again; what we are working out in Princeton today is not what it would have been under his leadership, but we can, and will, do our best to make the new Department of Statistics something of which Sam would have been proud.

For thirty years he kept Fine Hall statistics in balanced contact with mathematics on the one hand and with a wide variety of applications on the other, showing clearly by his example how it was best to combine both. His recognition of the dangers of tight Gaussian assumptions led him to pioneer with non-parametric methods. His recognition of the growing importance of computing came very early; the first punched card equipment on the Princeton campus occupied the room next to his office.

As a unified Princeton statistics comes into being and grows, we will do all we can to continue his tradition. We will emphasize the need for combining contact with mathematics and contact with applications. We will do all we can to bring statistics, computer science, and the use of computer facilities ever closer together. We will try to be ever more realistic in understanding the problems of the real world and in formulating those pale copies of real problems, whose solutions serve to guide us as we face reality. We can do no less if we are to follow his noble tradition.

REFERENCE

[1] Samuel Stanley Wilks (1906-1964). 1964 Yearbook of the American Philosophical Society, 147-154.

TARGET COVERAGE PROBLEMS

William C. Guenther
University of Wyoming, Laramie, Wyoming

Much of the material contained in this paper is a review of literature which has appeared in many different publications. The definition of a single shot coverage problem which was given in a paper by Guenther and Terragno [1] is extended to a multiple shot case. The results which were reviewed in reference 1 appear here in abstracted form since they are useful for the new extension. Some models for the multiple shot case are considered in detail. The latter include some for which results have not been previously published. It is hoped that this paper will be a coordinating force for future research.

In recent years a large number of publications have appeared on probability problems arising from ballistic applications. Many of these papers and reports are concerned with topics which are often referred to as coverage problems. A definition of a coverage problem, which yields many interesting models as special cases, appears in a paper by Guenther and Terragno [1] and will be reproduced here. That definition was for the single shot case but only minor modifications are required to extend it to a multiple shot situation. Further modifications may be necessary if it is desired that the definition yield certain other problems, which have already been investigated or may be formulated in the future, as special cases.

Although most work in this field has been restricted to the two-dimensional case, some applications are meaningful in three dimensions. It is doubtful that the coverage problem has any useful interpretation in more than three dimensions. We will use n-dimensional notation not only because it includes the cases $n = 2$ and $n = 3$ but also because results one derives can occasionally be used in unexpected places where n dimensions are meaningful.

For brevity we will use the notation $X_i = (x_{i1}, x_{i2}, \ldots, x_{in})$ and $\int dF(X_i)$ will represent an n-fold integral.

DEFINITION FOR THE SINGLE SHOT CASE. Before attempting to define a coverage problem, let us consider a special case which will help to introduce some of the essential ideas and language. Suppose that a point target is located at the origin of a two-dimensional coordinate system. A weapon with killing radius R is aimed at the origin with the intention of destroying the point target. When the weapon arrives at the target, the latter is located at $X_2 = (x_{21}, x_{22})$, a randomly selected position within or on a circle of radius D centered at the origin (see Figure 1). That

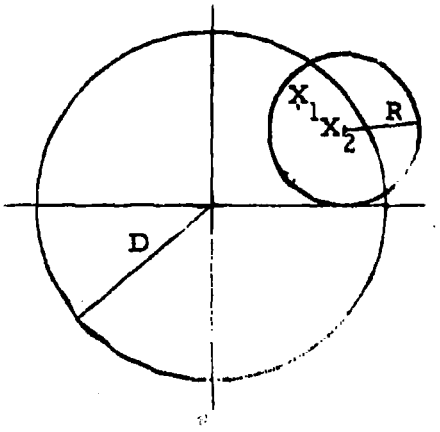

Fig. 1. X_2 is point target and weapon has killing radius R.

is, the probability density function of X_2 is

$$g(x_{21}, x_{22}) = \frac{1}{\pi D^2}, \qquad 0 \leq x_{21}^2 + x_{22}^2 \leq D^2.$$

Assume that aiming errors are circularly normally distributed with unit variance so that the center of the lethal circle $X_1 = (x_{11}, x_{12})$ has p.d.f.

$$f(x_{11}, x_{12}) = \frac{1}{2\pi} \exp[-\frac{1}{2}(x_{11}^2 + x_{12}^2)] \quad .$$

Now a given point X_2 will be destroyed if the impact point of the weapon is within R units of X_2. The probability that this happens is

$$h(x_{21}, x_{22}) = \int_{C_1}\int f(x_{11}, x_{12})\, dx_{11}\, dx_{12}$$

where C_1 is the region $(x_{11}-x_{21})^2 + (x_{12}-x_{22})^2 \leq R^2$. The probability of destroying the target (that is, the probability that the impact point is within R units of the target given that the target is as likely to be at one point as at any other within the circle of radius D) is

$$P(R,D) = \int_{C_2}\int h(x_{21}, x_{22})\; g(x_{21}, x_{22})\; dx_{21}\, dx_{22}$$

where C_2 is the region $x_{21}^2 + x_{22}^2 \leq D^2$. The evaluation of P(R,D) for any number of dimensions is discussed in Section 2 of reference 1 and is mentioned in the abstract of that paper which appears in the next section.

Now let us formulate the definition of a coverage problem for the single shot case. Let X_1 be the impact point of the weapon, X_2 be the position of the target at the time of impact, $P_1(X_1, X_2)$ = probability of destroying the target for given values of X_1 and X_2 (sometimes called the damage function), $F(X_1)$ = the distribution function of the impact point, $G(X_2)$ = the distribution function of X_2. Then

$$P_2(X_2) = \int_{-\infty}^{\infty} P_1(X_1, X_2)\, dF(X_1)$$

= probability a given X_2 is destroyed

and

$$P(\cdot) = = \int_{-\infty}^{\infty} P_2(X_2)\; dG(X_2)$$

= probability of destroying a point target whose position is governed by $G(X_2)$.

We will define a single shot coverage problem as the computation of a probability of the type $P(\cdot)$, that is, the evaluation of

$$P(\cdot) = \int_{-\infty}^{\infty} \int_{-\infty}^{\infty} P_1(X_1, X_2)\, dF(X_1)\, dG(X_2) \quad . \tag{1}$$

All three functions $P_1(X_1, X_2)$, $F(X_1)$, and $G(X_2)$ (and consequently $P(\cdot)$) will in general depend upon parameters.

Although the order of integration in (1) has proven to be the most efficient in the majority of problems which have been studied, there is no reason why that order cannot be reversed if it is profitable to do so. This change gives

$$P(\cdot) = \int_{-\infty}^{\infty} \int_{-\infty}^{\infty} P_1(X_1, X_2)\, dG(X_2)\, dF(X_1) \quad . \tag{2}$$

Several special cases are worthy of consideration. If

$$\begin{aligned} &\text{(a)}\ P_1(X_1, X_2) = 1, && X_1 \in \text{region } C_1 \text{ (usually a sphere)} \\ &\qquad\qquad\ = 0, && \text{otherwise} \\ &\text{(b)}\ g(X_2) = 1, && X_2 = B = (b_1, \ldots, b_n) \\ &\qquad\qquad\ = 0, && \text{otherwise,} \end{aligned} \tag{3}$$

then (1) reduces to

$$P(\cdot) = \int_{C_1} dF(X_1) \tag{4}$$

which is the probability content of region C_1 under distribution $F(X_1)$. If (a) of (3) is satisfied (sometimes called a zero-one damage function)

but $G(X_2)$ does not concentrate all the probability at one point, then (1) reduces to

$$P(\cdot) = \int_{-\infty}^{\infty} \int_{C_1} dF(X_1)\, dG(X_2) , \tag{5}$$

where in general C_1 is defined in terms of both X_1 and X_2.

If X_2 is uniformly distributed over a region C_2, that is

$$g(X_2) = \frac{1}{V(C_2)}, \qquad X_2 \in C_2 \tag{6}$$

$$= 0, \qquad \text{otherwise}$$

where $V(C_2)$ is the volume of C_2, and the damage function is zero-one, then $P(\cdot)$ can be interpreted as the expected fraction of overlap of the region of total destruction and a target area C_2. To see this integrate in reverse order. Given a value of X_1 (see Figure 2)

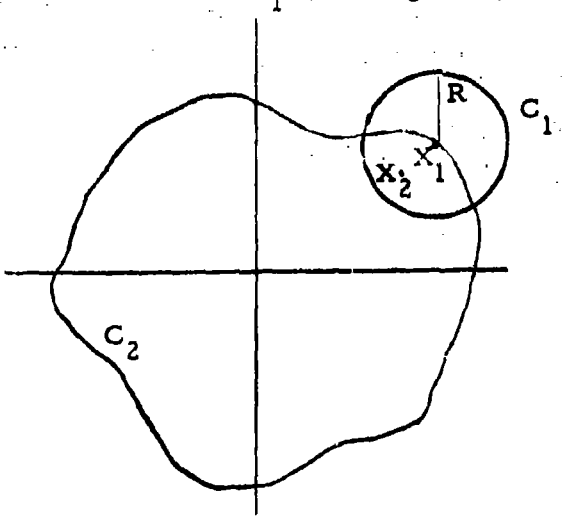

Fig. 2. Circular area of total destruction and target area C_2.

X_2 is captured if it lies in the region common to C_1 and C_2. The probability that happens is

$$\int_{C_1 \cap C_2} \frac{1}{V(C_2)} \, dX_2 = \frac{V(X_1)}{V(C_2)}$$

where $V(X_1)$ is the volume common to C_1 and C_2 for given X_1. Then integrating over X_1 we get

$$\int_{-\infty}^{\infty} \frac{V(X_1)}{V(C_2)} \, dF(X_1) = E\left[\frac{V(X_1)}{V(C_2)}\right]$$

which is, by definition, the expected fraction overlap. Multiplying the latter result by $V(C_2)$ gives $E[V(X_1)]$ or the expected overlap.

When the damage function is not of the zero-one type and X_2 has the density (6), then $P(\cdot)$ can again be interpreted as the fraction of the target area destroyed. This is best seen by writing $P(\cdot)$ as

$$P(\cdot) = \int_{C_2} P_2(X_2) \frac{1}{V(C_2)} \, dX_2$$

and observing that since $P_2(X_2)$ can be interpreted as the fraction of the point X_2 destroyed, $E[P_2(X_2)]$ is the fraction of the target area C_2 which is destroyed. Morganthaler [2] has used this interpretation.

SOME SPECIFIC RESULTS FOR SINGLE SHOT CASE--GUENTHER-TERRAGNO PAPER. A comprehensive review of results for the single shot case has been published by Guenther and Terragno [1]. This paper lists 58 references of which about 30 deal directly with target coverage. A thorough knowledge of results for the single shot case is extremely helpful in the multiple shot situation. This section will be an abstract of that paper.

For most models discussed in the review it is assumed that X_1 has density

$$f(X_1) = f(x_{11}, \ldots, x_{1n})$$

$$= \left[(2\pi)^{\frac{1}{2}n} \prod_{i=1}^{n} \sigma_{1i} \right]^{-1} \exp\left[-\frac{1}{2} \sum_{i=1}^{n} (x_{1i}/\sigma_{1i})^2 \right]. \tag{7}$$

Section 1 is devoted to probability content problems, special cases of (4) with the region C_1 being $\sum_{i=1}^{n} (x_{1i}-b_i)^2 \leq R^2$. Thus the point B is destroyed if the point of impact is within R units of the fixed point. If all $\sigma_{1i}^2 = \sigma^2$, then $P(\cdot)$ is the integral of a non-central chi-square density function with n degrees of freedom and non-centrality parameter $\sum_{i=1}^{n} b_i^2/\sigma^2$. Very extensive tables exist for n=2, adequate tables for n = 3(1)30(2)50(5)100. Results are less abundant if the variances are not equal. However, for B = o, n = 2, 3 and B $\neq$ 0, n = 2, existing tables seem to be quite adequate.

Section 2 describes some special cases of (5). The most interesting results are obtained by using (7) with equal variances for the density of X_1 and $\sum_{i=1}^{n} (x_{1i}-x_{2i})^2 \leq R^2$ for C_1. Thus, if X_1 is within R units of X_2, X_2 is destroyed. For these cases the probability can be expressed as the integral

$$P(\cdot) = \int_{-\infty}^{\infty} H\left(\frac{R^2}{\sigma^2}; n, \frac{r^2}{\sigma^2}\right) dG(X_2) = \int_{-\infty}^{\infty} H\left(\frac{R^2}{\sigma^2}; n, \frac{r^2}{\sigma^2}\right) dQ\left(\frac{r}{\sigma}\right) \tag{8}$$

where $H\left(\frac{R^2}{\sigma^2}; n, \frac{r^2}{\sigma^2}\right)$ is the non-central chi-square distribution function

with n degrees of freedom and non-centrality parameter $\sum_{i=1}^{n} x_{2i}^2/\sigma^2 = r^2/\sigma^2$, $Q(r/\sigma)$ is the distribution function of r/σ (which is, of course, determined by $G(X_2)$). The evaluation of the integral (8) is discussed for the cases:

I. The distribution of X_2 gives equal weight to each point on $\sum_{i=1}^{n} x_{2i}^2 = D^2$, no weight elsewhere. That is, X_2 is uniformly distributed over the surface of a sphere of radius D centered at the origin.

II. X_2 is uniformly distributed within or on a sphere of radius D centered at the origin. Thus,

$$g(X_2) = \frac{1}{V(D)}, \quad \sum_{i=1}^{n} x_{2i}^2 \leq D^2$$

$$= 0, \quad \text{elsewhere}$$

where $V(D)$ is the volume of the sphere.

III. X_2 has a density $g(X_2)$ taking on the form (in spherical coordinates)

$$p(r,a_1,\ldots,a_{n-1}) = (2D\pi^{n-1})^{-1}, \quad 0 \leq r \leq D$$
$$0 \leq a \leq \pi, \; i=1,\ldots,n-2$$
$$0 \leq a_{n-1} \leq 2\pi$$

$$= 0, \quad \text{elsewhere}$$

so that the spherical coordinates are each independently and uniformly distributed.

IV. r/σ has a gamma distribution.

V. r^2/σ^2 has a gamma distribution.

VI. r/σ has a beta distribution.

Finally, a case not falling under (8) in which X_1 and X_2 both have density (7) (but with different variances) is discussed. Perhaps II is the most interesting since it generalizes a well known result by Germond [3]. For this case

$$(9) \qquad P(\cdot) = P\left(\frac{R}{\sigma}, \frac{D}{\sigma}\right) = H\left(\frac{R^2}{\sigma^2};\ n+2,\ \frac{D^2}{\sigma^2}\right) + \left(\frac{R/\sigma}{D/\sigma}^n\right) H\left(\frac{D^2}{\sigma^2};\ n,\ \frac{R^2}{\sigma^2}\right)$$

and evaluation is accomplished by using tables of the non-central chi-square distribution [4].

In Section 3 a few models with damage function

$$P_1(X_1, X_2) = \exp\left[-\sum_{i=1}^{n} (x_{2i}-x_{1i})^2/2\,\lambda^2\right]$$

are discussed. Again X_1 is assumed to have density (7). Then $P(\cdot)$ is evaluated for

I. Same as Case I of Section 2.

II. Same as Case II of Section 2 except that unequal variances are permitted in (7).

III. Same as Case III of Section 2.

IV. Same as Case V of Section 2.

V. Both X_1 and X_2 have density (7) but with different variances.

EXTENDING THE DEFINITION TO THE MULTIPLE SHOT CASE. Again, having a special problem in mind will help in constructing the definition. Let us consider the following case discussed by Jarnagin

and Di Donato [5]. A big bomb is aimed at a point target located at the origin of a two-dimensional coordinate system. When the weapon arrives at the target, the latter is located at X_2, a randomly selected position within or on a circle of radius D. Assume that aiming errors for the big bomb are circularly normally distributed with unit variance. That is, when the big bomb detonates its position X_3 is governed by the density

$$f_3(x_{31}, x_{32}) = \frac{1}{2\pi} \exp\left[-\frac{1}{2}(x_{31}^2 + x_{32}^2)\right].$$

At detonation the big bomb scatters N bomblets, each with lethal radius R, with impact points uniformly and independently distributed over a circle of radius A. Thus, the density of X_1, the impact point of a bomblet, is for given X_3

$$f_{13}(X_1 \mid X_3) = \frac{1}{\pi A^2}, \qquad (x_{11}-x_{31})^2+(x_{12}-x_{32})^2 \leq A^2$$
$$= 0, \qquad \text{otherwise.}$$

Now, given that the target is at X_2 and the big bomb detonates at X_3, X_2 is captured by a bomblet if X_1 is within a distance R of X_2 (see Figure 3). The probability that this happens is

$$P_S = \int_{C_1} \frac{1}{\pi A^2} \, dX_1$$

where C_1 is the region $(x_{11}-x_{21})^2+(x_{12}-x_{22})^2 \leq R^2$. The target will be captured if it is covered by at least one bomblet. This happens with probability $1-(1-P_S)^N$ because of the independence condition. The probability that the target will be captured regardless of where the big bomb detonates is

$$h(X_2) = \int_{-\infty}^{\infty} [1 - (1-P_S)^N] \, f_3(X_3) \, dX_3 .$$

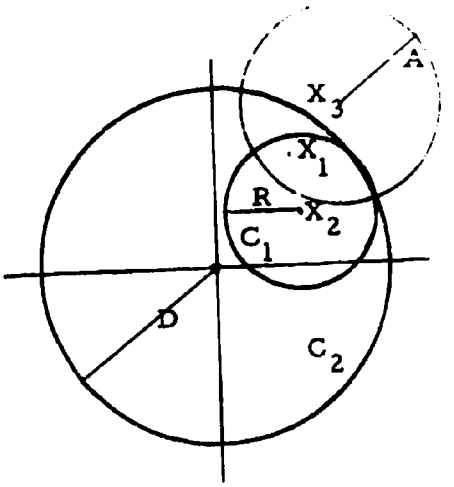

FIG. 3. Big bomb detonates at X_3, bomblet at X_1. Target is at X_2.

Finally, the probability that the target will be captured no matter where it is located is

$$\int_{C_2} h(X_2)\ g(X_2)\ dX_2$$

where C_2 is the region $x_{21}^2 + x_{22}^2 \leq D^2$ and

$$g(X_2) = \frac{1}{\pi D^2}\ ,\quad x_{21}^2 + x_{22}^2 \leq D^2$$

$$= 0\ ,\quad \text{otherwise.}$$

This problem will be discussed further in a later section.

To generalize the above result let X_3 = the impact point of the big bomb, $F_3(X_3)$ = the distribution function of X_3, X_1 = impact point of

a bomblet, $F_{13}(X_1 \mid X_3)$ = conditional distribution of X_1 given X_3, the same for each of the N bomblets with all N impact points being independently distributed, X_2 = position of target when the bomblets impact, $G(X_2)$ = distribution function of the point target, $P_1(X_1, X_2)$ = probability of destroying the target for given values of X_1 and X_2, P_S = probability of capturing the target for any one bomblet given X_3 and X_2. Then

$$P_S = \int_{-\infty}^{\infty} P_1(X_1, X_2)\ dF_{13}(X_1 \mid X_3)$$

and

$$P(\cdot) = \int_{-\infty}^{\infty} \int_{-\infty}^{\infty} [1 - (1-P_S)^N]\ dF_3(X_3)\ dG(X_2) \tag{10}$$

is the probability of destroying the target. Expanding the binomial under the integral in (10) leads to the alternate form

$$P(\cdot) = \sum_{k=1}^{N} (-1)^{k+1} \binom{N}{k} \int_{-\infty}^{\infty} \int_{-\infty}^{\infty} P_S^k\ dF_3(X_3)\ dG(X_2). \tag{11}$$

We will define an n-dimensional coverage problem as the evaluation of a probability of the type given by (10) or (11).

If X_3 has density

$$f_3(X_3) = 1, \quad X_3 = B \text{ (a fixed point)} \tag{12}$$
$$= 0, \quad \text{otherwise}$$

then (10) reduces to

$$P(\cdot) = \int_{-\infty}^{\infty} [1 - (1-P_S)^N] \, dG(X_2) \tag{13}$$

where $X_3 = B$ in P_S. Formula (13) yields $P(\cdot)$ for N shots aimed independently at B (at the origin if B = 0). Further if N = 1, (13) becomes

$$\int_{-\infty}^{\infty} \int_{-\infty}^{\infty} P_1(X_1, X_2) \, dF(X_1) \, dG(X_2) \ ,$$

the single shot formula (where $F(X_1) = F_{13}(X_1 \mid B)$).

SOME SPECIAL CASES OF FORMULA (13).

Big Bomb Hits Origin with Probability 1, Zero-One Damage Function

Assume that aiming errors of the big bomb are governed by the p.d.f. of (12) with B = 0 and that X_2 is uniformly distributed over a sphere of radius D centered at the origin, that is, has p.d.f.

$$g(X_2) = [V(D)]^{-1}, \quad \sum_{i=1}^{n} x_{2i}^2 \leq D^2 \quad \text{(region } C_2\text{)} \tag{14}$$

$$= 0 , \quad \text{otherwise}$$

where V(D) is the volume of sphere of radius D. We will also assume that the density of X_1 given X_3 is

$$f_{13}(X_1 \mid X_3) = [(2\pi)^{\frac{1}{2}n} \prod_{i=1}^{n} \sigma_{1i}]^{-1} \exp[-\frac{1}{2} \sum_{i=1}^{n} (x_{1i}-x_{3i})^2/\sigma_{1i}^2] \tag{15}$$

with $\sigma_{1i} = \sigma$, i=1,2,...,n and where $x_{3i} = 0$, i=1,2,...,n because the big bomb hits the origin with probability 1. Then

$$P_S = \int_{C_1} dF_{13}(X_1 \mid 0)$$

where C_1 is the region $\sum_{i=1}^{n} (x_{1i}-x_{2i})^2 \leq R^2$. It is well known that this integral has the value

$$P_S = H\left(\frac{R^2}{\sigma^2}; n, \frac{r^2}{\sigma^2}\right) \tag{16}$$

where $r^2 = \sum_{i=1}^{n} x_{2i}^2$. Hence

$$P(\cdot) = P\left(\frac{R}{\sigma}, \frac{D}{\sigma}\right) = \int_{C_2} \left\{1 - \left[1-H\left(\frac{R^2}{\sigma^2}; n, \frac{r^2}{\sigma^2}\right)\right]^N\right\} \frac{1}{V(D)}\, dX_2$$

$$= \sum_{k=1}^{N} (-1)^{k+1} \binom{N}{k} \int_0^D \left[H\left(\frac{R^2}{\sigma^2}; n, \frac{r^2}{\sigma^2}\right)\right]^k \frac{n r^{n-1}}{D^n}\, dr.$$

The multiple integral converts to a single integral by virtue of the result on page 248 of [1]. We know from Formula (9) that the single integral in (17) can be expressed in terms of H functions for $k = 1$. A corresponding result for $k \geq 2$ may be possible but it is unknown at the present time.

For the case n=2, Jarnagin [6] has prepared tables of (17) for R/σ = .005(.005).05(.01).10(.02).20(.05)1(.1)2(.2)4(.5)10, D/σ = .05, 1.(.1)4(.5)12, N = 1(1)20. Also included is an inverse table giving the number of bomblets N required to make $P(\cdot)$ = .05(.05).95 for the range of D/σ given above and with R/σ ranging over values required to make N go from 1 to 999.

Big Bomb Hits at Point B with Probability 1, Exponential Damage Function

Assume that the damage function is

$$P_1(X_1, X_2) = \exp\Big[-\frac{1}{2}\sum_{i=1}^{n}(x_{2i}-x_{1i})^2/\lambda^2\Big] \tag{18}$$

and that the p. d. f. of X_1 given $X_3 = B$ is given by (15) with $x_{3i} = b_i$, $i=1, 2, \ldots, n$. Then an easy integration yields

$$P_S = \frac{\lambda^n}{\prod_{i=1}^{n}(\sigma_{1i}^2+\lambda^2)^{\frac{1}{2}}} \exp\Big[-\frac{1}{2}\sum_{i=1}^{n}(x_{2i}-b_i)^2/(\sigma_{1i}^2+\lambda^2)\Big] .$$

Expanding the binomial in (13) we can write

$$P(\cdot) = \sum_{k=1}^{N}(-1)^{k+1}\binom{N}{k}\int_{-\infty}^{\infty}\frac{\lambda^{nk}}{\prod_{i=1}^{n}(\sigma_{1i}^2+\lambda^2)^{\frac{1}{2}k}} \exp\Big[(-\frac{k}{2})\sum_{i=1}^{n}\frac{(x_{2i}-b_i)^2}{(\sigma_{1i}^2+\lambda^2)}\Big]\, dG(X_2) . \tag{19}$$

First assume that X_2 is uniformly distributed over an ellipsoid whose center is at the origin and whose axes are parallel to the coordinate axes. Then

$$g(X_2) = [V(C_2)]^{-1}, \quad \sum_{i=1}^{n}(x_{2i}/a_i)^2 \leq 1 \quad \text{(the region } C_2\text{)}$$

$$= 0, \quad \text{otherwise}$$

where $V(C_2)$ is the volume of C_2. Then if we let $k^{\frac{1}{2}}(x_{2i}-b_i)/(\sigma_{1i}^2+\lambda^2)^{\frac{1}{2}} = y_i$, the probability (19) becomes

(20)
$$P(\cdot) = \sum_{k=1}^{N} \frac{(-1)^{k+1} \binom{N}{k} \lambda^{nk} (2\pi)^{\frac{1}{2}n}}{V(C_2)\, k^{\frac{1}{2}n} \prod_{i=1}^{n} (\sigma_{1i}^2 + \lambda^2)^{\frac{1}{2}(k-1)}} J_k$$

where

$$J_k = \int_{C_{2k}} f_0(Y)\, dY ,$$

$f_0(Y)$ is the standard normal density in n dimensions, and C_{2k} is the region

$$\sum_{i=1}^{n} \frac{\left(y_i + \dfrac{b_i \sqrt{k}}{(\sigma_{1i}^2 + \lambda^2)^{\frac{1}{2}}} \right)^2}{k^2 / a_i^2 (\sigma_{1i}^2 + \lambda^2)} \leq 1 .$$

Tables from which J_k can be obtained when n=2 have been prepared by Germond [7], DiDonato and Jarnagin [8], Lowe [9], and Rosenthal and Rodden [10]. If $b_1 = b_2 = 0$ so that the ellipse is centered at the origin, then J_k can be evaluated from the tables published by Esperti [11], Harter [12], DiDonato and Jarnagin [13], and Marsaglia [14]. All the above tables are described by Guenther and Terragno [1]. Groves [15] derived (20) for the case n = 2 and includes a 16 page table of J_k for this case (with $b_1 = b_2 = 0$) in his report.

If all $\sigma_{1i} = \sigma$, and $a_i = D$, then

$$J_k = H\left[\frac{k^2}{D^2(\sigma^2 + \lambda^2)} ;\ n,\ r^2 \right]$$

where

$$r^2 = \frac{k}{\sigma^2 + \lambda^2} \sum_{i=1}^{n} b_i^2 .$$

Further if $B = 0$, then J_k reduces to a central chi-square probability. For both the latter two cases many tables are available and a description of these tables is found in Section 1 of [1].

If in (19) we take $B = 0$, $\sigma_{1i} = \sigma$ and assume that $G(X_2)$ gives equal weight to each point on the sphere $\sum_{i=1}^{n} x_{2i}^2 = D^2$, then (19) reduces to

$$P(\cdot) = \sum_{k=1}^{N} (-1)^{k+1} \binom{N}{k} \frac{\lambda^{nk}}{(\sigma^2 + \lambda^2)^{nk/2}} \exp\left[\frac{kD^2}{2(\sigma^2+\lambda^2)}\right] \tag{21}$$

since everything comes out in front of the multiple integral except $dG(X_2)$ which when integrated over the whole space yields 1. For a $G(X_2)$ so chosen, X_2 picks its position at random on the surface of the sphere. The answer is the same, of course, no matter how $G(X_2)$ assigns probability on the surface of the sphere but uniform assignment is the most realistic model.

As one further model let us assume that $B = 0$ and X_2 has p. d. f.

$$g(X_2) = [(2\pi)^{\frac{1}{2}n} \prod_{i=1}^{n} \sigma_{2i}]^{-1} \exp[-\frac{1}{2} \sum_{i=1}^{n} (x_{2i}/\sigma_{2i})^2] \ . \tag{22}$$

Then (19) readily reduces to

$$P(\cdot) = \sum_{k=1}^{N} (-1)^{k+1} \binom{N}{k} \frac{\lambda^{nk}}{\prod_{i=1}^{n} [(\sigma_{1i}^2+\lambda^2)^{(k-1)} (k\sigma_{2i}^2+\sigma_{1i}^2 + \lambda^2)]^{\frac{1}{2}}} \ .$$

SOME SPECIAL CASES OF FORMULA (10).

The Jarnagin-DiDonato Model

Let us return to the example which we used to introduce multiple shot coverage problems but generalize the discussion to n-dimensions.

Then X_1 given X_3 is uniformly distributed over a sphere of radius A centered at X_1 so that

$$f_{13}(X_1 \mid X_3) = [V(A)]^{-1}, \quad \sum_{i=1}^{n} (x_{1i}-x_{3i})^2 \leq A^2 \quad \text{(region } C_3\text{)}$$

$$= 0, \quad \text{otherwise,}$$

X_2 is uniformly distributed over a sphere of radius D centered at the origin so that it has the p. d. f. given by (14), and

$$f_3(X_3) = [(2\pi)^{\frac{1}{2}n} \prod_{i=1}^{n} \sigma_{3i}]^{-1} \exp\left[-\tfrac{1}{2} \sum_{i=1}^{n} (x_{3i}/\sigma_{3i})^2\right]. \tag{23}$$

Here V(A) is the volume of a sphere of radius A, We will assume that $\sigma_{3i} = \sigma$, $i=1,2,\ldots,n$ and for convenience (as DiDonato and Jarnagin have done) we will take $\sigma = 1$ which means all distances are expressed in standard units. The damage function is

$$P_1(X_1, X_2) = 1, \quad \sum_{i=1}^{n} (x_{1i}-x_{2i})^2 \leq R^2. \quad \text{(region } C_1\text{)}$$

Then

$$P_S = \int_{C_1} \frac{1}{V(A)} \, dX_1 = \frac{V(t^2)}{V(A)}$$

where $t^2 = \sum_{i=1}^{n} (x_{2i}-x_{3i})^2$ and $V(t^2)$ is the volume common to C_1 and C_3. Hence, since all functions appearing in (10) are known, the 2n-fold integral could be written down with the integrand expressed in terms of X_2 and X_3.

Some simplification is possible. We seek $E[u(t^2)]$ where $u(t^2) = 1 - (1-P_S)^N$. If the density of t^2 were known, then $P(\cdot)$ could be expressed as a single integral with integrand in t^2. We know from working with single shot coverage problems that the density of t^2 given $r^2 = \sum_{i=1}^{n} x_{2i}^2$ is non-central chi-square with non-centrality parameter r^2. This is

$$h(t^2; n, r^2) = \frac{1}{2}\left(\frac{t}{r}\right)^{(n-2)/2} \exp\left[-\frac{1}{2}(t^2+r^2)\right] I_{(n-2)/2}(tr) \tag{24}$$

where $I_{(n-2)/2}(x)$ is the modified Bessel function of order $(n-2)/2$. The density function of r^2 (see [1], p. 248 for the density of r) is

$$g(r^2) = \frac{n(r^2)^{(n-2)/2}}{2D^n}, \qquad 0 \leq r^2 \leq D^2$$

$$= 0, \qquad \text{otherwise.}$$

Hence the joint distribution of t^2 and r^2 is $h(t^2; n, r^2)\, q(r^2)$ and

$$P(\cdot) = \int_0^{(A+R)^2} \int_0^{D^2} u(t^2)\, h(t^2; n, r^2)\, q(r^2)\, dr^2\, dt^2, \tag{25}$$

a double integral.

For the 2-dimensional case a further simplification is possible since (24) is then symmetric in t^2 and r^2. Thus, in (25) the integration of r^2 yields $H(D^2; 2, t^2)$ so that

$$P(\cdot) = \int_0^{(A+R)^2} \frac{u(t^2)}{D^2}\, H(D^2; 2, t^2)\, dt^2 . \tag{26}$$

The Jarnagin and DiDonato report includes over 100 pages of graphs which yield the $P(\cdot)$ of (26). Two cases are considered. For Case I, $R < A$ and $20 \leq N \leq 500$ for various values of D, A, and πR^2. For Case II, $R > A$ and $1 \leq N \leq 20$ for selected values of R, D, A. The Case I graphs give $\pi D^2 P(\cdot)$ while the set for Case II give $P(\cdot)$ directly. Various approximations to $P(\cdot)$ are discussed.

From a practical point of view the most interesting case is $R < A$. For this situation it is immediately apparent that bounds on the $P(\cdot)$ of (26) are

$$[1 - (1 - \frac{R^2}{A^2})^N] \int_0^{(A-R)^2} \frac{1}{D^2} H(D^2; 2, t^2)\, dt^2 < P(\cdot)$$

$$< [1 - (1 - \frac{R^2}{A^2})^N] \int_0^{(A+R)^2} \frac{1}{D^2} H(D^2; 2, t^2)\, dt^2 . \tag{27}$$

Both integrals appearing in (27) can be expressed in terms of H functions by using (9). The H functions in turn can be evaluated by using the tables of Hayman, Govindarajulu, and Leone [4]. Of course, the smaller the R the closer the bounds will be.

EXPONENTIAL DAMAGE FUNCTION, DETONATION POINTS OF BIG AND LITTLE BOMBS NORMALLY DISTRIBUTED. Assume that the damage function is given by (18), the density of X_1 given X_3 by (15), and the density of X_3 by (23). Then a straight forward evaluation yields

$$P_S = \int_{-\infty}^{\infty} P_1(X_1, X_2)\, f_{13}(X_1 \mid X_3)\, dX_1$$

$$= \frac{\lambda^n}{\prod_{i=1}^{n} (\sigma_{1i}^2 + \lambda^2)^{\frac{1}{2}}} \exp\left[-\frac{1}{2} \sum_{i=1}^{n} (x_{3i} - x_{2i})^2 / (\sigma_{1i}^2 + \lambda^2)\right] .$$

The same kind of evaluation next gives

$$(28)\qquad \int_{-\infty}^{\infty} P_S^k f_3(X_3)dX_3 = \frac{\lambda^{kn} \exp\left[\left(\frac{-k}{2}\right) \sum_{i=1}^{n} x_{2i}^2/(k\sigma_{3i}^2+\sigma_{1i}^2+\lambda^2)\right]}{\prod_{i=1}^{n} [(\sigma_{1i}^2+\lambda^2)^{(k-1)} (k\sigma_{3i}^2+\sigma_{1i}^2+\lambda^2)]^{\frac{1}{2}}}.$$

To write down $P(\cdot)$ as given by (10) we need finally to integrate (28) over the range of X_2.

For several distributions of X_2 $P(\cdot)$ is obtained very quickly. We will consider:

Case I: $\sigma_{3i} = \sigma_3$, $\sigma_{1i} = \sigma_1$ and $G(X_2)$ gives equal weight to each point on the sphere $\sum_{i=1}^{n} x_{2i}^2 = D^2$. Then with the same reasoning used to obtain (21) we get

$$(29)\qquad P(\cdot) = \sum_{k=1}^{N} (-1)^{k+1} \binom{N}{k} \frac{\lambda^{kn} \exp\left[-kD^2/2\,(k\sigma_3^2+\sigma_1^2+\lambda^2)\right]}{[(\sigma_1^2+\lambda^2)^{(k-1)} (k\sigma_3^2+\sigma_1^2+\lambda^2)]^{n/2}}.$$

Case II: The density of X_2 is given by (14). Letting

$$y_i = \frac{\sqrt{k}\, x_{2i}}{\sqrt{k\sigma_{3i}^2+\sigma_{1i}^2+\lambda^2}}$$

and recalling that

$$V(D) = \pi^{n/2} D^n/\Gamma\left(\frac{n+2}{2}\right)$$

we get

$$P(\cdot) = \sum_{k=1}^{N} (-1)^{k+1} \binom{N}{k} \frac{\lambda^{kn}\, \Gamma(\frac{n+2}{2})\, 2^{n/2}}{D^n\, k^{n/2} \prod_{i=1}^{n} (\sigma_{1i}^2 + \lambda^2)^{(k-1)/2}}$$

(30)

$$\cdot \int_{C_1} \frac{1}{(2\pi)^{n/2}} \exp\left[\frac{1}{2} \sum_{i=1}^{n} y_i^2\right] dy_1 \ldots dy_n$$

where C_1 is the region $\sum_{i=1}^{n} (k\sigma_{3i}^2 + \sigma_{1i}^2 + \lambda^2)\, y_i^2/k \leq D^2$. The evaluation of standard normal integrals over ellipsoidal and spherical regions is discussed in Section 1.3 of [1].

Case III. The density of X_2 is given by (22). A routine integration yields

$$P(\cdot) = \sum_{k=1}^{N} (-1)^{k+1} \binom{N}{k} \frac{\lambda^{kn}}{\prod_{i=1}^{n} [(\sigma_{1i}^2 + \lambda^2)^{(k-1)} (\sigma_{1i}^2 + k\sigma_{2i}^2 + k\sigma_{3i}^2 + \lambda^2)]^{\frac{1}{2}}}. \tag{31}$$

CONCLUDING REMARKS. Although the definition of a coverage problem which we have given can be further generalized, many of the interesting models which have received attention are special cases of the definition as we have given it. Certainly there are models which may be of interest other than those covered in the Guenther-Terragno review and in this paper.

In this review we have considered only the zero-one damage function and the exponential damage function given by (18). Many others have been proposed. For example, another possibility that has some merit is

$$P_1(X_1, X_2) = 1, \qquad \sum_{i=1}^{n} (x_{1i} - x_{2i})^2 \leq R^2$$

(32)

$$= \exp\left\{-\frac{1}{2}\left[\sum_{i=1}^{n} (x_{1i} - x_{2i})^2 - R^2\right]/\lambda^2\right\}, \quad \sum_{i=1}^{n} (x_{1i} - x_{2i})^2 > R^2.$$

The damage function (32) is found in [1] but the topic is not pursued. Other damage functions are mentioned in [16] and [17].

The first step for a potential researcher in the field of coverage problems is to select a useful and realistic model. Having made that choice, the remainder of the task confronting an investigator is mainly numerical. It is possible that most or all of the computation required is already available in the literature if one knows where to look. Even if no such results are in existence, chances are excellent that probabilities of interest can be evaluated if one is clever enough in handling special functions and computers.

Work on target coverage problems has suffered from a mass duplication of effort. This is in part due to (a) some company publications being difficult if not impossible to obtain, (b) results having been published not only in obscure publications but also in many different journals so that it is difficult to keep current in the field, and (c) some papers being difficult to read unless one has background in both probability and target coverage.

REFERENCES

1. William C. Guenther and Paul J. Terragno, "A Review of the Literature on a Class of Coverage Problems," The Annals of Mathematical Statistics 35, 232-260 (1964).

2. George W. Morganthaler, "Some Target Coverage Problems," Biometrika 48, 313-324 (1961).

3. G. E. Haynam, Z. Govindarajulu, and F. C. Leone, "Tables of the Cumulative Non-Central Chi-Square Distribution," AD 426 500 Office of Technical Service, U. S. Department of Commerce, Washington, D. C. 20230 (1962).

5. M. P. Jarnagin, Jr. and A. R. DiDonato, "Expected Damage to a Circular Target by a Multiple Warhead," NWL Report No. 1936, U. S. Naval Weapons Laboratory, Dahlgren, Virginia (1964).

6. M. P. Jarnagin, Jr., "Expected Coverage of a Circular Target by Bombs all Aimed at the Center," NWL Report No. 1941, U. S. Naval Weapons Laboratory, Dahlgren, Virginia (1965).

7. H. H. Germond, "Integration of the Gaussian Distribution over an Offset Ellipse," Rand Report No. P-94, The Rand Corporation, Santa Monica, California (1949).

8. A. R. DiDonato and M. P. Jarnagin, Jr., "Integration of the General Bivariate Gaussian Distribution over an Offset Ellipse," NWL Report No. 1710, U. S. Naval Weapons Laboratory, Dahlgren, Virginia (1960).

9. J. R. Lowe, "A Table of the Integral of the Bivariate Normal Distribution over an Offset Circle," Journal of the Royal Statistical Society, Series B 22, 177-187 (1960).

10. G. W. Rosenthal and I. J. Rodden, "Tables of the Integral of the Elliptical Bivariate Normal Distribution over Offset Circles," Lockheed Report No. IMSD-800619, Sunnyvale, California (1961).

11. R. V. Esperti, "Tables of the Elliptical Normal Probability Function," Defense Systems Division, General Motors Corporation, Detroit, Michigan (1960).

12. H. Leon Harter, "Circular Error Probabilities," Journal of the American Statistical Association 55, 723-731 (1960).

13. A. R. DiDonato and M. P. Jarnagin, Jr., "A Method for Computing the Generalized Circular Error Function and Circular Coverage Function," NWL Report No. 1768, U. S. Naval Weapons Laboratory, Dahlgren, Virginia (1962).

14. George Marsaglia, "Tables of the Distribution of Quadratic Forms of Ranks Two and Three," Boeing Scientific Research Laboratories Report No. D1-82-0015-1, Seattle, Washington (1960).

15. Arthur D. Groves, "A Method for Hand-Computing the Expected Fractional Kill of an Area Target with a Salvo of Area Kill Weapons," Ballistic Research Laboratories Memorandum Report No. 1544, Aberdeen Proving Ground, Maryland (1964).

16. Operations Evaluation Group, "Probability-of-Damage Problems of Frequent Occurrence," OEG Study 626, Office of the Chief of Naval Operations, Washington, D. C. (1959).

17. Frank McNolty, "Kill Probability When Lethal Effect is Variable," Operations Research 13, 478-482 (1965).

MAXIMUM LIKELIHOOD ESTIMATION FOR UNBALANCED FACTORIAL DATA*

H. O. Hartley
Institute of Statistics
Texas A&M University

1. INTRODUCTION. The statistical literature is abundant with results concerning the design and analysis of factorial experiments. Most of these results relate to design experiments whose intricate balance usually provides orthogonal contrasts for the estimation of parameter functions for which inferences are desired. The consequences of such designs are statistical efficiency of estimation with exactness of estimation theory and simplicity of computational procedures thrown in as 'fringe benefits'.

Unfortunately, however, in basic and operation research there are many situations where the scientist is forced to draw inferences from data which have not arisen from carefully balanced factorial experiments mainly because part of the origin of his data is beyond his control. Thus we may be concerned with an analysis of operational data in a chemical plant attempting to relate the quality and yield of the output to various types and sources of input materials, to different types of catalysts, to various modes of operating the plant such as temperature and pressure levels and running times. Even if it is possible to control the change in the various input factors it will often not be possible to conduct balanced experiments. Again in genetical research concerned with heritability studies we may study certain traits of the progeny resulting from the mating of a number of sires each to a different set of dames. We may try to arrange for the 'breeding pens' of the progeny trail to have an equal number of dames in each but the progeny resulting from each mating is beyond the control of the experimenter, resulting in an 'unequal number nested classification' of data. Again, in medical research we may wish to compare the follow-up of patients who have received different treatments. Such follow-up data are often classified with regard to numerous concomitant characteristics concerning the medical history, environmental and genetical background of patients resulting in data arranged in completely unbalanced factorial patterns. There is clearly no possibility of a designed experiment here.

---

*This paper gives only a summary of some of the results derived in more detail by Hartley, H. O. and Rao, J. N. K. "Maximum Likelihood Estimation for the Mixed Analysis of Variance Model" submitted for publication in Biometrika.

We do not need to add further examples of this kind; indeed it is generally recognized that they will outnumber, by far, the situations of data from balanced experiments.

In the case of balanced designs the estimation problem for the constants and variances involved in the linear model theory of the experimental data has been extensively treated: Confining ourselves to just one reference on variance estimation, optimality properties of the classical analysis of variance procedures have already been demonstrated for various balanced designs (see e.g., Graybill (1961)). However, results for unbalanced factorial and nested data are much more restricted: Henderson (1953) has suggested a method of unbiased estimation of variance components for the unbalanced two-way classification but his method is computationally cumbersome for a mixed model and when the numbers of classes is large. Searle and Henderson (1961) have suggested a simpler method also for the unbalanced two way classification with one fixed factor containing a moderate number of levels and a random factor permitted to have quite a large number of levels. Bush and Anderson (1963) have investigated for the two-way classification random model the relative efficiency of Henderson's (1953) method and two other methods, A and B, based on the respective methods of fitting constants and weighted squares of means described by Yates (1934) for experiments based on a fixed effects model which also provide unbiassed estimates of variance components. Possibilities of generalizations are indicated. In all the above methods the estimates of any constants in the model are computed from the 'Aitken Type' weighted least squares estimators based on the exact variance-covariance matrix of the experimental responses which involves the unknown variance ratios. The estimation of the latter is then based on various unbiassed procedures so that little is known about any optimality properties of any of the resulting estimators. However, all these methods reduce to the well known procedures based on minimal sufficient statistics in the special cases of balanced designs.

The method of maximum likelihood estimation here developed differs from the above in that maximum likelihood equations are used and solved for both the estimates of constants and variances. This method has apparently not been used by the above authors (and is indeed 'rejected' by Bush and Anderson, 1963) because the computational effort is not (in their view) warranted by the known properties of maximum likelihood estimation. This point is well taken. However, we have nevertheless undertaken to develop this theory on the following grounds:

(a) Within reason and with the help of suitable numerical techniques the argument of computational labor looses its stigma with the progress in computer technology.

(b) Our technique of maximum likelihood estimation provides a numerical analysis for the completely general mixed model and does not require the development of new devices whenever a more involved situation of unbalanced factorial data arises. Moreover, it provides the basis for a completely general 'analysis of variance test' procedure in the form of 'likelihood--ratio tests'.

(c) We have established large sample optimality properties and it is already apparent that for small experiments the amount of computational labor is quite comparable with that involved in alternatives. Here our technique will permit Monte Carlo evaluations of small sample variances (on the lines made by Bush and Anderson) for the maximum likelihood estimators. For really large experiments (such as arise with certain genetical problems) the large sample optimality properties of maximum likelihood estimators should provide a clear justification of additional computer time (if any).

(d) Recent researches in identifying minimal sufficient statistics for the estimation of the parameters (see e.g., Hultquist and Graybill, (1965) Furukawa (1960)) is at this time confined to several special designs. Since a universal method of identifying such statistics when they exist is not available it is a considerable (small sample) advantage of maximum likelihood estimators that they will automatically be functions of such statistics whenever they exist.

(e) Our estimates of variance components are always ≥ 0 (see section 4) and whilst the alternative estimators could be modified to also be ≥ 0 they would thereby loose the property of unbiassedness which is the main justification of their use.

2. SPECIFICATION OF THE GENERAL MIXED MODEL. The specification of the general mixed model will be sufficiently general to cover most of the situations of unbalanced factorial data arising in practice.

On the other hand, it utilizes certain specific features which distinguish analysis of variance models from a completely general linear model involving both 'constants' as well as random variables.

The linear model here treated is given by

$$y = X\alpha + U_1 b_1 + \ldots + U_c b_c + e \tag{1}$$

where

X is an $n \times k$ matrix of known fixed numbers

U_i is an $n \times m_i$ matrix of known fixed numbers

α is a $k \times 1$ vector of unknown constants

b_i is an $m_i \times 1$ vector of independent variables from $N(0, \sigma_i^2)$

e is an $n \times 1$ vector of independent variables from $N(0, \sigma^2)$.

The random vectors $b_1, b_2, \ldots, b_c$, and e are mutually independent and y is given by (1).

We assume that the design matrices X and U_i are all of full rank i.e., the rank of X is k and the rank of U_i is m_i. In terms of analysis of variance terminology the vector of constants α comprises in its elements all levels of all fixed factors, i.e., the levels of all fixed main effects and interactions appropriately re-parameterised so that the design matrix X has full rank. For the c random factors we are keeping the components separate since all elements of b_i have the same unknown variance σ_i^2. Usually (with analysis of variance models) each y is associated with precisely one level of the i^{th} random factor so that the design matrix U_i will have in each row precisely one 1 and the remaining $m_i - 1$ elements zero. We therefore assume that the U_i have this property which imples that all $m_i \times m_i$ matrices $U_i' U_i$ are diagonal.

One additional important assumption must be made about the design matrices which may be described as a condition for estimability of the α and σ_i^2: Denote by

$$m = \sum_{i=1}^{c} m_i \tag{2}$$

the total number of levels in all random components. Then the adjoined $n \times (k+m)$ matrix

$$M = (X \mid U_1 \mid \ldots \mid U_c) \tag{3}$$

is assumed to have as a base an $n \times r$ matrix W of the form

$$W = (X \mid U^*) \tag{4}$$

where the $n \times (r-k)$ matrix U^* must contain at least one column from each U_i so that

$$k + c \leq r \leq k + m. \tag{5}$$

3. THE LIKELIHOOD EQUATIONS. From (1) it is obvious that y follows a multivariate normal distribution with variance--covariance matrix

$$\sigma^2 H = \sigma^2 \{ I_n + \gamma_1 U_1 U_1' + \ldots + \gamma_c U_c U_c' \} \tag{6}$$

where

$$\gamma_i = \sigma_i^2 / \sigma^2 \quad . \tag{7}$$

Hence the likelihood of y is given by

$$L = (2\pi)^{-\frac{1}{2}n} \sigma^{-n} \mid H \mid^{-\frac{1}{2}} \exp \{-(y - X\alpha)' H^{-1} (y - X\alpha)/2\sigma^2\} . \tag{8}$$

The differentiation of the log likelihood

$$\lambda = \text{Log } L \tag{9}$$

with regard to a, σ and γ_i yields the equations

$$\frac{\partial \lambda}{\partial a} = \sigma^{-2} \{X' H^{-1} y - (X' H^{-1} X) a \} = 0 \tag{10}$$

$$\frac{\partial \lambda}{\partial \sigma} = -\frac{n}{\sigma} + \frac{1}{\sigma^3} (y - Xa)' H^{-1} (y - Xa) = 0 \tag{11}$$

and

$$\frac{\partial \lambda}{\partial \gamma_i} = -\tfrac{1}{2} \text{ tr } \{H^{-1} \frac{\partial H}{\partial \gamma_i} \} - \frac{1}{2\sigma^2} (y - Xa)' \frac{\partial H^{-1}}{\partial \gamma_i} (y - Xa)$$

$$= -\tfrac{1}{2} \text{ tr } \{H^{-1} U_i U_i'\} + \frac{1}{2\sigma^2} (y - Xa)' H^{-1} U_i U_i' H^{-1} (y - Xa). \tag{12}$$

Whitlst it has long been recognized that equations (10) and (11) readily yield the maximum likelihood estimates $\tilde{a}$ and $\tilde{\sigma}^2$ as functions of the γ_i involved in H, the solution of equations (12) i.e., $\frac{\partial \lambda}{\partial \gamma_i} = 0$ has not been attempted in the past. We give in the next section a numerical procedure of solving the simultaneous equation (10), (11), and $\frac{\partial \lambda}{\partial \gamma_i} = 0$ given by (12).

4. SOLUTION OF THE MAXIMUM LIKELIHOOD EQUATIONS BY STEEPEST ASCENT. As mentioned in 3. the equations (10) and (11) are readily solved for a and σ^2 in terms of the γ_i: -- We obtain the familiar answers for 'weighted least squares'

$$\tilde{a} = (X' H^{-1} X)^{-1} (X' H^{-1} y) \tag{13}$$

and

$$n \tilde{\sigma}^2 = y' H^{-1} y - (X' H^{-1} y)' (X' H^{-1} X)^{-1} (X' H^{-1} y) . \tag{14}$$

Equations (13) and (14) yield $\tilde{\alpha}$ and $\tilde{\sigma}^2$ in terms of the y and γ_i. We require symbols for this functional relationship and write in place of (13) and (14)

(15) $$\alpha = \tilde{\alpha}(\gamma_i)$$

and

(16) $$\sigma = \tilde{\sigma}(\gamma_i) \ .$$

Substitution of (15) and (16) in (12) and equating to zero would yield c simultaneous equations for the c values of γ_i. The solutions of these equations are now obtained as the asymptotic limits of a system of c simultaneous differential equations, namely the equations of steepest ascent given by

(17) $$\frac{d\gamma_i}{dt} = \frac{\partial\lambda}{\partial\gamma_i} \left(\tilde{\alpha}(\gamma_i), \tilde{\sigma}(\gamma_i), \gamma_i\right)$$

where the k + 1 + c argument function $\frac{\partial\lambda}{\partial\gamma_i}(\alpha, \sigma, \gamma_i)$ is given by the right hand side of (12) and (15) and (16) are substituted for α and σ.

The variable of integration, t, in (17) is auxiliary and the numerical integration of (17) commences at initial trial values ${}_o\gamma_i$ (usually chosen as consistant estimators) so that

(18) $$\gamma_i = {}_o\gamma_i \quad \text{at } t = 0.$$

It can now be shown that as $t \to \infty$

(19) $$\lim_{t \to \infty} \gamma_i(t) = \tilde{\gamma}_i \text{ (say)}$$

and

(20) $$\lim_{t \to \infty} \frac{\partial\lambda}{\partial\gamma_i} \left(\tilde{\alpha}(\gamma_i), \tilde{\sigma}(\gamma_i), \gamma_i\right) = 0 \ .$$

Therefore, $\tilde{\gamma}_i$ together with $\tilde{a}(\tilde{\gamma}_i)$ $\tilde{\sigma}(\tilde{\gamma}_i)$ represent a solution of the maximum likelihood equations (10), (11), and $\frac{\partial \lambda}{\partial \gamma_i} = 0$ given by (12). It should be noted that although the limit along a specific path of integration is unique as $t \to \infty$ it does not follow that there is only one solution of the maximum likelihood equations since a change in the starting point ${}_o\gamma_i$ may give rise to a different path of integration.

Finally we should comment on a modification of our steepest ascent integration which ensures that $\gamma_i = 0$ along the path: First observe that the log likelihood is a differentiable function of $\tau_i = \gamma_i^{\frac{1}{2}}$ which is symmetrical at $\tau_i = 0$. It follows that if τ_i is used as a parameter in place of γ_i we have

$$\frac{\partial \lambda}{\partial \tau_i} = \frac{\partial \lambda}{\partial \gamma_i} \cdot 2\tau_i \quad . \tag{21}$$

Therefore, the steepest ascent differential equations (17) can be replaced by

$$\frac{d\tau_i}{dt} = 2\tau_i \frac{\partial \lambda}{\partial \gamma_i} (\tilde{a}(\gamma_i), \tilde{\sigma}(\gamma_i), \gamma_i) \; . \tag{22}$$

The integration would commence at positive values ${}_o\gamma_i$ but should the path of integration reach a point where one or several of the $\tau_i = 0$, a new integration would be started at that point and the one or several τ_i would be held at $\tau_i = 0$ for the rest of the integration path. The limit as $t \to \infty$ will again be a solution of the likelihood equations

$$\frac{\partial \lambda}{\partial \tau_i} = 0, \quad \frac{\partial \lambda}{\partial a} = 0, \quad \frac{\partial \lambda}{\partial \sigma} = 0. \tag{23}$$

This procedure ignores and avoids any possible solutions of the likelihood equations with $\gamma_i < 0$.

It would carry us to far afield if we were to discuss in this paper computational details of solving the system of c ordinary first order differential equations (17) or (22). It suffices to state that a large step (high order) Runge-Kutta procedure (see e.g., Henrici (1962)) is found to be quite serviceable. For large n (i.e., $n \geq 50$) numerical inversion of the n x n matrix H involved in (12), (13), and (14) can be completely avoided by reducing this task to operations involving only matrix inversions of order m x m where $m = \Sigma\, m_i$ on lines similar to Henderson et al (1959). The relevant equation is

$$H^{-1} = I - Z\,(Z'Z + I)^{-1}\,Z' \tag{24}$$

where

(25) Z is the adjoined n x m matrix

$$Z = (\sqrt{\gamma_1}\,U_1 \mid \ldots \mid \sqrt{\gamma_c}\,U_c) .$$

With the help of (24) the computational work is quite manageable on high speed computers and a program is in preparation covering data for which $n \leq 500$, $c \leq 5$ $k \leq 150$, $m \leq 150$. The computer time on the IBM 7094 is estimated to range between 5 minutes and 2 hours largely depending on the magnitudes of m and k.

REFERENCES

Bush, N. and Anderson, R. L. (1963). "A Comparison of Three Different Procedures for Estimating Variance Components." Technometrics, 5, 421-40.

Furukawa, N. (1960). "The Point Estimation of the Parameters in the Mixed Model." Kumamoto J. Sci. A, 5, 1-43.

Graybill, F. A. (1961). An Introduction to Linear Statistical Models, Vol. 1. McGraw-Hill Book Company, Inc.

Graybill, F. A., Martin, F. and Godfrey, G. (1956). "Confidence Intervals for Variance Ratios Specifying Genetic Heritability." Biometrics, 12, 99-109.

Henderson, C. R. (1953). "Estimation of Variance and Covariance Components." Biometrics, 9, 226-52.

Henderson, C. R., Kempthorne, O., Searle, S. R. and Von Krosigk, C. M. (1959). "The Estimation of Environmental and Genetic Trends from Records Subject to Culling." Biometrics, 15, 192-218.

Henrici, P. (1962). Discrete Variable Methods in Ordinary Differential Equations. John Wiley & Sons, Inc.

Hultquist, R. A. and Graybill, F. A. (1965). "Minimal Sufficient Statistics for the Two-Way Classification Mixed Model Design." J. Amer. Stat. Assoc. 60, 182-92.

Searle, S. R. and Henderson, C. R. (1961). "Computing Procedures for Estimating Components of Variance in the Two-Way Classification Mixed Model." Biometrics, 17, 607-16.

Yates, F. (1934). "The Analysis of Multiple Classifications with Unequal Numbers in the Different Classes." J. Amer. Stat. Assoc. 29, 51-66.

LIST OF ATTENDEES

Alley, Bernard	US Army Missile Command
Anctil, Albert A.	Army Materials Research Agency
Anderson, Virgil L.	Purdue University
Atkinson, John C.	Edgewood Arsenal
Bailey, Milton	US Naval Supply Res & Dev Facility
Barksdale, Thomas H.	Fort Detrick
Barnett, Bruce D.	Picatinny Arsenal
Bechhofer, Robert	Cornell University
Bell, Raymond	BRL, Aberdeen Proving Ground, Md.
Biser, Erwin	Fort Monmouth
Bohidar, Neeti R.	Fort Detrick
Boldridge, A.	TECOM
Bombara, E. L.	Marshall Space Flight Center
Brown, George A.	Thiokol Chemical Corp., Denville, NJ
Brown, William A.	Dugway Proving Ground
Bruce, C.	RAC
Bruno, O. P.	BRL, Aberdeen Proving Ground, Md.
Bulfinch, Alonzo	Picatinny Arsenal
Cameron, Joseph M.	National Bureau of Standards
Carrillo, J. V.	White Sands Missile Range, New Mexico
Carter, F. L.	Fort Detrick
Chernack, Gilbert	Thiokol Chemical Corp., Denville, NJ
Chrepta, M. M.	Fort Monmouth
Ciuchta, Henry P.	Edgewood Arsenal
Cohen, A. C.	University of Georgia
Couington, George F.	Picatinny Arsenal
Cousin, Thomas	BRL, Aberdeen Proving Ground, Md.
Cox, Paul C.	White Sands Missile Range, New Mexico
Curtis, William E.	Picatinny Arsenal
D'Andrea, Mark M.	US Army Material Research Agency
DeCicco, Henry	US Army Munitions Command
Dick, John S.	US Army
Dressel, F. G.	Army Research Office-Durham
Duff, James B.	Fort Belvoir
Dutoit, Eugene	Picatinny Arsenal
Dziobko, John	Picatinny Arsenal
Ehrenfeld, Sylvain	New York University
Eisenhart, Churchill	National Bureau of Standards
Fetters, William B.	Naval Propellant Plant, Indian Head, Md.
Fontana, W.	US Army Electronics Laboratory
Foohey, Sean P.	Research Analysis Corporation

Foster, Walter D.	Fort Detrick
Futterer, Arnold T.	Edgewood Arsenal
Galbraith, A. S.	Army Research Office-Durham
Geshner, John A.	Picatinny Arsenal
Groenewoud, Cornelius	Cornell Aeronautical Lab., Buffalo, N. Y.
Grubbs, Frank E.	BRL, Aberdeen Proving Ground
Guenther, William C.	University of Wyoming
Gupta, Shanti S.	Purdue University
Hall, Charles A.	White Sands Missile Range
Hanson, Fred S.	White Sands Missile Range
Harris, Bernard	University of Wisconsin
Harshbarger, Boyd	Virginia Polytechnic Institute
Hartley, H. O.	Texas University
Hassell, Louis D.	Picatinny Arsenal
Heacock, Frederick E.	LOH Field Office, St. Louis, Missouri
Hecht, Edward C.	Picatinny Arsenal
Helvig, T. N.	Honeywell, Inc.
Howard, B. A.	US Army Weapons Command
Hunter, J. Stuart	Princeton University
Jacobus, David P.	WRAIR
James, Peter G.	Bureau of Medicine, FDA
Jenkins, Andrew H.	Redstone Arsenal
Jessup, Gordon L.	Fort Detrick
John, Frank J.	Watervliet Arsenal
Kirby, William	BRL, Aberdeen Proving Ground
Kocornik, Richard W.	Picatinny Arsenal
Kolodny, Samuel	Harry Diamond Labs.
Krueger, Albert C.	Picatinny Arsenal
Landerman, J.	ONR
Lavin, George I.	BRL, Aberdeen Proving Ground
Lawrence, Myron C.	USAF, Oprs. Analysis Ofc., Wash., D.C.
Lehnigk, Siegfried H.	Redstone Arsenal
Levy, Hugh B.	Picatinny Arsenal
Little, Robert E.	University of Michigan
Lucas, H. L.	North Carolina State University
Lum, Harry S.	Fort Detrick
Lum, Mary D.	Wright-Patterson Air Force Base
Macy, Donald M.	US Army Aviation Materiel Command
Mandelson, Joseph	Edgewood Arsenal
Mann, H. B.	University of Wisconsin, Math Res Center
Mannello, Edmund L.	Picatinny Arsenal
Manthei, James H.	Edgewood Arsenal

Margolin, Barry H.	Fort Monmouth
Masaitis, Cesiovas	Ballistic Research Laboratories
Mazzio, Vincent J.	US Army Natick Laboratories
McBroom, C. W. O.	Walter Reed Hospital
McKeague, Robert L.	USA Ammunition Procurement & Supply Agcy.
McLaughlen, G.	NRB
McLean, Robert A.	University of Tennessee
McMains, Forest	Picatinny Arsenal
McMullen, W. C.	Naval Supply, R&D
Miller	Picatinny Arsenal
Miller, Morton	Scherring RC
Mioduski, Robert	BRL, Aberdeen Proving Ground
Moore, James R.	BRL, Aberdeen Proving Ground
Mowchan, Walter	BRL, Aberdeen Proving Ground
Nagorny, George W.	Naval Base, Philadelphia, Pa.
Nelson, Harold	Hercules Power Co.
Nickel, J. A.	University of Oklahoma
Olivieri, Peter G.	Nuc Rel Div, QAD, Dover, N.J.
Orleans, B. S.	BU Ships
Osiecki, Charles H.	Picatinny Arsenal
Palmer, J. D.	University of Oklahoma
Parks, Albert	Harry Diamond Laboratories
Parrish, Gene B.	Army Research Office-Durham
Pell, William H.	National Science Foundation
Pliml, James R.	LOH Field Office, St. Louis, Missouri
Provost, Robert G.	U. S. Army Missile Command
Revusky, Samuel H.	Fort Knox, Kentucky
Riggs, Charles W.	Fort Detrick
Rinkel, Richard C.	Research Analysis Corporation
Rose, Carol D. (Mr.)	US Army Tank-Automotive Center
Rosenthal, Arnold J.	Celanese Corporation of America
Rosenblatt, Joan R.	National Bureau of Standards
Rothman, David	Rocketdyne, A Division of NAA
Rotkin, I.	Harry Diamond Laboratories
Saboe, John C.	International Resist. Co.
Sarakwash, Michael	Thiokol Chemical Corporation
Schlenker, George J.	U. S. Army Weapons Command
Schmidt, Th. W.	Army Research Office-Durham
Scholten, Roger W.	The Boeing Company
Selig, Seymour M.	Office of Naval Research
Selman, Jerry H.	U. S. Army Munitions Command

Sloane, Harry S.	Dugway Proving Ground
Slutter, Carl G.	Picatinny Arsenal
Smoot, Perry R.	AMRA, Watertown, Mass.
Solomon, Herbert	Stanford University
Somody, Edward V.	Aberdeen Proving Ground
Starr, Selig	Army Research Office-Washington
Strauch, R.	Vitro Laboratory
Tang, Douglas B.	Walter Reed Army Institute of Research
Tilden, Donald A.	Picatinny Arsenal
Tingey, H. B.	University of Delaware
Uherka, David J.	U. S. Army Natick Laboratories
Vick, James A.	Edgewood Arsenal
Walner, Arthur W.	US Naval Applied Science Laboratory
Webb, S. R.	Rocketdyne, A Division of NAA
Webster, Robert D.	Picatinny Arsenal
Weinstein, Joseph	Fort Monmouth
Weintraub, Gertrude	Picatinny Arsenal
Wiesenfeld, Louis	Picatinny Arsenal
Williams, Burton L.	White Sands Missile Range
Willoughby, Weldon	BRL, Aberdeen Proving Ground
Youden, W. J.	George Washington University